
Università degli Studi di Napoli “Federico II”
Facoltà di Ingegneria



Tesi di Dottorato

Antonio Formisano

Seismic upgrading of existing RC buildings
by means of metal shear panels:
design models and full-scale tests

*Il Coordinatore del Corso:
Prof. Dr. Ing. Federico M. Mazzolani*

Dottorato di Ricerca in Ingegneria delle Costruzioni
XIX Ciclo

ACKNOWLEDGEMENTS

During my PhD Course there were a lot of people who supported and helped me, allowing the elaboration of this dissertation.

First of all, I would like to express my deep and sincere gratitude to my Tutor and my Master Prof. Federico Massimo Mazzolani, who offered me the possibility to join His glamorous research group. He guided me during the whole Doctoral Course by means of His illuminant teaching activities, believing in me and offering me the opportunity to improve my erudition in the Structural Engineering field through the involvement in numerous research topics. His ingeniousness, experience, competence, seriousness, tirelessness determination and enthusiasm, together with His extraordinary human qualities, have represented a clear reference for my studies and for my life. The affection and the gratitude I prove for Him are unlimited.

I am much grateful to Prof. Raffaele Landolfo, who helped me in the Doctoral studies, always having encouragement words for me. Really I have esteem and admiration for Him, not only in the academic framework. His great professionalism and human qualities were for me a clear example to be followed.

I am very grateful to Prof. Gianfranco De Matteis, who guided me during the whole Doctoral period, giving me the opportunity to study the topic of the present thesis and also allowing to deep my knowledge in many other research activities. His competence and enthusiasm have represented an important stimulus for my activity.

I would like to thank Prof. Bruno Calderoni, Dr. Gaetano Della Corte and Dr. Beatrice Faggiano for the useful teachings provided me during the PhD Course.

I am also grateful to Dr. Simeone Panico and Eng. Marco Maruzzelli for their aid provided respectively in the experimental and the numerical activities developed in the current thesis.

I thank all my fellow Engineers who shared with me the experience of the PhD period. A particular mention is devoted to Enrico Barecchia and Giuseppe Brando, for their friendship, and especially to my colleague and friend Gianmaria Di Lorenzo, for the sincere suggestions and constructive criticisms he gave me.

A special thank to the D.A.P.S. librarian and my friend Carmine Citro for his help in the bibliographical research and for all the beautiful times enjoyed together in these three years.

In the framework of my research activity I respectfully acknowledge the financial support given by the International research project PROHITECH “Earthquake Protection of Historical Buildings by Reversible Mixed Technologies” and the theme n.5 “Development of innovative approaches for the design of steel and composite structures” of the National research project RELUIS “Innovative materials and approaches for seismic design and mitigation of structural vulnerability”, both coordinated by Prof. Federico M. Mazzolani.

Also I extend my acknowledgements to the Brollo-Marcegaglia Company, for the free furniture of the steel sheeting used in the experimental activity, and to the BOVIAR Company, especially in the person of Eng. M. Catanese, for measurement operations provided during the tests performed in the framework of the present thesis.

An immense acknowledgement is devoted to the members of my family, for their sacrifices, affection and patience proved me during these years. They gave me an exemplar style of life, permitting me to understand the real values which my existence must be based on. The love and the admiration I prove for them cannot be described in so few words.

Last but not least, I wish to express my deep gratitude to my love Anna, for her encouragement, emotional and material involvement and unlimited support offered me during my studies. Without her presence, the elaboration of such a thesis should not be possible. For this reason the dissertation herein presented is dedicated to her.

To Anna

List of Contents

Introduction

MOTIVATION AND SCOPE	1
SUMMARY	3

Chapter I

Seismic vulnerability of RC buildings

1.1 INTRODUCTION	7
1.2 SEISMIC HAZARD	9
1.3 SEISMIC VULNERABILITY AND PROTECTION	14
<i>1.3.1 General</i>	14
<i>1.3.2 Vulnerability assessment techniques</i>	17
1.4 EARTHQUAKE RISK MODELLING	19
<i>1.4.1 Loss estimation</i>	19
<i>1.4.2 The seismic risk definition</i>	21
1.5 THE BEHAVIOUR OF EXISTING RC BUILDINGS	23
1.6 SEISMIC RETROFITTING TECHNIQUES	32
<i>1.6.1 General</i>	32
<i>1.6.2 Seismic rehabilitation schemes</i>	33

1.6.3 Rehabilitation approaches	35
<i>1.6.3.1 Local intervention methods</i>	<i>38</i>
1.6.3.1.1 Injection of crack	39
1.6.3.1.2 Shotcrete (guniting)	40
1.6.3.1.3 Steel plate adhesion	40
1.6.3.1.4 Steel jacketing	41
1.6.3.1.5 Fibre reinforced polymers (FRPs)	42
<i>1.6.3.2 Global intervention methods</i>	<i>44</i>
1.6.3.2.1 RC jacketing	44
1.6.3.2.2 External buttresses	45
1.6.3.2.3 Addition of RC walls	45
1.6.3.2.4 Base isolation	47
1.6.3.2.5 Steel bracings	48
1.6.3.2.6 Steel Plate Shear Walls (SPSWs)	49

Chapter II

State-of-the-art review on steel plate shear walls

2.1 INTRODUCTION	51
2.2 THE SHEAR WALL SYSTEMS	54
2.3 COMPACT SHEAR PANELS	61
<i>2.3.1 General</i>	<i>61</i>
<i>2.3.2 Design criteria</i>	<i>62</i>
<i>2.3.3 Theoretical and numerical modelling</i>	<i>66</i>

2.3.4 <i>Experimental research activities</i>	68
2.4 SLENDER SHEAR PANELS	98
2.4.1 <i>General</i>	98
2.4.2 <i>Design criteria</i>	99
2.4.3 <i>Theoretical and numerical modelling</i>	103
2.4.4 <i>Experimental research activities</i>	106
2.5 APPLICATIONS	128

Chapter III

Numerical evaluation of the metal shear panels response and set-up of design criteria

3.1 INTRODUCTION	137
3.2 COMPACT SHEAR PANELS	138
3.2.1 <i>Preliminary analyses</i>	138
3.2.2 <i>Numerical simulation of experimental tests</i>	150
3.2.3 <i>Parametric study</i>	160
3.3 SLENDER SHEAR PANELS	165
3.3.1 <i>Simulation of an experimental test</i>	165
3.3.1.1 <i>The reference experimental basis</i>	165
3.3.1.2 <i>Analysis methods</i>	167
3.3.1.3 <i>FEM model calibration</i>	171
3.3.2 <i>Parametric study</i>	183

3.3.2.1 Foreword	183
3.3.2.2 The shear panel – frame system	184
3.3.2.2.1 Foreword	184
3.3.2.2.2 Simplified interpreting models	185
3.3.2.2.3 Influence of the column stiffness	186
3.3.2.3 Influence of the aspect ratio	189
3.3.2.3.1 Foreword	189
3.3.2.3.2 Panels with “compact” shape	190
3.3.2.3.3 Panels with “slender” shape	194
3.3.2.4 Influence of intermediate ribs	197
3.3.2.4.1 Design of intermediate stiffeners	197
3.3.2.4.2 The numerical results	199
3.3.2.5 Concluding remarks	202

Chapter IV

The building under investigation

4.1 INTRODUCTION	203
4.2 THE ORIGINAL BUILDING	206
4.2.1 The division in sub-structures	210
4.2.2 The selected RC module	214
4.2.3 The material mechanical features	218
4.3 EXPERIMENTAL DYNAMIC TESTS	222

4.3.1 General	222
4.3.2 Acquisition systems	224
4.3.3 Direct impulse test (instrumented hammer)	226
4.3.4 Indirect impulse test (falling mass)	229
4.3.5 Comparison between test results	230
4.4 NUMERICAL DYNAMIC INVESTIGATION	231
4.4.1 The numerical model	231
4.4.2 The numerical modal analysis results	233
4.4.3 Calibration of the numerical model according to experimental results	239
4.5 THE PUSHOVER ANALYSES	242
4.5.1 General	242
4.5.2 The numerical study	244
4.5.3 Preliminary experimental test and calibration of the FE model	251

Chapter V

Seismic retrofitting methodology and design of existing buildings by means of metal shear panels

5.1 INTRODUCTION	256
-------------------------	------------

5.2 THE FEMA 273 GUIDELINES	259
5.2.1 General	259
5.2.2 The seismic rehabilitation	262
5.2.2.1 As-built information	262
5.2.2.2 Rehabilitation objectives	264
5.2.2.3 Rehabilitation methods	272
5.3 THE ATC-40 PROVISIONS	277
5.3.1 General	277
5.3.2 Non-linear static analyses	278
5.3.2.1 Foreword	278
5.3.2.2 Capacity	280
5.3.2.3 Demand	283
5.3.2.4 Conversion of the capacity curve into the capacity spectrum	284
5.3.2.5 Bilinear representation of the capacity spectrum	288
5.3.2.6 Estimation of damping and reduction of the response spectrum	290
5.3.2.7 Determination of the performance point	294
5.4 THE ADOPTED PROCEDURE	298
5.5 ANALYSIS OF THE BASE RC STRUCTURE	301

Chapter VI

Numerical and experimental activities on the RC structure upgraded with metal shear panels

6.1 INTRODUCTION	308
6.2 APPLICATION OF STEEL SHEAR PANELS	309
6.2.1 The base material	309
6.2.2 The shear wall system	311
6.2.2.1 The shear panel design	311
6.2.2.2 Design of the external steel frame	312
6.2.2.3 The steel frame insertion in the RC structure	316
6.2.2.4 The insertion of transversal stiffeners	320
6.2.2.5 Panel-to-frame and panel-to-panel connections	321
6.2.2.6 Installation of shear walls	324
6.2.3 The numerical modelling	325
6.2.3.1 The ABAQUS model	325
6.2.3.2 The SAP model	328
6.2.4 The experimental test	331
6.2.4.1 Loading devices and measurement instruments	331
6.2.4.2 The obtained results	334
6.2.5 Interpretation of test results	342
6.3 APPLICATION OF PURE ALUMINIUM SHEAR PANELS	346
6.3.1 General	346
6.3.2 Design of the shear wall system	346

6.3.3 The adopted base material	347
6.3.4 The numerical modelling	350
6.3.4.1 The ABAQUS model	350
6.3.4.2 The SAP model	351
6.3.5 The experimental test	352
6.3.5.1 The intervention set-up	352
6.3.5.2 The obtained results	352
6.3.6 Interpretation of test results	360

Chapter VII

Comparison of solutions and results: steel versus aluminium and numerical versus experimental

7.1 INTRODUCTION	364
7.2 COMPARISON AMONG EXPERIMENTAL RESULTS	364
7.3 EXPERIMENTAL – NUMERICAL COMPARISONS	372
7.3.1 RC structure retrofitted with steel shear panels	372
7.3.2 RC structure retrofitted with pure aluminium shear panels	376

<i>Concluding remarks</i>	379
----------------------------------	-----

<i>References</i>	384
--------------------------	-----

Introduction

MOTIVATION AND SCOPE

Nowadays the seismic protection of buildings from quake ground motions represents one of the main targets of the international scientific community in the Civil Engineering field. Over the last decades, lessons learned from more severe earthquakes ((Northridge, U.S.A. 1994; Kobe, Japan, 1995; Izmit, Turkey, 1999; Athens, Greece, 1999; ChiChi, Taiwan 1999; San Giuliano di Puglia, Italy, 2002) showed many examples of bad performance of existing structures, mainly represented by both masonry and reinforced concrete (RC) buildings. In particular, many gravity-load designed (GLD) RC structures collapsed due to clear reasons, i.e. bad quality of materials, rough execution, lack of appropriate design, inobservance of code provisions and so on (Mazzolani and Gioncu, 2000).

The need of protection against both damage and collapse for this type of structures underlined the importance to improve the existing structural design codes for seismic zones aiming at both safeguarding human lives and limiting injures and loss of functionality in buildings and facilities after a high intensity seismic event.

Several technical solutions are currently available for improving the performance of existing structures vulnerable to earthquakes, they going from active to passive dissipating devices, as well as base isolation.

In general, seismic repairing/upgrading structural systems can be classified according to the following typologies (Mazzolani et al., 2004):

1. Systems based upon reparation and/or upgrading of existing structural elements, which change their local behaviour aiming at improving the global response of the structure.
2. Systems based on the addition of new structural elements, which globally operate for improving the structure seismic response.

Among systems belonging to the first category, a large number of seismic rehabilitation/reparation techniques has been studied and successfully applied. With reference to the current available systems, epoxy injections, steel plating or concrete jacketing and the use of fibre reinforced polymers can be mentioned.

On the other hand, type 2 systems are very useful for seismic upgrading of buildings where purposely-designed lateral-load resisting structures are absent. A correct design of such systems is based on the idea to eliminate or reduce the plastic deformation demand to the existing structure by adding supplemental energy dissipating devices, according to the “Damage Tolerant Structures (DTS)” approach (Wada et al., 1992). As it is well known, the current trend for seismic design is based on the concept that energy introduced into structures by severe seismic actions has to be dissipated from beams and columns thanks to their plastic deformation capacity. As a consequence damages of primary structural elements even for moderate-intensity earthquakes occur. Contrary, the “Damage Tolerant Structures” approach consists in the use of sacrificial devices, under form of passive, active or hybrid protection systems, which modify the dynamic properties of the primary structure and/or increase its dissipative capacities aiming at reducing the dynamic response of the whole structure. In the current practical applications, the main interest is related towards passive control systems, which are able to maintain constant both the fundamental period and the damping capacity of the structure during the seismic motion, without the intervention of any external power source, as instead happens in the active and hybrid control systems.

In such a framework, metal based technologies are often considered as the most satisfactory technical solutions, because of the effectiveness, practicality and economy (Mazzolani, 2006a). They mainly consist in adding new structural elements which collaborate with the existing structure, varying its

static scheme and operating at global level as supplemental energy dissipation passive systems.

Among used metal devices, bracing systems, under form of concentric, eccentric and buckling restrained types, may significantly improve safety of existing buildings against lateral collapse, they being designed according to modern knowledge of earthquake engineering. Such solutions are very affordable, but, as they rely on steel yielding for dissipation, they are also affected by the problem of residual deformations of the structure after the earthquake. This drawback could be overcome by means of innovative shape-memory alloys (SMA) solutions, which, based on the super-elastic properties of such materials, allow a self-centring capacity of the structure after the earthquake. In the last case, the energy dissipation could be integrated through the addition of viscous damping devices.

In the framework of passive control systems based on the metal technology, while steel braces have been widely studied and applied for retrofitting operations, the use of metal shear panels for protecting the primary structural members from seismic damages is recently developing only. Nevertheless, the use of such innovative systems composed by sacrificial panels, whose functioning is mainly based on shear yielding of metal elements activated by means of structure interstory-drifts, has been almost exclusively addressed for retrofitting of existing steel structures. For this reason, the possibility to effectively use metal shear panels in order to upgrade existing reinforced concrete structures represents the main target of the present study.

SUMMARY

Over the last decades metal shear panels were firstly used as complementary structural elements made of lightweight sheetings connected to an external supporting frame by means of steel bolts, rivets or spot welds.

Subsequently, it was proved that they could considerably contribute to increase the seismic performance of framed structures especially under wind and moderate-intensity earthquakes. Nevertheless, they were not efficient in case of strong earthquakes due to the occurrence of shear buckling phenomena which decreased significantly their dissipation capacity. For this reason, the

last evolution of panel systems allowed the improvement of their dissipative behaviour by means of the adoption of either appropriate stiffeners or low-yield strength metals, which increased the buckling threshold and facilitated the shear yielding of material. In addition, the possibility to exploit the stiffening effect of panels also at the serviceability limit state, represented another important prerequisite of such seismic protection devices. Finally, the evaluation of the contribution provided by metal shear panels for seismic retrofitting of existing RC structures was studied. Such a kind of application seems to be very interesting, since the insertion of shear panels within existing structures could represent an effective way to increase their strength, stiffness and energy dissipation capacity, making them able to withstand seismic actions. Lightness, versatile ductility, strength and stiffness, architectural function as complementary or substitutive cladding elements of the existing ones, little flexural interaction with beams and columns are a few of the important advantages that make metal panel systems competing of others conventional and innovative existing systems in the seismic retrofitting field.

Nevertheless, apart few theoretical studies and experimental applications limited to laboratory experiences, the deep examination of the possible advantages deriving from the use of metal shear panels for seismic retrofitting interventions has not yet been done. As a consequence, in the framework of the ILVA-IDEM research project, which has been coordinated by Prof. F.M. Mazzolani in order to evaluate the effectiveness of different metal based techniques for seismic upgrading of an existing RC structure (Mazzolani, 2006b), the possibility to prove the efficiency of such systems has represented a precious and unique unrepeatable opportunity to improve their knowledge on both design and analysis methods.

In order to achieve such a target, in the **first Chapter**, as a preliminary study phase, the seismic behaviour evaluation of existing RC buildings, with particular reference to the gravity-load designed ones, has been done by means of the analysis of appropriate seismic vulnerability assessment techniques. Then, once the fundamental lacks of such structures have been evidenced, a wide overview on the possible seismic protection systems, starting from conventional methodologies up to the introduction of innovative devices, has been presented.

In the **second Chapter** a complete review of state-of-the-art on steel plate shear walls, with reference to both compact and slender shear panels, has been performed. In particular, for each panel typology, design criteria, theoretical and numerical modelling studies and experimental research activities have been illustrated in detail. Finally, some applications developed worldwide on such systems have been shown.

In the **third Chapter** a wide numerical analysis on both compact and slender shear panels has been developed. Firstly, both parametric studies and numerical simulation of experimental tests on stiffened pure aluminium shear panels have been carried out. Then, in a second investigation phase, the behaviour of slender steel shear panels has been analysed by means of both refined and simplified numerical models and theoretical methods. In particular, a parametric analysis on such systems has been carried out by varying both the aspect ratio and the thickness of the plate and by evaluating the influence provided by intermediate stiffeners. Finally, the obtained results have provided useful information for the correct design of slender steel plates in shear.

In the **fourth Chapter** the experimental campaign developed within the ILVA-IDEM research project, focusing the attention on the sub-structure devoted to the application of metal shear panels, has been presented. After the identification of the mechanical features of structure materials, the dynamic behaviour of the module under study, obtained under experimental way, has been numerically reproduced by means of the calibration of a finite element model. In conclusion, on the basis of a preliminary experimental cyclic test performed on the original RC structure, some pushover numerical analyses have been carried out in order to evaluate the building performance under lateral loads.

In the **fifth Chapter** both the seismic retrofitting methodology and design of existing buildings by means of metal shear panels have been discussed and applied. Based on the provisions given by FEMA 273 and ATC-40 American guidelines, the seismic performance of the building under investigation has been evaluated. Later on, a reliable procedure in the framework of the

“performance based design” has been implemented aiming at improving its behaviour by means of the introduction of an appropriate shear panel configuration able to provide the strength and stiffness prerequisites requested for seismic retrofitting design of the original structure.

In the **sixth Chapter** both numerical and experimental activities on the analysed RC structure equipped with metal shear panels have been illustrated. On the basis of the results deriving from seismic retrofitting design, both steel and pure aluminium shear panel configuration arrangements have been defined according to a simplified analytical procedure and then checked by adopting a sophisticated FEM model. Finally, after the global numerical analyses of the whole system, the full-scale test of the upgraded structure has been carried out and the achieved results have been interpreted, confirming the effectiveness of the adopted retrofitting devices.

In the **seventh Chapter** the experimental test results have been compared each other and with the numerical analysis ones.

Finally, interesting conclusions on the beneficial effects provided by metal shear panels for the seismic upgrading of existing RC buildings have been drawn.

Chapter I

Seismic vulnerability of RC buildings

1.1 INTRODUCTION

The wide patrimony of RC buildings designed by seismic codes before the modern ones and eventually located into zones subjected to a new seismic classification underlines in precise way the importance to put into evidence effective procedures able to evaluate the safety level of existing structures (Pecce et al., 2004).

In fact, the evaluation of the RC building resistant capacity is of great interest in the practice and also in the research field for both the assessment of the seismic vulnerability and the choice of opportune retrofitting solutions to be applied. Actually RC buildings represent a consistent part of the construction patrimony of all Countries (in Italy over 50%) and a remarkable part of them has been built either without the application of any seismic code or adopting poor criteria of anti-seismic design.

In particular it is important to observe that the great part of existing multi-storey RC framed structures presents in-plane and in-elevation irregularities. Besides, the scarce care of constructive details (anchoring and overlapping of metal bars, joint details) strongly reduce the structural resources in terms of strength, stiffness and dissipation capacity in the plastic field.

As a consequence, under medium-high intensity earthquakes, RC framed buildings could undergo wide damages to members (beams and columns) and

joints, which could produce partial or global collapses, avoiding the exploitation of the available whole resources of the structure.

For this reason, the detailed analysis of existing RC structures represents a topic of a remarkable interest in the field of seismic engineering, where many researchers coming from all over the World are engaged in order to define accurate and/or simplified methodologies for the evaluation of their seismic vulnerability, considered as the quantification of structural and non-structural performances of buildings under earthquakes.

The large attention dedicated to the evaluation of the seismic capacity of existing RC buildings is also correlated to the peculiar nature of the problem, which requires to operate on a structure whose technical information are often not available. So, the limited knowledge of the construction determines the difficulty to individuate with sufficient accuracy some its structural characteristics, i.e. the material properties, the amount and the disposition of steel bars, the constructive details, the eventual physiological and/or pathological degradation conditions, etc. Therefore, the availability of the technical documentation of buildings is of a fundamental importance.

When such a specific documentation is absent or the adoption of direct investigation methodologies (in-situ and laboratory tests, detailed analysis of technical drawings, etc.), is not possible, the knowledge of the construction period of the building represents an useful parameter for the structural analysis. In fact, from the constructive epoch of the building the following information can be obtained:

- the code used for seismic design;
- design methods and execution techniques;
- constructive typologies frequently adopted.

In general terms, putting together the above information, the typical features of RC buildings belonging to a certain period can be individuated. In particular, the normative analysis allows to define, for each epoch, the mechanical properties of steel and concrete, the minimum percentage of steel bars, the dimensional provisions and the allowable check methods.

In such a way, useful indications on both actions and material resistance values can be achieved, while information on stresses used in the calculations, on the location of steel bars and on the care of structural details could be not available.

Aiming at acquiring such information, technical manuals can be used in order to have more precise indications on both the calculation methodology and the percentage of steel bars to be used in the different structural elements. Then, in order to verify if such provisions are followed in the professional practice, the examination of the design of real buildings, which can be found from public technical structures, construction companies and professional technical studies, is carried out. Such design provisions, other than represent important check elements about the information achieved from both codes and manuals, allow to acquire useful prescriptions on the constructive practice used in different seismic zones, providing the possibility to evaluate the vulnerability of the group of buildings located in each of them.

On the other hand, the analysis of a single building having strategic importance or with a significant public destination of use is recently assuming a more relevant interest.

In fact the new seismic Italian code (OPCM 3431, 2005) introduces new tools for the analysis of the seismic vulnerability of existing RC framed buildings in order to design an eventual seismic retrofitting or adjustment intervention. The innovative provisions of such a procedure, which are already considered in the more advanced European (EN 1998-1-1, 2005) and International (SEAOC, 1995; FEMA 273, 1997) codes, are illustrated in detail in the present Chapter.

1.2 SEISMIC HAZARD

Generally it is believed that the seismic protection of human life is merely a technological problem, based on both the technology of structural systems inside the construction and the technology of some artificial devices (Gavarini, 1991). Surely technology is a very important topic in the field of seismic engineering, but it is not able to solve every problem. So, an attempt to consider the question of seismic safety as a whole does not seem useless.

What do we request range to a building to be built in a seismic area? The answer is not unique. Certainly one is to prevent its collapse or, at least, that the collapse probability should be kept under a given limit during a fixed time period. In such a way we can avoid, or keep within acceptable limits, injuries to human life. Being such an approach the main target of modern seismic

studies, we can accept, as technical codes usually do, some damage to secondary parts of the structure and also to the construction itself. Such an approach may be accepted for “ordinary” buildings, but it cannot be proposed for monumental ones, because a light damage for the general safety may be serious for a single element, like for example a painted wall; on the other hand, a light structural damage, or a damage to a non-structural element, may cause the interruption of an essential function in a “strategic” building or may be the origin of a panic phenomenon, with tragic consequences, in important buildings like schools.

Therefore, it is evident that the first element to be evaluated for the realization of constructions in seismic areas is the type of protection we need for the building, while another aspect to be focused concerns the protection level we want to ensure. Sometimes there is confusion among such concepts and this should be avoided: for example one may think that, to ensure the building functionality, it is sufficient to rise the level of design forces, while it is quite evident that this is not correct or, at least, not sufficient.

The level of protection to be assured for a building, which is diversified in relation to the destination type of the construction itself, should be related to the probability that the undesired seismic effect may happen.

Such a concept must be associated to the global expected damage from occurring earthquakes within a region and within a given period of time, which is measured by seismic risk. The assessment of the seismic hazard, which involves different topics and professional disciplines, is required for the preparation of earthquake loading regulations aiming at determining the seismic actions for projects requiring special study, for areas where no codes exist or for various earthquake risk management purposes (Vayas et al., 2005).

In existing seismic urban areas, the seismic risk depends on many factors, namely:

- the seismicity of the zone, related to the intensity and the frequency of expected earthquakes;
- the nature of the soil in the area;
- the seismic vulnerability of single buildings;
- the artistical/historical value of the buildings themselves;
- the monetary value of buildings;
- the presence and the number of people in the area;

- the urban vulnerability, related to the possible consequences of panic phenomena in narrow streets, passages, stairs and so on.

When part of a design process, seismic hazard assessment implies all of the studies involved in Boxes 2-4 of Figure 1.1, involving also the material on site characteristics including a list of geological hazards.

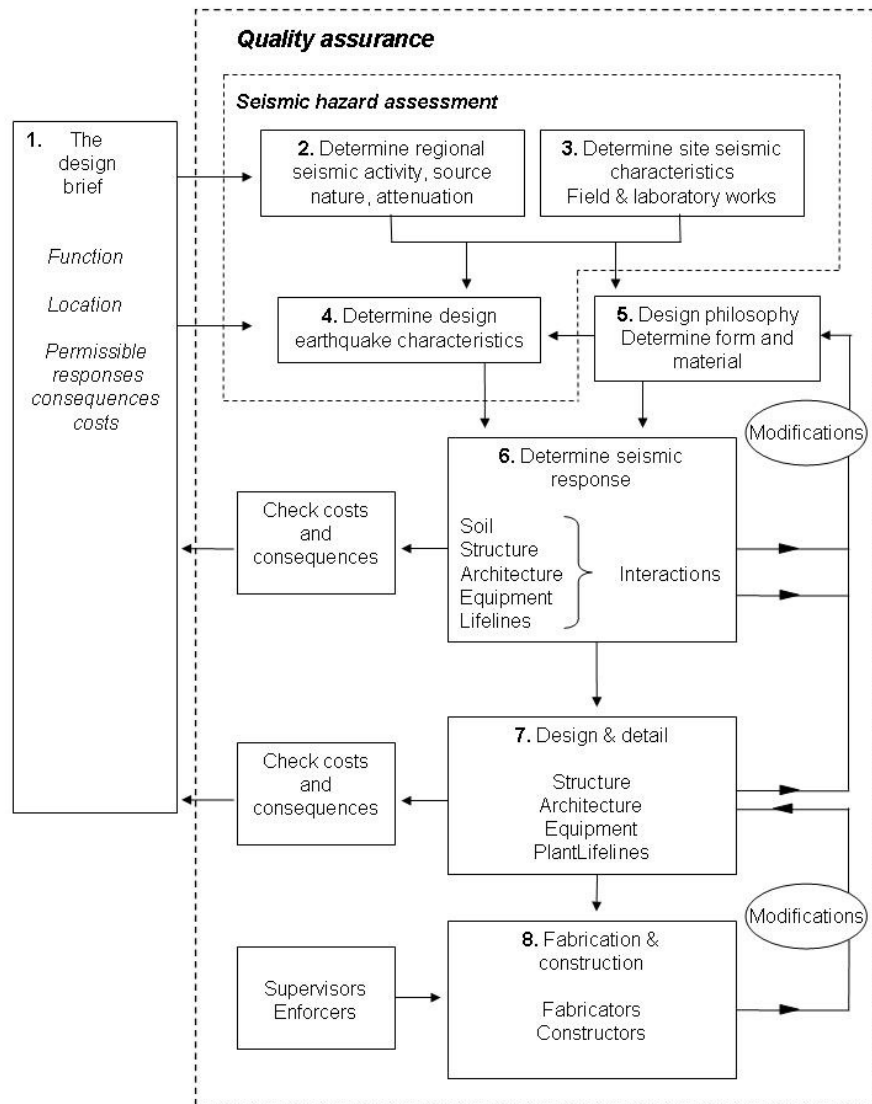


Figure 1.1: Simplified flowchart for the design and construction of earthquake resistant infrastructures

Of the above subject areas, the major attention is to be paid to the seismic activity, which is evaluated through studies of three main components, namely crustal strain, fault activity and historical seismicity. These three components are complementary, but for the best results should be used together. In particular, the seismicity of a given zone is generally defined either by the maximum expected macro seismic intensity or by the maximum ground acceleration. In the framework of the seismic risk mitigation of existing areas, the first definition appears to be more suitable for two reasons:

- 1) the macroseismic intensity has a better correlation with the seismic behaviour of old buildings;
- 2) a more continuous subdivision of the intensity is more appropriate for reinforcement purpose.

For the purpose of assessing risk, the most suitable definition of seismicity is given by the knowledge of the return period as a function of the macroseismic intensity and the exceedance probability, defined as the probability $p(i/t)$ to overcome the intensity $I=i$ in a time t . Such an information, if available in every place of a territory, enables to draw isoprobable curves.

Moreover, it is very important to improve the seismicity definition by providing indications on the possible local amplification due to the nature of the ground and the consequent possible modification of the response spectrum. Such an information is necessary when major monumental buildings, for which an exact evaluation of the seismic action allows to better estimate the risk and so to limit the reinforcement operations to the minimum requested level, are considered.

Besides, the seismic risk depends not only on the seismicity and the vulnerability, but also on the exposure, which is on the number of human lives multiplied by the presence time (i.e. the occupancy) and/or the economic construction value, that is the economic value of its content and the artistic/historical value of the building.

Thus, the assessment of the exposure is an important operation which is not difficult to perform and must not be underestimated. As a consequence, for such an activity suitable rules should be established.

When the analysis of the above topics has been carried out, the risk hazard can be assessed both for new and existing buildings.

In particular, in case of new constructions, the regulations are aimed to ensure that a given level of risk, implicitly or explicitly considered as acceptable, is not overcome. On the other hand, for existing structures the risk level can be first assessed and then reduced, if necessary. In such a case the first problem is to establish policies, which in principle deal with any of the previously mentioned factors, able to lead to the desired reduction of risk. Then, the subsequent step based on the strengthening of the single building is only one of the available means. In fact the correct definition of a risk reducing process may generally take into account some constraints and should always be optimised. With respect to constraints, it seems necessary to distinguish different risk types, which should be separately considered:

- risk for people, dealing with possible injuries to human life;
- risk for not monetary values, such as the artistical/historical value of the buildings and/or of portions of urban areas;
- risk measurable in monetary terms, due to material damage;
- risk connected with urban aspects.

More in detail, for design or risk assessment purposes, the evaluation of the seismic hazard consists of the following basic steps:

- Definition of the nature and location of earthquake sources;
- Magnitude-frequency relationships for sources;
- Attenuation of ground motion with distance from source;
- Determination of ground motions at the site having the required probability of exceedance.

Being essentially seismic risk and hazard statements forecasts of future situations, they can be considered as uncertain events. Seismic hazard assessments are attempts to forecast the likely future seismic activity rates and strengths, based on the knowledge of the past and the present, and significant uncertainties arise partly because both the processes involved are not fully understood and the data are generally poor and variable in quantity. For reasonable credibility, considerable knowledge of both historical seismicity, illustrated in non-numerical terms by seismicity maps, and geology need to be used, together with an appropriate analysis of uncertainties. Where available, the knowledge of other geophysical or seismological factors may also be helpful, particularly if regional seismic activity patterns are evaluated. Once both the estimated future seismic-activity rates and acceptable risks are

known, appropriate earthquake loadings for the proposed structure, having a mean recurrence range depending on the failure consequences, may be determined.

Due to the difficulty regarding the seismic hazard evaluation, different design criteria, from well codified to inadequate or inexistent, have been adopted in several areas of the World. As a consequence, depending on the location and nature of the project interested, seismic risk evaluation ranging from none through arbitrary to thorough-going may be required.

In the seismic hazard assessment the terms deterministic and probabilistic do not have the same meanings they possess when they are commonly used: this is recognized by the frequent use of terms semi-deterministic or semi-probabilistic, where the word *semi* means part rather than half. Then, the probabilistic approach to seismic hazard evaluation takes into account for the uncertainties surrounding the values of variables under quantitative way. So, in a fully probabilistic assessment, the uncertainties of all the explicit and implicit variables would be formally taken into consideration.

Of course, in practice, being some of the parameters to define uncertainties not enough known, a fully probabilistic analysis would generally be excessive and financially unrealistic. Therefore, some components of the hazard assessments are necessarily of the deterministic type, i.e. the choice of the magnitude of the design earthquake.

However, in any given study, the approach should be chosen according to the nature of the project and also tailored to the region seismicity, including the quantity and quality of the available seismicity data.

1.3 SEISMIC VULNERABILITY AND PROTECTION

1.3.1 General

One of the key questions that any society must analyse is the level of protection to provide to people and equipments. The earthquake protection term refers to all those activities which can be taken into account for either decreasing the effects of earthquakes or reducing future physical or economic losses and human casualties. Such an expression, having a meaning similar to the earthquake risk mitigation one, which instead refers to interventions for

strengthening the built environment, includes human, financial, social and administrative aspects of reducing earthquakes effects. Therefore, earthquake protection is an expensive operation which must compete for limited resources with other priorities for individual and public expenses, such as health care and environmental protection.

In this sense it is very difficult to precisely define the benefits that could be obtained by this expense area, it being in common with many other ones. In fact often earthquakes are seen as a remote threat, contrasting with the planning timescale of governments, adult taxpayers or corporations and even then very unlikely to be fatal; so it is very complicated to raise public enthusiasm for spending money on protection except that in the immediate aftermath of an earthquake. Overspending on protection will waste resources, restricting economic development and economic growth and these opportunity costs are easier to perceive. Therefore the set-up of the right level of protection and the consequent evaluation of alternative protection strategies, which are two of the great importance topics dealing with the seismic risk of historical buildings, depends on the earthquake intensity expected in the site of interest.

In such a context, it can be observed that all over the World there are a large number of earthquake intensity scales, part of them representing modification or adaptation of previous ones, which take their origin from the request of seismologists to classify the quake ground motions without instrumental measurements. The most common ones are the Modified Mercalli (MM) scale, a 12-point scale used in USA, the European Macroseismic Scale (EMS), based on the MM one and used in Europe, the Japanese Meteorological Agency (JMA) scale, a 7-point scale used in Japan, and other scales similar to the MM one which are used in USSR and China.

Currently, intensity scales are used to make a quick assessment of the geographical extent of earthquakes in the initial reconnaissance in order to guide the emergency services.

Any discussion about earthquake protection must be based on the identification of the distribution of the vulnerability around the World.

Vulnerability may be defined as the “weakness” versus assigned external actions of a structure or a system. Generally the vulnerability assessment,

which is finalised to the evaluation of the seismic risk, concerns a population of objects rather than individual items.

The vulnerability evaluation can be performed at different levels: at the upper limit, the full structural analysis on single constructions, as it is typically defined by codes, may be considered, even if this kind of approach is not properly judged as a vulnerability assessment. On the other hand, a very simple and rapid approach can be carried out, it being able to provide an evaluation of the problem in a few minutes.

The vulnerability assessment is often useful due to its capacity to give practical information on population such a built-up areas and large systems: in such cases the unavoidable uncertainties correlated to the appraisal of single objects do not influence, on a statistical basis, the survey as a whole.

A vulnerability survey is based on the collection of information on a given number of important parameters which can be performed filling one or more forms or adopting an expert system implemented on a personal computer.

The obtained information may be summarised within a vulnerability index to be utilised in a risk model or may be used as a global input to perform several analysis, such as hypotheses and costs of retrofitting, cost-benefits analyses, optimal strategies for large scale interventions, etc. These analyses, which may be executed defining suitable models, deal with uncertainties and often include the evaluation of different nature data, represented by engineering information, synthetic judgements, cultural values, drawings, photos, texts, historical items, social implications and so on.

As far as only the numbers are considered, the models may be of a numerical type, they being affected by the uncertainty of the information defined on a probabilistic basis, but when other types of information are introduced other approaches must be considered. In this case suitable information tools able to help in the evaluation and decisions to take are developed and used.

Earthquake vulnerability is heavily concentrated in the poorer countries of the World. In the same way, it is recognised that also in the wealthiest countries there is a significant earthquake vulnerability among the poorest members of society who are sometimes forced to live in old weak buildings. In such a context, it is essential not to overlook the political dimension of

allocating priorities for earthquake protection within a society in which all members feel vulnerable.

1.3.2 Vulnerability assessment techniques

In the last years one of the main interests of the research activity in the field of earthquake engineering has been devoted to the necessity to predict the vulnerability of existing structures by means of the development of appropriate assessment techniques.

In technical literature several procedures have been proposed, they being generally classified into three categories (Yakut, 2004).

The simplest and quickest method, known as walk-down or street survey, requires data collected from a brief inspection of the building only. Parameters typically used are the location, the age, the structural system and the number of stories of the building, its vertical and plan irregularities, the material used and the workmanship quality.

The purpose of such rapid evaluation techniques is to identify highly vulnerable buildings which must be analysed through future investigations.

FEMA 154 (1988) and FEMA 310 Tier 1 evaluation (1998) fall into this category.

When a more detailed and reliable assessment is required, preliminary assessment techniques, belonging to the second category, are used. In addition to the data collected from the street analysis, information on both the size and orientation of structural components, material properties and layout are needed.

This procedure, which requires the access to the building and the comprehensive investigation of technical drawings, is not implemented by means of sophisticated and time-consuming analysis of the building, but some quick calculations are performed only. The success of such techniques depends on both the availability and quality of data.

The structural capacity of the construction, which is usually expressed in terms of an index, is checked against an anticipated demand. So, the expected performance of the building is predicted by this comparison.

FEMA 310 Tier 2 evaluation (1998) is the widely used preliminary assessment techniques.

The deep investigation of buildings through refined structural analyses falls into the third category of vulnerability assessment. The comprehensive information on both the geometrical properties and details of the components, as well as the mechanical properties of materials are achieved from structural drawings and as-built features of the building. Linear or non-linear analysis techniques are used to determine the building response for an anticipated seismic action. Such response quantities are then compared with assigned accepted values in order to arrive at a decision regarding the expected performance of the structure.

ATC-40 (1996), FEMA 273 (1997) and FEMA 310 Tier 3 (1998) procedures are among the techniques most largely used at this assessment level, which is used in site-specific applications and is able to capture architectural features, material quantity as well as detailing of the components to a certain extent.

Among three assessment phases, the preliminary quick evaluation is the most widely used technique when a reliable assessment is needed.

Several preliminary assessment techniques, depending on the size of lateral load resisting elements only, have been proposed by many researchers.

Hassan and Sozen (1997), as well as Gulkan and Sozen (1999), developed simple vulnerability indexes based on both the orientation and the cross-sectional size of vertical elements located into low- and mid-rise (up to seven stories) reinforced concrete buildings.

The Hassan and Sozen method required that both shear and infill walls normalised with respect to the total floor area of the building in order to compute the wall index. The column areas, normalised in the same way, were used to determine the column index. Then, such indexes were examined graphically to define the relative vulnerability of a group buildings.

Gulkan and Sozen showed that the ground floor drift was influenced by the wall and column areas. Unlike its simplicity, the major drawback of this procedure was the assumption that the material quality and as-built properties of the building were uniform. Although the construction quality and code compliance might be considered reasonably uniform for many Countries, the effect of concrete strength on this force-based performance assessment was ignored. Moreover, the effect of well-accepted secondary factors, such as soft storey, short column and vertical irregularity, were not taken into account.

The vulnerability assessment techniques above illustrated, enclosed within a very large range of seismic resistance evaluation procedures of existing constructions, represent an effective procedure used to define the vulnerability index of a building or a set of buildings. The knowledge of such indexes is very useful for determining the damaging level that could occur into buildings subjected to earthquake attacks.

1.4 EARTHQUAKE RISK MODELLING

1.4.1 Loss estimation

The estimation of possible future losses is a very important topic to be evaluated in earthquake-prone Countries.

In such a framework different types of loss estimation can be used, they being depending on both the nature of the problem and the study purposes. In particular such approaches include scenario studies, probabilistic risk analysis and potential loss studies.

In the first study, the assessment of the effects of a single earthquake on a Country is done. A “maximum probable” or “maximum credible” magnitude earthquake is often assumed based on known geological faults or probabilistic seismic source zones. Commonly, historical significant earthquake, such as the 1906 San Francisco event or the 1923 Great Tokyo earthquake, are used as scenarios to evaluate their effects on present-day portfolios. Scenario studies are used to estimate the losses from an extreme case, to check the financial resilience of a company or institution to withstand that loss level and also to estimate the resources to be used for handling the emergency. In this way the number of people killed, injured and buried by collapsing buildings or made homeless is assessed. Then the resources necessary for minimising disruption, rescuing people buried, accommodating the homeless and minimising the recovery period can be estimated.

The second study phase concerns probabilistic risk analysis, in which both the calculation of all potential losses and the probability that such losses occurring from each of different sizes and locations of earthquakes can take place are defined. Such an approach generates a loss exceedance probability (EP) curve for a building or a group of buildings, defining the level of loss

that would be experienced with different return periods. The EP curve, which is used to calculate the average annual loss to be employed in defining insurance rate setting and risk benchmarking, provides the probability that different levels of loss can occur. Probabilistic analysis can be used to assess EP curves for the number of buildings destroyed, lives lost and total financial costs over a given period of time. So, the probable effects of mitigation policies on reducing earthquake losses can be estimated. Also the relative effects of different policies to reduce expected losses can be compared or the change in risk over tie can be examined.

Finally, in potential loss studies the definition of expected hazard levels within a Country is performed in order to show the location of communities that could suffer heavy losses. In this framework the maximum historical intensity or the peak ground acceleration level associated with a long probabilistic return period is usually mapped across an area. So, the effect of such an intensity on the communities within that area is evaluated aiming at identifying the most risk ones. In Table 1.1 the different users of loss estimation and the corresponding types of required output are summarised.

Table 1.1: Users of loss estimation and corresponding information needed

Who	Why	Information needed
Physical planner	Identify high-risk locations	Risk mapping
Building owners	Identify high-risk buildings Plan mitigation strategies	Building-by-building vulnerability studies
Insurers and reinsurers	Set insurance premium rates Structure risk transfer (reinsurance) deals Identify possible losses Reduce risks	Annualised loss and exceedance probability curves
Civil protection agencies	Plan size and location of emergency services	Estimation of fatalities an injuries, damage, homelessness
Building regulators	Determine optimum resistance levels	Cost-benefits studies

Due to the importance of loss modelling, in the last decade many refined computer models for the computation of probable losses, using scenario studies or probabilistic ones, have been developed. The most advanced models

have been used to help the international insurance and reinsurance industries, which have huge financial exposure in seismic zones, to assess their likely losses.

Being the available knowledge about earthquakes and their recurrence patterns of uncertain type, the estimation of future losses are extrapolated from the statistical distribution of earthquakes observed in the past and are based on the probabilistic determination of the seismic risk. In the current context, the term risk and the associated ones hazard and vulnerability, have been formally defined by an international agreement.

1.4.2 The seismic risk definition

The term earthquake risk refers to the expected losses into a given element susceptible at risk within an assigned future time period. Such elements may be a building, a group of buildings or a city, the human population of that building or settlement or also the economic activities associated with either. According to the way in which the element at risk is defined, the risk may be measured in terms of either expected economic loss or number of lives lost or the extent of physical damage to property, depending from the availability of appropriate measures.

In particular, the term specific risk is referred to risks or loss estimations which are expressed in percentage terms with respect of the maximum possible loss. Such a risk type, which is commonly used for evaluating the financial losses of properties, refers to the ratio between the cost of repair of the property and the repair cost ratio, intended as the global cost related to the total replacement.

Another important term to specify is the hazard one, which is the probability of occurrence of an earthquake within a specific period of time in a given area. According to the type of analysis to be carried out, the earthquake may be specified in terms of either its source characteristics, that are commonly specified as magnitude, or its effects at a particular site.

When considering the hazard of ground shaking, the site characteristics of the earthquake are expressed in terms of intensity, such as EMS or modified Mercalli ones, or in terms of peak ground acceleration (PGA) or some other parameters derived from measured characteristics of the ground motion.

As already seen for risk, hazard may be expressed either in terms of average expected rate of occurrence (or average return period, intended as its inverse) of a specific seismic event or on a probabilistic basis.

Moreover, the potential for other collateral hazards from ground liquefaction, landslide, tsunami and direct damage in the fault rupture zone can be considered as an alternative to ground shaking. In such cases a characteristic hazard parameter, expressed in the same way of the one used for ground shaking hazard, must be defined.

Finally the deepening of the significance of the vulnerability term is needed. Such a word, as already mentioned in the Section 1.3.1, is usually used to define the degree of loss of a given element (or a set of elements) susceptible at risk which results from a specified hazard level (i.e. the occurrence of a known severity earthquake).

In particular, the vulnerability of an element is represented by the ratio between the expected loss and the maximum likely one. For this reason, it assumes values comprised between 0 and 1. Generally, the measure of loss, which depends on the risk element, can be obtained as the ratio between the killed or injured people and the total population, as a repair cost ratio or as the physical damage degree defined on an appropriate scale. When a large set of buildings is considered, it may be defined in terms of the portion of buildings experiencing a particular damage level.

However the specification of the average vulnerability only is inadequate for loss assessment purposes, being the losses distribution within the set of elements considered at risk very large. So, the evaluation of the damage degree of elements such as buildings is generally expressed by means of a damage distribution in terms of histograms.

As for hazard, it is clear that the vulnerability to one size of event is only a partial definition of the total vulnerability, which must be specified for all probable events which may cause any loss or damage. Therefore, the total vulnerability for an element at risk is an assembly of the separate vulnerability distributions for each seismic event which may be taken into account.

Therefore, vulnerability functions can be combined with the hazard data in order to estimate the possible losses distribution for all probable earthquakes in a given period of time, thus determining the risk of a given element or a set of elements (Figure 1.2).

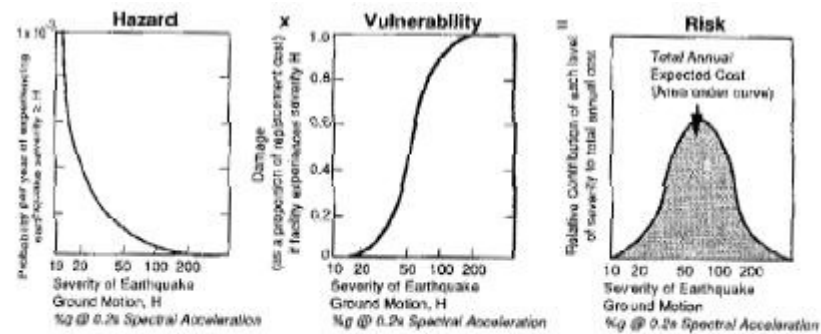


Figure 1.2: Definition of the seismic risk, intended as hazard multiplied for vulnerability

Finally, once that structures have been declared as susceptible at seismic risk, in order to avoid their damageability under earthquake attacks, the preliminary evaluation of possible vulnerability sources should be done, as it will be shown in the next Section, where the seismic behaviour of existing RC buildings, with particular reference to gravity load designed ones, has been largely illustrated.

1.5 THE BEHAVIOUR OF EXISTING RC BUILDINGS

The individuation of the seismic performance of existing buildings by means of vulnerability assessment techniques and the related determination of their susceptibility at seismic risk allows to point scrupulous attention on that constructions which are very vulnerable to earthquake attacks. Among them, particular reference has to be made to framed RC structures, which are able to absorb the horizontal action effects thanks to both the flexural capacity and the continuity of beams and columns. Under earthquakes, the members of such structures, if correctly designed and characterised by appropriate constructive details, can develop plastic hinges able to absorb the energy produced by the ground motion. In this way the structure, which can withstand displacements greater than the design ones, is declared as a ductile type.

Generally, ductile RC structures must possess the following characteristics:

- formation of plastic hinges;
- sufficiently ductile beam-to-column joints in order to carry the load cycles induced by earthquakes;

- resistance hierarchy criterion, which allows the formation of plastic hinges in the beams before the columns (weak beams – strong columns concept).
- presence of a sufficient number of stirrups well anchored in both members and joints so to avoid a quick degradation of their resistance under alternate loadings;
- effective wrapping effect produced by concrete in the zones prone to develop plastic hinges by means of the disposition of an adequate amount of closed stirrups;
- minimum percentage of steel bars in the structural parts where plastic hinges could develop;
- appropriate overlapping length of steel bars in favourable zones (compressed concrete) protected by an appropriate number of stirrups.

With regard to the first aspect, the creation of a sufficient number of plastic hinges in the structure, due to the combined effect produced by both gravity loads and seismic forces, is directly correlated to its stability.

Nevertheless, the major part of existing RC buildings, especially the ones built in Italy in the period between 1960 and 1970 and located in not-seismic zones, have been designed without adequate seismic rules and therefore able to withstand exclusively vertical loads (Gravity Load Designed - GLD).

In fact, during violent seismic events (California, 1994; Japan, 1995; Turkey, 1999; Greece, 1999), a not satisfactory behaviour of such structures has been observed. In fact, in many cases they showed a deficient behaviour characterized by both a low ductility of beam-to-column joints and the absence of an appropriate resistance hierarchy able to provide global type collapse mechanisms. Other problems observed were generally represented by the lack of in plane and/or in elevation regularity, the elevated torsional deformability and the presence of short columns which determined a not satisfactory seismic behaviour of the building.

In particular, the common seismic deficiencies evidenced by reinforced concrete buildings are correlated to the following aspects (Lew, 2005):

- 1) global strength;
- 2) global stiffness;
- 3) configuration;
- 4) load path;

- 5) inadequate component detailing;
- 6) diaphragm effect;
- 7) foundation system.

Global strength usually refers to the lateral strength of the vertical lateral force-resisting system. For degrading structural systems characterised by a negative post-yield slope on the pushover curve, a minimum strength requirement may be required. In fact, in certain cases, added strength, which affect the expected inelastic displacement of the structure, may reduce non-linear demands into acceptable ranges. A deficient behaviour in terms of global strength is common into old buildings either due to a complete lack of seismic design or a design based on early building codes with inadequate strength requirements, which are directly related to unacceptable demand-to-capacity ratios within elements of the lateral load-resisting system.

Global stiffness is related to the stiffness of the global lateral load-resisting system, although such a deficiency may not be critical at all levels. In framed buildings critical drifts occurred in the lowest levels and the interventions to be performed aimed at reducing these structural displacements. The most common cause of inobservance of standard provisions is due to the excessive drift demands on the existing poorly detailed components.

Configuration irregularities are related either to the plane development or the vertical extension of buildings. Plane irregularities require extraordinary demands on elements due to either the torsional response or the diaphragm shape. Indeed, vertical irregularities are due to an irregular vertical distribution of mass or stiffness between floors which produces force or displacement concentration at certain levels. Such negative features are infrequently considered in the original design of old buildings and, therefore, rehabilitation measures are normally required to mitigate their effects.

The load path is usually considered to extend from each mass in the building to the supporting soil. As an example, for cladding panels, the path would include their connection to supporting floors, the diaphragm and collectors which deliver the load to components of the primary lateral load - resisting system, the continuity of the above components to the foundation and the loads transfer between foundation and soil. A discontinuity or inadequate strength in the load path could prevent the positive attributes of the seismic system from being effective. Many load path deficiencies are difficult to

classify because the strength lack may be considered as part of another element. For example, an inappropriate construction joint in a shear wall could be considered a load path deficiency or a shear wall lack in the global strength category.

In the current context, detailing regards the design decisions affecting the components behaviour beyond the strength determined by nominal demand in the non-linear range. A poor confinement of concrete gravity columns is an example of a detailing deficiency. In such a case, when old buildings are considered, the expected drifts due to seismic events will exceed the deformation capacity of these columns, leading to possible degradation and collapse. In fact, even if the design for gravity loads is adequate, the post-elastic behaviour is unsuitable due to insufficient configuration and spacing of ties. The identification of detailing deficiencies is useful to introduce mitigation strategies which may guarantee acceptable performances without the addition in the structure of new lateral force-resisting systems.

The main purpose of diaphragms in the global seismic scheme is to act as a horizontal beam spanning among lateral load-resisting systems. The deficiencies detected in terms of lack of diaphragm include inadequate shear or bending strength, stiffness or reinforcing around openings or re-entrant corners. Insufficient local shear transfer to lateral force-resisting system or inadequate collectors are classified as load path deficiencies.

Foundation system deficiencies can occur within the foundation itself or can interest an inappropriate transfer mechanism between foundation and soil. Deficiencies include lack of bending or shear strength between foundation and beams, insufficient axial capacity or detailing of columns and weak and degrading connections among structural elements. Transfer deficiencies include excessive settlement or bearing failure, excessive rotation, inadequate tension capacity of deep foundations or loss of bearing capacity due to liquefaction.

Based on these circumstances, the key concepts of the modern seismic codes are based on the achievement of the following objectives:

- prevent a non structural damage under seismic events of moderate intensity, which can frequently occur during the life of the structure.
- prevent a structural damage, reducing the not structural one, when seismic events of moderate intensity, which can happen less frequently, occur.

- avoid the structural collapse danger under high intensity earthquakes.

These prerequisites are able to provide different performance levels for the structures, according to the methodology of the "Performance Based Design", in the certainty that the principal purpose of the different design criteria is to allow the evaluation of the desired performances of the structure under the applied load conditions.

All these considerations underline a series of problems in the evaluation of the seismic behaviour of existing RC structures. Generally, all resistant mechanisms, resulting either of brittle type or sensitive to the cyclic degradation, have to be correctly evaluated by means of adequate calculation models in order to obtain reliable results in the evaluation of the actual seismic resistance. In this framework we can observe that RC structures, designed according to the modern codes and especially by following the provisions given by the new seismic italian code (OPCM 3431, 2005), must possess an adequate ductility, expressed as the energy dissipation capacity in the plastic field, without undergoing significant strength reductions under the effects of both vertical and horizontal actions. These conditions are satisfied if particular care to the definition of the constructional details is given. In such a context, by evaluating the constructional details of RC structures designed for carrying vertical loads only, the deficiencies reported in Figure 1.3 can be mainly recognised.

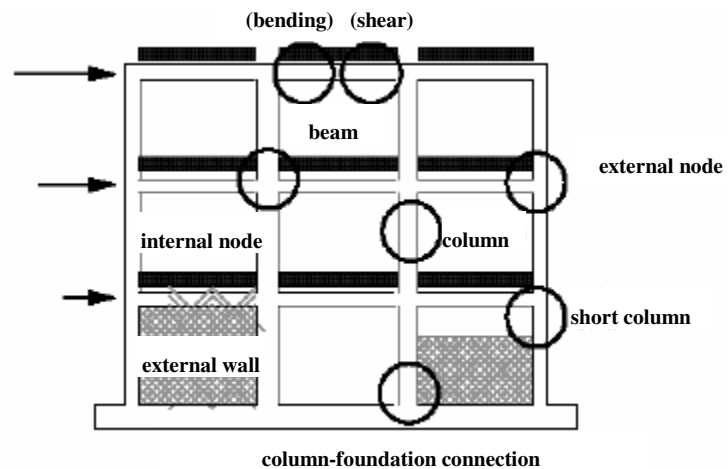


Figure 1.3: Examples of typical problems occurring in RC buildings designed for gravity loads only (Verderame, 1999)

Usually, the structural system of existing RC buildings is composed by resisting frames placed in one direction only, perpendicular to the floor slab orientation. Such frames are usually realised by means of emergent beams but, in some cases, beams having the same depth of the slab are of concern. Therefore, in the other direction, they are connected by the slab only, without any specific beam. The structural elements of these constructions are designed without any reference to the effect of horizontal forces (including explicitly also the wind action). As a consequence, flexible resisting systems having a very poor ductility are adopted.

The typical lacks of GLD buildings, according to the evidences reported in previous experimental and theoretical studies (Bracci et al., 1995), are:

1. the weakness of the columns in comparison to the beam-to-column connections, which can determine a soft-storey mechanism (Figures 1.4 a, b);
2. the minimum reinforcement of the concrete in terms of bars and stirrups, especially in the zones prone to develop plastic hinges (Figures 1.4 c, d);
3. absence of an adequate steel bars reinforcement in the critical plastic zones (Figures 1.4 e, f);
4. absence of suitable transversal reinforcement in the beam-to-column joints (Figures 1.4 g, h);
5. discontinuous bending reinforcement in correspondence of connections (Figures 1.4 i, l).

Also, the behaviour of connection can represent a critical aspect for the seismic design of RC buildings due to the adoption of inappropriate constructive details. In such a case, slipping phenomena of the bars, especially in case of employment of smooth bars without enough extremity hooks, can occur especially in the external joints, which appear to be the most critical parts of the structure, but also in the intermediate ones, in case of not continuous longitudinal reinforcements. Besides, the absence of adequate quantity of stirrups at the beam-to-column intersection, due to the high shear stresses, can determine the collapse of the joint.

Many studies carried out on a number of RC buildings realized before 1970 have underlined as the calculation formalities of the structural elements conceived for withstanding gravitational loads do not differ significantly from the ones designed after the introduction of the Italian law 1086/71. The main constructional differences between the structural typologies characterising

these two constructive epochs are represented by the adopted materials. For columns, shear failure can occur especially in short elements (i.e. in the staircases frames), with a consequent fragile behaviour of the whole structure. In addition, the poor confining due to either the reduced quantity or the incorrect detailing of the stirrups can induce a bending crisis of the first level columns, with the consequent instability of compressed bars, the unthreading of tensile ones and the crushing of the not confined compressed concrete. The columns are generally calculated considering the vertical loads only (subjected to simple compression) and the analyses performed on existing buildings (Masi and Vona, 2004) showed that in the implemented structural models the flexural effects caused from the wind action or the eccentricity due to the application of vertical loads were considered only. As a consequence, the dissipative capacities of the structure are very low: in this case unfavourable partial type collapse mechanisms could occur with possible local shear crises. In fact the beams show a reduced ductility due to either shear or the slipping of the bars in the joints, while the columns, designed for carrying vertical loads, result in high stiffness and low strength elements which exhibit the formation of plastic hinges at their base.

For this reason, in GLD frames fragile collapse mechanisms highly sensibility to the application of cyclic action, usually occur: sophisticated calculation models are required in order to achieve realistic results in the evaluation of their seismic performances. In fact, according to the previous considerations, the columns damage strongly conditions the structural behaviour, since it usually determines the introduction of temporary supports able to sustain vertical loads. On the other hand, the damage of beams, which is commonly detected in RC buildings, does not affect seriously the safety of the whole structure in terms of global collapse. In Figures 1.4 c, d, e, f significant examples of damages occurred in RC beam and columns are reported. The damage of RC shear walls does not condition the whole stability of the structure because they can withstand the vertical loads also after the occurrence of typical transversal cracks produced by earthquakes, which are visible in Figures 1.4 m, n. Also, the damage occurred in the beam-to-column connections (Figures 1.4 i, l) must be considered with particular care, because it produces a strength reduction of structural elements, determining an uncontrolled redistribution of stresses.

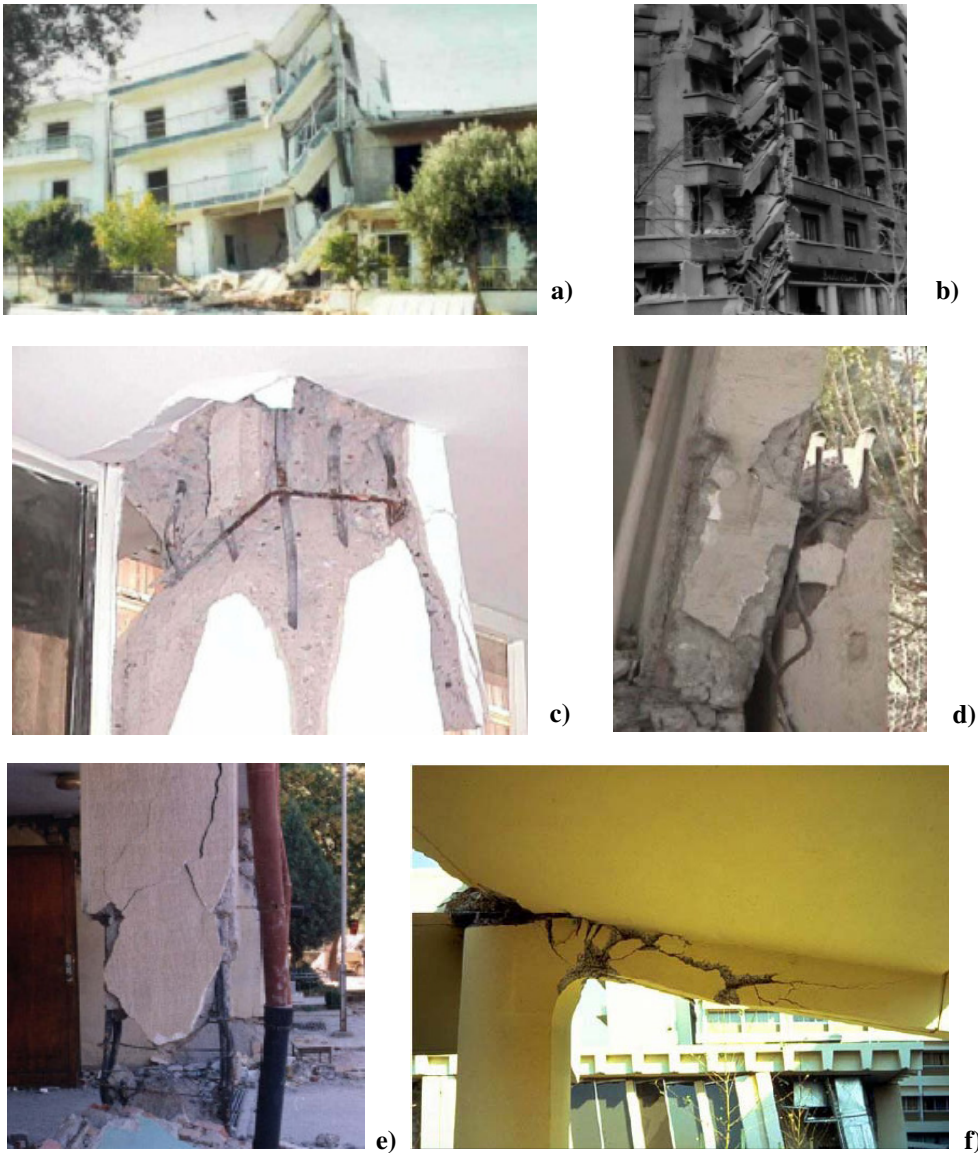


Figure 1.4: Damages in RC structures: soft-storey collapse (a); partial collapse due to soft-storey mechanism (b); column failure due to insufficient stirrups (c); column failure due to insufficient development length at the top (d); insufficient detailing at the joint (e); beam failure due to lack of steel bars (f); connection failure due to insufficient detailing near connection zone (g, h); failure of beam-to-column connections (i, l) and shear cracking in concrete shear walls (m, n) (continues)



Figure 1.4: Damages in RC structures: soft storey collapse (a); partial collapse due to soft-storey mechanism (b); column failure due to insufficient stirrups (c); column failure due to insufficient development length at the top (d); insufficient detailing at the joint (e); beam failure due to lack of steel bars (f); connection failure due to insufficient detailing near connection zone (g, h); failure of beam-to-column connections (i, l) and shear cracking in concrete shear walls (m, n)

In conclusions, considering that members and connections of RC buildings were severely damaged by past earthquakes, the identification of uncertainty in all component susceptible to undergo seismic effects and the consequent quantification of the risk to social systems and subsystems allow to develop risk-reduction strategies and to implement mitigation actions by means of the introduction of retrofit and rehabilitation techniques, whose study represents the topic of the next Section.

1.6 SEISMIC RETROFITTING TECHNIQUES

1.6.1 General

In the last decades the occurrence of severe earthquakes worldwide confirmed the deficiencies of existing structure, with particular reference to reinforced concrete ones. As a consequence, the experience collected from field observations and the related development of accurate analyses led to the improvement of both the knowledge level and the evolution of seismic codes.

In this field the interest of the research community is focused on buildings which do not comply with current seismic codes and exhibit deficiencies, such as poor detailing, discontinuous load paths and lack of capacity design provisions. Therefore, the retrofitting of such buildings by means of the introduction of rehabilitation schemes able to provide cost-effective structural solutions must be carried out. So, many intervention methods used in the past have been revised according to the new seismic code requirements and innovative techniques based on the use of new materials have been also developed.

In the current Section, the term rehabilitation is used to include all types of intervention methods, such as repairing, retrofitting and strengthening, which can be effectively used in order to reduce the earthquake vulnerability of buildings. According to the above classification, the term repairing, which deals with the as-built system, is defined as reinstatement of the original characteristics of a damaged section or element, while the “strengthening” one is referred to the intervention which allows, depending on the desired performance, to enhance one or more seismic response parameters (strength, stiffness, ductility, etc.).

1.6.2 Seismic rehabilitation schemes

The main aspect to underline in the framework of seismic rehabilitation of existing buildings is the definition of performance objectives which depends on the following several factors (Thermou and Elnashai, 2005):

- the structural type and the importance of the building;
- its historical significance and its role in post-earthquake emergencies;
- the construction materials;
- socio-economic issues correlated to the economic consequences deriving from business interruption.

More in detail, cost vs. importance of the structure is a significant factor, especially when the building is of cultural and/or historical interest, while the available workmanship and the level of quality control define the feasibility of the proposed intervention approach. Moreover, the duration of work, together with the consequent interruption of building use, and the disruption to occupants should be considered. In the same way, the functionality and aesthetical compatibility of the intervention scheme with the existing building, as well as the reversibility of the scheme when it is not accepted on a long-term basis, should also be evaluated. Finally, socio-economic factors have to be judged aiming at deciding both the level and type of intervention. In fact, there were documented cases where aesthetic and psychological issues dictated the rehabilitation strategies. As an example, after the Mexico City earthquake (1985), where external bracings were popular due to the feeling of confidence in the occupants, the use of such systems was adopted for making safe the structures.

All these factors can be specified as limits of one or more response parameters (stresses, strains, displacements, etc.) and, consequently, different limit states have to be correlated to the level of the seismic action.

The choice of an appropriate rehabilitation scheme, together with the definition of the intervention level to apply in the buildings having deficient behaviour, is a rather complex operation which depends on many different nature factors. In the context of the selection of a suitable intervention level, the most common strategies to be taken into account are:

- restriction or change of the building use;
- partial demolition and/or mass reduction;

- addition of new lateral load resisting systems;
- member replacement;
- transformation of non-structural into structural components;
- local or global modification of elements and system;
- introduction of base isolation systems, as well as either passive or active vibration control devices.

On the other hand, when the seismic retrofit of buildings is quite expensive and disruptive, the alternative of “no intervention” or “demolition” must be taken into consideration.

From a technical point of view, the selection of the suitable intervention to be carried out must be based on the compatibility with the existing structural system, the materials used for repairing and available technologies.

A convenient way to deep the engineering issues regarding the retrofit procedure is to break down the process into steps.

The first step involves the collection of information for the as-built structure, such as the structural system configuration, material strength, reinforcement detailing, non-structural components (i.e. external walls, which significantly influence the seismic response of the structure), foundation system and the level of damage. Such information can be acquired from visits to the site, construction drawings, engineering analysis and interviews with the original contractor.

The rehabilitation objective is selected from earthquake hazard levels and various pairs of performance targets, which are defined according to an acceptable damage level.

The building performance can be qualitatively described in terms of the following parameters:

- safety of people during and after the event;
- cost and feasibility of restoring the building to pre-earthquake conditions;
- length of repairing time;
- economic or historic impact on the community.

On the other hand, variations of the actual building performance could be associated with the following aspects:

- unknown geometry and member sizes;
- deterioration of materials;

- incomplete site data;
- variation of ground motion that can occur within a small area;
- incomplete knowledge and simplifications related to modelling and analysis phases.

Then, in the subsequent phase, the rehabilitation method, which is selected starting from the selection of an analysis procedure, is set-up in order to evaluate the building performance. Preliminarily, the rehabilitation measures are defined and the assessment of the analysis results is done, while in a second phase the check of the selected rehabilitation design is performed. Such an analysis procedure must be able to meet the fixed requirements through an analysis of the building.

A separate analytical evaluation is performed for each combination of building performance and seismic hazard specified in the assumed rehabilitation objective. If the rehabilitation design fails to comply with the acceptance criteria for the selected objective, the interventions must be redefined or an alternative strategy has to be considered.

1.6.3 Rehabilitation approaches

The aims of seismic rehabilitation can be described by the following procedures (Figure 1.5) (Fukuyama and Sugano, 2000):

- to recover original structural performance;
- to upgrade original structural performance;
- to reduce seismic response.

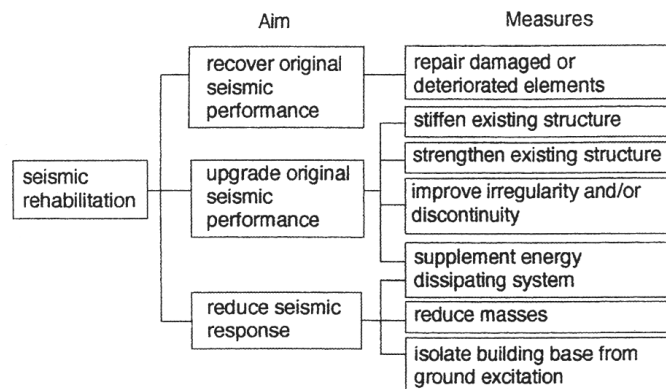


Figure 1.5: Seismic rehabilitation strategy and measures

The combined use of such rehabilitation techniques is employed in order to reduce the buildings vulnerability.

In particular, aiming at recovering the original structural performance, damaged or deteriorated portions of a building may be repaired with adequate material or replaced with new elements or materials.

On the other hand, in order to upgrade the original performance of buildings, several strengthening operations can be used (Figure 1.6). Besides, the stiffening of the building represents an useful operation for reducing its large displacements under horizontal actions. Irregularity or discontinuity of stiffness or strength distribution, which may result in failure or large distortion at a particular portion of the building, must be eliminated by changing the structural configuration. In this field another effective approach may be the one which increase the number of energy dissipating devices in the structure in order to enhance the building damping and to reduce the seismic response.

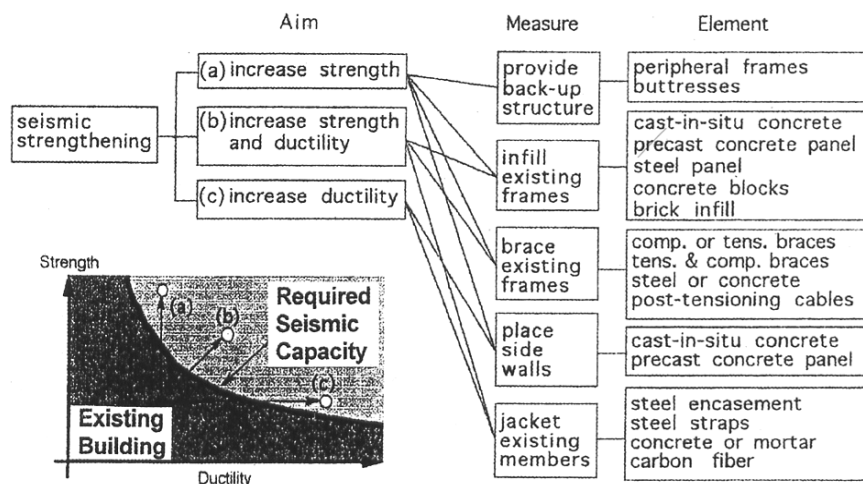


Figure 1.6: Typical strengthening methods

Other than the possibility to reduce the building masses, another concept to reduce seismic response is to isolate existing structures from the ground excitation aiming at increasing their fundamental period. This is an important approach for important buildings which must be functioned after an earthquake or which must preserve expensive and valuable contents.

Schematic concepts of seismic strengthening, seismic isolation and energy

dissipation are shown in Figure 1.7.

In the whole, according to the rehabilitation aims above reported, two general approaches for the seismic rehabilitation project can be recognized (Moehle, 2000).

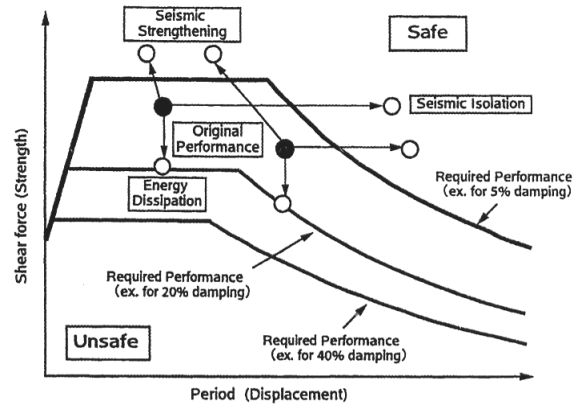


Figure 1.7: Seismic strengthening, seismic isolation and energy dissipation techniques for improving the seismic response of buildings

The first method, illustrated in Figure 1.8, involves local modification of isolated components of the structural and non-structural system. In this analysis the objective is to increase the deformation capacity of deficient components, so that they will not reach their specified limit state as the building responds at the design level. Common approaches include addition of concrete and steel or fibre reinforced polymer composite (FRPC) jacketing.

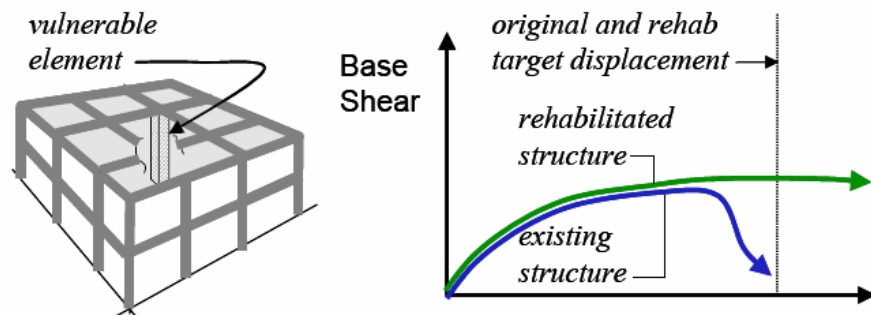


Figure 1.8: Rehabilitation approaches: local modification of the structural system

The second approach, reported in Figure 1.9, involves the global modification of the structural system so that the design demands on the existing structural and non-structural components, often denoted by target displacement, are less than their capacities.

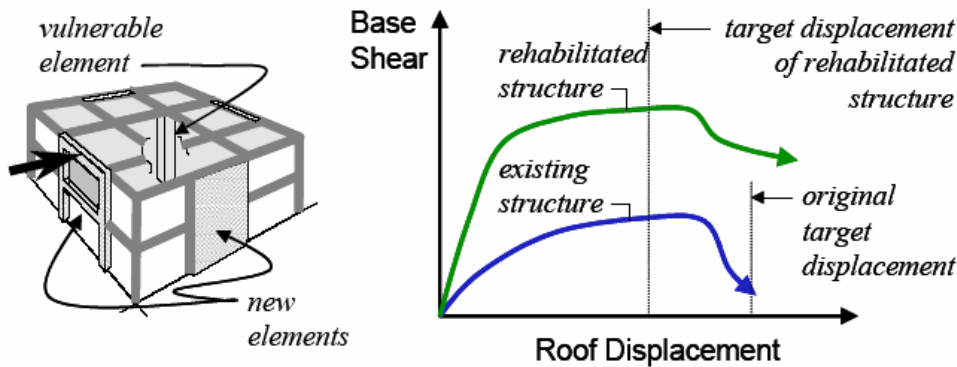


Figure 1.9: Rehabilitation approaches: global modification of the structural system

The most common techniques used following this approach include addition of structural walls, steel braces or base isolators. In this context, while passive energy dissipation schemes are usually used for RC frames, even if the displacement required for these structures is often beyond the displacement capacities of the existing components, techniques based on active control concept are rarely adopted.

Recent application showed that global modification schemes are more common than local modification ones. However, difficulties in developing accurate models of foundation flexibility and conservative acceptance criteria for existing components require the use of some combination of the above two approaches, which are treated in detail in the next Sections.

1.6.3.1 Local intervention methods

The local modification of isolated structural and non-structural components of buildings aims at increasing their deformation capacity in order to avoid the attainment of their limit state. Local intervention techniques, which are applied to a group of members that suffer from structural deficiencies, may be

used aiming at obtaining the desired behaviour of seismically designed structures by means of the methods illustrated one by one in the current Section.

1.6.3.1.1 Injection of crack

The most versatile and economical repairing method of RC structures is based on the crack injection process, whose effectiveness depends on the capacity of adhesive epoxy materials to penetrate under pressure into the fractures of the damaged concrete (Figure 1.10 a). In fact, while shear and flexural cracks are continuous and provide free passage for the epoxy, longitudinal ones, developing along reinforcing bars due to bond failure, are usually narrow and discontinuous and, therefore, difficulties in the use of adhesive materials may occur. Such a repairing technique can be used in small and large crack widths (up to 5-6 mm), while in case of larger fractures, up to 20 mm wide, cement grout is the appropriate material for injection (Figure 1.10 b).

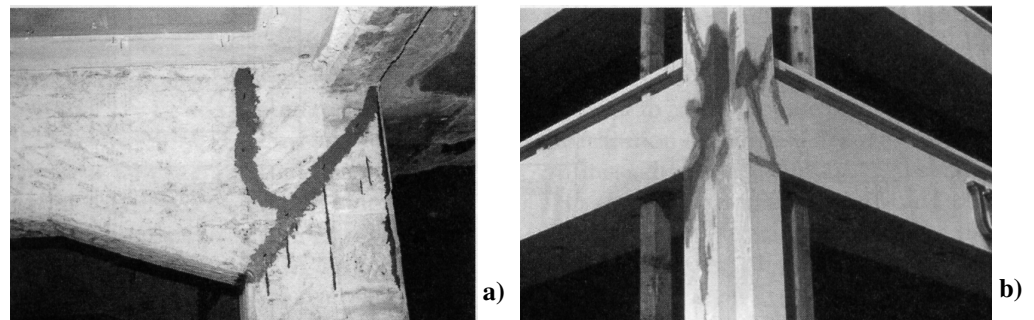


Figure 1.10: Repairation of beam-to-column joints: application of the epoxy resin (a) and cement grout injections (b)

In the first phase of the process loose material is removed; then the surface trace of cracks is fully sealed with epoxy paste, leaving only surface-mounted plastic nozzles, whose spacing depends on both the crack width and the epoxy viscosity at the application temperature, for injection. Finally, the intervention is concluded when epoxy is expelled from the next higher nozzle. Once the repair epoxy has set, the nozzles, which are bent and tied firmly, can be cut flush and sealed with an epoxy-patching compound prior to rendering of the affected members.

Flexural tests on both RC beams and beam-to-column joints showed that this process, other than eliminate the unattractive appearance of wide cracks, is able to restore the original capacity of damaged components.

1.6.3.1.2 Shotcrete (gunite)

Shotcrete, realised under form of either dry-mix or wet-mix types, is used, alone or in combination with other retrofit schemes, for repairing RC and masonry structures. Due to both its low water/cement ratio and high-velocity impact, it achieves excellent bond to most component surfaces. In particular, the impact velocity of the material toward the application surface is dependent upon both the exit velocity and the nozzle distance from the surface, which must be clean, sound and damp.

Where bond is important, the impact angle of the equipment, to be used very close to the application surface, must be around 90°. When the shotcrete strikes the application surface, some of the larger and harder aggregate particles tend to ricochet. Due to the nature of its composition, rebound is not able to obtain significant strength and should not be allowed in the final work. The amount of rebound is affected by the following factors:

- orientation of the receiving surface;
- shotcrete mix-design;
- amount of reinforcing steel embedment;
- cross-section thickness;
- impact velocity;
- spraying technique.

1.6.3.1.3 Steel plate adhesion

Such a technique can be mainly used for improving both the shear and flexural strength of beams. When thick steel plates have to be used, it is advisable to apply several thin layers in order to minimise interfacial shear stresses.

Moreover, for such interventions, the complete understanding of both the short- and long-term behaviour of adhesives used, as well as information concerning the concrete-steel adhesion, is required.

The execution of the bonding work is also of great importance to achieve a

composite action between the adherent parts. Prevention of premature debonding or peeling of externally bonded plates is the most critical aspect of the design.

1.6.3.1.4 Steel jacketing

The steel jacketing consists of the global encasement of the column through thin steel plates connected to its surface by means of non-shrink grout (Figure 1.11 a). A steel cage (Figures 1.11 b, c) can be considered an alternative to the complete column jacketing. In this case steel angles are positioned at the corners of the column cross-section and either transversal straps or continuous steel plates are welded on them. In particular, the straps are often laterally stressed either by special wrenches or by preheating to temperatures of about 200-400° prior to perform welding operations. As in the case of steel jacketing, the space between concrete and steel cage is filled through the use of non-shrink grout. If corrosion or fire protection is needed, a grout concrete or shotcrete cover may be provided.

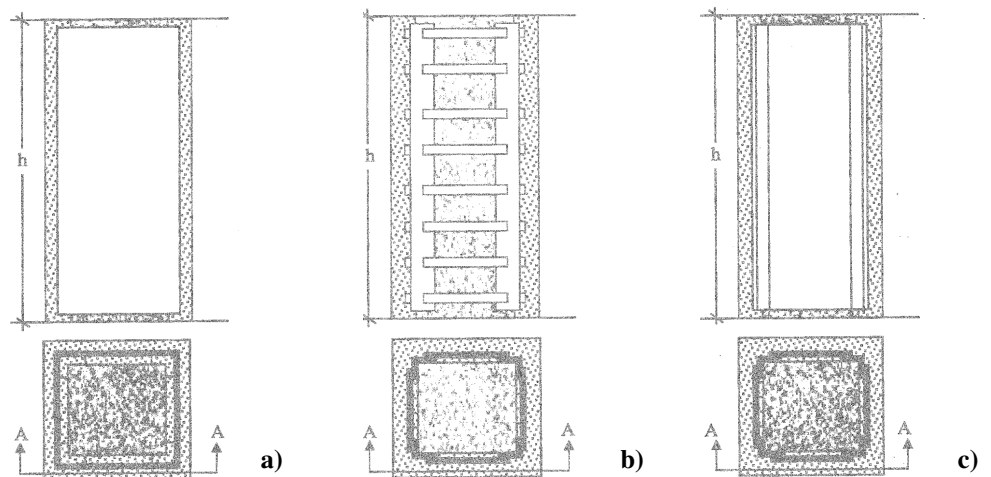


Figure 1.11: Repairation of columns: steel jacketing (a) and steel cage technique using steel straps (b) or steel plates (c)

The rehabilitation technique based on the use of corrugated steel plates can be effectively used for jacketing columns and beam-to-columns joints, by

making always use of non-shrink grout for filling the gap between concrete and steel parts. In particular, in case of deficient connections, a gap between the beam jacket and the column face is provided in order to reduce the flexural strength enhancement of the beam, which may cause excessive forces to develop in both the joint and the column.

1.6.3.1.5 Fibre reinforced polymers (FRPs)

In structural applications, especially when dead weight, space or time restrictions exist, the use of fibre reinforced polymers is considered very attractive thanks to their ease of application.

FRP composites, which can be realised with constituents such as carbon (CFRP), glass (GFRP) and aramid (AFRP), present strength levels higher than the ones offered by steel, but their use is often limited by strain limitations (Figure 1.12 a). Such materials, which are very sensitive to transverse actions and cannot transfer local shear (i.e. interfacial failure), are unable to carry compressive loads. Their behaviour is linear up to failure without any significant yielding or plastic deformations. Differently from steel, some fibres are anisotropic. Such an anisotropy conditions also the thermal expansion coefficient in both longitudinal and transverse directions. In addition, being the transversal strength less than the longitudinal one, bond deterioration and splitting of concrete can occur. These effects can also cause lateral stresses and low-cycle fatigue under repeated thermal cycling.

The choice of an appropriate retrofit scheme based on the use of composite materials results in a very great flexibility, depending on the selection of many factors, such as the fibres type, their orientation, their thickness and the plies number. In this way the attainment of the strength hierarchy at both local (single elements upgrading) and global (achievement of a desired global mechanism) levels is guaranteed.

The effectiveness of strengthening operations depends on both the available anchorage length and/or the type of attachment at the FRP ends and the laminates thickness. Failure of FRP reinforcement may occur either through de-bonding of the material at the interface with concrete or by tensile fracture, often at a stress lower than the material tensile strength, due to a strength concentration (i. e. at rounded corners). In many cases, according to

experimental results, the failure mechanism of FRP elements is due to combined effects between de-bonding and fracture.

The selection of both constituents (Figures 1.12 b, c) and details used to realise the composite significantly affect the environmental durability. In fact, environmental conditions can change failure modes of composites, even if performance levels are unchanged, and can also weaken the FRP-concrete interface, producing the modification of the failure mechanism and, sometimes, the change of performance.

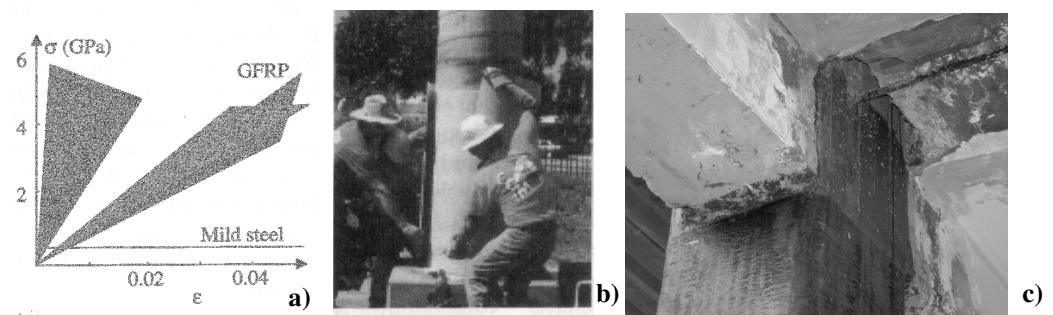


Figure 1.12: Composite materials: comparison with mild steel (a) and application of prefabricated shells (b) and sheets (c)

For columns, shear failure, confinement failure of the flexural plastic hinge region and lap splice de-bonding can be accommodated by the use of FRP. Such failure modes and the associated retrofit operations should be viewed together, since retrofitting for one deficiency may shift the problem to another location and/or failure mode without automatically improving the global performance. As an example, a shear-critical column strengthened with carbon wraps over its central region is expected to develop flexural plastic hinges at its ends, which must be retrofitted for the desired confinement levels. Besides, lap splice regions have to be checked not only for the required clamping force to develop the capacity of the longitudinal column reinforcement, but also for confinement and ductility of flexural plastic hinges.

On the other hand, FRPs can be used for shear and flexural strengthening of beams. Epoxy-bonded laminates or fabrics extending in the compression zone or epoxy-bonded FRP fabrics wrapped around the beam are usually used for such operations.

Finally, composite materials can be applied also for reinforcing connections and walls. In particular, in case of beam-to-column joints, jacketing interventions are usually used to replace missing transverse reinforcement in the connection.

1.6.3.2 Global intervention methods

In case of systems with high flexibility or when no continuous transverse load path is available, then global intervention techniques are introduced for seismic rehabilitation of existing RC buildings. The most well known global retrofit schemes are presented hereafter.

1.6.3.2.1 RC jacketing

Reinforced concrete jacketing is one of the most common methods applied for the rehabilitation of concrete members. Such an intervention can be considered as a global strengthening technique if the longitudinal reinforcement located in the jacket passes through holes drilled in the slab and new concrete is used in the beam-to-column joint (Figure 1.13). Contrary, if such a reinforcement operation stops at the floor level, then jacketing is considered a member intervention technique.

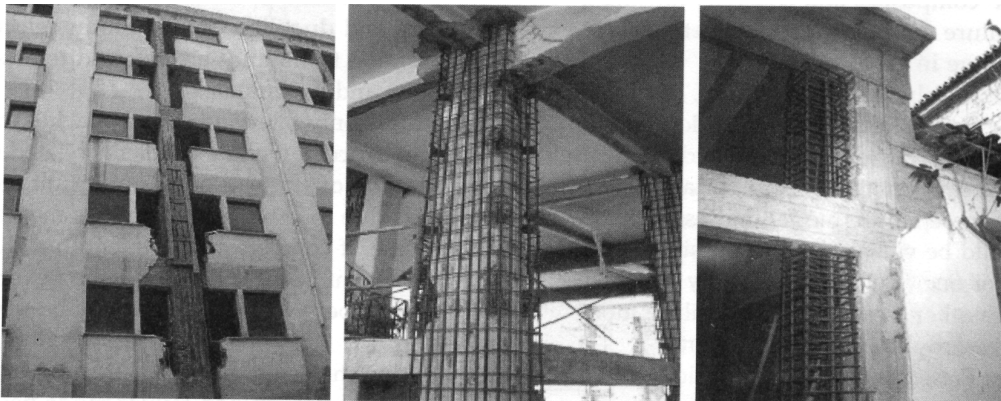


Figure 1.13: Reinforced concrete jacketing technique

This technique allows to have an uniform distribution of the lateral load capacity throughout the building, avoiding concentrations of lateral load-

resisting systems. On the other hand, the presence of beams requiring most of the new longitudinal bars in the jacket can be considered as a disadvantage of the method. Due to the column presence, cross ties for the new longitudinal bars, which are not located at the jacket corners, are difficult to provide.

Nowadays, no specific design rules exist for dimensioning and detailing of jackets aiming at reaching assigned performance targets. Another disadvantage is represented by the uncertainty characterising the bond between the jacket and the member. Moreover, slip and shear stress transfer at the member-jacket interface are dominant considerations in the application of RC jacketing technique.

1.6.3.2.2 External buttresses

External buttresses are used in order to increase the lateral strength of the whole structure aiming at reducing or eliminating the disruption of use of the buildings. This intervention, which is used in common with the realization of RC walls, requires the introduction of a new foundation scheme, which would be eccentric with respect to the buttress axis for avoiding excavation under the building.

The building strengthening by means of a set of external buttresses presents two intricate problems:

- the buttress stability may be critical because, differently from the structure, it is not loaded vertically downwards. In this case, the only vertical action applied on the buttress is its self-weight, which could produce the foundation uplifting, even causing over-turning problems.
- the connections between buttresses on one hand and the building on the other hand is far from be simple. In order to ensure full interaction and load sharing when the structure is laterally loaded, the buttress should be connected to the floors and columns at each level. So, the connection area is subjected to unusual stress levels, which require a particular attention.

1.6.3.2.3 Addition of RC walls

Among global strengthening methods of existing structures, the addition of RC shear walls is one of the most used systems, it being very efficient in

controlling global lateral drift and, therefore, to reduce damage in frame members.

In the design process, particular attention must be paid to the following aspects:

- plan and vertical distribution of walls;
- transfer of forces to walls through floor diaphragms;
- struts and collectors;
- integration and connection of the wall into the existing building;
- load transfer to foundations.

The design of walls takes place as in the new structures, providing the plastic hinge zones at their base with boundary well-confined elements, they being sufficiently detailed for flexural ductility and also capacity-designed in shear throughout their height. Besides, such elements are over-designed under flexural actions above the plastic hinge region in order to ensure that:

- inelasticity or pre-emptive failure will not take place elsewhere in the wall before the formation of plastic hinges at their base;
- the new wall remain elastic above the zone prone to develop a plastic hinge.

The most convenient way to insert new shear walls is to infill such elements into bays strategically selected of existing frames. If the wall is located within the whole area of the bay, then it incorporates beams and columns, the latter acting as its boundary elements (Figure 1.14).

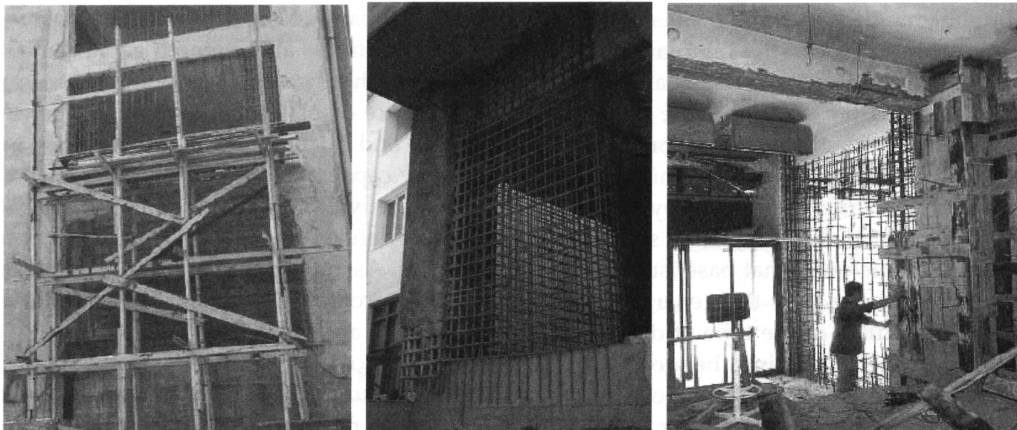


Figure 1.14: Cast-in-place infill walls

When the web of the wall is required to be added only, the shotcreting against a light formwork or a partition wall is performed. In the latter case, shotcrete is used aiming at increasing the adherence between existing and new materials. As an alternative to the cast-in-place infill wall technique, the addition of pre-cast panels, which should be designed to behave monolithically, can be proposed. In such a context, the infill wall should be also designed with enough shear strength in order to develop flexural yielding at its base.

In addition, particular attention must be paid to the reinforcing of the foundation for resisting the overturning moment and the necessity to integrate the new element with the remaining part of the structure. In this framework it is important to underline that interventions on foundations are usually expensive and disruptive; thus the use of such a technique for buildings having lack in the foundation system is not advisable.

1.6.3.2.4 Base isolation

The base isolation technique is mainly used when the need of rehabilitation interests critical or essential facilities, buildings with expensive and valuable contents and structures for which high levels of performance are required.

The isolation devices, which are inserted at the bottom or at the top of the first floor columns, significantly reduce the seismic impact on the building and its contents. The use of such a technique could require retrofitting interventions, such as the addition of a floor diaphragm, which is employed in order to connect all the columns above the isolators, and the strengthening of the first floor columns by means of the cross-sections enlarging, the addition of reinforcing bars or the realisation of new resistant elements.

The installation of isolators within the structure requires the cutting of columns, the temporary support of the above structure weight, the insertion of devices and the transfer of load to vertical elements. These operations are not simple, because they must take place without causing damage to people and elements (structural and non-structural) of the building.

Many efforts have been recently made to extend this valuable strategy to inexpensive housing and public buildings. The results of research programs conducted in this field showed that this seismic protection method can be both

cost-effective and functional for small buildings subjected to high seismic actions. In particular, a comparative study performed by Bruno and Valente (2002) on conventional and innovative seismic protection strategies concluded that base isolation gives a higher degree of safety than the one provided by many energy dissipation devices. Moreover, the comparison between conventional and innovative devices showed that shape memory alloys are more effective than rubber isolators in reducing seismic vibrations.

1.6.3.2.5 Steel bracings

Steel bracings can be a very effective method for global strengthening and stiffening of buildings. The advantages of such a system are the ability to accommodate openings, the minimal added weight to the structure and, in case of external steel systems, minimum disruption to the function of the building and its occupants. Besides, possible interventions on foundations are not required because steel bracings are usually installed between existing members. Increased loading on the existing foundation is possible at the bracing locations; therefore, in this case, probable interventions on the foundation system must be evaluated. In addition, the connection between the existing concrete frame and the bracing elements should be carefully treated because it results to be very vulnerable under seismic actions.

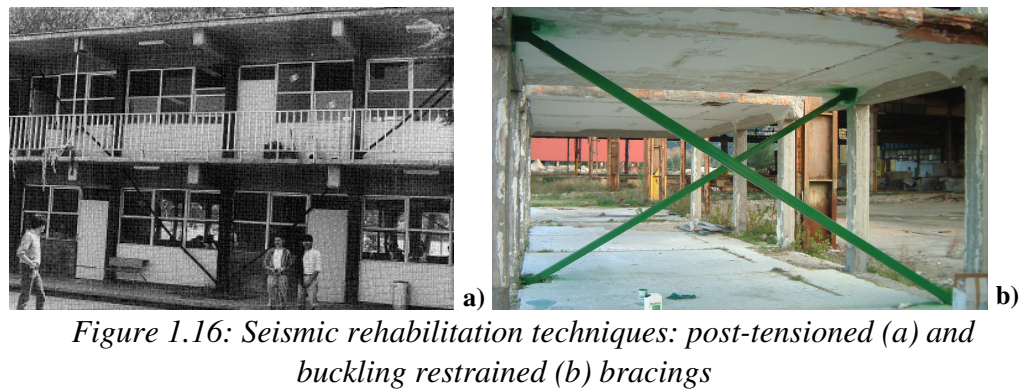
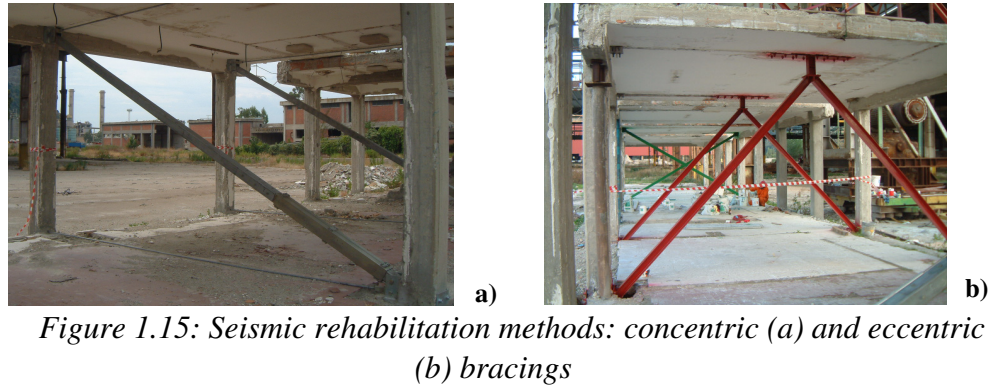
Several configurations of bracing systems, under form of concentric and eccentric types, may be installed within the bays of a RC frame aiming at providing a significant increase of the horizontal capacity of the structure.

Concentric steel bracing systems have been investigated for the rehabilitation of non-ductile RC buildings by many researchers. In such a field, the intervention carried out in Bagnoli, an area surrounding Naples, is noteworthy (Figure 1.15 a) (Cardone et al., 2004).

On the other hand, in the last years the use of eccentric steel bracings in the rehabilitation of RC structures has lagged behind concentric steel bracing applications due to the lack of sufficient research and information about the design, modelling and behaviour of the combined steel-concrete system. Nevertheless, full-scale experimental investigations on an existing RC building retrofitted with eccentric steel bracings have been recently carried out (Figure 1.15 b), providing useful information on both the RC beam-steel link

connection details and the implementation of a reliable link model to be used in the numerical analyses (D'Aniello et al., 2006).

Finally, also post-tensioned steel bracings (Figure 1.16 a) (Miranda and Bertero, 1990), as well as buckling restrained bracings (BRBs) (Figure 1.16 b) (Della Corte et al., 2005), can be effectively used for seismic upgrading of reinforced concrete buildings.



1.6.3.2.6 Steel Plate Shear Walls (SPSWs)

An alternative to steel bracings is represented by Steel Plate Shear Walls (SPSWs), which consist of one storey high and one bay wide steel plates installed vertically within a building frame and connected to the surrounding beams and columns. The infill plates may be stiffened or unstiffened and the beam-to-column interface may have moment-resisting or shear connections. In

particular, stiffeners have to be added to the plate, determining additional fabrication costs, in order to avoid buckling phenomena of the compressed wall zones, which can be considered one of the disadvantages of SPSWs.

In structures equipped with steel plate shear walls, due to relatively large inelastic deformations of the panel, the connections of the boundary frame can undergo relative large cyclic rotations and inter-storey drifts.

Such a system showed high seismic performances and also demonstrated advantages from the economic point of view, such as reduction of the construction time, limited weight transferred to the foundation system in comparison to RC shear walls, high initial stiffness and large energy dissipation capability.

In addition, the great ductility and the large dissipation capacity provided by steel plate shear walls can be exploited for seismic rehabilitation of existing RC buildings.

Nevertheless, in this field, potential problems occurred due to the choice of an effective connection system to relate steel and RC parts, the ductility incompatibility between the ductile SPSWs and non-ductile RC frame and the high shear force and curvature ductility demand induced by the panel tension field mechanism on the surrounding RC structure. For these reasons, the use of such a rehabilitation system, which presents few applications only into steel buildings, has not been deeply analysed.

Therefore, the possibility to use steel plate shear walls as effective seismic retrofitting systems of existing RC structures represents the target of the present study. The analysis of such systems, which can be used as an alternative to steel bracings, must begin with both an accurate investigation on their behaviour and a complete overview of all applications developed worldwide, which represent the objectives of the next Chapter.

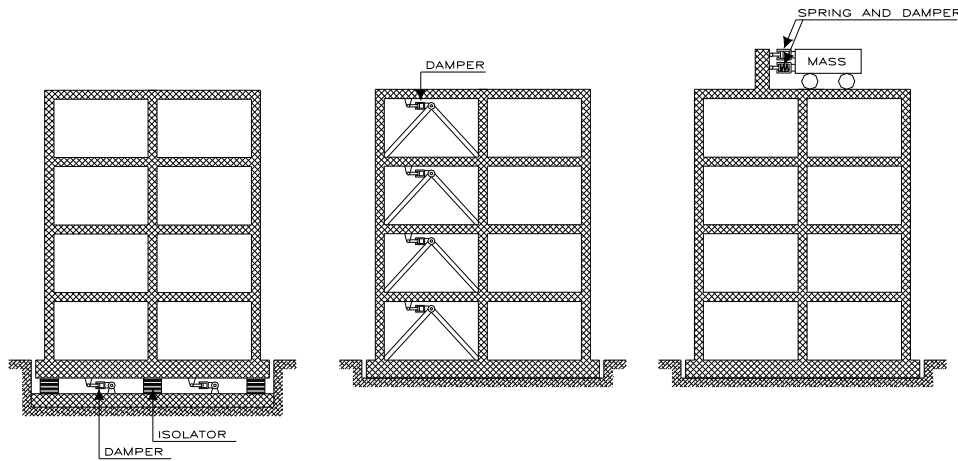
Chapter II

State-of-the-art review on steel plate shear walls

2.1 INTRODUCTION

As it is well known, the current seismic design concept of framed structures consists to entrust the energy dissipation role under strong earthquakes to the beams and columns which, thanks to their plastic deformation capacities, have to dissipate the input seismic energy (Gioncu and Mazzolani, 2002). A direct consequence of such an approach is the occurrence of damage to the primary structure even for moderate-intensity earthquakes. A new approach in the seismic design, also known as Damage Tolerant Structures approach (Wada et al., 1992), is based on the adoption of passive seismic protection devices, acting as sacrificial elements during seismic events, which otherwise could damage structural and non-structural elements.

In the passive control systems any external power sources are not required and the dynamic properties of the structure, such as fundamental period and damping capacity, remain constant with seismic ground motion. Such systems can be classified into three categories: base isolation, energy dissipation and mass effect devices (Figure 2.1) (Panico, 2004).



a. Seismic isolation

Sliding or Rolling Mechanism:

- Ball bearings
- Slide plate bearings
- Sliding layers

Flexible elements:

- Multi-rubber bearings
- Double columns
- Flexible piles

b. Energy dissipation

Hysteretic type:

- Metal-yielding type
- Friction type

Viscous type:

- Viscous dampers
- Viscoelastic devices

c. Mass effect

- Mass spring type
- Pendulum type
- Sloshing of liquid

Figure 2.1: Classification of passive control systems

In the base isolation systems, elongating the natural period through isolators the acceleration response of the structure is reduced. The seismic isolation devices are usually installed between the foundation and the structure or between two relevant parts of the structure itself, as in the case of the suspension buildings. The isolation of a building can be done by means of sliding or rolling mechanisms (ball bearings, slide plate bearings, sliding layers), as well as flexible elements (multi-rubber bearings, double columns, flexible piles).

The mass effect systems are based on supplementary masses connected to the structure by means of springs and dampers in order to reduce the dynamic response of the structure. These devices are tuned to the particular structural frequency so that when that frequency is excited, the devices will resonate out of phase with structural motion, dissipating energy by inertia forces applied on

the structure by such masses. The structural response control technology by mass effect mechanism can be mainly applied by tuned mass dampers as mass-spring systems and pendulum systems and by tuned liquid dampers systems based on sloshing of liquid.

Finally, the energy dissipation systems consist of special sacrificial devices that act as hysteretic and/or viscous damper, absorbing the seismic input energy and protecting the primary framed structure from damage. The hysteretic dampers include devices based on yielding of metal and friction, while viscous dampers include both devices operating by deformation of viscoelastic solid and fluid materials (viscoelastic dampers) and the ones operating by forcing fluid materials to pass through orifices (viscous dampers).

In this framework, with reference to metal-based devices, the majority of the adopted systems belong to the categories of diagonal bracing and shear walls.

In the first case, the dissipative function is carried out by either ductile braces (Clark et al., 2000) or Added Damping Added Stiffness (ADAS) elements placed along diagonals or at the top of chevron bracings (Aiken and Whittaker, 1993), while the presence of diagonals provides stiffness and strength.

In shear walls systems, stiffening, strengthening and dissipative functions are carried out by either the basic sheeting constituting the panel or by the connecting system between shear panels and the bearing structure (Pinelli et al., 1996). Even though both types of the above solutions have been proposed, the former appears more effective and promising.

In fact, on one hand, the adopted plates, when rigidly connected to the external frame, may easily provide high in-plane strength and stiffness, while, on the other hand, the possibility to have a quite uniform shear stress distribution throughout the plate, ensures a large energy dissipation capacity due to the large size of yielded material. Shear walls systems give also the other advantages respect to other lateral load resisting systems, as moment resisting frames, namely steel savings, speed of erection, reduced foundation cost, increased usable space in buildings, in addition to the cladding function they have.

In the next Sections, shear wall systems, which are typical energy dissipation systems currently used both in steel and RC framed structures, will be analyzed and discussed. They are mainly based on metallic-yielding approach and are activated by the relative interstorey drift occurring during the loading process of the structure. They will be examined in relation to the different adopted arrangements, the dissipative mechanisms and used materials, showing also the benefits related to their use. In addition, a wide overview on both analytical and experimental studies developed worldwide on metal plate shear walls will be done and finally some applications based on such systems will be shown.

2.2 THE SHEAR WALL SYSTEMS

Shear walls represent one of more convenient passive control systems used to control the dynamic response of framed buildings subjected to low and high intensity earthquakes. Firstly, they can be used as basic seismic resistance system under earthquake loading, due to their considerable lateral stiffness and strength. In addition, due to the large energy dissipation capacity related to the large plate portions where plastic deformations take place, they are very effective for seismic protection of structures under strong loading conditions, producing a dissipative action which is activated by interstorey displacements.

The seismic protection systems based on shear walls consist of a series of plates that, generally located either around a service area or in the perimetral frames of the structure, realize a central stiffening nucleus able to absorb the effects of horizontal forces. Within this category, the use of metal plates for shear walls represents an innovative bracing system, effectively able to confer to the building a remarkable resistance against seismic and wind actions. These devices, which have a low erection cost and high speed of installation, are usually obtained by inserting a metallic panel, which represents the main lateral load-resisting element, inside a frame composed by steel beams and columns. Typically, the beams are positioned at floor levels, while the column location is controlled by architectural requirements.

Shear panels have to be considered as bi-dimensional elements having depth and width of the same dimension order, while the thickness results small and not comparable to the previous ones. When these structural systems are

loaded transversally to the plane, because of a low second moment of area of the cross section, they do not offer significant strength and stiffness. In such a case the panels can be used when they assume the shape of trapezoidal sheetings only. On the other hand, when the actions are applied in their plane, shear panels offer a very good behaviour, with large strength and stiffness, also for resisting overturning moments due to lateral loads.

Steel shear walls were firstly used in the late 1920s as cladding panels without any structural purpose (Cohen and Powell, 1993). However, further studies proved their significant influence on the global behaviour of structure, since the measured displacements were smaller than the computed ones (Miller and Serag, 1978). In order to take profit of their presence, it was proposed to include explicitly the stiffness and strength of cladding panels into structural models, so to improve the performance of low- and medium-rise moment resisting frames under wind and seismic loads. Generally, cladding were made of lightweight steel panels, mainly based on corrugated sheeting and sandwich panels, simply connected to supporting frame by means of steel bolts, rivets or spot welds (Nilson, 1960). However, in recent studies, it has been proved that they can considerably contribute to increase the seismic performance of steel framed structure, especially under moderate-intensity earthquakes (Figure 2.2 a), while their contribution at the ultimate limit state is quite limited owing to poor dissipative behaviour (Figure 2.2 b) (De Matteis, 2002).

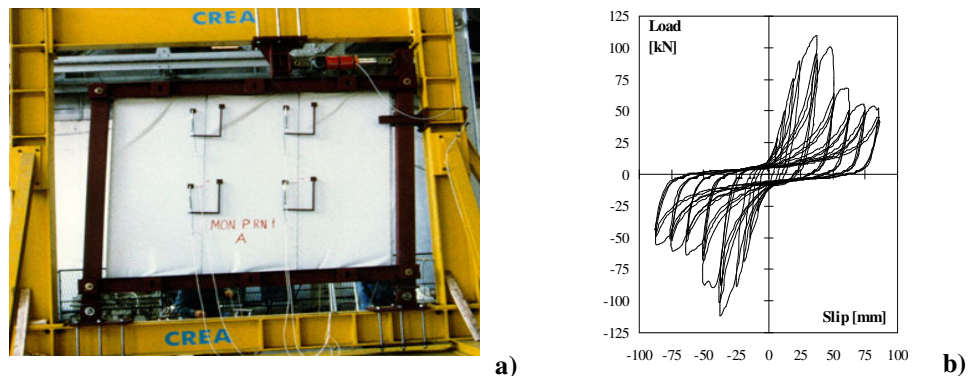


Figure 2.2: Lightweight sandwich steel panels: a) tests performed at the Crea Laboratory under the coordination of the University of Naples; b) cyclic behaviour of the tested device

In the subsequent research phase, shear panels made of steel plates continuously and rigidly connected to the external frame were proposed in order to be used as primary system in absorbing external lateral actions, while beams and columns had only the role of carrying out stationary loads (Kulak 1991). Then, dissipative requirements were added by adopting special cladding-to-frame connections (Figure 2.3) in order to increase the damping of the main structure, since the thin metal plates adopted were not able to significantly contribute to the energy dissipation (Pinelli et al., 1996).

The alternative was to avoid shear buckling of the plate, by adopting appropriate stiffeners configurations (Tanaka et al., 1998).

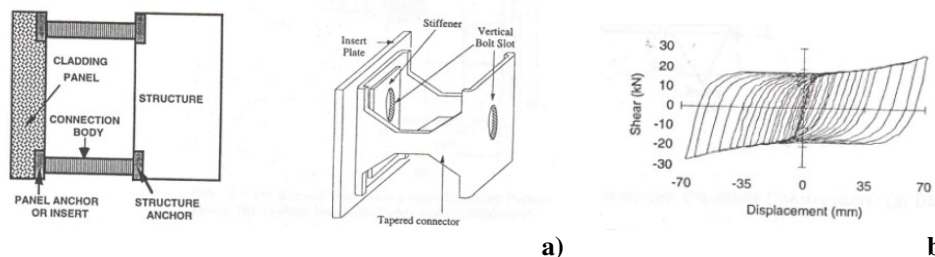


Figure 2.3: Panel based on dissipative connections: advanced tapered connector tested at the University of Florida (a) and its cyclic behaviour (b)

Steel plate shear walls inserted into framed buildings can be conformed according to two different configurations (Liu and Astanek-Asl, 2000).

The first solution, defined as standard system, is the one in which the connections among members are schematised as pinned joints (Figure 2.4 a): in such a case the only seismic-resistant system is represented by the shear wall, while the remaining part of the structure must be designed in order to carry vertical loads only. Considering that also hinged beam-to-column connections are able to absorb some amount of the flexural moment, which is between 20% and the 70% of the plastic moment of the connected beam, it is evident that also the primary structure participates to the absorption of the acting horizontal actions. In this case the members must be opportunely rigid and resistant so that the dissipation mechanism can develop correctly through the whole shear panel surface: therefore it is necessary that the beams should be designed for remaining in the elastic field while the columns must not

suffer buckling phenomena.

The second solution, defined as dual system, foresees that the beam-to-column connections are of moment-resisting type: the reaction frame participates significantly to the absorption of horizontal actions, providing an additional contribution to the lateral resistance provided by steel shear walls (Figure 2.4 b).

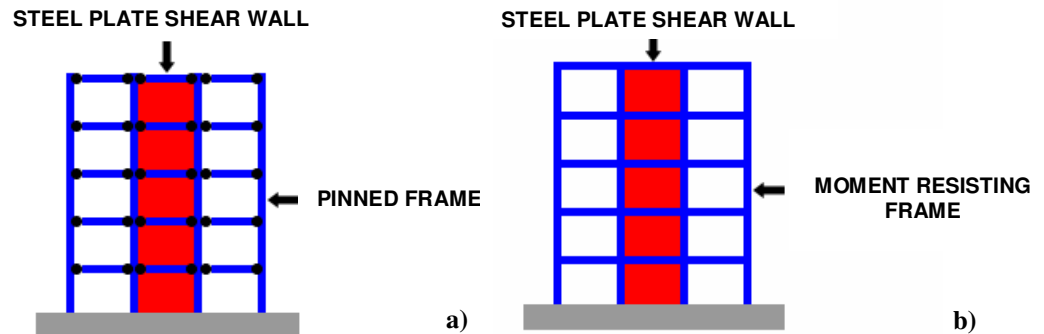


Figure 2.4: Shear walls configuration: a) standard system; b) dual system

In such a case the members have to be designed to support the tension field mechanism produced by the panel, with particular attention to the formation of plastic hinges in the surrounding members. Considering that also the framed structure participates to the absorption of lateral forces, it should be designed in order to absorb a part of these actions which must be determined according to the ratio between the lateral stiffness of the two systems (steel frame and shear wall).

The connection between shear panels and the members of the surrounding frame, which can be either of simple or moment-resistant type, can be realized by using bolts or by welding the panel to appropriate plates fixed to the beams and columns.

The selection of an appropriate structural configuration of shear wall systems for controlling the structure response under both wind and seismic actions represents an important task for structural engineers. At this aim, several structural configurations of panels can be adopted in multilevel buildings. The most common ones are: single wall (Figure 2.5 a), coupled

walls (Figure 2.5 b), out-rigger walls (Figure 2.5 c) and mega-truss (or mega-frame) wall configuration (Figure 2.5 d).

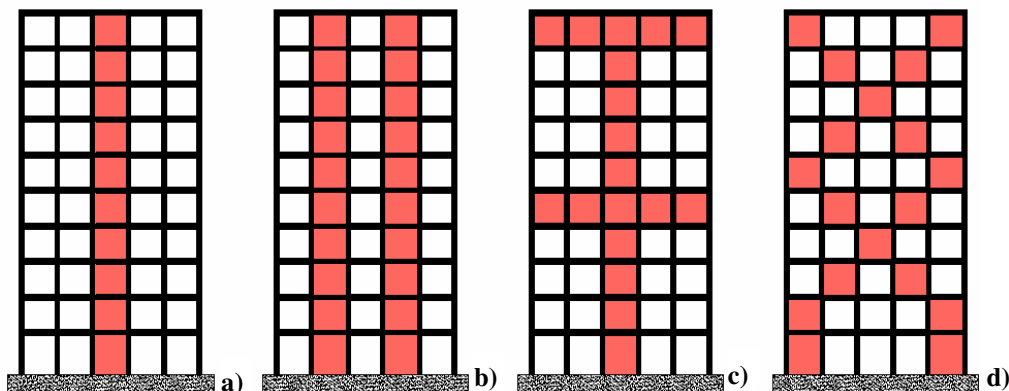


Figure 2.5: Structural configurations of shear walls: a) single wall; b) coupled walls; c) out-rigger walls and d) mega-truss (or mega-frame) walls

Moreover, steel plate shear walls, when applied in framed buildings, can be inserted also into the single mesh of the frame according to the following basic arrangements:

- as large panels rigidly and continuously connected along columns and beams of the frame mesh, serving also as cladding panels (Figure 2.6 a);
- as smaller elements installed in the frameworks of a building at nearly middle height of the storey and connected to rigid support members for transferring shear forces to the main frames, according to either bracing, or partial bay or pillar type configurations (Figures 2.6 b, c, d).

Comparing the current system with the traditional steel bracing ones (concentric or eccentric braces), it has to be observed that the former allows to easily realize some openings, required by the presence of windows and doors, by means of the insertion of opportune stiffening elements surrounding the same open surface (Figure 2.7 a). Another solution that can be effectively employed for allowing the presence of large openings in steel walls is to use two separate steel shear walls connected among them through the floors beams (Figure 2.7 b).

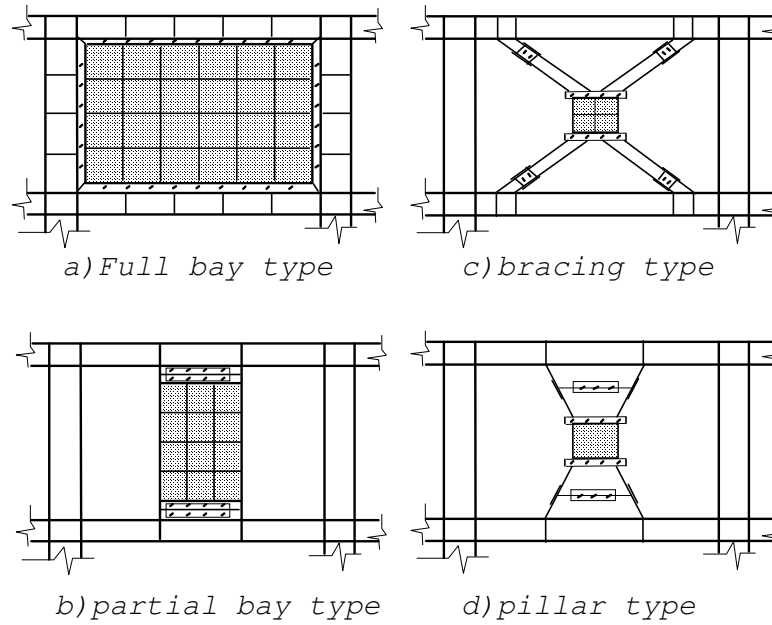


Figure 2.6: Typical arrangements of steel shear panels

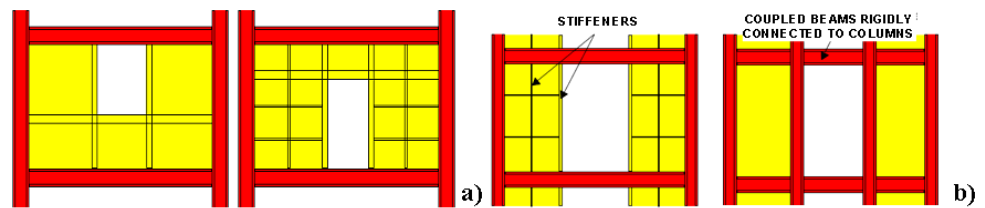


Figure 2.7: Presences of openings in simple steel plate shear walls (a) and adoption of coupled steel plate shear walls for openings realization (b)

In shear panels the energy dissipation takes place mainly for shear mechanism, by means of either pure shear stress action (Figure 2.8 a) or tension field action (Figure 2.8 b) (De Matteis et al., 2005a). In the latter, owing to the high slenderness of plate, premature shear buckling in the elastic field occurs and the lateral shear forces are carried by means of diagonal tensile stresses developing in the web plates parallel to the directions of the principal stresses. Such a behaviour produces not only a poor dissipative behaviour, with a pronounced slip-type hysteretic response, but also a strong

flexural interaction with beams and columns of the primary frame. A pure shear dissipative mechanism would be preferable, it allowing to have both a stable inelastic cyclic behaviour and a uniform yielding spread over the entire panel.

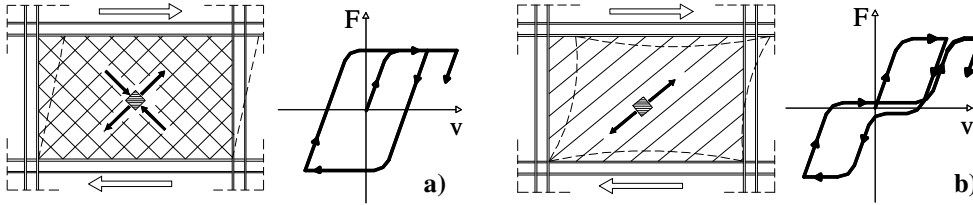


Figure 2.8: Shear energy dissipation mechanisms: pure shear (a) and tension field (b)

In addition, shear panels with pure shear mechanism are also able to enhance the energy dissipation capacity of the whole structure, acting as sacrificial devices, absorbing a large amount of seismic input energy and protecting the primary framed structure from relevant structural damages. Therefore, they can act as hysteretic dampers, whose dissipative function is activated by the interstorey drifts occurring during the deformation of the structure subjected to horizontal actions.

In order to have a pure shear dissipative mechanism, shear panels have to be designed and ribbed in such a way to avoid any buckling phenomenon up to the required plastic deformation level. In a stiffened shear panel, it is possible to have both the local shear buckling of the portion of plate enclosed within longitudinal and transversal stiffeners and global shear buckling where the stiffeners, due to their limited second moment of area, are involved in the buckling shape of the shear plate. Therefore, it is necessary to use suitable stiffeners, by adopting longitudinal and transversal ribs having adequate flexural second moment of area and conferring an appropriate width-to-thickness ratio to the whole plate.

Steel shear walls behaving with a pure shear dissipative mechanism are also identified as "compact shear panels", because they yield in shear without the occurrence of buckling phenomena. Whereas the steel shear panels dissipating energy by means of the tension field action are also denoted as "slender shear panels" because they are expected to buckle in elastic field. An

intermediate category of shear walls is instead identified as "non-compact shear panels", where shear yielding has been already reached when buckling occurs (AISC, 1999).

The behaviour of both compact and slender shear panels will be presented in the next Sections, aiming at illustrating design criteria, analytical studies and main applications developed in the last years.

2.3 COMPACT SHEAR PANELS

2.3.1 General

Differently from unstiffened shear panels, which dissipate energy through the metal yielding along tension diagonals only and are characterized by cyclic behaviour with pronounced degradation of stiffness and strength owing to out-to-plane displacements produced by shear buckling of the plate, stiffened shear panels present a dissipative mechanism due to pure shear deformation thanks to inhibited buckling due to the lateral confining action carried out by the insertion of suitable ribs.

Nevertheless, the need to use stiffened plates in order to delay shear buckling in the plastic field represent a very expensive solution, especially under the fabrication point of view. As an alternative to the use of stiffened plate, the adoption of Low Yield Strength (LYS) steels, can be proposed, they having E/f_y ratios greater than the ordinary steels and, therefore, allowing a larger width-to-thickness ratio for shear buckling of steel plate. The low yield strength steel is a type of steel that, due to small amounts of carbon and alloying elements, has a nominal yield stress of about 90-120 MPa, the same Young modulus as conventional steel and a nominal elongation over 50%. It is to be considered that the low yield point ensures the energy dissipation yet for smaller deformation levels, as in the case of wind and moderate earthquakes, working as dampers also at the serviceability limit state.

Owing to not easy availability of LYS steel on the world market, the use of the wrought aluminium alloy EN-AW 1050A, known as pure aluminium, as metallic material to build shear panels has been proposed (De Matteis et al., 2003). Thanks to its low percentage of alloying elements, the pure aluminium, having a high degree of purity (99.50%), is able to give a yield stress lower

than LYS steel and, simultaneously, due to the lower specific weight, to reduce the overloading on structural elements.

In addition, in order to improve its mechanical features, the base material can be subjected to a heat treatment, favouring the increase of the ductility and the conventional yield stress reduction.

A qualitative comparison between low yield steel, a typical mild steel and pure aluminium alloy, before and after heat-treatment, is shown in Figure 2.9, where the mechanical features of heat-treated aluminium alloys are also reported. For this reason, pure aluminium should be particularly adequate for the fabrication of dissipative devices based on metal yielding.

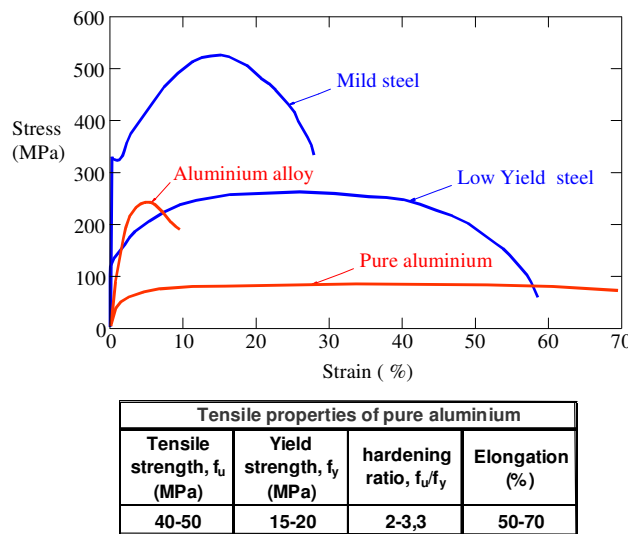


Figure 2.9: Comparison of stress-strain relationship between typical steels and aluminium alloy with degree of purity of 99.50% (Aluminium and Aluminium Alloys – ASM specialty handbook)

2.3.2 Design criteria

A dissipative shear panel based on metallic yielding technology is able to provide a stable cyclic behaviour if it is designed in such a way to avoid any buckling phenomenon before the plastic deformations occur. For this reason it is necessary to check that the yielding of the panel takes place for loading

levels lower than the ones corresponding to the buckling of the panel itself (De Matteis et al., 2005b). This aim is reached if the following condition is applied:

$$\tau_{cr} \geq \alpha \tau_y \quad \text{with} \quad 1 \leq \alpha \leq \frac{\tau_u}{\tau_y} \quad (2.1)$$

where α is the material hardening ratio, τ_u is the ultimate shear stress and τ_y is the yielding shear stress.

In a stiffened shear panel the shear buckling phenomenon can be both of local type and of global type (Figure 2.10). In the first case the instability waves are confined within the portion of plate enclosed by longitudinal and transversal stiffeners (Figure 2.10 a). Contrary, in the case of global buckling, owing to their limited second moment of area, the stiffeners are involved in the buckling shape according to a flexural buckling form (Figure 2.10 b).

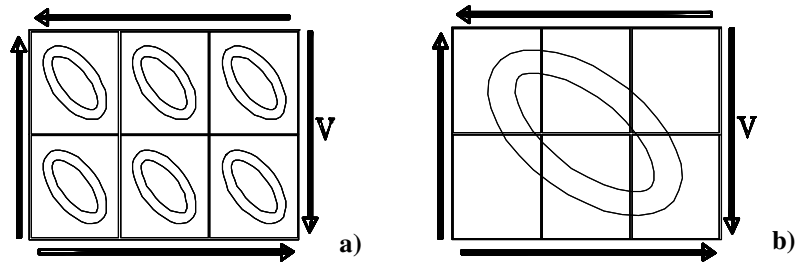


Figure 2.10. Shear buckling phenomena for stiffened shear panel: a) local; b) global

The buckling problem of shear plates in the plastic field has been approached by extending at the inelastic range the formulas valid in the elastic range, by replacing the Young's modulus with an appropriate reduced modulus $E_r = \mu E$, where $\mu < 1$ is the plasticity factor (Bleich, 1952). In this way the critical shear stress can be obtained by using the same formula of elastic buckling (Timoshenko and Gere, 1961):

$$\tau_{cr} = k_\tau \frac{\pi^2 \mu E}{12(1-\nu^2)} \left(\frac{t_w}{b_w} \right)^2 \quad (2.2)$$

where ν is the Poisson's modulus and k_τ is the shear buckling coefficient, which depends upon the boundary restraints and the aspect ratio a/b_w , where a

is the spacing of transverse stiffeners, b_w and t_w are depth and thickness of the plate, respectively. For instance, by making reference to compact shear panels made of aluminium alloy, the plasticity factor μ was determined by applying the unified theory of plastic buckling for an infinitely long plate of 24 ST aluminium alloy in uniform shear (Stowell, 1948). Stowell gave the values of μ in the form of curves plotted versus the intensity of the shear stress τ . It was found that μ is nearly independent of the degree of restraint at the long edges and its values may be well approximated by a function of the tangent-modulus E_t according to the $\sqrt{E_t/E}$ -curve, which provides conservative values for the critical shear stress. The limit value of the normalized slenderness parameter $\bar{\lambda}_w$, which allows the fulfilment of eq. (2.1), may be obtained by eq. (2.2) by assuming the Poisson modulus ν equal to 0.33 :

$$\tau_{cr} = k_\tau \frac{\pi^2 \mu E}{12(1-\nu^2)} \left(\frac{t}{b} \right)^2 \geq \alpha \tau_y \Rightarrow \bar{\lambda}_w = \sqrt{\frac{\tau_y}{\tau_{cr}}} = \frac{0.81}{\sqrt{k_\tau}} \frac{b_w}{t_w} \sqrt{\frac{f_y}{E}} \leq \sqrt{\frac{\mu}{\alpha}} \quad (2.3)$$

Equation (2.3) shows that the limit value of slenderness parameter $\bar{\lambda}_w$ decreases to the increasing of the hardening ratio α and to the decreasing of the plasticity factor μ , which is the tangent-modulus in the plastic field in related to. The slenderness parameter $\bar{\lambda}_w$ can be also evaluated according to the EC9 provisions (EN 1999-1-1, 2006):

$$\bar{\lambda}_w = \frac{0.81}{\sqrt{k_\tau}} \frac{b_w^*}{t_w} \sqrt{\frac{f_y}{E}} \leq \frac{0.48}{0.4 + 0.2\alpha} \quad (2.4)$$

$b_w^* = b_{w1}$ for local buckling and $b_w^* = b_w$ for overall buckling (Figure 2.11).

The shear buckling coefficient k_τ can be calculated by the relationships given by the EC9 for local and overall buckling.

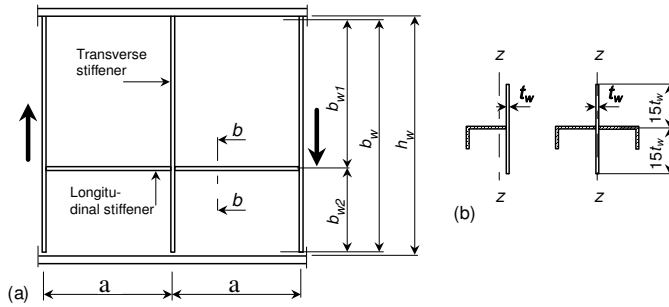


Figure 2.11. Geometrical parameters for stiffened shear panels

The main geometrical parameters influencing the monotonic and cyclic behaviour of compact shear panels are the width-to-thickness b/t ratio of the single plate portions and the normalised stiffness parameter γ_{st} , the latter defined by the following equation:

$$\gamma_{st} = \frac{E \cdot (I_{st}/n_{st})}{bD} = \frac{12 \cdot (1 - \nu^2) \cdot (I_{st}/n_{st})}{b \cdot t^3} \quad (2.5)$$

According to EC9, the second moment of area of the applied ribs I_{st} is assumed as the sum of second moments of the n_{st} intermediate transverse stiffeners placed on the panel surface.

The monotonic and the cyclic response of shear panels may be described in terms of normalized shear strength F/F_{02} (F being the panel shear strength and F_{02} the nominal shear strength related to an uniform shear stress corresponding to the conventional elastic limit) and the shear deformation level γ , given by the ratio between the global shear panel displacement Δ and the panel depth H .

According to previous numerical analysis carried out in the last years (De Matteis et al., 2004b; 2005b), the performance of a compact shear panel having $H/b = 1.5$ for different shear deformation levels γ can be synthetically represented into a design chart (Figure 2.12), where for a fixed design value of shear strength $F/F_{0.2}$ and plastic shear strain γ , both the b/t ratio and the optimum value of the stiffness parameter $\gamma_{st,opt}$ are given. In particular, $\gamma_{st,opt}$ is defined as the value of γ_{st} corresponding to the attainment of the maximum value of the panel shear strength, for a given b/t ratio and a required plastic deformation γ . In the same chart the limit curves related to the attainments of premature buckling phenomena can be provided. In fact, the right side of the diagram (large b/t values) is related to the attainment of elastic buckling ($\tau_{cr} \leq \tau_{0.2}$). The corresponding elastic buckling curve clearly represents a limit for the use of shear panels as dissipative devices. Obviously, such buckling phenomena could be either of local or global type, depending on the panel configuration. In particular, global buckling is more relevant for reduced shear deformation levels, where the applied ribs have a lower flexural stiffness. Shear panel configurations falling on the right of the above buckling curve can be defined as “slender”, meaning that they suffer buckling phenomena before being involved into plastic deformations. Similarly, the buckling curve depicted on the left side of the above charts (small b/t values) is representative

of panel configurations where the buckling phenomena occur for shear stress (τ_{cr}) equal or larger than the one corresponding to the attainment of the design deformation demand (τ_y) (plastic buckling curve). Shear panel configurations falling on the left of the above buckling curve can be defined as “compact”, meaning that they do not suffer buckling phenomena up reaching the required plastic deformation. As a consequence, shear panel configurations falling between plastic buckling curve and elastic buckling curve can be defined as “semi-compact”, meaning that suffer buckling phenomena while undergoing plastic deformation.

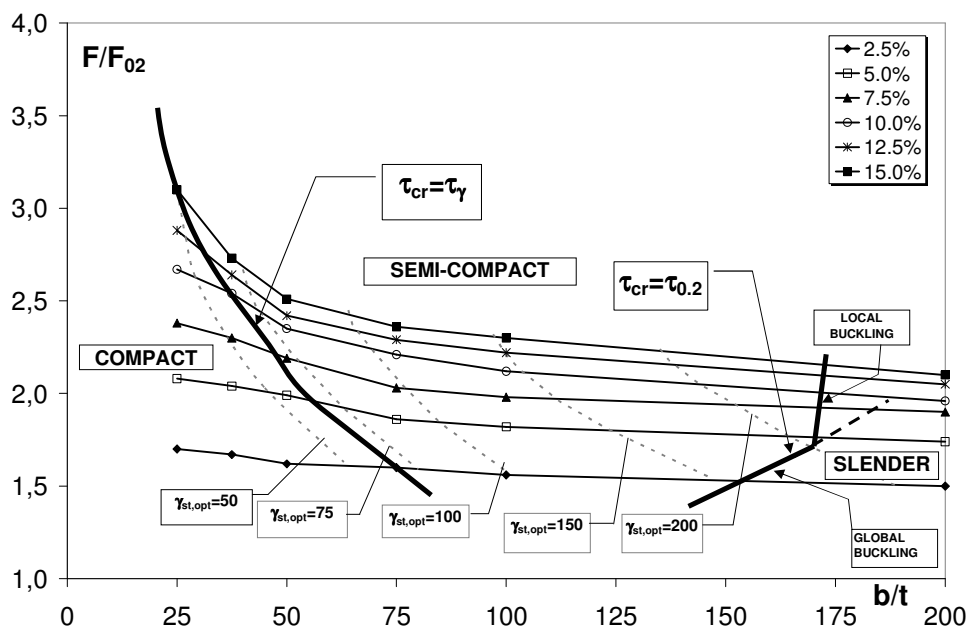


Figure 2.12: Design chart for pure aluminium shear panels

2.3.3 Theoretical and numerical modelling

Introduction of shear panels into steel framed structures allows the improvement of structural performance levels under lateral loads due to the increase of stiffness, strength and ductility. In addition, compact shear panels are also able to enhance the energy dissipation capacity of the whole structure, acting as sacrificial devices, absorbing a large amount of seismic input energy

and protecting the primary framed structure from relevant structural damages. Therefore, compact shear panels can act as hysteretic dampers, whose dissipative function is activated by interstorey drifts occurring during the loading process of the structure. On the other hand it has to be taken into account that stiffening effect provided by shear panels produces an important increase of lateral stiffness of the whole structure and therefore the shifting of the structural period into the range of higher spectral acceleration. Such an effect should be considered in the design process, where compact shear panels can be compared to concentric bracings (Figure 2.13) (Panico, 2004).

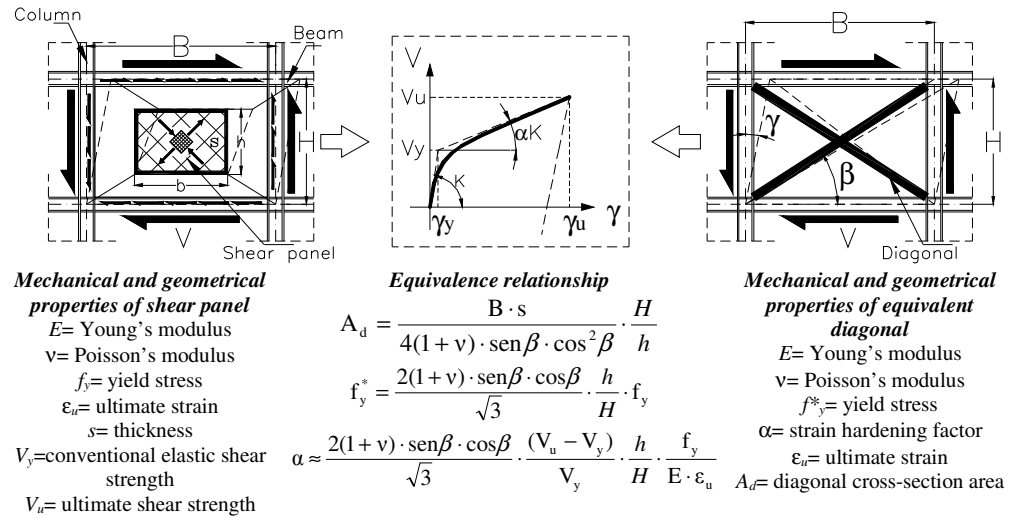


Figure 2.13: Equivalence between shear compact shear panel and X-bracing model

Generally, owing to their large lateral flexibility, bare frames designed according to strength, and therefore with reference to the ultimate limit state only, are not able to meet also serviceability limit state requirements prescribed by current structural codes. Hence, shear panels may be profitable used also as upgrading system, which provides the complementary rigidity to the frame to fulfil minimum stiffness requirements. In this way, the whole structure has to be intended as a composite (dual) system, where the primary structure exhibits elastic deformations only under moderate earthquakes, while it becomes a useful supplementary energy dissipation system for medium and high intensity earthquakes, developing plastic hinges in beams and columns.

On the other hand, shear panels have to be intended as the main energy dissipative system, supplying also additional lateral stiffness and strength to the whole structure (Figure 2.14). Design criteria for a dual system have to be applied aiming at optimising the structural performance of the whole structure to allow the achievements of predefined performance targets keeping the minimum fabrication costs. The main variables are stiffness and strength ratios between the primary structure and the complementary one, which should be determined following a sort of trial and error procedure.

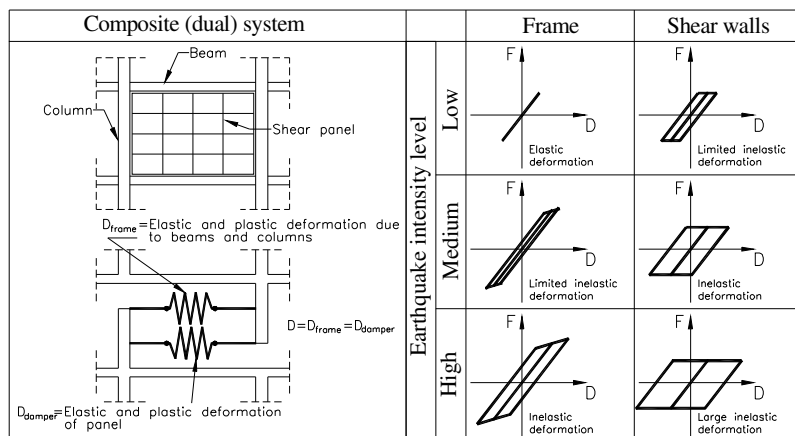


Figure 2.14: Schematized modeling for frame-shear wall combined systems

2.3.4 Experimental research activities

During 70's, stiffened steel shear walls were used in Japan in new constructions and in U.S.A. for seismic retrofit of the existing buildings as well as in new buildings. In the recent years, "low-yield point (LYP)" steel plates and pure aluminium shear panels, which have been mainly developed in Japan and Italy, respectively, have been successfully used as base elements to realise metal plate shear walls. Such devices belong to the so-called compact shear panels category, whose goal is to prevent buckling of the steel plate prior to its shear yielding. A large investigation on the main research activities developed for compact shear panels is provided hereafter.

As a pionieristic intervention, Nakashima et al. (1994) tested and interpreted the cyclic behaviour of steel shear wall panels made of "low yield"

steel. The stress-strain curve of such a steel, developed by Nippon Steel in Japan and designated by BT-LYP 100, is reported in Figure 2.15 a, where the comparison with the mechanical features of both SS400 steel (equivalent to A36 one) and SM490 steel (equivalent to A572, Grade 50 one) is also depicted. In particular, the used low yield steel had the same Young modulus as conventional mild steels, a yield stress about 1/3 of that of ASTM A36 and an ultimate strain 1.5-2 times larger than the A36 one. These properties gave relatively early yielding of this type of steel and sustained energy dissipation capability. Experimental cyclic tests performed on low-yield steel have provided very stable hysteresic loops and relatively large dissipative capacity, as result from Figure 2.15 b.

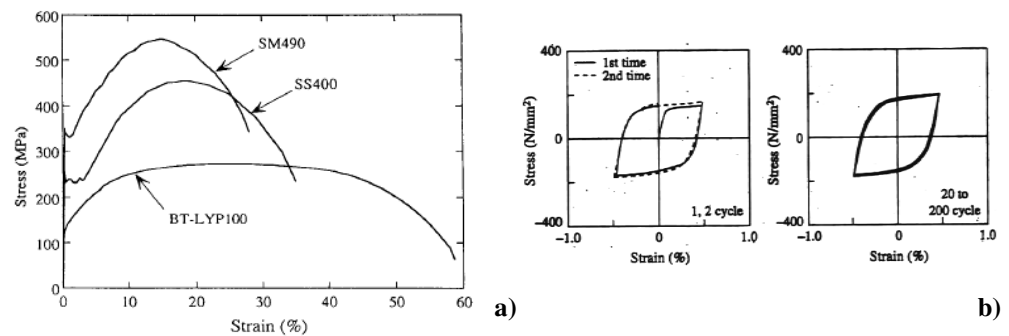


Figure 2.15: Comparison of stress-strain curves between low-yield steel and mild steel (a) and hysteresic behaviour of low-yield steel (b)

Experimental tests were performed on a prototype building equipped with hysteretic dampers made of the mentioned low-yield steel, as illustrated in Figure 2.16 a. The shear panel specimen consisted of a 6 mm thick plate enclosed within upper and lower blocks represented by flanges, made of SM490 steel, which were designed to be both stiff and strong in order to guarantee the complete development of plasticization into the panel only. At this aim, the panel was stiffened with 6 mm thick and 90 mm wide ribs, made of SM490 steel, which were fillet-welded all around to the shear panel and flanges. In particular, two horizontal and two vertical stiffeners, located on each panel side at 1/3 and 2/3 of its height and, therefore, able to subdivide the plate into nine parts, were adopted. In order to evaluate the stiffeners influence on the panel response, two other types of shear panel specimens were

designed and tested. The first was the same of the previously illustrated one, except that the horizontal stiffeners were omitted, while the other was unstiffened. Six specimens were fabricated for the test: three having stiffeners on both panel sides (called standard type), two with vertical stiffeners only and one without stiffeners (Figure 2.16 b).

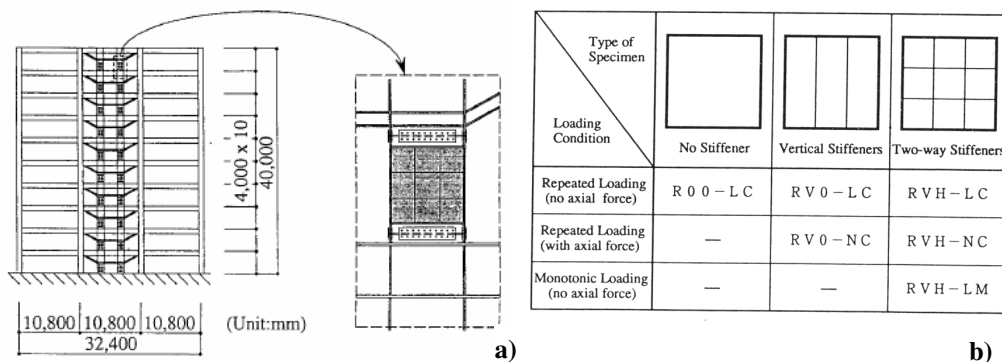


Figure 2.16: Nakashima et al.'s experimental activity (1994): prototype building including low-yield steel shear panels (a) and types of tested specimens together with applied loading conditions (b)

In the experimental activity the loading set-up shown in Figure 2.17 a was used. The specimen was securely clamped to the girders of the retaining structure by means of high tension bolts. Displacements were applied to the top of the specimen by using a horizontally placed jack and the presence of axial loads was also taken into account in some tests. One standard type specimen was loaded monotonically, while the other ones were subjected to cyclic loads according to the history shown in Figure 2.17 b, where on the y-axis the horizontal displacements of the panel top over the yielding one are reported.

The test results showed that yielding interested the entire plate in a pure-shear condition, giving a large energy dissipation capacity, as shown in Figure 2.18, where the behaviour of the unstiffened panel under monotonic load and the hysteretic loops of the tested devices are reported.

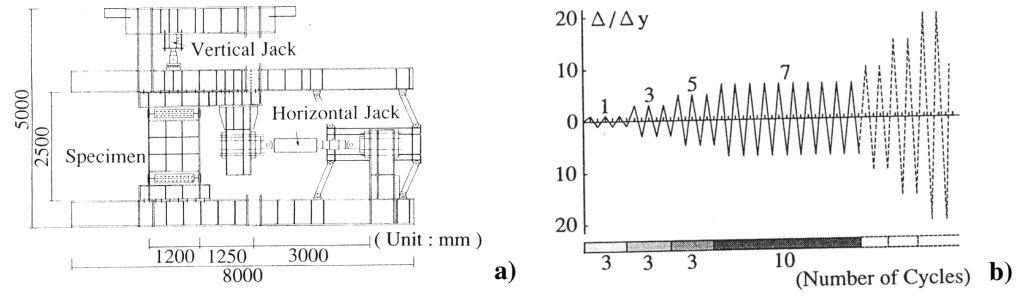


Figure 2.17: Nakashima et al.'s experimental activity (1994): test equipment(a) and cyclic loading history (b)

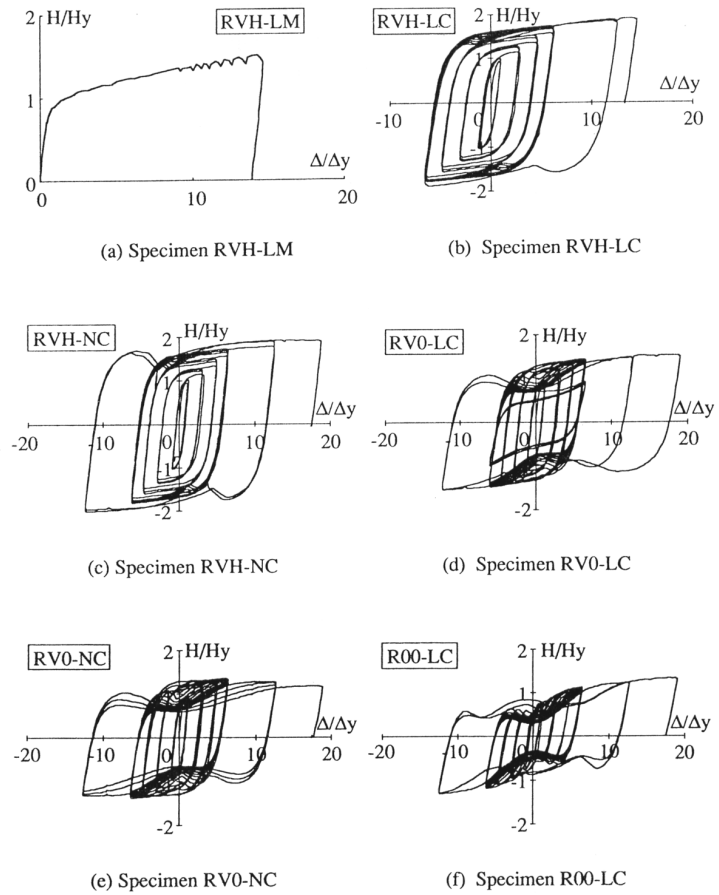


Figure 2.18: Nakashima et al.'s experimental activity (1994): response of tested shear panels

In the whole, the following conclusions were drawn:

- shear panels made of low-yield steel and stiffened with horizontal and vertical ribs exhibited a very stable hysteretic behaviour with the better energy dissipation capacity;
- degradation in strength, stiffness and energy dissipation was exacerbated by the growth of out-of-plane deformations of the plate after buckling;
- strain-hardening under load reversals was very conspicuous.

In particular, the quantification of the significant strain-hardening behaviour associated with the low-yield steel under shear conditions, which represents a paramount importance aspect in estimating the energy dissipated by such devices, has been treated in (Nakashima, 1995).

In this work, three shear panel specimens, having thickness of 6, 9 and 12 mm and made of BT-LYP 100 steel, were confined by four flanges realised with SM490 steel (Figure 2.19 a). Experimental tensile tests carried out on coupons extracted from low-yield steel (LYS) shear panels provided the results illustrated in Figure 2.19 b and summarised in Table 2.1.

The loading set-up used in the experimental tests, in which the jack position was adjusted so that the loading centreline coincided with the mid-height of the specimen, is shown in Figure 2.20 a.

For each type of specimen, both one monotonic and one cyclic test were performed. In particular, the cyclic tests were characterised by the history depicted in Figure 2.20 b, where the ordinate indicates the horizontal displacement applied to the panel divided by its net height. Two cycles were applied to the panel for each drift angle selected starting from 1/441 to 1/17.

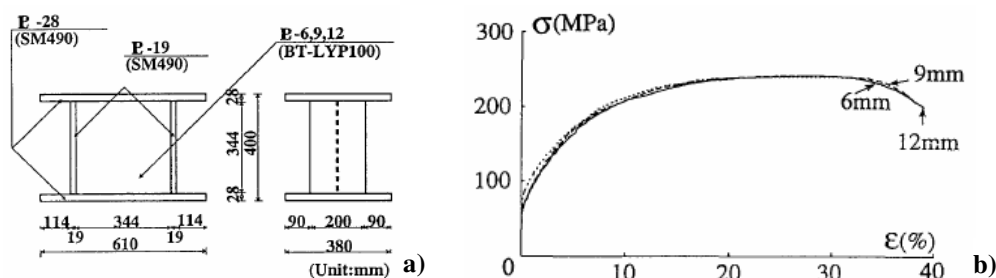


Figure 2.19: Nakashima's experimental activity (1995): geometrical dimensions of tested panels (a) and stress-strain curves of LYSs used in the test (b)

Table 2.1: Material properties of specimens tested in the Nakashima's experimental investigation (1995)

Material (1)	Nominal thickness of shear panel (mm) (2)	Yield stress (MPa) (3)	Maximum stress (MPa) (4)	Rupture strain (%) (5)	Young's modulus (GPa) (6)
BT-LYP100	6.0	98.8 ^a	235.0	53	198
BT-LYP100	9.0	88.2 ^a	237.1	56	201
BT-LYP100	12.0	85.8 ^a	236.2	52	204
SM490	19.0	347.0	529.0	27	207

^a0.2% offset yield stress.

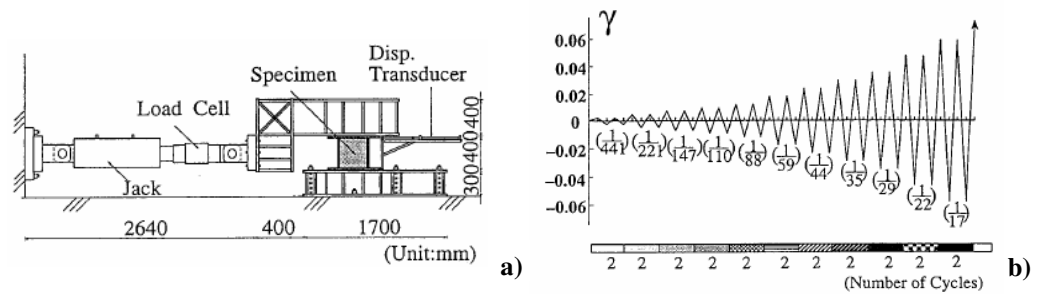


Figure 2.20: Nakashima's experimental activity (1995): loading apparatus (a) and loading history (b) used in the test

Figure 2.21 shows the results of experimental monotonic tests performed on tested specimens in the normalised horizontal force (H'/H_y) vs. drift angle plane. In such tests it was noted that normalised yielding force was larger for panels with smaller thickness. After yielding, the horizontal force increased progressively, reaching values more than three times greater than the initial yielding ones at the drift angle of 0.05.

Figure 2.22 illustrates H'/H_y vs. γ relationships obtained from cyclic loading tests. For all tested specimens, initial yielding occurred at the same force level detected in the monotonic tests. Strain-hardening was significant both in the cycles with the same drift angle and in those with increasing shear strain levels. The degree of strain-hardening was demonstrated by comparing the experimental hysteretic loops with the ones obtained from a test performed on a conventional mild steel shear panel. Besides, it was verified that the energy dissipated by tested shear panels was larger (1.65 and 1.95 times after

cycles with drift angles of 0.011 and 0.059, respectively) than the ones provided by an equivalent linearly elastic and perfectly plastic model.

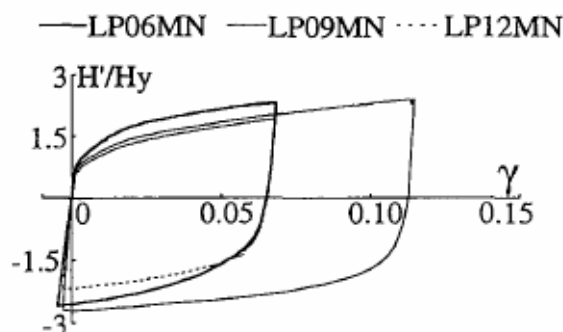


Figure 2.21: Nakashima's experimental activity (1995): results of monotonic tests

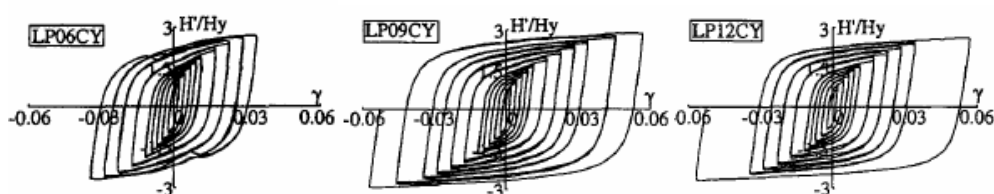


Figure 2.22: Nakashima's experimental activity (1995): results of cyclic tests

The hysteretic behaviour of specimens was well simulated by a multisurface model based on the choice of appropriate parameters. As an alternative, hysteresis models, which can be easily incorporated into earthquake response analysis of structures, were proposed due to the possibility to more simply simulate the LYS shear panels behaviour (Nakashima et al., 1995).

Nakagawa et al. (1996) experimentally investigated the hysteretic behaviour of low-yield strength (LYS) steel plate shear walls by means of two tests performed on both a single wall and a three-storey steel frame equipped with shear panels. The material used for steel panels, which was close to the pure iron chemical composition due to the very small amount of both carbon and alloying elements, presented the stress-strain curve reported in Figure 2.23 a, where the comparison with the mechanical features of the conventional

mild steel JIS SN400 is carried out. From the comparison it is apparent that LYS steel, which has no clear-cut yield shelf, is characterised by a yield strength about 1/3 of the SN400 one, a low yield ratio and an excellent ductility.

In the first experiment, the specimens were made of 1700x1700 mm LYS steel panels having thickness of 4.5 mm and ribbed with 6 mm steel plates made of JIS SN400 steel. Each specimen was inserted within a high-stiffness loading frame, having pin joints at its four corners, by means of high-strength bolts (Figure 2.23 b).

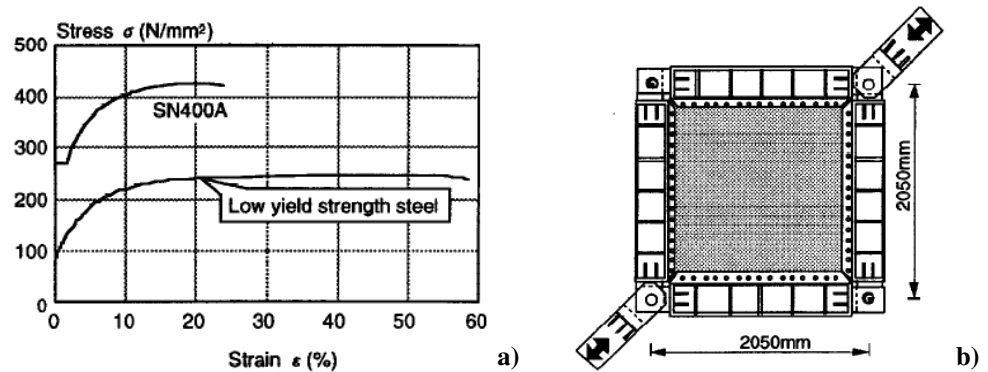


Figure 2.23: Nakagawa *et al.*'s experimental activity (1996): low-yield steel adopted for shear panels (a) and the specimen configuration in the first experiment (b)

The experimental parameters were both the ribs arrangement and their spacing and height: the variation of such factors led to the preparation of five specimens (Figure 2.24), two of them realised according to the configuration reported in Figure 2.24 a. Two different rib arrangements were adopted: on each side of the plate, defining a grid-type scheme (Figure 2.24 a), and located in one direction only on each side, defining a non-grid type scheme (Figure 2.24 b, c, d). In particular, the latter configuration was also used to realise a specimen having the same number of plate portions considered in the panel with the grid-type scheme (Figure 2.24 a).

The hysteretic curves of tested specimens are shown in Figure 2.25 in the average shear stress – shear strain plane. The panels exhibited stable and large hysteretic loops and did not appreciably differ in the cumulative loop area.

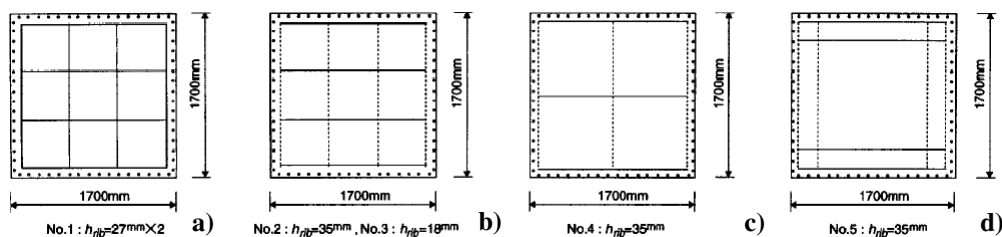


Figure 2.24: Nakagawa et al's experimental activity (1996): shear panel configurations tested in the first experiment

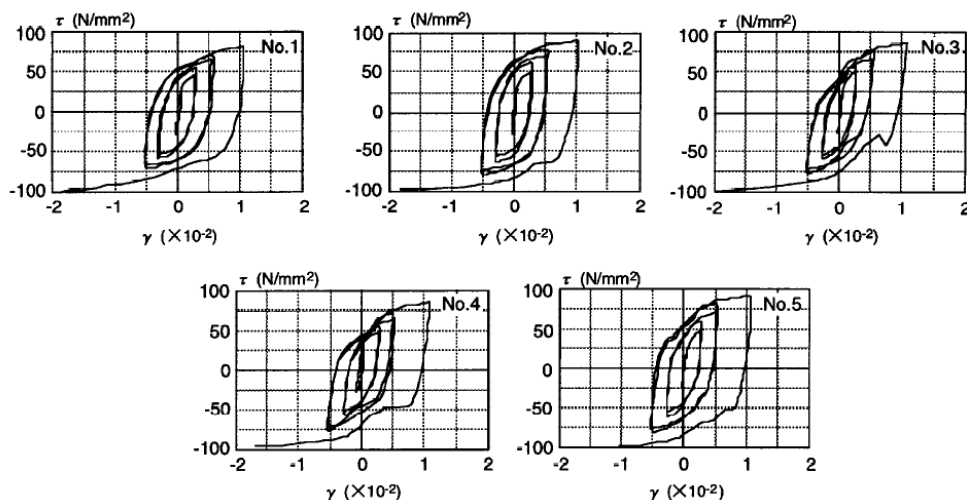


Figure 2.25: Nakagawa et al's experimental activity (1996): hysteretic loops of tested specimens

In the first specimen configuration, stiffened in the two directions on both sides (Figure 2.24 a), the ribs effectively restrained the panel and confined the buckling waves within the single plate portions, while in the non-grid type specimens the out-of-plane deformation of ribs developed, producing the change from a local buckling mode to a global buckling one for large displacements.

The second test was performed aiming at investigating the behaviour of a three-storey steel plate shear wall subjected to both horizontal and highly variable vertical forces (Figure 2.26 a).

The frame members were designed in order to remain in the elastic field under a drift angle of $1/200$; the panels, 4.5 mm thick, were connected to the beams and the columns by means of high-strength steel bolts. According to the results of the first experiment, the LYS steel plates presented a d/t ratio equal to 110 so that their hysteretic loops would not develop the slip-like hysteretic behaviour up to a drift angle of $1/200$.

The ribs, made of SS400 steel and having height of 70 mm in order to ensure the out-of-plane stiffness of the panel, were fillet welded to the plate and arranged following the non-grid type scheme.

The specimen was loaded cyclically according to the history depicted in Figure 2.26 b, where on the ordinate the drift angle of the second storey is reported.

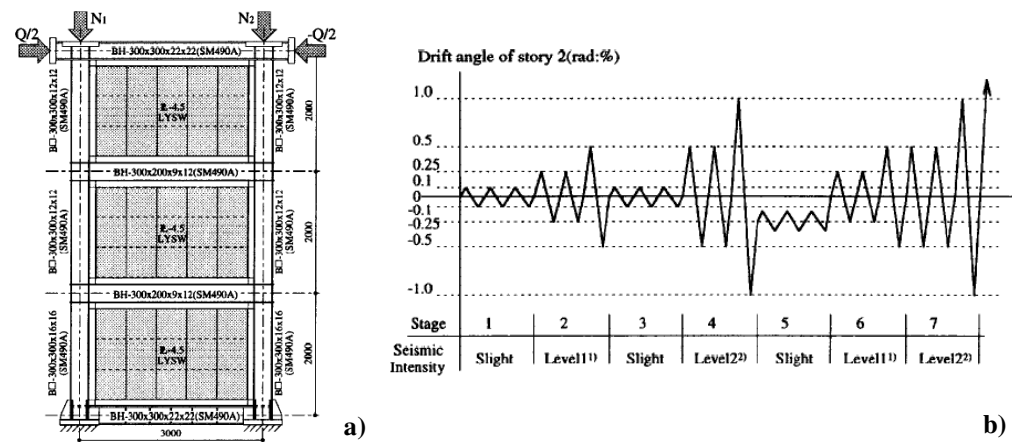


Figure 2.26: Nakagawa *et al.*'s experimental activity (1996): specimen (a) and loading pattern (b) used in the second test

The experimental results, reported in terms of shear load Q – drift angle R for the second storey in the loading stages 1 to 4 and 5 to 7 (Figure 2.27), showed that panels plastically buckled at the drift angle of $1/400$ in the stage 2, even if this effect was not visible in the hysteretic loops. In fact, up to stage 4, the hysteretic curves gradually increase in strength with strain hardening, showing stable spindle-shaped loops. After stage 5 the hysteretic loops did not become completely spindle-shaped under the influence of the large buckling deflection. However the ribs were not deflected out of the panel plane in the final cycle, confirming to have a sufficient stiffness.

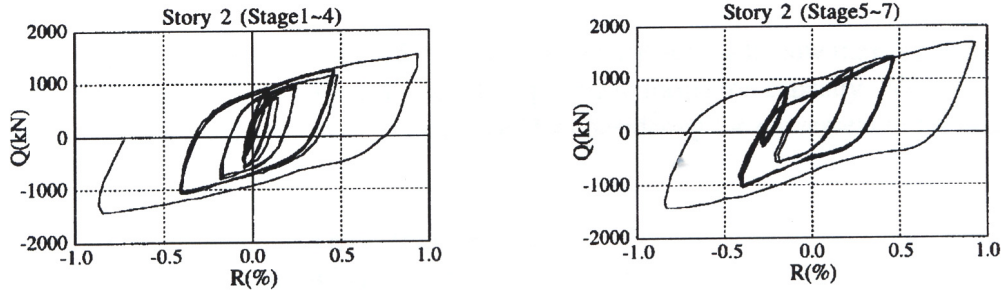


Figure 2.27: Nakagawa et al's experimental activity (1996): hysteretic cycles of the tested second specimen

Finally, it was demonstrated that LYS panels presented a sufficient damping performance when cyclically loaded in a rigid frame subjected to a highly variable vertical load, showing a behaviour similar to that of a single shear panel.

Tanaka and Sasaki (2000) tested cyclically sixteen LYS shear panel specimens, subdivided into four series, in order to achieve both a hysteretic model of such dampers and design estimation formulae for determining their performances. The shear panel configurations, which are shown in Figure 2.28, were inserted into three types of loading apparatus (Figure 2.29). A complete overview of all tested specimens is reported in Table 2.2.

The generic specimen consisted of a LYP-100 steel shear panel enclosed within two frame flanges and two end plates. The shear panels, realised according to two configuration types (square and rectangular shaped), were either unstiffened or reinforced by ribs.

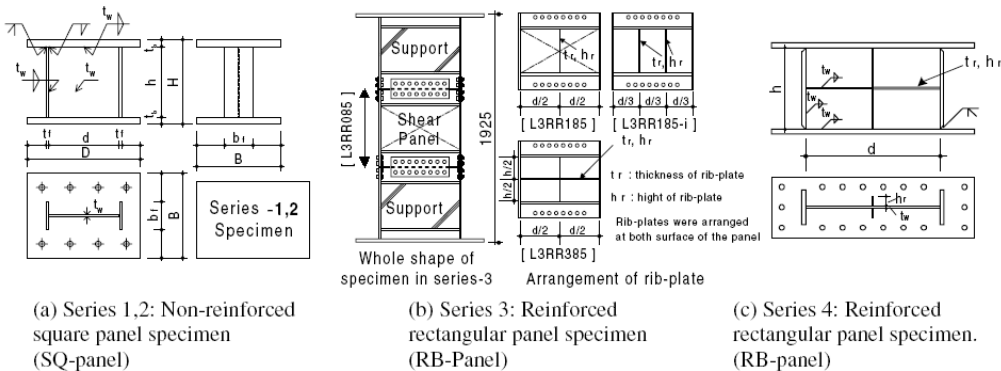


Figure 2.28: Tanaka and Sasaki's experimental activity (2000): the four series of tested specimens

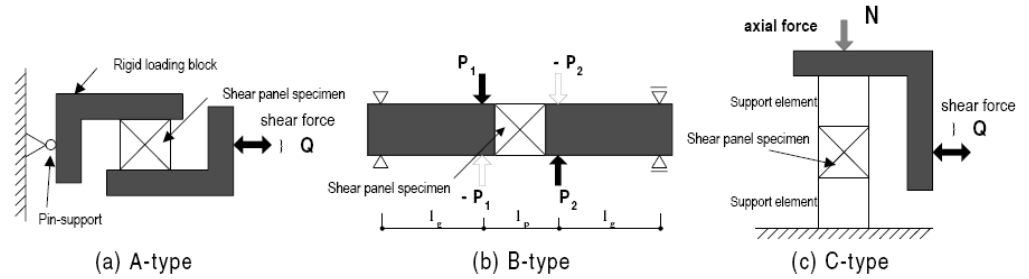


Figure 2.29: Tanaka and Sasaki's experimental activity (2000): the three types of testing apparatus

Table 2.2: List of shear panel specimens tested in the Tanaka and Sasaki's experimental activity (2000)

Test Series	Specimen	Configuration										Property of used steel								Type of loading
		d (mm)	H (mm)	t _w (mm)	b _f (mm)	t _f (mm)	t _r (mm)	h _t (mm)	d/t _w [(d/t _w) _{eq}]	(d/t _w) _B	w _f p (tf/cm ²)	w _f B (tf/cm ²)	Y.R. (elong.)	t _f p (tf/cm ²)	t _f B (tf/cm ²)	Y.R. (elong.)				
1	L1SR020	167	164	8.6	100	8.5			19.3	0.67	0.84	2.49	0.34	39.0	3.59	5.34	0.67	29.8	A	
	L1SR040	249	249	6.0	101	8.8			41.2	1.42	0.84	2.49	0.34	39.0	3.59	5.34	0.67	29.8	A	
	L1SR050	249	248	4.9	100	8.8			50.7	1.74	0.84	2.49	0.34	39.0	3.59	5.34	0.67	29.8	A	
	L1SR060	249	249	4.0	100	8.8			62.2	2.14	0.84	2.49	0.34	39.0	3.59	5.34	0.67	29.8	A	
2	L2SR033	300	300	9.0	101	11.9			33.1	1.16	0.87	2.56	0.34	60.1	3.91	5.34	0.73	42.6	B	
	L2SR050	300	299	6.2	101	12.0			48.0	1.73	0.86	2.74	0.31	56.5	3.91	5.34	0.73	42.6	B	
3	L3RR085	668	384	5.1	175	16.0			[85.8]	2.88	0.77	2.36	0.33	63.5	3.41	5.36	0.64	26.3	C	
	L3RR185	668	384	5.1	175	16.0	6.0	50.0	[63.7]	2.14	0.77	2.36	0.33	63.5	3.41	5.36	0.64	26.3	C	
	L3RR285-1	668	384	5.1	175	16.0	6.0	50.0	[48.3]	1.62	0.77	2.36	0.33	63.5	3.41	5.36	0.64	26.3	C	
	L3RR385	668	384	5.1	175	16.0	6.0	50.0	[43.0]	1.44	0.77	2.36	0.33	63.5	3.41	5.36	0.64	26.3	C	
	L3RR285-2	668	384	5.1	175	16.0	6.0	50.0	[48.3]	1.62	0.77	2.36	0.33	63.5	3.41	5.36	0.64	26.3	C	
	L3RR285-3	668	384	5.1	175	16.0	6.0	50.0	[48.3]	1.62	0.77	2.36	0.33	63.5	3.41	5.36	0.64	26.3	C	
4	L4RR385-1	668	400	6.0	175	16.0	6.0	50.0	[37.2]	1.28	0.84	2.49	0.34	34.7	3.65	5.31	0.69	30.2	B	
	L4RR385-2	668	400	6.0	175	16.0	6.0	50.0	[37.2]	1.28	0.84	2.49	0.34	34.7	3.65	5.31	0.69	30.2	B	
	L4RR385-3	668	400	6.0	175	16.0	6.0	50.0	[37.2]	1.28	0.84	2.49	0.34	34.7	4.06	4.57	0.89	32.0	B	
	L4RR385-4	668	400	6.0	175	16.0	6.0	50.0	[37.2]	1.28	0.84	2.49	0.34	34.7	0.91	2.51	0.36	46.9	B	

Test results showed that fracture occurred in all specimens (Figure 2.30). In particular, in case of square panels with width (d) over thickness (t_w) ratio smaller than 33, crack occurred at their side end, very close to the welding connecting the plate and the flange. On the other hand, for square specimens having width-to-thickness ratio larger than 48, fracture happened at the panel centre caused by cyclic and reversal plate-bending due to buckling of the plate. Contrary, for rectangular panels, crack occurred at the panel centre or at the panel zone where welding connected the ribs, as shown in Figures from 2.30 c to 2.30 g, where the effectiveness of the reinforcing effect produced by stiffeners is visible.

In Figure 2.31 the hysteretic loops provided by square panels having

different width-to-thickness ratios are compared. From the comparison it is apparent that when such a ratio become small (below 40), a more satisfactory dissipative behaviour of the panel occurs. On the other hand, the dissipative performance of rectangular-shaped specimens having three different details of reinforcing rib-plates is illustrated in Figure 2.32.

In conclusion empirical equations were introduced in order to estimate the maximum strength and the allowable deformation of panels, whose hysteretic behaviour was simulated by the Skeleton Shift Model, which was able to well reproduce the test results.

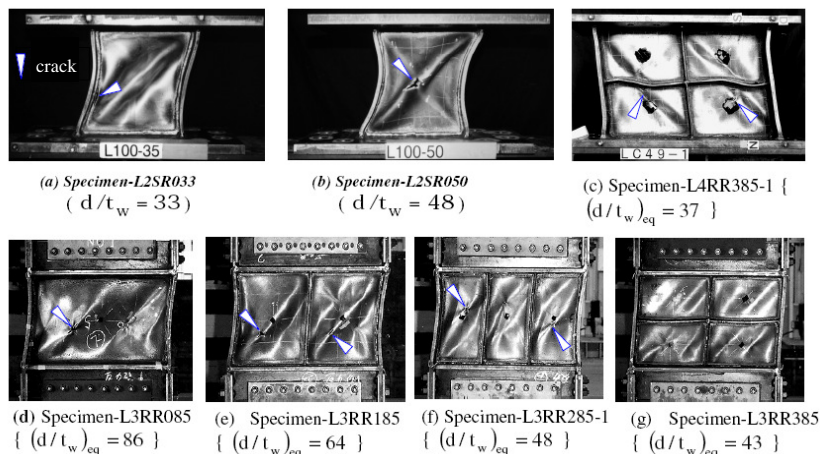


Figure 2.30: Tanaka and Sasaki's experimental activity (2000): typical fracture modes of tested specimens

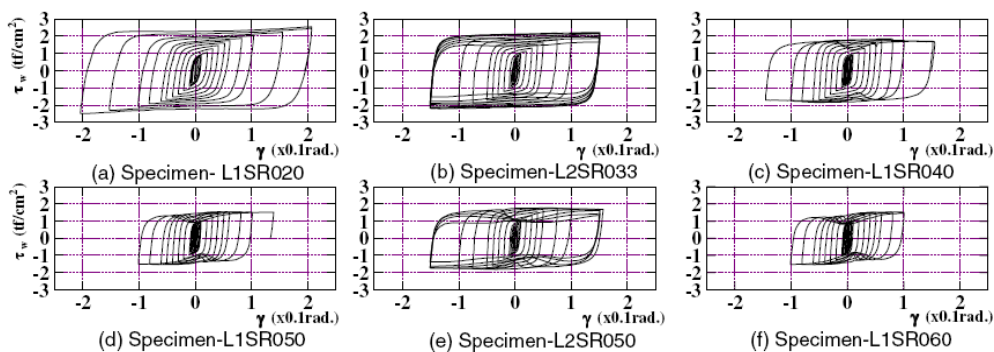


Figure 2.31: Tanaka and Sasaki's experimental activity (2000): hysteretic behaviour of square-shaped panels

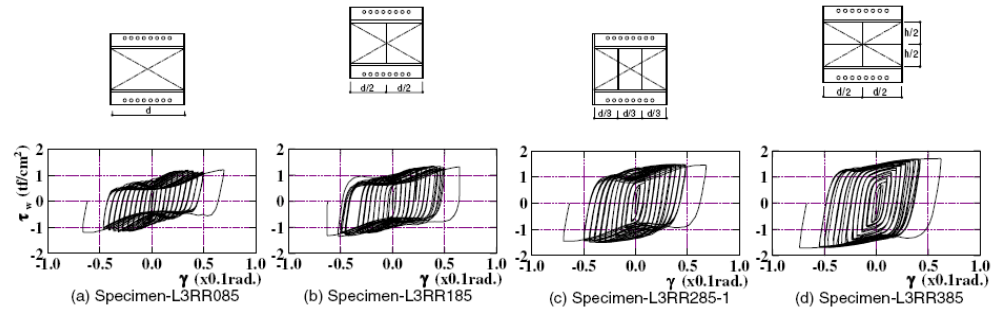


Figure 2.32: Tanaka and Sasaki's experimental activity (2000): hysteretic behaviour of rectangular-shaped panels

Katayama et al. (2000) investigated the behaviour of hysteretic dampers made of low-yield strength steel under dynamic loading.

The specimen under study was realised by using a wide flange roll-formed section, made of SN400B steel, from which firstly a rectangular webbed part (500x560 mm) was cut out. Then, the opening in the rolled section was filled by fillet welding a LYP-100 rectangular plate (520x580x6 mm) (Figure 2.33 a). The loading apparatus used for test is illustrated in Figure 2.33 b, where it is evident that the displacement was applied quasi-statically and dynamically to the top of the specimen by means of a horizontally placed actuator.

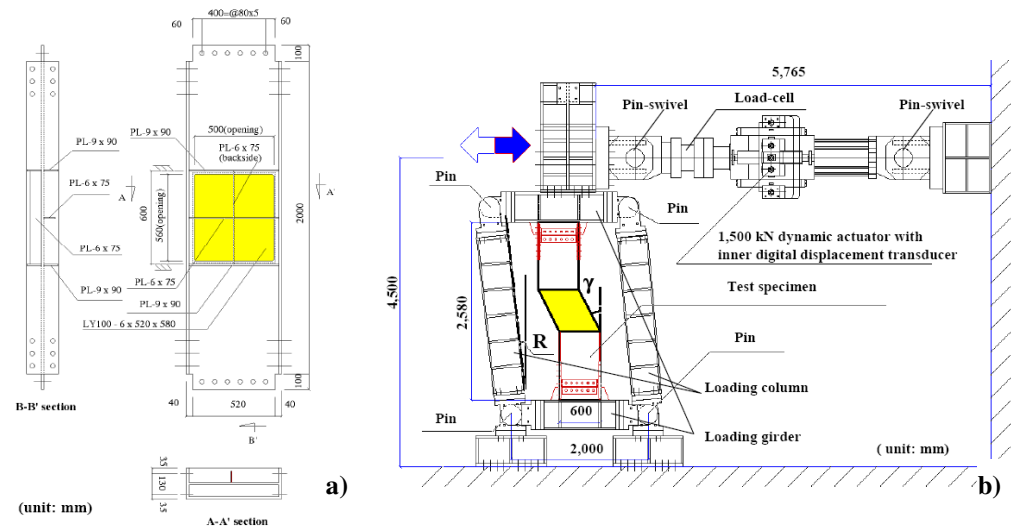


Figure 2.33: Katayama et al.'s experimental activity (2000): the tested specimen (a) and the loading apparatus (b)

Six specimens were prepared and two patterns of loading history were planned (incremental and earthquake responses). In particular, two specimens were loaded cyclically with dynamic (1.0 Hz) and quasi-static (0.5 mm/sec) speeds, according to the history shown in Figure 2.34 a, where the ordinate indicates the drift angle R . The other ones were loaded randomly with dynamic (real time) and quasi-static (0.5 mm/sec) speeds. Two time histories were used, they being represented by the storey drift response of the second story in a 4-storey building against JMA Kobe earthquake and artificial Yokohama ground motion (Figure 2.34 b).

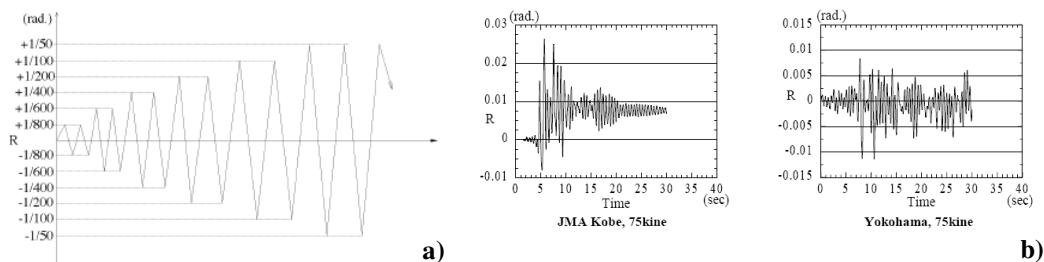


Figure 2.34: Katayama et al.'s experimental activity (2000): incremental loading history (a) and random response of storey drift angles (b)

Figure 2.35 a illustrates the results of the incremental loading tests, showing the difference in terms of hysteretic behaviour between the application of dynamic (solid line) and quasi-static (broken line) loadings. In such tests significant out-of-plane deformation and crack were not observed.

Strain-hardening, which was significant in both specimens, produced the shear stress increase of the shear wall damper. Nevertheless, although such an effect was also caused by strain rate, its contribution was 20% at most and no more 6% even when the drift angle reached its maximum value.

On the other hand, random loading tests showed that the shear stress increase was not so much as that of LYP 100 steel, because shear buckling may contribute to restrain the damper shear stress increment. The final response of the damper in terms of shear stress – shear strain hysteretic curves is reported in Figure 2.35 b, where both the behaviour under dynamic (solid line) and quasi-static (broken line) loading are plotted.

From these results it was evident that the damper could resist large earthquakes several times. Besides, the total energy dissipation capacity of

dampers under dynamic loading was larger than the static loading one, due to the fact that shear resistance under dynamic loading increased by the effect of strain rate.

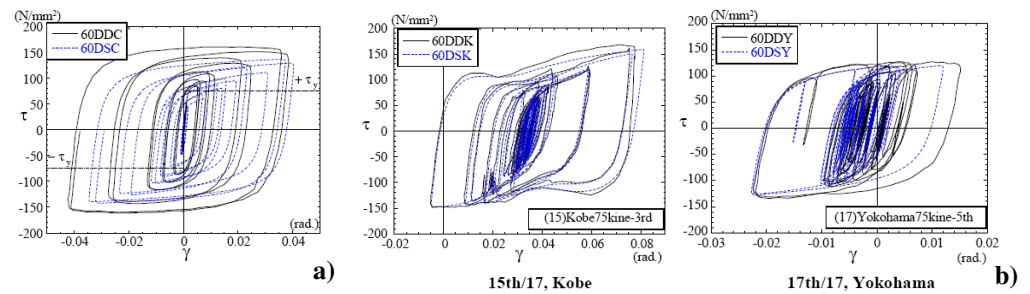


Figure 2.35: Katayama *et al.*'s experimental activity (2000): results of incremental (a) and random (b) loading tests

Vian and Bruneau (2004) tested four single bay, single storey steel plate shear walls made of LYS. The surrounding frame, composed by steel members realised with steel having yield stress of 345MPa, measured 4000x2000 mm and presented a reduced beam section (RBS) at each beam-to-column connection (Figure 2.36 a). The infill panels, 2.6 mm thick, were made of LYS steel having yielding and ultimate stress equal to 165 and 300 MPa, respectively.

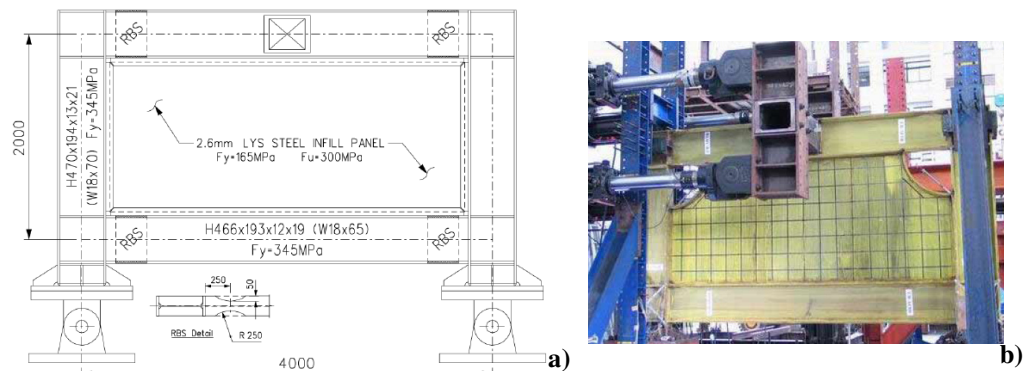


Figure 2.36: Vian and Bruneau's experimental activity (2004): typical specimen dimensions (a) and the panel with the top corners cut-out (b)

Four specimens were prepared for test: two panels were made of solid plates (type S), while the other two presented some perforations, with the presence of either the top corners cut-out and reinforced to transmit forces to the surrounding frame (type CR) (Figure 2.36 b) or twenty 200mm-diameter holes in order to reduce the system strength (type P) (Figure 2.37 a).

All specimens were tested by using a cyclic quasi-static loading protocol similar to the ATC-24 one. The displacement history shown in Figure 2.37 b was applied horizontally to the top beam centre by using four actuators.

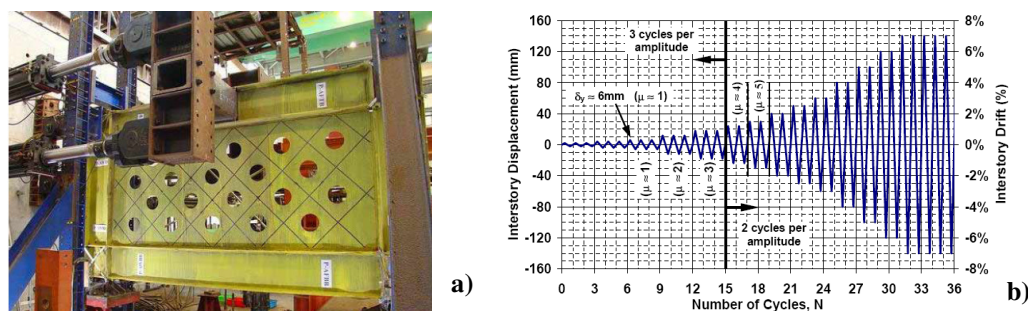


Figure 2.37: Vian and Bruneau's experimental activity (2004): the panel with holes before testing (a) and the applied displacement loading history (b)

In the panel type P, whose hysteretic cycle is reported in Figure 2.38 a, small fractures were found at corners at the test conclusion, occurred when a drift of 3% was reached (Figure 2.38 b). In such a phase a weld failed in the continuity plate at the top of a column and other damages and distortions of the specimen made the test impossible to continue.

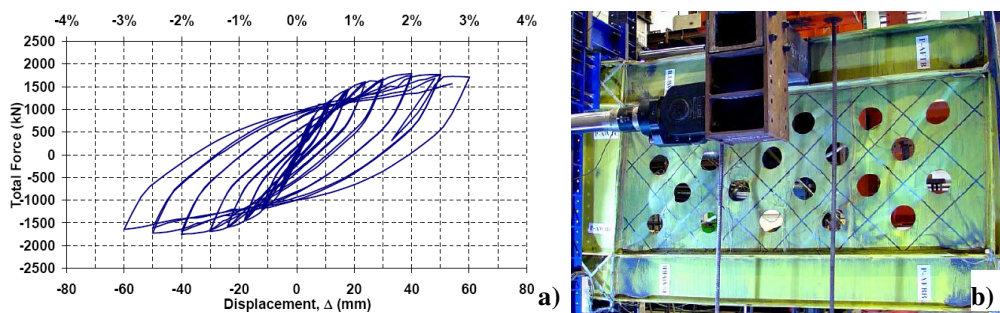


Figure 2.38: Vian and Bruneau's experimental activity (2004): hysteretic cycles (a) and final configuration (b) of the specimen type P

The specimen type CR, whose hysteresis is depicted in Figure 2.39 a, exhibited stable behaviour for relatively limited drift. The loading detail twisted both the top beam and the columns. Web local buckling occurred in the bottom beam RBS connections after a drift of 1.5%, even if the global behaviour was not affected until rupture of the bottom flange of the bottom beam in the reduced beam section connections (drift equal to 2.5%). The yielding phase of both the panel and the bottom beam RBS connection, corresponding to a drift of 1.5%, is shown in Figure 2.39 b.

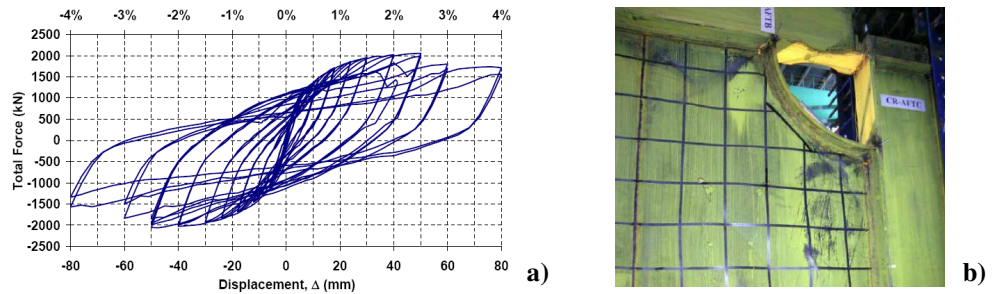


Figure 2.39: Vian and Bruneau's experimental activity (2004): hysteretic cycles (a) and yielding (b) of the specimen type CR

One of the tested solid panel specimen (type S) exhibited a stable hysteretic behaviour (Figure 2.40 a), even if the same problems occurred in the other tests (twisting of columns and damages to the top beam) were visible. The test ended for the same reason already seen for the specimen type CR. In this case, a numerical pushover analysis was developed by means of the SAP program in order to simulate the panel behaviour, giving good results (Figure 2.40 b).

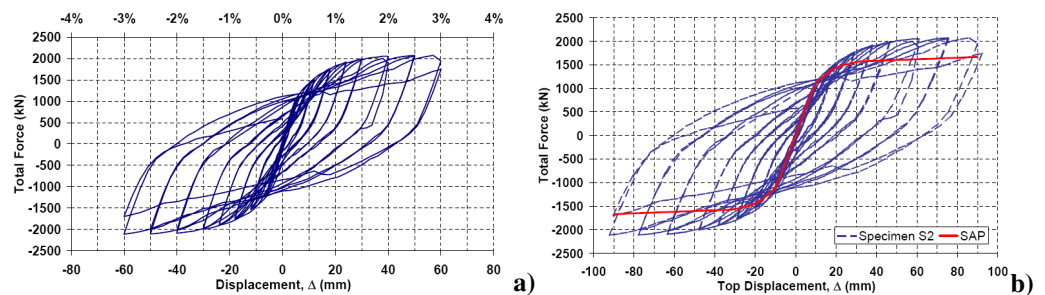


Figure 2.40: Vian and Bruneau's experimental activity (2004): hysteretic cycles (a) and numerical simulation (b) of the specimen type S

However, all specimens were characterised by stable hysteretic cycles with very little pinching until the significant accumulation of damage at large drifts occurred. In addition, the use of RBS details may result in a more economical design for beams anchoring an SPSW system at the top and bottom of a multi-storey frame.

In the framework of the study on compact shear panels, in the recent years the use of plates made of aluminium alloys has been introduced as effective passive control devices for seismic protection of steel structures.

Rai and Wallace (1998) applied aluminium shear-links in order to modify the behaviour of chevron-type ordinary concentric braced frames, where a double-T shaped aluminium beam was comprised between the tops of diagonal braces and the beam from the above floor (Figure 2.41 a). The purpose of the study was to describe the inelastic cyclic behaviour of the shear link, by evaluating the influence of several factors, namely the effects of different aluminium alloys, the arrangement of transverse stiffeners and strain rates on the energy dissipation capacity of such devices. Aluminium was chosen because of its low-yield strength which enabled the use of thicker webs and reduced the web buckling problems.

In the experimental program the shear link, 51.6 mm deep and 152.4 long, was isolated from the proposed bracing configuration and tested in the vertical direction, it being turned through 90° with respect to its original position (Figure 2.41 b).

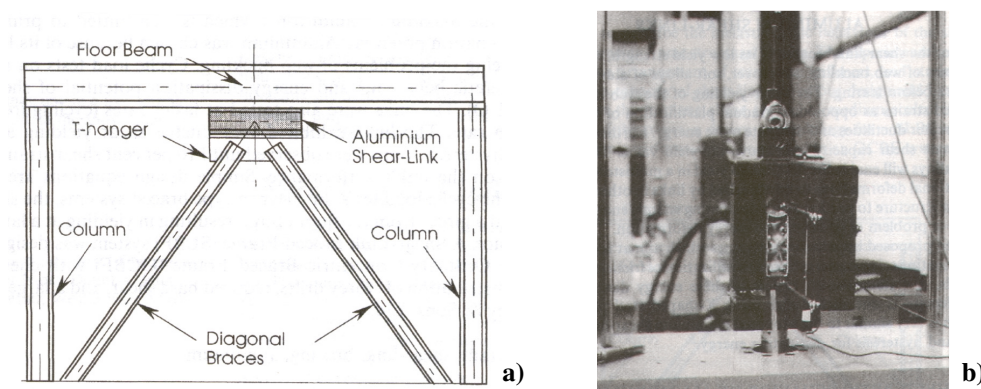


Figure 2.41: Rai and Wallace's experimental activity (1998): the bracing system based on the use of an aluminium alloy shear link (a) and details of the testing apparatus (b)

The load was transferred from the actuator to the specimen through a pair of rigid L-shapes fixtures which moved up and down with the actuator. The specimen was bolted to in-plane vertical legs of the top and bottom fixture. The second vertical length of the top fixture was laterally braced to the vertical leg of the bottom fixture to prevent out-of-plane bending and twisting of the specimen.

Two different specimens were tested, they being differentiated in the dimensions of their flange width only. The increase of the flange width was due to the possibility to use more fasteners in order to avoid the bolt slippage observed in the specimens tested for the material characterization. Two different aluminium alloys (3003 and 6061 – temper O), whose mechanical features are reported in Table 2.3, were used for the web of specimens. Besides, two different arrangements of transverse stiffeners were grove-welded to the link: in the first, ribs were provided at the ends of the link, while in the other two intermediate stiffeners were also added. The typical geometrical dimensions of the tested specimen is illustrated in Figure 2.42.

Table 2.3: Properties of aluminium alloys used in the Rai and Wallace's investigation (1998)

Aluminium alloys (1)	0.2% yield stress (MPa) (2)	Tensile strength (MPa) (3)	Ultimate strain (mm/mm) (4)	Young's modulus (GPa) (5)
3003-O	35.2	109.2	0.2396	62
6061-O	52.8	126.3	0.2961	69

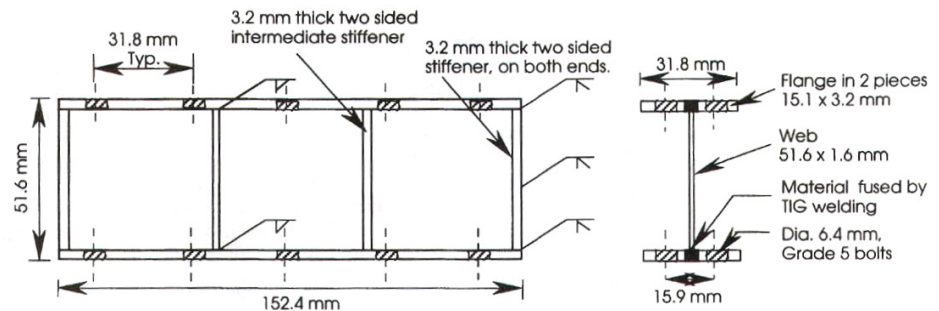


Figure 2.42: Rai and Wallace's experimental activity (1998): geometrical details of a typical tested specimen

Specimens were subjected to sinusoidal input waves: for quasi-static tests, a typical loading program began with three cycles at 8.3 MPa, then followed by three cycles at 20.7 MPa, which was near the expected yield stress of the web material. Besides, in order to understand the effect of different strain rates on the shear link behaviour, specimens were tested at three cycling frequencies (5, 10 and 17 Hz).

A typical shear stress – strain hysteretic behaviour of a shear link with only end stiffeners is shown in Figure 2.43 a. Such a device exhibited very ductile shear yielding and excellent energy dissipation capacity. The first yielding of the web occurred at the first cycle and this process, characterised by stable loops, continued up to a strain equal to 0.1. Then, for a strain of 0.2, a quick degradation of strength was observed but, despite the visibly distressed end stiffeners, the specimen retained good capacity. After this phase, for each load reversals, some loss of stiffness was observed due to bolt slippage at the specimen-loading fixture connection. The yielded and buckled unstiffened specimen at the end of the test is illustrated in Figure 2.43 b.

In the experimental activity the specimen with intermediate stiffeners showed the same inelastic response of the unstiffened one. This was due to the fact that the intermediate ribs, which were not welded to the link, were not effective in controlling the plastic web buckling, they allowing the passage of buckling waves among sub-panels (Figure 2.43 c).

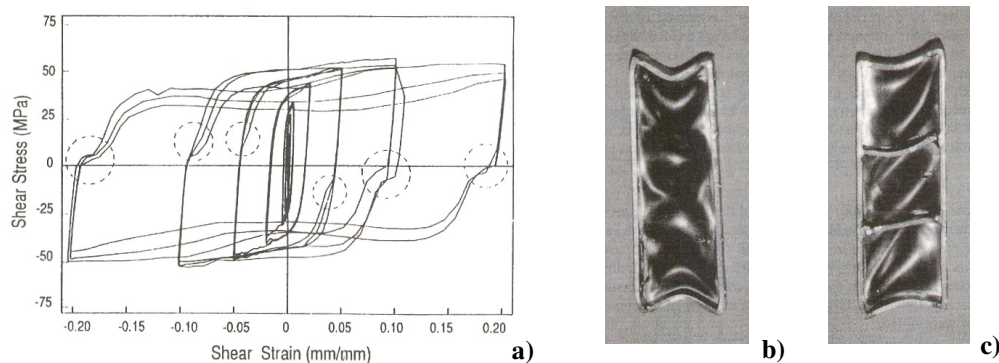


Figure 2.43: Rai and Wallace's experimental activity (1998): typical hysteretic behaviour of the unstiffened shear link (a) and deformed shape of unstiffened (b) and stiffened (c) specimens at the end of the tests

In the whole, unpinched and fully hysteretic loops were observed until 10% of shear strain for all tested specimens and a relatively small influence of strain rates was observed on the link performance. Finally, simple equations, based on data achieved from the cyclic loading tests, were developed aiming at designing the analysed shear links.

Foti and Zambrano (2004) proposed a shear panel made of both aluminium alloy and steel for preserving the structural integrity of civil structures subjected to seismic loads. The device was realised by inserting a 2 mm thick AW-8006 aluminium alloy plate within two 6.5 mm thick steel plates, which presented some openings and offered a lateral stiffness to the panel (Figure 2.44 a).

On the basis of previous experimental quasi-static tests (Foti and Diaferio, 1999), two different kinds of panels were used, they being differentiated for the type of connection among plates only. In the first solution, the mentioned three plates were connected by means of epoxy resin and steel bolts, while in the second one the plates brazing was used as a connection element.

The two types of devices were mounted on a frame connected to a 5.6 x 4.6 m shaking table having three degrees of freedom (two horizontal and one vertical). The frame used for tests, which was made of four HEA100 columns and HEA280 beams, presented a V-bracing system, consisting of HEB100 diagonals, connected to the upper nodes of the frame and the top of the panel by means of M10 bolts. The frame was also stiffened with two diagonals in order to avoid torsional oscillations. A mass of 8500 Kg was added to the top of the frame in order to simulate the vertical loads which acted on the real structure.

A global view of the specimen inserted in the frame for shaking table tests, which were performed at the Laboratório Nacional de Engenharia Civil (LNEC) in Lisbon, is reported in Figure 2.44b.

The earthquake used in the test was the Aigio (E-W component) earthquake scaled by a factor of two, whose spectrum is characterised by a maximum peak ground acceleration of 0.54 g and a duration of 6 sec. The tests, which were performed at increasing level of PGA, demonstrated that both types of aluminium panels (brazed and bolted) offered large dissipation capacity, without losing their initial stiffness. It was also noticed that hysteretic cycles of bolted and brazed panels were similar in shape and in size

In conclusion it was found that the tested frame was able to withstand even catastrophic events without damages, they being exclusively concentrated in the panel, which could be easily replaced without causing the interruption of the building activities. In addition, the comparison of the experimental results showed that the brazed panels behaviour was not completely satisfactory for the lower plasticization capacity and the delamination danger that showed up in the most severe test conditions. Finally, the test results showed the importance to perform the detailed design of such devices in order to avoid buckling phenomena, to transfer properly the shear force among the plates and to make possible their plasticization at low level of the input seismic intensity. For these reasons the choice of the stiffeners, the type of connection among the plates and the plate thickness can be considered as crucial points of a correct design procedure for the design of compact metal shear panels.

In the framework of the investigation on the energy dissipation capacity of aluminium stiffened shear panels, the results of six shear cyclic experimental tests carried out at the Department of Structural Analysis and Design of the University of Naples “Federico II” are noteworthy (De Matteis et al., 2005c; 2006b).

The choice of aluminium is really innovative in the field of seismic engineering and it was justified by both low yield strength and high ductility, which could be further improved through proper heat treatment.

Tested shear panel specimens had in-plane dimensions 1500x1000 mm and a thickness of 5 mm and were made of two different alloys, namely AW1050A and AW5154A, whose stress-strain curves, before and after heat treatment, are reported in Figures 2.46 a, b, respectively.

The former is characterised by a high degree of purity and was chosen for its very low yield strength (about 20 MPa after heat treatment), higher hardening and larger ductility. Instead, the latter is more easily available on the market and was considered for a useful comparison.

The panels were ribbed by means of either welded stiffeners, connected to the plate by means of the spot-welding technique in order to reduce the sheeting shape distortion produced by shrinkage, or bolted steel channel section stiffeners.

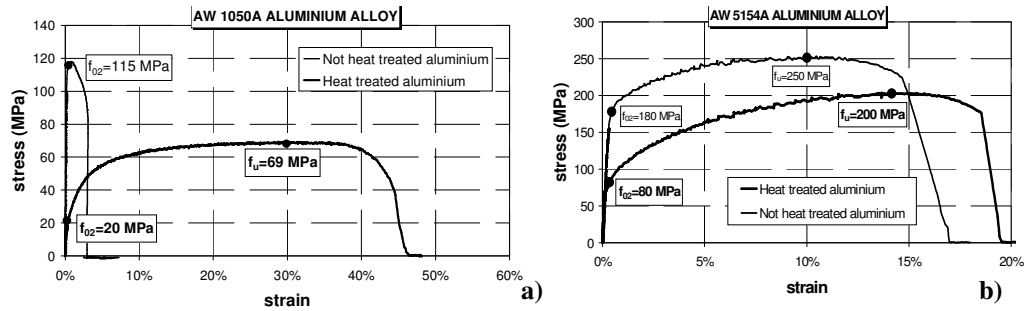
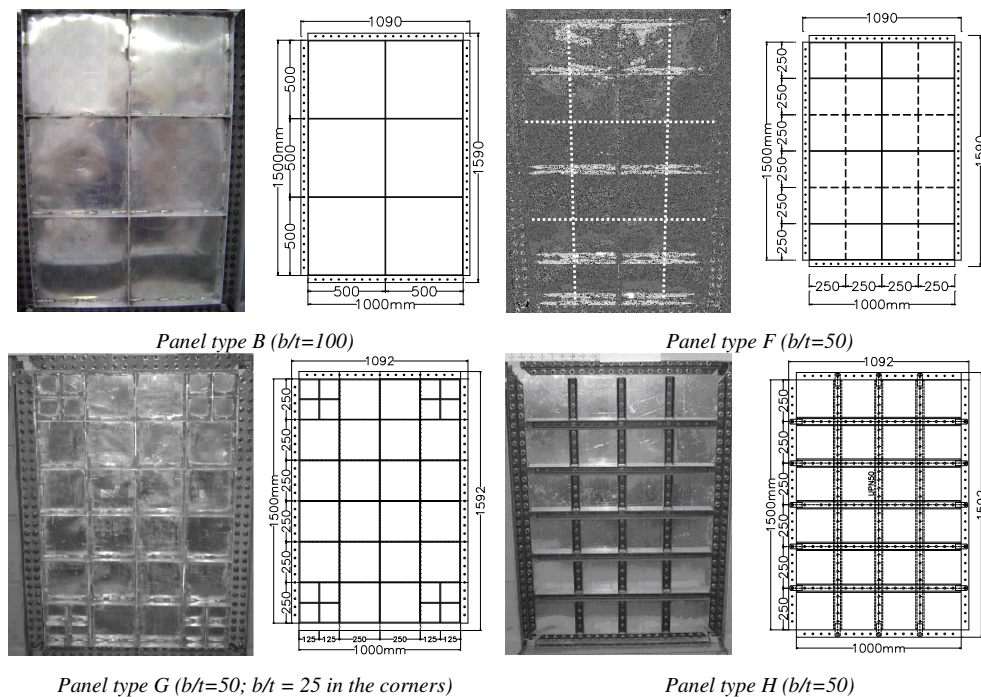


Figure 2.46: De Matteis et al.'s experimental activity (2005c, 2006b): results of tensile tests before and after heat treatment on the AW1050A (a) and the AW5154A (b) aluminium alloys adopted for shear panels realisation

In the experimental program, four different types of panel configurations were considered, presenting different geometry of the applied ribs (Figure 2.47).



Panel type G (b/t=50; b/t=25 in the corners)

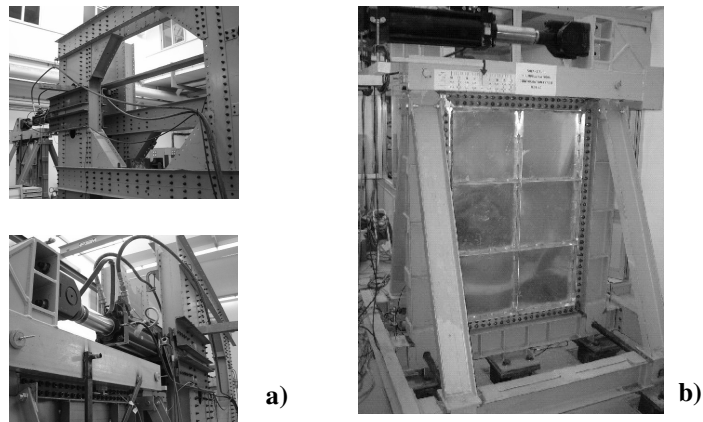
Panel type H (b/t=50)

Figure 2.47: De Matteis et al.'s experimental activity (2005c, 2006b): geometrical configuration of tested aluminium alloys shear panels

For panel type B, the ribs were placed on both sides of the plate according to square fields 500 mm of side length. Contrary, panel configuration type F was stiffened with ribs alternatively placed on the two sides of the plate in order to obtain square fields 250 mm of side length and to balance the out-of-plane deflection induced by welding process. Panels with configuration type G and H were successively designed in order to overcome some drawbacks pointed out in the first four cyclic tests carried out on panels type B and F.

Panel type G, having a $b/t=50$, presented a slenderness ratio which was reduced to $b/t=25$ in the corners in order to delay the local buckling of the panel. In addition, the ribs were applied on both sides of the plate rather than alternatively as for panel type F. Panel type H had a configuration similar to the panel type F one, but it was ribbed by means of steel channels (UPN50). This choice came from the necessity to eliminate the geometrical and mechanical imperfections induced by the welding process of stiffeners. Panels type B and type F were fabricated considering both AW 1050A and AW 5154A aluminium alloy, while the latter two specimens were made of AW 1050A aluminium alloy only. Therefore, in total six different shear panels specimens were considered and tested.

The shear load on the panels was applied by means of a servo-hydraulic actuator (Figure 2.48 a) which was connected to the top beam of an articulated steel frame composed by very rigid members and equipped with lateral out-of-plane braces (Figure 2.48 b).



*Figure 2.48: De Matteis et al.'s experimental activity (2005c, 2006b):
the adopted testing apparatus*

Test specimens were connected to the loading steel frame by steel cover plates with friction high-strength grade 8.8 steel bolts, having a diameter of 14 mm and a pitch of 50 mm.

The main results of the experimental tests were represented in terms of the average shear stress τ applied on the horizontal panel side and the equivalent shear strain γ , which comprised only the part related to the panel shear deformation, since the slips occurring in the panel connections, as well as the displacements of the reaction frame, were deducted from the global applied displacement.

The obtained hysteretic curves for panels type B and type F made of AW 1050A aluminium alloy, together with the applied displacement histories, are shown in Figures 2.49 and 2.50, respectively. In the same figure, some pictures illustrating the main collapse phase of tested specimens are also provided.

The global cyclic response of the tested panels was rather dissipative, even though, in the initial part of the loading process, the behaviour was conditioned by some slipping phenomena due to initial imperfections and local buckling of some lower plate portions due to normal stresses equilibrating the flexural moment on the base of the plate.

Such a loading condition produced a significant “pinching” effect on the shape of the shear stress – shear strain curve. Nevertheless, due to the stable post-buckling behaviour, a significant increase of the global stiffness and dissipative capacity of systems was evident, especially for panel type F, when the applied shear strain increased. Then, due to rib buckling, the shear stress – shear strain diagram showed a sort of “double bulge” effect.

Finally, a noticeable strength degradation occurred for large displacements and global buckling phenomena developed up to the complete collapse of the systems, which was due in both cases to failure of surrounding connections.

The shear loading tests above illustrated were carried out also on the panels type B and type F made of AW 5154A aluminium alloy. In this case, due to both higher material strength and reduced load capacity of the adopted actuator in tension, the applied deformation histories on the panels were not symmetric.

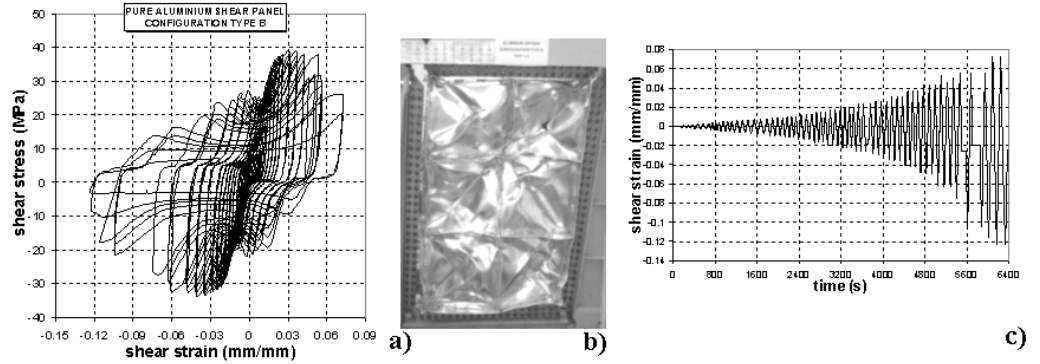


Figure 2.49: De Matteis et al.'s experimental activity (2005c, 2006b): hysteretic loops (a), final deformed shape (b) and applied shear deformation history (c) of AW 1050A panel type B

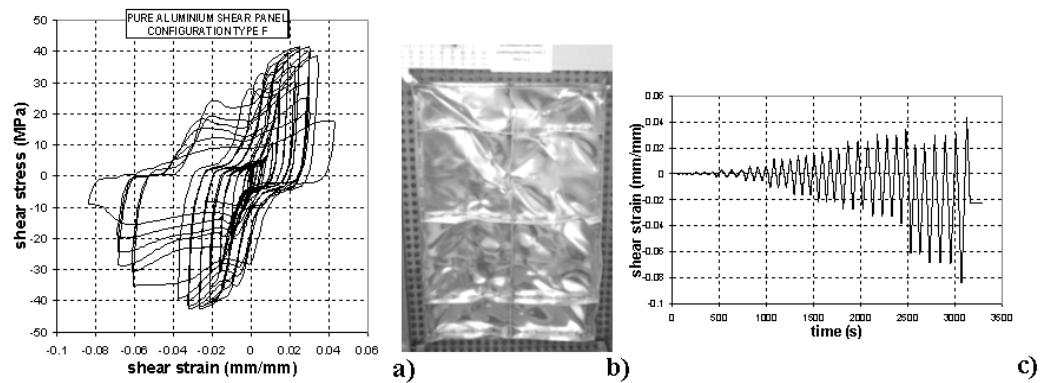


Figure 2.50: De Matteis et al.'s experimental activity (2005c, 2006b): hysteretic loops (a), final deformed shape (b) and applied shear deformation history (c) of AW 1050A panel type F

The obtained results, reported in terms of shear stress-equivalent shear strain curves, are provided in Figures 2.51 a and b for panels type B and type F, respectively. They clearly evidenced a slip-type hysteretic response, with a reduced dissipative capacity in comparison to AW 1050A alloy shear panels. This was due to larger material strength, which means higher plate mechanical slenderness.

For panel type G, thanks to the fact that ribs were placed in the same position on both sides of the plate, the measured initial out-of-plane

displacements were very limited. The strengthening of the four corners favoured the development of shear buckling phenomena on the entire surface of the panel, with buckle waves always enclosed within the plate portions framed by ribs (Figure 2.52). After the attainment of the maximum panel strength, a quick degradation of resistance begun owing to both local tearing of material and premature collapse of perimeter connections. Nevertheless, even if the failure of surrounding connections did not allow the exploitation of the whole plastic resources of base material, it has to be observed that the obtained cyclic performance was significantly improved with respect to the previous specimens.

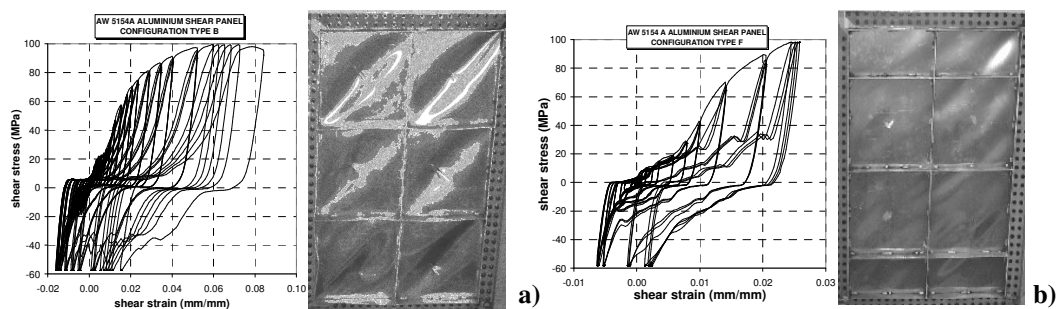


Figure 2.51: De Matteis et al.'s experimental activity (2005c, 2006b): hysteretic loops and final deformed shape of panel type B (a) and type F (b) made of AW 5154A aluminium alloy

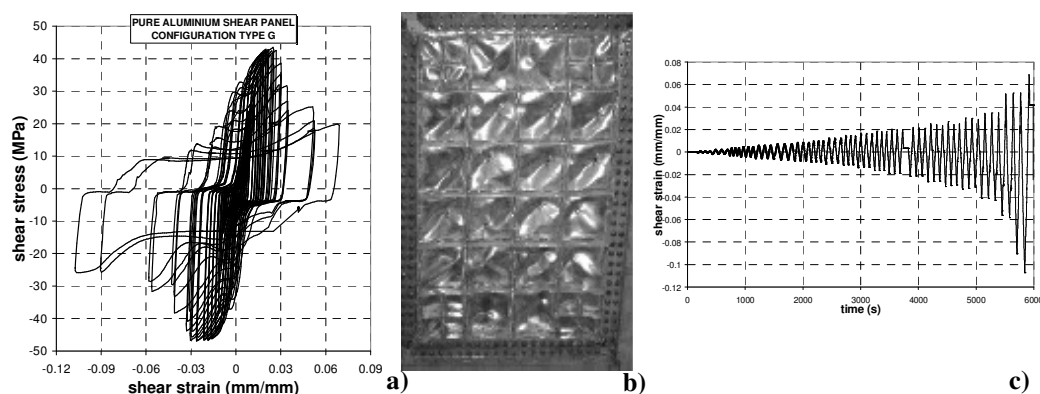


Figure 2.52: De Matteis et al.'s experimental activity (2005c, 2006b): hysteretic loops (a), final deformed shape (b) and applied shear deformation history (c) of AW 1050A panel type G

Thanks to the particular type of the adopted stiffening system, panel type H exhibited a ductility much higher than the previous tested specimens, with more regular hysteretic cycles (Figure 2.53). This allowed reaching a complete shear yielding of the panel, avoiding that the premature collapse of some panel portions could compromise the global cyclic performance of the system. Besides, the adoption of pinned joining of applied ribs by means of perimeter cover plates allowed the failure of the surrounding connections to be not influential. Also, it is worth noticing that in the final collapse configuration of the panel type H, the bolted ribs were not involved in any buckling phenomena.

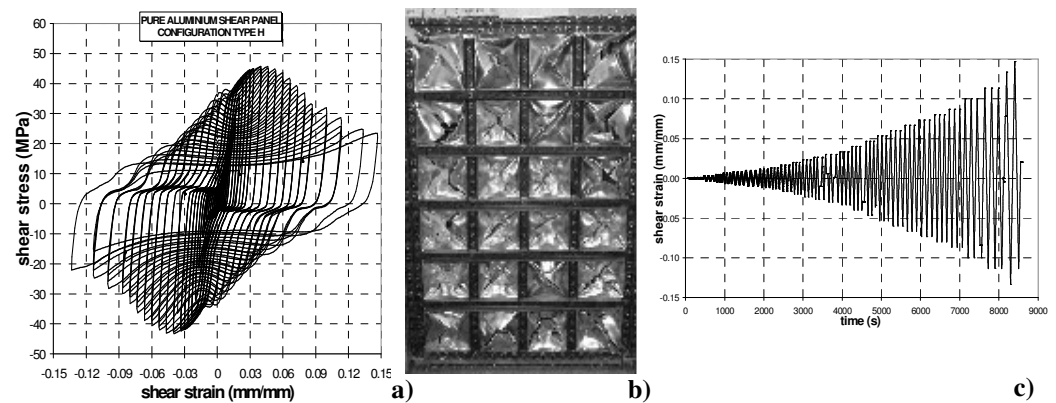


Figure 2.53: De Matteis *et al.*'s experimental activity (2005c, 2006b): hysteretic loops (a), final deformed shape (b) and applied shear deformation history (c) of AW 1050A panel type H

Finally, from the examination of test results, the identification of two different shear panel classes, namely dissipative shear panels and stiffening shear panels, according to the adopted base material, was done.

In particular, AW 5154A aluminium alloy shear panels should be more properly classified as stiffening devices, providing a structural behaviour similar to the one experienced by slender steel plates in shear. On the other hand shear panels made of AW 1050A could be surely classified as dissipative devices, since they exhibited a structural behaviour characterised by large hysteretic cycles and large ductility with a pure shear plastic collapse

mechanism. In fact, in such cases, the experienced buckling phenomena did not condition the attainment of the maximum shear strength of tested systems.

2.4 SLENDER SHEAR PANELS

2.4.1 General

In the framework of passive control devices used to resist lateral forces into new and existing buildings, apart the applications based on the use of stiffened and low-yield strength metal panels, which could result expensive from both the economic and fabrication point of view, the solution foreseeing the adoption of unstiffened steel shear walls, giving rise to the so-called slender shear panels, has been successfully developed in the last years. In fact, such walls, lighter and more ductile than reinforced concrete ones, allow both an increase in the speed of erection and the possibility to exploit more wide spaces in the building. Moreover, steel savings as much as 50% have been achieved in structures employing slender shear panels rather than a comparable moment resisting frame.

The main advantages in using unstiffened shear panels are enhanced strength, stiffness and ductility, stable hysteretic characteristics and a large capacity for plastic energy absorption.

In particular, the strength and ductility of thin steel plate shear walls make them very suitable in buildings in seismic high-risk zones. For this reason, they are also useful for upgrading of existing buildings since their light weight can often avoid the necessity of extensive modification of the substructure. Besides, in retrofit scenarios, the insertion of steel plate shear walls may require reinforcing of boundary columns, which can drastically increase retrofit costs. In this context, the use of light-gauge steel plates, which yield at lower force values in comparison to the more thick ones, may provide a very effective and economic retrofitting solution.

Steel plate shear walls made of slender panels in most existing buildings have been designed to resist earthquakes without buckling. Nevertheless, the buckling of the plate is not synonymous of failure. In fact, the post-buckling strength of a thin steel plate, which can be several times its elastic buckling

resistance, can provide substantial strength, stiffness and ductility, as it was demonstrated for plate girder webs (Basler, 1961).

In the next Sections, based on a wide overview of both analytical studies and experimental research activities developed on thin steel plate shear walls in the last years, the substantial economic advantages and the significant contribution offered to the building response under earthquake attacks in terms of strength, stiffness and energy dissipation capability by using such devices are presented.

2.4.2 Design criteria

For the characterization of the slender shear panels behaviour, several studies have been carried out, being based on the evident analogy existing between them and the web of a stiffened beam. In fact, in steel plate shear walls, the columns to which the panels are anchored can be assimilated to the beam flanges, the panel to the web and the horizontal members at each level can be considered as the transversal stiffeners of the same beam.

Based on such an analogy, several analytical methods, which have been also checked by a number of experimental tests, have been developed, allowing the determination of the characteristics of shear panels in terms of stiffness and strength. Before the occurrence of buckling phenomena, the typical stress state in a shear panel is shown in Figure 2.54 a.

The principal stresses characterising such an element present an inclination of 45° in both directions (Figure 2.54 b).

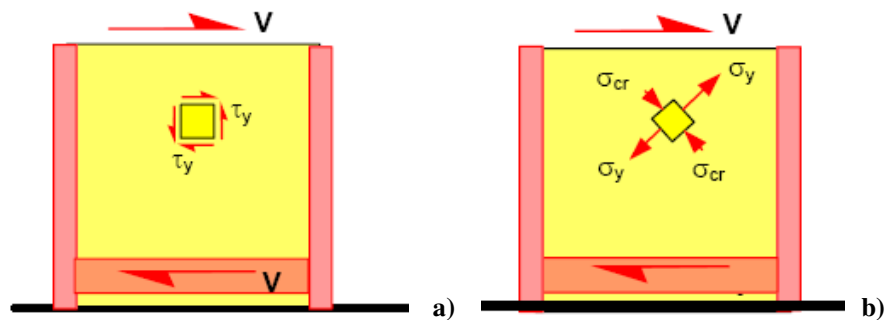


Figure 2.54: Stress state on the web of a stiffened beam subjected to shear (a) and corresponding principal stresses (b)

The behaviour of shear panel is linear until the critical stress of the panel is reached and the web panel presents buckling phenomena with out-of-plane displacements. Starting from this point the resistant mechanism developed in the plate is modified: when the critical stress τ_{cr} is attained, the compression stress does not increase anymore, while the tensile one increases up to reaching the yielding strength of the plate material.

The tension field mechanism provides a meaningful post-buckling strength, which presents in the post-critical field a stable behaviour. Therefore, the critical load of the panel P_{cr} does not represent a limit value for the ultimate resistance of shear panels.

In particular, when the plate thickness is very small, the shear instability occurs for reduced value of the shear load and, consequently, the shear strength of the panel is governed by the tension field mechanism only. The typical formulation used to evaluate the critical tangential stress for rectangular plates subjected to pure shear is the following:

$$\tau_{cr} = k \cdot \frac{\pi^2 \cdot E}{12 \cdot (1 - \nu^2)} \cdot \left(\frac{t}{d} \right)^2 \quad (2.6)$$

where k , defined as plate factor, depends both from the b/d ratio and the boundary conditions of the same plate. Many Authors have provided useful indications about the exact value to be adopted for this parameter, considering several constraint conditions along the borders and different values of the aspect ratio of the plate. Two different approaches to analyse the panel behaviour after the stability loss due to shear can be adopted. The first one is based on the use of a simplified model, which accounts for the main characteristics of the buckled shear panel, while the second one aims at solving the problem on the basis of the non-linear theory of flexible plates. In this context, only the first approach is considered because it is more simple to be implemented and also existing studies have shown that it converges towards the same results.

Buckling of a shear plate develops for a shear force $V_{cr} = \tau_{cr} \times b \times t$ and phenomena with the presence of showy humps of the web or rather with a sort of wrinkling in the direction of the principal compression stress appear. The increase of the external load involves a redistribution of the initial stresses which are characterised by the increase of the tensile stress σ_1 , while the compression one σ_2 is unchanged (Figure 2.55 a). If the web is very thin, the

stress value σ_2 can be neglected, allowing the formulation of the following hypotheses:

- the web is not able to withstand loads in the direction normal to the humps;
- the resistant capacity in the direction of the principal tensile stress will be provided only.

The hypothesized stress field is composed by a certain number of tensile diagonals which fully carry the increase of the external load: this is the so-called tension field mechanism. This theory was shown for the first time by Wagner (1931), which hypothesized the development in the web of a field of tensile stresses along a direction inclined of an angle ϑ in comparison to the horizontal one (Figure 2.55 b), determining its value when the web resulted very thin and the flanges had enough stiffness to not interfere with the tension field mechanism.

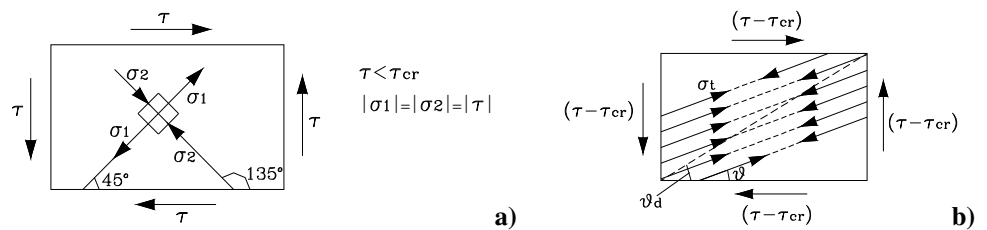


Figure 2.55: Principal stresses on shear plate (a) and the development of the tensile stresses after buckling (b) (Wagner, 1931)

The first method able to predict with a good approximation the ultimate capacity of web panels has been proposed by Basler (1961), which established that, when the flanges were so flexible to not oppose to the lateral load produced by the tension field, the beams reached the collapse when the web panel developed a yielding band, externally to the diagonal extension, as shown in Figure 2.56. In addition Basler affirmed that in the two triangular zones adjacent to the yielding zones the shear stresses resulted equal to the critical one τ_{cr} . Obviously, the hypothesis on the incapability of the flanges to carry out the lateral loads coming from the web resulted very conservative.

From the above considerations it was clear that Wagner and Basler faced the study of two totally opposite situations: the first Author considered the web endowed with rigid flanges, while the second one considered the employment of very flexible flanges, neglecting their flexural stiffness.

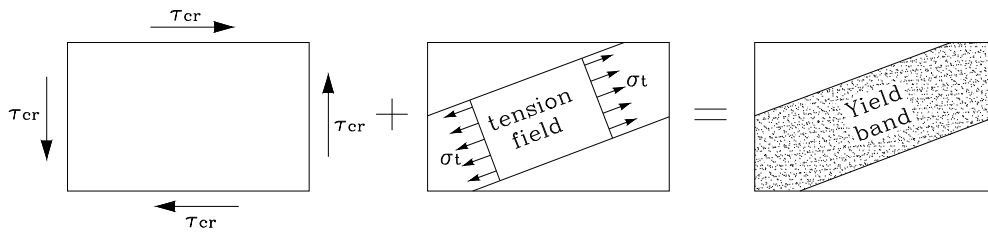


Figure 2.56: The development of the tension field mechanism (Basler, 1961)

When adopting such models for predicting the behaviour of steel shear walls, it has to be considered that generally the columns have a significant flexural stiffness, thus influencing the inclination angle of the generated tension field action and affecting the correct estimation of the shear panel strength.

The idea to profit for the post-buckling strength also for SPSWs was firstly developed by Thorburn et al. and experimentally verified by Timler and Kulak in 1983. These studies were executed for appraising the strength, the ductility and the dissipative capacity of thin steel shear panels. The obtained results showed that these systems offered particular resistance to the horizontal actions induced on the structure, providing:

- high ductility
- poor degradation under cyclic loadings
- optimal initial stiffness and, when the surrounding frame was characterised by rigid joints, high over-strength
- significant values of the dissipated energy

In the above study, the following conclusions were drawn:

- the buckling strength of shear panels was usually neglected, since the reduced thickness produced visible out-of-plane deflections even before the load application.
- the tension field presented an inclination with respect to the horizontal direction different from the one of the web panels of stiffened beams, having the large column stiffness an important role in the development of the tension field mechanism.

2.4.3 Theoretical and numerical modelling

On the basis of the conclusions reported in the previous Section, Thorburn, Kulak and Montgomery (1983) investigated on the post-buckling resistance of steel panels subjected to shear. Starting from the study carried out by Basler and from diagonal tension field theory developed by Wagner, they provided useful indications for interpreting the behaviour of SPSWs after the instability occurrence, when a tension field mechanism developed to resist the applied lateral loads. Thorburn et al. introduced two analytical models in order to determine the stiffness offered by slender steel panels under the considered load condition. In both of them any contribution offered from the panels in the compression phase was neglected. Moreover, in the two models, it was assumed that the columns were continuous for all the height of the wall and that hinged beam-to-column joints were applied. The first model, known under the name of *equivalent diagonal* (Figure 2.57 a), schematised the thin panel as a single diagonal in each frame field. It was shown that for infinitely rigid members the panel thickness (t) could be obtained from the area of the single equivalent diagonal through the following relationship:

$$t = \frac{2 \cdot A \cdot \sin\Theta \cdot \sin(2 \cdot \Theta)}{L \cdot \sin^2(2 \cdot \alpha)} \quad (2.7)$$

On the other hand, for flexible columns, characterised by $I_c=0$, where I_c is their second moment of area, the following formulation is applicable:

$$t = \frac{2 \cdot A \cdot \sin(4 \cdot \beta)}{L \cdot \tan\beta} \quad (2.8)$$

where A is the area of the equivalent diagonal member, L is the beam length, h_s is the height of the relevant frame field and α is the inclination of the generated tension field. This angle, which can be considered equal to β for deformable columns, in case of infinitely rigid columns was obtained from the following relationship

$$\tan^4\alpha = \frac{1 + \frac{L \cdot t}{2 \cdot A_c}}{1 + \frac{h_s \cdot t}{A_b}} \quad (2.9)$$

where A_b and A_c are the beam and column cross section area, respectively.

The beams were assumed rigid because the diagonal tension field develops on both sides, thus providing balanced internal forces. Only for the upper beam of the last storey, the tensile loads were not balanced, requiring the necessity to model the beam with the real stiffness. The two cases were dealt as limit conditions of the real system behaviour and the thickness of the panel comprised among the results of these cases was found acceptable. It was recommended that the equivalent single diagonal model, due to its simplicity, was used to evaluate the member (beams and columns) dimensions and the panel thickness only.

The second approach, also developed by Thorburn et al., is known as *strip model* and is shown in Figure 2.57 b. In such a method, the panel is represented as a series of inclined strips, hinged to the members ends of the external reaction frame, which have a transversal section A_s equal to the strips width multiplied by the panel thickness, according to the following formula:

$$A_s = \frac{(L \cos \alpha + h_s \cdot \sin \alpha)}{n} \cdot t \quad (2.10)$$

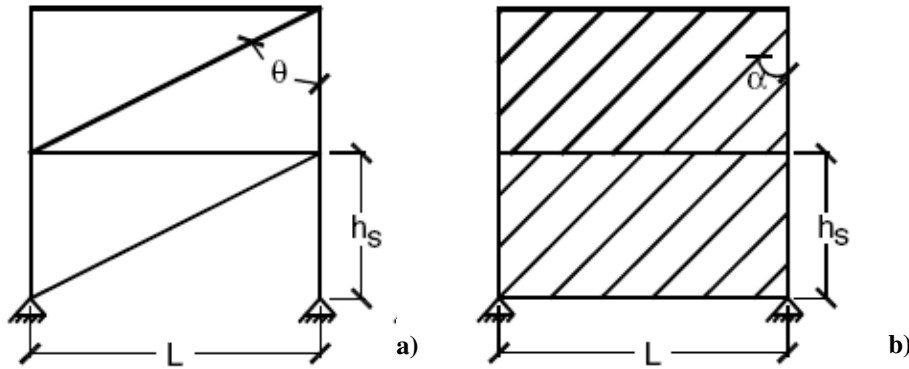


Figure 2.57: Shear panels modelling: equivalent diagonal method (a) and strip model (b)

The inclination angle α of the strips, which are oriented as the principal tensile stresses, was expressed by means of the following relationship:

$$\tan^4 \alpha = \frac{1 + \frac{L \cdot t}{2 \cdot A_c}}{1 + \frac{h_s \cdot t}{A_b} + \frac{h_s^4 \cdot t}{360 \cdot I_c \cdot L}} \quad (2.11)$$

where L , h_s and t are the panel width, height and thickness, respectively, A_b and A_c are the cross sectional area of the frame beams and columns, respectively, and I_c is the second moment of area of the columns.

In such a model, in which the cases of rigid and flexible columns are still considered as limit cases, the initial stiffness of the panel (pre-buckling stage) and the beneficial effect of the material hardening were neglected. The Authors suggested that the minimum number of strips to be used for an adequate modelling of each panel field should be equal to ten. Starting from the strip model theory and applying a plastic analysis on the panel, it was possible to develop equations that allowed to obtain the ultimate strength of different types of SPSW useful for their preliminary dimensioning. The ultimate resistance of the panel (V) could be obtained based on the ultimate resistance of the single strip by using the following relationship:

$$V = \frac{1}{2} f_y t L \sin 2\alpha \quad (2.12)$$

where f_y is the yielding strength of the base material.

The Canadian code for steel structures (CAN/CSA-S16-01, 2001) considered explicitly the use of slender shear walls in seismic areas, recognizing two categories of SPSWs: the type *LD* (walls realised with panels having limited ductility) and the type *D* (walls characterised by ductile panels). The main difference between the two categories was that the shear wall type *D* considered moment resisting beam-to-column connections.

The design procedure of steel plate shear walls developed by the Canadian code was based on a preliminary pre-dimensioning, considering the equivalent diagonal model. The use of simplified static relationships allowed the determination of the action on the diagonal member starting from the lateral design forces. Therefore, the cross-sectional area of the equivalent brace was easily determined for a specific value of the material yielding stress. Then, by using eq. (2.7) the panel thickness could be evaluated. The strip inclination angle α was determined according to eq. (2.11) according to the strip model theory. In addition, aimed at avoiding the collapse of columns, the Canadian code prescribed that the second moment of area of the columns was greater than $0.00307 t h_s^4 / L$, where t is the panel thickness, h_s is the inter-storey height single level and L is the bay width. For seismic applications, the above code provided additional requirements such as, for type *D* walls, correct

checking of the load carrying capacity of the columns. Finally, value of the shear strength of the wall was given by the following relationship:

$$V_{re} = 0.5 \cdot R_y \cdot F_y \cdot t \cdot L \cdot \sin(2\alpha) \quad (2.13)$$

where R_y is the behavioural factor ratio.

2.4.4 Experimental research activities

The first research program to investigate the behaviour of steel plate shear walls used as stiffening systems for buildings was the one carried out by Mimura and Akiyama (1977), who developed a method in order to predict the behaviour under monotonic and cyclic loadings of slender panels. In particular, the behaviour of the global system (frame+panel) in terms of force-displacement response was assumed as the sum of the single contributions offered both by the panel and the external frame.

Timler and Kulak (1983) tested a single full-scale steel shear wall realised with slender panels in order to verify the analytical formulation carried out by Thorburn, Kulak and Montgomery (1983).

The experimental test (Figure 2.58) was based on the use of two panels inserted in a steel frame, having dimensions of 3750x2500 mm and a thickness of 5 mm.

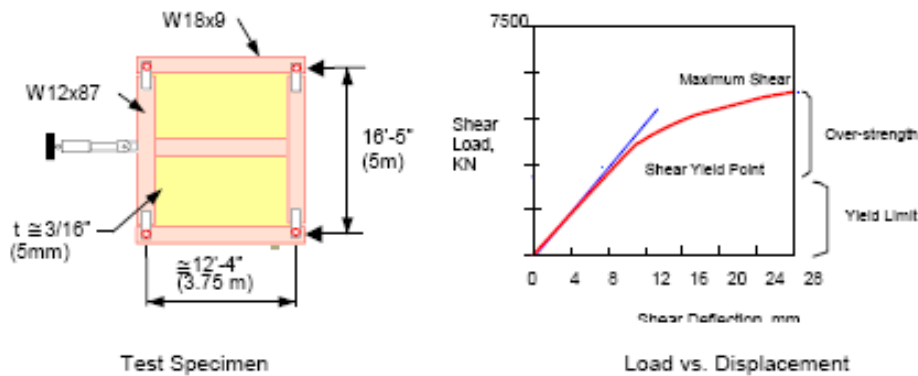


Figure 2.58: The model tested by Timler and Kulak (1983)

Columns and beams were realized with W310x129 (W12x87) and W460x144 (W18x97) profiles, respectively, which were joined by means of hinged connections. No axial forces to simulate the presence of gravitational

actions were applied. The loading history initially considered three initial cycles characterized by a maximum drift equal to $h_s/400$, as prescribed by the Canadian code, then followed by a final pushover until the attainment of the system collapse.

The maximum load of failure was 5395 kN. When the limit drift was attained, the inclination angle of the tensile tension field in the central zone of the panel was found to be variable between 44 and 56 degrees. The failure of the system was attained due to the cracking of the welding used to connect the thin panel to the plates anchored to the members. This behaviour limited the load carrying capacity of the system. In order to interpret the experimental test, the strip model was employed, giving rise to very satisfactory results for the interpretation of the whole force-displacement curve of the system.

Basis on this experimental activity, the Authors revised the formulation for determining the inclination of the tension field α , according for the effects of the columns flexibility as stated in eq. (2.11).

Tromposch and Kulak (1987) conducted an experimental activity on large scale steel shear panels (Figure 2.59), which was very similar to the ones tested by Timler and Kulak.

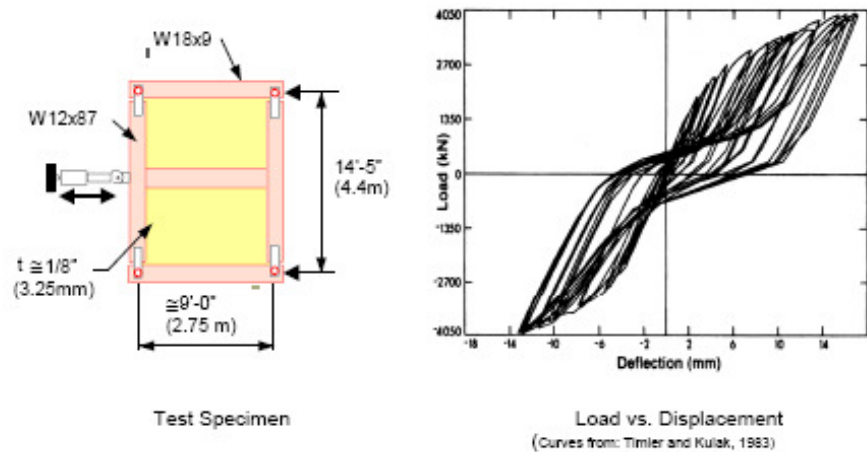


Figure 2.59: The model tested by Tromposch and Kulak (1987)

The main differences were due to different dimensions of the single panel (2750 x 2200 x 3.25 mm), in the use of bolted, instead of welded, beam-to-

column connections, in the presence of larger beams, realised with W610X241 (W24X62) profiles, in the column pre-loading, in order to simulate the effects of gravitational loads, and in the adopted loading history, considering both cyclic and monotonic loading tests. In cyclic tests, 28 reversible cycles, with the maximum value of the applied load equal to the 67% of the system ultimate strength, were performed. The maximum displacement obtained during the loading phases was 17 mm (equal to $h_s/129 = 0.8\%$ drift). After this sequence of cycles, the current pre-loading in the columns was eliminated and a subsequent monotonic loading phase up to the complete collapse of the system was performed. The ultimate final displacement was equal to 71 mm ($h_s/31 = 3.2\%$ drift).

The failure was caused by the bolts slip in the beam-to-column connection and by the failure of the welding between the panel and the steel plates connected to the frame members. However the definitive collapse of the system was not reached, since the test was stopped because the hydraulic jacks attained the maximum loading capacity. The hysteretic experimental cycles, although showing a significant pinching effect, evidenced a good and stable energy dissipation capacity.

The equivalent strip model, which was used for the prediction of the experimental results, provided good results for the evaluation of both the ultimate strength and the envelope of the cyclic response. For achieving this result, it was necessary to consider the connection among the members as rigid for low load levels and as pinned after the bolt slip was occurred. In addition, it was shown that, accounting for the distribution of the residual stresses in the panel weldings, more precise results could be obtained. Finally Tromposch and Kulak also applied some changes to the model proposed by Mimura and Akiyama (1977) for the prediction of the hysteretic behaviour of SPSW, neglecting their stiffness in the pre-buckling phase and considering that the whole stiffness was provided by the reaction frame only until that the displacements were sufficient to activate the tension field mechanism in the shear plate.

Caccese, Elgaaly and Chen (1993) performed an experimental investigation on the effects that the slenderness ratio of the shear plates and the possible types of beam-to-column connections (hinged or moment resisting) played on the shear wall behaviour. They examined five single-bay three-stories steel

frames, modelled in a length scale 1/4, in which 1245 x 2870 shear panels, having inter-storey heights among sub-panels of 838 mm and a residual zone of 229 mm above the third level to allow the anchorage of the tension field, were inserted (Figure 2.60).

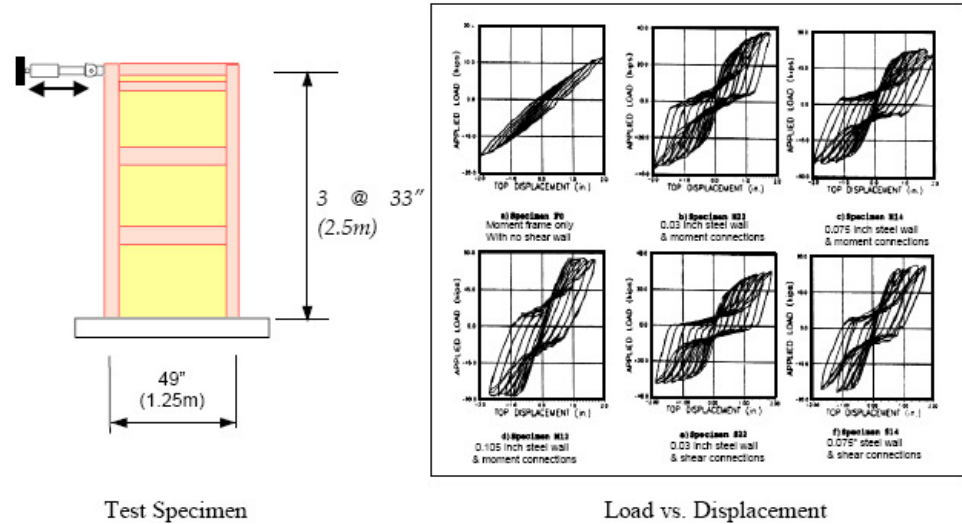


Figure 2.60: The model tested by Caccese, Elgaaly and Chan (1993)

Two series of specimens, differentiated each other with reference to the employed connection type, were tested under monotonic and cyclic loads (Table 2.4).

Table 2.4: Details of steel shear wall specimens tested in the Caccese et al.'s experimental activity (1993)

Specimen number (1)	Nominal Plate Thickness		Slenderness ratio d/t (4)	Beam-column connection (5)
	Gage (2)	mm (in.) (3)		
F0	—	0	—	type 1
M22	22	0.76 (0.0299)	1,639	type 1
M14	14	1.90 (0.0747)	656	type 1
M12	12	2.66 (0.1046)	468	type 1
S22	22	0.76 (0.0299)	1,639	type 2
S14	14	1.90 (0.0747)	656	type 2

The panels were welded to the external reaction steel frame. Different configurations were obtained by varying the panels thickness and the type of beam-to-column connections. The adopted thicknesses were of 0.76, 1.90 and 2.66 mm for moment-resisting connections, while 0.76 and 1.90 mm were employed for hinged connections.

The load was exclusively applied on the upper part of the system and the columns were not axially loaded. The load program consisted in 24 cycles, increasing progressively the displacement up to a maximum value of 50.8 mm (2% drift). Then, in order to obtain the complete collapse of the system, the load was increased monotonically up to the maximum displacement allowed by the jack. The deformed shape of some of tested specimens at the force peak value corresponding to the 24th cycle is shown in Figure 2.61.

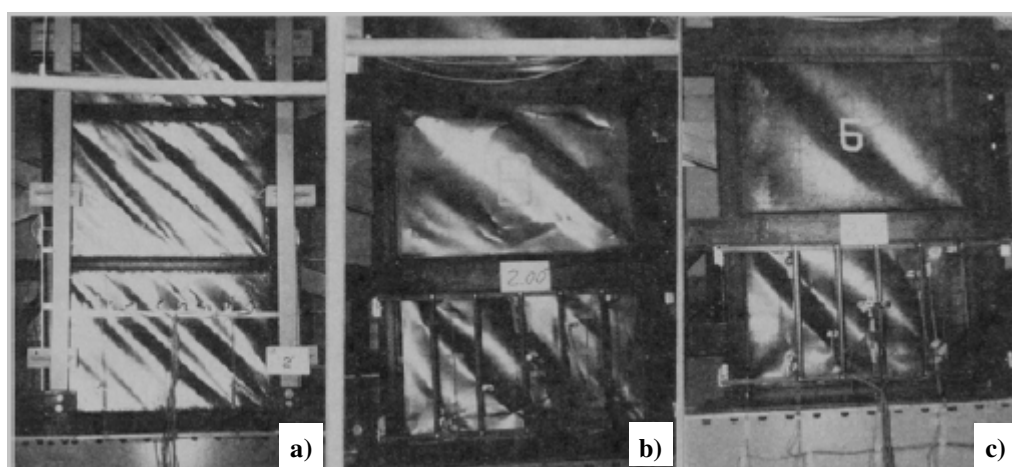


Figure 2.61: Caccese et al.'s experimental activity (1993): deformed shapes of M22 (a), M14 (b) and M12 (c) specimens at the end of the test

The performed experimental tests evidenced that the failure mechanism depended on the applied panel thickness: while slenderest panels yielded before the members of the external frame, exhibiting any collapse, in panels with higher thickness the failure was governed by column buckling without plastic involvement of shear panels.

It was observed that when the columns instability determined the system failure, further increases of the panels thickness caused negligible effects on the load carrying capacity of the shear wall. Therefore, it was remarked that

the columns of a shear wall system should be carefully designed aimed at obtaining the panel yielding before the attainment of buckling phenomena. In addition, it was noticed that the employment of rigid, instead of hinged, beam-to-column connections did not determine any substantial difference on the behaviour of shear walls. This result was due to the fact that even thin panels, when completely welded to the frame, create moment-resisting connections for the frame members.

Elgaaly, Caccese and Du (1993) applied both a finite element model and a model based on a revision of the equivalent strips method to simulate the experimental results obtained by Caccese et al (1993a, b).

When employing the first method, a non linear analysis was carried out by using a mesh of 6x6 elements for representing the panels in each frame field, while beam elements were used to model the frame members. The panels thickness, according to the experimental tests, was assumed equal to 1.9 and 2.7 mm and moment resisting beam-to-column connections were hypothesized. For both cases the failure load was determined by elastic buckling of the columns. Comparing the numerical results with the experimental ones it was noticed that the finite element model overestimated both the strength and the stiffness of the system. These discrepancies were attributed to the difficulty in modelling of both the initial panel imperfections and the out-of-plane deformations of the frame members.

Shear panels with a thickness of 1.9 mm was also modelled by using the strip model technique, adopting twelve strips in each frame field. The inclination angle of the strips was established equal to 42.8 degrees, which fit well with the results of the finite element model. Assuming for the steel of the strips an elastic - perfectly plastic behaviour, the model produced reasonable results with respect to the experimental ones. It was also noticed that the employment of an empirical tri-linear material stress-strain law allowed a further improvement of the previously achieved results. Besides, an analytical model based on the employment of the strip model was calibrated to foresee the cyclic hysteretic behaviour of slender panels.

Xue and Lu (1994) carried out an analytical study on three-bays – twelve-storeys moment resisting frames, having the intermediate bay stiffened by shear walls. The object of this research study was represented by the evaluation of the results produced by the use of different beam-column and

plate-frame connections on the performances of the global system. Four different combinations of connections were taken into account: a) moment-resisting beam-to-column connections and panels fully connected to the frame elements; b) moment-resisting beam-to-column connections and panels connected to the frame beams only; c) shear type beam-to-column connections and panels fully connected to the frame elements; d) shear type beam-to-column connections and panels connected to the frame beams only. The external bays of the frame under examination presented width of 9144 mm, while the internal one (stiffened by panels) was characterised by a width of 3658 mm. The storey height of all levels was equal to 3658 mm, except for the first one, which measured 4572 mm. The panel thickness, which was unchanged in all the examined configurations, varied along the wall height, decreasing from the top towards the lower part of the building. The finite element analysis considered the beams and the columns as elastic mono-dimensional elements, while the panels were modelled using shell elements with an elastic-plastic behaviour. The initial imperfections of the panel were considered by taking into account a configuration similar to the first eigenmode. Each model was analysed by a pushover analysis with lateral forces applied to every level. It was observed that the type of beam-to-column connections in the field where the panels were inserted presented a meaningless effect on the global behaviour of the system, since varying the panel-to-column connection type only a low increase of the system ultimate strength was obtained. On the basis of the achieved results, it was concluded that the optimal system configuration was the one based on hinged beam-to-column connections in combination with shear panel and the connection of the shear panel on the beams only, because in such a way the shear forces inside the column were drastically reduced, avoiding the occurrence of premature buckling phenomena.

Driver, Kulak, Kennedy and Elwi (1997) carried out a large scale test of a multi-level shear walls, having moment-resisting beam-to-column connections, in order to better identify the elastic stiffness, the first yielding, the ductility and the energy absorption capacity of the system, investigating on the stability of the hysteresis cycles and on the factors which caused the failure mechanism of the shear wall (Figure 2.62).

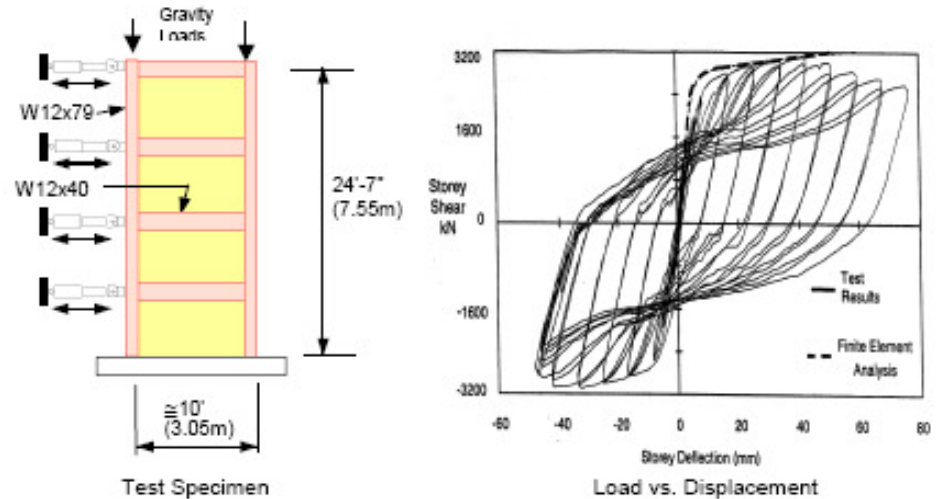


Figure 2.62: The model tested by Driver, Kulak, Kennedy and Elwi (1997)

The shear wall, having width of 3050 mm, was articulated on four levels, each one of 1829 mm height, except for the first one, which was 1927 mm height. The panel thickness adopted for the first two and the last two levels was 4.8 and 3.4 mm, respectively. A rigid beam was used at the top level in order to anchor the tensile stresses developed in the panel, which was connected to the frame by means of plates welded to steel profiles. The cyclic test performed on the system, with the load applied under quasi-static way, was made of 35 cycles, with a progressive increase of the lateral displacement.

From the observation of the corresponding force-displacement experimental curve, the yielding displacement and the corresponding base shear value were equal to 8.5 mm and 2400 kN, respectively. For a base shear force equal to 3000 kN and a displacement three times greater than the yielding one, both the yielding of the panel and of the first level beam-to-column connection, occurred. The local buckling of the first level column flange occurred for a displacement equal to four times the yielding one (δ_y), while severe fractures in the panels of the first level and local instabilities of the same column were observed for $\delta = 6 \delta_y$. At that moment the structure reached the 95% of the ultimate strength. The failure occurred when the applied displacement was equal to nine times the yielding one and the force reached the 85% of the maximum panel strength due to the complete collapse of the welding of the base of the column. Analyzing the hysteretic cycles of

each shear panel, it was noticed that the bottom shear panel absorbed the greater part of the input energy with an excellent ductility and a stable behaviour. The system was also modelled under analytical way, considering both the finite element model and the equivalent strips method. A good agreement was obtained in terms of both ultimate strength and initial stiffness of the system. However, for high displacements, the proposed model overestimated the panel stiffness. Such a discrepancy was due to the difficulty to correctly account for the second order geometric effects. Also, the equivalent strip model provided results in a good agreement with the experimental ones. A revision of the hysteretic model proposed by Tromposch and Kulak (1987) was also presented considering separately the contribution of the MRF and the panel contribution. The two components were empirically analysed by assuming a bi-linear hysteretic behaviour. The combination of these responses provided a tri-linear behaviour of the compound system that fit well the experimental results.

Rezai (1999) performed the first experimental dynamic test with shaking table on shear walls realized with steel panels (Figure 2.63).

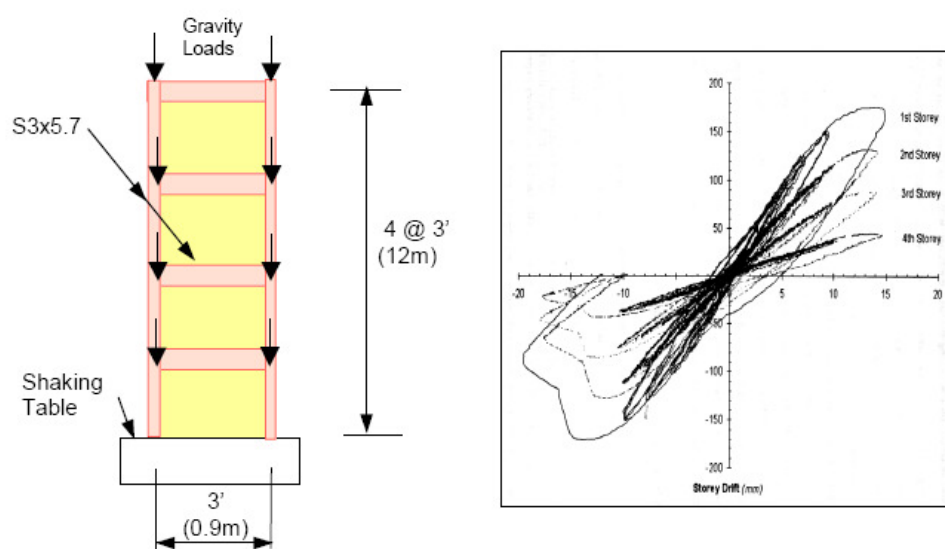


Figure 2.63: The model tested by Rezai (1999)

This study had the main purpose to appraise the reliability of the prescriptions provided by Canadian code for this structural typology. A four

levels and one span steel frame, having a width of 918 mm and inter-storey height of 900 mm, was considered. The shear panels, having a thickness of 1.5 mm, were connected to 2.5 mm steel plates welded to the frame members. An elaborate reaction frame was designed in order to prevent out-of-plane failure of elements at each level. The gravity load and the mass for the dynamic vibrations were provided by steel flats located at every level. Four different earthquakes recordings, considering different levels of peak ground acceleration, were used for exciting the system. Additionally impact and vibration tests were performed too. Due to the limited capacity of the shaking table, shear panels did not undergo large plastic deformation in all the performed tests. A reduced dissipation energy was observed only in the first two levels, with a limited yielding of the first level columns and at the base of shear panels.

Lubell, Prion, Ventura and Rezai (2000) tested two shear wall systems: the first system having four levels panels and the second one composed by a single shear plate (Figure 2.64).

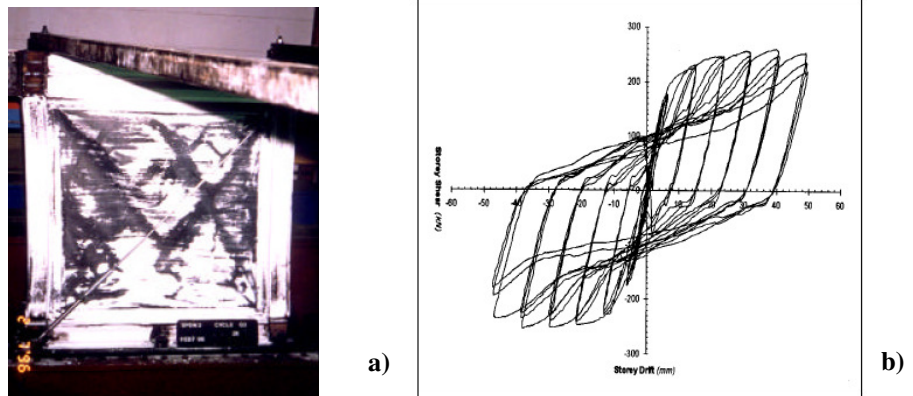


Figure 2.64: The model tested by by Lubell, Prion, Ventura and Rezai (2000): the specimen at the test conclusion (a) and its hysteretic response in the load-displacement plane (b)

All the systems presented panels having thickness of 1.5 mm, width of 900 mm and a width-to-depth ratio equal to 1, while the beam-to-column connections were of rigid type. Quasi-static cyclic loads were applied according to the provisions specified by the ATC 24 protocol (1992).

The one-level system was loaded up to 7 times the yielding structural displacement and exhibited a collapse of the contrast frame due to the excessive out-of-plane displacement of the upper part of the system. The ultimate strength was about 200 kN, with a yielding resistance of 180 kN corresponding to a displacement of 9 mm. Having to prevent out-of-plane displacements of the frame, on the same system was performed a second test, after the upper beam had been adequately stiffened. In this case the yielding was about 190 kN for a displacement (δ_y) of 3 mm, while an ultimate strength of 260 kN was obtained, corresponding to a displacement equal to $4\delta_y$. The failure was due to the column which manifested some fractures after suffering meaningful plastic rotations. The significant increase of both the ultimate resistance and the stiffness was attributed to the larger stiffness of the upper beam, which allowed a correct tension field anchorage.

The four-levels system was analysed under an uniform distribution of lateral load, while the gravitational load was simulated by positioning steel flats to every level. First yielding appeared for a value of the base shear equal to 150 kN and a first level lateral displacement of 9 mm. The system failure due to the global buckling of columns occurred for a displacement equal to 1.5 times the yielding one. From the observation of the hysteretic cycles of each panel, it was observed that the first one, presented the most significant damage. It is worth noticing that this behaviour was observed for all the experimental tests performed on multi-level shear walls, as those carried out by Driver et al. (1997) and Rezai (1999). Also, a significant compression of the columns and a fragile collapse of the walls were observed when significant displacements were applied. Such phenomena caused the exigency to over-design the columns of a shear wall in order to guarantee the plasticization of shear panels only. In addition, also in this case, the equivalent strip model was implemented for evaluating the accuracy of the modelling technique. From the performed analysis, it was observed that the model over-estimated the elastic stiffness of both the one level and the four-levels systems, but the yielding and the ultimate resistance were well appraised. Nevertheless, when the upper rigid beam was present, the strip model provided better results in the prediction of the initial stiffness.

Mo and Perng (2000) tested RC frames reinforced with steel trapezoidal plates in order to estimate the effectiveness of these devices as upgrading

system for absorbing lateral actions. The RC structure was represented by a simple frame, having width of 1125 mm and height of 900 mm, composed by 150x150 mm beams and columns with steel rebars percentage defined according to the ACI 1995 prescriptions. The tested panels presented different thickness (0.3, 0.4, 0.5 and 1.0 mm) and were connected to the steel members by means of bolts. Based on the performed cyclic tests in quasi-static regime, the hysteresis response of shear panels was always characterised by a significant pinching effects, even if a good ductility was obtained. In the test carried out on the panel having thickness of 0.3 mm, the failure of the connection with the frame members was recorded, while panels with thickness of 0.4 and 0.5 mm exhibited a better plastic behaviour with ductility factor equal to 3.89 and 2.89. In the case of the panel having thickness of 1.0 mm it was observed a brittle failure mechanism, because the frame elements collapsed before the yielding of the panel. The experiment results were also compared with those related to different reinforcing methods of RC structures, including the adoption of typical shear walls. The reinforcement with trapezoidal sheetings conferred a reduced ultimate strength but a greater ductility and dissipation energy in comparison to the typical shear walls, while it presented a greater resistance, ductility and energy dissipation capacity. It was concluded that, in order to assure a ductile failure of the system, the panel thickness should be limited within well confined fixed limits aiming at avoiding both the local collapse of panel-frame connections and the failure of the surrounding frame members.

Sabouri-Ghomi and Roberts (1991) developed a general method for the analysis of shear walls characterised by different configurations of panels, with and without openings and with and without flexural stiffeners. The proposed analytical model, known as Plate Frame Interaction (PFI), could easily be applied in the engineering practice, it allowing the design of both the panel and the frame members, without considering the interaction existing between two structural components.

Analysing a single shear panel, the following assumptions were made:

- the columns were rigid to neglect the shear deformations induced by the panel action and to develop an uniform tensile stress state in the plate during the post-critical phase;

- the difference between the intensity of the tensile stresses on the two beam sides was reduced and the bending of the beam due to the tension field mechanism was negligible;
- the panel could be considered as simply connected along the members;
- the pre-critical phase of the panel was neglected;
- both the panel and the frame member behaviour was idealized by means of elasto-perfectly plastic behaviour.

The panel, having depth d , width b and thickness t , presented a behaviour characterized by the force-displacement diagram of Figure 2.65 a, where in the point C a stiffness variation due to shear buckling phenomena is evident. Such a point is characterized by the attainment of the critical strength F_{cr} and a shear displacement, corresponding to U_{cr} , expressed through the followings relationships:

$$F_{wcr} = \tau_{cr} \cdot b \cdot t \quad U_{wcr} = \tau_{cr} \cdot d / G \quad (2.14)$$

where G is the shear elastic modulus of the panel material.

In the post critical phase the panel did not lose the load carrying capacity since the diagonal tension field is activated. If θ is the inclination angle of the tensile bands with respect to the horizontal direction, maximum strength of shear panel subjected to horizontal actions is provided by the following relationship:

$$F_{wu} = b \cdot t \cdot \left(\tau_{cr} + \frac{\sigma_{ty} \cdot \sin 2\theta}{2} \right) \quad (2.15)$$

where σ_{ty} is the maximum tensile stress attainable in the panel.

The corresponding value of the elastic limit displacement of the shear panel is:

$$U_{we} = \left(\frac{\tau_{cr}}{G} + \frac{2 \cdot \sigma_{ty} \cdot \sin 2\theta}{E} \right) \cdot d \quad (2.16)$$

Once the elastic limit displacement and the ultimate strength of the panel are known, the point D of Figure 2.65 a can be determined, allowing the definition of the secant stiffness of the system, taking into account both the elastic phase (pure shear behaviour) and the post buckling one:

$$K_w = \frac{\tau_{cr} + \frac{\sigma_{ty} \cdot \sin 2\Theta}{2}}{\tau_{cr} / G + \frac{2 \cdot \sigma_{ty} \cdot \sin 2\Theta}{E}} \cdot \frac{b \cdot t}{d} \quad (2.17)$$

It can be noted that the elastic limit displacement of the panel is not influenced by its thickness, especially when the critical shear stress is zero. On the other hand, the maximum panel strength essentially depends on both the thickness and base panel width, the influence of the panel depth d being negligible.

It can be also observed that for high b/d ratios the panel essentially works in shear, since the bending deformations are limited. In addition, when such a ratio is very high ($b/d \gg 1$), the tension field develops involving the beams only, without anchoring to the columns.

The inclination of the tension field bands can be assumed equal to 45° , corresponding to a mean value of the range ($35^\circ - 55^\circ$) experimentally determined by other Authors (Timler and Kulak, Lubell and Rezai). In fact, using the limit values of the above range, the Authors observed that a reduction of 6% and 12% in terms of ultimate strength and stiffness, respectively, was recorded. Therefore, it was concluded that the error due to the adoption of an inclination angle of 45° could be considered to be negligible.

To overcome the limitations previously imposed in the definition of the PFI model, Sabouri-Ghomi et al. (2003) introduced some correction factors in the relationships characterizing both the ultimate resistance and the elastic limit displacement of the panel, providing the following expressions:

$$F_{wu} = b \cdot t \cdot \left(\tau_{cr} + \frac{C_{m1} \cdot \sigma_{ty} \cdot \sin 2\Theta}{2} \right); U_{we} = \left(\frac{\tau_{cr}}{G} + \frac{2 \cdot C_{m2} \cdot \sigma_{ty} \cdot \sin 2\Theta}{E} \right) \cdot d \quad (2.18)$$

The factors C_{m1} and C_{m2} depend on several parameters like the column stiffness, the beam-to-column connection, the members-panel connection, etc. According to the experimental activities performed from several Authors it was found that these correction factors ranged between 0.8 and 1 for C_{m1} and between 1 and 1.7 for C_{m2} .

As far as the reaction frame is concerned (Figure 2.65 b), it is characterised by a not negligible lateral resistance only if the beam-column connection is rigid.

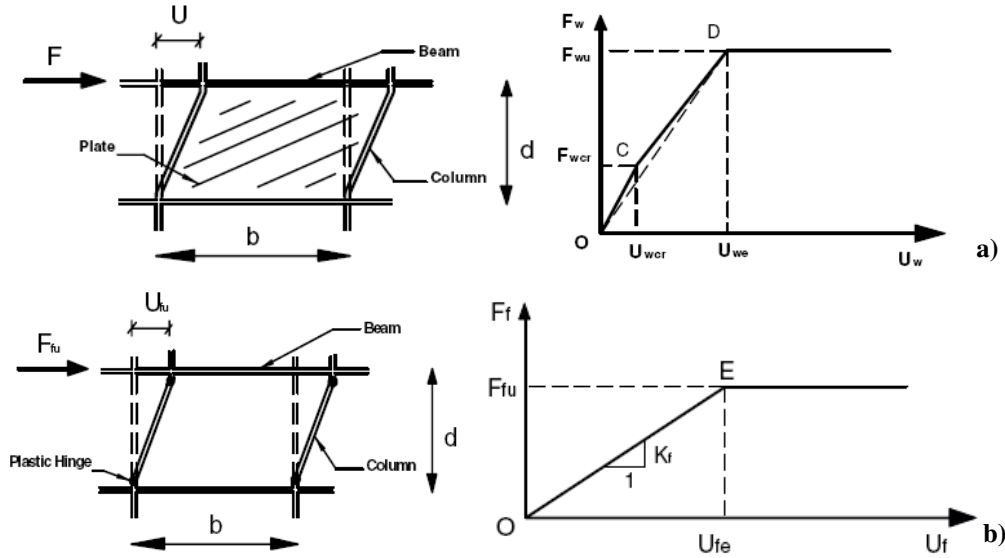


Figure 2.65: The PFI method developed by Sabouri-Ghomi and Roberts (1991): force-displacement diagram of the panel (a) and the frame (b)

Considering that the beams are rigid, the lateral strength and the elastic limit displacement of the frame are equal to:

$$F_{fu} = \frac{4 \cdot M_{fp}}{d} \quad U_{fe} = \frac{M_{pf} \cdot d^2}{6 \cdot E \cdot I_f} \quad (2.19)$$

where M_{pf} and I_f are the plastic moment and the second moment of area of the columns, respectively. As a consequence the frame stiffness is equal to:

$$K_f = \frac{24EI_f}{d^3} \quad (2.20)$$

By composing the behaviour of the frame and of the panel, it is possible to determine the global behaviour of the compound system, which is defined by a three-linear behaviour (Figure 2.66 a). In order to ensure a panel plasticization before the frame yielding, the panel stiffness should be significant larger than the frame one. In order to activate correctly the tension field action, the frame members must be opportunely designed, assuming a scheme of continuous beam (hinged frame) according to the followings relationships:

$$M_{pf} = \frac{\sigma_{ty} \cdot t \cdot d^2 \cdot \cos^2 \Theta}{8} \quad \text{for columns} \quad (2.21)$$

$$M_{pf} = \frac{\sigma_{ty} \cdot t \cdot d^2 \cdot \sin^2 \Theta}{8} \quad \text{for beams} \quad (2.22)$$

Also the axial force in the columns has to be carefully considered, while the strength of the beam has to be checked for the one belonging to the top floor. The validity of the model has been confirmed by analyzing previous experimental tests and calibrating the obtained results through the previously described corrective coefficients, obtaining a substantial coincidence of results, as depicted in Figure 2.66 b.

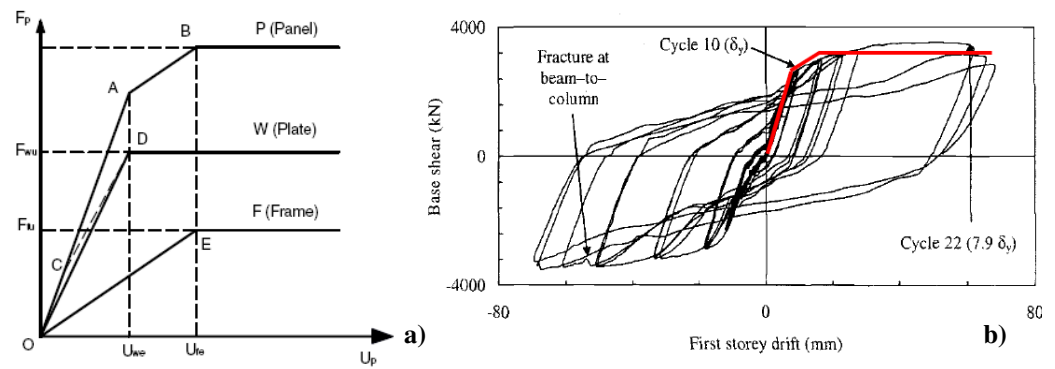


Figure 2.66: The PFI method developed by Sabouri-Ghomi and Roberts (1991): force-displacement diagram of the composed (frame+panel) system (a) and comparison with the experimental result (b)

Astaneh-Asl and Zhao (2002) carried out a research finalized to the study of the shear panels behaviour under cyclical loads.

The experimental test was performed on a system composed by a panel connected both to a composed steel-concrete column (filled type) and to steel beams and columns (Figure 2.67).

The shear panel was endowed with a stiffening plate, located at the mid-height and connected by means of bolts to the steel columns. The panel was 9.5 mm thick, while the thickness of the stiffening plate was 6.4 mm.

The connection between the panel and the W18x86 profiles was realised by means of continuous welds. Also, the beam-to-column connection was realised through a complete penetration welding. The hollow circular columns, having diameter of 610 mm and thickness of 7.9 mm, were filled up of concrete along its whole height.

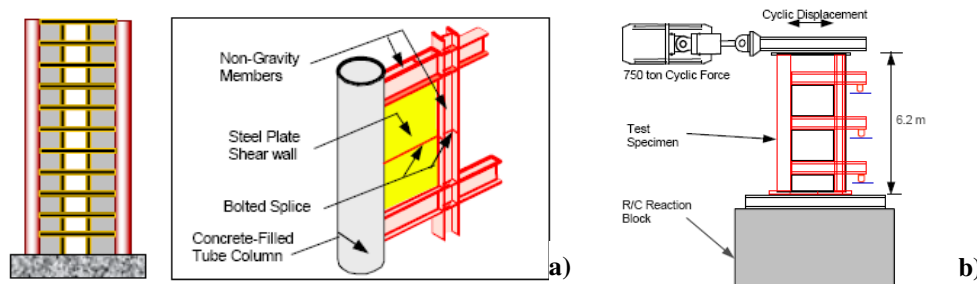


Figure 2.67: The characteristic module (a) and details of the test (b) carried out by Astaneh-Asl and Zhao (2002)

Two tests were performed, which supplied the following results (Figure 2.68):

1. The tested system, shear wall plus contrast frame, behaved in ductile way and tolerated a great number of inelastic cycles under applied actions: in particular the seismic-resistant elements (panel, inner columns and beams) developed plastic behaviour and dissipated a great amount of energy;
2. the behaviour of the shear wall was similar to the one of the web panels subjected to shear. For low values of the relative displacement the system remained in the elastic field but, after the exceeding of a drift equal to 0.6%, the panel showed the typical tension field mechanism;
3. the composed column during the experimental phase remained in the elastic field, while in the beam ends developed plastic hinges, having great rotations in the plastic field;
4. the welded connection between the panel and the frame members did not present failures, showing a ductile behaviour.

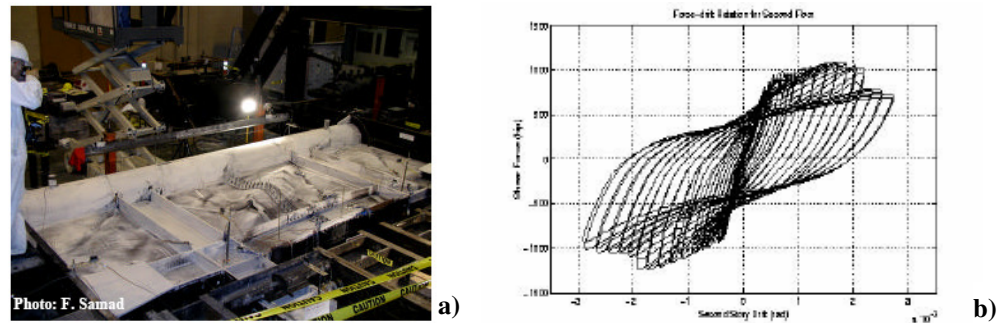


Figure 2.68: Final deformed shape (a) and hysteric diagram (b) of the shear panel tested by Astaneh-Asl and Zhao (2002)

Berman and Bruneau (2003) carried out an experimental study to determine the feasibility of light-gauge SPSWs for seismic retrofitting of buildings. The building under consideration was a four storeys hospital located in a high seismicity zone and characterised by moment resisting steel frames. The choice of thin steel panels for retrofitting operations was due to the necessity to minimise the demand on the structure, avoiding further column strengthening, and to prove alternative type connections, since they developed small forces in the connections with the surrounding frame.

Two different specimens were used: a 1 mm thick steel plate and a 0.75 mm thick corrugated sheeting with corrugations oriented at 45° to match the inclination angle of the tension field for the flat infills. Three single storeys light gauge steel plate shear walls, denominated as F1, F2 and C1, were designed: the first two utilised 1 mm thick steel plates, while the latter was characterised by corrugated infills.

Tensile tests performed on coupons extracted from the same base sheeting provided a yield stress equal to 150, 225 and 325 MPa for specimens F1, F2 and C1, respectively. The connections between infills and the surrounding frame, whose members were designed in order to remain elastic during testing, were made by using epoxy resins (specimens F1 and C1) or welding (specimen F2).

The specimens, having an aspect ratio of 0.5 (3660 mm width by 1830 mm height), were mounted between a 1100 kN static actuator and a stiff reaction frame, as shown in Figure 2.69. Figures 2.70 a, b show specimens C1 and F2 prior to testing.

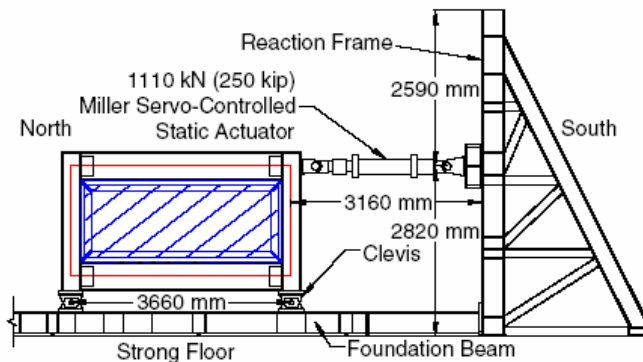


Figure 2.69: The testing set-up used in the Berman and Bruneau's experimental activity (2003)

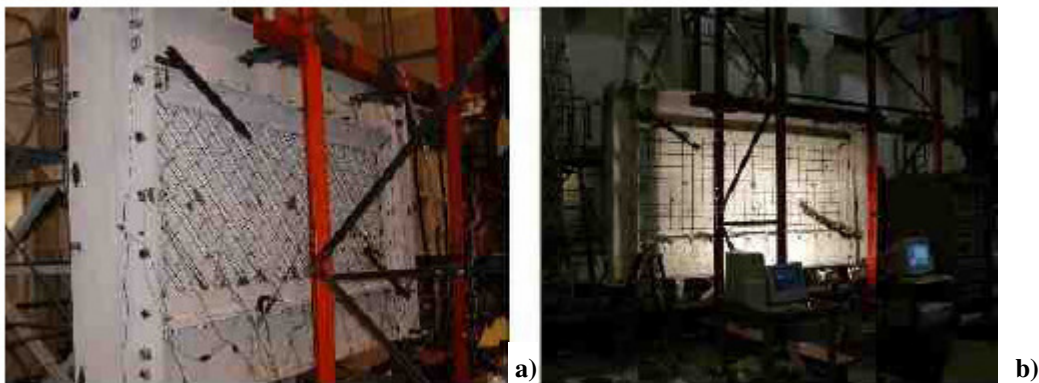


Figure 2.70: Berman and Bruneau's experimental activity (2003): specimens C1 (a) and (F2) (b) prior to testing

For the sake of example, the hysteretic curve of specimen F2, which exhibited the most desirable behaviour, is reported in Figure 2.71 a, where pinched but stable hysteretic loops, demonstrating the ductile behaviour that can be achieved with steel plate shear walls, are observed. For this specimen, yielding at 0.29% drift, the ultimate failure occurred from fractures in all four corners. Such cracks, appeared for a displacement equal to 2 times the yielding one (δ_y), did not have significant impact on the capacity of the specimen until $12 \delta_y$, when they reached a remarkable size (Figure 2.71 b). For this reason, the flat infill with the welded connections had substantially superior behaviour when compared to the other two specimens. In fact, on one

hand, it was observed that there was no substantial advantage to using infills with corrugated profiles (specimen C1), despite their enhanced buckling strength, because their failure mode was determined to be fracture of the infill at locations of repeated local buckling.

On the other hand it was also proved that the use of epoxy resin as connection element in the specimen F1 did not provide a satisfactory behaviour, due to its failure before panel yielding. Finally the moments in the beams and columns were shown to be small for all specimen and the variation of the strain across the infills was insignificant.

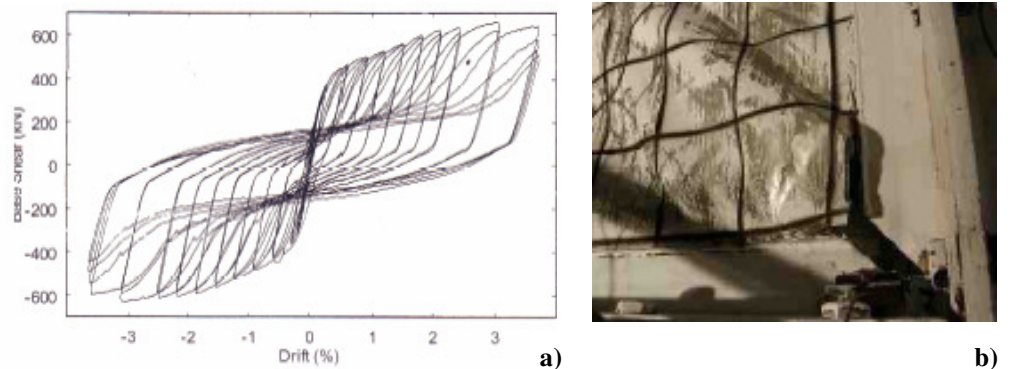


Figure 2.71: Berman and Bruneau's experimental activity (2003): hysteretic loops (a) and fracture (b) observed in the specimen F2

Berman, Celik and Bruneau (2004) carried out experimental tests in order to estimate the behaviour under cyclical loads of both concentric braces (CBFs), realized with tubular profiles and integrated by open section Cold Formed Steel Studs (CFSSs) which acted as reaction elements for diagonals for increasing their critical load and avoiding buckling phenomena, and steel plate shear walls (SPSWs). The experimental campaign, carried out on systems designed according to the prescriptions given by the American (AISI, AISC LFRD Specifications and AISC Seismic Provisions, 1999) and Canadian (CAN/CSA-S16-01, 2001) codes, was based on the execution of 6 tests: two tests on shear walls (slender and trapezoidal sheetings) and four tests on concentric bracings (two tests on single and other two tests on double diagonals). In particular, the employed bracing systems can be synthesized as follows (Figure 2.72): 1) *FP*, slender 1 mm thick panel; 2) *CP*, trapezoidal

sheeting with thickness of 0.75 mm; 3) *B1*, single diagonal concentric brace integrated with CFSS; 4) *B2*, single diagonal concentric brace; 5) *B3*, St. Andrew cross braces integrated with CFSSs; 6) *B4*, St. Andrew cross braces.

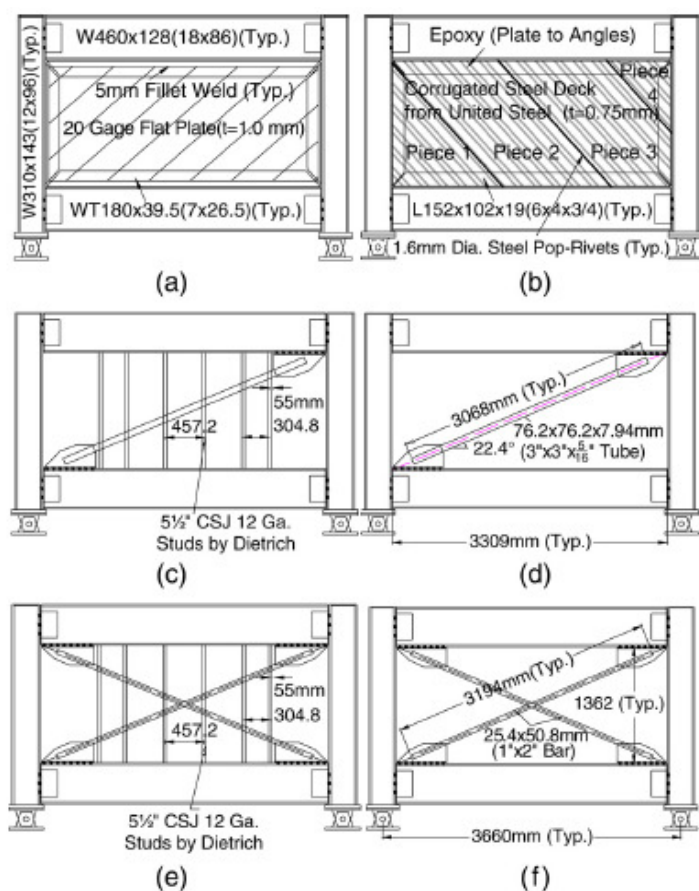


Figure 2.72: Configurations of the systems tested by Berman, Celik and Bruneau (2004): a) FP; b) CP; c) *B1*; d) *B2* ; e) *B3* ; f) *B4*

The tested systems, subjected to cyclic loadings according to the provisions established by the ATC-24 protocol (1992), have provided the experimental response reported in Figure 2.73, where it is also possible to evaluate the contribution in terms of dissipated energy given by the reaction steel frame only.

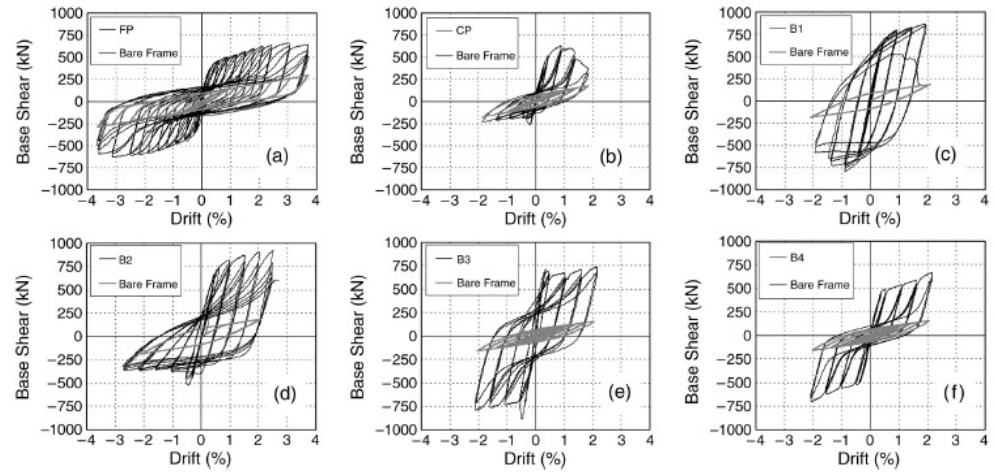


Figure 2.73: Hysteretic curves of the systems tested by Berman, Celik and Bruneau (2004): a) FP; b) CP; c) B1; d) B2 ; e) B3 ; f) B4

From the experimental comparison it is evident that the *FP* type shear wall provides the better performance in terms of ductility, presenting stable hysteretic cycles, even if it is characterised by a strong pinching effect for displacement in the plastic field greater than 3.

It can be noticed that, both in terms of the accumulated energy for each cycle and total dissipated energy one, the slender shear wall (*FP*) and the St. Andrew cross braces integrated with CFSSs (*B3*) have the same dissipative capacity for ductility values up to 4 (Figure 2.74).

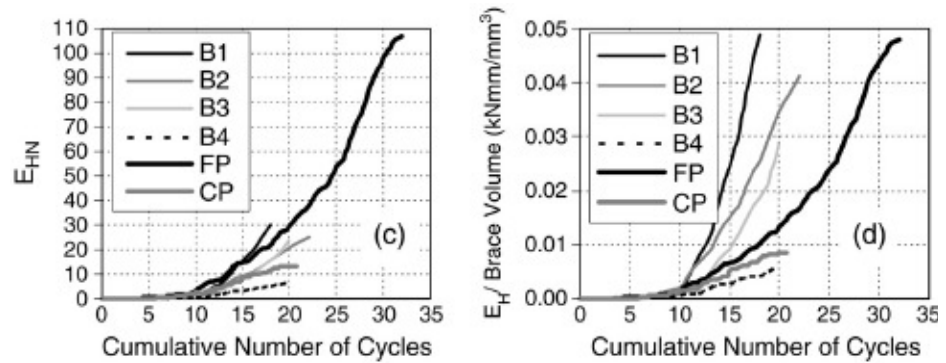


Figure 2.74: Comparison among different systems tested by Berman, Celik and Bruneau (2004) in terms of normalised energy dissipation

2.5 APPLICATIONS

Since 70's, steel shear walls have been used as primary lateral load resisting systems in several modern and important structures. Firstly stiffened steel shear walls were used in Japan in new constructions and in USA both in new buildings and for seismic retrofitting of the existing ones. On the other hand, in the last two decades, unstiffened steel plate shear walls were used in buildings in USA and Canada. In some cases, the steel plate shear walls were covered with concrete forming a somewhat composite shear wall. In the following a brief summary of the applications of both stiffened and unstiffened steel plate shear walls is provided (Astaneh-Asl, 2001).

The first significant application of steel plate shear walls occurred in 1970 in Tokyo, where a 20-story office building, known as Nippon Steel Building, was equipped with stiffened steel shear panels able to carry without buckling lateral actions only.

The lateral load resisting system of the building in longitudinal direction was a combination of moment frame and steel plate shear wall units, the latter according to a H configuration, while in transverse one consisted of steel plate shear walls only (Figure 2.75 a). The thickness of steel plates, horizontally and vertically stiffened by means of channel profiles (Figure 2.75 b), ranged from 4.76 to 12.7 mm.

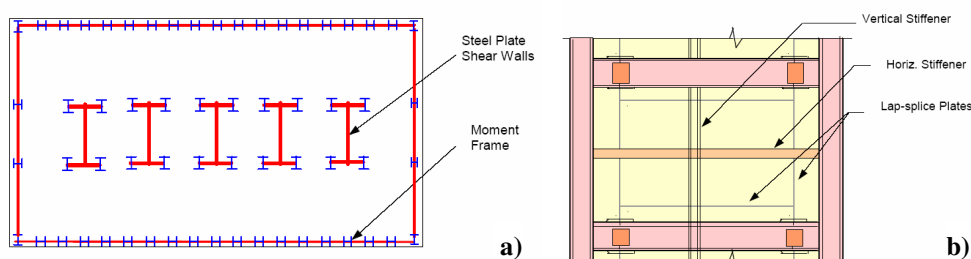


Figure 2.75: The Nippon Steel Building: typical floor plan (a) and details of steel shear walls (b)

Another application was done into a 53-storeys high-rise building in Tokyo, whose structure, initially designed using reinforced concrete shear walls, finally consisted of moment perimeter frame and T shaped stiffened

steel shear walls. Figure 2.76 shows a plan view and a cross-section of the building.

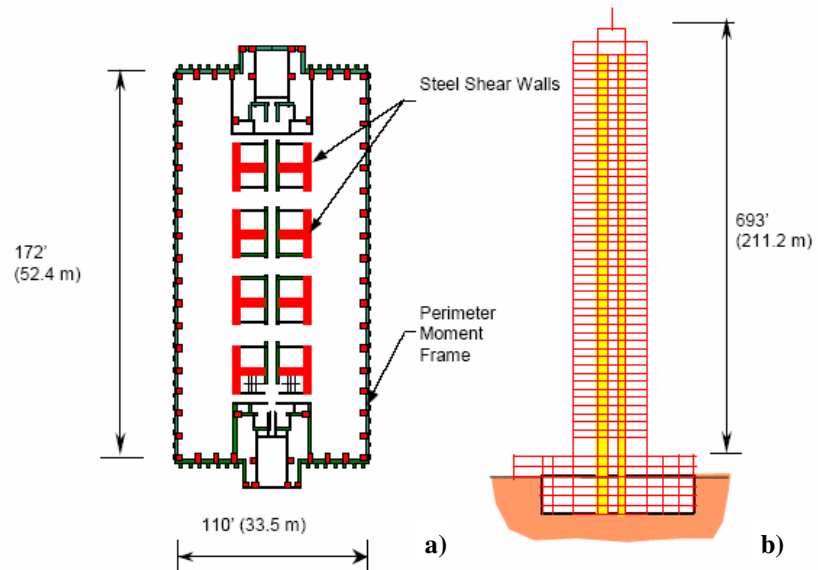


Figure 2.76: Plan (a) and transverse (b) sections of the 56-storeys building in Tokyo

The wall panels were about 3080 mm high and 5082 mm long and were provided by vertical stiffeners on one side and horizontal stiffener on the other side. The panels were connected to boundary box and H steel columns by using bolted connections.

One of the most important buildings endowed with steel plate shear walls was the 35-storeys high-rise building in Kobe, which was realised in 1988 and subjected to the 1995 Kobe earthquake, without suffer significant damage (Figure 2.77).

The structural system in this building consisted of a dual system composed by steel moment frames and both RC and steel shear walls. RC shear walls were located in the three basement levels, while composite and stiffened walls were used in the first and second floors and above the second floor, respectively. Figure 2.78 shows the typical floor and vertical sections of the building.



Figure 2.77: The 35-storeys building with shear walls in Kobe (in the background) sustained minor damage during earthquake (1995), while the City Office building (in the foreground) lost its 3 top floors

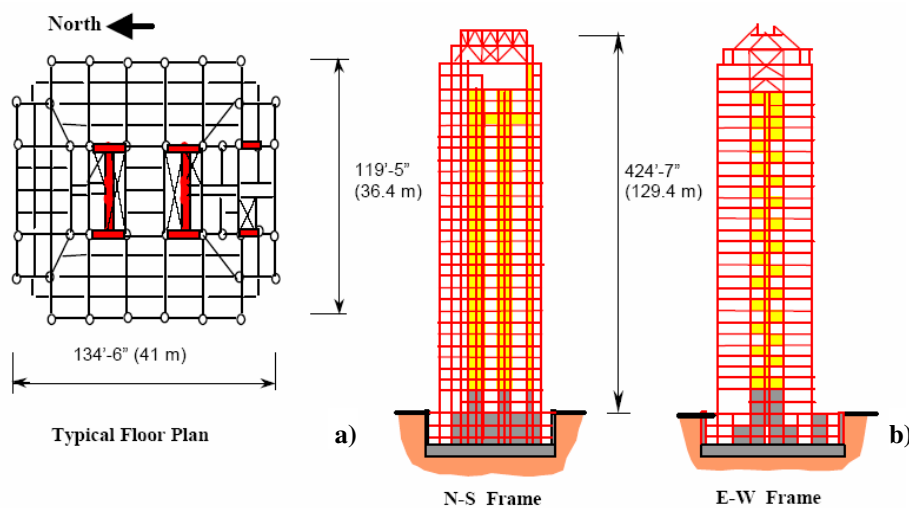


Figure 2.78: Structural plan view (a) and vertical sections (b) of the 35-storeys building in Kobe

The study on the seismic performance of this building (Fujitani et al., 1996) indicated that the damage could consist of both local buckling of stiffened

steel plate shear walls on the 26th storey and a permanent roof drift of both 225mm in northerly and 35mm in westerly directions. The results of inelastic analyses of this structure reported in Fujitani et al. (1996) indicates also that soft stories may have formed at floors between 24th and 28th level of the building. A visual inspection of the structure two weeks after the earthquake did not show any sign of visual damage (Kanada and Astaneh-Asl, 1996).

In the same Country, “low-yield point (LYP)” steel plates have been recently developed and successfully used as steel plate shear walls. The mechanical features of low yield steel, already presented in the previous Sections, allow to realise devices able to dissipate effectively the energy introduced in the structure by quake ground motions. Figure 2.79 shows a building where the low yield point steel is used under form of stiffened shear panels in the core elevator / stairwell shaft of the building..



Figure 2.79: A view of building equipped with Low Yield Point (LYP) steel plate shear walls and a close-up of the walls

Figure 2.80 shows another example of recent application of low-yield point (LYP) steel plate shear walls in a 31-storeys building in Japan. According to Yamaguchi et al. (1998), the LYP steel used in this structure had a 2% offset proof stress (yield point) of 11.6 –17.4 ksi and an ultimate elongation exceeding 50%.

The panels, having thickness comprised between 6.35 and 25.4 mm, were 4600 mm wide by 2800 mm high and presented both horizontal and vertical stiffeners. The prefabricated LYP wall units were connected to the boundary beams and columns by using friction bolts. The walls, designed to remain

elastic under wind load, yielded under the “Level 1” earthquake. The designers reported that, as a result of using low yield steel, the drift values decreased about 30%. In addition, it was demonstrated that the arrangement of LYP steel shear walls in an alternate pattern should reduce bending effects, preventing also the accumulation of gravity load in the wall. As a result, such walls were mainly subjected to shear, whereas relatively small bending effects due to lateral loads were absorbed by moment frames.

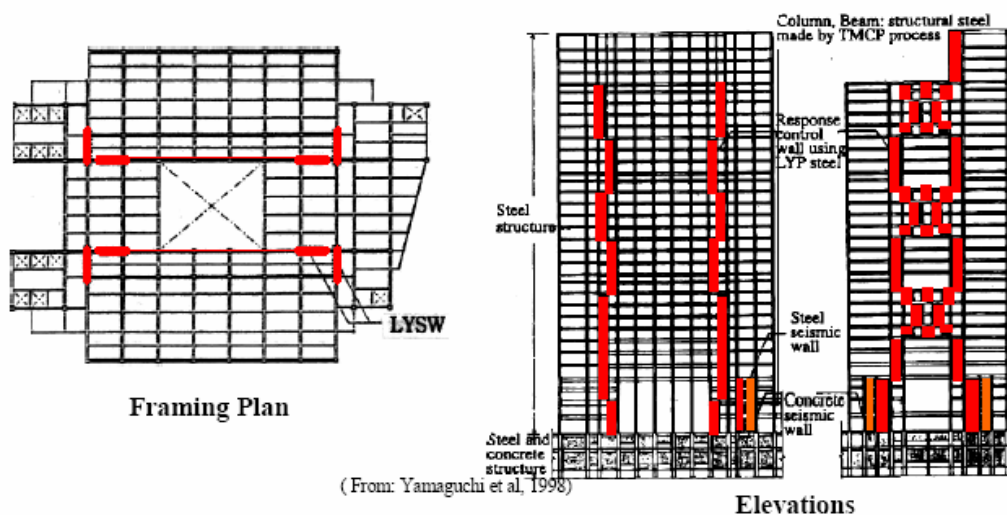


Figure 2.80: Framing plan and elevations of the 31-storeys building in Japan reinforced with low-yield steel shear walls

Not only in Japan, but also in USA there are numerous applications of steel shear walls. A very good example related to the efficient use of such devices in areas with low seismicity but with relatively high wind loads is given by a 30-storeys hotel in Dallas (Texas, USA) (Figure 2.81). Such a building presented steel braced frame in longitudinal direction and steel plate shear walls in the transverse one. The shear walls were able to carry about 60% of the tributary gravity load, while the wide flange columns at the boundary of shear walls resisted the remaining 40%. In this way a significant amount of steel in beams and columns was saved. In particular, the steel used in the shear wall system was 1/3 less than the one necessary in an equivalent structure realised with steel moment resisting frame (Troy and Richard, 1988). Even if

the wind was the governing lateral load, under the design wind force, the maximum drift was 0.0025 only. This was due to relatively high in-plane stiffness of steel plate shear walls.



Figure 2.81: A view of the 30-storeys building in Dallas

Also in a very high seismicity area such as California the use of steel shear walls has been done. The building equipped with steel panels was the new Sylmar Hospital (Figure 2.82 a), which replaced for the reinforced concrete Olive View Hospital that partially collapsed during the 1971 San Fernando earthquake and had to be demolished. The new structure consisted of a steel structure with concrete shear walls in the lower two stories and steel plate shear walls in the perimeter walls of the upper four floors. The used steel shear wall panels were 7700 mm wide and 4774 mm high with thickness variable from 15.8 to 19 mm. They also presented some openings and intermediate stiffeners, as shown in Figure 2.82 b. The steel panels were bolted to plates welded on the columns. The horizontal beams, as well as the stiffeners, were double channels welded to the steel plate to form a box shape, as shown in Figure 2.82 b. According to the designers, (Youssef, 2000) and (Troy and Richard, 1988) the double channel box sections were used to form torsionally stiff elements at the boundaries of steel plates and to increase buckling capacity of the panels.

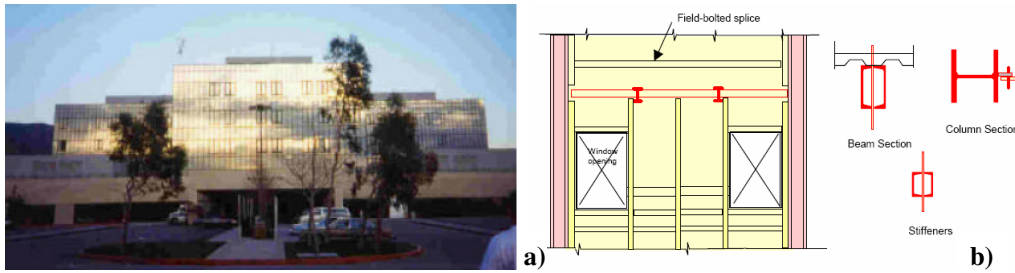


Figure 2.82: Sylmar hospital (California): global view (a) and used steel plate shear walls (b)

The walls were designed for global buckling capacity of the stiffened walls as well as local buckling capacity of the panels bounded by the stiffeners. The tension field action capacity was not used, although the designers acknowledged its presence and considered the strength of tension field action as a “second line of defense” mechanism in the event of a maximum credible earthquake.

The structure was shaken by the 1987 Whittier earthquake and seven years later by the 1994 Northridge earthquake. The investigation of damage to this building in the aftermath of the 1994 Northridge earthquake indicated that there were severe damages to some non-structural elements, such as suspended ceilings and sprinkler system, resulting in the breakage of a number of sprinklers and flooding of some floors. The non-structural damages were clearly indicator of very high stiffness of this structure, which was also the cause of relatively large amplification of accelerations from the ground to the roof level.

Currently, the tallest building with steel plate shear walls in a very highly seismic area of the United States is a 52-storeys building in San Francisco, which has been recently realised. The building, whose rendering is shown in Figure 2.83, is a residential tower with 48 stories above ground and four basement parking levels. In such a building the gravity load carrying system consisted of four large concrete-filled steel tubes at the core and sixteen concrete-filled smaller steel tube columns in the perimeter. The floors outside the core consisted of post-tensioned flat slabs and inside the core and lower floors were typical composite steel deck-concrete slab.

The main lateral load resisting system of the structure consisted of a core made of four large concrete filled steel tubes, one at each corner of the core,

together with steel shear walls and coupling beams. In particular, steel shear walls were connected to concrete filled steel tubes by coupling beams. The shear wall units were primarily shop-welded and bolt spliced at the site at each floor mid-height. The only field welding was the connection of the girders and steel plate shear wall to the large concrete-filled steel tube columns.



Figure 2.83: Rendering of the 52-storeys residential building in San Francisco (California)

A further application of SPSWs will be foreseen into a 22-storeys office building in Seattle (Washington), whose rendering view is depicted in Figure 2.84. The lateral load resisting system will consist of:

- a core with four large concrete filled tubes on its corners;
- steel plate shear walls;
- coupling beams connecting the tubes to each other in one direction and steel braced frames in the other.

Analogously to the 52-storeys structure above discussed, also in this building the steel plate shear wall system will be primarily shop-welded, field bolted with only steel plates and girders welded to the round columns in the

field. Four round concrete-filled tubes will carry the bulk of gravity in the interior of the building. The I-shaped columns within the steel box core will not participate in carrying gravity and will be the main part of the lateral load resisting system, which can be considered to be a dual system of steel shear wall and special moment-resisting frames.



Figure 2.84: A rendering of the 22-storeys office building in Seattle

Chapter III

Numerical evaluation of the metal shear panels response and set-up of design criteria

3.1 INTRODUCTION

In the current Chapter a wide numerical investigation on both compact and slender shear panels has been developed.

Firstly, a preliminary parametric numerical study framed within a large experimental activity recently undertaken at the Department of Structural Analysis and Design of the University of Naples “Federico II” on compact shear panels made of pure aluminium has been carried out. In the numerical investigation stiffened shear panels made of four different metals (two wrought aluminium alloys, LYS steel and mild steel) have been analyzed by sophisticated FEM models in order to outline the influence of the material features on the response of shear panels, emphasising also the different effect of the buckling paths, namely global shear buckling of the panel, flexural buckling of the stiffener and local buckling of the single panel portions. This study has been also able to provide appropriate design charts, allowing the determination of optimal panel configurations in relation to the performance required to shear panels in terms of strength and deformation capacity. Then, on the basis of the above mentioned experimental activity on stiffened pure aluminium shear panels, the numerical simulation of some test results,

selected starting from the conclusions of the numerical study, has been done by means of the implementation of a sophisticated FEM model. Afterwards, a wide numerical analysis has been carried out considering panels with different rib configurations, aiming at emphasizing the influence of the main behavioural parameters on the dissipative capacity of the system. In particular, numerical cyclic analyses have been carried out considering different displacement demand levels, comparing the performance of shear panels characterised by different rib depths. In addition, economical considerations about the most suitable configuration to be adopted as a passive control device into new and existing structures in relation to the estimated displacement demand have been drawn.

In a second investigation phase the behaviour of slender steel shear panels has been analysed. After the implementation of a refined FEM model calibrated on the basis of available experimental results, a parametric analysis on slender steel shear panels has been carried out. In order to assess the influence of the geometry on the structural behaviour of shear plates, the theoretical behaviour of thin steel panels in shear, based on existing simplified methodologies, has been analysed and then compared with the results obtained by an extensive numerical study carried out by means of accurate finite element models. The comparison between theoretical and numerical results has been developed with reference to different values of thickness and by varying the aspect ratio of the plate. Moreover, the influence of intermediate stiffeners has been investigated. In the whole the obtained results have provided useful information for the correct design of slender steel plates in shear to be used as stiffening and strengthening devices in new and existing framed structures.

3.2 COMPACT SHEAR PANELS

3.2.1 *Preliminary analyses*

In the present Section, as a preliminary phase of the experimental campaign undertaken at the University of Naples “Federico II” on stiffened pure aluminium shear panels, which has been widely described in the Chapter 2, parametric studies have been performed in order to define appropriate shear

panel configurations, based on the choice of optimum values of their geometrical parameters (width-to-thickness ratio and flexural rigidity of applied stiffeners), to be used as dissipative devices for passive seismic protection of framed buildings. The reference experimental activity has been based on the use of 5 mm thick aluminium panel specimens, measuring 1500 by 1000 mm, which have been inserted into a very rigid and pinned steel frame equipped with lateral braces. Such panels were stiffened with longitudinal and transversal open rectangular-shaped stiffeners, which have been drawn from the same aluminium sheets utilized for the plates. Different rib arrangements were considered in order to assess their influence on the ductility and hysteretic behaviour of aluminium shear panels. In the current investigation, for a defined rib arrangement, the optimal spacing and depth have to be selected accordingly, in order to fulfil the requirements given in the Chapter 2 and in particular to ensure a shear buckling of the plate delayed after the shear yielding with a preliminary hardening ratio α .

Aiming at developing an appropriate parametrical study, appropriate FEM models have been set up so to investigate the effect of the main influential parameters on the performance of the structural system under consideration (Panico et al., 2003; De Matteis et al., 2004a). In particular, in this phase of the study, the shear panel under consideration is characterized by stiffeners alternatively placed on each side of the plate in order to have 4 x 6 portions having dimensions of 250 x 250 mm (“type F” in Figure 3.1c).

The monotonic and cyclic behaviour of such panels with different configurations in terms of aspect ratio and stiffener depth have been investigated by using the ABAQUS non linear numerical analysis program (Hibbitt et al., 2004), taking into account the influence of geometrical imperfections, the actual inelastic properties of the material, the influence of ribs and the interaction with the surrounding loading frame.

In particular, beam and column members of the loading frame are obtained by using double channel profiles (depth equal 200 mm) and connected to each other with pin joints at the four corners (Figure 3.1 a). They have been modelled by using B31 BEAM elements, while S4R SHELL finite elements have been used to model aluminium plate and the stiffeners. The bolted connection system between panel and frame has been modelled by using SPRING elements characterized by large stiffness values. As a result of a

preliminary mesh sensitivity study, a mesh of 50x50 mm has been considered. The input load is applied to the top beam of the external lateral reaction frame.

A global view of the implemented FEM model is shown in Figure 3.1 b).

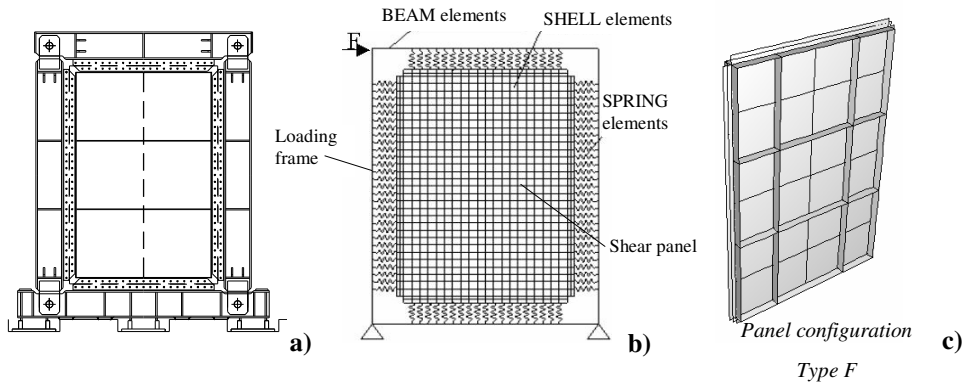


Figure 3.1: FEM modelling: the considered shear panel geometry (a), preliminary (b) and final (c) FEM model

The influence of initial geometrical imperfections induced by fabrication phases, shrinkage of welds and out-of-plane deflection of boundary loading frame on the mechanical behaviour of thin plates under shear load has been evaluated by an appropriate imperfection sensibility study related to both shape and magnitude of the imperfections. With regard to the shape, the following imperfections have been assumed:

- out-of-plane displacement applied to a corner of the panel;
- initial deformed shape determined according to the first critical mode;
- initial deformed shape determined according to a combination of the first four critical modes;

With regard to the maximum amplitude of imperfections, the following values have been considered:

- 1.5 mm corresponding to 1/1000 of H_p ;
- 3.0 mm corresponding to 1/500 of H_p ;
- 15.0 mm corresponding to 1/100 of H_p ;

where H_p is the panel height. By comparing the corresponding monotonic response under shear loading, any significant difference has been noted, demonstrating the slight sensitivity of the system under consideration to geometrical imperfections (De Matteis et al., 2004b). For this reason in the

following analyses, geometrical imperfections have been included by considering an out-of-plane displacement equal to 3.0 mm applied to one upper corners of the panel.

In order to provide major generality to the results of the following parametric study, in the developed numerical model, the eccentricity between external frame members and the internal plate element due to connecting system and also the cross-section dimension of the frame members have been neglected. Namely, the frame member axes have been considered coincident with the plate edges (Figure 3.1 c) (De Matteis et al., 2005a).

In the current numerical model, as base material for shear panels, four different metals have been considered. In fact, in addition to LYS steel and almost pure aluminium (EN-AW 1050A) that have been already assumed as convenient materials to build up dissipative metal shear panels (De Matteis et al., 2003; Nakagawa et al., 1996), a different aluminium alloy (EN-AW 5154A) and a traditional Fe360 steel have been considered as well. The former has been chosen because it is an aluminium alloy with a quite large ductility and a reasonably limited strength, easily available on the market, it being commonly used in the marine and shipbuilding industry. The latter has been selected for comparative reasons, it being the material more economical and easily available. The above material selection allows the comparison in terms of performance of shear panel made with materials having different yielding strength, elastic modulus and also hardening features. It is worth noticing that the two aluminium alloys considered in this study are commercial materials that have been subjected to heat treatment to improve their mechanical features (reduce the yield stress and increase the ductility). Therefore, the relevant stress-strain relationships have been defined according to material tests carried out at the Laboratory of the Department of Structural Analysis and Design of the University of Naples “Federico II”. Contrary, for LYS steel and mild steel Fe360, a Ramberg-Osgood model and a tri-linear constitutive law have been used, respectively. In particular, the former model has been defined on the basis of existing experimental results (Nakashima et al., 1994). The mechanical features of the considered materials are listed in Table 3.1, where $f_{0.2}$ indicates either the conventional yield strength (aluminium alloys and LYS steel) or the yield strength f_y (Fe360 steel), while the assumed stress-strain relationships are drawn in Figure 3.2.

Table 3.1: Metal materials considered in the numerical analyses

Material	$f_{0.2}, (f_y)$ (Nmm ⁻²)	f_u (Nmm ⁻²)	ϵ_u (%)	E (Nmm ⁻²)	$E/f_{0.2}$	$\alpha = f_u/f_{0.2}$
Fe360 steel	(235)	360	25	210000	893	1.53
LYS steel	86	254	40	210000	2441	2.95
Pure aluminium (EN-AW 1050A)	21.3	80	45	70000	3286	3.76
Aluminium alloy (EN-AW 5154A)	75.2	203.6	18	70000	931	2.71

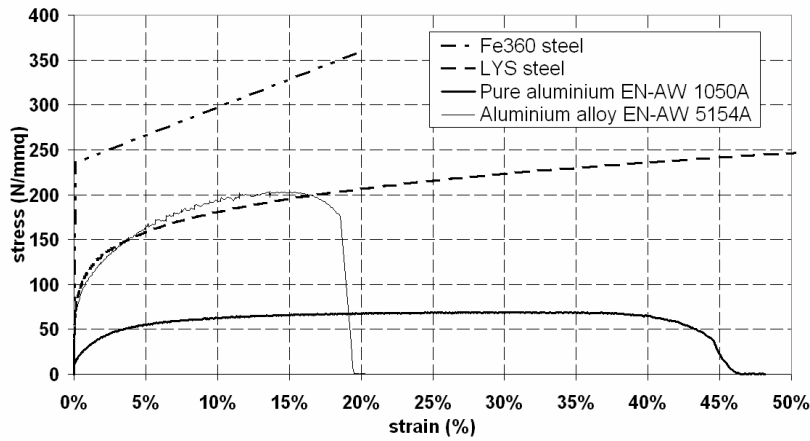


Figure 3.2: Assumed stress-strain curves for metal materials under consideration

The aim of the study is to define useful design tools for the selection of shear panels made with different base materials in order to ensure a suitable behaviour of the panel under both monotonic and cyclic loading conditions in relation to the shear deformation demand. Based on the panel configuration type F previously defined, the numerical study has been carried out ranging the width-to-thickness ratio of the plate elements and the second moment of area of the ribs (De Matteis et al., 2005b). In particular, the stiffness of the ribs has been changed by varying their depth, while their thickness has been assumed equal to the one of the sheeting. The analyses have been carried out by assuming width-to-thickness ratios b/t equal to 25, 37.5, 50, 75, 100 and 200, where the distance between the ribs b is constant and equal to 250 mm,

while the thickness of the plate t ranges from 1.25 mm to 10 mm. The b/t ratios and the corresponding values of examined depths of the ribs h_{st} are given in Table 3.2.

Table 3.2: Depth of ribs h_{st} (in mm) for the considered configuration

$b/t=25$	$b/t=37.5$	$b/t=50$	$b/t=75$	$b/t=100$	$b/t=200$
0	0	0	0	0	0
10	10	10	10	5	5
20	20	20	20	10	10
40	40	30	30	20	15
60	50	40	40	30	20
80	60	50	45	40	25
100	70	60	50	45	30
110	80	70	55	50	32
118	92	77	60	55	35
120	100	80	70	60	40
150	120	100	80	70	45
185	144	120	93	78	51

It is worth noting that for each ratio b/t , the case of ribs having a second moment of area equal to $I_{st,lim}$ has been also considered (bold numbers in Table 3.2), where $I_{st,lim}$ is the limit value beyond which the stiffeners may be considered as “rigid”. It is assumed as sum of moments of inertia of the n_{st} intermediate transverse stiffeners placed in the panel and it has been calculated according to EC3 (EN 1993-1-1, 2005) and EC9 (EN 1999-1-1, 2006) provisions, considering that $b/h_w < \sqrt{2}$, where h_w is the width of panel equal to 1000 mm.

For each value of b/t ratio, the second moment of area $I_{st,lim}$, the corresponding limit values of the stiffener depth $h_{st,lim}$ and the corresponding normalized stiffness parameter $\gamma_{st,lim}$ are listed in Table 3.3, where the normalized stiffness parameter γ_{st} is calculated by the following equation, where a constant value of Poisson’s ratio $\nu=0.3$ has been assumed:

$$\gamma_{st} = \frac{E \cdot (I_{st}/n_{st})}{bD} = \frac{12 \cdot (1-\nu^2) \cdot (I_{st}/n_{st})}{b \cdot t^3} \quad (3.1)$$

Table 3.3: $I_{st,lim}$ values according to EC3 and EC9

b/t	$I_{st,lim} \text{ (mm}^4\text{)}$	$\gamma_{st,lim}$	$h_{st,lim} \text{ (mm)}$
25	24.000.000	210	118
37,5	7.111.111	210	92
50	3.000.000	210	77
75	888.889	210	60
100	375.000	210	50
200	46.875	210	32

The monotonic analyses of the several examined configurations of panel have been given in terms of $F/F_{0.2} - \gamma$ curves, where $F_{0.2}$ is the yielding shear force calculated by assuming an uniform distribution of yielding shear stress (evaluated according to either f_y or $f_{0.2}$, see Table 3.1) along the width of panel $B=1000$ mm and γ is the shear deformation. All the analyses have been worked up to 20% of shear deformation, which can be considered as a limit value for practical applications.

In Figure 3.3, for the sake of comparison, $F/F_{0.2} - \gamma$ curves for a value of b/t equal to 25 are presented for each material. They highlight the increased effect of depth ribs on the global plastic response of shear panels. The comparison among different materials clearly emphasises that the best performance in the plastic range is provided by the AW 1050 aluminium alloy, it being characterised by the highest strain hardening and the most convenient $E/f_{0.2}$ ratio. On the contrary, the worst performance is exhibited by Fe360, which is characterised by a poor post-elastic behaviour and by a larger value of yield strength, strongly increasing the susceptibility of shear panel to buckling. It is also emphasised that the performance of LYS steel and AW 5154 aluminium alloy are very similar to each other, they being characterised by similar values of yielding strength.

Anyway, it can be noticed that in all the cases, for each b/t ratio, for increasing values of ribs stiffness, the obtained $F/F_{0.2} - \gamma$ curves approach a sort of envelope curve, which correspond to the plastic failure of the system. As far as the stiffener depth decrease, the separation from the envelope curve is representative of global buckling involving the stiffeners. Then, the post-buckling behaviour is characterized by tension field mechanism, which can be either of local or global type, depending on rib stiffness, which can be such to

exclude them or not from the buckling mechanism. Also, typical collapse mechanisms of examined shear panels are shown in Figure 3.4.

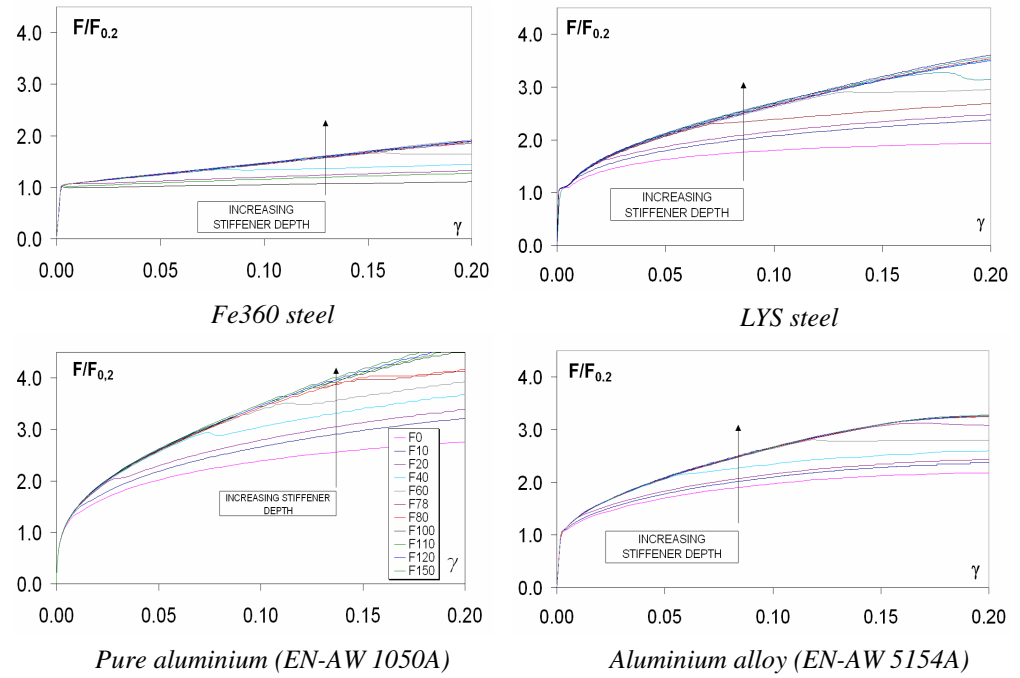


Figure 3.3: $F/F_{0.2}$ - γ curves for panel configuration characterised by $b/t = 25$ and different stiffeners depth

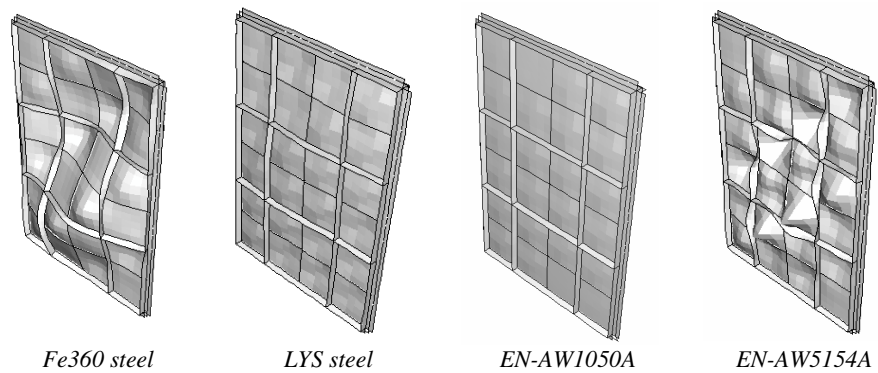


Figure 3.4: Typical buckling mechanisms for analysed shear panels

It can be noticed as for a given shear panel configuration ($b/t = 100$, $h_{st} = 40$ mm) and shear deformation ($\gamma = 10\%$), the deformation mechanism of the

system is material dependent. In particular, the obtained out-of-plane displacements of shear panels show as the shear buckling phenomenon (of global and local type) is decreasing going from Fe360 steel to pure aluminium.

In Figure 3.5, the shear strength levels $F/F_{0.2}$ for all the examined cases are plotted as a function of the normalised stiffness parameter γ_{st} for a typical value of shear deformation $\gamma = 7.5\%$. These curves allow the definition of an optimal value of the stiffness parameter ($\gamma_{st,opt}$). In fact, such curves show that the shear strength of the system increases with the rib stiffness up reaching a maximum value identified by the curve plateau. Therefore, $\gamma_{st,opt}$ can be defined as the one corresponding to the attainment of such a maximum value of the shear strength. Obviously, the optimal value of the stiffness parameter ($\gamma_{st,opt}$) regarding the material under consideration, depends on the prefixed value of shear deformation level γ , which could be intended as the design deformation demand for shear panels.

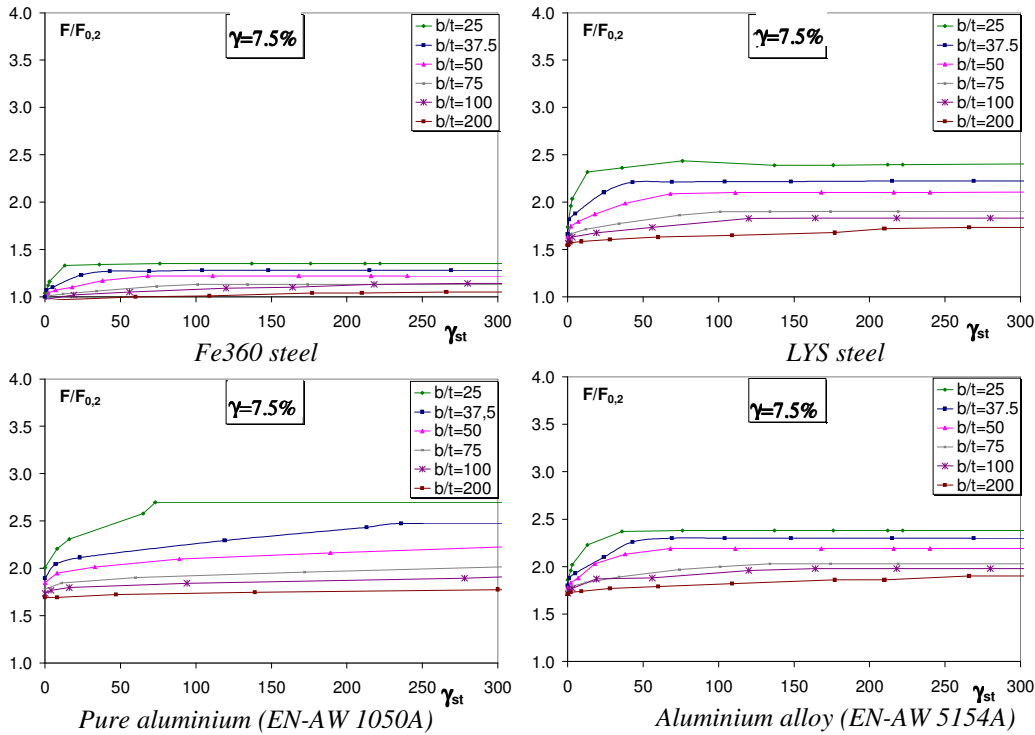


Figure 3.5: $F/F_{0.2} - \gamma_{st}$ curves for shear deformation $\gamma = 7.5\%$

For each material, the results obtained for different shear deformation levels (γ ranging from 2.5% to 15%) can be summarized into single design charts (Figure 3.6), where for a given design value of shear strength $F/F_{0.2}$ and shear strain γ , both the b/t ratio and the optimum value of the stiffness parameter $\gamma_{st,opt}$ are obtained.

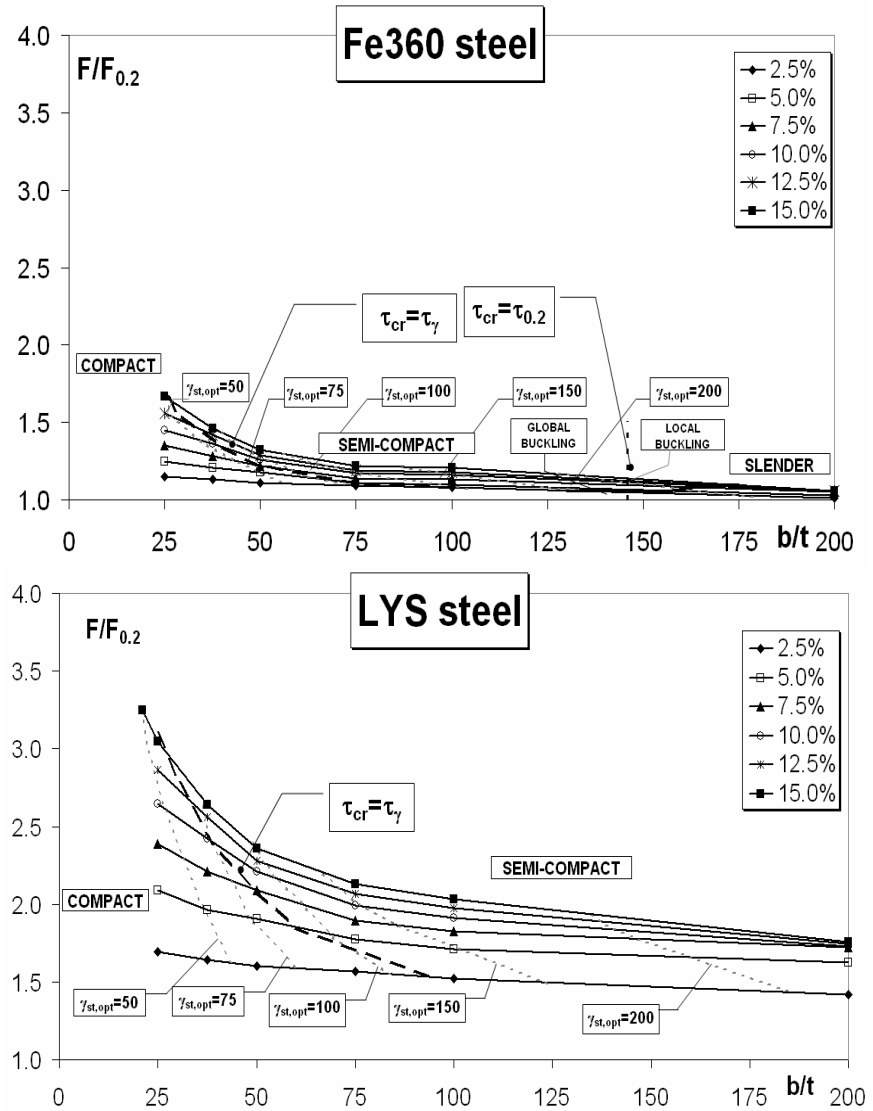


Figure 3.6: Design chart for shear panels (continues)

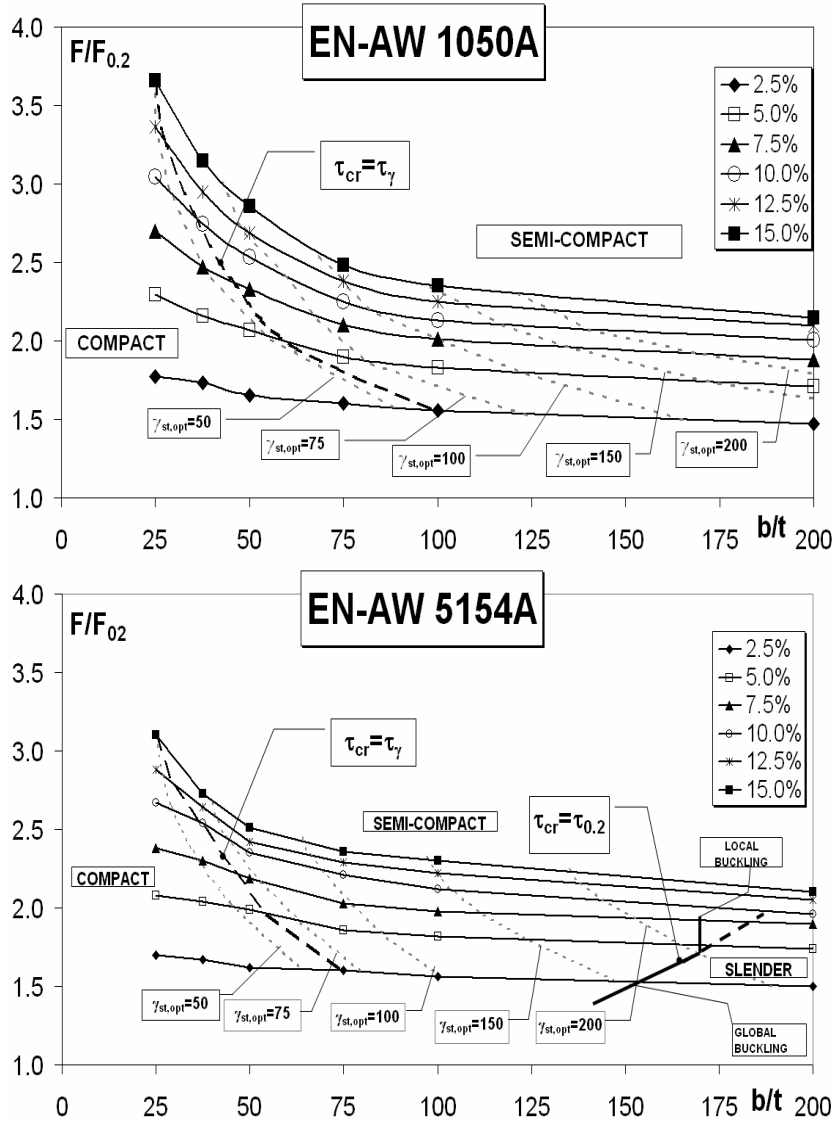


Figure 3.6: Design chart for shear panels

In the same charts the limits related to the attainments of buckling phenomena are reported as well. In particular, the buckling limits placed on the right side of the diagram (large b/t values) are related to the attainment of elastic buckling ($\tau_{cr} \leq \tau_{0.2}$) (elastic buckling curve), which clearly represents a limit for the use of shear panels as a dissipative device. Obviously, such

buckling phenomena could be either of local or global type, depending on the panel configuration. In particular, global buckling is more relevant for reduced shear deformation levels, where the applied ribs have a lower flexural stiffness. Shear panel configurations falling on the right of the above buckling curve can be defined as “slender”, meaning that they suffer buckling phenomena before being involved into plastic deformation. Similarly, the buckling curves depicted on the left side of the above charts (small b/t values) are representative of panel configurations where the buckling phenomena occur for shear stress (τ_{cr}) equal or larger than the one corresponding to the attainment of the design deformation demand (τ_γ) (plastic buckling curve). Shear panel configurations falling on the left of the above buckling curve can be defined as “compact”, meaning that they do not suffer buckling phenomena up reaching the required plastic deformation. As a consequence, shear panel configurations falling between plastic buckling curve and elastic buckling curve can be defined as “semi-compact”, meaning that suffer buckling phenomena while developing plastic deformation.

From the comparison of the above diagrams in relation to the different materials, the following considerations can be drawn:

- LYS and AW 1050 aluminium alloy shear panels clearly allow a better exploitation of the system characteristics, as it appears from the attained $F/F_{0.2}$ ratios. They allow the use of reduced rib stiffness (γ_{st}) and/or larger local slenderness ratio b/t for a given plastic deformation demand (γ). It can be also noticed that in such a case all the analysed panel configuration fall into the “compact” and “semi-compact” range, and the plastic buckling curve ($\tau_{cr} \geq \tau_\gamma$) is moved towards larger values of b/t ratios.
- For a defined shear deformation level and for a specific b/t ratio, AW 1050 aluminium alloy shear panels allow to obtain the maximum strength level $F/F_{0.2}$ with the minimum value of the rib stiffness in comparison to the other materials.
- For a reduced strain hardening factor α , the obtained curves show a significant reduction of their variability range, emphasising the possibility of a reduced exploitation of the system post-elastic resources.

In conclusion, by the comparison of four metals, it appears that pure aluminium shear panels provide a better performance, due to the exploitation of their plastic characteristics in terms of both strain hardening and ductility,

allowing the use of ribs with a lower flexural stiffness and also of larger b/t ratios. On the contrary, the traditional Fe360 steel exhibited a poor post-elastic behaviour owing to both a larger value of yield strength and a lower strain hardening. Also, aluminium alloy AW 5154A and LYS steel provide a similar performance, which is intermediate between the above ones. Finally, the numerical study allowed to identify for each material the ranges of b/t ratio where shear buckling phenomena take place in the elastic phase, during the plastic phase or after a predefined value of plastic shear deformation γ , allowing the correct definition of “slender”, “semi-compact” and “compact” shear panel classes.

3.2.2 Numerical simulation of experimental tests

In the present Section, aiming at evaluating the dissipative capacity of pure aluminium stiffened shear panels, a numerical investigation is developed, varying the configuration of the applied ribs. In particular two typologies of shear panels, endowed with ribs applied by means of discontinuous welds and already tested (see Chapter 2), have been considered for the execution of the numerical study. The first one (identified as “Panel type B”) presents the stiffeners located in the same position on both plate sides, determining square portions with a base dimension of 500 mm (Figure 3.7 a). The second one (identified as “Panel type F”) is characterised by ribs alternatively placed on the two sides of the plate, defining square panel portions of 250mm side length (Figure 3.7 b).

Aiming at developing a parametrical study to investigate the effect of the main influential parameters on the performance of the structural systems under consideration, two FEM models have been set up by using the ABAQUS non linear numerical analysis program (Hibbit et al.,2004) (Figure 3.8). In a subsequent phase of the research, the numerical models should be used as a sort of virtual laboratory to develop useful design methods, which take into account all the main parameters conditioning the seismic response of the systems, as well as to define optimum geometrical configurations of shear panels in relation to the required deformation capacity and energy dissipation capability.

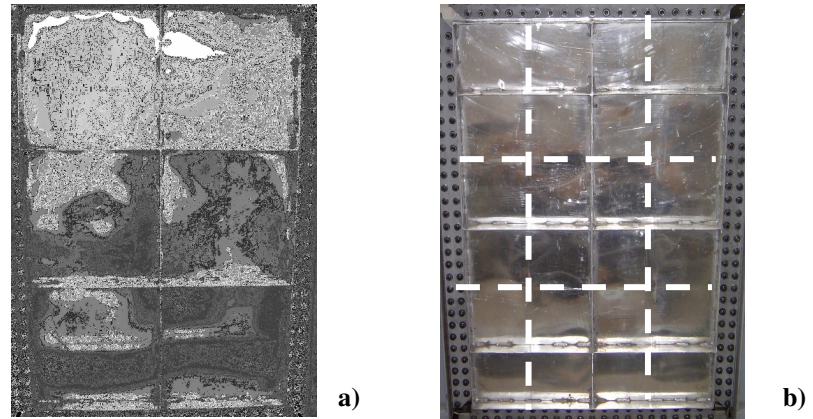


Figure 3.7: The tested shear panels: type B (a) and type F (b)

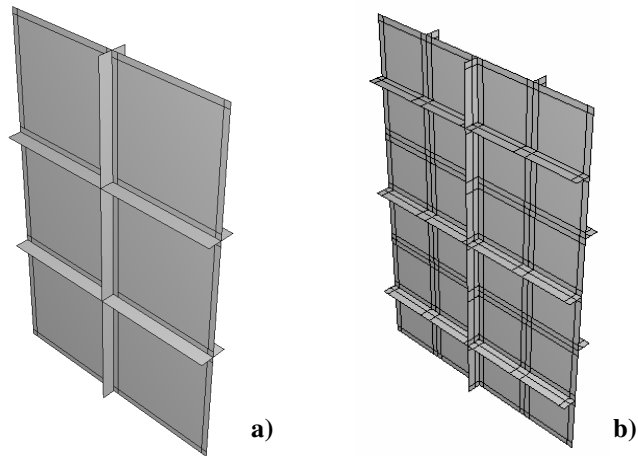


Figure 3.8: Numerical models: panel type B (a) and type F (b)

The base material has been modelled taking into account its actual non linear behaviour, according to performed uniaxial tensile tests. In addition, for evaluating the influence of the heat affected zone (HAZ) of panel portions deriving from the presence of welding connections between ribs and the aluminium sheet, a reduced conventional yield stress $f_{0.2}$, which has been assumed equal to half of the primitive one, has been considered for a distance of 25 mm from the spot-weld locations. On the contrary, the ultimate stress f_u and the corresponding ultimate deformation ϵ_u of the HAZ have been assumed as for the non-affected material.

Beams and columns of the external frame have been modelled by using a two-node linear B31 BEAM element, while the S4R SHELL finite element has been used to model the aluminium sheeting and the stiffeners.

In the FEM models, the actual eccentricity between the external frame members and the internal plate element due to the connecting system and the size of the member cross-sections has been considered (De Matteis et al., 2005 a). The steel frame-to-panel connection, which is realised by means of tightened steel bolts located for each 50 mm, has been introduced in the model by considering that no slip between the different parts occurs. This has been modeled by using the TIE constraint in the ABAQUS program library, which has been applied on the panel sides and the corresponding frame member. The same command has been used to model the interaction between the stiffeners and the aluminium plate. In particular, for ribs located only on one panel side, fixed connection points has been considered every 50 mm, for simulating the presence of welds. In this case, appropriate contact conditions were used for the remaining parts of the stiffeners-plate interface. On the other hand, for ribs located in the same position on both panel faces it was possible to assume a continuous tie.

According to the experimental lay-out, the external load was applied to the top beam of the external lateral reaction frame. The system response has been obtained by applying the modified Riks algorithm, which uses the Newton-Raphson procedure and belongs to the “arc-length” analysis method. In this algorithm the equilibrium condition is determined by iterative runs which move along the same equilibrium curve.

A preliminary mesh sensitivity study has been carried out for shear panel type B in order to determine the optimal discretization able to provide the best compromise between accuracy of results and analysis time consuming (Formisano et al., 2006b). In particular, the results of three different numerical models, characterised by a mesh with square elements having side equal to 12.5 mm, 25 mm and 50 mm (named Bm12.5, Bm25 and Bm50, respectively), have been compared in terms of monotonic curves and energy dissipation capacity for the same significant displacement levels observed during the experimental test (Figure 3.9).

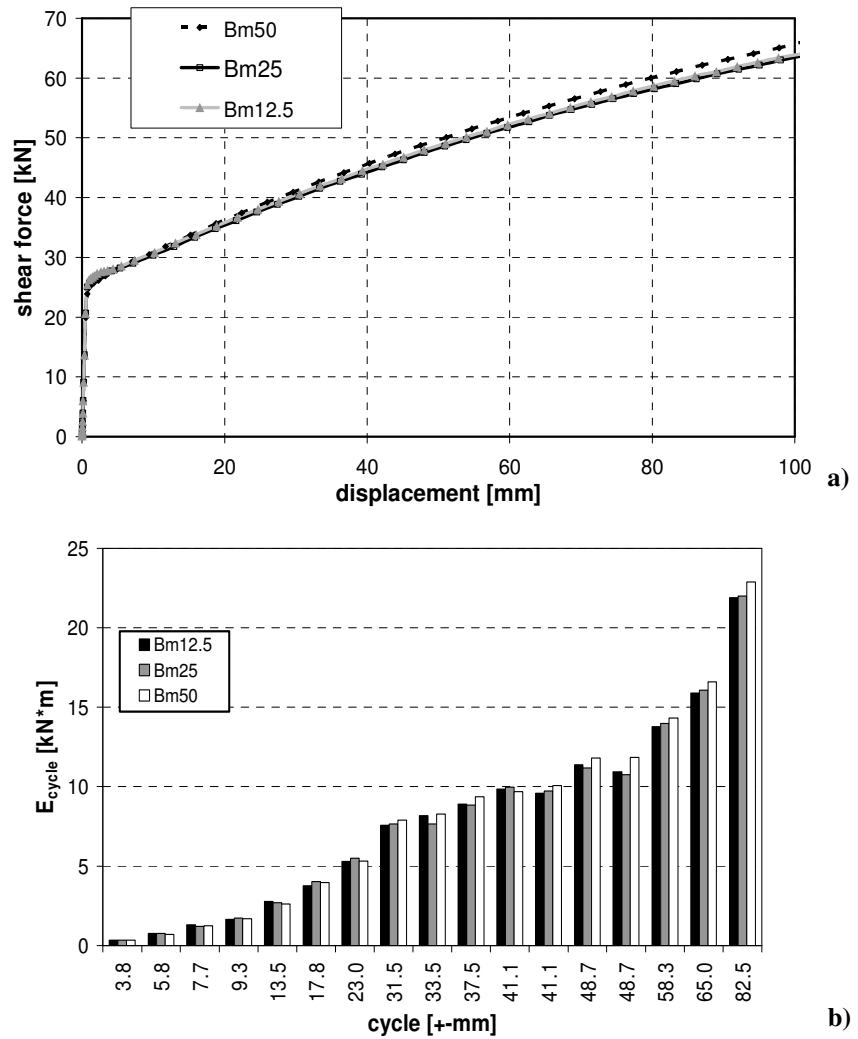


Figure 3.9: Results of mesh sensitivity study: monotonic response (a) and energy dissipation capacity (b) of analysed shear panels

From the examination of the obtained results, it is apparent that the best mesh to be adopted is the one characterised by 25x25 mm base elements, as the slightly lower accuracy level offered in comparison to the one with 12.5x12.5 mm elements is compensated by the high reduction of analysis time (approximately three times).

The mesh adopted for performing the following analyses is shown in Figure 3.10 for both shear panel type B and type F.

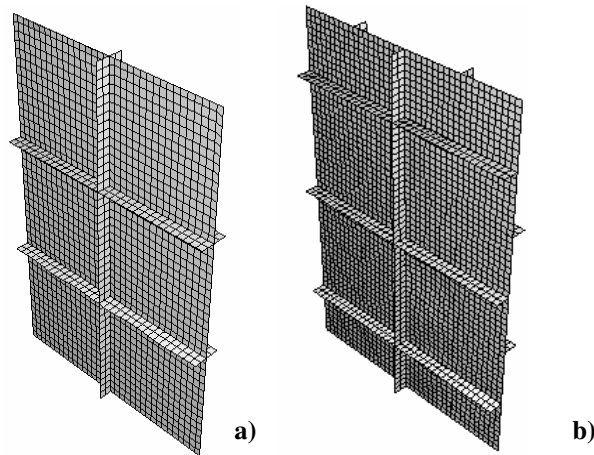


Figure 3.10: Adopted mesh: shear panel type B (a) and type F (b)

The mechanical behaviour of thin plates under shear load can be significantly influenced by initial geometrical imperfections induced by fabrication phases, shrinkage of welds and out-of-plane deflection of boundary loading frame. On the basis of previous buckling analyses (De Matteis et al., 2004a), the imperfection shape has been assumed according to the first buckling mode. Anyway, in order to improve the accuracy of the numerical simulation, a detailed survey of the initial out-of-plane displacement of tested shear panels has been carried out. In particular, the actual imperfection level has been assumed in the two numerical models considering the maximum out-of-plane of the middle point of each panel portion revealed on the initial testing specimen. Then, for each panel portion, a sinusoidal shape of the imperfection has been assumed, with a zero value on the boundary stiffeners (Figure 3.11).

According to the numerical models above defined, in the following, numerical and experimental results are compared, considering the main parameters characterising the behaviour of the systems in terms of dissipated energy, secant global stiffness and equivalent viscous damping ratio, which are defined in Figure 3.12.

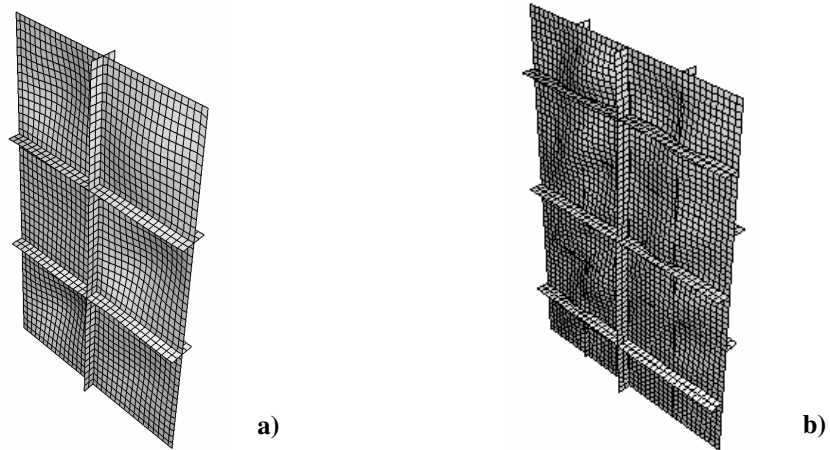
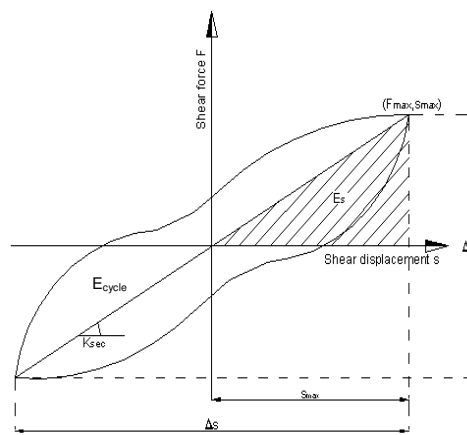


Figure 3.11: Initial imperfection shape of shear panel type B (a) and type F (b)



$$E_{cycle} = \frac{1}{8} \Delta F \cdot \Delta s$$

$$v_{eq} = \frac{1}{4\pi} \frac{E_D}{E_S}$$

$$K_{sec} = \frac{\Delta F}{\Delta s}$$

Figure 3.12: Definition of dissipated energy (E_{cycle}), equivalent viscous damping (v_{eq}) and secant shear stiffness (K_{sec})

The comparison is proposed for hysteretic loops characterised by medium-high lateral displacement only. In fact, it has to be considered that the main aim of the whole study is to propose a system able to provide a significant dissipative capacity in a wide deformation range.

In addition, since the elastic strength of the adopted material is extremely limited, the initial stresses and the effect of welding have a significant and not easily predictable influence on the response of the system in the early deformation stages. At this phase of the research, exact information on the effect of residual stresses to be accounted in the model are not available yet.

Therefore, they have not been incorporated into numerical models. This should explain the discrepancies of results in the very initial phases of the loading process. On the contrary, for large deformations, the reliability of the proposed numerical model is clearly evident (Figures 3.13 and 3.14) (Formisano, 2006).

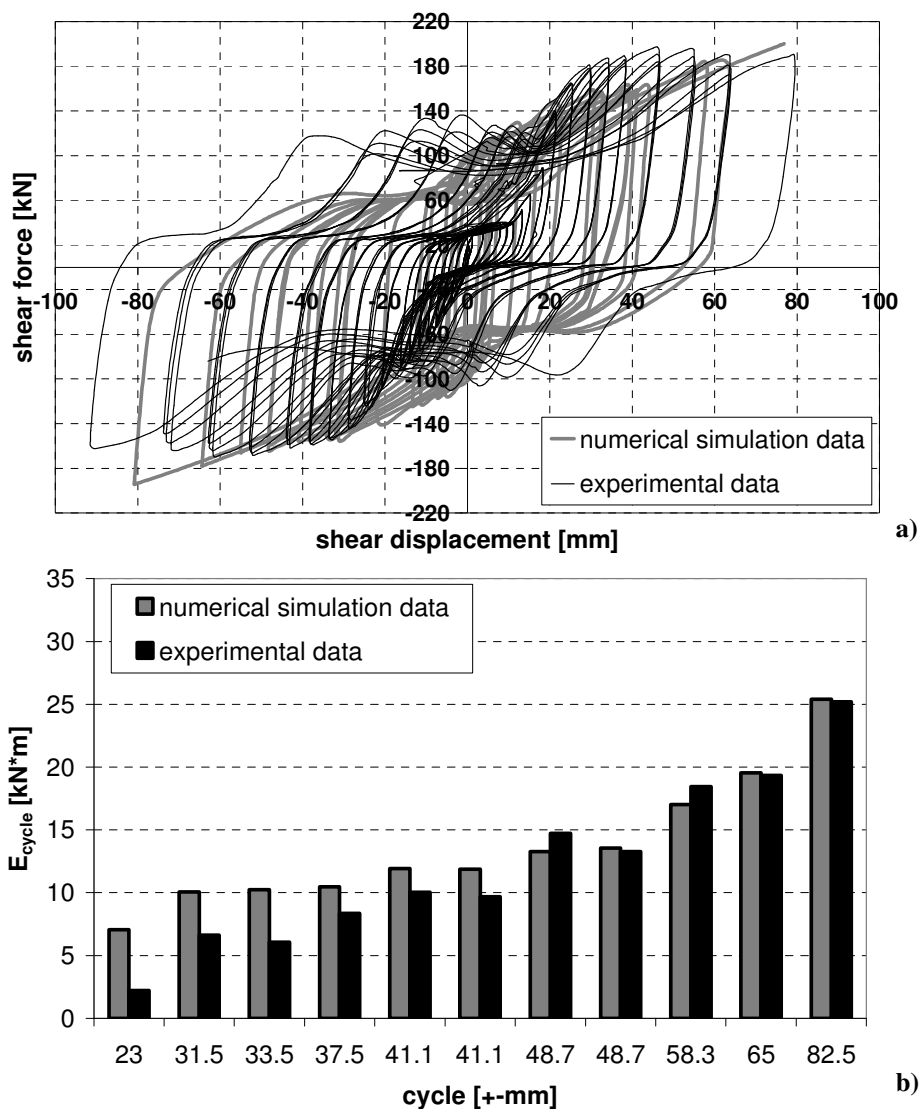


Figure 3.13: Comparison between experimental and numerical results for the panel type B: (a) cyclic behaviour, (b) dissipated energy, (c) secant global stiffness, (d) equivalent viscous damping ratio (continues)

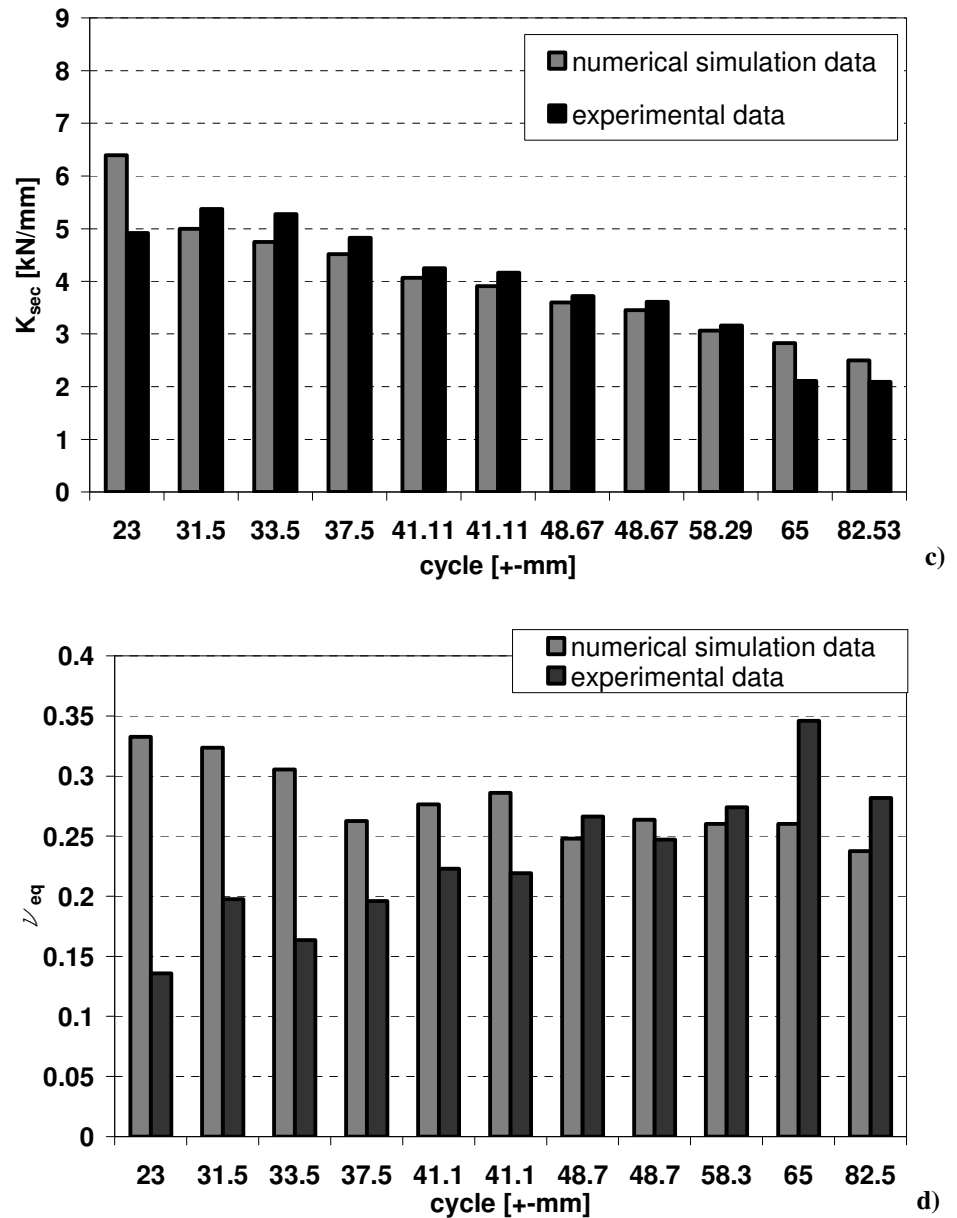


Figure 3.13: Comparison between experimental and numerical results for the panel type B: (a) cyclic behaviour, (b) dissipated energy, (c) secant global stiffness, (d) equivalent viscous damping ratio

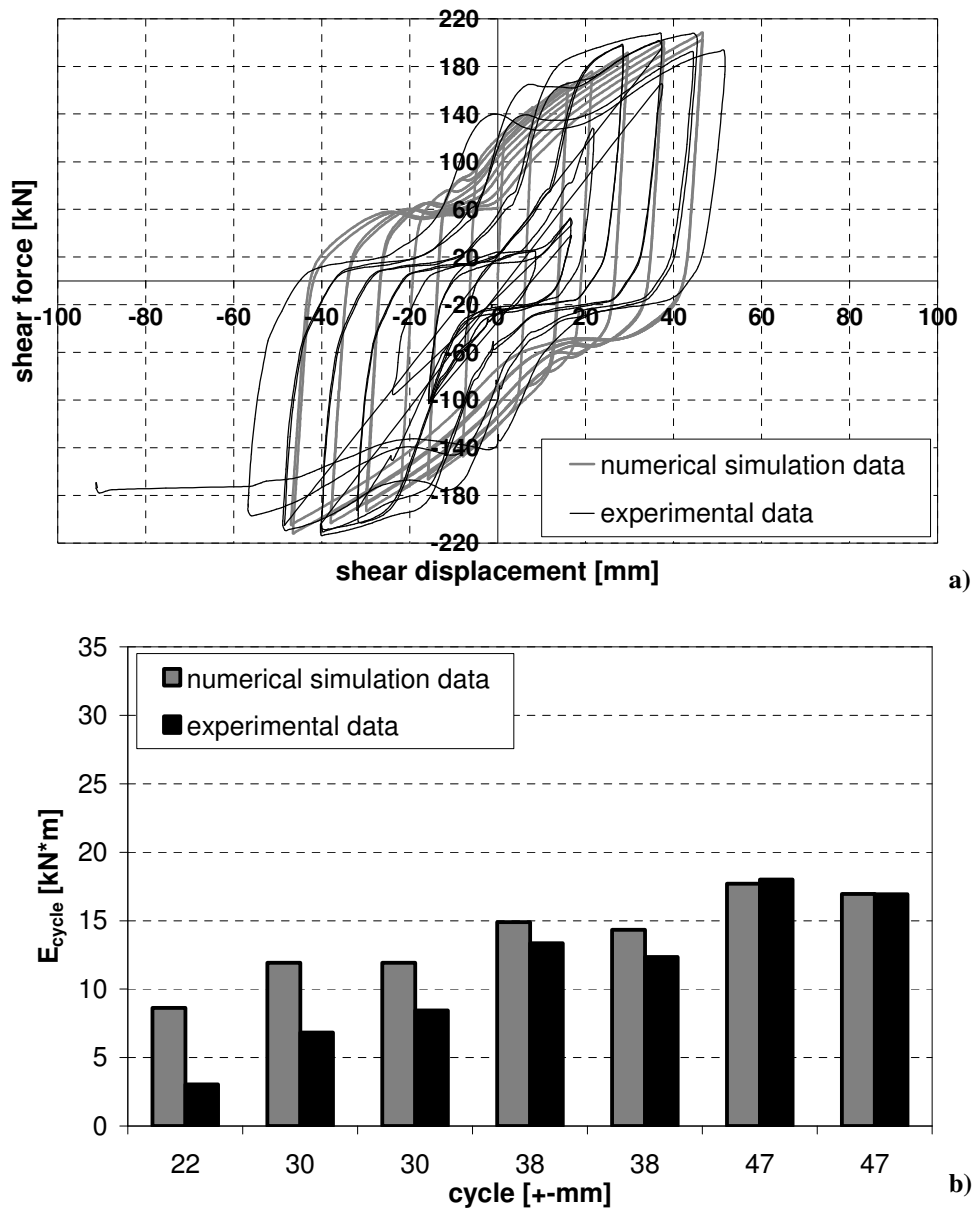


Figure 3.14: Comparison between experimental and numerical results for the panel type F: (a) cyclic behaviour, (b) dissipated energy, (c) secant global stiffness, (d) equivalent viscous damping ratio (continues)

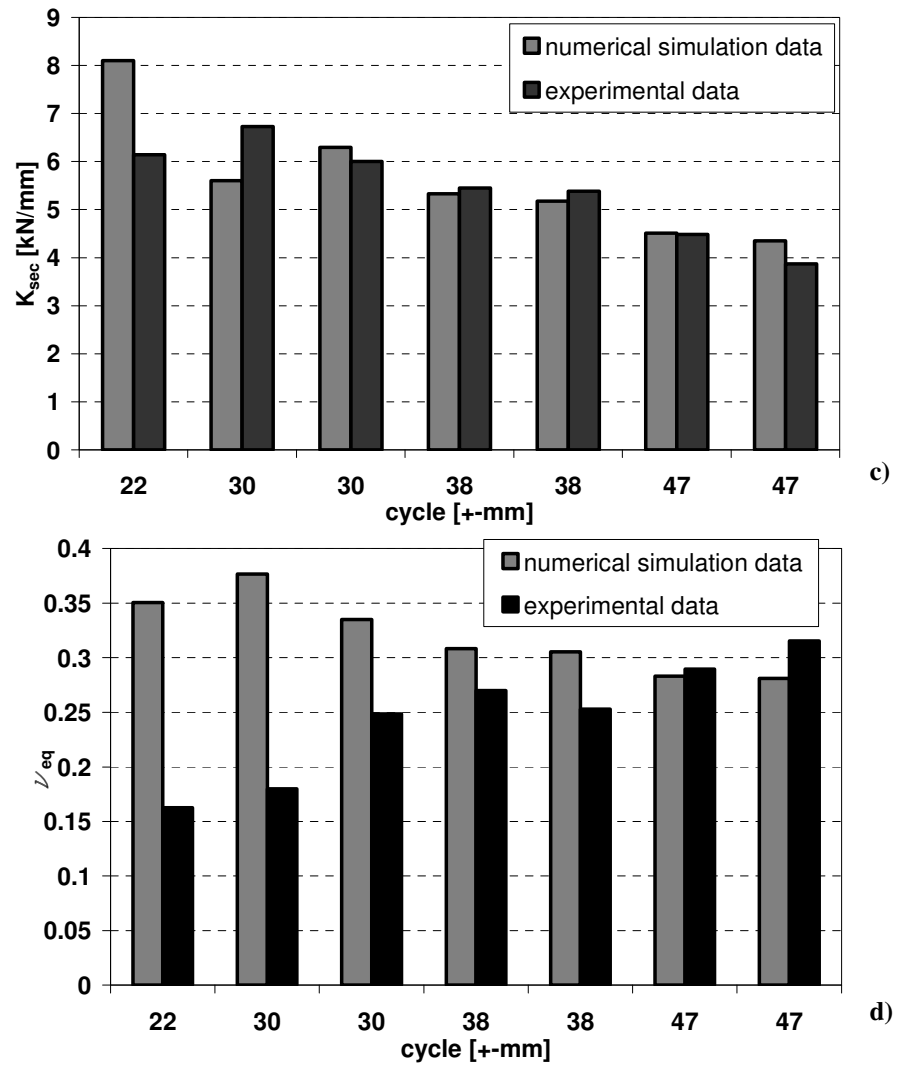


Figure 3.14: Comparison between experimental and numerical results for the panel type F: (a) cyclic behaviour, (b) dissipated energy, (c) secant global stiffness, (d) equivalent viscous damping ratio

In fact, when significant displacements are applied, it is apparent that the implemented FEM model provides accurate results in terms of both shear stress-shear strain curves and the main global features of the systems (energy dissipation capacity, global secant stiffness and equivalent damping ratio).

The proposed numerical model is also able to well identify the collapse

mode exhibited by tested specimens as it appears from the comparison in terms of deformed shapes shown in Figures 3.15 and 3.16 for panel type B and F, respectively, which are related to a deformation amplitude of about ± 40.00 mm.

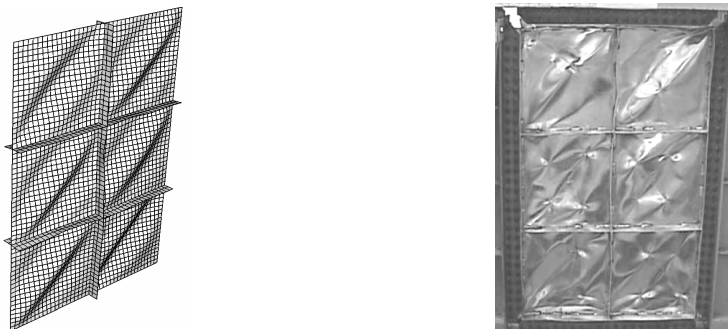


Figure 3.15: Numerical – experimental comparison in terms of deformed shape for panel type B

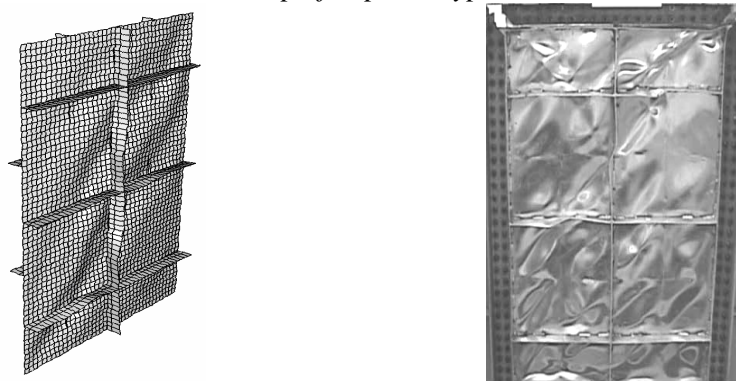


Figure 3.16: Numerical – experimental comparison in terms of deformed shape for panel type F

3.2.3 Parametric study

Based on the above FEM model, it is possible to modify the main geometric parameters conditioning the response of the systems aiming at determining the optimal configuration of the shear panels in terms of energy dissipation capability (Formisano et al., 2006d).

In the following, a parametrical analysis carried out on both panel types B and F, by varying the rib flexural stiffness, is presented. The analysed shear panels are identified with the “Apx” acronym, where “A” denotes the specific

configuration (B or F), “p” represents the analysis typology (parametric) and “x” defines the rib depth.

For each shear panel, ten hysteretic loops, characterised by displacement amplitudes varying from ± 10 mm to ± 100 mm, have been considered. In particular, a comparison between the different configurations in terms of hysteretic cycles is represented in Figure 3.17, showing how the occurring buckling phenomena cause different pinching effects on the behavioural curves. Moreover, the obtained results for both panel types, in terms of dissipated energy, are provided in Figure 3.18.

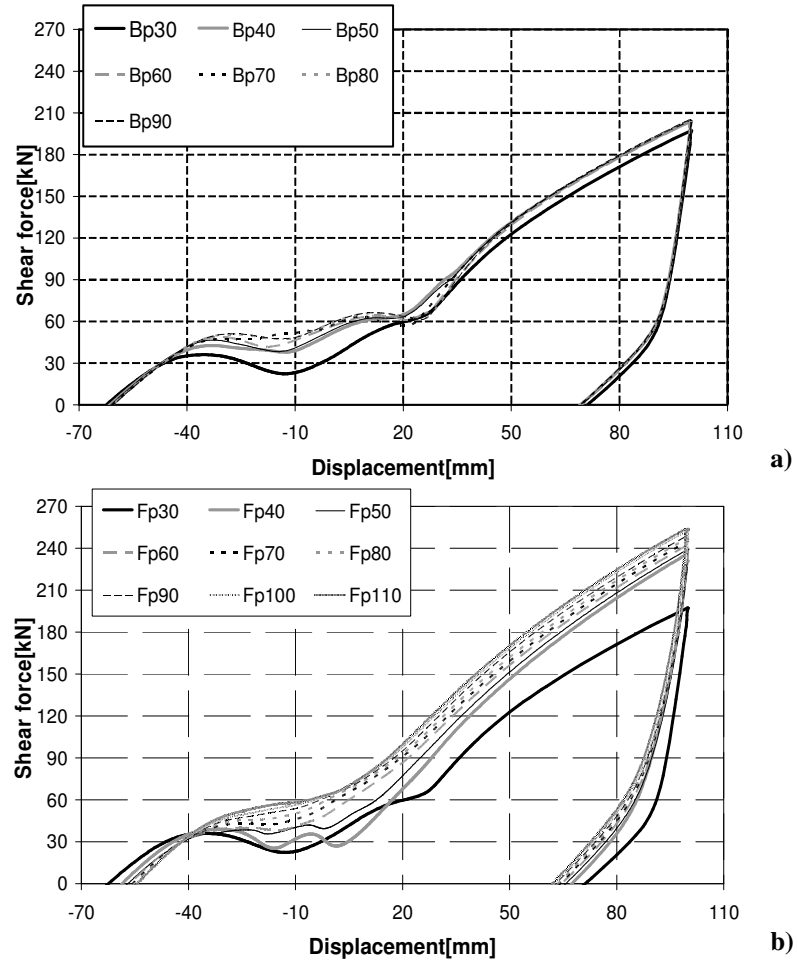


Figure 3.17: Parametric analysis results: hysteretic loops for shear panel type B (a) and F (b)

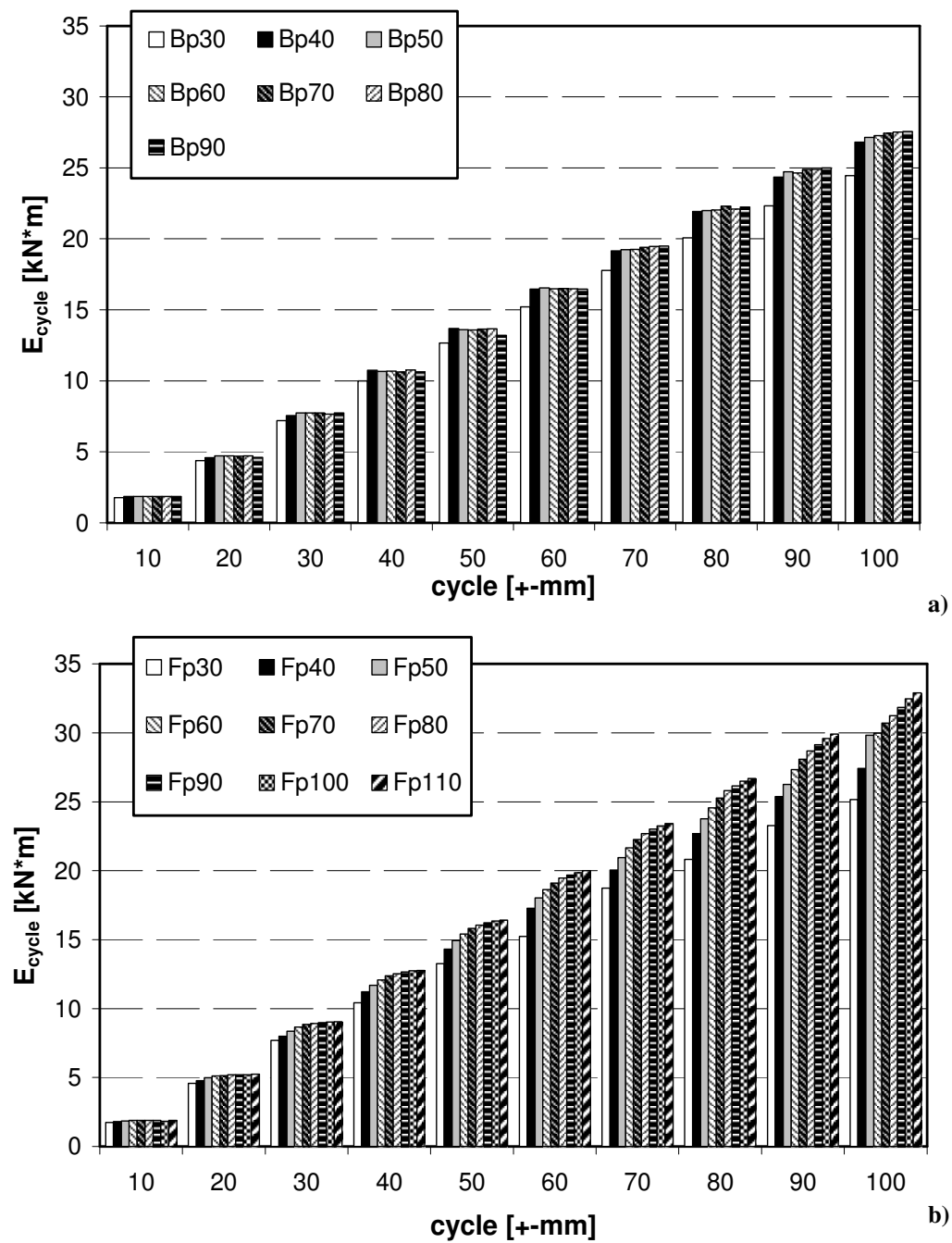


Figure 3.18: Parametric analysis results: dissipated energy for shear panel type B: (a) and F (b)

It is apparent that the shear panel type F provides a better mechanical performance than the type B one. However, it requires a higher realization cost due to a larger employment of material. Therefore, in order to determine the most suitable configuration to be adopted, a careful evaluation is necessary, depending on the demanded performance level.

Besides, it is evident that shear panel type B configurations present a substantial convergence of results for stiffener depths higher than a value comprised between 40mm and 50mm. Such a kind of behaviour is due to the capacity of ribs, of depth equal to 50mm, to confine the buckling phenomena in the single portions of the shear panel.

It is interesting to observe that European Standards classify the stiffeners as “rigid”, when they behave as transverse ribs having a total second moment of area equal to (Höglund, 1997):

$$I_{st,lim} = 1.5 \cdot \frac{B^3 \cdot t^3}{a^2} \quad (3.2)$$

For shear panel type B such a limit value ($I_{st,lim,B}$) is equal to $75 \times 10^4 \text{ mm}^4$, corresponding to a rib depth of 46mm. Hence, the obtained results confirm the accuracy of the formulation provided by EC9 (EN 1999-1-1, 2006).

Obviously, from an economical point of view, this means that the most attractive shear panel type B configuration is the one characterised by rib depth of 50 mm.

On the other hand, for shear panel type F, EC9 provides a limit value of the total second moment of area of stiffeners ($I_{st,lim,F}$) equal to $300 \times 10^4 \text{ mm}^4$, corresponding to a rib depth of 88mm.

From the obtained results it is evident that, even for higher values of rib depth, the corresponding dissipated energy increases, although with lower scatters, without the attainment of any convergence. Such a situation is probably due to the presence of discontinuous welds, which do not realize a completely effective connection among different parts as implicitly considered by EC9.

For this reason, when ribs are not located on the same position on the two sides of the plate, a major attention for the actual arrangement of welds has to be paid. In order to analyse such an effect, two additional shear panel type F configurations have been considered.

The first one (named Fp88-c, where “c” is the acronym of continuous) is characterised by the prescribed limit rib depth, but considering a continuous welding connection between stiffeners and plate.

The second one (Fp53-ds, where “ds” is the acronym of double side), has ribs located in the same position on the two sides of plate and is characterised by a stiffeners total second moment of area equal to the optimal value suggested by EC9.

The obtained results are shown in Figure 3.19 where, for the sake of comparison, the output data of the shear panel type Fp90 are illustrated as well. From the same figure it is clearly evident that an effective continuous connection entails better results in terms of global dissipated energy.

In conclusion it has been established that panel type F, due to a more rational arrangement of applied ribs, results to be more effective in terms of energy dissipation capability in comparison to the type B one, although more expensive in terms of fabrication costs.

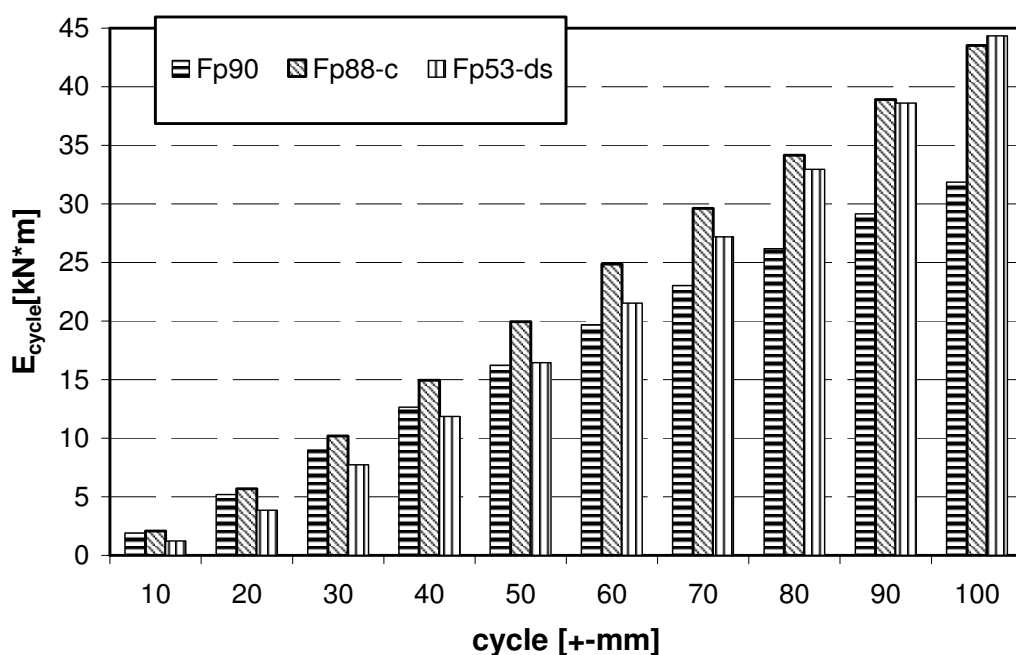


Figure 3.19: Dissipated energy for shear panels having different stiffener-to-plate connections

3.3 SLENDER SHEAR PANELS

3.3.1 Simulation of an experimental test

3.3.1.1 The reference experimental basis

The experimental activity used to calibrate an effective FEM model for simulating the slender steel shear panels behaviour is the one developed by Berman and Bruneau (2003) for seismic retrofitting of a hospital made of steel. Such an experimental campaign has been deeply described in the Section 2.4.4. Within this activity, the attention has been focused on the test performed on the 1 mm thick steel panel (specimen type F2), which provided the most interesting results.

Such a specimen, 3660 mm wide by 1830 mm high ($b/d=0.5$), was made of a mild steel, whose stress-strain behaviour is reported in Figure 3.20. It was welded to a surrounding steel frame made of members designed in order to remain in the elastic field under the tension field action developed by the plate.

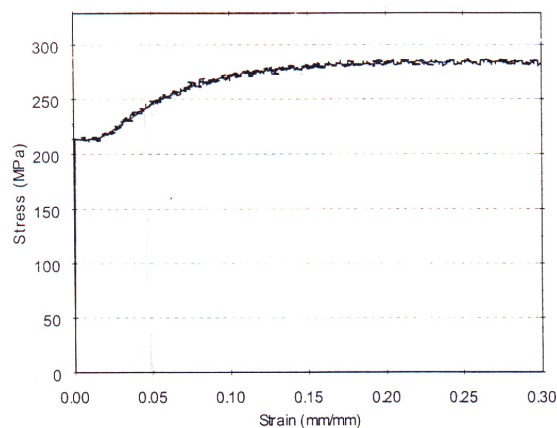


Figure 3.20: Stress-strain behaviour of the panel specimen type F2 tested in the Berman and Bruneau's experimental activity (2003)

The loading cyclic history applied to the panel, defined according to the procedure given by ATC-24 (1992), considered cycles impressed under quasi-static conditions with control of both forces and displacements (Figure 3.21).

The behaviour exhibited from the compound panel-frame structure is illustrated in Figure 3.22 a in the base shear – inter-storey drift plane.

According to the PFI method developed by Sabouri-Ghomi and Roberts (1991), which hypothesised that the panel and the frame could work under parallel way, it is possible to extrapolate from the global compound system response the one provided by steel panel only (Figure 3.22 b).

Such a panel behaviour will be simulated by the FEM model implemented in the next Section

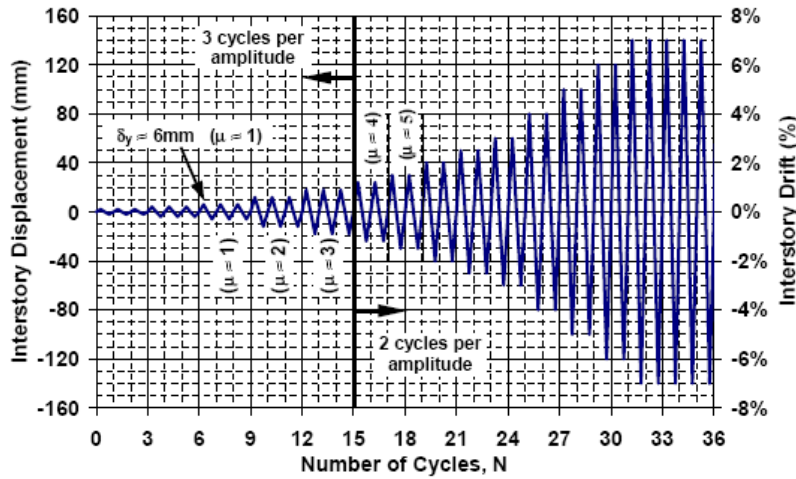


Figure 3.21: The cyclic loading history applied to the panel specimen type F2 in the Berman and Bruneau's experimental activity (2003)

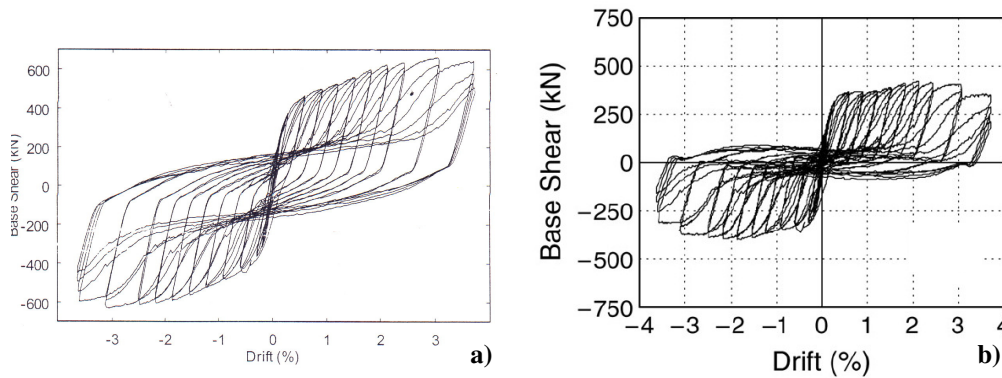


Figure 3.22: Experimental response of the frame-panel system (a) and contribution provided by the shear panel only (b)

3.3.1.2 Analysis methods

In the following a brief discussion about the numerical analysis methods used in the current finite element modelling of slender steel shear panels is given.

In particular, the attention has been focused on both the eigenvalues analysis, useful to evaluate both the elastic critical load and the buckling modes of the system, and the modified Riks method, implemented in order to follow the evolution of the shear panel response in the shear force – lateral displacement plane (Hibbitt et al., 2004).

The first analysis type is performed because the elastic instability problems can be considered as equal to eigenvalues ones (Baker and Pekoz, 2001). The procedure implemented in ABAQUS for the resolution of such problems allows to consider both the initial perturbation affecting the system, before the load application, and the consequent deformations deriving from such actions.

Considering an initial perturbation P applied to the system and the corresponding tangent stiffness $[K_p]$, if we apply a load variation λ_Q , the stiffness variation due to this load is $[K_Q]$ and the load-displacement relationship corresponding to the load $P+\lambda_Q$ will assume the following expression:

$$([K_p] + \lambda[K_Q])\{d\} = \{F\} \quad (3.3)$$

where:

$\{d\}$ = nodal displacements vector;

$\{F\}$ = nodal forces vector.

When $\{F\}=0$, because eq. (3.3) could admit a solution different from zero, the resolution of such a problem is reduced to a classic equivalence problem which is presented in the following way:

$$([K_p] + \lambda[K_Q])\{\phi\} = \{0\} \quad (3.4)$$

where λ is the multiplier of the critical load and $\{\phi\}$ are the buckling modal shapes.

If the applied perturbation P is zero, the eq. (3.4) assumes the following expression:

$$([K] + \lambda[K_g])\{\phi\} = \{0\} \quad (3.5)$$

where:

$[K]$ = initial stiffness matrix;

$[K_g]$ = geometrical stiffness matrix.

The second analysis type used in the FE modelling is the modified Riks method, which is generally used in order to obtain nonlinear static equilibrium solutions for unstable problems, where the load-displacement response exhibits the type of behaviour sketched in Figure 3.23, where the load and/or the displacement may decrease as the solution evolves.

The traditional methods based on the control of either force or displacement fail in the prediction of this unstable behaviour (Figure 3.24); therefore several methods have been proposed and applied to resolve such problems. Of these, the most successful seems to be the modified Riks algorithm; so a version of this method has been implemented in ABAQUS.

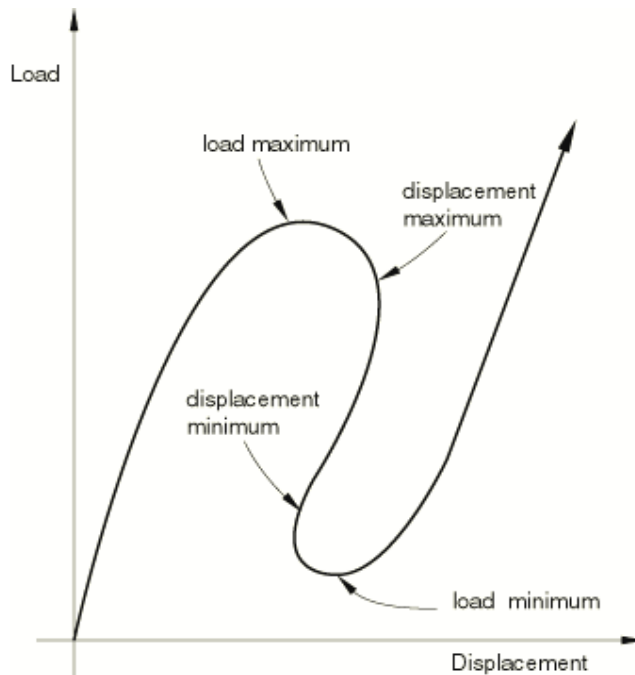


Figure 3.23: Typical unstable static response

The essence of the method is that the solution is viewed as the discovery of a single equilibrium path in a space defined by the nodal variables and loading parameters. Development of the solution requires that this path must be traversed as far as required. In particular, the Riks method, which uses the load magnitude as an additional unknown, solves simultaneously for loads and displacements. Therefore, another quantity must be used to measure the

progress of the solution; for this reason ABAQUS uses the “arc length” l along the static equilibrium path in load-displacement space. This approach provides solutions regardless of whether the response is stable or unstable.

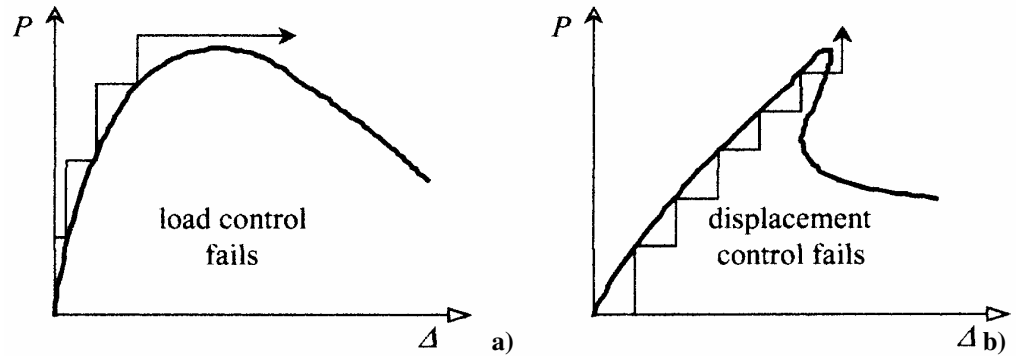


Figure 3.24: Fails of traditional load (a) and displacement (b) control methods

If the Riks step is a continuation of a previous history load, any loads applied at the beginning of the step are treated as “dead” loads with constant magnitude. The load magnitude defined in the Riks step is referred to as a “reference” load. All prescribed loads are ramped from the initial (dead load) value to the reference specified ones.

In the Riks step the load increases under proportional way and its current magnitude, P_{total} , is defined by the following relationship:

$$P_{\text{total}} = P_0 + \lambda (P_{\text{ref}} - P_0) \quad (3.6)$$

where P_0 is the “dead load,” P_{ref} is the reference load vector and λ is the “load proportionality factor”. ABAQUS prints out the current value of the load proportionality factor, which is found as part of the solution, at each increment.

The basic algorithm to solve the nonlinear equilibrium equations remains the Newton method; therefore, at any time there will be a finite radius of convergence.

An initial increment in arc length along the static equilibrium path, $\Delta\lambda_{\text{in}}$, is provided when the step is defined. The initial load proportionality factor, $\Delta\lambda_{\text{in}}$, is computed as:

$$\Delta\lambda_{in} = \frac{\Delta l_{in}}{l_{period}} \quad (3.7)$$

where l_{period} is a user-specified total arc length scale factor (typically set equal to 1). This value of $\Delta\lambda_{in}$ is used during the first iteration of a Riks step.

For subsequent iterations and increments the value of λ is computed automatically, so the control over the load magnitude is not performed. The value of λ is part of the solution. Minimum and maximum arc length increments, Δl_{min} and Δl_{max} , can be used to control the automatic incrementation.

When this procedure is applied, it is possible to observe that many of the materials (and possibly loadings) of interest have path-dependent response. For these reasons, it is essential to limit the increment size. In the modified Riks algorithm, as it is implemented in ABAQUS, the increment size is limited by moving a given distance along the tangent line to the current solution point. Then the research for equilibrium in the plane, which is orthogonal to the same tangent line and passes through the obtained point, is carried out (Figure 3.25).

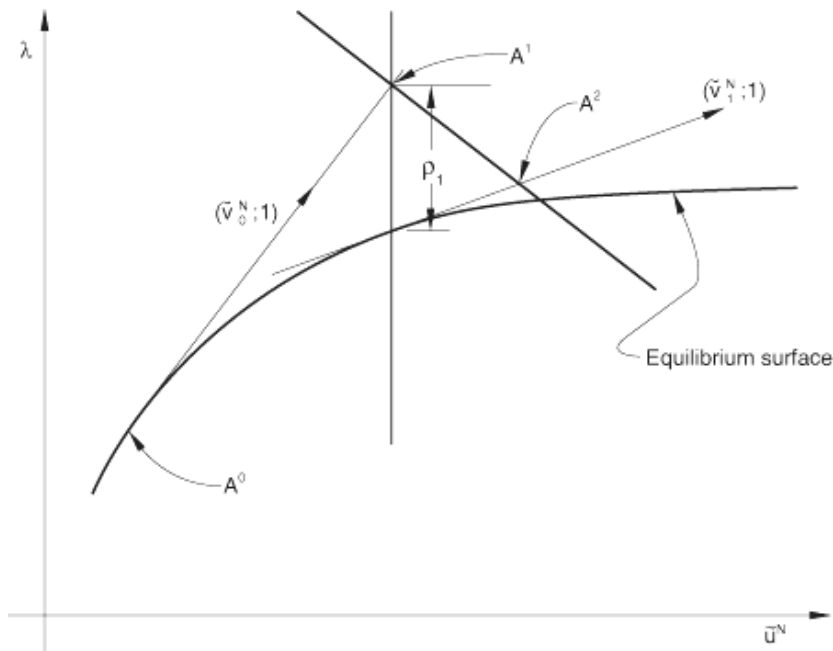


Figure 3.25: Modified Riks algorithm

3.3.1.3 FEM model calibration

The prediction of the behaviour of slender steel shear panels represents a non-linear problem which cannot be resolved by means of closed-form solutions; therefore it requires exclusively a numerical approach able to take into account both the geometrical and mechanical non linearities which affect the system performance. For this reason the implementation of finite element models represents the only way to follow in this direction.

FE modelling is a very complex operation from which the more or less accuracy in predicting the real system behaviour could depend. So, in this framework, large attention has to be done to the choice of suitable modelling criteria, such as by selecting both appropriate mesh and initial imperfections.

The main target of this study is to simulate the single slender panel behaviour under monotonic loading aiming at establishing which parameters could influence their response.

To this purpose, in such a study phase, a sophisticated FEM model by means of the ABAQUS non linear numerical analysis program (Hibbitt et al., 2004) has been calibrated on the basis of the above available experimental results.

As already mentioned, the system under study is composed by an external steel frame filled by a slender steel shear panel which is welded to appropriate plates fixed to the frame members.

The shear panel has been modelled by means of type S4R shell finite elements having 6 degrees of freedom for each node and accounting for the out-of-plane behaviour of the panel. Since the translational degree of freedoms are independent from the rotational ones, with this element the transversal deformations due to shear are automatically considered. Also, in this case, the distribution of the 3D deformation field is obtained starting from the deformation of the four Gauss integration points located on the middle surface of each shell element.

The frame members have been represented by means of cubic two-nodes elements (type B31) able to take into account both bi-axial flexural actions and axial strains and cross-section deformations.

The beam elements have been modelled according to the profiles (W460x128 e W310x143) used in the experimental test. The behaviour of the members cross-section has been described through 13 integration points: five

in each flange and five in the web, the latter having two points in common with flanges (Figure 3.26).

In this way the stresses in the middle plane of both the flanges and the web, by neglecting their variability through thickness, are described.

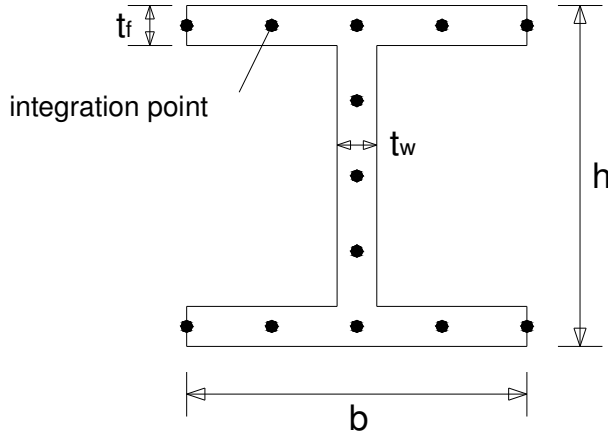


Figure 3.26: Characterisation of beam elements

According to the experimental evidence, since pinned joints have been used to characterise the beam-to-column connections, the type of linear elements employed for the steel members modelling assumes a not relevant importance. Therefore, the choice of B31 elements has been dictated by the compatibility with the selected shell ones aiming at modelling the more appropriate frame-to-panel interaction, which has been represented by the TIE constraint, a command belonging to the ABAQUS commands library.

The TIE command allows to create a constraint between two nodes by means of the following equations:

$$u_i - u_j = 0 \quad (3.8)$$

$$v_i - v_j = 0 \quad (3.9)$$

being u and v the horizontal and vertical component of the displacement, respectively, and i, j the two corresponding nodes.

After the definition of the element types used to represent the system elements, the structural modelling has been performed through the progressive definition of a sequence of steps which allow to assign the geometrical and mechanical properties of parts, as well as both the loading and constraint conditions.

The implementation and the visualization of the numerical model is made possible by using the graphical pre-processor of the software, known as ABAQUS/CAE.

The geometrical dimensions of both steel members and shear panel have been assigned according to the real ones. In particular, frame members have been modelled respecting the geometrical dimensions of profiles (W460x128 e W310x143) used in the experimental test (Figure 3.27).

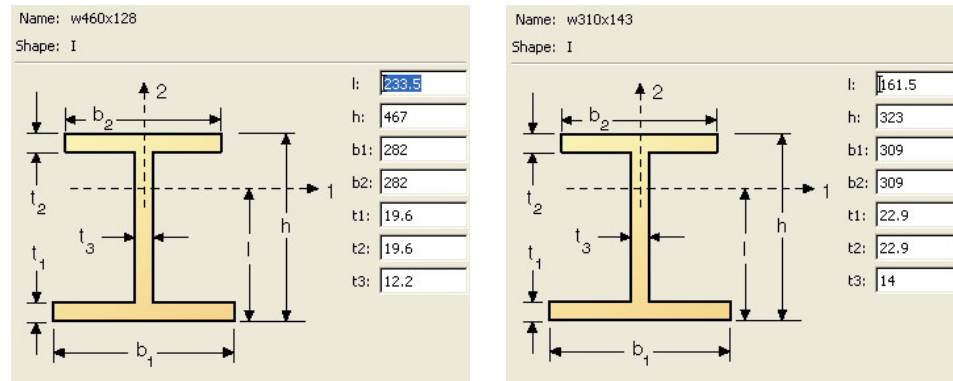


Figure 3.27: Dimensions of the beams (a) and columns (b) cross-section

The panel material, which is a steel whose mechanical features are reported in Figure 3.20, has been assigned to the program by considering its true stress – true strain curve, defined according to the following equations:

$$\sigma_{\text{true}} = \sigma (1 + \epsilon) \quad (3.10)$$

$$\epsilon_{\text{pl}} = \epsilon - \sigma/E \quad (3.11)$$

On the other hand, Fe430 steel having an elasto-perfectly plastic behaviour has been used to characterise the frame members.

Then, in the step assembly, all the elements above described have been put together in order to obtain the composed frame-panel system (Figure 3.28).

According to the experimental layout, pinned joints have been used in the frame beam-to-column connections and out-of-plane displacements of the frame have been restrained.

The system has been loaded by means of a lateral force applied to the top beam of the frame. Then, the choice of the more appropriate mesh to be used in the FEM model has been done. Structured elements have been adopted due to the simplicity to check their insertion in the model. Two different

discretization types have been considered, they being represented by square elements with side length of 25 (Figure 3.29 a) and 50 mm (Figure 3.29 b).

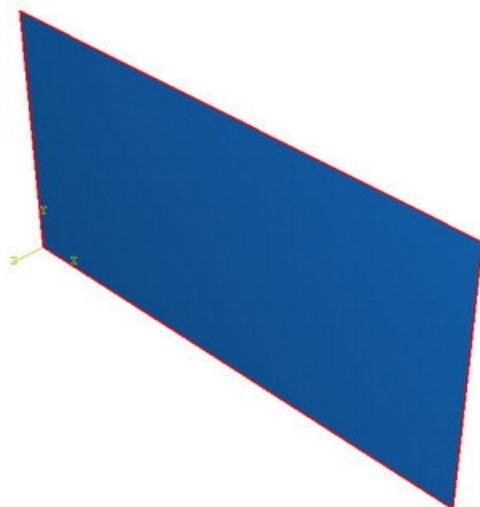


Figure 3.28: Frame-to-panel assembly

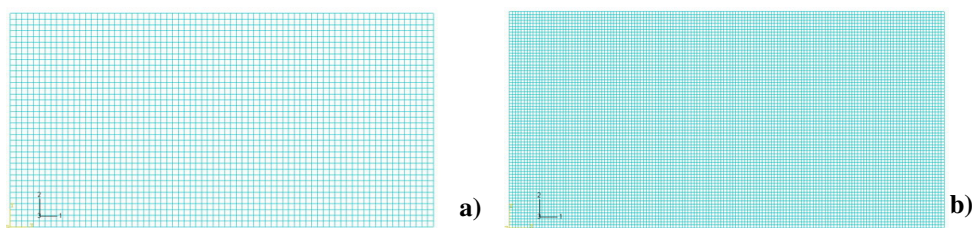


Figure 3.29: Finite element mesh with 50 mm (a) and 25 mm (b) side length

In the FE modelling, as previously described, both the buckling and the modified Riks analyses have been performed in order to introduce the geometrical imperfections in the model, which have been considered as the buckled deformed shape corresponding to the attainment of the elastic critical load, and to follow the evolution of the system behaviour in the lateral force – displacement plane, respectively.

In the buckling analysis, for both the examined panel configurations, characterised by a different mesh, the first four critical modes presented eigenvalues very close each other; thus, the selection of the first critical one

has been justified. The first four buckled shapes of the system meshed with elements of 50 mm side length are reported in Figure 3.30.

On the other hand, the effect of mechanical imperfections in the system has not been taken into account due to the lack of information about both the magnitude and distribution of residual stresses.

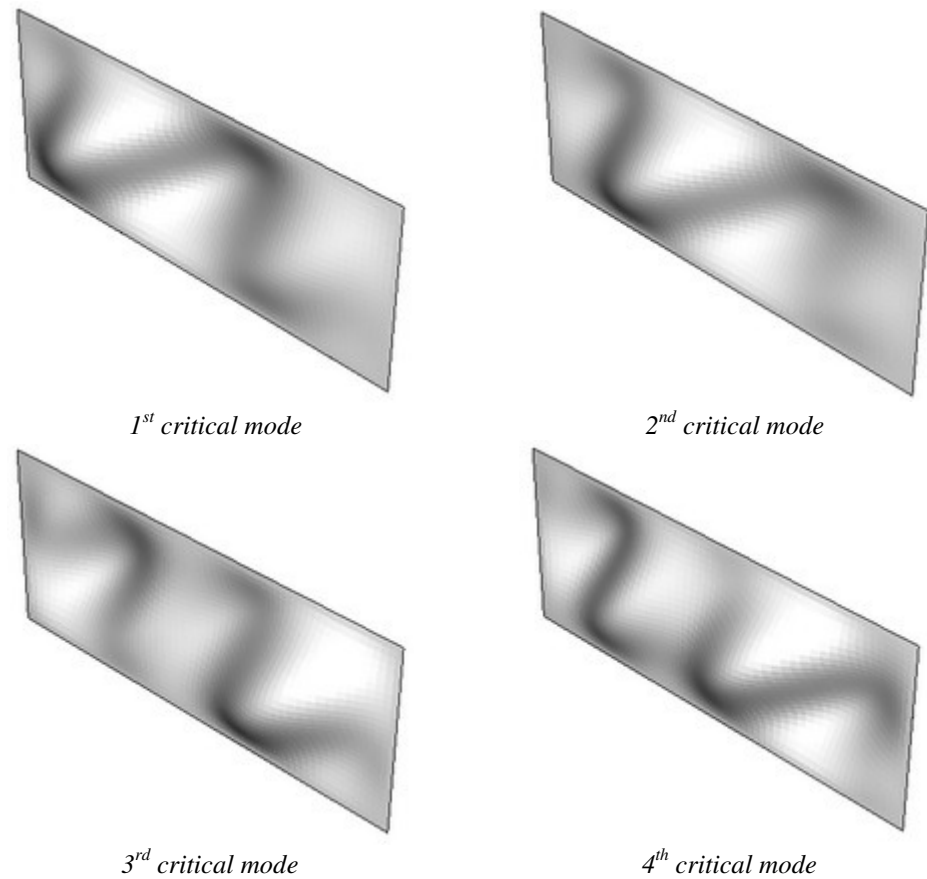


Figure 3.30: Buckled deformed shapes of the system with mesh of 50 mm side length (out-of-plane displacements amplified by 300)

The results of the numerical analyses carried out on both panel configurations are illustrated in Figure 3.31, where it is apparent that any behavioural difference among curves is detected.

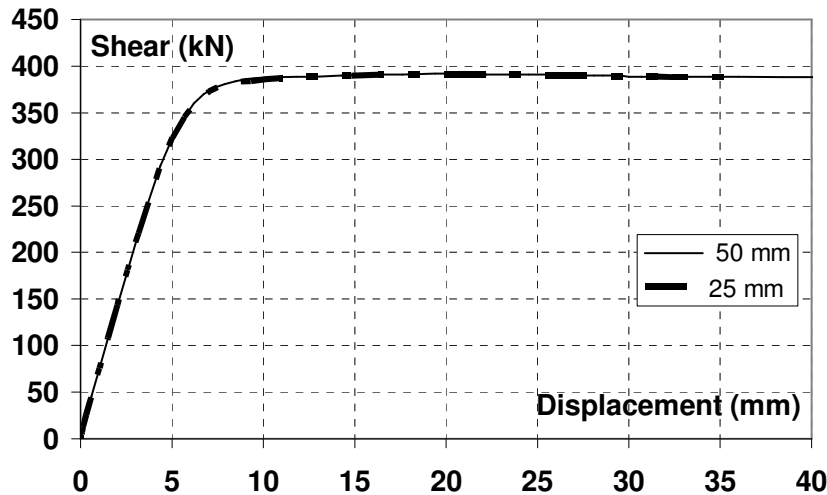


Figure 3.31: Numerical results deriving from the application of FEM models characterised by different mesh

For this reason, in the following the panel with mesh of 50 mm side length has been used only. The maximum strength and stiffness exhibited by the system are equal to 391 kN and 85000 Nmm^{-1} , respectively. The panel behaviour is governed by the tension field mechanism only, due to the very low value assumed by the shear corresponding to the attainment of the elastic critical mode (3.57 kN).

The maximum numerical resistance of the system is equal to the theoretical one, calculated by considering a tension field inclination angle equal to 45° , which is determined in the following way:

$$V = \frac{1}{2} F_y t L \sin 2\alpha = 0,5 \cdot 214 \cdot 1 \cdot 3660 \cdot \sin 90 = 391 \text{ kN}$$

On the other side, the panel has a theoretical stiffness equal to:

$$K = \frac{E L \cdot t}{4 h_s} = 103000 \text{ Nmm}^{-1}$$

which represents a value greater (about 17%) than the one achieved under numerical way. This difference is due to the fact that in the numerical model the panel is connected to an infinitely rigid frame. In order to consider the real interaction between the frame and the panel, according to the theory

developed by Sabouri-Ghomi et al. (2003), appropriate corrective coefficients have been introduced.

The first factor C_{m1} is assumed equal to 1, being the numerical system strength equal to the theoretical one, while the displacement corrective coefficient C_{m2} , given by the ratio between the theoretical and the numerical stiffness, assumes a value equal to 1.2, which is comprised in the range $[1 \div 1,7]$ provided by the same Authors.

The comparison between theoretical and numerical results in the shear force – inter-storey drift plane is provided in Figure 3.32.

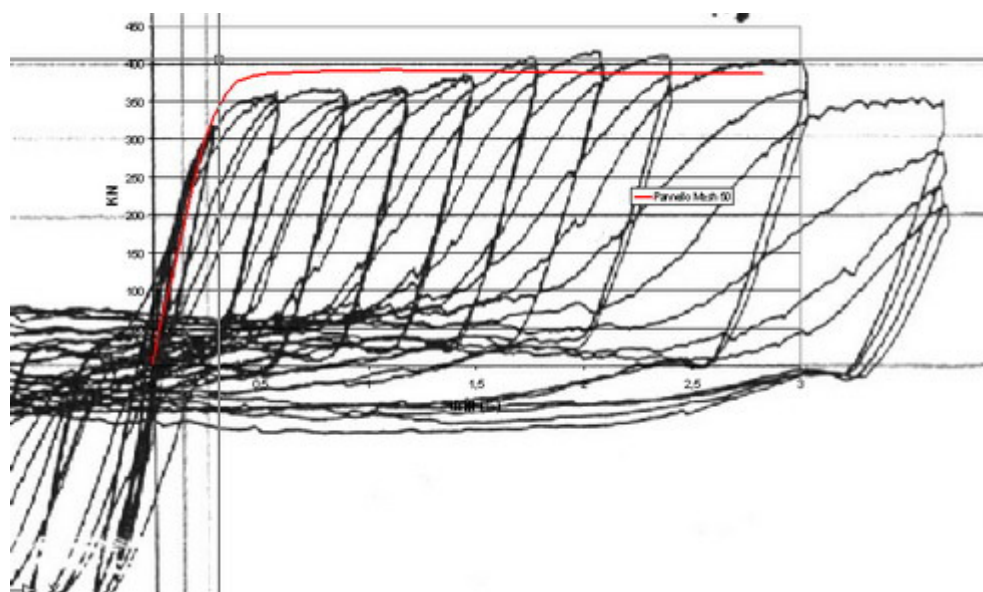


Figure 3.32: Numerical simulation curve of the Berman and Bruneau's experimental cyclic test (2003)

From the comparison it is evident that the numerical curve does not envelop very well the cyclic behaviour of the panel. In particular, it is observed that the numerical stiffness is lower than the experimental one, while the maximum numerical panel strength is greater than the one characterising the initial loading cycles.

As a consequence, in order to improve the obtained results, a new finite element modelling has been done by considering the real dimensions of the panel plate, whose actual width and height are represented by the net distance

between the column and beam flanges, respectively. In such a way, according to the theoretical relationships previously introduced, a more rigid and less resistance shear panel is obtained.

To this purpose, by varying the location of the profiles axis in the plane of their cross-section, new geometrical properties of the used beams and columns have been considered (Figure 3.33).

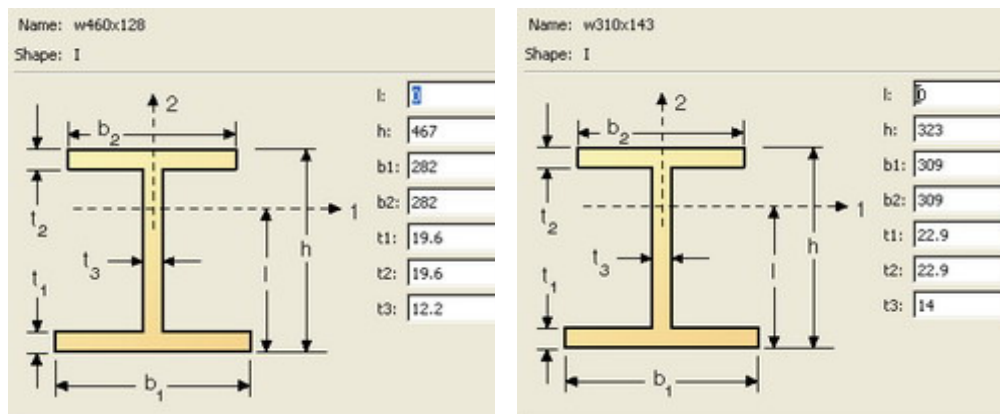


Figure 3.33: Geometrical characteristics of beams (a) and columns (b) used in the improved FEM model

The results deriving from the application of the new FEM model are depicted in Figure 3.34.

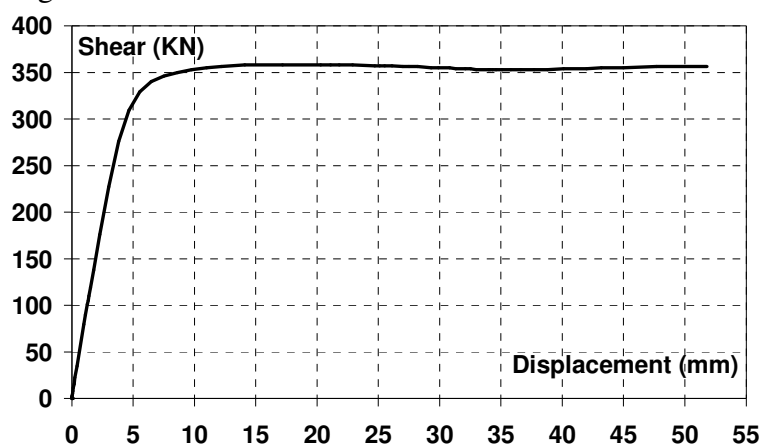


Figure 3.34: Numerical response of the tested shear panel (improved FEM model)

From the force-displacement diagram, a maximum panel strength equal to 360 kN, corresponding to the elastic limit displacement equal to 5 mm, and a stiffness of about 110000 Nmm^{-1} are observed. Under the theoretical point of view the following results have been achieved:

$$V = \frac{1}{2} F_y t L \sin 2\alpha = 0,5 \cdot 214 \cdot 1 \cdot 3660 \cdot \sin 90 = 360 \text{ KN}$$

$$K = \frac{E L \cdot t}{4 h_s} = 126000 \text{ Nmm}^{-1}$$

It is apparent that in both cases the same strength value is obtained, while a numerical-theoretical scatter in terms of stiffness is still visible. The corrective coefficient to be introduced aiming at considering the real panel-frame behaviour is:

$$C_{m2} = \frac{K_t}{K_r} = 1,17$$

which is always comprised in the range provided by the PFI method.

Now, by considering the comparison between experimental and numerical results (Figure 3.35), a very well agreement is observed in terms of both initial stiffness and maximum strength.

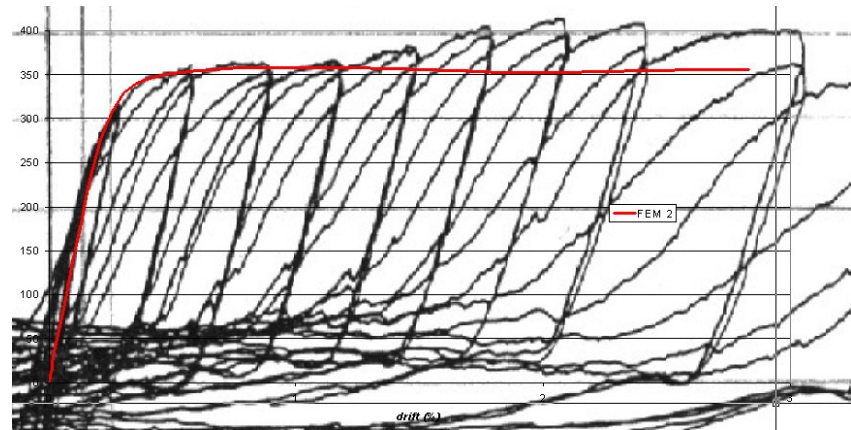


Figure 3.35: Experimental-numerical comparison (improved FEM model)

The scatter detected in terms of resistance when significant plastic excursions of the panel occur is due to the fact that in the pushover numerical analysis the panel deformations are not able to activate the strain-hardening

resources of the material. Contrary, during cyclic test, an accumulation of deformations in the plastic field allows to exploit such a material feature.

In addition, the stiffness detected in the final loading phases of the experimental test is reduced with respect to the numerical simulation one due to the fractures evidenced in the panel corners zones, which are the first parts to exhibit a plastic behaviour. Nevertheless, considering also that such a reduction does not compromise the final strength of the system, the effectiveness of the implemented numerical model is confirmed.

In the following the numerical results related to the significant steps occurred during the loading simulation phases (Figure 3.36), are reported in terms of both stress states and deformations of the shear panel.

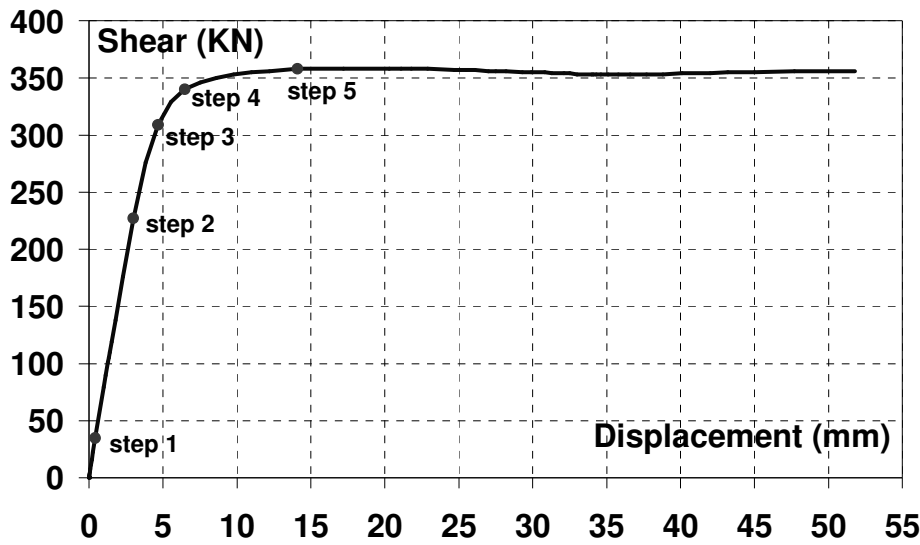


Figure 3.36: Significant steps detected in the numerical response of the simulated shear panel

In the first step, characterised by a load equal to about 1/10 of the maximum one, the activation of the tension field mechanism in the plate occurs. In this phase the corners are the most stressed and deformed zones of the panel (Figures 3.37 a, b).

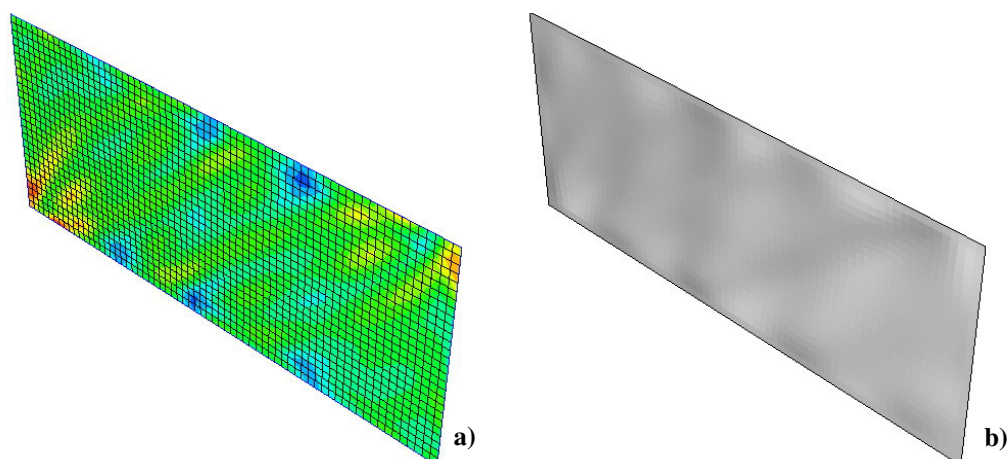


Figure 3.37: The first loading step: stress state (a) and deformed shape (amplification factor equal to 100) (b) of the tested shear panel

In the second step, when a load of 214 kN corresponding to a displacement of 2.19 mm is attained, according to the experimental results, diagonal tensile bands develop in the plate with the formation of plastic zones in the corners (Figures 3.38 a, b)

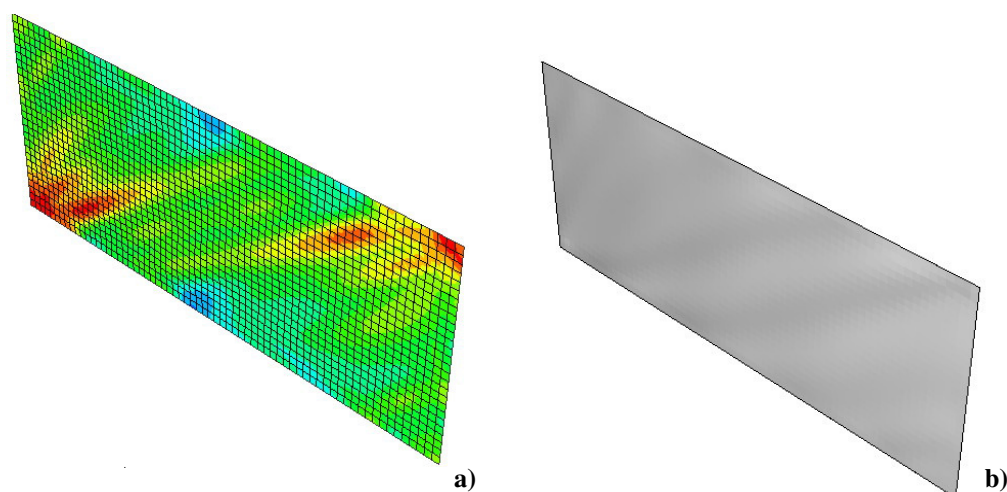


Figure 3.38: The second loading step: stress state (a) and deformed shape (amplification factor equal to 3) (b) of the tested shear panel

In the third step, corresponding to the attainment of a lateral force equal to 85% of the maximum one, the panel shows large zones, especially along the diagonals and in the corners, where the maximum material strength is reached (Figures 3.39 a, b). Starting from this point, the system stiffness decreases.

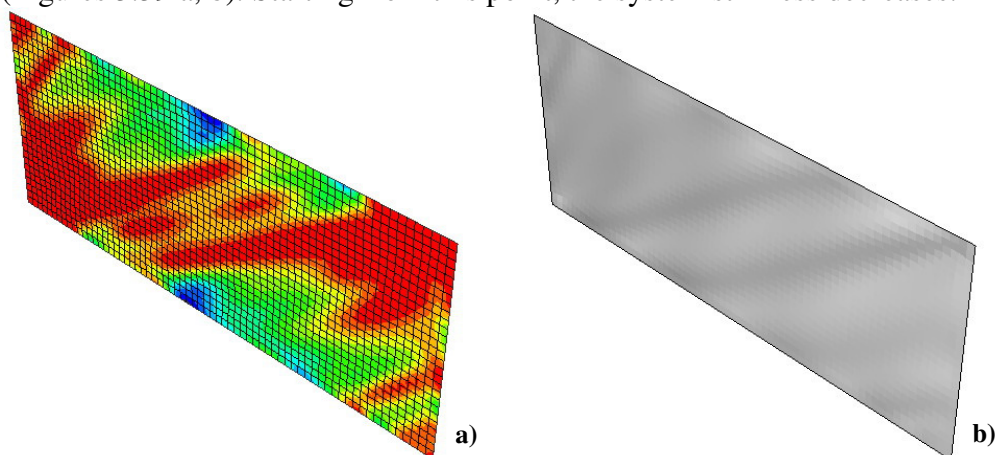


Figure 3.39: The third loading step: stress state (a) and deformed shape (amplification factor equal to 2)(b) of the tested shear panel

In the fourth phase, when the applied load (344 kN) is very close to the maximum one, the system, which is subjected to a displacement of 4.28 mm, exhibits a quasi-fully plastic behaviour (Figures 3.40a, b). In such a step the panel stiffness is strongly reduced.

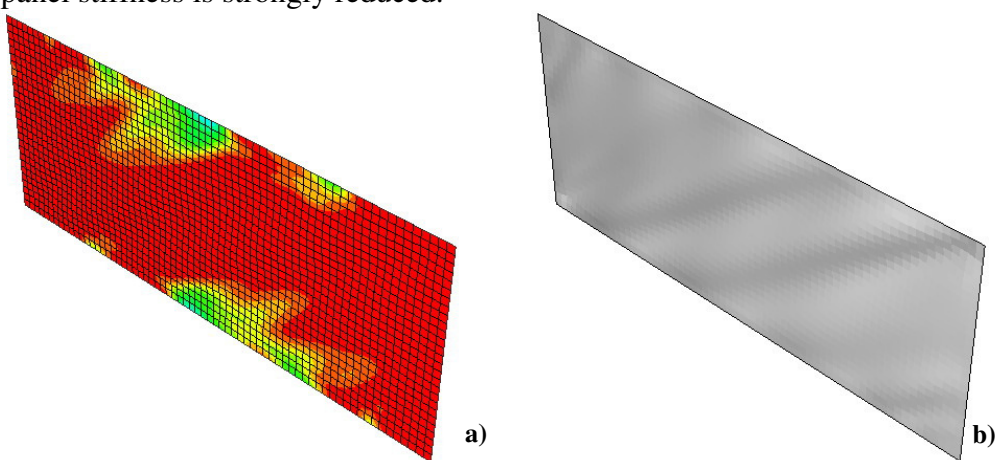


Figure 3.40: The fourth loading step: stress state (a) and deformed shape (amplification factor equal to 2) (b) of the tested shear panel

Finally, in the final step of the loading process (step 5), when the maximum panel strength, corresponding to a displacement of 12.7 mm, is attained, a fully plastic behaviour of the system is observed (Figure 3.41 a). In such a phase, where the stiffness tends to zero, the out-of-plane displacements of the panels are very pronounced (Figure 3.41 b).

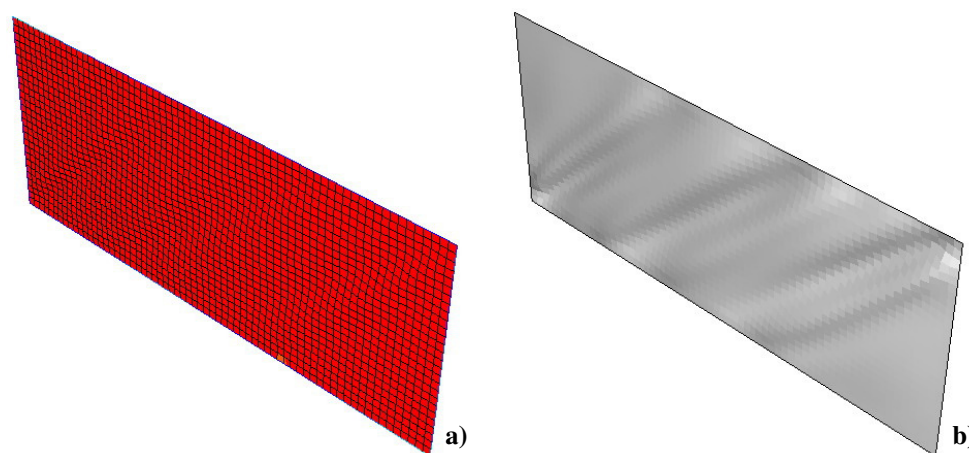


Figure 3.41: The fifth loading step: stress state (a) and deformed shape (b) of the tested shear panel

3.3.2 Parametric study

3.3.2.1 Foreword

The numerical simulation of the Berman and Bruneau's experimental activity carried out in the previous Section allows to have a useful computational tool to predict the slender steel shear panels behaviour, which is conditioned by two main parameters, namely the aspect ratio (b/d) and the thickness (t) of the plate. In particular, the b/d ratio influences the effectiveness of the tension field mechanism, which determines the behaviour of the plate after the occurrence of buckling phenomena and up reaching the ultimate strength.

Other than accurate numerical models, implemented by means of finite element programs, the behaviour of thin shear panels can be assessed by means of simplified numerical and theoretical methods, whose validity has been confirmed by the study carried out by different Authors (Timler, 2000).

In the current Section the numerical results related to a refined parametric study performed for evaluating the influence of the main parameters, including the adoption of intermediate stiffeners, on the panel behaviour are presented. Then, such results have been compared with the ones determined by applying the mentioned simplified methods, based on both the strip model theory and the PFI method, in order to check their reliability for predicting the behaviour of slender shear panels (Formisano et al., 2006a).

3.3.2.2 The shear panel – frame system

3.3.2.2.1 Foreword

In order to define the behaviour of slender shear walls, the structural analogy existing with the behaviour of a stiffened girder may be applied (Timler, 2000). In fact, the columns where the shear plates are anchored can be compared to the beam flanges, the shear plate to the web of a girder and the horizontal beams placed at each level can be considered as the transversal stiffeners of the web girder. Nevertheless, the above analogy may be limited by a different stiffness ratio between the single parts of the system. In particular, a reduced flexural stiffness of the shear wall columns could cause a significant modification of the tension field inclination angle, avoiding that the resisting mechanism is activated on the whole panel surface. To this purpose, Kuhn et al. (Thorburn et al., 1983) established the minimum value of the second moment of area of columns in order to avoid their excessive deformation under the loads transferred by the shear plate:

$$I_c \geq \frac{0,00307 t h_s^4}{L} \quad (3.12)$$

This problem is not relevant for the intermediate beams of shear walls. In fact they are subjected on both sides to a stress state induced by shear plates which have the same intensity but opposite sign, hence they do not produce any effect (Figure 3.42).

On the contrary, upper and lower beams of a shear wall must possess a sufficient flexural stiffness in order to absorb the stresses developed by the shear panels. With regard to columns, their stiffness is an important parameter for both the force distribution within the panel and the definition of the global

system flexibility. This is due to two separate effects: the flexural deformation of columns, which depends on the applied cross-section, and the horizontal forces generated by the tension field developed into the panel.



Figure 3.42: Effect of the tension field mechanism on the intermediate beam of a steel plate shear wall

3.3.2.2.2 Simplified interpreting models

Among proposed theoretical methods for interpreting the behaviour of slender shear panels, the PFI model (Sabouri-Ghomi and Roberts, 1991) allows the application of the following simplified relationships to determine the stiffness (K_w) and the ultimate strength (F_{wu}):

$$F_{wu} = b \cdot t \cdot \left(\tau_{cr} + \frac{\sigma_{ty} \cdot \sin 2\Theta}{2} \right) \quad K_w = \frac{\tau_{cr} + \frac{\sigma_{ty} \cdot \sin 2\Theta}{2}}{\tau_{cr}/G + \frac{2 \cdot \sigma_{ty} \cdot \sin 2\Theta}{E}} \cdot \frac{b \cdot t}{d} \quad (3.13)$$

where $\tau_{cr} = k \cdot \frac{\pi^2 \cdot E}{12 \cdot (1 - \nu^2)} \cdot \left(\frac{t}{d} \right)^2$ is the critical shear stress and the plate

factor k is a coefficient depending on both the $a=b/d$ ratio and the boundary conditions of the panel. In particular, when the slenderness ratio b/t of the applied shear plate is quite large, the pre-critical behaviour of the panel can be neglected assuming $\tau_{cr} = 0$. In addition, also the relationship related to the evaluation of the panel stiffness can be simplified, obtaining the following expression:

$$K = \frac{E \cdot L \cdot t}{4 \cdot d} \quad (3.14)$$

where L is the shear plate width.

A more refined method to define the shear panel behaviour in the post-critical field is provided by the Strip Model, which interprets the behaviour of the plate by means of inclined strips having the same panel thickness t and a cross-section A_s given by the following expression:

$$A_s = \frac{(L \cdot \cos \alpha + h_s \cdot \sin \alpha)}{n} \cdot t \quad (3.15)$$

where n is the number of stripes (at minimum equal to ten), in which the panel is subdivided and α represents their inclination angle corresponding to the diagonal tension field inclination. Such a method can be simply implemented by means of commercial finite element programs, like the SAP 2000 (Computer and Structures, Inc., 2003), modelling the stripes as trusses able to develop tensile plastic hinges (Figure 3.43).

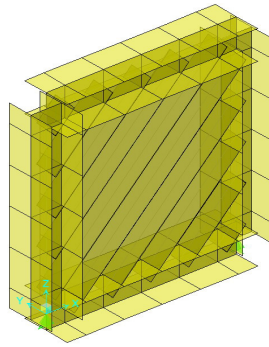


Figure 3.43: Modelling of the shear panel by means of Sap 2000 (strip model theory)

3.3.2.2.3 Influence of the column stiffness

In order to evaluate the main influential parameters affecting the system flexibility, a preliminary numerical analysis, which is based on a finite element modelling of a 1000x1000x1 mm shear panel inserted within a reaction steel frame realised with coupled UPN profiles (Figure 3.44 a), has been carried out by varying the column and beam stiffness. The finite element model is implemented by means of the ABAQUS non linear numerical analysis program (Hibbitt et al., 2004), where the shear plate and the frame members are modelled by using four nodes bi-dimensional having reduced integration (S4R type) and two-node linear (B31 type) elements, respectively.

On the basis of a preliminary sensitivity study, a mesh having square elements of 25 x 25 mm, which provide the best compromise between accuracy of results and analysis time consuming, has been used for the plate (Figure 3.44 b).

The material used for the shear panel is a DX56D steel, which is a mild steel with limited elastic strength employed in the field of cold-formed thin walled sheeting and profiles according to the UNI EN 10142 code provisions (1992); S275 steel, characterised by an elastic-perfectly plastic behaviour, has been employed for the frame members.

The mechanical features of the panel material, which is the same used in the experimental activity presented in the Chapter 6, have been preventively estimated by means of a tensile test on steel coupons, providing yield and ultimate stress values equal to 305 and 340 MPa, respectively, and ultimate strain larger than 30% (Figure 3.45).

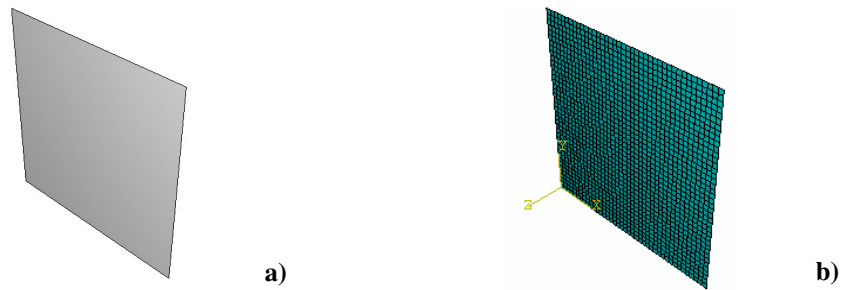


Figure 3.44: The implemented numerical model (a) and the used mesh (b)

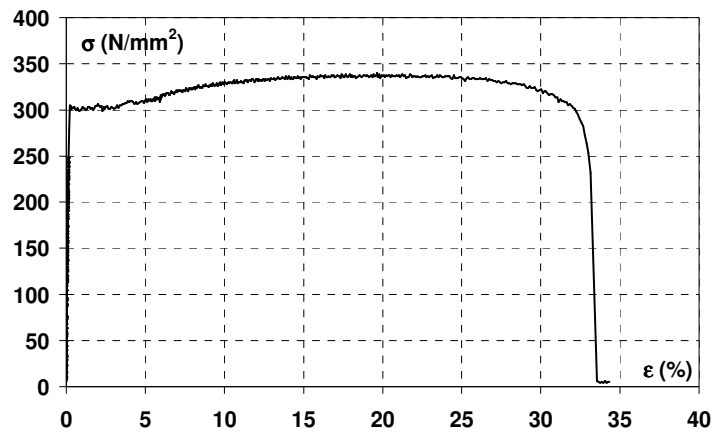


Figure 3.45: Stress-strain curve of the steel used for the shear panels

In the FEM models, the actual eccentricity between the external frame members and the internal plate element due to the connecting system and the size of the member cross-sections has been considered (De Matteis et al., 2005 a, b). The steel frame-to-panel connection has been introduced in the model by considering that no slip between the different parts occurs. This has been modelled by using the TIE constraint in the ABAQUS program library, which has been applied between the panel sides and the corresponding frame members. In the numerical analysis the external load was applied to the top beam of the external lateral reaction frame. The system response has been obtained by applying the modified Riks algorithm, which uses the Newton-Raphson procedure and belongs to the “arc-length” analysis method. In this algorithm the equilibrium condition is determined by iterative runs which move along the same equilibrium curve.

In the numerical model, aiming at verifying the influence exerted by the columns stiffness, steel frame members having different depth have been considered, as indicated in Table 3.4.

Table 3.4: Analysed shear plate configurations

Analysed configuration	Member profile	Second moment of area [mm⁴]
1	2 UPN 140	605 x 10 ⁴
2	2 UPN 160	925 x 10 ⁴
3	2 UPN 180	1350 x 10 ⁴
4	2 UPN 200	1910 x 10 ⁴
5	2 UPN 220	2690 x 10 ⁴

The member profiles have been selected starting from the minimum dimension stated by eq. (3.12), which provides a second moment of area equal to $620 \times 10^4 \text{ mm}^4$. Based on the performed numerical analysis, the shear stress - shear strain curves of analysed shear panel configurations have been obtained. The results are provided in Figure 3.46 in terms of equivalent uniform shear strain τ (which is the applied shear force F divided by the shear resistant area of the plate $A = 1000 \text{ mm}^2$) versus the shear deformation γ (assumed equal to the interstorey drift angle), where the influence of the column stiffness is noticeable.

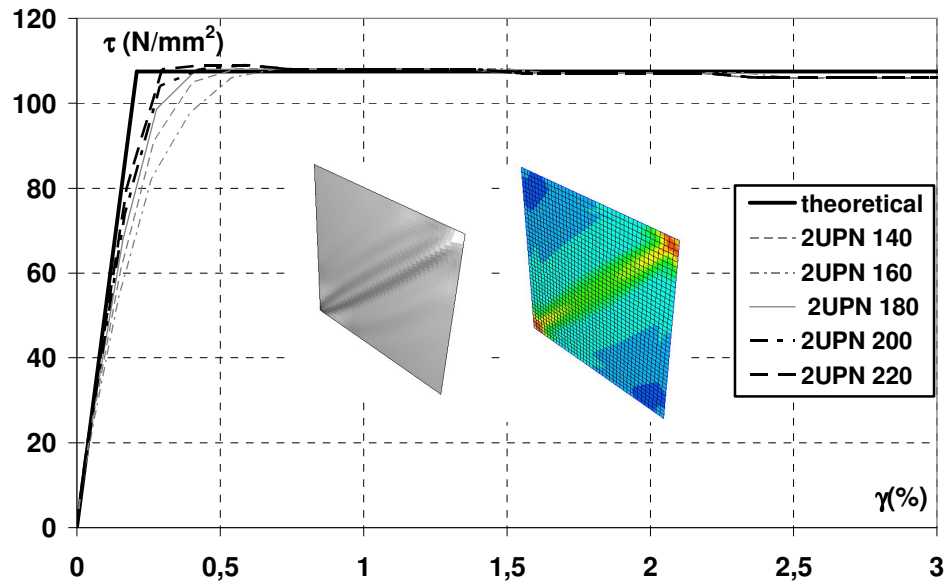


Figure 3.46: τ - γ curves of shear panel systems obtained by varying the frame members

It can be observed that the system stiffness tends toward the theoretical one as the column height increases. It is also evident that more rigid columns allow a more uniform distribution of the diagonal tension field within the panel. As a consequence, for such configurations, the corresponding curves of Figure 3.46 present a less pronounced non linear behaviour, allowing the attainment of the panel full plastic behaviour for smaller displacement levels, which become quite close to the theoretical one.

3.3.2.3 Influence of the aspect ratio

3.3.2.3.1 Foreword

The purpose of the current study is to analyse by numerical and theoretical ways the behaviour of shear panels, enclosed into a reaction steel frame, having a b/d aspect ratios ranging between 2.5 and 0.8. Such limit values are suggested by the Canadian code (CSA, 2001) in order to guarantee the development of a correct plastic mechanism.

The finite element model has been developed by means of the ABAQUS numerical code. The obtained results have been compared with the theoretical ones, namely the Plate Frame Interaction (PFI) method, developed by Sabouri-Ghomi & Roberts (1991), and the Strip Model, introduced by Thorburn et al. (1983).

3.3.2.3.2 Panels with “compact” shape

Among panels having a b/d ratio ranging between 0.8 and 2.5, which here are defined as “compact” shape panels, three different aspect ratios (0.8, 1.0 and 2.0) have been analysed. In all cases shear plates have been inserted into a reaction steel frame composed by coupled UPN 220 profiles (Figure 3.47).

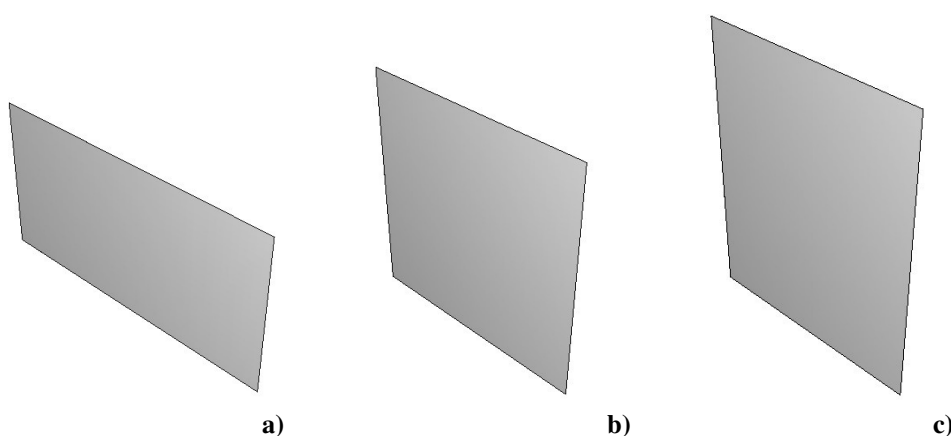


Figure 3.47: Geometry of analysed shear panel shapes: a) $b/d = 2.0$, b) $b/d = 1.0$, c) $b/d = 0.8$

The results of the numerical study performed on the selected configurations have underlined as the behaviour is only slightly different from each other. In fact, the corresponding shear stress τ – shear strain γ curves do not present any difference in terms of stiffness and maximum strength, as evidenced in Figure 3.48. In the same figure the theoretical behaviour of shear plates determined by the PFI method (Sabouri-Ghomi and Roberts, 1991) is depicted, showing as the latter is able to adequately interpret the behaviour of slender shear panels subjected to horizontal actions. This is also confirmed by the stress state developed in the panels, after the occurrence of buckling phenomena,

which evidences an inclination angle of tensile bands close to 45° (Figure 3.49).

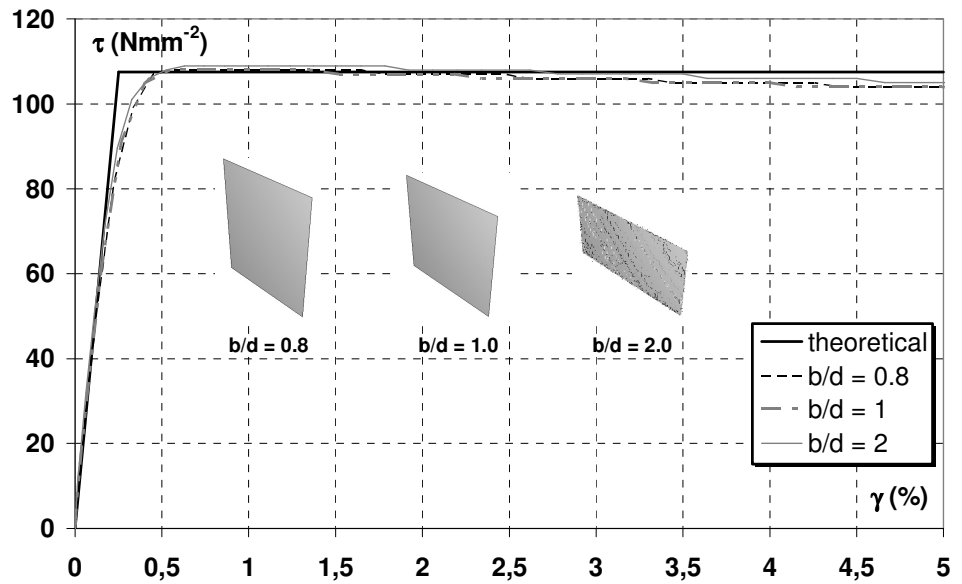


Figure 3.48: Numerical response of analysed shear panels

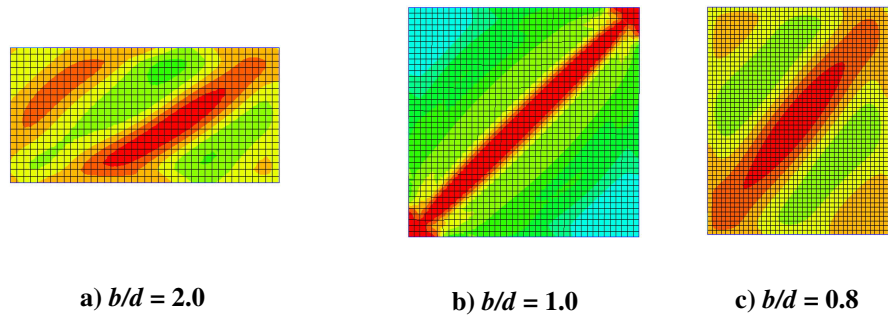


Figure 3.49: Tension field developed in the analysed shear panels

In addition, by comparing the results obtained by the application of the Abaqus model and the ones related to the Strip Model, in case of panel geometric configuration $b/d = 1.0$, a very good agreement can be noticed (Figure 3.50).

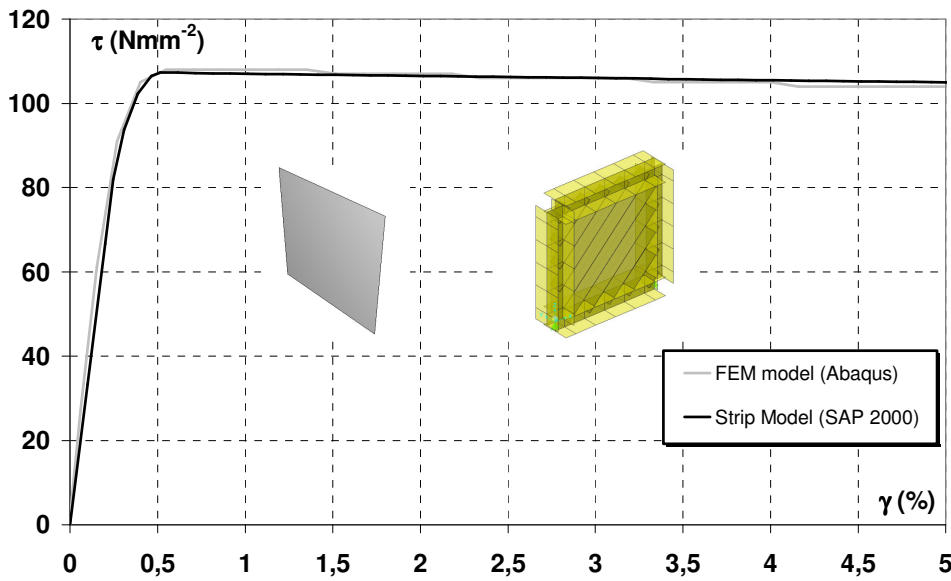


Figure 3.50: Numerical comparison between the numerical result (Abaqus model) and the application of the Strip model for the panel configuration with $b/d = 1.0$

Additional analyses have been carried out in order to establish the influence of the b/t ratio on the behaviour of slender panels having aspect ratios enclosed in the above range. The numerical investigation has been developed on a 1000x1000 mm panel having different thickness values (see Figure 3.51). The comparison of the obtained results in terms of τ – γ curves shows that the panel behaviour remains substantially unchanged. The only discrepancy is related to the initial stiffness. This can be explained considering that, for panels having constant shape ratio and boundary conditions, the critical load is proportional to the square thickness while the strength increases linearly with t . Therefore, the ratio between the panel critical load ($F_{cr,n}$) and its maximum strength (V) becomes more and more significant for larger plate thickness (t) (Table 3.5). From the same table it is also evident that the numerical evaluation of the panel critical load ($F_{cr,n}$) is very close to the one obtained from the application of the Timoshenko linear theory ($F_{cr,t}$) (Timoshenko and Woinowsky-Krieger, 1959). As a consequence, panels

having larger thicknesses show a slight increment of both strength and stiffness (see Figure 3.51).

Table 3.5: Percentage scatters between the numerical critical load ($F_{cr,n}$) and the maximum strength (V) of panels

	Thickness [mm]			
	1	2	3	4
$F_{cr,n}$ [kN]	2,65	20,70	68,90	161,30
$F_{cr,t}$ [kN]	2,71	21,69	73,21	173,5
V [kN]	107,5	219,0	331,0	444,0
C_v [%]	2,46	9,45	20,81	36,33

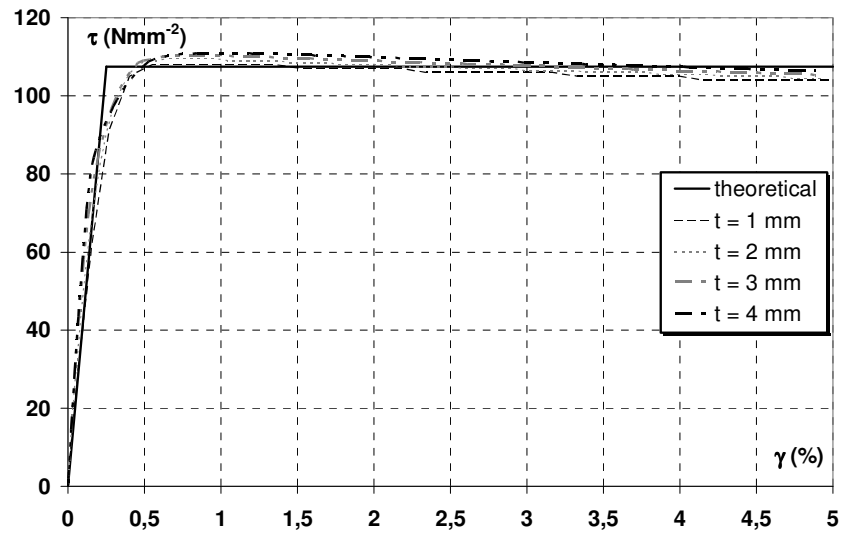


Figure 3.51: Results of numerical analysis carried out on panels having $b/d = 1.0$ and different thicknesses

Therefore it can be concluded that the behaviour of shear panels having b/t ratio close to 200 cannot be correctly interpreted neglecting the pre-critical phase, according to the eq. (3.13), considering an initial shear stiffness under pure shear actions equal to:

$$K = \frac{G}{d} b t \quad (3.16)$$

where G is the shear elastic modulus of the material.

3.3.2.3.3 Panels with “slender” shape

In the following the shear panel having aspect ratio $b/d < 0.8$ is analysed. In particular, two panel configurations, having aspect ratio equal to 0.67 and 0.50, are taken into consideration by means of both finite element models and simplified models (PFI, Strip model). In Figure 3.52, the results of the numerical FEM analysis are shown. In the same figure, the theoretical response predicted by the method provided in Section 3.2 is depicted.

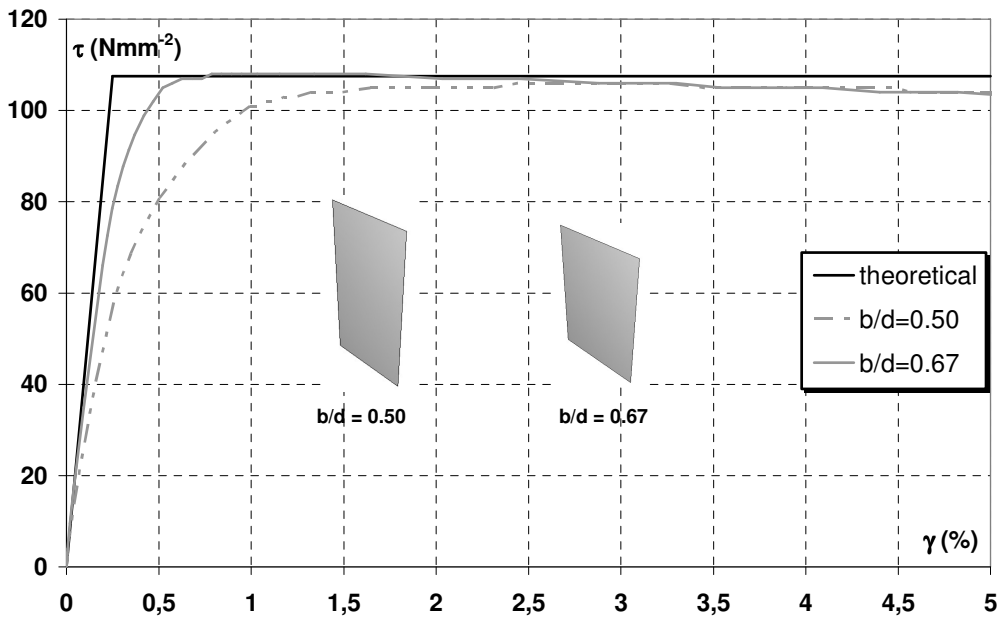


Figure 3.52: Structural response of analysed slender shear panels

The corresponding comparison evidences that the response of the examined systems changes significantly. In particular, when the b/d ratio decreases, the shear panel presents a more flexible behaviour, reaching the ultimate strength for large displacements only. For this reason, the PFI method, which provides a panel stiffness significantly greater than the actual one, is not able to predict

the behaviour of such a system. This phenomenon is due to two different reasons, namely the tension field inclination, which is greater than 45° (Figure 3.53), and the flexibility of the surrounding columns, which are directly interested, especially in the middle panel height, by the effects due to diagonal tensile stresses. Although the tension field inclination is greater than 45° , the ultimate strength obtained by FEM analysis for large displacements is the same achieved by the application of the theoretical method due to the fact that, during the loading phase, a rotation of the tensile stress state occurs (Figure 3.54).

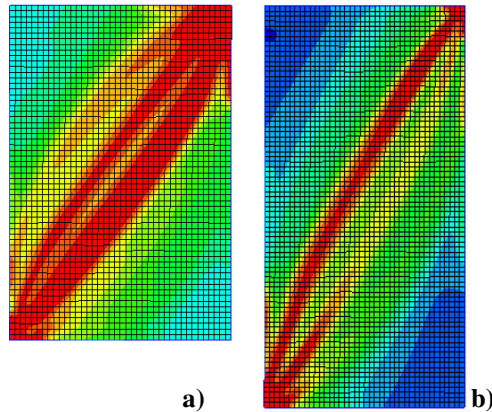


Figure 3.53: Tension field mechanism for the analysed panels: $b/d = 0.67$ (a) and $b/d = 0.50$ (b)

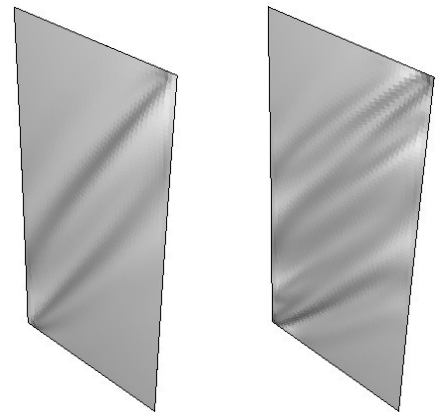


Figure 3.54: Variation of the tensile bands inclination during the loading phase ($b/d = 0.50$)

With reference to the panel having a b/d ratio equal to 0.50, the comparison between numerical and theoretical results shows some discrepancies, due to the larger flexibility evidenced by the strip model curve, although both models provide the same ultimate strength which is attained at the same deformation amplitude (Figure 3.55).

For the same shear panel configuration, the behaviour for different thicknesses has been evaluated. The comparison is provided in Figure 3.56 in terms of shear stress – shear strain curve.

It is apparent that the behaviour of the system is not significantly affected by the plate thickness, confirming the importance of the b/d ratio which, when lower than 0.8, causes a strong increase of system flexibility.

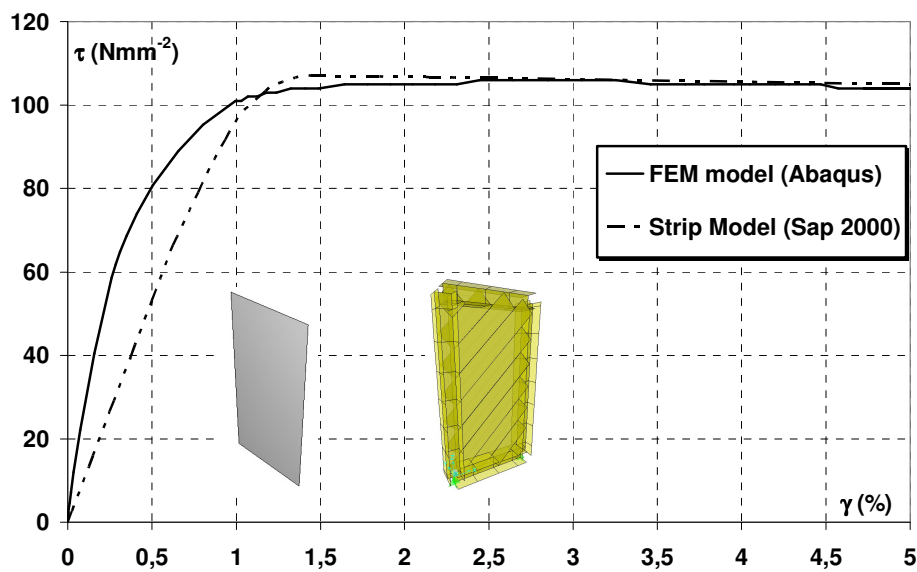


Figure 3.55: Comparison between numerical and theoretical curves for shear panel with $b/d = 0.50$

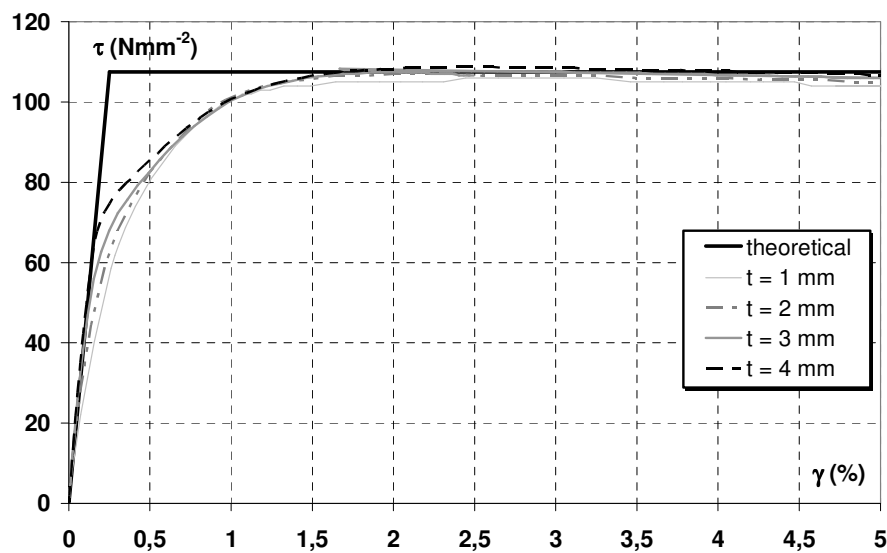


Figure 3.56: Numerical responses of the shear panel having $b/d = 0.50$ and different thicknesses

3.3.2.4 Influence of intermediate ribs

3.3.2.4.1 Design of intermediate stiffeners

In the previous Section, it has been clearly stated that the behaviour of shear panels having aspect ratio less than 0.8 is not satisfactory. Therefore, in the following the possibility to apply intermediate horizontal stiffeners in order to control the development of the tension field mechanism is investigated. To this purpose two different methods are applied: the first approach is based on the insertion of an intermediate beam within the reaction steel frame, so to consider two different sub-panels. The second approach is instead based on the introduction of two fishplates located on both panel sides aiming at realising an intermediate stiffener. In the former, both a smaller column deformability and a stable tension field mechanism, characterised by an inclination angle of 45° , are achieved. On the other hand, aiming at reaching such benefits, the intermediate beam must be not necessarily connected to the shear panel, but it should be able to avoid out-of-plane buckling of the plate.

When applying the second proposed solution, the shear walls behave as a stiffened girder web, presenting a reduced b/d ratio and consequently an increased critical stress. The stiffener dimensions can be evaluated by the elastic analysis of stiffened plates (Timoshenko and Woinowsky-Krieger, 1959). In such a way it is possible to determine the minimum value of the second moment of area of the stiffener I_o able to prevent its instability under the developing stress state load. Such a value is obtained by determining the relative flexural stiffness γ_{st} between the plate and the stiffeners:

$$\gamma_{st} = \frac{E \cdot I}{D \cdot d} = \frac{12 \cdot (1 - \nu^2) \cdot I}{t^3 \cdot d} \quad (3.17)$$

which assumes for steel the following expression:

$$\gamma_{st} = 10.92 \frac{I}{t^3 \cdot d} \quad (3.18)$$

The above relationship is applied neglecting the post-critical reserves that shear panels exhibit after the occurrence of buckling phenomena.

In order to exploit the panel strength resources in the post-critical field, the ECCS recommendations (1988) suggested to consider stiffeners with an increased relative flexural stiffness γ^* :

$$\gamma^* = \gamma_{st} \xi \quad (3.19)$$

where the coefficient ξ , depending from both the stiffeners position and the stresses type, assumes values equal to 4 and 2.5 for ribs having open and closed cross-section, respectively.

Aiming at determining the optimal second moment of area of intermediate stiffeners to be inserted on the panel surface, reference to the formulae given by EC3 ((EN 1993-1-1, 2005) may be made:

$$\frac{a}{h_w} < \sqrt{2} \Rightarrow I_{st} \geq \frac{1,5 h_w^3 t^3}{a^2}; \quad \frac{a}{h_w} \geq \sqrt{2} \Rightarrow I_{st} \geq 0,75 h_w^3 t^3 \quad (3.20)$$

where a and h_w are the panel base and height, respectively. Therefore, in the analysed case, the following rib stiffness is determined:

$$\frac{a}{h_w} = 1 < \sqrt{2} \Rightarrow I_{st} \geq \frac{1,5 h_w^3 t^3}{a^2} = \frac{1,5 \cdot 1000^3 \cdot 1^3}{1000^2} = 1500 \text{ mm}^4 \quad (3.21)$$

The selected stiffening type is realised with steel fishplates, placed on both sides of the panel, which are connected to the base plate by means of steel bolts. In particular, by adopting a stiffener depth equal to 200 mm and being in the analysed case $\xi = 4$, two fishplates having thickness of 4 mm must be used aiming at guaranteeing a stable development of tensile bands within each panel field. Based on the execution of numerical analyses on slender shear panels endowed with stiffening plates having thickness t ranging between 2 and 5 mm, the effectiveness of the selected fishplates is shown in Figure 3.57.

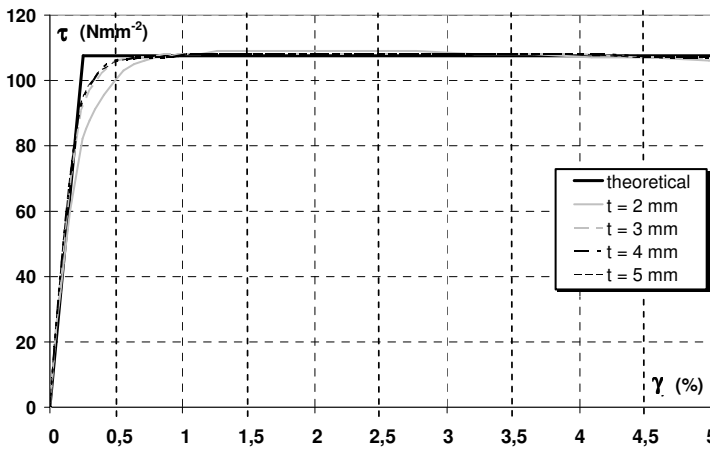


Figure 3.57: Results of numerical analysis carried out on slender shear panels ($b/d = 0.5$) endowed with fishplates having different thicknesses

3.3.2.4.2 The numerical results

Once an appropriate intervention to improve the response of slender shear panels (aspect ratio less than 0.8) has been defined, a refined FEM model has been developed in order to determine the actual behaviour of the system (Figure 3.58). The comparison shows that the numerical curves related to slender shape shear panels endowed with intermediate beam and stiffeners ($t = 4$ mm) are characterised by a constant stiffness up to the attainment of the maximum panel strength, as it was observed for “compact” shape panels (see Figure 3.59).

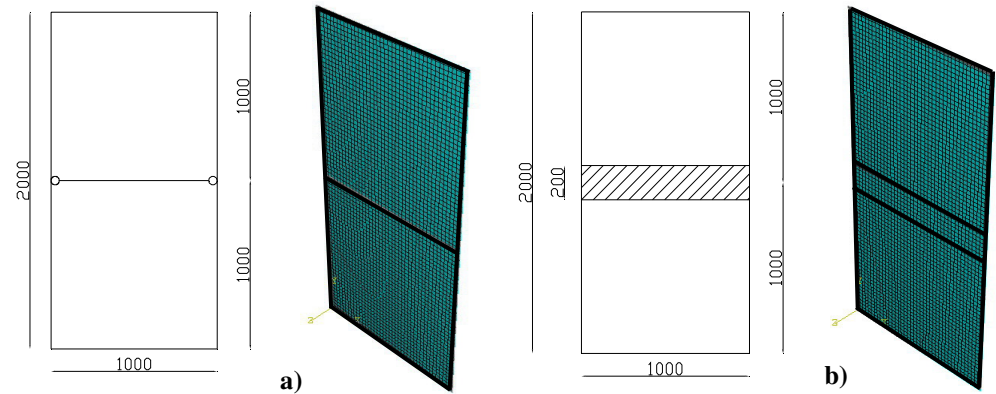


Figure 3.58: Geometry and numerical model of analysed slender shape shear panel endowed with an intermediate beam (a) and intermediate stiffeners (b)

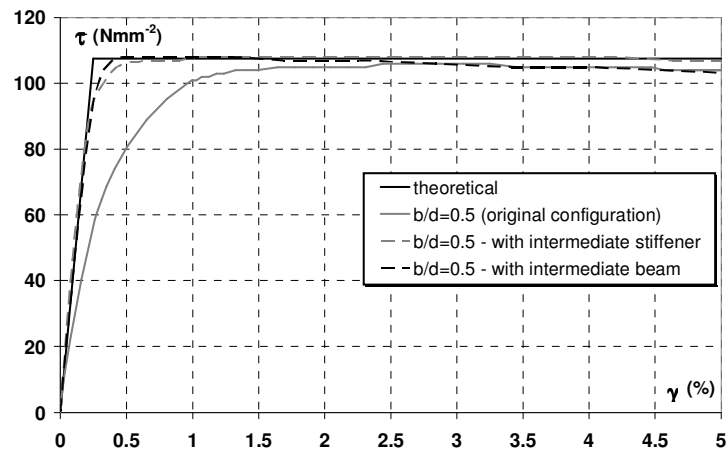


Figure 3.59: Behaviour of slender shape shear panels ($b/d = 0.5$) with and without intermediate stiffeners

In addition, such curves appear to be very close to the theoretical one. In fact, for both shear panels the inclination angle of the tension field is about 45° , allowing the involvement of the whole plate surface in the load resisting mechanism (Figure 3.60). Such a result is also apparent from Figure 3.61, where the deformed shape of two shear panels is depicted.

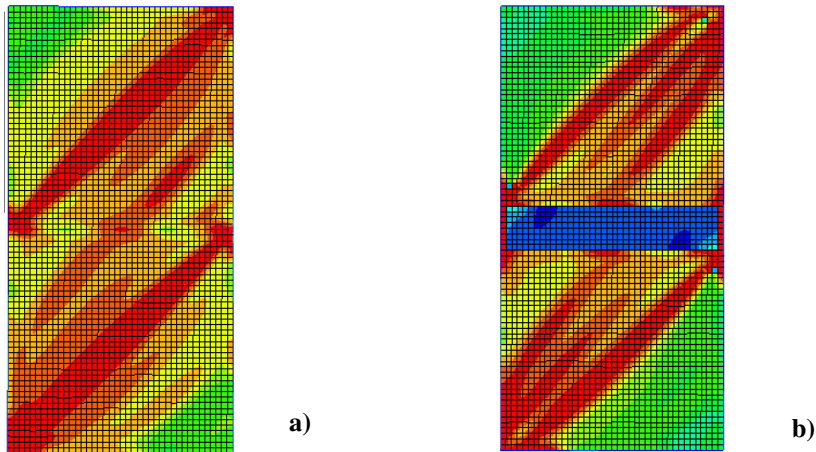


Figure 3.60: Stress state developed in the analysed shear panel: endowed with an intermediate beam (a) and with stiffening fishplates (b)

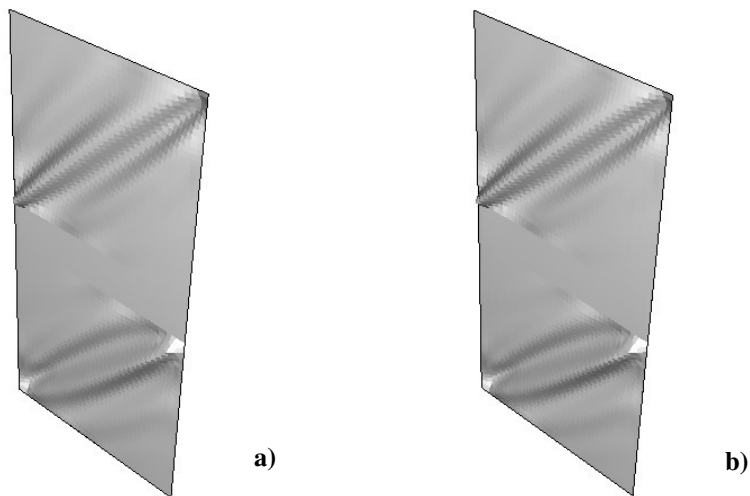


Figure 3.61: Deformed shape of the analysed shear panel: endowed with an intermediate beam (a) and with stiffening fishplates (b)

Finally, in Figures 3.62 and 3.63, the results obtained by the strip model (SAP 2000) for the analysed systems are compared with the numerical results obtained by the application of the refined FEM model, showing a good agreement in terms of both maximum strength and stiffness.

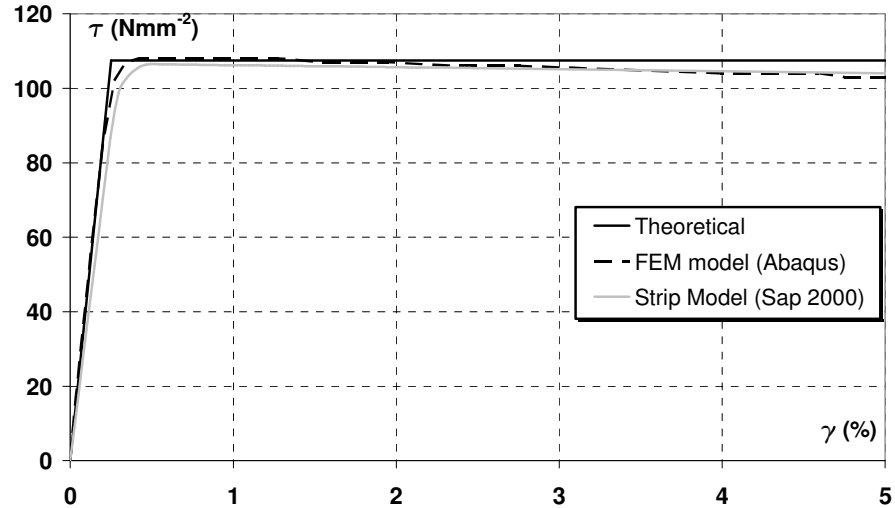


Figure 3.62: Comparison between the theoretical and numerical results of a slender shape shear panel ($b/d = 0.50$) endowed with an intermediate beam

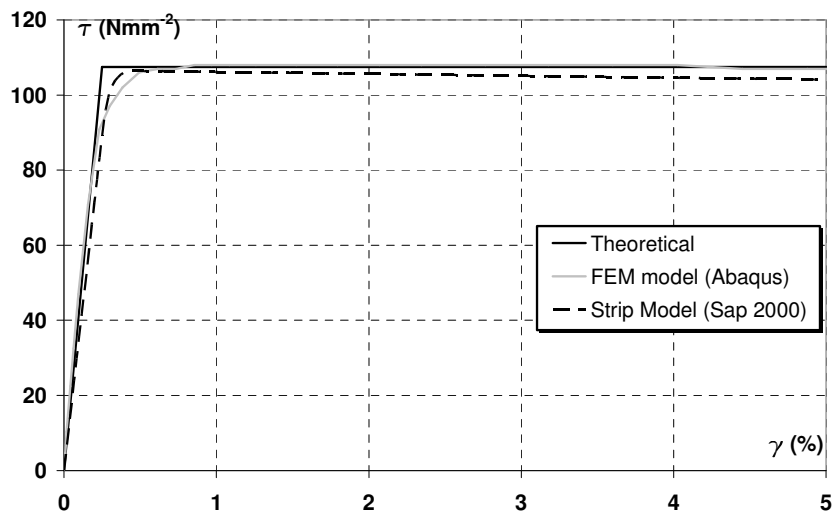


Figure 3.63: Comparison between the theoretical and numerical results of a slender shape shear panel ($b/d = 0.50$) endowed with intermediate stiffeners

3.3.2.5 Concluding remarks

In the current study the behaviour of slender steel shear panels characterised by different thicknesses and aspect ratios has been investigated under theoretical and numerical ways. The numerical analysis, which has been carried out by means of the ABAQUS non linear FEM program, have shown that when the b/d ratio ranges between 0.8 and 2.5, the shear panel presents a high initial stiffness, which remains constant until the maximum capacity is attained. Such a condition is due to the fact that the tension field mechanism developing in the post-critical field remains stable during the loading phase, without suffering any variation of the inclination angle. At the same time it has been observed that the available simplified theoretical (PFI method) and numerical (Strip Model) models are able to adequately interpret such a behaviour.

On the other hand, slender steel shear panels having an aspect ratio less than 0.8 are more flexible, the diagonal tension field being characterised by an inclination angle larger than 45° . Aiming at improving the behaviour of slender shape shear panels, two stiffening systems, based on placing an intermediate beam in the reaction frame and two coupled fishplates on the panel surface, have been analysed. In particular, the optimal thickness used for fishplates, firstly determined on the basis of provisions given by the EC3 code, has been subsequently verified by means of numerical analyses. Finally, it has been observed that both solutions provide the same beneficial effect on the shear response of the steel panel, allowing a global behaviour similar to the one of “compact” shape shear plates, therefore confirming the possibility to apply effectively simple technological solutions to improve the structural performance of the system when subjected to shear forces.

Chapter IV

The building under investigation

4.1 GENERAL

In the framework of the seismic retrofitting of reinforced concrete (RC) buildings by means of advanced and innovative techniques based on the use of metallic devices, the possibility to enrich the knowledge on the use of metal shear panels under both the experimental and theoretical point of view came from the availability of a real RC building located in the Bagnoli district of Naples (Mazzolani, 2006a). Within this area, a very important industrial plant producing steel, known as ILVA (former Italsider), was realised (Figure 4.1).



Figure 4.1: The Italsider industrial plant in Bagnoli (Naples)

Recently, the European Community decided to reduce the Italian steel production; therefore, many iron and steel industries were closed. Being the Bagnoli site a very attractive area from both the residential and tourist point of views, the existing plant of the steel mill was immediately closed. So, many buildings were demolished and others will be destroyed in the next future.

However it was recognized that several of these buildings presented a cultural value in the field of Structural Engineering, since they represented the construction practice for residential and industrial RC constructions during 60's – 70's in the South of Italy.

According to the design procedures and technical standards applied to buildings before 1980, when Naples was not considered as a seismic area, such structures, which were realised either without or with small attention to the effect of lateral actions, belonged to the gravity load designed (GLD) buildings category.

Besides, such structures were subjected to deterioration of component materials (concrete and steel), which were exposed to highly aggressive environmental conditions due to the their location in a contemporary coastal, industrial and metropolitan area, more and more influenced by the atmospheric pollution.

Therefore, the necessity to eliminate such structures allowed to transform the demolishing area into a field- research laboratory. Consequently the research project was “christen” with the acronym of “ILVA-IDEM” (ILVA Intelligent DEMolition) (Mazzolani, 2006b).

This activity, which started in 2000, represents a kind of natural conclusion of many years of cooperation activities between this steel industry and the University of Naples “Federico II” (Pagano and Mazzolani, 1966).

The need to evaluate the structural vulnerability of such buildings and, therefore, to select appropriate methods for their upgrading and/or rehabilitation, are fundamental operations aiming at conferring to the building the strength, stiffness and ductility requirements which are representative of the functionality established in compliance to the socio-economical development plan of the site.

In fact, the interest of the scientific community in this field is growing in order to reduce damages to existing buildings. These problems can be ascribed both to seismic phenomena, frequently occurred on the Italian territory, and to

the deterioration of building during their life, which is often derived either to the surrounding environment actions or to the change of both the functional and static scheme, in many cases made ignoring any technical standards.

The consequent socio-economic injuries, which could increase with time if no adequate interventions are adopted, induced to start several investigation campaigns on both masonry and RC buildings located on the Italian territory.

In addition, a lot of both theoretical studies and laboratory experiments on the techniques based on the above methods have been carried out. Nevertheless, even if laboratory tests are valuable, they presents some limitations due to the difficulty to correctly reproduce the real boundary conditions of the structure, to consider the scale-effect in reduced scale models and to reproduce actual structural defects, such as construction tolerances, bad execution, reinforcing bars corrosion and/or concrete degradation.

With regard to this aspect, the importance of taking advantage of an existing building used as a large scale specimen would be evidenced as a precious and unique unrepeatable occasion to improve the knowledge on both design and analysis methods. In fact, the opportunity to execute all of necessary investigations on such a structure allows on one hand to evaluate its structural vulnerability and on the other hand to identify the appropriate retrofitting technique, by comparing the efficiency of different technical solutions for both seismic reinforcing and upgrading of RC structures.

Besides, the major part of recent studies mainly examines each methodological solution independently from the others. Therefore, the surplus value of the current experimental investigation consists on both the analysis of a real building and the comparison of different technologies in the field of seismic upgrading, which are two paramount aspects of Earthquake Engineering. A number of both institutional and industrial partners have cooperated for the research activity herein presented. On the institutional side, three Italian Universities and one Italian public Institution were engaged. On the side of Industries, there were nine participants offering their economic and technological support. The research group components are listed in Table 4.1.

In addition, also many national and international Institutions and Research Projects (CNR, MIUR, RELUIS, PROHITECH) have supported the execution of such an experimental campaign.

Table 4.1: The ILVA-IDEM research group

INSTITUTIONAL PARTNERS	INDUSTRIAL PARTNERS	ACTIVITY
University of Napoli Federico II	BagnoliFutura	Site coordination and safety control
University of Chieti G.D'Annunzio	Italrecuperi	Demolition works
University of Basilicata	TIS	Special dissipative devices
Italian Dept. of Civil Protection	Dr. R. Del Gado & TECNO IN	Experimental measurements
	STRAGO	Experimental measurements
	Degussa CC Italia	Composite materials and advanced concretes
	Technobuilding Services	RC rehabilitation
	ALGA	Rubber bearings
	Giugliano Costruzioni Metalliche	Steelworks
	GIAN.BI.	Steelworks
	TIC	Steelworks
	Carannante	Steelworks
	CO.GE.FER.	Steelworks

4.2 THE ORIGINAL BUILDING

The original structure, which was designed and realised in 70's to serve as an office building, is a regular reinforced concrete building with framed structure and masonry infills designed to resist gravity loads only (Faggiano et al., 2006). The building configuration at the beginning of the investigation activities is illustrated in Figure 4.2, where both the north-east and the north-west sides are represented.



Figure 4.2: North-east (a) and north-west (b) sides view of the original RC building

The construction, which develops on two storeys (first storey and roof) with rectangular 41.60 m x 6.50 m floors, presents a single bay in the transversal direction and twelve bays in the longitudinal one (Figure 4.3). The total height of the building is 6.60 m, it being characterised by two inter-storeys heights equal to 3.30 m (Figure 4.4).

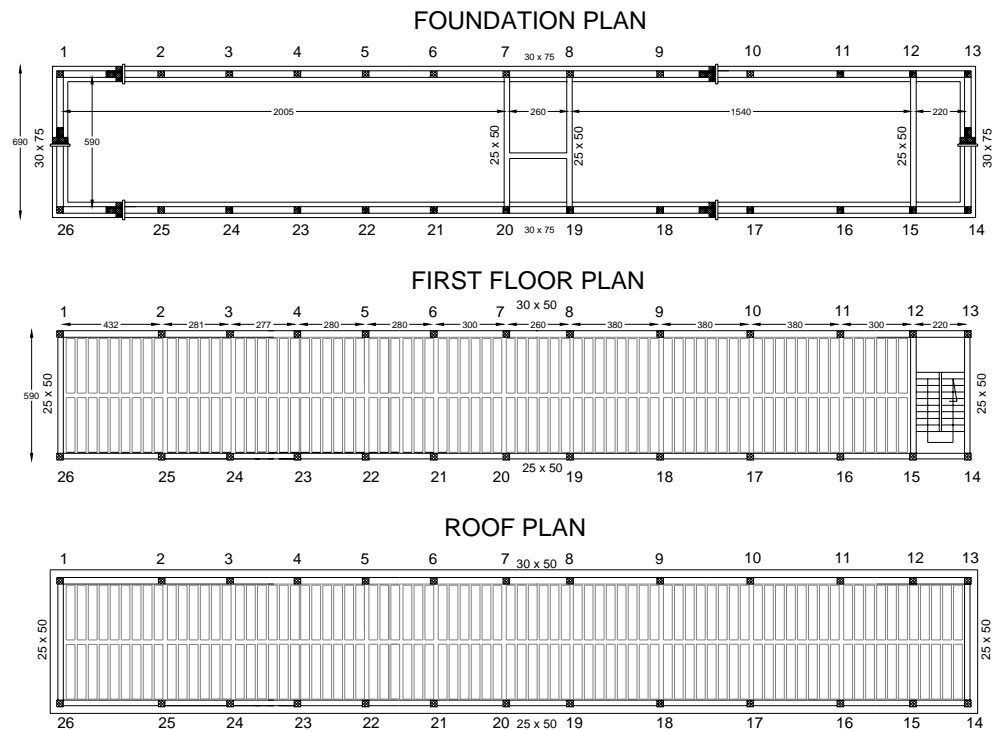


Figure 4.3: Plan configurations of the building at different levels (length unit: cm)

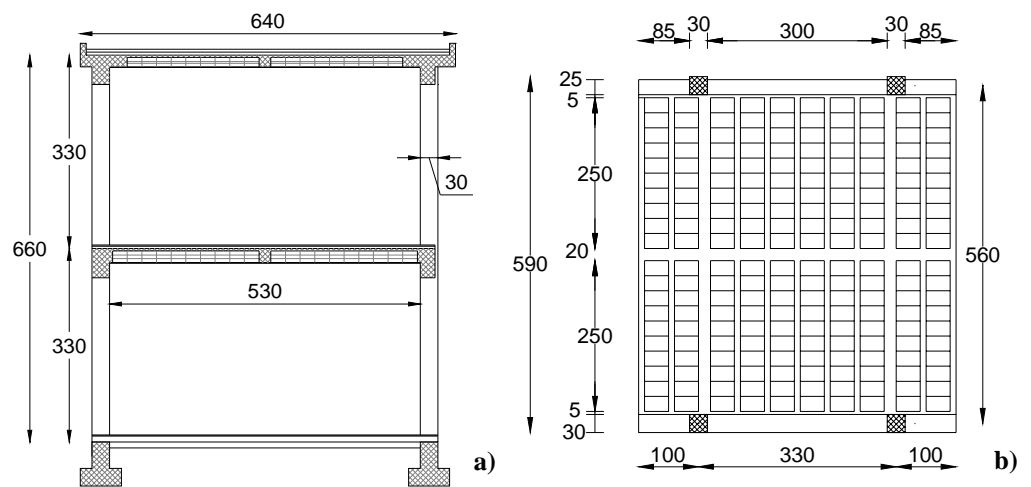


Figure 4.4: Transversal section (a) and detail of the slab (b) of the structure (length unit: cm)

As it is visible in Figure 4.3, direct foundations, which are realised with inverse T cross-section beams, are located along the building perimeter. The same disposition occurs both for the first and the second level beams. Only where staircases are located, namely in the central part and on one side of the building, transversal beams, having a rectangular 25 x 50 cm cross-section, connect the perimeter beams. At the first floor, 25 x 50 cm rectangular beams are located on three sides of the building, while along the south side 30 x 50 cm T-section beams are used. In the transverse direction, the lateral strength is supplied by 26 columns having 30 x 30 cm square cross-section.

Floors are made by reinforced concrete and hollow tiles mixed slabs, which are 24 cm and 20 cm high at the first and second floor, respectively. In the main direction of slabs, two types of floor beams, having both the same height and steel reinforcement but with different width (10 - 20 cm) are used. In particular, the larger floor beams are placed in order to connect transversally the columns. Besides, in the middle part of the slabs, a transverse 20 cm wide beam is located, it being used with the role of load shearing among the longitudinal floor beams.

Façade walls are composed by three layers: an external part of 4 cm thick tile blocks, an intermediate layer of 12 cm thick semi-hollow tile blocks and an internal coat made of 10 cm thick semi-hollow light concrete blocks. The latter layer type is also used to realise partition walls.

The steel reinforcements used for all structural elements are depicted in Figures 4.5 and 4.6. In particular two longitudinal $\phi 12$ bars and transversal $\phi 8$ stirrups, 25 cm spaced, are used for floor beam reinforcement. Besides, transversal $\phi 6$ bars, 40 cm spaced, are located at the extrados. On the other hand, longitudinal perimeter beams are reinforced at the top with two $\phi 8$ bars and at the bottom with two $\phi 8$ and 1 $\phi 12$ bars and transversal $\phi 8$ stirrups, 20 cm spaced. Columns are reinforced by four $\phi 12$ longitudinal bars and transversal $\phi 8$ stirrups, 20 cm spaced. Foundation beams are reinforced at both the upper and the lower side with four $\phi 14$ bars and transversal $\phi 8$ stirrups, 30 cm spaced.

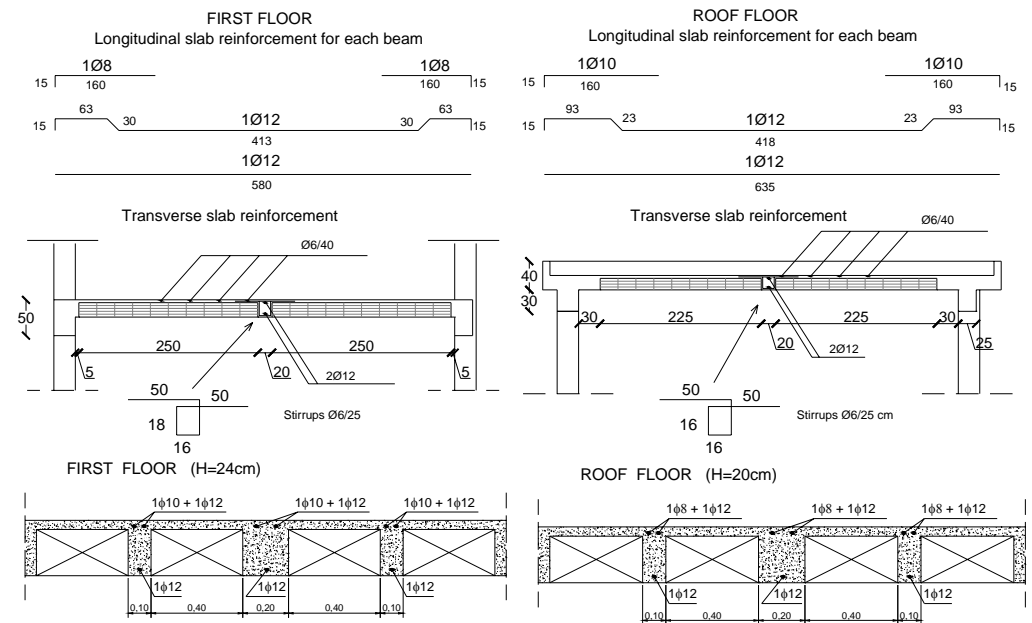


Figure 4.5: Steel reinforcement of the floor beams (length unit: cm)

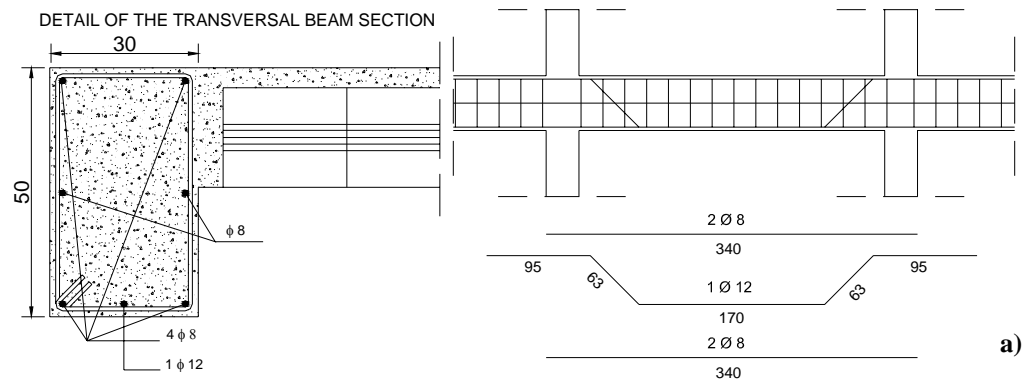


Figure 4.6: Steel reinforcement of beams (a), foundation beams (b) and columns (c)(length unit: cm) (continues)

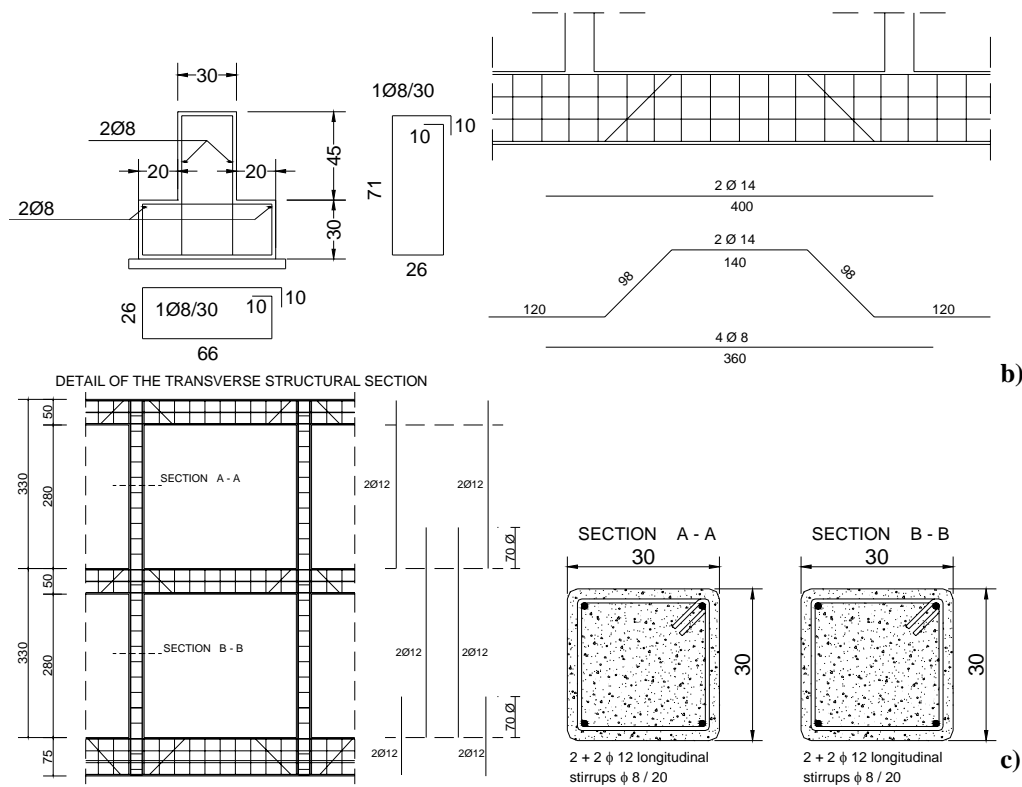


Figure 4.6: Steel reinforcement of beams (a), foundation beams (b) and columns (c)(length unit: cm)

4.2.1 The division in sub-structures

The strong regularity of the structure under investigation suggested to divide the building into six smaller similar sub-structures, herein referred to as structural modules, aiming at increasing the potential number of specimens to be tested with different upgrading solutions. In this way, a unique opportunity to investigate the effects of seismic rehabilitation and strengthening on a uniform comparative basis was provided (Valente et al., 2006).

To this purpose, firstly the elimination of completion elements from the original RC structure has been done. Then slabs were cut at both the first and the second level floors. The sequence of demolition phases is illustrated in Figure 4.7, whereas the six obtained sub-structures are shown in Figure 4.8.



Figure 4.7: Demolition activities: removing of partition (a) and internal (b) walls and cutting of slabs (c)

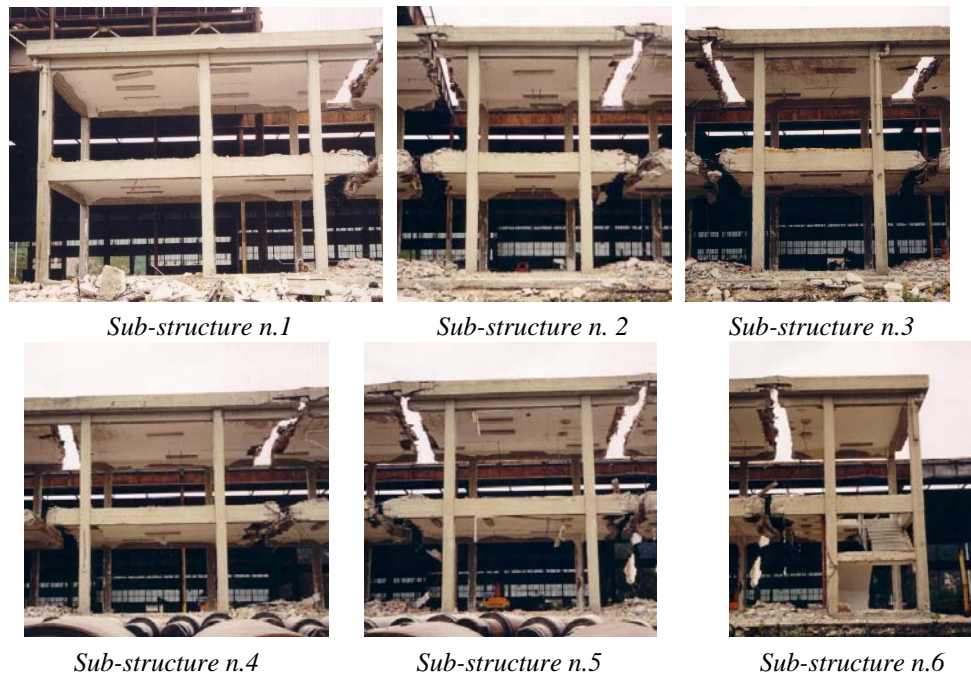


Figure 4.8: The obtained six modules

The geometry of each module has been acquired by means of the detection of the structural member sizes, the slab arrangement, the steel reinforcement and so on. The sub-structures from 2 to 5 present the same geometrical typology, they having two column alignments in the transverse direction, with few differences in bay spans along the longitudinal direction. On the other hand the modules at the building ends (n.1 and n.6) are different from the central ones. In fact, the module n.1 consists of three transverse column alignments and two unequal bays in the longitudinal direction, while the n.6 one is occupied by the staircase, having its structure realised with knee beams.

Figure 4.9 shows the building divided into six separate sub-structures, highlighting the different seismic upgrading systems chosen for testing.

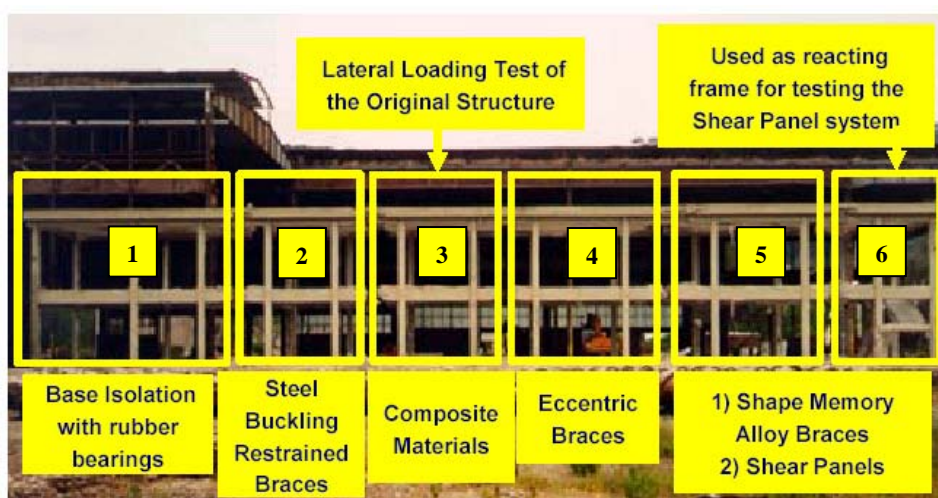


Figure 4.9: Different systems considered for seismic upgrading

In particular, the following techniques have been applied:

- Module n.1: base isolation with neoprene bearings (Figure 4.10 a).
- Module n. 2: buckling restrained bracings (BRBs) (Figure 4.10 b). In such a case, the unbonded brace typology has been adopted, it being obtained by inserting steel rectangular plates between two box profiles which have the function to stabilise the internal element from eventual lateral deformations, so that it could absorb external actions.

- Module n. 3: carbon – fiber reinforced polymers, under form of strips and sheets, applied to the columns in order to modify the structure collapse mechanism (Figure 4.10 c).
- Module n. 4: eccentric bracings (EBs), characterised by an inverse Y scheme (Figure 4.10 d).
- Module n. 5: shape memory alloys (SMAs) applied under form of concentrating bracings (Figure 4.10 e). SMAs have super-elastic characteristics which, opportunely used, confer to the anti-seismic devices a strong self-centring capacity able to drastically reduce or nullify the residual deformations of frames due to the excursion in the plastic field of structural members subjected to earthquake effects. After the mentioned application, such a module has been used to evaluate the effectiveness of the intervention based on the use of metal shear panels, which represents the main purpose of the present study.
- Module n. 6: used for the extraction of specimens (concrete and steel bars) tested for the material characterisation and as a retaining structure for the module n.5, which was tested under lateral loads in the longitudinal direction of the building (Figure 4.10 f).



Figure 4.10: Anti-seismic devices applied on the six modules (continues)



Figure 4.10: Anti-seismic devices applied on the six modules

Fifteen full-scale tests on the sub-structures retrofitted with the above mentioned systems have been carried out, including three tests on the bare RC structures.

4.2.2 The selected RC module

As cited in the previous Section, the module n. 5 has been chosen to be upgraded with metal shear panels (Figure 4.11).



Figure 4.11: General view of module n. 5

The geometrical configuration of the sub-structure is characterised by a rectangular plan with dimensions of 6.30 x 5.90 m and two floors with heights on the ground of 3.55 m and 6.81 m, respectively, with not practicable roof.

The slab thickness is equal to 24 cm and 20 cm for the first and the second floor, respectively. Both slabs have a middle transversal floor beam and are supported by emergent rectangular beams (30 x 50 cm and 25 x 50 cm) placed along the longitudinal direction at the first level. On the other hand, at the second level, the beams have a T cross-section with the same width and the same height of the first level one. In the transverse direction, lateral strength is essentially provided by columns, which have square cross-section with 30 cm of side and are reinforced with four longitudinal steel bars $\Phi 12$, placed at the corners of the section. Square steel stirrups $\Phi 8$ were placed in the columns with 300 mm spacing. No complementary elements are located at the first floor, excluding a plaster layer, having thickness of 4 cm, located on the intern side of the slab. Contrary, at the roof floor, both a 5 cm thick slope slab, realised with sand and mortar, and waterproofing layers are located. The foundation structure is composed by two reverse T-shaped beams placed in longitudinal direction.

The geometry of the sub-structure has been measured and data about the structural member sizes, the slab arrangement, the steel reinforcements and so on, have been acquired and briefly summarised in Figure 4.12, in which the structural sections of the RC module are reported too.

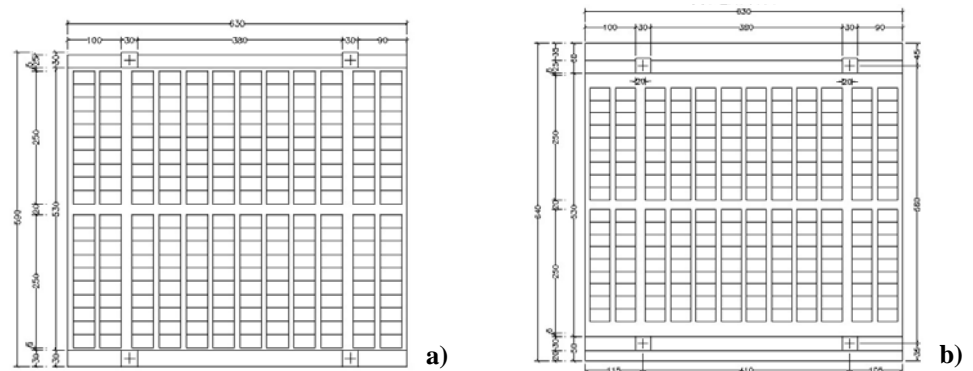


Figure 4.12: Geometrical characteristics and some structural details of the module n. 5: first level (a) and roof (b) floors, transversal (c) and longitudinal (d) sections, first floor (e) and roof (f) slab cross-section, first level (g) and roof (h) beams and column cross-section (i) (continues)

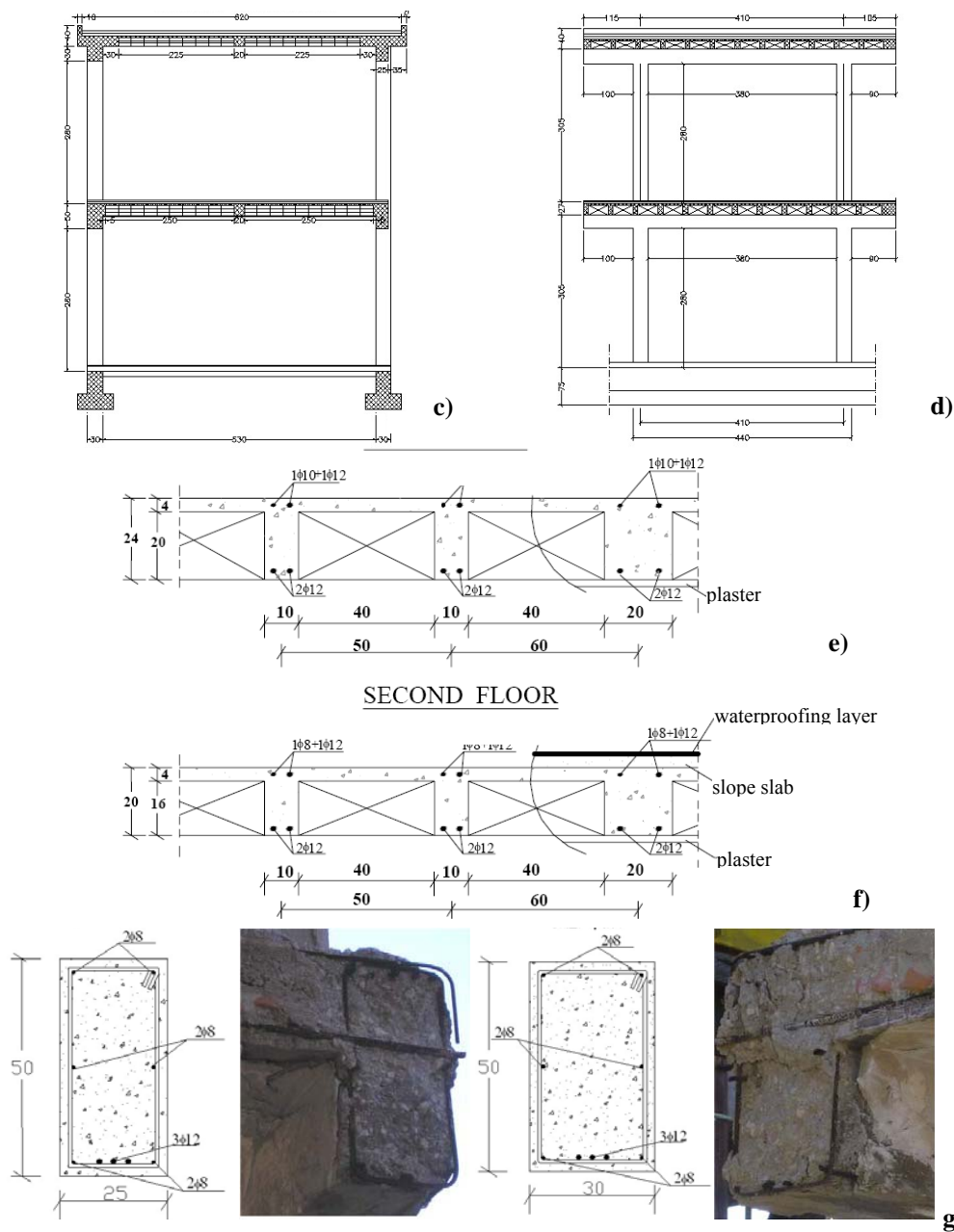


Figure 4.12: Geometrical characteristics and some structural details of module n. 5: first level (a) and roof (b) floors, transversal (c) and longitudinal (d) sections, first floor (e) and roof (f) slab cross-section, first level (g) and roof (h) beams and column cross-section (i) (continues)

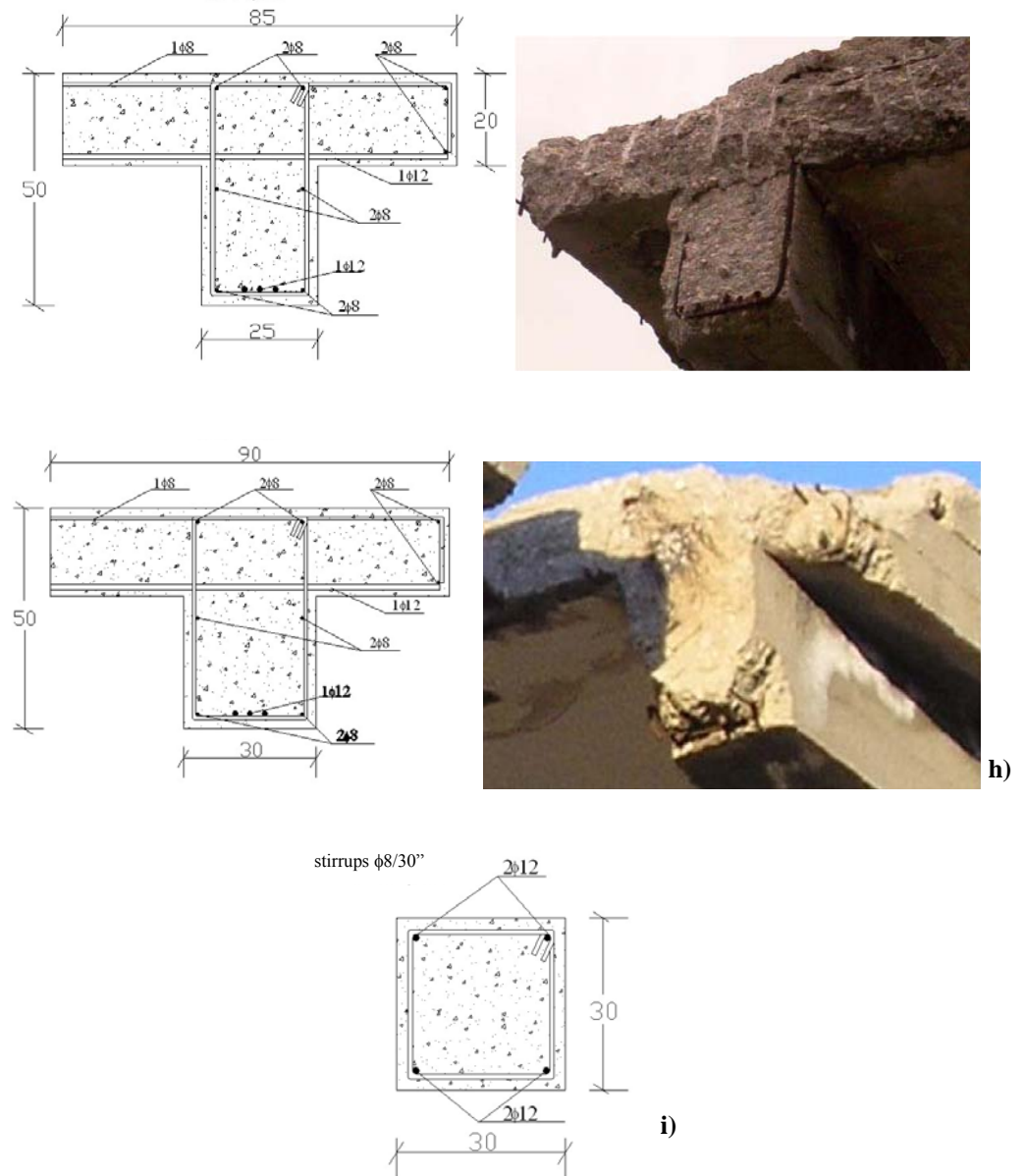


Figure 4.12: Geometrical characteristics and some structural details of module n. 5: first level (a) and roof (b) floors, transversal (c) and longitudinal (d) sections, first floor (e) and roof (f) slab cross-section, first level (g) and roof (h) beams and column cross-section (i)

Such a module was initially tested in the weak direction (transversal direction) for the application of the intervention proposed by the University of Basilicata, based on concentric diagonals made-up with a mixed technology of shape-memory alloys and viscous dampers as upgrading system.

4.2.3 The material mechanical features

As a first step of the research activity, the evaluation of the mechanical characteristics of the structure materials has been done.

The main mechanical properties of both concrete and steel bars have been determined by means of laboratory tests carried out on specimens directly extracted from the existing structural members (Faggiano et al., 2006). Also, a number of non destructive tests (NDTs) were performed on concrete elements aiming at evaluating both the quality and the distribution of their properties in the structure. The knowledge of such features is very important both for addressing the seismic behaviour of the RC structure under study and calibrating a refined numerical model.

Three concrete cylinders, which were removed from the module n.6 (Figure 4.13), have been subjected to compression tests (Figure 4.14), whose resulting stress-strain curves are reported in Figure 4.15. In addition, both the Young modulus and the axial compression strength of the concrete specimens, together with their mean values, are given in Table 4.1.



Figure 4.13: Extraction of cylindrical concrete specimens from the module n.6

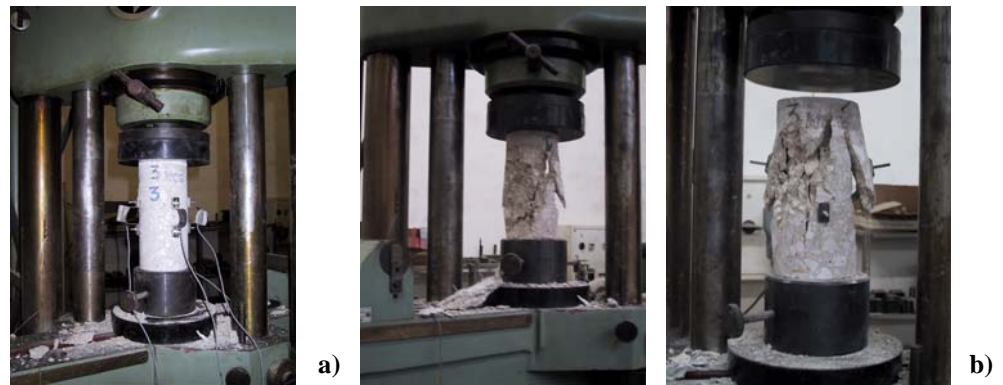


Figure 4.14: Concrete specimen subjected to compression test: initial (a) and collapse (b) phases

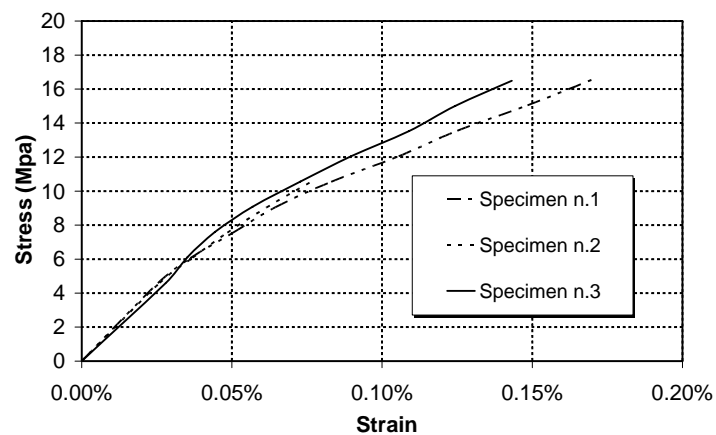


Figure 4.15: Stress-strain curves of tested concrete specimens

Table 4.1: Mechanical properties of concrete specimens

Specimen n.	Unit weight (kg/m ³)	Elastic modulus (MPa)	Strength (MPa)
1	2244	17692.0	20.5
2	-	16666.7	21.0
3	2235	16129.2	19.9
Average	2239	16829.3	20.5

On the other hand, NDTs consisted in the measurement of the ultrasonic pulse velocity (V) and the rebound index of the sclerometer (I_r), which can be correlated with the Young modulus and the strength of the concrete. Such tests were performed for all columns at their middle height (Table 4.2); moreover, in order to catch the variability of concrete properties along the member development, the measurement of features at both the base and the top of one column only (column n.1) was carried out, as shown in Table 4.3, where T (top), M (middle) and B (base) indicate three different positions of the column n.1 where measurement operations have been performed.

Table 4.2: Non destructive tests on the middle height of tested columns

Column n.	Floor n.	Section -	V (m/s)	Ir -
1	2	M	3920	38.6
1	1	M	3800	33.1
2	2	M	4039	28.4
2	1	M	4050	38.1
3	2	M	4039	28.4
3	1	M	4090	38.0
4	2	M	3810	32.4
4	1	M	4145	35.0

Table 4.3: Non destructive tests performed at different points of the column n.1

Column n.	Floor n.	Section -	V (m/s)	Ir -
1	2	T	2930	35.1
1	2	M	3920	38.6
1	2	B	4168	38.9
1	1	T	3790	32.5
1	1	M	3800	33.1
1	1	B	3910	32.3

From the obtained values it is observed that the concrete resistance increases from top to bottom of the column, showing that the elastic

deformation capacity is not uniform along the columns height; furthermore, some scatters in the average values measured at the middle height of columns exist.

The definition of V and I_r and their combination allow to obtain the Young modulus and the concrete strength, which were equal to 17214 MPa and 21.4 MPa, respectively. In such a framework, it is important to observe that the obtained values are only slightly different from the laboratory ones.

Furthermore, tensile tests on both longitudinal steel bars ($\phi 10$ and $\phi 12$) and stirrups ($\phi 8$) extracted from beams and columns of the module n.5 have been performed. The obtained results are summarised in Table 4.4, where with Φ the nominal diameter of bars is indicated. It is worth noticing that, according to available technical drawings, the nominal strength values of concrete (cylindrical) and steel were of 20 MPa and 380 MPa, respectively. The values reported in Table 4.4 show a variation of the yield stress and the ultimate stress equal to about $\pm 20\%$ and $\pm 10\%$, respectively.

Table 4.4: Experimental mechanical properties of steel bars

Specimens n.	Φ (mm)	Length (mm)	Yielding load (kN)	Ultimate load (kN)	Ultimate Stress (MPa)	Yielding Stress (MPa)
1	8	1040	29.0	33.0	656.5	576.9
2	8	975	-	41.0	815.7	-
3	8	500	23.1	33.4	664.5	459.6
Average					712.2	518.25
4	10	558	39.5	59.2	753.8	502.9
5	10	520	38.9	58.8	748.7	495.3
6	10	485	-	62.7	798.3	-
Average					766.9	499.1
7	12	850	44.1	73.8	652.5	389.9
8	12	570	53.1	82.2	726.8	469.5
9	12	860	53.0	79.0	698.5	468.6
Average					692.6	442.7

Such a change of properties suggests a quite different behaviour of rebars, which is testified by the force-displacement curves plotted in Figure 4.16.

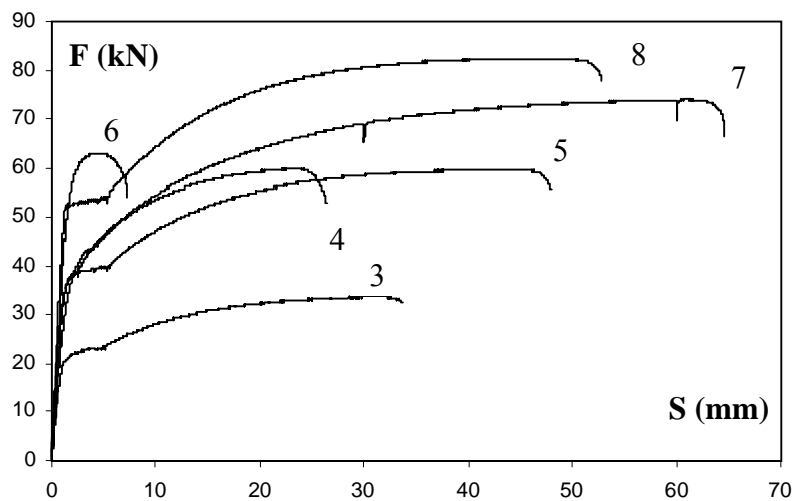


Figure 4.16: Stress-strain curves of steel bars

In the same Figure 4.16, it is noticed that:

- a well defined yield plateau is detected for three specimens only;
- a brittle rupture is observed in one case only;
- the results do not depend on the rebars diameter.

In the whole, the scatter among mechanical properties of materials should determine a different dynamic behaviour of the single sub-structures, whose investigation under excitation actions will be presented in the next Section.

4.3 EXPERIMENTAL DYNAMIC TESTS

4.3.1 General

The dynamic identification represents the reference basis for implementing numerical models able to reproduce the experimental response of structures subjected to seismic actions.

Generally, the results obtained from theoretical models of the structures do not interpret very well their actual behaviour due to the difficulty to simulate both the real constitutive laws of constituent materials and the existing

boundary conditions and the modifications which the structure undergoes during its life.

When sufficient information on the real structural behaviour are available, then the theoretical model can be corrected in order to reduce the existing differences. In fact, a theoretical model improved according to experimental results can be used aiming at individuating structural damaging phenomena and deterioration of the materials mechanical features. Such models could become a valid design tool when the effects of either structural changes or the variation of the applied forces is analysed.

Therefore, in order to implement a valid theoretical model of the sub-structures under study, the National Seismic Service of the Department of Civil Protection, in cooperation with the University of Chieti/Pescara, performed dynamic tests, modal identification and FE model calibration (Valente et al., 2006).

Since the mentioned modules should be upgraded or strengthened to resist seismic loads, the target of the work has been represented by both the definition of accurate numerical models to be used in the design phase and the identification of the structural dynamic properties in order to achieve information for upgrading/strengthening assessment.

Besides, the availability of similar structures represented an unique opportunity to execute comparative tests involving different experimental techniques and different theoretical/numerical methodologies in presence of structural uncertainties.

In this framework, four main analysis phases were conducted:

- 1) modal testing, in order to provide data for further processing;
- 2) modal identification, used to extract frequencies, modal shapes and damping properties from the recorded data;
- 3) damage identification, for detecting and localising defecting regions in the structure;
- 4) model updating, aiming at achieving tuned and predictive finite element models.

Three different excitation techniques able to provide either time or frequency data and forced or free decaying responses were used in the dynamic tests:

- direct impulse, by means of an impacting hammer;

- ground shaking, by using a falling mass;
- harmonic forcing, applied through the use of an electrodynamic shaker.

In this way a wide range of different data endowed with dissimilar noise to signal ratio and frequency content has been achieved.

Differently from the harmonic tests performed by means of vibrodine, the impulse techniques allow to activate all eigenmodes of the structure, but with an intensity not comparable with the one characterising the same harmonic tests. Among impulse tests, the one with impacting hammer allows to select and modify both the point and the direction of the applied force, which can be also measured. The tests based on the falling mass provide a great amount of energy, but both the frequency content and the spatial distribution of the applied action are less controllable than the ones based on the use of impacting hammers. For this reason, they are limited to structures with small dimensions, as the one under study.

In such a framework, it is necessary to observe that the irregularity of cuts performed at floor levels, even if the stiffness distribution at different levels was unchanged, produced some difference in the distribution of the plane masses. Furthermore, the division of the building into modules has produced localised damaging effects which could not be easily detected from visual inspection. Therefore, damage detection and localization was achieved during the execution of experimental dynamic tests.

Finally, starting from this investigation, in order to catch the real structural dynamic behaviour, the initially implemented FEM model of the module under study, developed on the basis of the in-situ survey data, has been calibrated on the basis of experimental data by means of the insertion of appropriate reduction factors of the flexural and shear stiffness of beams and columns.

4.3.2 Acquisition systems

The dynamic response of the structure was recorded by using a modular acquisition system based on telemetric data transmission, which allowed for large flexibility during the execution of tests (Valente et al., 2006). Such a system is composed by a set of four independent four channel acquisition units. Each structural module was instrumented with both two acquisition units and an independent unit able to measure the excitation force.

The acquisition units are endowed with a built in 16 bit A/D converter and non volatile internal memory for local storage of data. They communicate under wireless way with a notebook which is the central acquisition unit for remote storage and management of the data.

In Figure 4.17 a typical acquisition unit used in the tests is shown inside the transport case together with the cable connections to the transmitting devices (on the right) and to one accelerometer (on the left).

The on/off status of the system was triggered according to prefixed threshold values calibrated against the environmental noise. The sampling frequency, which was set to 250 Hz to handle with the structural frequency and to avoid aliasing, was increased up to 1000 Hz for the hammer tests to capture the impulse excitation.

The dynamic behaviour of the structural modules was characterised in terms of acceleration response. To this purpose, unidirectional force balance accelerometers, having offset of ± 0.50 g and linear behaviour up to 100 Hz, were used, they being particularly effective for low to modest vibration amplitudes.

The sensors positioning is generally dictated by preliminary optimization analyses which allow to minimise the number of accelerometers to be used without reducing the information included in the recorded time histories. In the current case, being immediate the choice of the best sensors placement due to both the regularity of the structural scheme and the validity of the rigid diaphragm hypothesis, any optimization procedure is not required.

Therefore, due to a large axial over bending stiffness ratio of columns, the modules will behave ideally according to a shear type scheme, where the floors present a plane rigid body motion. As a consequence, three measurement points per floor are necessary only. However, in order to enlarge the dynamic response, the accelerometers have been placed in three of the four vertexes of each floor (positions 1-3-4 and 5-7-8), as depicted in Figure 4.17 b.

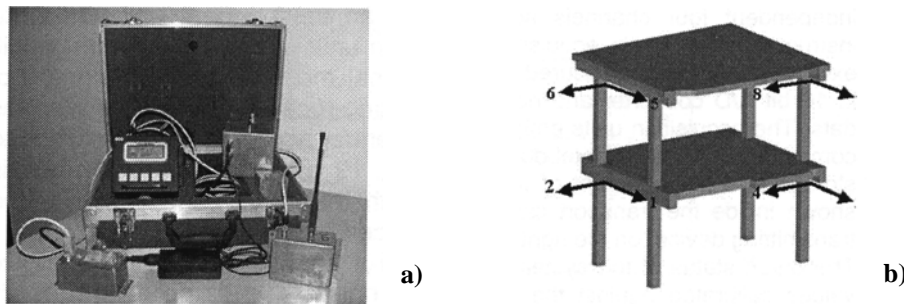


Figure 4.17: Local acquisition unit (a) and positioning of accelerometers (b)

Finally, at the light of the numerical activities involving the calibration of the initial FEM model, particular care was taken in the disposition of accelerometers as close as possible in the theoretical beam-to-column joints in order to reduce the geometric differences between the measurement points and the numerical model nodes.

In the following, the experimental direct and indirect impulse tests (instrumented hammer and falling mass) related to the sub-structure under study (module n. 5) are presented and discussed only.

4.3.3 Direct impulse test (instrumented hammer)

Impulse forces on the structures can be usually obtained by using an impacting device. In the case under investigation, an instrumented hammer (Figure 4.18 a) has been used, it being able to excite significantly a sub-structure having limited mass and geometrical dimensions.

The impacting hammer is provided with a load cell used to measure both the duration and the frequency content of the applied impulse. Such parameters can be adjusted by tuning the stiffness of the hammer head. In fact the frequency range effectively excited by this type of device is controlled by the stiffness of the contact surfaces and by the impacting head mass. Since a system resonance occurs at the frequency given by the square root of the contact stiffness over impacting mass ratio, it is important to underline that above this value the deliver of the energy into the structure is difficult to achieve. If the materials are very stiff, the duration of the pulse is very short and a large frequency range covered by the impact is obtained. Such a large range is also achieved when light impacting mass tests are performed.

One of the difficulties related to the use of such an excitation technique is to ensure the tests repeatability with respect to the hammer position and orientation relative to the impacted surface. Simultaneously, multiple impacts or hammer bounces must be carefully avoided.

In the case under study, the hammer was impacted at each beam-to-column joint of the two floors in the two directions (Figure 4.18 b). Each test was repeated twice for checking purposes, so that a total of 32 impulse tests were performed.

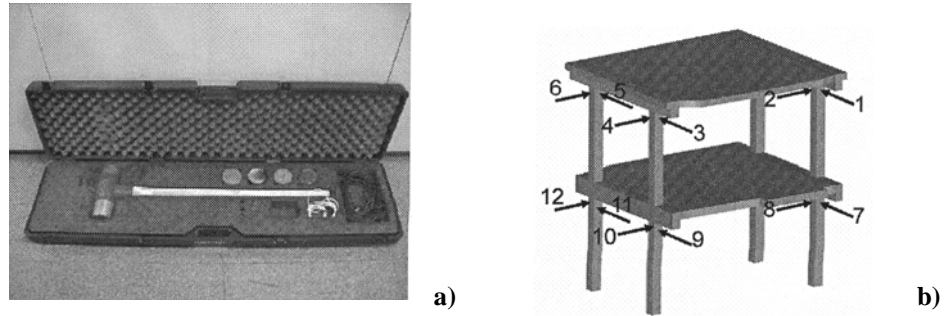


Figure 4.18: Instrumented hammer (a) and points subjected to impact (b)

An example of the impulse force obtained with the hammer is given in Figure 4.19, where the recorded impulse waveform is plotted together with the frequency content of the delivery energy.

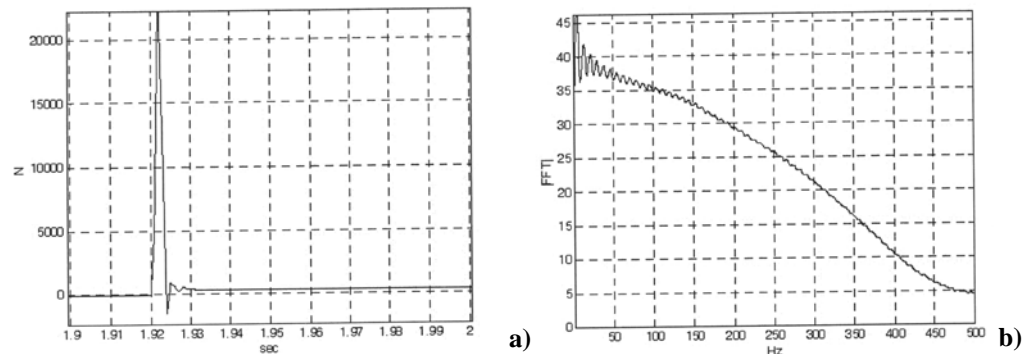


Figure 4.19: Waveform (a) and frequency content (b) of the hammer impulse force

In particular, an impulse excitation of less than 2/1000 sec. duration has been applied, as illustrated in Figure 4.19 a, while an energy distribution with

decaying amplitude over a wide frequency range is shown in Figure 4.19 b. Nevertheless, since the amplitude decay is less than 5% in the frequency range of interest (0-50 Hz) and do not exceed 12% in the interval 0-100 Hz, a flat energy spectrum can be assumed. In Figure 4.20 a typical structural response to the impulse force released by the impacting hammer is shown together with the Fourier transform (FFT) of the time history.

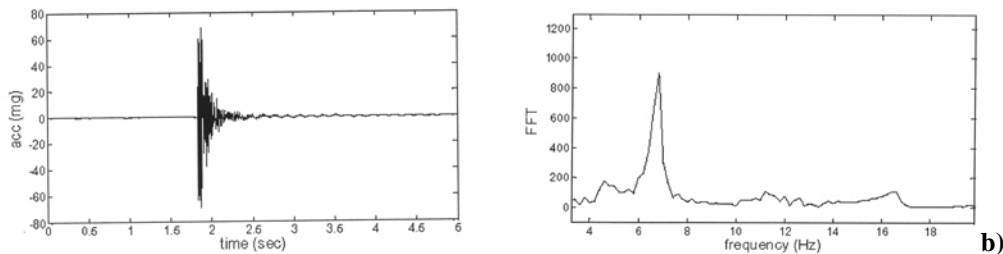


Figure 4.20: Structural response (a) and FFT of the response (b) to impact hammering

The peak impulse acceleration is about 0.05 and the true free decaying response starts at about half of that value. The frequency content of the response shows that one structural mode at about 7 Hz is significantly excited only, even if global and local modes appear, the latter generally present to a different extent in function of the impacting location.

In conclusion, from the hammering tests, the modal parameters depicted in Figure 4.21 have been drawn.

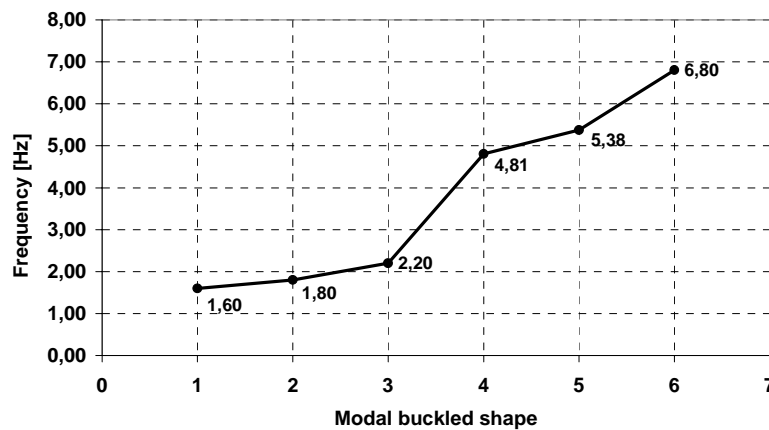


Figure 4.21: Experimental frequencies of the module n. 5

4.3.4 Indirect impulse test (falling mass)

The indirect impulse excitation is realised by impacting a falling body, having mass M and located at a height h , on the ground (Figure 4.22 a). Assuming that the impact is fully inelastic, the energy transferred to the ground is Mgh , being g the gravity constant. Therefore, being the energy governed by M and h , it may be adapted to the dimensions and characteristics of the structure in order to feed the required energy. In the tests, different positions of the mass have been considered, they being all able to excite the structural module under consideration (Figure 4.22 b).

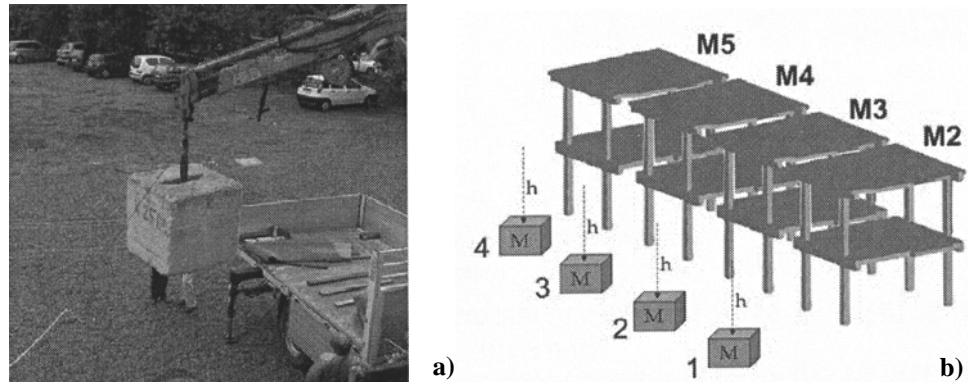


Figure 4.22: Falling mass (a) and its different positions assumed during the tests (b)

With this kind of test, the vibrations are transmitted to the structure similarly to the seismic actions, but from their comparison two main differences are noticed, they being represented by the waveform and the spatial distribution of the acceleration field. In fact, the waveform is a single shock type wave characterised by a very limited duration and a wide frequency content. Besides, the acceleration field cannot be considered as spatially uniform because the plan dimensions of the structure are not negligible with respect to the distance of the impact point. Nevertheless, such an aspect can be advantageously exploited. Actually, the rotational modes, with low values of the seismic participation factor, can be excited as well as the translational or flexural modes by a proper selection of the impact point.

4.3.5 Comparison between test results

The results presented in the previous Sections have shown that some differences exist among different excitation techniques used in the experimental activity, they being related to the manner in which the energy is transmitted to the structure and to the dynamic response of the structure itself.

In particular, even if steady state responses can be achieved by the use of shakers only, the free decaying ones can be obtained also by means of impulse devices. With reference to this last aspect, the comparison between the response achieved with the falling mass and the one related to the use of the impact hammer, both recorded at the same measurement point, is illustrated in Figure 4.23.

If both test devices are suitably designed, the same peak values are obtained. Nevertheless, quite different waveforms of the free decaying response have been achieved from experimental tests. In the first case (Figure 4.23 a), an apparent higher damper response is observed, while in the second one (Figure 4.23 b) the free vibrations, which persist for a longer time, are apparently related to a well defined frequency.

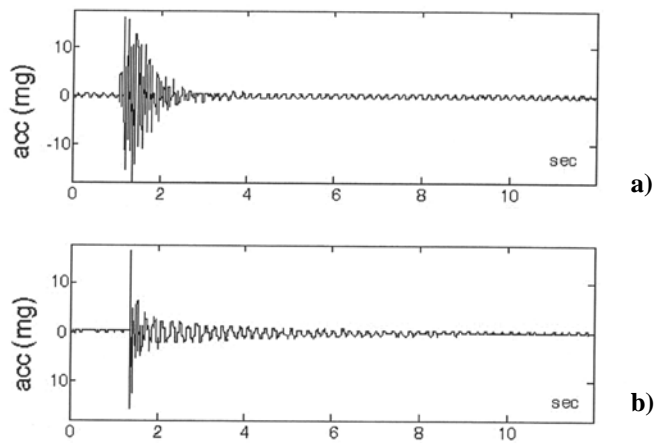


Figure 4.23: Free vibrations from impulse tests: hammer (a) and falling mass (b)

When the same responses are plotted in the frequency domain by means of the Fourier transforms, different conclusions can be obtained, as shown in

Figure 4.24. In fact, in this case, a similar FFT magnitude at the resonant frequency occurred; therefore, the same energy is supplied from the structure at the main vibration mode.

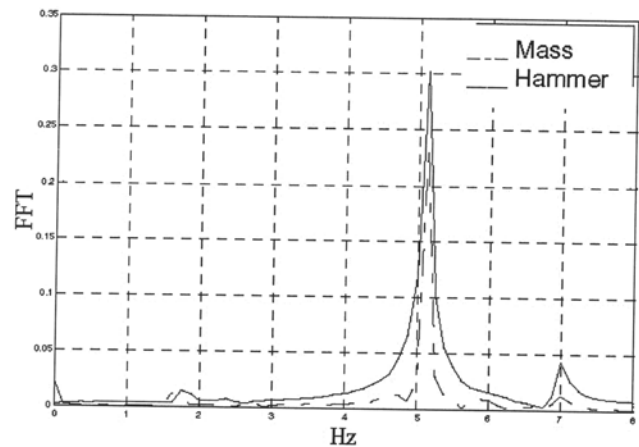


Figure 4.24: Comparison between FFTs of the performed impulse tests

However, the falling mass technique is able to provide stronger energy concentration than the impacting hammer one. On the contrary, the latter is more effective in exciting multiple modes of the structure at higher degree.

4.4 NUMERICAL DYNAMIC INVESTIGATION

4.4.1 The numerical model

The knowledge of the experimental structural dynamic properties has allowed the calibration of a finite element model of the RC structure, which has been constructed by means of the SAP2000 ver. 8.23 non linear numerical program (Computer and Structures, Inc., 2003).

All structural elements of the module, including floor beams at both levels, the repartition floor beam and the transversal large floor beams, have been modelled as beam elements. Both the transversal beams and the repartition floor beam of the generic level have been subdivided in relation to the number

of floor beams in order to better reproduce the real geometrical scheme of the structure and to evaluate with care the distribution of the solicitation characteristics.

The mechanical features of steel and concrete have been considered in the model according to the results of experimental tests performed on such materials in the Section 4.5.

In the structure numerical model the infinitely stiff behaviour of floors has been hypothesised, it being introduced by means of the *diaphragm* command available in the SAP library. With such an option, each floor is characterised by three dynamic degrees of freedom only.

The structural mass at each floor has been concentrated in specific points, know as *master joints*, which coincide with the centre of mass of the floors theirselves.

Three-dimensional and plan views of the sub-structured under modelling are illustrated in Figure 4.25.

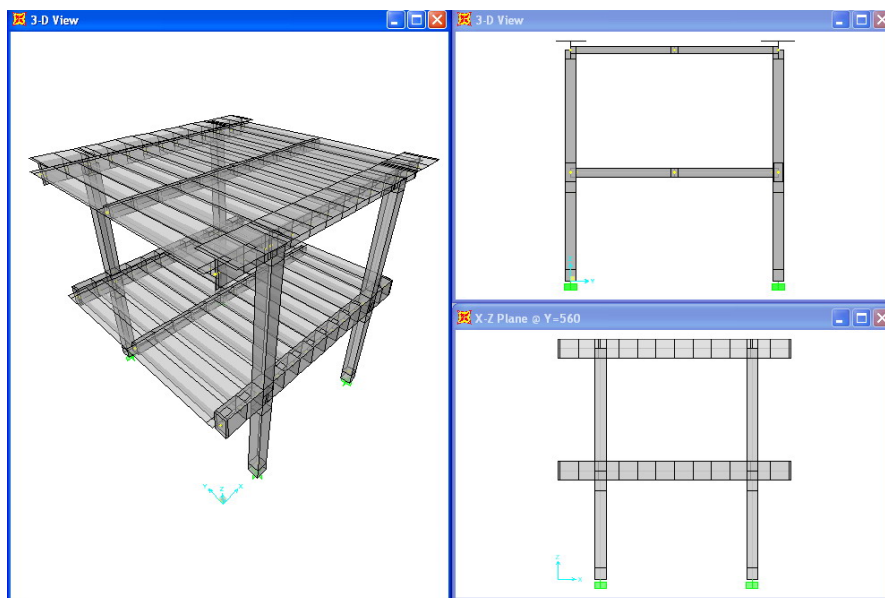


Figure 4.25: Numerical model of the sub-structure n.5

Subsequently, on the basis of both performed geometrical surveys and available technical drawings, the self-weight of each floor has been determined, it being approximated to 3 kNm^{-2} . Then, considering an

accidental load equal to 2 kNm^{-2} , according to the destination of use of the original building, and calculating the weight incidence per meter of all structural sections, the distributed loads applied on each element of the model has been defined (Figure 4.26).

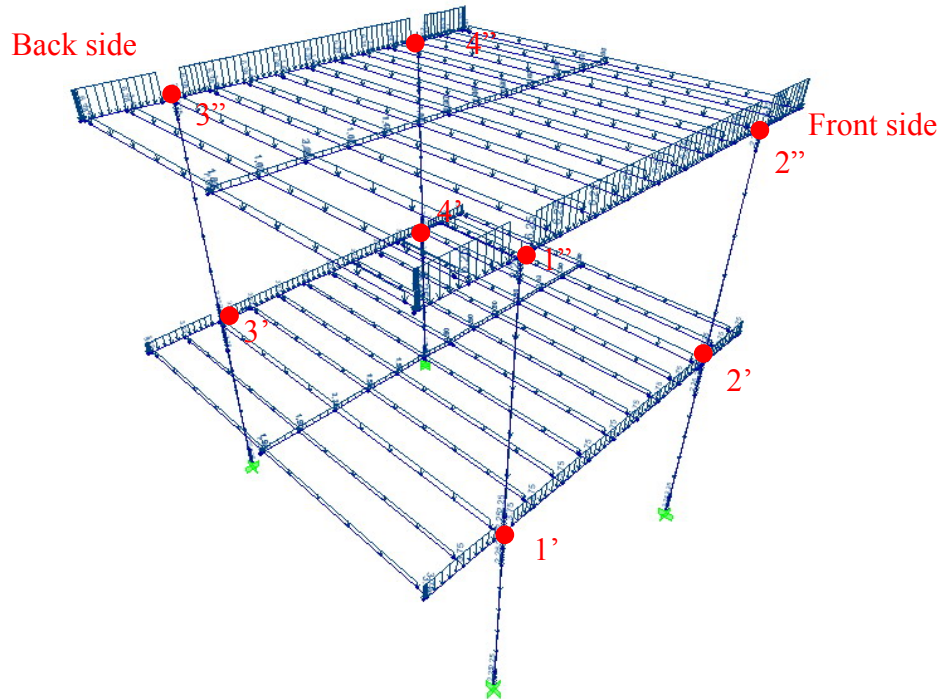


Figure 4.26: Distributed loads applied on the module under study

4.4.2 The numerical modal analysis results

The dynamic properties of the structure in terms of both periods and modal shapes have been obtained by means of the above illustrated numerical model.

In a preliminary study phase, being known the geometrical dimensions of the structural members, a rigorous calculation of masses excited during the seismic oscillation of the building has been performed.

Therefore, the evaluation of the seismic mass of each floor, firstly neglecting the contribution of accidental loads which were not present on the structure, has been done, it being approximately equal to $17500 \text{ N s}^2 \text{ m}^{-1}$.

Subsequently, by considering at both levels a X-Y reference system having origin in the centre of gravity of the column n.1 cross-section (see Figure 4.26), the barycentre of two floors has been determined by evaluating the static moment (S) provided by each structural element (floors, beams and columns), at each level in both directions, with respect to the assumed reference system (Tables 4.5, 4.6 and 4.7).

Table 4.5: Evaluation of static moments of the first level elements

Element	Mass [Kg]	d_x [m]	d_y[m]	S_x [Kgm]	S_y [Kgm]
Floor	11064	2.00	2.80	30979.20	22128
Front beam	2138	2.00	0.00	0.00	4275
Back beam	1781	2.00	5.57	9930.50	3562.50
Column 1	630	0.00	0.00	0.00	0.00
Column 2	630	4.10	0.00	0.00	2583
Column 3	630	0.00	5.60	3528	0.00
Column 4	630	4.10	5.60	3528	2583
TOTAL	17503	-	-	47965.70	35131.50

Table 4.6: Evaluation of static moments of the second level elements

Element	Mass [Kg]	d_x [m]	d_y[m]	S_x [Kgm]	S_y [Kgm]
Floor	9310.50	2.00	2.80	26069.4	18621
Front beam	3562.50	2.00	0.00	0.00	7125
Back beam	3634	2.00	5.57	20258.20	7267.50
Column 1	247.50	0.00	0.00	0.00	0.00
Column 2	247.50	4.10	0.00	0.00	1014.75
Column 3	247.50	0.00	5.60	1386	0.00
Column 4	247.50	4.10	5.60	1386	1014.75
TOTAL	17497	-	-	49099.60	35043

Table 4.9: Determination of the second floor rotational mass

Element	L_X [m]	L_Y [m]	Mass [Kgs ² m ⁻¹]	d_{XG} [m]	d_{YG} [m]	I_0 [Kgs ² m]	I_t [Kgs ² m]	I_{zt} [Kgs ² m]
Floor	6.30	4.70	949.08	0.003	0.006	4886.19	0.04	4886.23
Front beam	5.70	0.80	363.15	0.003	2.81	1002.60	2859.74	3862.34
Back beam	0.30	0.90	370.41	0.003	2.77	1027.90	2839.66	3867.56
Column 1	0.30	0.30	25.23	2.00	2.81	0.38	299.88	300.26
Column 2	0.30	0.30	25.23	2.10	2.81	0.38	309.64	310.02
Column 3	0.30	0.30	25.23	2.00	2.79	0.38	298.12	298.50
Column 4	0.30	0.30	25.23	2.10	2.79	0.38	307.88	308.26
TOTAL								13833.17

The seismic and rotational mass values obtained from the above calculations have been applied in the master joints of the two levels and the modal analysis of the structure has been performed. The achieved results, expressed in terms of both vibration periods and participating masses, are illustrated in Tables 4.10 and 4.11, respectively.

Table 4.10: Periods and frequencies extracted from the FE structural model

Vibration mode	Period sec	Frequency cycle/sec	Frequency rad/sec	Eigenvalue rad ² /sec ²
1	0.461238	2.1681	13.622	185.57
2	0.359932	2.7783	17.457	304.73
3	0.292813	3.4152	21.458	460.45
4	0.142846	7.0006	43.986	1934.8
5	0.129727	7.7085	48.434	2345.8
6	0.10274	9.7333	61.156	3740.1

Table 4.11: Participating mass coefficients of the structure in the modal analysis

Vibration mode	Period	SumUX	SumUY	SumRZ
	sec	%	%	%
1	0.461	0	85	0
2	0.360	89	85	12
3	0.293	89	85	89
4	0.143	89	100	89
5	0.130	100	100	89
6	0.103	100	100	100

From the results it is apparent that the first vibration period is enclosed in the typical range $[0.2\div 0.6 \text{ sec}]$ provided in the technical literature for RC buildings similar to the one under study and that no interference between modes is detected, as it is visible in Figure 4.27.

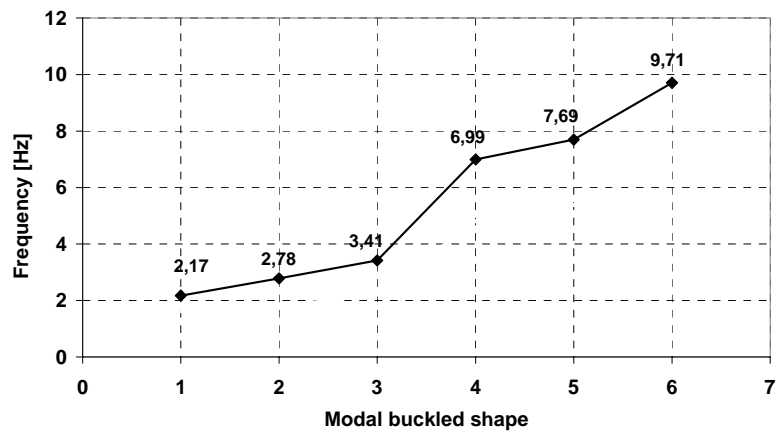


Figure 4.27: Vibration frequencies extracted from the numerical model of the structure

Besides, the diagram illustrating the variation of participating mass factors vs. modal shapes (Figure 4.28) evidences a regular modal behaviour of the

building. In particular, the first vibration mode, which excites the major part of the structural mass, appears to be of translational type along the transversal direction, whereas starting from the second mode, coupled translational modes, due to the asymmetry of the structure in the two directions, are visible.

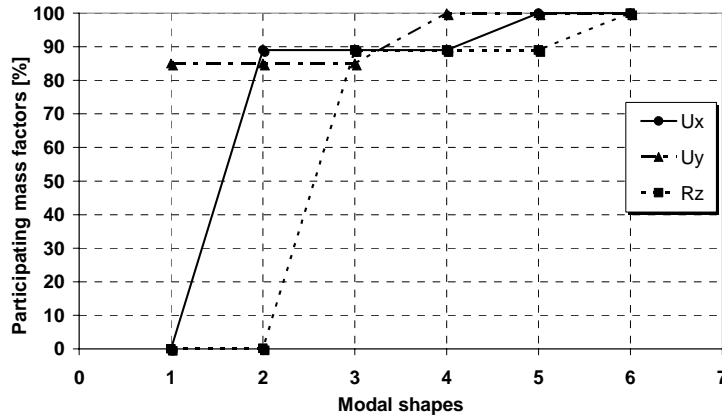


Figure 4.28: Participating mass coefficients of the structure in the modal analysis

The implemented numerical model provides the results depicted in terms of vibration periods in Figure 4.29, where the comparison with the experimental ones is performed.

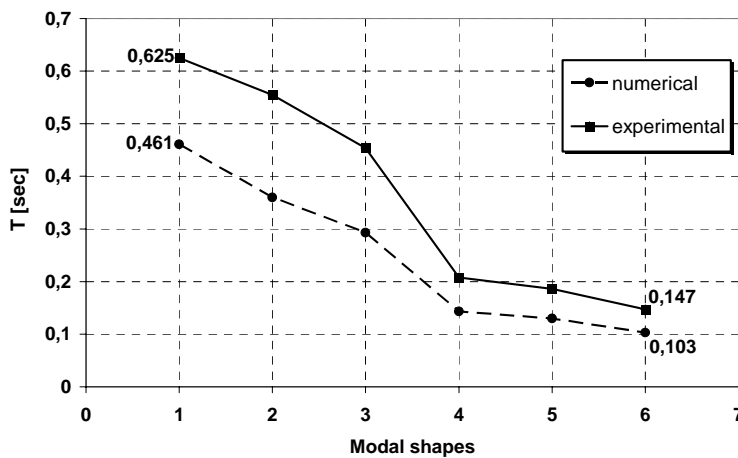


Figure 4.29: Experimental-numerical comparison in terms of vibration periods (T)

As it is observed from the above figure, the numerical curve is different from the experimental one, with discrepancies ranging from 26% (1st mode) to 30% (6th mode). Such a different behaviour is due to the structural members degradation (Figure 4.30), which reduces the stiffness of the module, modifying its response in terms of both frequency and vibration period. Therefore, the consequences deriving from these phenomena have been incorporated in the numerical model, according to the provisions given in the next Section.



Figure 4.30: Degraded aspect of floor (a), beam (b) and column (c)

4.4.3 Calibration of the numerical model according to experimental results

As previously stated, the degradation phenomenon conditioning the behaviour of structural members should be considered in the numerical model in order to calibrate the experimental results. In particular, in order to account for cracking of concrete, the numerical model was set-up according to a bending and shear stiffness of beams and columns suitably reduced. For this aim, several provisions provided by both current technical literature and design standards were used, such as FEMA - “Prestandard and Commentary for the Seismic Rehabilitation of Buildings” (ATC/BSSC, 1997), Paulay & Priestley - “Seismic Design of Reinforced Concrete” (Paulay and Priestley, 1992) and the new seismic Italian code (OPCM 3431, 2005). These suggest to reduce both the bending and shear stiffness until to the values listed in Table 4.12.

Table 4.12: Stiffness reduction factors adopted in the numerical modelling

FEMA 356			Paulay & Priestley			OPCM 3431/05		
Member	Bending stiffness	Shear stiffness	Member	Bending stiffness	Shear stiffness	Member	Bending stiffness	Shear stiffness
Beam	0.5 EI	0.4 EA _w	Beam	0.4 EI	0.4 EA _w	Beam	0.5 EI	0.5 EA _w
Column	0.7 EI	0.4 EA _w	T-shaped Beam	0.35 EI	0.4 EA _w	Column	0.5 EI	0.5 EA _w
			Column	0.6 EI	0.4 EA _w			

In Figure 4.31, the numerical results in terms of vibration periods T , obtained applying the reductions factors of the above Table 4.12, are shown.

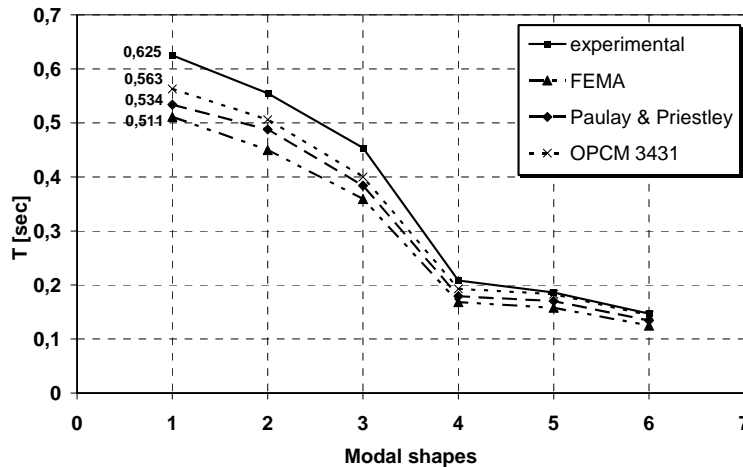


Figure 4.31: Comparison between numerical and experimental results in terms of vibration periods

A good agreement between theoretical and experimental results is noticed when the OPCM reduction factors have been used. In this case, the theoretical-experimental scatters detected in terms of the first three fundamental periods range from 9.9% to 19%. In order to further reduce the discrepancy between numerical and experimental results, new reduction factors have been proposed. They are very similar to the OPCM ones and are listed in Table 4.13.

Table 4.13: Proposed stiffness reduction factors

Member	Bending stiffness	Shear stiffness
Beam	0.5 EI	0.5 EA _w
Column	0.4 EI	0.5 EA _w

In Figure 4.32, the numerical values of the fundamental period obtained by using the proposed reduction factors, together with the experimental ones, are shown. In the same figure the results based on the full values of the geometrical properties of member cross-sections are also depicted. In Figure 4.33, the first six vibration modes are drawn.

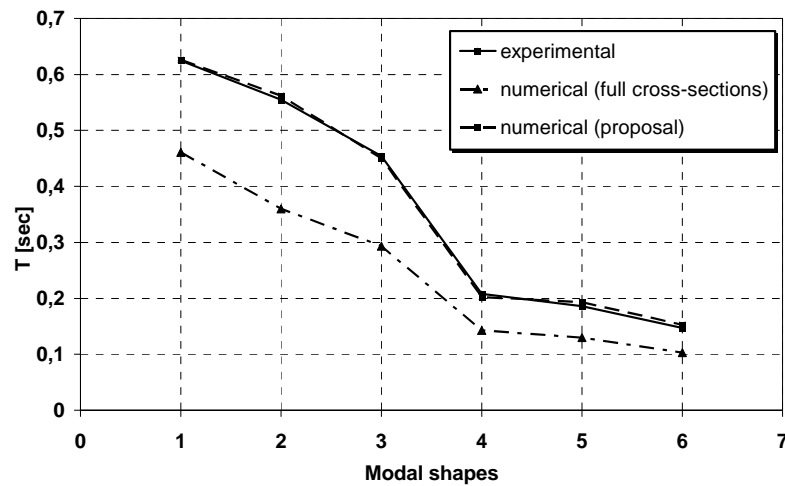


Figure 4.32: Comparison between the experimental vibration periods and the numerical ones obtained by means of the suggested reduction factors

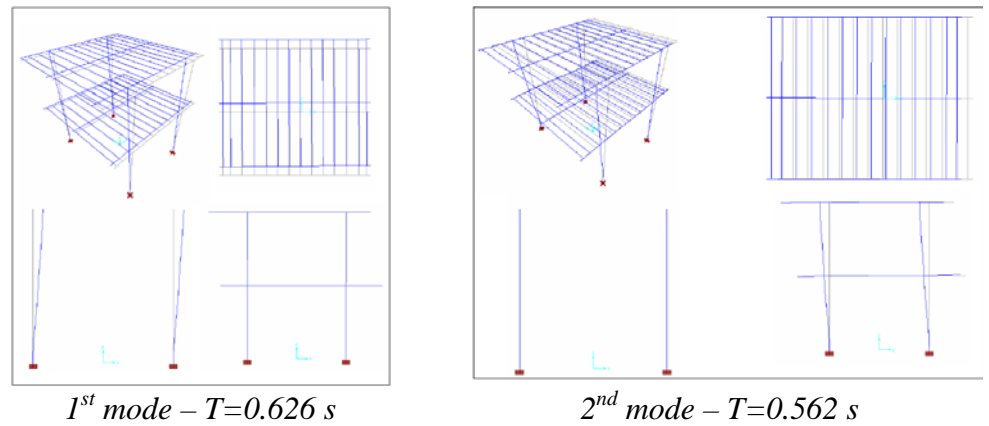


Figure 4.33: Modal deformed shapes of the structure corresponding to the first six vibration modes (continues)

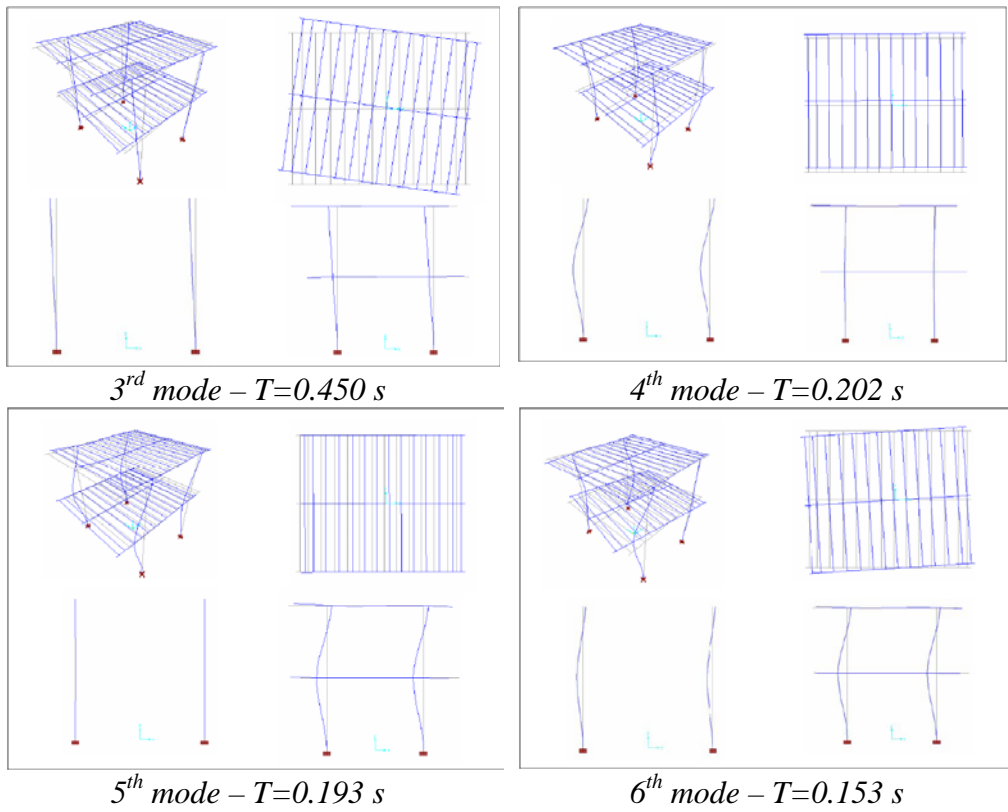


Figure 4.33: Modal deformed shapes of the structure corresponding to the first six vibration modes

4.5 THE PUSHOVER ANALYSES

4.5.1 General

Aiming at understanding the seismic behaviour of the building under investigation, appropriate non-linear pushover analyses have been carried out, they being able to evaluate the global available structural ductility. In this framework, the basis concept is that the total capacity of the structure to withstand seismic actions can be described from the behaviour of the structure itself when it is subjected to a system of equivalent static forces which are

increased up to the attainment of collapse, considered as the capacity to sustain the vertical loads only.

The used force system must be able to simulate under realistic way the effects produced by seismic actions. Nevertheless, such effects depend on the structure response and, therefore, the force system should change continuously during the analysis. Instead, for simplicity of calculation, the force distribution, which is assigned in order to excite the fundamental vibration mode of the structure (it being predominant for buildings having period less than 1 sec), is assumed constant during the analysis.

The potentiality of such a methodology consists of the knowledge of the structure behaviour at each increment of the applied external action, in the spirit of concentrated plasticity models, where plastic hinges develop up to collapse, corresponding to the attainment of a kinematic mechanism.

This procedure, which should require the use of a non-linear calculation code, can be also implemented by means of a series of sequential elastic analyses, according to the provisions given by ATC-40 (1996) and FEMA 273 (1997) American codes. In this way, the final curve representative of the structure capacity is expressed in the base shear vs. top displacement diagram.

In order to perform pushover analyses, the plastic hinges properties must be defined for each structural element, having a ductility which allows to withstand vertical loads beyond the elastic limit. The schematic model of the plastic hinge behaviour, according to the FEMA 273 indications, is illustrated in Figure 4.34.

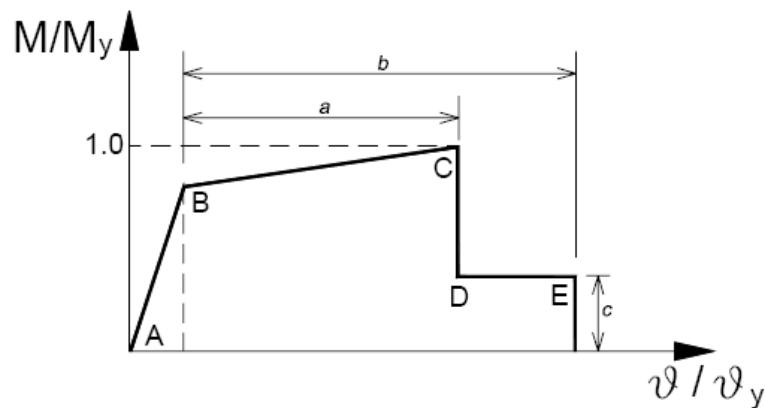


Figure 4.34: The plastic hinge behaviour according to FEMA 273 provisions

The distance a represents the plastic hinge rotation which develops in the structural component end starting from the yielding phase (point B) up to the conclusion of the strain-hardening one (line B-C). Instead, the distance b is representative of the failure plastic rotation, considering also the deformation developing after the strength degradation (line D-E). Finally, the distance c indicates the residual component strength.

The values of such distances are provided by the FEMA 273 guidelines as a function of the following parameters:

$$\frac{\rho - \rho'}{\rho_{BAL}} \quad (4.3)$$

where ρ e ρ' represent the ratio between the steel bars area and the concrete one in the tensile and compressed fibre, respectively, while ρ_{bal} indicates the same ratio in the tensile fibre corresponding to the balanced failure ($\epsilon_{cu} = 0.0035$; $\epsilon_{su} = 0.01$);

$$\frac{V}{b_w d \sqrt{f'_c}} \quad (4.4)$$

where V is the design shear of the component. It is calculated considering the sum of the shear due to vertical loads and the shear equilibrating the resisting moments developed by plastic hinges :

$$V = \frac{M_U^{SX} + M_U^{DX}}{L} \pm \frac{qL}{2} \quad (4.5)$$

$$\frac{P}{A_g f'_c} \quad (4.6)$$

where P is the design axial force.

Besides, only closed stirrups having pitch less than $d/3$, where d is the component height, and able to absorb a shear more than $3/4$ of the design one are considered as effective transversal reinforcements.

4.5.2 The numerical study

Based on the above numerical model, some static pushover tests have been performed in order to evaluate the lateral load bearing of the bare structure in

terms of both strength and ductility. The mechanical properties of plastic hinges have been defined according to both ATC 40 and FEMA 273 provisions, according to the procedure given in the previous Section.

In the first analysis phase, being unknown the collapse mechanism of the structure, the plastic hinges have been positioned in the points susceptible to develop inelastic rotations, such as columns and floor beams ends. Besides, the presence of stirrups has not been considered due to the inobservance of prerequisites provided by the FEMA guidelines.

Subsequently, once that both the reference (see eqs. from 4.3 to 4.6) and modelling parameters for beams (Table 4.14) and columns (Table 4.15) have been determined, the numerical model has been completed by assigning the $M-N$ domain of the structural sections.

Table 4.14: Modelling of beams plastic hinges

Reference parameters		Modelling parameters			Check parameters				
					Component type				
$\frac{\rho - \rho'}{\rho_{bal}}$	$\frac{V}{b_w \cdot d \cdot \sqrt{f'_c}}$	a	b	c	Performance levels				
					Primary		Secondary		
					<i>IO</i>	<i>LS</i>	<i>CP</i>	<i>LS</i>	<i>CP</i>
≤ 0.0	≤ 3	0.02	0.03	0,2	0.005	0.01	0.02	0.02	0.03
≤ 0.0	≥ 6	0.01	0.015	0,2	0.0015	0.005	0.01	0.01	0.015
≥ 0.5	≤ 3	0.01	0.015	0,2	0.005	0.01	0.01	0.01	0.015
≥ 0.5	≥ 6	0.005	0.01	0,2	0.0015	0.005	0.005	0.005	0.01

Table 4.15: Modelling of columns plastic hinges

Reference parameters		Modelling parameters			Check parameters				
					Component type				
$\frac{\rho - \rho'}{\rho_{bal}}$	$\frac{V}{b_w \cdot d \cdot \sqrt{f'_c}}$	a	b	c	Performance levels				
					Primary		Secondary		
					<i>IO</i>	<i>LS</i>	<i>CP</i>	<i>LS</i>	<i>CP</i>
≤ 0.1	≤ 3	0.006	0.015	0,2	0.005	0.005	0.006	0.01	0.015
≤ 0.1	≥ 6	0.005	0.012	0,2	0.005	0.004	0.005	0.008	0.012
≥ 0.4	≤ 3	0.003	0.01	0,2	0.002	0.002	0.003	0.006	0,1
≥ 0.4	≥ 6	0.002	0.008	0,2	0.002	0.002	0.002	0.005	0.008

Each pushover analysis has been performed taking into account the $P-\Delta$ effects induced by gravity loads. A first pushover analysis has been carried out in transversal direction (Y) considering the plastic hinges concentrated at the

ends of beams and columns and by applying a triangular distribution of lateral loads. The main problems were related to both the actual position of the hinges and their effective bending resistance, which has been reduced accounting for the damaging effects of members deriving from the previous experimental test performed on the structure upgraded with shape memory alloy braces. As shown in Figure 4.35 b, the collapse mechanism takes place for soft-floor at the first storey with plastic hinges located at the ends of columns. Maximum base shear and top displacement are equal to 89.5 kN and 0.053 m, respectively, with the first yielding occurring at 49.8 kN of base shear (Figure 4.36).

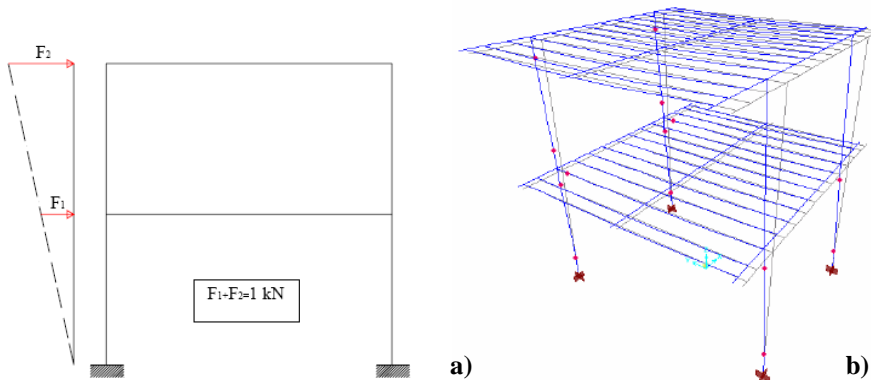


Figure 4.35: The pushover analysis (Y – direction): load distribution (a) and formation of plastic hinges (b)

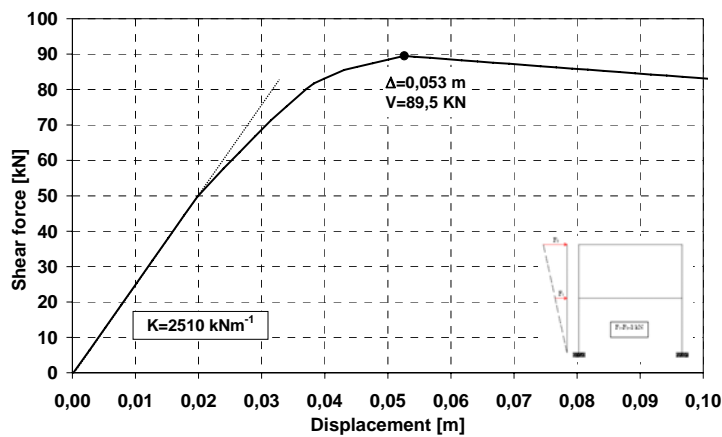


Figure 4.36: Pushover curve of the module tested in the transversal (Y) direction

A second pushover analysis was performed without considering any degradation of the structural members. The comparison with the previous analysis is shown in Figure 4.37.

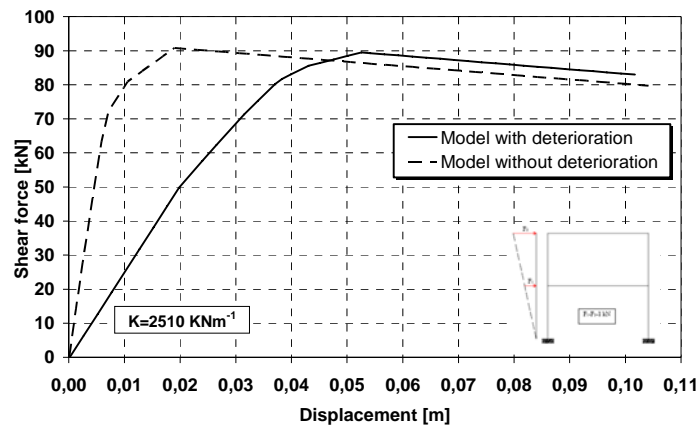


Figure 4.37: Comparison between results of numerical pushover analyses performed on structural models with and without members degradation (transversal direction)

In order to consider both the actual length of plastic hinges and the rigid behaviour of a part of the slabs thickness, a slight correction of the numerical model has been made. In particular, the position of plastic hinges has been changed. In fact, the geometrical off-set of plastic hinges has been made in the real structure until to place them in correspondence of both the upper and lower base of beams. In this way, a little increase of the maximum base shear is obtained, as shown in Figure 4.38.

In the new structural model, the maximum value of the base shear is increased of 9.2%, so reaching 97.7 kN, which corresponds to 28.4% of the structural weight.

The same analysis type has been performed when the lateral load distribution is applied in the opposite direction in comparison to the previous one (-Y direction). The obtained kinematic behaviour, reported in Figure 4.39, shows that, also in this case, a soft-storey mechanism occurs with creation of plastic hinges at both the column and the transversal large floor beams ends.

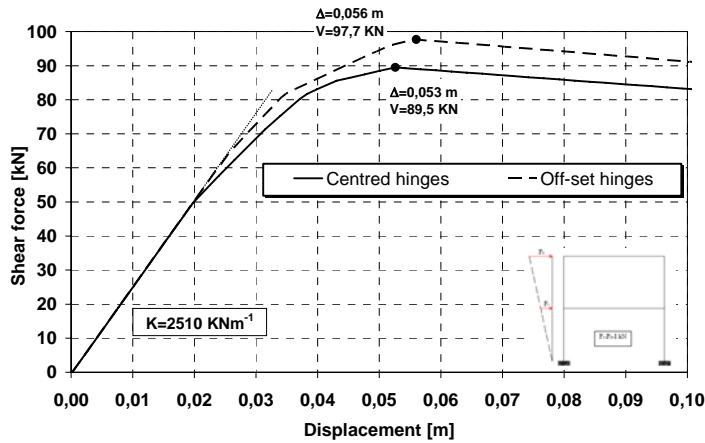


Figure 4.38: Comparison between results of pushover analyses carried out in the transversal direction on the structure with and without hinges off-set

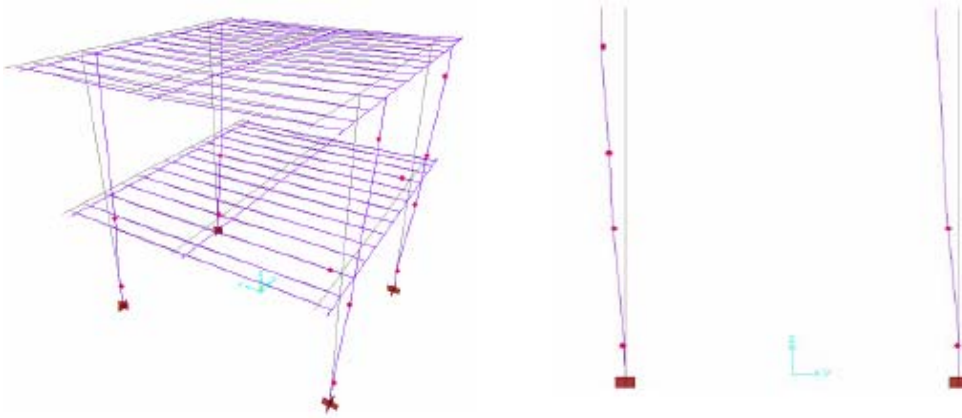


Figure 4.39: The pushover analysis (-Y direction): collapse mechanism

The comparison between pushover curves obtained from the analysis performed in the two opposite directions is depicted in Figure 4.40, where it is apparent that the structure, even if it presents in both case the same stiffness, shows a different behaviour in terms of the attained maximum strength. Such a behaviour is probably due to the presence of two frames, located orthogonally to the direction of the applied load, having beams with different geometrical dimensions.

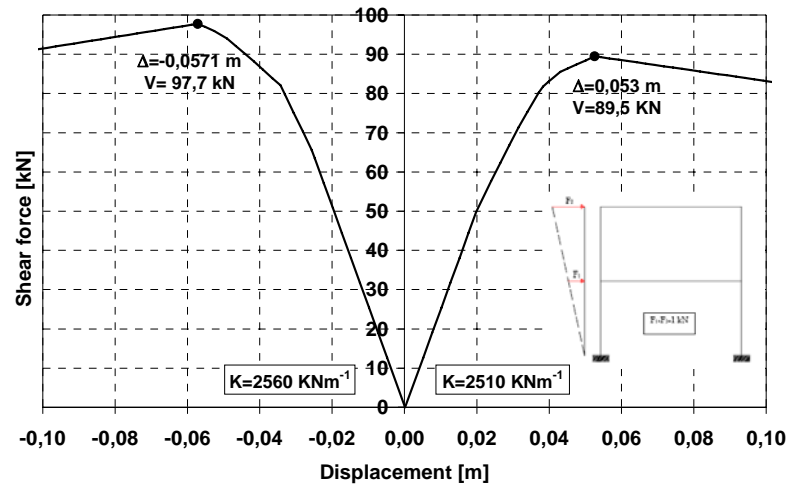


Figure 4.40: Comparison between pushover curves obtained from analyses performed in the transversal direction (+Y; -Y)

An analogous pushover analysis has been also performed in the direction parallel to emergent beams (longitudinal direction – X). The corresponding curve is shown in Figure 4.41, where the numerical response of the sub-structure along the transverse direction (Y) is depicted as well.

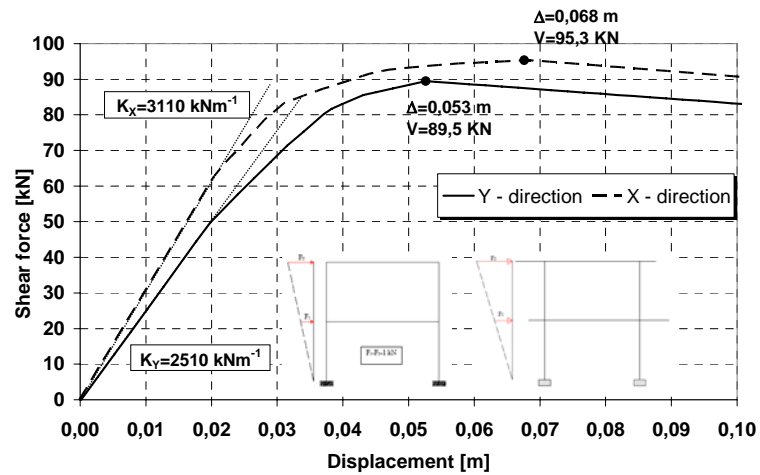


Figure 4.41: Comparison between numerical pushover analyses in X and Y directions

As it was easily predictable, the bare frame is stiffer in the longitudinal

direction than in the transversal one. Such a behavioural difference, evaluated in the order of about 24 %, is due to emergent beams positioned along the longitudinal direction. Also, the maximum base shear in X-direction is larger than the Y-direction one as well, their difference being of 6.6% only. This is due to the mechanism collapse that, in both cases, is governed by the formation of plastic hinges in the columns, which have the same plastic bending moment in both directions. Aiming at evaluating the inelastic response of the structure according to the geometrical disposition (at the ground floor only) of the upgrading system to be used, a pushover analysis in X-direction, with lateral load applied at first floor only, has been performed as well. The relevant pushover curve, drawn in Figure 4.42, shows a maximum base shear of 98.9 kN corresponding to a displacement measured at the first floor equal to 0.0196 m, about 1/2 of the second floor one. It is worth noticing that, in this case, the lateral stiffness is almost twice than the one previously obtained in the same direction. On the other hand, in both cases, due to the detected collapse mechanism, which is always governed by plastic hinges in the columns, the same maximum base shear is achieved. Such a curve will be compared with the experimental one, allowing the FEM model calibration.

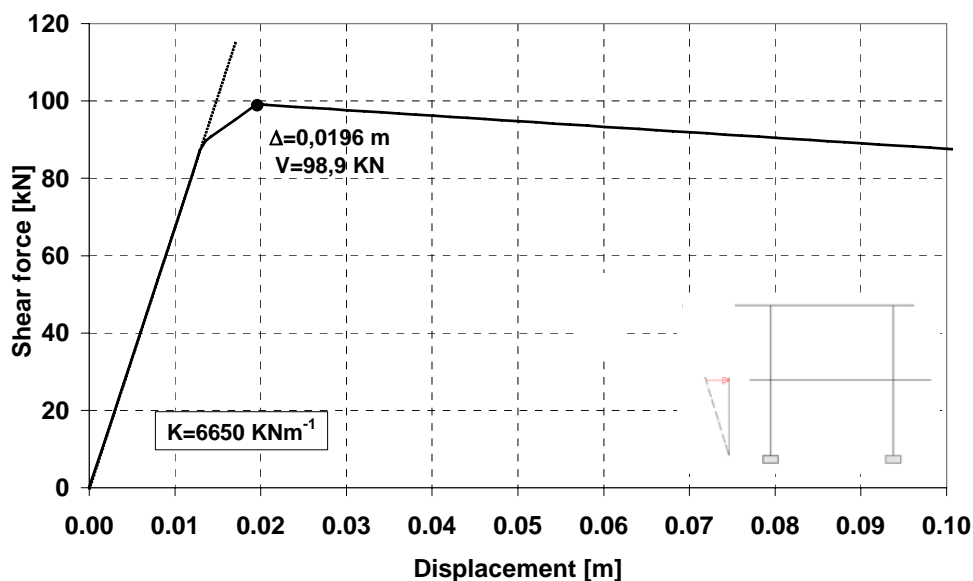


Figure 4.42: Pushover analysis in the X-direction with lateral load applied to the first floor only

4.5.3 Preliminary experimental test and calibration of the FE model

Previous numerical pushover analyses have been performed without taking into account the damage of the structural members of the RC module caused by the experimental pull-out test carried out in the transversal direction on the same structure upgraded with shape memory alloy bracings. In such a test, plastic hinges took place at the ends of the columns of the first floor, with a consequent reduction of the flexural load bearing capacity in the longitudinal direction as well. Serious damages, also due to poor presence of stirrups, occurred at the ends of the columns for a length of about 30 cm, where both cracking of the concrete and buckling of the longitudinal bars were noticeable (Figure 4.43).



Figure 4.43: Damage at the column ends due to the previous experimental pushover test in the transversal direction

Such a damage highlighted an inadequate residual flexural resistance of the columns. Therefore, in order to guarantee an adequate safety of the building as well as to avoid the torsional effects during succeeding pushover tests in the longitudinal direction, two steel X-bracings have been placed at the first floor of the framed structure in the transversal direction (Figure 4.44). During their installation, a local restoring intervention of the columns in correspondence of the damaged zones has been also made.



Figure 4.44: Installation of transversal X-bracings

As a reaction system for performing the experimental test on the module n. 5, the RC frame corresponding to the module n. 6 of the original RC building has been used. In such a sub-structure two steel V-bracings, made of coupled UPN140 channel profiles and connected to both foundation beams and the first floor slab, have been also installed for strengthening purposes (Figure 4.45).

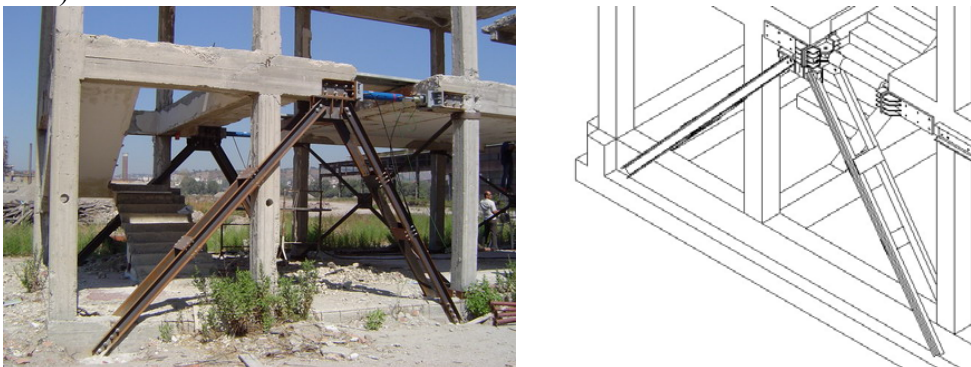


Figure 4.45: The reaction structural system (module n. 6 strengthened by steel V-bracings)

Two hydraulic jacks, both with a load capacity of 150 kN in compression and 75 kN in tension, were placed at the top of the V-bracings and pin joined to the slab ends in order to transfer axial load only (Figure 4.46).

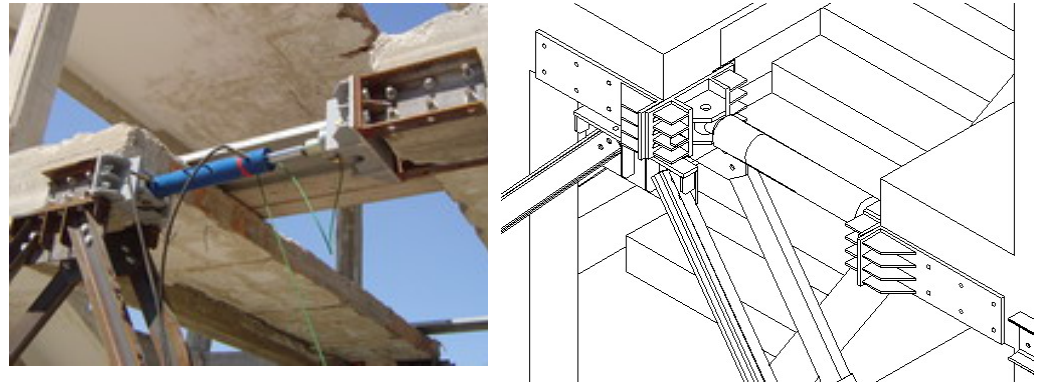


Figure 4.46: Application of pin-joined hydraulic jacks to the sub-structure

The experimental test was carried out by using a cyclic loading history, whose steps are listed in Table 4.16. The main purpose of the test was to know the stiffness of the bare RC structure.

Table 4.16: Loading history adopted in the cyclic experimental test on the module n. 5

Step	Initial force [kN]	Intermediate force [kN]	Final force [kN]
1	0	10	0
2	0	16	0
3	0	20	0
4	0	20	0
5	0	-16	0
6	0	-20	0
7	0	20	0

The experimental results of the cyclic test are depicted in Figure 4.47, where a comparison in terms of stiffness with the theoretical monotonic curve

is also shown.

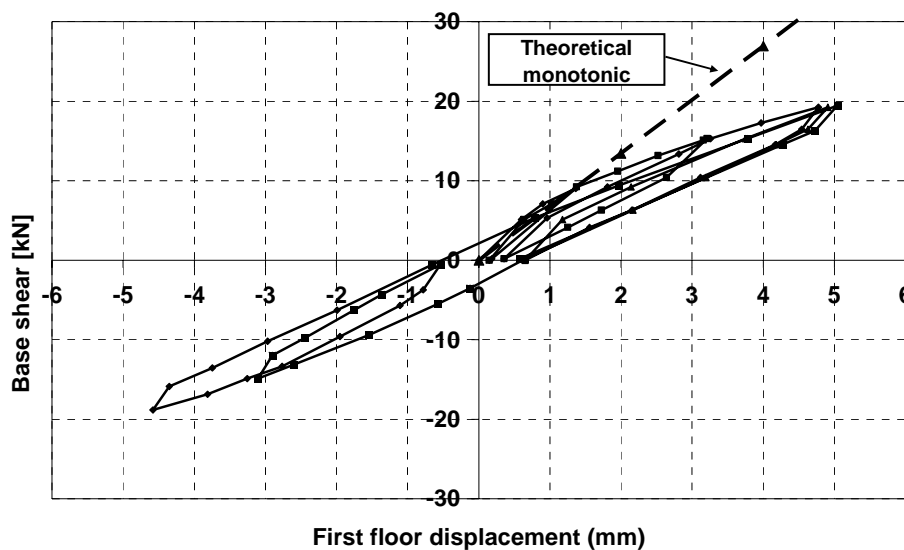


Figure 4.47: Experimental pushover test carried out on module n. 5 and comparison with the theoretical monotonic curve

The above comparison shows that the theoretical behaviour is remarkably different with respect to the experimental one. In particular, the theoretical stiffness is significantly larger than the actual one, starting from displacements larger than 1 mm. Such a result is due to the softening effect provided by the local damaging of the column ends. Aiming at improving the numerical model of the structure, both the bending and shear stiffness have been reduced at $0.2 EI$ and $0.3 EA_w$, respectively, for a length of 30 cm from the members end. Besides, the plastic moment of the hinges has been calculated without considering both the buckled bars in compression and the concrete cover of beams and columns. In Figure 4.48, both the experimental cyclic curve and the final theoretical monotonic one are depicted. From the comparison it is apparent that, neglecting the initial phase of the test and considering the column ends completely cracked, the two curves present the same stiffness.

Finally, in Figure 4.49, for the sake of comparison, both the initial numerical curve (without accounting for the initial structural damage of the RC frame) and the final numerical one calibrated on the basis of the

experimental bare RC structure stiffness, therefore introducing the previously mentioned reduction coefficients, are shown. In the same figure, such curves are compared with the foreseeable real response of the bare RC structure, which has not been determined due to the fact that the test stopped before the creation of initial plastic hinges.

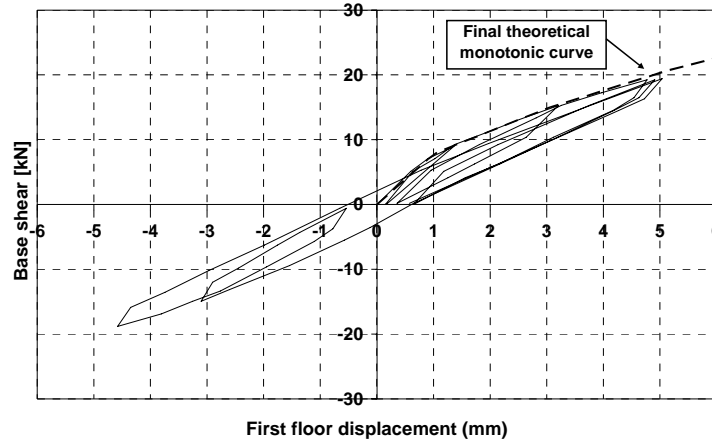


Figure 4.48: Comparison between the experimental cyclic curve and the corrected theoretical monotonic one

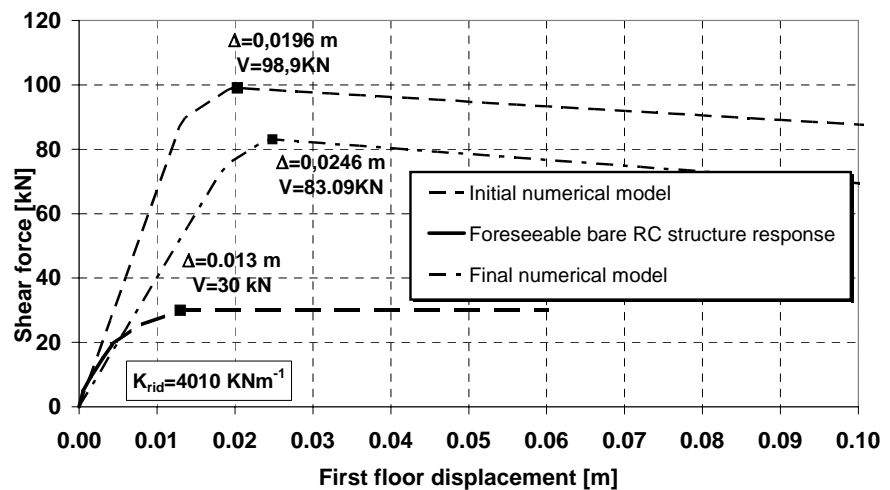


Figure 4.49: Monotonic pushover curves of the module n. 5, neglecting and accounting for the initial damage

Chapter V

Seismic retrofitting methodology and design of existing RC buildings by means of metal shear panels

5.1 INTRODUCTION

In several Countries, like USA, Japan and New Zealand, subjected to high intensity seismic events, the problem of the evaluation of the seismic safety of existing buildings has been analysed with particular emphasis due to the importance of this topic in terms of both people safety and safeguarding of the construction patrimony. Within the seismic European code, the framework of the reparation and the seismic strengthening of buildings is inspired to the FEMA 273 American guidelines "NEHRPs Guidelines for the seismic rehabilitation of buildings" (1997). Such a methodology is founded upon the explicit definition of pre-determined design objectives and on the acceptability criteria connected to the structural performances.

The definition of the rehabilitation objectives, namely the performances required to the buildings as a function of the earthquake intensity, represents a consolidated trend for the American guidelines emanated after 1994 (Hamburger and Moehle, 2000) (Figure 5.1), resulting very interesting both for the clarity of formulation and for the ability to localize the critical elements of a structure. At the base of such a formulation there are several studies and experimental tests which have allowed to correlate determined

damage and functionality scenarios with the results provided by structural analysis.

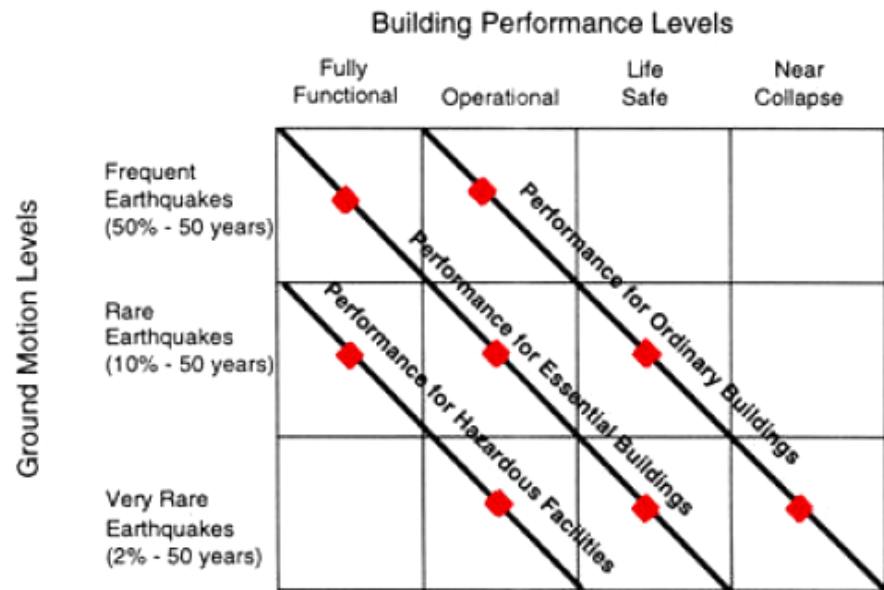


Figure 5.1: Performance objectives stated in the recent American codes and guidelines

The methodology can be applied for both a rapid screening, whose principal target is to underline the sure and the clearly uncertain cases (FEMA 178, 1992 and FEMA 310, 1998), and a systematic and detailed analysis (FEMA 273, 1997) of structural and not structural components.

The FEMA 178 manual provides a first level procedure: it recognizes some positive characteristics that, based on the behaviour of the buildings during past earthquakes, are considered as effective for the protection of the human life. Some of them are substantially of qualitative type (regularity, redundancy, etc.), while other ones must be verified through numerical immediate checks (quick checks). If the building possesses these positive characteristics for the structural typology to which it belongs, as well as for the foundation and the non structural components, it is considered in conformity with the guidelines, and therefore it is able to guarantee the life safety under the design seismic event. On the other hand, if some

characteristics are not present, then the building has some lacks which must be deepened. Detailed checks related to the relief weak points can be carried out, so to understand if they can be considered of such a type. If these lacks are confirmed by the more detailed checks, then it is necessary to foresee interventions that remove or mitigate such problems.

The FEMA 273 provides the basis for the analysis of buildings taking into account their real behaviour under earthquake, aiming at interpreting the performance exhibited by such structures in the non linear field. These guidelines, differently from the procedure provided by the Italian codes, which foresee the reduction of the design seismic force by a behavioural factor accounting for the structural ductility, consider the elastic seismic actions with the purpose to underline the distribution of the critical zones of the building. The reason of this formulation is that existing structures, with particular reference to the RC ones, have not been generally designed and realized for guarantying a ductile behaviour of the single components.

Some acceptability criteria for the main parameters (coefficient of ductility, rotation of plastic hinges) are defined as a function of different performance levels, both for structural as well as not structural components and for the whole RC building, considering the type of bars, the entity of the stresses (axial loads in the columns and shear in the beams) and the conformity of the structure to the anti-seismic prescriptions.

Among different analysis methods that can be adopted, non linear procedures implicate dynamic or static equivalent (pushover) analyses: the former method, which is based on direct integration of accelerograms that respects specific prerequisites, generally provides results very sensitive to the numerous geometric and material parameters of the model. The latter method is more standardised, providing less variable results, and aims at determining the deformations of every principal structural element to be compared with the limit values corresponding to the assumed performance objectives.

The pushover analyses are based on incremental loading processes, which simulate the effect of static forces, equivalent to the seismic actions. All the structural components are continuously checked and the analysis stops when particular conditions at the ultimate limit state are attained.

In order to determine the performance point of a structure under a fixed earthquake level, it is necessary to intersect the structural capacity with the

demand due to the considered seismic action in the so-called acceleration - displacement response spectrum (ADRS) plane. In the practise this intersection is not immediately determinable because the demand is a function of the equivalent viscous damping ratio of the structure which must be calculated on the basis of the hysteretic characteristics of the structure itself by means of an iterative procedure according to the provisions given by the ATC-40 American code (1996).

For this reason, the detailed analysis of the FEMA 273 guidelines, together with the ATC-40 provisions, has been performed in the current Chapter in order to establish the seismic performance of the building under investigation.

5.2 THE FEMA 273 GUIDELINES

5.2.1 *General*

The FEMA 273 “NEHRP Guidelines for the Seismic Rehabilitation of Buildings” contains a systematic guidance which makes able designers to formulate effective and reliable rehabilitation approaches that will limit the expected earthquake damage to a specified range for existing buildings subjected to specified levels of ground motions.

In particular, this document is intended to be applied to all building - regardless of importance, occupancy, historic features and size - that by some criteria are deficient in their ability to resist the effects of earthquakes. It also applies to the structural elements of buildings, such as shear walls or frames, and their constituent components, such as a column in a frame or a boundary member in a wall, as well as to non-structural components, that is ceilings, partitions, mechanical/electrical systems, etc.. In addition to techniques for increasing strength and ductility of systems, the guidelines provide rehabilitation techniques for reducing seismic demand, such as the introduction of isolation or damping devices.

For this reason, such a publication can represent both a reference document for building regulatory officials and a solid base for the future development and implementation of building code provisions and standards based also on the use of innovative rehabilitation systems.

The document consists of two parts: the Guidelines volume, which provides requirements and procedures, and the Commentary one, which is able to explain in detail the indications of the first part. A companion volume titled “Example Applications” contains information on typical deficiencies, rehabilitation costs and other useful explanatory information.

Nevertheless, this document should not be considered as a design manual, textbook or handbook. In fact, despite the instructional examples and explanations found in the Commentary and Example Applications volume, other supplementary information and instructional resources have to be required to use this document appropriately.

On the other hand, FEMA 273 cannot be considered neither a code nor a standard. The conversion of the Guidelines into a normative context represents a hard operation, which should be performed with particular care, requiring a lot of time.

In the whole, the document is intended to be suitable both for voluntary use by owners and design professionals, as well as for adaptation and adoption into model codes and standards.

This document contains several new features that depart significantly from previous seismic design procedures used in the design of new buildings.

First of all, methods and design criteria to achieve four different levels of seismic performance are defined, they being known as Collapse Prevention, Life Safety, Immediate Occupancy and Operational. These levels are discrete points on a continuous scale describing the building’s expected performance, or alternatively, how much damage, economic loss and disruption may occur.

Three Structural Performance Levels and four Non-structural Performance Levels are used to form the four basic Building Performance Levels listed above. The definition of different possible rehabilitation targets vs. specified levels of earthquake intensity, also defined in both the ATC-40 (ATC, 1996) and the VISION 2000 project (SEAOC, 1995), has contributed to develop the performance based design methodology. The guidelines have allowed to codify the performance targets, the acceptability criteria related to the attended performance and the analysis tools for their evaluation. Thanks to these contributions, in the last years a large diffusion of the above methodology, which have inspired the emanation of the recent codes, has been recorded.

Afterwards, simplified and systematic rehabilitation methods have been introduced. In particular, simplified rehabilitation, which may be applied to certain small buildings specified in the Guidelines, have the primary purpose to reduce seismic risk by seeking Limited Objectives.

Partial rehabilitation measures, which target high-risk building deficiencies, are included as Simplified Rehabilitation techniques, which use equivalent static force analysis procedures found in most seismic codes for new buildings.

Systematic Rehabilitation, which may be applied to any building, foresees the check of each existing structural element, the design of new ones and the verification of acceptable global interaction for expected displacements and internal forces. The Systematic Rehabilitation Method focuses on the nonlinear behaviour of structural response by means of procedures not previously emphasized in seismic codes.

Four distinct analytical procedures can be used in Systematic Rehabilitation:

- Linear static;
- Linear dynamic;
- Non linear static;
- Non linear dynamic.

The selection of the more appropriate analytical method is based upon the building characteristics. The linear procedures admit the traditional use of a linear stress-strain relationship, but they adjust both overall building deformations and material acceptance criteria to permit better consideration of the probable nonlinear characteristics of the system seismic response. The nonlinear static procedure, often called “pushover analysis,” uses simplified nonlinear techniques to estimate seismic structural deformations. The nonlinear dynamic procedure, commonly known as nonlinear time history analysis, requires considerable judgment and experience to be performed and, therefore, may be used within appropriate limitations only.

In the framework of Performance Levels and Ranges, the guidelines assume that performance can be measured using analytical results such as storey drift ratios or strength and ductility demands on individual components or elements. In order to enable structural verification at the selected Performance Level, stiffness, strength, and ductility characteristics of many

common elements and components have been derived from both laboratory tests and analytical studies and then considered under standard format in the document.

The seismic demand inputs for the various analysis techniques are selected within the ones provided by United States Geological Survey (USGS) aiming at updating the 1997 *NEHRP Recommended Provisions* for new buildings. In such a context, national probabilistic maps were developed for ground motions with a 10% chance of exceedance in 50 years, a 10% chance of exceedance in 100 years and a 10% chance of exceedance in 250 years. These probabilities correspond to earthquakes that are expected to occur, on average, about once every 500, 1000, and 2500 years. Key ordinates of a ground motion response spectrum for these various cases allow the user to develop a complete spectrum at any site.

Finally, the knowledge of local seismicity, costs of rehabilitation and local socioeconomic conditions factors is used to determine an appropriate rehabilitation objective which conditions the choice of the rehabilitative intervention.

5.2.2 The seismic rehabilitation

The basic approach for seismic rehabilitation design includes the following steps, they being presented in the order in which they would typically be performed in the rehabilitation process:

- obtain as-built information on the building and determine its characteristics, including whether the building has historic importance;
- select a rehabilitation objective;
- select an appropriate rehabilitation method.

The detailed description of the above steps is herein presented.

5.2.2.1 As-built information

The first step, which foresees the acquisition of the base constitutive elements of the building, represents the procedure commonly adopted for any evaluation process. In the current recognition, while modern codes encourage

the construction of new buildings having good seismic performances, including regular configuration, structural continuity, ductile detailing and appropriate quality materials, many existing buildings were designed and constructed without these features and contain characteristics, such as unfavorable configuration and poor detailing, that preclude application of building code provisions for their seismic rehabilitation.

The as-built building configuration consists of the identification of both the type and arrangement of existing structural elements and components composing the gravity- and lateral-load resisting systems, as well as the nonstructural components. In this phase it is important accounting for both the intended load-resisting elements and components and the effective ones. The latters may include structural elements conforming to codes, non conforming ones and nonstructural elements participating in resisting gravity, lateral, or combined gravity and lateral loads, whether or not they are able to respect the function assigned them by the original designers. Existing load paths should be identified, considering the effects of any modifications (e.g., additions, alterations, rehabilitation, degradation) since original construction. Potential discontinuities and weak links should also be identified, as well as irregularities that may have a detrimental effect on the building response to lateral demands.

The project calculations should include documentation of these characteristics under form of drawings or photographs, integrated by appropriate descriptive texts. Existing characteristics of the building and site should be obtained from the following sources, as appropriate:

- field observation of exposed conditions and configuration;
- available construction documents, engineering analyses, reports, maintenance histories and manufacturers' literature and test data;
- reference standards and codes from the period of construction;
- destructive and non-destructive examination and testing of selected building components;
- interviews with building owners, managers, the original constructors, contractors and the local building official.

As a minimum, at least one visit to the site should be performed to obtain detailed information regarding both building and geotechnical conditions, as well as issues related to adjacent structures. In such a way it is possible to

evaluate if the available construction documents are representative of existing conditions. If the building has historic features, it is also important to identify its location; in this case particular care should be taken in the investigation process to minimize the impact of the work on the mentioned properties.

Furthermore, structural analysis of the buildings seismic behaviour requires a good knowledge of the existing components (e.g., beams and columns), their interconnection and the properties of constituent materials.

The component strength must be determined for two basic purposes:

- to allow calculation of its ability to deliver load to other elements and components;
- to determine its capacity to resist forces and deformations.

The component deformation capacity must be calculated to allow validation of overall element and building deformations and their acceptability for the selected rehabilitation objectives. In general, such capacities are calculated as “expected values”, accounting for the mean material strengths as well as the probable effects of strain hardening and/or degradation.

The knowledge of such components should be obtained by visual surveys of condition, destructive and nondestructive testing and field measurement of dimensions, as appropriate. Even with an exhaustive effort to maximize knowledge, uncertainty will remain regarding the validity of computed component strength and deformation capacities. To account for this uncertainty, a knowledge factor, κ , is utilized in the capacity evaluations. Two possible values exist for κ , based on the reliability of available knowledge classified as either minimum or comprehensive.

When only a minimum level of knowledge is available, a κ value of 0.75 shall be included in component capacity and deformation analyses. Instead, a κ value of 1.0 may be used where comprehensive knowledge and understanding of the components configuration has been obtained.

5.2.2.2 Rehabilitation objectives

The second step represents the basis for the rehabilitation design. Each rehabilitation objective consists of one or more specifications of a seismic demand (hazard level) and corresponding damage state (building performance

level). In the substance, they are statements of the desired performance when the building is subjected to earthquake demands of specified severity. Building performance can be described qualitatively in terms of :

- safety of occupants during and after seismic events;
- cost and feasibility of restoring the building to initial condition;
- period of time necessary for repairing;
- economic, architectural, or historic impacts on the larger community.

These performance characteristics are directly related to the extent of damage sustained by the building, which is categorized as a building performance level.

Each of these levels consists of both a structural performance level, which defines the permissible damage to structural systems, and a nonstructural one, which defines the permissible damage to nonstructural building components and contents.

A series of three discrete structural performance levels may be used in constructing project rehabilitation objectives: *Immediate Occupancy* (S-1), *Life Safety* (S-3) and *Collapse Prevention* (S-5). Two Structural Performance Ranges are defined to allow design for structural damage states which are intermediate in comparison to the ones represented by the discrete performance levels, which are *Damage Control* (S-2) and *Limited Safety* (S-4). In addition, there is the S-6 designation, which is used to indicate *structural performance not considered*, to cover the situation where only nonstructural improvements are made.

A series of three discrete Nonstructural Performance Levels can be considered: *Operational Performance Level* (N-A), *Immediate Occupancy Performance Level* (N-B) and *Life Safety Performance Level* (N-C). There is also a *Hazards Reduced Performance Range* (N-D) and a fifth level or category (N-E) in which nonstructural damage is not limited.

For the definition of the above levels, numbers indicate the Structural Performance Level, while letters are used for nonstructural performance level. Four performance levels commonly used in the formation of building rehabilitation objectives are described: Operational (1-A), Immediate Occupancy (1-B), Life Safety (3-C) and Collapse Prevention (5-E).

Operational level is obtained combining the immediate safeness level and the non-structural functionality one. Buildings guaranteeing such

performances do not undergo significant damage in both their structural and non structural parts and, therefore, are not characterised by interruption of use. All buildings should guarantee such a performance level under earthquakes with low return periods; contrary, for more severe seismic actions, designs based on this functionality level should result too expensive, they being acceptable for strategic structures only.

Immediate Occupancy is obtained combining the structural and non structural performance related to the immediate safeness. Buildings satisfying this objective suffer no damage to structural elements and minimum damage to non-structural parts. For this reason, they are utilised also after earthquake, even if some reparation interventions are required. The risk for human people is very low.

Life safety is given by the combination between the structural performance and the non structural one for the safety of human lives. Buildings guaranteeing such performances can undergo large, but controlled, damaging effects to both structural and non structural components. For allowing return of people, reparation works, often economically not convenient, are performed. As a consequence, in many cases, it is necessary to foresee the rehabilitation intervention of the whole structure, performed in the light of an accurate benefits-costs study. In this case, risk for people lives is very low.

Collapse prevention avoids the structural collapse without taking into account the vulnerability of non structural elements, whose failure should compromise the human lives. However, avoiding the collapse of the building, very large losses are excluded. Structures offering such performances could result unrecoverable economically.

The combination of both structural and non structural performances is used to define the overall performance of the building (Table 5.1).

The *rehabilitation objective* selected as a design basis will determine the cost and feasibility of any rehabilitation project, as well as the benefit to be obtained in terms of improved safety, reduction in property damage and interruption of use in case of future earthquakes. Table 5.2 presents a matrix indicating the broad range of rehabilitation objectives: each cell of the matrix represents a single target.

A qualitative representation of foreseeable costs related to rehabilitation interventions vs. performance objectives, the latter conditioned by both

earthquake severity and performance levels, is shown in Figure 5.2, where it is apparent that higher costs are necessary for more ambitious performance targets.

Table 5.1: Performance levels of the building

Non structural performance levels	Levels of structural performances					
	S-1 <i>Immediate safeness</i>	S-2 <i>Controlled damage</i>	S-3 <i>Life safety</i>	S-4 <i>Limited safety</i>	S-5 <i>Collapse prevention</i>	S-6 <i>Not considered</i>
N-A functionality	1-A (OL)	2-A	N.R.	N.R.	N.R.	N.R.
N-B safeness	1-B (IO)	2-B	3-B	N.R.	N.R.	N.R.
N-C life safety	1-C	2-C	3-C (LS)	4-C	4-D	5-D
N-D limited risk	N.R.	2-D	3-D	4-D	5-D	6-D
N-E not considered	N.R.	N.R.	N.R.	4-E	5-E (CP)	NO

Table 5.2: Rehabilitation objectives

		Building Performance Levels			
		Operational Performance Level (1-A)	Immediate Occupancy Performance Level (1-B)	Life Safety Performance Level (3-C)	Collapse Prevention Performance Level (5-E)
Earthquake Hazard Level	50%/50 year	a	b	c	d
	20%/50 year	e	f	g	h
	BSE-1 (~10%/50 year)	i	j	k	l
	BSE-2 (~2%/50 year)	m	n	o	p

k + p = BSO
k + p + any of a, e, i, m; or b, f, j, or n = Enhanced Objectives
o = Enhanced Objective
k alone or p alone = Limited Objectives
c, g, d, h = Limited Objectives

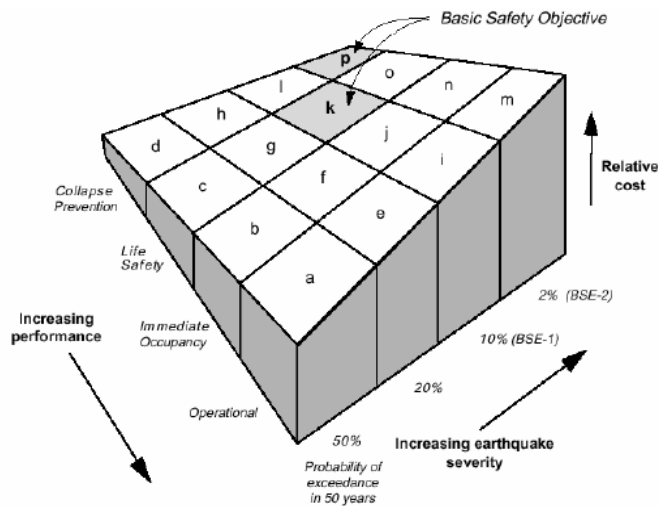


Figure 5.2: Surface indicative of costs related to different rehabilitation objectives

Generally, the *Guidelines* make reference to two levels of earthquake hazards that are particularly useful for the formation of Rehabilitation Objectives. These are defined in terms of both probabilistic and deterministic approaches and are named as Basic Safety Earthquake 1 (BSE-1) and Basic Safety Earthquake 2 (BSE-2). With the purpose to consider explicitly both the extreme and rare seismic events, the BSE-1 and BSE-2 earthquakes are typically taken as earthquakes having 10% and 2% of exceedance probability in 50 years, respectively, except in regions near major active faults. In these regions the BSE-1 and BSE-2 may be defined based on the deterministic estimation of earthquakes.

The goal of a rehabilitation project may be to satisfy a single rehabilitation objective (for example, Life Safety for the BSE-1 earthquake) or multiple Rehabilitation ones (i.e. Life Safety for BSE-1 earthquake, Collapse Prevention for BSE-2 earthquake and Immediate Occupancy for an earthquake with a 50% probability of exceedance in 50 years). A specific analytical evaluation should be performed to confirm that a rehabilitation design is capable of meet each desired Rehabilitation Objective selected as a goal for the project.

A desirable goal for rehabilitation is to achieve the Basic Safety Objective (BSO), which has performance and hazard levels consistent with seismic risk traditionally considered acceptable. At this aim, building rehabilitation must be designed to obtain both the Life Safety Performance Level (3-C) for BSE-1 earthquake demands and the Collapse Prevention Level (5-E) for BSE-2 earthquake demands.

Buildings meeting the BSO are expected to have little damage from the relatively frequent, moderate earthquakes that may occur, but significantly more damage from the most severe and infrequent seismic events. The level of damage to buildings rehabilitated to the BSO may be greater than that expected in properly designed and constructed new buildings.

Alternative objectives that provide higher (Enhanced Objectives) and lower (Limited Objectives) performance levels are also described.

On one hand, any rehabilitation objective intended to provide performance greater than the BSO one at either the BSE-1 or BSE-2, or both, is known as enhanced objective. Such performances can be obtained in two ways:

- Directly, designing for a higher Performance Level than Life Safety for the BSE-1 or a higher Performance Level than Collapse Prevention for the BSE-2.
- Indirectly, with the design controlled by some other selected Performance Level and hazard that will provide better than BSO performance at the BSE-1 or BSE-2.

On the other hand, any Rehabilitation Objective intended to provide performance lesser than the BSO one is called with the Limited Objective term. Such a target, which may consist of either Partial Rehabilitation or Reduced Rehabilitation, should be considered when the rehabilitation measures:

- do not create or make a more severe structural irregularity;
- do not result in a reduction in the capability of the structure to resist lateral forces or deformations;
- do not produce increase of seismic forces into any components having not adequate capacity to resist these forces, unless this component behaviour is still acceptable considering the whole structural performance;
- are detailed and connected to the existing structure;

- do not create or make more severe unsafe conditions.

In particular, any rehabilitation program that does not fully address the lateral-force-resisting capacity of the complete structure is termed Partial Rehabilitation. The portion of the structure that is addressed in Partial Rehabilitation should be designed for a target Rehabilitation Objective and planned so that additional rehabilitation could be performed later to meet fully that objective. Contrary, Reduced Rehabilitation programs address the entire building's lateral-force-resisting capacity, but not at the levels required for the BSO. Reduced Rehabilitation may be designed for one or more of the following objectives:

- Life Safety Performance Level (3-C) for earthquake demands that are less severe (more probable) than the BSE-1;
- Collapse Prevention Performance Level (5-E) for earthquake demands that are less severe (more probable) than the BSE-2;
- Performance Levels 4-C, 4-D, 4-E, 5-C, 5-D, 5-E, 6-D, or 6-E for BSE-1 or less severe (more probable) earthquake demands.

Building performance is a combination of the performance of both structural and nonstructural components. Table 5.3 describes the overall levels of structural and nonstructural damage that may be expected of buildings rehabilitated to the levels herein defined.

Table 5.3: Damage control and building performance levels

	Building Performance Levels			
	Collapse Prevention Level	Life Safety Level	Immediate Occupancy Level	Operational Level
Overall Damage	Severe	Moderate	Light	Very Light
General	Little residual stiffness and strength, but load-bearing columns and walls function. Large permanent drifts. Some exits blocked. Infills and unbraced parapets failed or at incipient failure. Building is near collapse.	Some residual strength and stiffness left in all stories. Gravity-load-bearing elements function. No out-of-plane failure of walls or tipping of parapets. Some permanent drift. Damage to partitions. Building may be beyond economical repair.	No permanent drift. Structure substantially retains original strength and stiffness. Minor cracking of facades, partitions, and ceilings as well as structural elements. Elevators can be restarted. Fire protection operable.	No permanent drift; structure substantially retains original strength and stiffness. Minor cracking of facades, partitions, and ceilings as well as structural elements. All systems important to normal operation are functional.
Nonstructural components	Extensive damage.	Falling hazards mitigated but many architectural, mechanical, and electrical systems are damaged.	Equipment and contents are generally secure, but may not operate due to mechanical failure or lack of utilities.	Negligible damage occurs. Power and other utilities are available, possibly from standby sources.
Comparison with performance intended for buildings designed, under the <i>NEHRP Provisions</i> , for the Design Earthquake	Significantly more damage and greater risk.	Somewhat more damage and slightly higher risk.	Much less damage and lower risk.	Much less damage and lower risk.

For comparative purposes, the estimated performance of a new building subjected to the BSE-1 level of shaking is indicated. These performance descriptions are estimates rather than precise predictions; therefore variation among buildings of the same Performance Level must be expected. Independent performance definitions are provided for structural and nonstructural components, each of them being classified as either primary or secondary. Generally, for a given performance level, acceptance criteria for primary elements and components are typically more restrictive than those for secondary elements and components.

In a typical building, nearly all elements, including many nonstructural components, will contribute to the building's overall stiffness, mass, and damping and consequently its response to earthquake ground motion. However, not all of these elements are critical to the ability of the structure to resist collapse when subjected to strong ground shaking. Nevertheless, the behaviour of all elements and components participating in the building's lateral response is considered, even if they are not normally considered as part of the lateral-force-resisting system. This allows to evaluate the different extent of damage experienced by each of these elements. Therefore, the concept of primary and secondary elements permits to differentiate between the performance required by elements which can be considered critical or not critical for the ability of buildings to resist collapse.

The presence of vulnerable elements makes the building susceptible at seismic risk, which can be attenuated into several ways. The occupancy of vulnerable buildings can be reduced, redundant facilities can be provided and nonhistoric buildings can be demolished and replaced. However, when all alternatives are considered, the options of modifying the building to reduce the risk of damage must be studied. Such corrective measures include stiffening or strengthening the structure, adding local elements to eliminate irregularities or tie the structure together, reducing the demand on the structure through the use of seismic isolation or energy dissipation devices and reducing the height or mass of the structure.

Appropriate building modifications can be determined using either the Simplified Rehabilitation Method or the Systematic Rehabilitation Method.

The former can be applied to many small buildings having regular configuration and located in moderate or low seismic zones. It requires less

complicated analysis than the complete analytical rehabilitation design procedures found under systematic rehabilitation. In many cases, simplified rehabilitation techniques, which are described for components, as well as for entire systems, represent a cost-effective improvement in seismic performance, even if they are often not able to qualify a specific Performance Level.

On the other hand, the Systematic Rehabilitation Method is intended to be complete, it containing all requirements to reach any specified Performance Level. It is an iterative process, similar to the one assumed in the design of new buildings, in which modifications of the existing structure are assumed for the purposes of a preliminary design and analysis and the results of the analysis are verified as acceptable on an element and component basis. If either new or existing components or elements are still inadequate, the modifications are adjusted and, if necessary, a new analysis and verification cycle is performed.

5.2.2.3 Rehabilitation methods

The purpose of building structural alterations and modifications, introduced in order to meet the selected rehabilitation objectives, is determined according to simplified or systematic methods.

The simplified methods allows to design rehabilitation measures without requiring analyses of the entire building response to earthquake hazards. This method is not applicable to all buildings and can be used to achieve limited rehabilitation objectives only. It may be used to obtain a rehabilitation objective consisting of the Life Safety Performance Level (3-C) for a BSE-1 earthquake for buildings meeting all of the following conditions:

- the building is conformed to selected model building types having limitations with regard to number of stories, regularity and belonging to seismic zones;
- a complete evaluation of the building is performed in accordance with FEMA 178 (1992), and the consequent identified deficiencies are addressed by the selected Simplified Rehabilitation Methods.

Any building may be partially rehabilitated to achieve a limited rehabilitation objective by using the simplified method, which may not be used for buildings intended to meet the BSO or any enhanced rehabilitation

objectives. For those buildings and other ones not meeting the limitations for the simplified method, the systematic method should be used.

In this case the basic approach must include the following conditions:

- The structure is analyzed to determine if it is adequate to meet the selected rehabilitation objective(s) and, in contrary case, to identify specific deficiencies. If initial analyses indicate that key elements or components of the structure do not meet the acceptance criteria, it may be possible to demonstrate acceptability by using more detailed and accurate analytical procedures.
- One or more rehabilitation strategies should be developed to address the deficiencies identified in the preliminary evaluation.
- A preliminary rehabilitation design should be developed according to the rehabilitation strategy.
- The structure and the preliminary rehabilitation measures should be analyzed to determine whether the rehabilitated structure is adequate to meet the selected rehabilitation objective(s).
- The process should be repeated as required until a design solution is obtained that meets the selected rehabilitation objective(s), as determined by the analysis.

Even if it is not required by any of the strategies, in the development of the rehabilitation design, an appropriate level of redundancy must be possessed by the rehabilitated lateral-force-resisting system of the building aiming at avoiding the global collapse when localized failure of few elements occurs.

In many cases, although some existing buildings have significant strength and stiffness, it is possible that some of their components do not have sufficient features (strength or deformation capacity) to satisfy the rehabilitation objectives. Therefore, the local modifications of few inadequate components, which improve the component performances, represent the more appropriate and economical strategy to be adopted.

This intervention foresees the execution of several measures, such as cover plating steel beams or columns or the addition of plywood sheathing to an existing timber diaphragm, which increase the element or component strength, allowing them to resist more earthquake induced force before the onset of damage.

Local corrective measures improving the ductility of a component allow it to resist large deformation levels with reduced amounts of damage, without necessarily increasing its strength. Examples of the current technique are the placement of a confinement jacket around a reinforced concrete column to improve its ability to deform without spalling or degrading reinforcement splices and the reduction of the cross section of selected structural components to increase their flexibility and response displacement capacity.

Other causes of undesirable earthquake performance are represented by stiffness, mass and strength irregularities, which can be detected by examining the distribution of structural displacement and inelastic deformation demand values when results of linear analyses are reviewed. If these values are unbalanced, with large concentrations of high values within one storey or at one side of a building, then an irregularity exists. Such irregularities are often caused by the presence of a discontinuity in the structure, such as the termination of a perimeter shear wall above the first storey. Simple removal of the irregularity may be sufficient to reduce demands predicted by the analysis to acceptable levels. However, such interventions may be inappropriate in the case of historic buildings, where the effect of possible alterations should be considered with care.

Effective corrective measures used either to remove or reduce irregularities and discontinuities, such as soft or weak storeys, include the addition of braced frames or shear walls within the soft/weak storey. Torsional irregularities can be corrected by the addition of moment frames, braced frames or shear walls to balance the distribution of stiffness and mass within a storey. Partial demolition can also be an effective corrective measure for irregularities, although this obviously has a significant impact on the appearance and utility of the building.

In addition, some flexible structures behave poorly under earthquakes because critical components and elements do not have adequate ductility or strength to resist the large deformations induced by quakes. For structures comprising many elements, an effective way to improve their performance is given by interventions able to reduce their deformability. This effect can be produced by the addition of new braced frames or shear walls within existing structures.

Some existing buildings have inadequate strength to resist lateral forces, exhibiting inelastic behaviour under low levels of seismic actions. The introduction of supplemental elements to strengthen the building lateral-force-resisting system allows to increase the threshold of the ground motion at which damage occurs. Shear walls and braced frames are effective elements for this purpose; however, since they may significantly stiffen the structure to which they are added, it is necessary that their dimensioning have to be done with main reference to the strength increase only. Moment resisting frames, being more flexible, may be more compatible with existing elements in some structures; however, they may not become as effective in the building response until existing brittle elements have been already damaged.

It is known that stiffness and mass of the structure are two of the primary characteristics which control the amount of force and deformation induced by the ground motion. In this direction, reductions in mass, which can be obtained through demolition of upper stories, replacement of heavy cladding and interior partitions or removal of heavy storage and equipment loads, produces the direct reduction of the above features.

Among innovative rehabilitation techniques, the base isolation one, based on the insertion of bearings between the superstructure and its foundations, is noteworthy. It produces a system with a fundamental response that consists of nearly rigid body translation of the structure above the bearings. Most of the deformation induced in the isolation system by the ground motion occurs within the compliant devices, which have been specifically designed to resist these concentrated displacements and can also have excellent energy dissipation characteristics. Such a double function results in greatly reduced demands on the existing elements of the structure, including contents and non-structural components. For this reason, seismic isolation is often an appropriate strategy to achieve Enhanced Rehabilitation Objectives. This technique is most effective for relatively stiff buildings with low profiles and large mass, whereas it is less effective for light and flexible structures.

Other technologies available for dissipating in a controlled manner the energy imparted into structures by earthquakes are represented by special devices, such as fluid viscous dampers, yielding plates or friction pads, which are able to reduce the structure displacements. The most common devices dissipate energy through frictional, hysteretic or viscoelastic processes. In

order to dissipate substantial energy, dissipation devices must typically undergo significant deformations through significant displacements applied to the structure. Therefore, these systems are most effective in structures that are relatively flexible and have some inelastic deformation capacity. Energy devices are most commonly installed in structures as components of braced frames. Depending on the characteristics of the damper, either static or dynamic stiffness is added to the structure, as well as energy dissipation capacity. In some cases, although the structural displacements are reduced, the forces delivered to the structure can be actually increased.

In the whole, all the described rehabilitation interventions can be effectively designed by means of systematic analysis methods only, allowing to obtain performance objectives more advanced than the base ones (BSO).

In the first phase of the procedure, a preliminary design, where both the extension and the configuration of corrective measures are defined, is performed aiming at estimating the interaction between the behaviour of all structural elements. After this phase, a mathematical model, in which all elements contributing to define the global resistance of the building to lateral loads are considered, is developed.

Finally, an analysis procedure, either of linear or non linear type, is selected aiming at simulating with sufficient approximation the real structure behaviour under earthquakes. In the final phase of the systematic approach all different elements are verified under applied forces or displacements when their behaviour is brittle or ductile, respectively.

Among analysis procedure, the non linear dynamic behaviour of structures can be simulated by means of non linear dynamic analysis in the time domain (time histories analyses). Nevertheless, the use of such a procedure is often not practicable. For this reason, recently simplified methods represented by non linear static analyses have been proposed, they being able to simulate with care the structure behaviour, as it will be illustrated in the next Section.

Non linear static procedure (NSP) may be used for any structure and any Rehabilitation Objective with the following exceptions and limitations:

- they should not be used for structures in which higher mode effects are significant, unless a linear dynamic procedure (LDP) evaluation is also performed. In order to determine if higher modes are significant, a modal response spectrum analysis should be performed for the structure

using sufficient modes to capture 90% of the mass participation. Besides, a second response spectrum analysis should be performed considering the first mode participation only. Higher mode effects should be considered in significant way if the shear in any storey, calculated from the modal analysis considering all modes required to obtain 90% of the mass participation, exceeds 130% of the corresponding storey shear resulting from the analysis considering the first mode response only.

- they should not be used unless comprehensive knowledge of the structure has been obtained.

The key parameters of non linear analysis procedures using pushover methods are capacity, demand and performance. The capacity is the ability of the structure to resist severe seismic actions. The demand is the representation of the quake ground motion. The performance represents the measurement of the capacity to absorb demand: the structure must be able to resist seismic demand in order that performance has to be compatible with design objectives. The deep explanation of such terms, together with the examination in detail of non linear static (pushover) analyses, is illustrated in the following Sections with reference to the provisions given by ATC-40 American report.

5.3 THE ATC-40 PROVISIONS

5.3.1 General

The ATC-40 American report “Seismic Evaluation and Retrofit of Concrete Buildings” was emanated by the Applied Technology Council (ATC) under the auspice of the California Seismic Safety Commission (CSSC) in 1996 in order to develop state-of-the-practice recommendations for seismic retrofitting provisions of vulnerable reinforced concrete structures and seismic risk decision tools.

The document is applicable to the overall existing RC structural system, as well as to its elements (concrete frames, shear walls, diaphragm and foundations) and components (columns, beams, walls, slabs and joints), even if the provided analytical procedures could be also used for new buildings.

Besides, consideration about non-structural systems and components has been also included in the elaborated report.

The methodology upon which the current document is based is the performance based design: both the evaluation and retrofit design criteria are expressed as performance objectives able to define desired levels of seismic performance when the building is subjected to specific intensities of seismic actions. In such a context, acceptable performance is measured by the level of structural and/or non structural damage expected from the quake ground motions. Damage is expressed in terms of inelastic deformation limits for various structural components and elements composing the RC structure.

As a consequence, the analytical procedure incorporated in the base methodology considers post-elastic deformations of the structure by means of non-linear static analysis methods. This kind of analytical procedure is more complex than the traditional force-based one, which provides prescriptive provisions for the design of new buildings. Even if the use of simplified non-linear static analysis procedures for seismic retrofitting of existing buildings has grown over the past 30 years, a large acceptance of this method will be achieved only when its capacity to identify structural deficiencies and to produce economical retrofit strategies better than conventional ones will be demonstrated. At this aim, in the next Sections the detailed illustration of the non-linear static analysis procedures, with particular reference to the capacity spectrum method, based on capacity and demand parameters, has been made.

5.3.2 Non-linear static analyses

5.3.2.1 Foreword

In the ATC-40 prescriptions various analysis methods, both elastic (linear) and inelastic (non-linear), are available for the analysis of existing RC buildings. Elastic analysis methods include both static and dynamic lateral force procedures and recommendations using demand capacity ratios. Although an elastic analysis provides a good indication of the elastic capacity of the structure and indicates where first yielding will occur, it cannot predict

both failure mechanisms and the force redistribution during progressive yielding phases.

Contrary, inelastic analysis procedures are able to show how buildings really work by means of the identification of their failure modes. Such analysis methods help engineers to better understand the structures behaviour when they are subjected to major earthquakes, resolving in this way some of the uncertainties associated with code and elastic procedures.

In the current framework, the most basic inelastic analysis method is the complete non-linear time history analysis, which at the moment is considered too much complex for general use. Therefore, simplified non-linear analysis methods have been developed, they including the following procedures:

- the capacity spectrum method (CSM), which uses the intersection of the capacity curve with a reduced response spectrum to estimate the maximum structural displacement;
- the displacement coefficient method (FEMA 273, 1997), which uses pushover analysis and a modified version of the equal displacement approximation to estimate the maximum displacement;
- the secant method (COLA, 1995), which utilises a substitute structure and secant stiffnesses.

The ATC-40 code emphasizes the use of non-linear static procedure, focusing its interest mainly in the capacity spectrum method, which provides a graphical representation of the global force-displacement capacity curve (i.e. pushover) of the structure and then compares it to the response spectra representations of the earthquakes demand. Such a method, which is a very useful tool in the evaluation and retrofit design of existing reinforced concrete buildings, provides an immediate and clear picture on the impact that different retrofit strategies could have on the performance of buildings under earthquake attacks. For this reason, the deep analysis of the above mentioned procedure, starting from the initial determination of the structural demand after the knowledge of the capacity of the building, represents the first step to follow in the definition of the retrofitting intervention based on the use of metal-based techniques.

5.3.2.2 Capacity

The global capacity of a structure depends on both the strength and the deformation capacities of the individual structure components. In order to determine capacities beyond the elastic limits, non linear analyses, such as the pushover ones, are required. These procedures use a series of sequential elastic analyses which are superimposed aiming at approximating a force-displacement capacity diagram of the whole structure. In particular, the overall structural capacity to sustain seismic forces can be effectively described from its behaviour under a system of equivalent static forces which are increased up to collapse, considered as the disability to continue to withstand vertical loads.

The applied force system must be able to simulate in realistic way the effects produced by seismic actions: since such effects depend on the structure response, the distribution of forces should change continuously during the analysis. For this reason recent proposals suggest to foresee the adaptation of force distribution in relation to the damaging level of the structure by means of adaptive pushover analyses. Nevertheless, in order to not complicate a procedure able to conjugate the adaptation to the real model with standardization features, the force distribution is assumed to be unchanged during analyses, it being able to represent the inertia forces distribution deriving from the fundamental vibration mode, assuming that it is predominant. Such an approximation is generally valid for buildings with fundamental periods up to 1 sec, whereas for more flexible structures also the other vibration modes must be considered. Besides, when during analysis localised damage mechanisms occur, it could be opportune to adopt force distributions congruent with them: for example, the occurrence of a soft-storey mechanism at the lower floor of a building may conduct to consider an uniform distribution of forces along its height.

The current procedure should require the use of a non linear calculation code, but, for simplicity, it can be performed under simplified way by means of superimposed sequential analyses, as suggested by both FEMA and ATC-40 recommendations, in order to reduce both the analysis time and possible scatters among results. In such a case, the structure capacity is represented by means of a curve in the base shear – top displacement plane. As a consequence, the building complex response is represented under form of a

one DOF non linear oscillator, allowing in this way a direct comparison with seismic demand reported in terms of response spectrum. In such an analysis, the mathematical model of the structure is continuously modified accounting for a reduced resistance of yielding components. A lateral force distribution is again applied until additional components yield. Such a process is continued until either the structure becomes unstable or an established limit is reached.

The main steps which allow the construction of the pushover curve are:

1) Application of a horizontal forces system proportional to the floor masses multiplied for modal coefficients related to the first vibration mode of the building model:

$$F_X = \frac{w_X \Phi_{1X}}{\sum_{X=1}^n w_X \Phi_{1X}} V \quad (5.1)$$

where:

w = floor mass;

Φ_{1X} = amplitude of the first vibration mode related to the X level;

V = base shear;

F_X = horizontal force corresponding to the X level.

For structures with soft storeys, the modal shape must be updated for each increment of excursion in the plastic field. For buildings with many storeys or with strong irregularities also the effects of other vibration modes must be taken into account.

2) Calculation of solicitations developed into structural elements due to the combination of the force system defined at the step 1 with gravity loads.

3) Determination of both the base shear and the roof displacement of the building.

4) Revision of the model (updating of the stiffness matrix), obtained by assigning a reduced stiffness to the elements having excursion in the plastic field.

5) Increase of horizontal forces applied to the updated numerical model of the building in order to allow the development of inelastic properties of other elements.

6) Addition of the rates of both base shear and top displacement to the previously determined ones.

7) Repetition of steps 4, 5 and 6 up to the attainment of one of the following limit states:

- instability due to P- Δ effects;
- distortions greater than the ones corresponding to the desired performance level;
- achievement of a deformation level for an element (or a group of elements) able to produce a significant strength reduction.

Following the above procedure, the pushover curve reported in Figure 5.3 can be plotted.

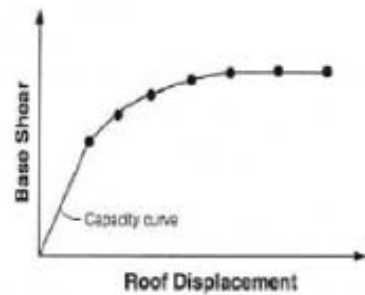


Figure 5.3: Example of a pushover curve

In order to define the global reduction of the structure resistance it is necessary either to reduce or to eliminate the stiffness of elements attaining a limit state. As a consequence, the entire procedure, starting from the step 1, must be repeated until to obtain a new capacity curve (Figure 5.4 a).

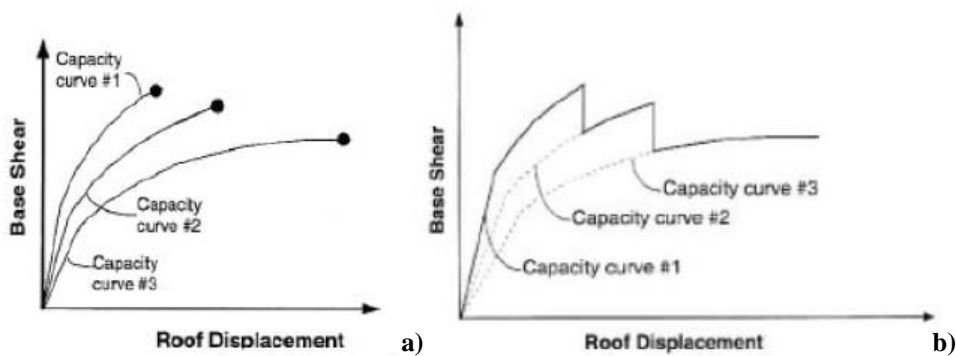


Figure 5.4: Progressive (a) and final (b) configuration of the capacity curve

The final capacity curve of the structure, accounting for the progressive reduction of the system strength, fillets the several obtained curves with vertical lines in correspondence of the attainment of different limit states, assuming the characteristic configuration of the sawtooth curve (Figure 5.4 b).

5.3.2.3 Demand

Ground motions during an earthquake produce into structures complex horizontal displacements patterns which may vary with time. Tracking this motion at every time-step in order to determine structural design requirements is judged impossible.

Traditional linear analysis methods use lateral forces to represent a design condition.

On the other hand, for non linear methods, it is more direct to use a set of lateral displacements as a design condition. For a given structure and ground, the displacement demand is an estimate of the maximum expected response of the building during the ground motion.

The effects produced into structures by seismic actions must be related to parameters able to measure the ground shaking, which is defined through a seismic hazard study able to provide probability curves related to motion parameters and referred to a given observation time period. Such a study is often referred to sites having standard features, which do not coincide necessarily with the ones characterizing the building soil under investigation. Therefore, the subsequent step consists in determining whether and how the base seismic action before defined could be modified in relation to the topographic, geomorphologic and mechanical properties of the soil. As a consequence, the seismic forces to be considered in the design phase are dependent on the soil conditions and cannot be described in terms of peak ground acceleration only. So, the combined effect of the acceleration amplitude with both the frequency content and the earthquake duration can be effectively described by means of the elastic response spectrum, which represents the maximum response induced by the ground motion into a simple elastic oscillator when both its vibration natural frequency and its damping ratio vary. Such response spectra are related to different seismic zones which are detected into seismic hazard maps developed by normative codes.

Once a capacity curve and demand displacement are defined, a performance check can be done. A performance check verifies that structural and non structural components are not damaged beyond the acceptable limits of the performance objective for the forces and the displacements implied by the displacement demand. The execution of such a check can be performed according to the capacity spectrum method after the conversion of the capacity curve into the capacity spectrum, as shown in the next Section.

5.3.2.4 Conversion of the capacity curve into the capacity spectrum

The use of the capacity spectrum method requires to convert the capacity curve, which is expressed in the base shear – roof displacement plane, into the so-called capacity spectrum, which is a representation of the capacity curve in the Acceleration-Displacement Response Spectra (ADRS) format (i.e. S_a vs. S_d).

Every point on a response spectrum curve is associated with a unique spectral acceleration S_a , spectral velocity S_v , spectral displacement S_d and period T . In order to convert a spectrum from the standard S_a vs. T format found in the building code into the ADRS one, it is necessary to determine the value of S_{di} for each point on the S_{ai} - T_i curve by means of the following equation:

$$S_{d_i} = \frac{T_i^2}{4\pi^2} S_{a_i} g \quad (5.2)$$

Standard demand response spectra contain a range of constant spectral acceleration and a second range of constant spectral velocity.

Spectral acceleration and displacement at period T_i are given by:

$$S_{a_i} g = \frac{2\pi}{T_i} S_v \quad S_{d_i} = \frac{T_i}{2\pi} S_v \quad (5.3)$$

In order to develop the capacity spectrum from the capacity (or pushover) curve, it is necessary to do a point by point conversion to the first mode spectral coordinates. Any point on the capacity curve having V_i and Δ_{roof} as coordinates is converted into the corresponding point (S_{ai} , S_{di}) on the capacity spectrum using the following relationships:

$$S_{a_i} = V_i / W / \alpha_1 \quad (5.4)$$

$$S_{d_i} = \frac{\Delta_{roof}}{(PF_1 \times \phi_{1,roof})} \quad (5.5)$$

where:

V = base shear;

W = building dead weight plus likely live loads;

Δ_{roof} = roof displacement;

$\phi_{1,roof}$ = roof level amplitude of the first mode;

α_1 = modal mass coefficient for the first natural mode of the structure;

PF_1 = modal participation factor for the first natural mode of the structure.

In particular, the latter two factors can be expressed by the following relationships:

$$PF_1 = \frac{\sum_{i=1}^N (w_i \phi_{i1}) / g}{\sum_{i=1}^N (w_i \phi_{i1}^2) / g} \quad (5.6)$$

$$\alpha_1 = \frac{\left[\sum_{i=1}^N (w_i \phi_{i1}) / g \right]^2}{\left[\sum_{i=1}^N w_i / g \right] \left[\sum_{i=1}^N (w_i \phi_{i1}^2) / g \right]} \quad (5.7)$$

where:

w_i/g = mass assigned to the level i ;

ϕ_{i1} = amplitude of mode 1 at level i ;

N = uppermost level in the main portion of the structure.

The participation factor and the modal mass coefficient vary according to the relative inter-storey displacement over the height of the building (Figure 5.5).

However, S_a vs. T representation of the response spectra is generally more familiar to most engineers, while the ADRS representation is often unknown. For this reason, in Figure 5.6, the same spectrum in the two formats have been plotted.

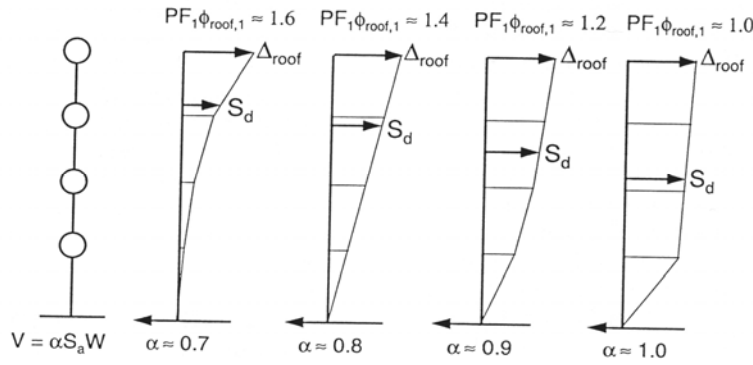


Figure 5.5: Relationships between participation factors and modal mass coefficients

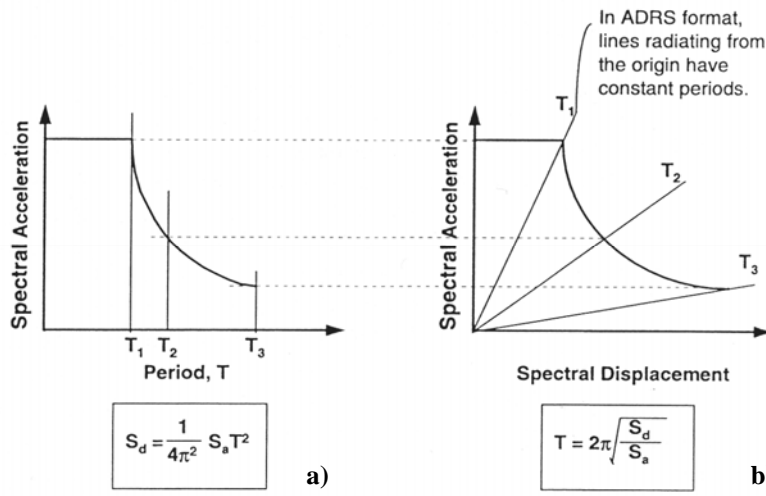


Figure 5.6: Traditional (a) and ADRS (b) formats for the response spectra representation

In the S_a vs. S_d representation, inclined lines starting from the origin have constant period T , which can be computed for any point on the spectrum by using the following relationship:

$$T = 2\pi \sqrt{\frac{S_d}{S_a}} \quad (5.8)$$

In a similar way, for any point on the traditional spectrum, the spectral displacement can be achieved by means of the following equation, which is directly obtained from eq. (5.8):

$$S_d = \frac{S_a T^2}{4\pi^2} \quad (5.9)$$

The same capacity spectrum superimposed on each of the response spectra graphics illustrated in Figure 5.6 is shown in Figure 5.7.

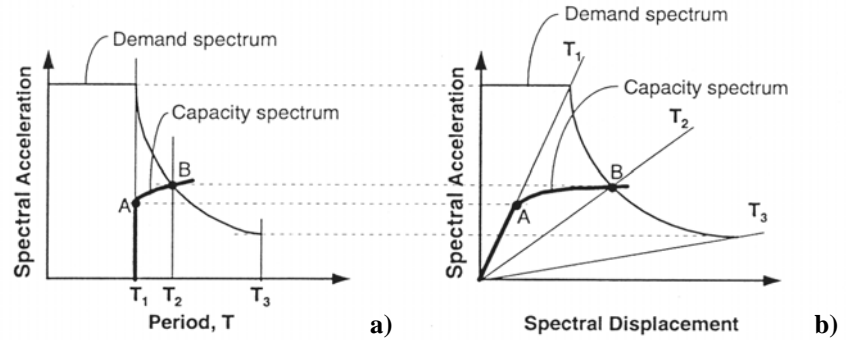


Figure 5.7: Capacity spectrum superimposed over response spectra in traditional (a) and ADRS (b) formats

In such a figure, in the S_a - T plane, the period, having a value equal to T_1 , remains constant up to the attainment of the point A and then increases until to T_2 when the point B is reached. This shows that, when the structure is subjected to inelastic displacements, the period increases. Even if the lengthening period is most apparent on the traditional spectrum plot, it is also clear in the ADRS plane, where the constant period lines radiate from the origin.

For the sake of example, Figure 5.8 indicates that, in the ADRS format, lines starting from the origin have constant period, which lengthens as the structure undergoes inelastic displacements. Points 1 and 2 lie on two different response spectra, but they are located on the same line departing from the origin, which corresponds to a period of 0.5 sec. Instead, in the same Figure 5.8, point 3 is positioned on the line with $T = 1$ sec. Therefore, for the capacity spectrum illustrated, when the structure is subjected to a displacement of 3.95 inches, the period passes from 0.5 to 1 sec.

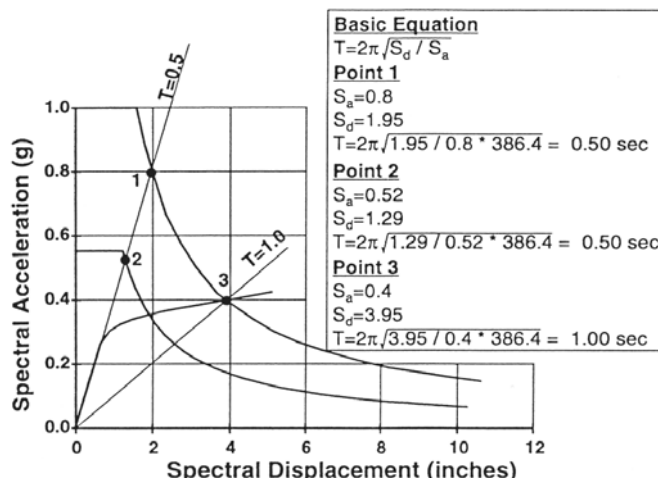


Figure 5.8: Period increment due to inelastic displacements applied to the structure in the ADRS plane

5.3.2.5 Bilinear representation of the capacity spectrum

A bilinear representation of the capacity spectrum is used to estimate both the effective damping and the appropriate reduction of the spectral demand. An example of this representation is illustrated in Figure 5.9.

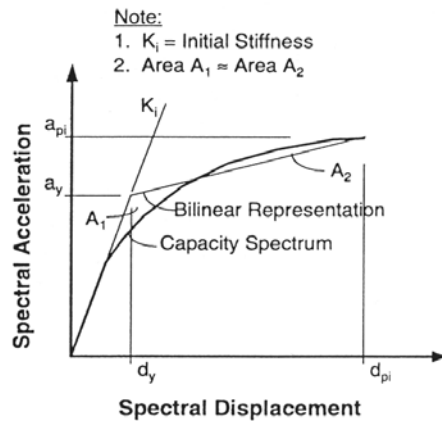


Figure 5.9: Bilinear representation of the capacity spectrum

From the figure it is evident that the construction of such a curve requires to define the point (a_{pi}, d_{pi}) . This point is the trial performance one which must be estimated in order to have a reduced demand response spectrum.

In fact, if the reduced response spectrum intersect the capacity spectrum at the estimated (a_{pi}, d_{pi}) point, then it can be considered as the performance point. Guidance on the estimate of this point can be provided by the equal displacement approximation method, according to the following procedure (see Figure 5.9):

- draw a line from the origin which represents the initial stiffness of the building;
- draw a second line back from the trial performance point (a_{pi}, d_{pi}) ;
- slope the second line such that when it intersects the first one at the point (a_y, d_y) , the area denoted with A_1 in the figure is approximately equal to the one designated with A_2 .

The intent to set area A_1 equal to A_2 one is to have equal area under the capacity spectrum and its bilinear representation, i.e. to have equal energy associated with each curve.

In the case of a “sawtooth” capacity spectrum, the bilinear representation should be based on the capacity spectrum curve describing the behaviour at the displacement d_{pi} , as depicted in Figure 5.10.

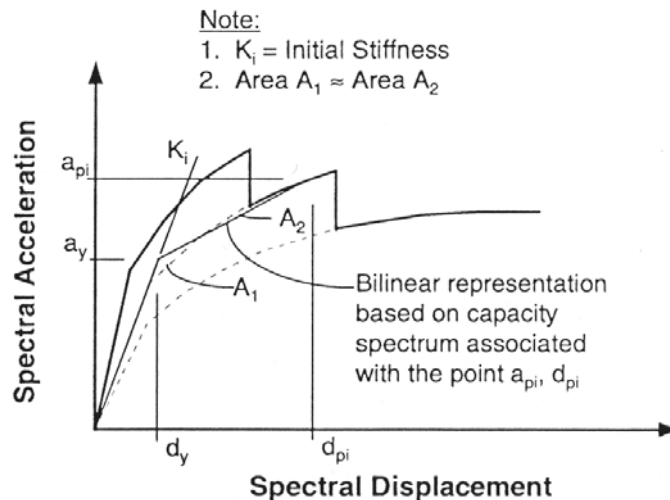


Figure 5.10: Bilinear representation of the capacity spectrum for a degrading system

5.3.2.6 Estimation of damping and reduction of the response spectrum

The damping occurring into a structure when it is subjected to seismic actions producing inelastic displacements can be considered as a combination of the viscous damping, which is inherent in the structure, and the hysteretic one.

Hysteretic damping is related to the area enclosed by loops which are produced when the earthquake force is plotted against the structure displacement. Such a damping component can be represented as equivalent viscous damping by using equations that are available in the literature.

On the other hand, the equivalent viscous damping, β_{eq} , associated with a maximum displacement of d_{pi} , can be estimated by the following relationship:

$$\beta_{eq} = \beta_0 + 0.05 \quad (5.10)$$

where:

β_0 = hysteretic damping represented as equivalent viscous damping;

0.05 = 5 % viscous damping inherent in the structure (assumed to be constant).

The term β_0 can be calculate according to the following equation (Chopra, 1995):

$$\beta_0 = \frac{1}{4\pi} \frac{E_d}{E_{S_0}} \quad (5.11)$$

where:

E_D = energy dissipated by damping;

E_{S_0} = maximum strain energy.

The physical significance of both terms E_D and E_{S_0} is shown in Figure 5.11.

E_D is the energy dissipated by the structure in a single load cycle, that is the area enclosed within a single hysteretic loop. E_{S_0} is the maximum strain energy associated with that motion cycle, that is the area of the hatched triangle.

Referring to the Figure 5.12, the term E_D can be calculated as:

$$E_D = 4(a_{pi}d_{pi} - 2A_1 - 2A_s - 2A_3) = 4(a_y d_{pi} - d_y a_{pi}) \quad (5.12)$$

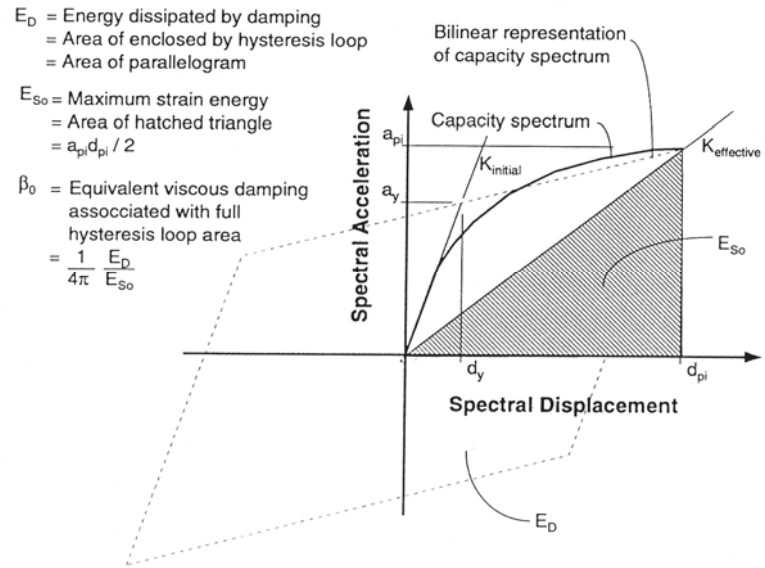


Figure 5.11: Derivation of damping for spectral reduction

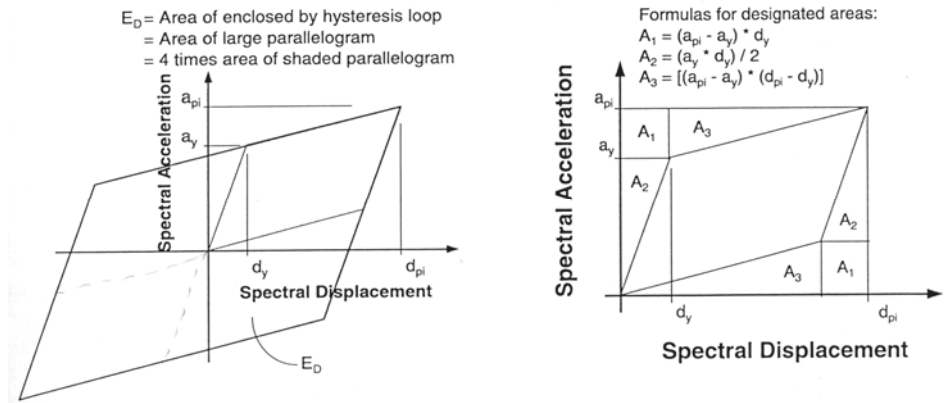


Figure 5.12: Derivation of energy dissipated by damping E_D

The term E_{So} can be determined according to the Figure 5.11 as:

$$E_{So} = a_{pi} d_{pi} / 2 \quad (5.13)$$

and when β_0 is written in terms of percent critical damping, the equation (5.10) becomes:

$$\beta_0 = \frac{63.7(a_y d_{pi} - d_y a_{pi})}{a_{pi} d_{pi}} \quad (5.14)$$

Therefore, β_{eq} assumes the following expression:

$$\beta_{eq} = \beta_0 + 5 = \frac{63.7(a_y d_{pi} - d_y a_{pi})}{a_{pi} d_{pi}} + 5 \quad (5.15)$$

β_{eq} can be used to estimate spectral reduction factors, obtained from relationships developed by Newmark and Hall, which are able to decrease the elastic response spectrum into a reduced one with damping greater than 5%.

In this framework it is important to observe that spectra should not be reduced at a damping value higher than 25% and that an absolute limit of 50% must be considered for β_{eq} .

The idealized hysteretic loop depicted in Figure 5.12 can be representative of a ductile building subjected to quake motions having relatively short duration and with an equivalent viscous damping less than approximately 30%.

For conditions greater than the previous ones, the idealized hysteretic loop lead to overestimate the equivalent viscous damping, because the actual cycle presents a reduced area, which is often caused by pinching phenomena. This is the case of reinforced concrete buildings, which are not ductile structures.

Therefore, in order to take into account the presence of imperfect hysteretic loops, the introduction of a damping modification factor, κ , able to reduce the viscous damping, has been done. As a consequence, the concept of effective viscous damping, β_{eff} , has been introduced, it being represented by the following relationship:

$$\beta_{eq} = \kappa \beta_0 + 5 = \frac{\kappa \cdot 63.7(a_y d_{pi} - d_y a_{pi})}{a_{pi} d_{pi}} + 5 \quad (5.16)$$

The κ -factor represents the more or less adaptation capacity of the hysteretic loop to the parallelogram area. It depends on the structural behaviour of the building, which is influenced by both the quality of the seismic resisting system and the duration of the ground shaking

With reference to different kinds of structures, indicated with Type A, B and C, three correspondent values have been assigned to the κ -factor:

- for structural behaviour type A, $\kappa=1$ (stable and full hysteretic loops);

- for structural behaviour type B, $\kappa=2/3$ (moderate reduction of the area within the hysteretic loops);
- for structural behaviour type C, $\kappa=1/3$ (poor hysteretic behaviour with a significant reduction of the loop area).

The ranges and limits for the κ -values assigned to the three structural behaviour types are summarized in Table 5.4 and illustrated in Figure 5.13.

Table 5.4: Damping modification factor values

Structural Behavior Type	β_0 (percent)	κ
Type A	≤ 16.25	1.0
	> 16.25	$1.13 - \frac{0.51(a_y d_{pi} - d_y a_{pi})}{a_{pi} d_{pi}}$
Type B	≤ 25	0.67
	> 25	$0.845 - \frac{0.446(a_y d_{pi} - d_y a_{pi})}{a_{pi} d_{pi}}$
Type C	Any value	0.33

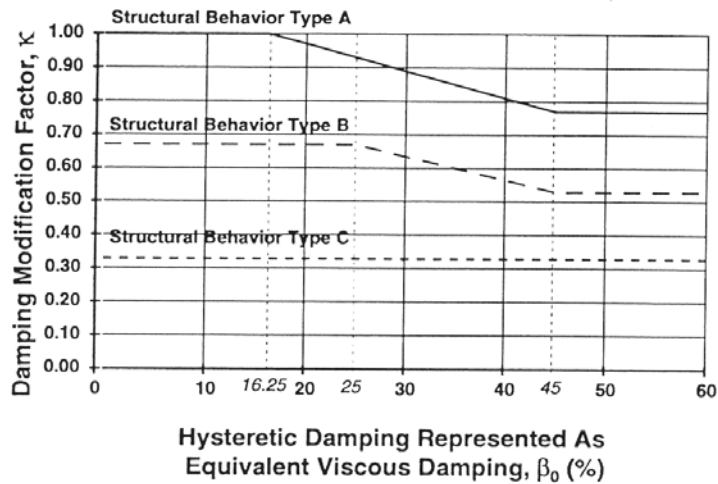


Figure 5.13: Damping modification factors for different structural behaviour types

5.3.2.7 Determination of the performance point

The performance point represents the maximum structural displacement expected for the demand earthquake ground motion.

With reference to the diagram of Figure 5.14, when the displacement d_i at the intersection of the demand spectrum and the capacity one is within 5% ($0.95d_{pi} \leq d_i \leq 1.05d_{pi}$) of the displacement of the trial performance point (a_{pi} , d_{pi}), then d_{pi} becomes the performance point. If such an intersection is not enclosed within the acceptable tolerance, a new point (a_{pi} , d_{pi}) is selected and the process is repeated.

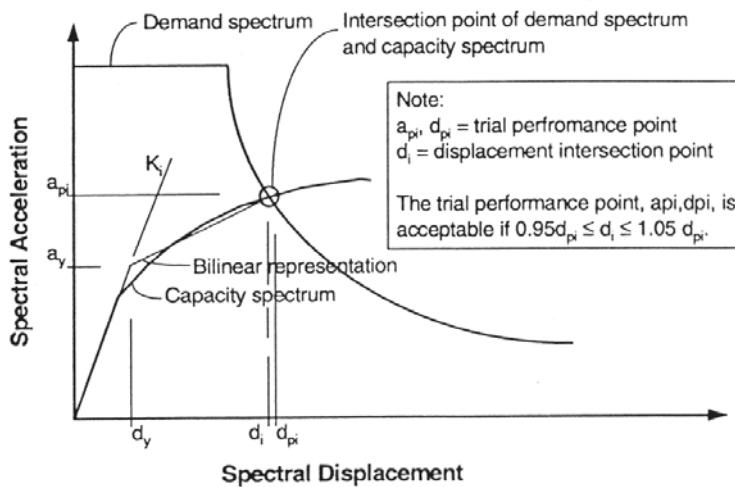


Figure 5.14: Determination of the performance point

When the capacity curve assumes the “sawtooth” configuration, which is characterized by several different capacity spectra accounting for degradation of elements, special attention must be paid to the performance point determination (Figure 5.15). In this case, the bilinear representation of the capacity spectrum is constructed for a single curve only. Because the analysis could be acceptable, the bilinear representation must be for the same single capacity spectrum curve which makes up the portion of the capacity spectrum where the intersection point occurs.

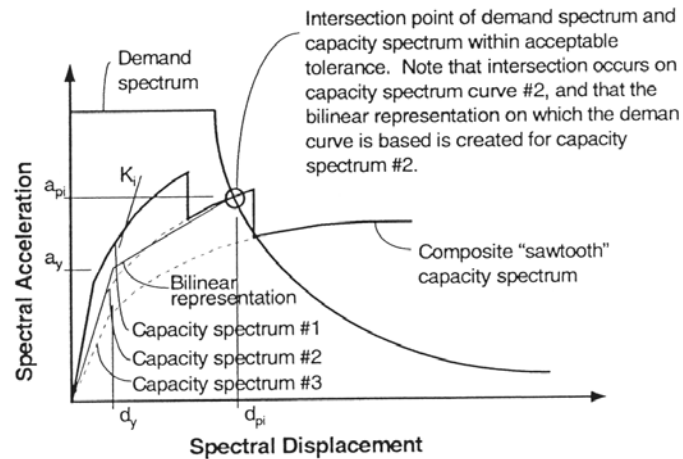


Figure 5.15: Intersection point between the demand spectrum and the sawtooth capacity one

Three different procedures for calculating the performance points are considered:

- Procedure A: it is an analytical method and represents the clearest and most direct application methodology. It may result convenient for spreadsheet programming.
- Procedure B: it is also an analytical method which makes a simplified assumption that is not performed in the other two procedures. This method assumes that not only the initial slope of the bilinear representation of the capacity curve remains constant, but also the point (a_y, d_y) and the post-yield slope result to be unchanged.
- Procedure C: it has been developed to provide a graphical solution using hand methods. It has been found that the performance point obtained in such a way is reasonably close to the one on the first try. Nevertheless, this procedure is the least transparent application methodology.

In the current dissertation, the procedure A, both for the accuracy of results and the better interpretation of the seismic retrofitting design provisions, has been deeply treated only. In this procedure, where iteration is done by hand or by spreadsheet methods in order to converge on the performance point, the following steps are performed:

- 1) Develop the elastic response spectrum as appropriate for the site.

- 2) Transform the capacity curve into a capacity spectrum. Plot the capacity curve on the same chart in which the 5% damped response spectra is plotted, as shown in Figure 5.16 a.
- 3) Select a trial performance point (a_{pi} , d_{pi}), as illustrated in Figure 5.16 b. The first choice of this point could be either the displacement obtained by applying the equal displacement approximation method or the end point of the capacity spectrum.

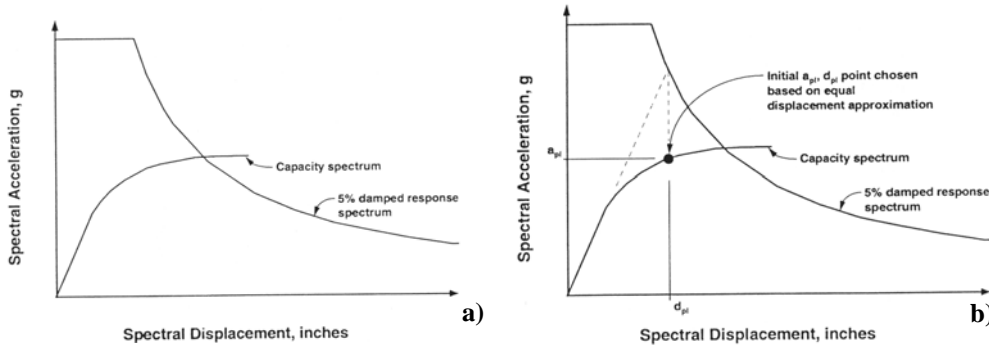


Figure 5.16: Step 2 (a) and step 3 (b) of the Procedure A for calculating the performance point

- 4) Develop a bilinear representation of the capacity spectrum, providing the result reported in Figure 5.17 a.
- 5) Calculate the spectral reduction factors and develop the demand spectrum. Draw the demand spectrum on the same diagram where the capacity spectrum is represented, as shown in Figure 5.17 b.

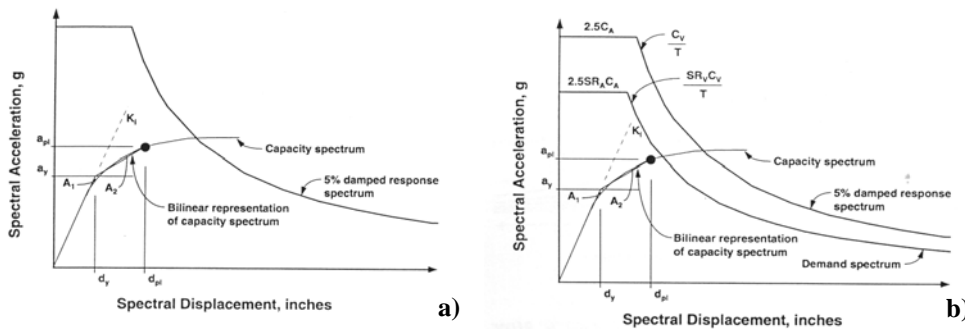


Figure 5.17: Step 4 (a) and step 5 (b) of the Procedure A for calculating the performance point

- 6) Determine if the demand spectrum intersects the capacity one at the point (a_{pi}, d_{pi}) or if the displacement (d_i) at which the demand spectrum intersects the capacity one is within the acceptable tolerance established for d_{pi} . The current procedural phase is illustrated in Figure 5.18.

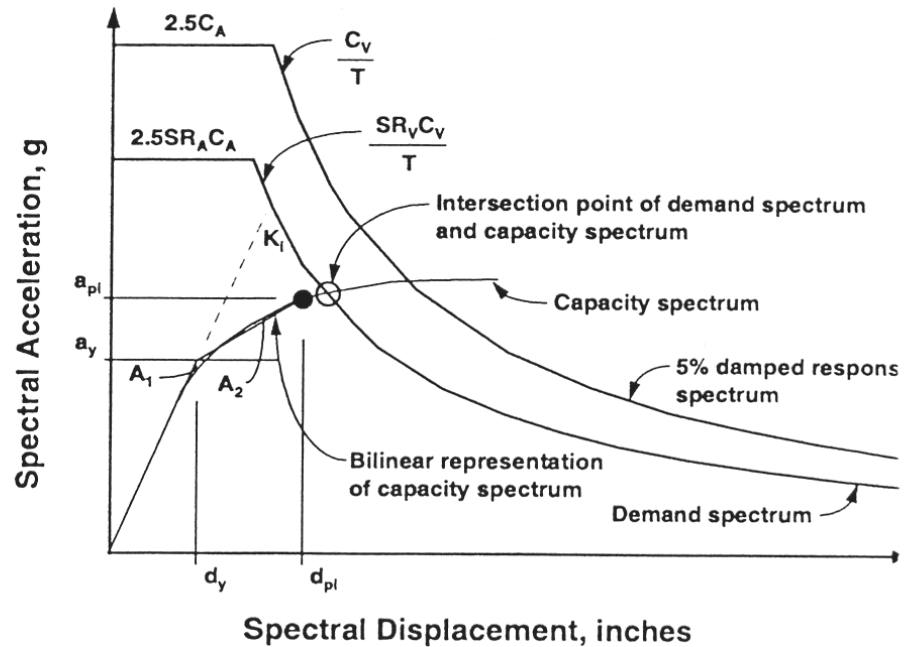


Figure 5.18: Step 6 of the Procedure A for calculating the performance point

- 7) If the demand spectrum does not intersect the capacity one within acceptable tolerance, then select a new (a_{pi}, d_{pi}) point and return to the step 4. In such a case this new point could be the intersection point determined in the step 6.
- 8) If the demand spectrum intersects the capacity spectrum within acceptable tolerance, then the trial performance point (a_{pi}, d_{pi}) is the performance point (a_p, d_p) and d_p represents the maximum displacement expected for the demand earthquake.

5.4 THE ADOPTED PROCEDURE

The use of metal shear panels for retrofitting existing structures can be explained through the example of Figure 5.19 (De Matteis and Mistakidis, 2003; Mistakidis et al., 2004). This figure illustrates the effect of the installation of shear panels on the capacity and demand curves for a retrofitted structure. The curve with the solid line is the capacity spectrum for the structure without shear panels. A performance point occurs for this unretrofitted structure at a spectral displacement of about 5.5 cm, resulting in a Structural Stability (SS) performance level. The curve with the dashed line is the capacity spectrum for the structure after the installation of shear panels. This curve indicates a structure that has both added stiffness and also larger strength. Due to the increase of the stiffness, the initial elastic period shifts from 0.92 sec to about 0.58 sec. However, the most important effect is the change on the demand spectra, and in particular in the larger damping capacity of the structure. For example, the reinforced structure achieves an effective damping of 30% for a displacement of 3.7 cm, while the unretrofitted structure achieves the same damping for a displacement of 5.5 cm. As a result, the performance point for the retrofitted structure shifts to a spectral displacement of about 3.7 cm, resulting in the attainment of Life Safety (LS) structural performance level. In order to perform a preliminary design, it is necessary to decide what target spectral displacement is desired for the retrofitted structure, and then, to determine the characteristics of the LYS panels that will shift the performance point to this spectral displacement.

Figure 5.20 illustrates how this information may be obtained for typical RC framed structure. In this figure, the capacity spectrum for the unretrofitted structure is shown with the solid line. Moreover, it is assumed that the designer, after the examination of the damage state of the structure as determined by the examination of the capacity curve, may easily determine the spectral displacement levels corresponding to the performance levels.

For this example structure, the spectral displacements that correspond to the Immediate Occupancy (IO), Life Safety (LS) and Structural Stability (SS) performance levels, are indicated in Figure 5.20.

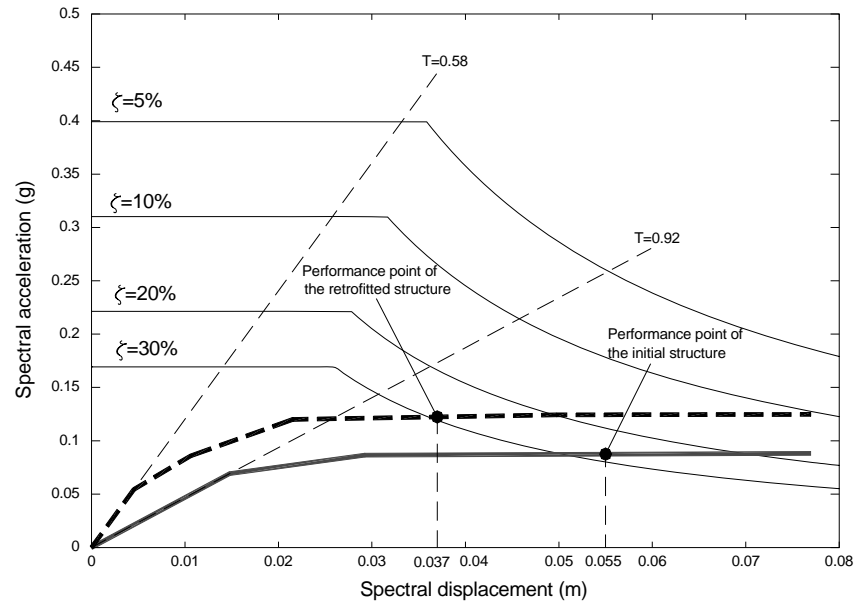


Figure 5.19: Effect of the installation of metal shear panels on the demand and capacity curves

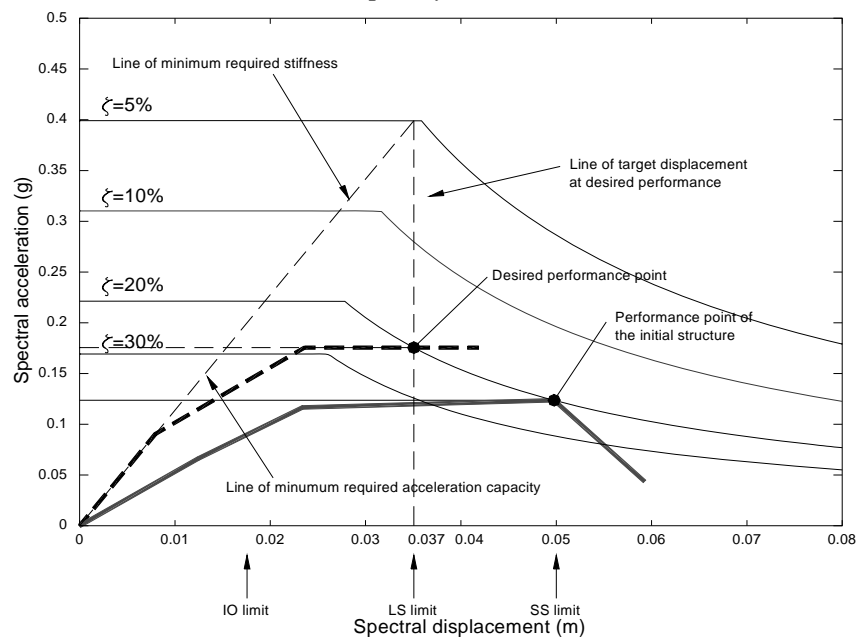


Figure 5.20: Preliminary retrofitting design of a RC structure endowed with metal shear panels

Therefore, this examined structure fails to fulfil even the Structural Stability performance level and therefore has to be retrofitted. Let us assume that the design engineer sets as a performance objective for the building the Life Safety one. Therefore, the target displacement for the retrofitted building is set equal to the displacement that corresponds to the Life Safety performance objective. This is illustrated in the Figure 5.20 by the vertical dashed line drawn at the corresponding spectral displacement.

The next step is to determine an appropriate initial stiffness for the retrofitted structure. As an approximation (based on the “equal displacements” simplifying assumption), an estimation of the initial period required for the retrofitted structure can be obtained by extending the vertical line that corresponds to the desired target displacement until it intersects with the elastic response spectrum (demand spectrum for 5% viscous damping). A radial line drawn from the origin of the demand/capacity spectrum plot through this intersection defines the minimum initial stiffness for the retrofitted structure T_{ret} , expressed as fundamental period. This period can be calculated from the following equation:

$$T_{ret} = 2\pi \sqrt{\frac{S_d}{S_{ae}}} \quad (5.17)$$

where S_d is the target displacement and S_{ae} is the spectral acceleration corresponding to the intersection of the target displacement line with the elastic response spectrum. The target stiffness for the retrofitted structure can be calculated from the equation:

$$K_{ret} = K_{ini} \left(\frac{T_{ini}}{T_{ret}} \right)^2 \quad (5.18)$$

where K_{ini} and T_{ini} are the initial stiffness and the period of the unretrofitted structure, respectively, and K_{ret} is the stiffness required for the retrofitted structure. Once the required stiffness has been determined, the stiffness K_p of metal shear panels can be determined from the equation

$$K_{ret} = K_{ini} + K_p \quad (5.19)$$

At this point, and in order to determine the strength of the retrofitted structure, it is necessary to make an assumption about its damping properties. As a simplifying assumption it is reasonable to consider that the retrofitted structure will be able to provide at least the same level of damping of the

initial structure. Therefore, the approximate solution for the performance point of the retrofitted structure is obtained as the intersection of the vertical line at the desired target spectral displacement with the demand spectrum that corresponds to the damping level of the initial structure. This point is annotated in the figure as the “desired performance point”. A horizontal line extending from the desired performance point to the y axis indicates the minimum spectral acceleration capacity required for the retrofitted structure.

Once this information is known, the required ultimate base shear capacity for the retrofitted structure can be obtained from the following equation:

$$V_{ret} = \frac{S_{a_{ret}}}{S_{a_{ini}}} V_{ini} \quad (5.20)$$

where V_{ini} is the ultimate base shear capacity of the initial structure, V_{ret} is the required ultimate shear capacity of the retrofitted structure, $S_{a_{ini}}$ and $S_{a_{ret}}$ are the ultimate spectral acceleration for the unretrofitted and retrofitted structures, respectively. Finally, the shear strength V_p of shear panels can be determined from the equation

$$V_{ret} = V_{ini} + V_p \quad (5.21)$$

Once the required stiffness and strength of shear panels have been determined, it is possible to develop a preliminary design of the shear panels. However, it should be emphasized, that while the presented approach is suitably accurate to lead to a preliminary design solution, it is extremely important that the actual demand and capacity spectra for the retrofitted structure should be formally computed as part of the final design process.

5.5 ANALYSIS OF THE BASE RC STRUCTURE

Based on the non linear analysis procedures given by FEMA and ATC-40 documents, the resistance of the base RC structure under lateral actions can be evaluated. In particular, once the structural geometrical and dynamic properties have been determined, it is possible to know the resisting capacity of each single element and, therefore, to evaluate, according to the results of the performed preliminary test (see Chapter 4), the behaviour of the bare RC structure subjected to horizontal forces applied in longitudinal direction to the

first storey only. In such a way the response of a one DOF system having the major part of the mass applied above the first level is achieved. The main target of the procedure is to determine the performance point of the structure subjected to the above mentioned loading condition, as stated by the ATC-40 procedures. To this purpose the pushover curve of the structure must be converted into the capacity spectrum one by applying the relationships provided in the Section 5.3.2.4. In the case under study the transformation is simple because the base shear obtained by pushover analysis must be divided for the structure weight (Figure 5.21).

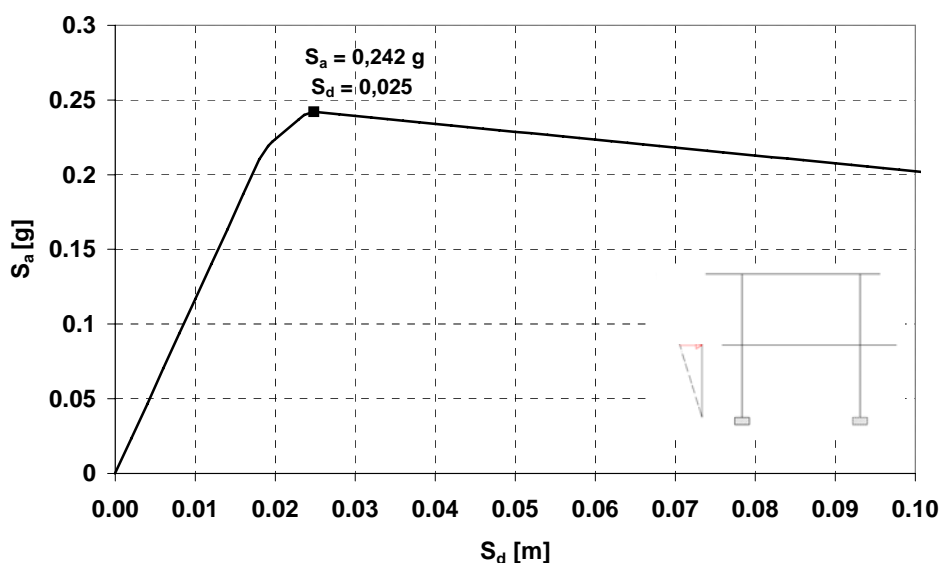


Figure 5.21: Capacity spectrum of the base RC structure

According to the seismic classification of areas provided by the new seismic Italian code (OPCM 3431, 2005), the structure under consideration is located in a second category seismic zone, characterised by a peak ground acceleration equal to 0.25 g, and is realised on a soil type *B*. Therefore, being known the elastic response spectrum, the seismic actions applied on the study building are defined (Figure 5.22). In addition, such a spectrum, which is generally represented in the S_a - T plane, can be plotted in the S_a - S_d one, also considering the spectral acceleration reduction obtained by accounting for different damping ratios (10%, 15% and 20%) (Figure 5.23).

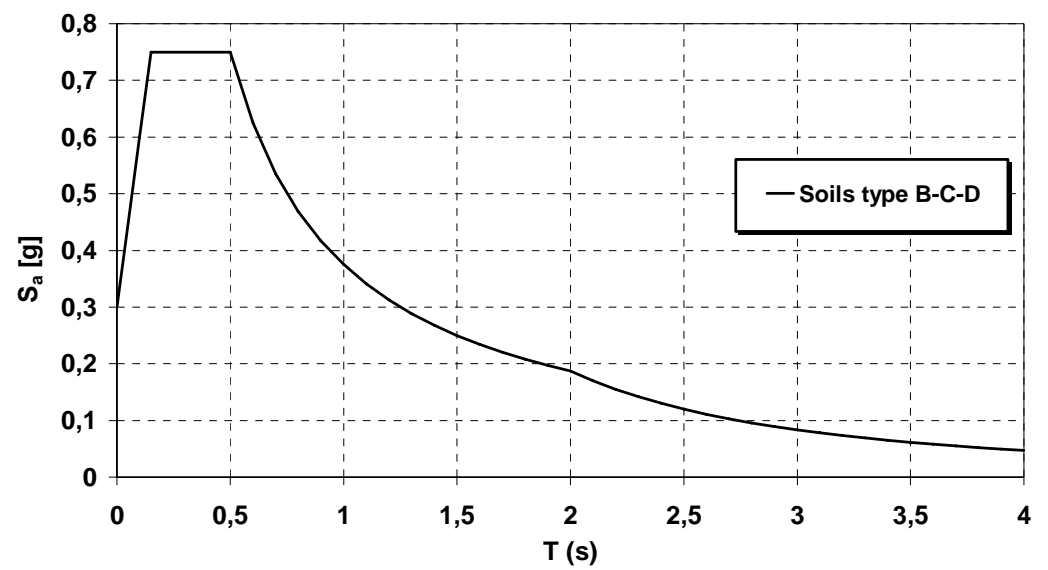


Figure 5.22: Elastic response spectrum for second category seismic zones ($a = 0.25$ g) and soil type B

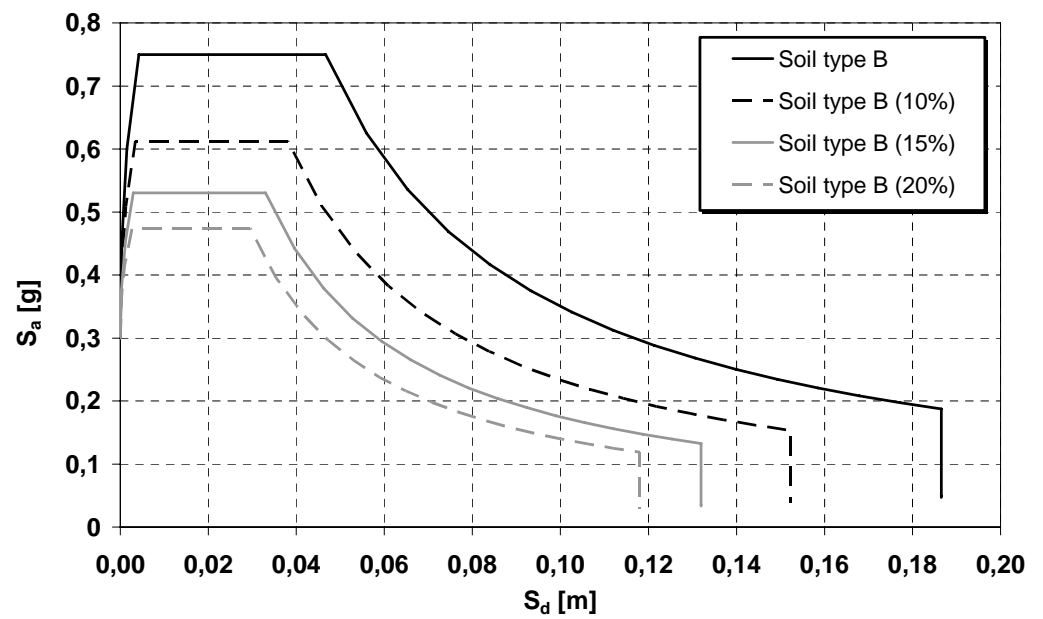


Figure 5.23: Elastic response spectra for soils type B and different damping ratios

In a first analysis phase, by inserting the structure capacity spectrum in the S_a - S_d plane, the performance point can be individuated by means of the equal displacement approximation method, which provides $a_i = 0.128$ g and $d_i = 0.072$ m (Figure 5.24).

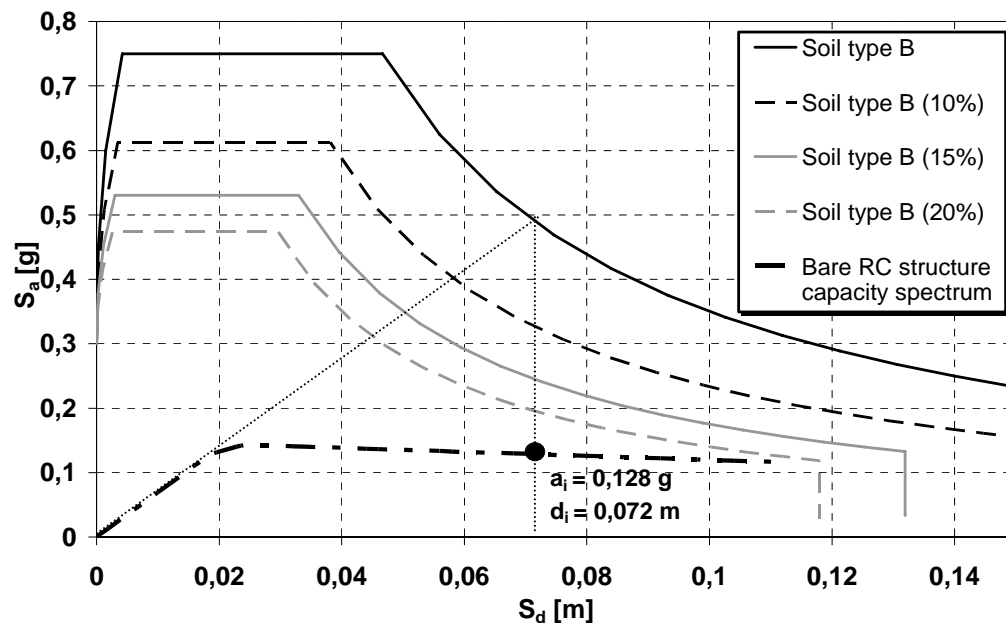


Figure 5.24: Estimation of the performance point by means of the equal displacement approximation method

Later on, the introduction of a damping modification factor κ has been done, it being equal to 0.33 according to the ATC-40 provisions for existing structures characterized by poor dissipative capacity. In fact, since the module is designed for gravity loads only and presents damages due to the pushover test performed in the transversal direction, then it can be classified in the above category.

Therefore, the application of the mentioned method, based on two iteration procedures only, conducts to the estimation of the performance point (Figure 5.25), characterised by the following parameters:

$$a_i = 0.130 \text{ g} ; \quad d_i = 0.064 \text{ m} ; \quad \beta_{eq} = 37\%$$

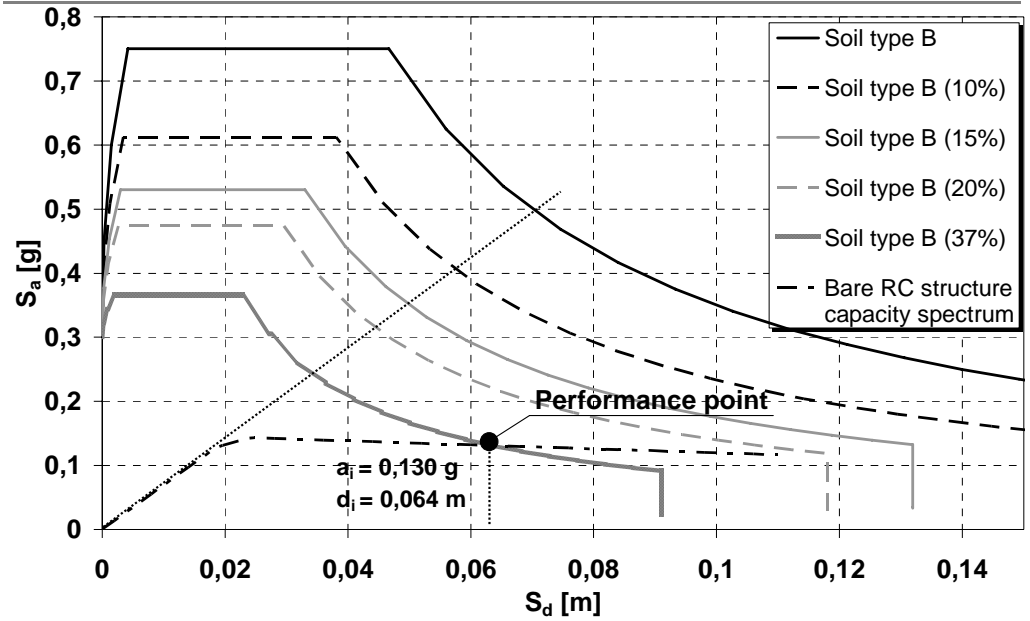


Figure 5.25: Determination of performance parameters of the bare RC structure

From the numerical analysis results it has been seen that such performance values are not resisted by the base structure, which exhibited the formation of a failure plastic hinge at a displacement of 0.056 m. For this reason, a seismic retrofitting intervention is necessary for increasing the structure performances.

To this purpose, the use of metal shear panels has been foreseen.

The first step to be performed is the determination of the initial stiffness of the retrofitted structure, obtained by establishing as a new performance point the one related to the attainment of the maximum rotation capacity of columns plastic hinges, which corresponds to the maximum resistance point illustrated in Figure 5.21. At this aim, the target design displacement of the first level of the RC structure under collapse conditions (*LS*) has been fixed equal to 2.5 cm, corresponding to an inter-storey drift (Δ/H) equal to about 1% (Figure 5.26).

By applying eqs. (5.17) and (5.18), the following results are achieved:

$$T_{\text{ret}} = 0.362 \text{ s} \quad K_{\text{ret}} = 15.53 \text{ kNmm}^{-1}$$

The knowledge of K_{ret} allows to determine the stiffness contribution (K_p) that panels should provide:

$$K_p = 11.5 \text{ kNmm}^{-1}$$

Since the pushover analysis provides a viscous damping coefficient inadmissible for the bare RC structure, then such a factor has been assumed equal to 20% for seismic retrofitting purpose. As a consequence, the shear strength of the reinforced module has been determined:

$$V_{ret} = 275.10 \text{ kN}$$

and from eq. (5.19) the shear panel resistance has been obtained as

$$V_p = 192 \text{ kN}$$

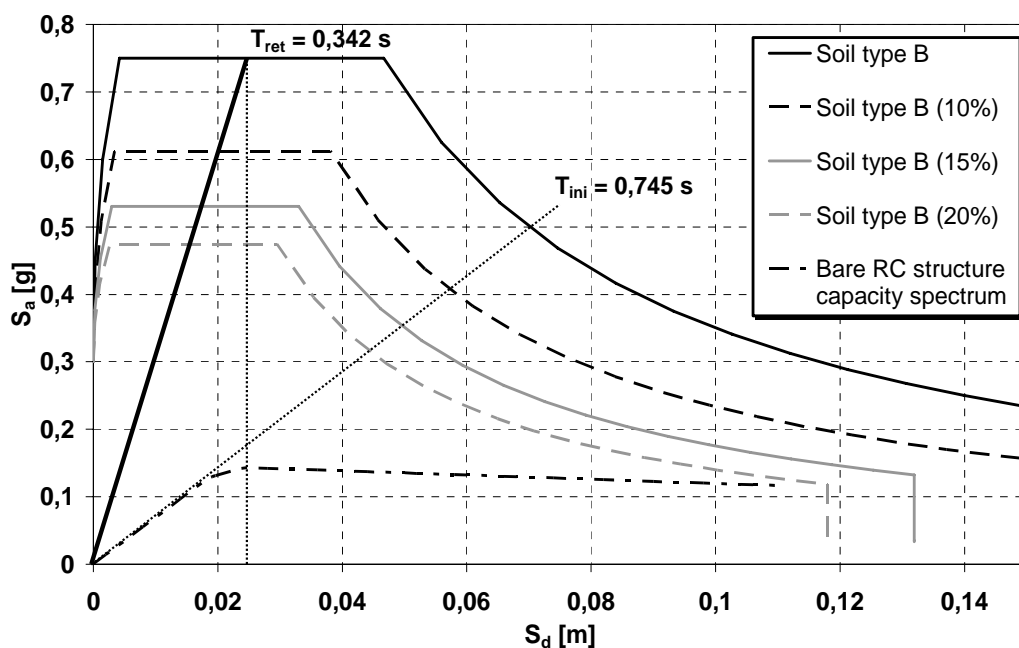


Figure 5.26: Determination of the retrofitted structure stiffness

Finally, on the basis of the proposed design methodology, the capacity curve of the reinforced structure has been defined in the spectral acceleration – spectral displacement (*ADRS*) plane (Formisano et al., 2005) (Figure 5.27).

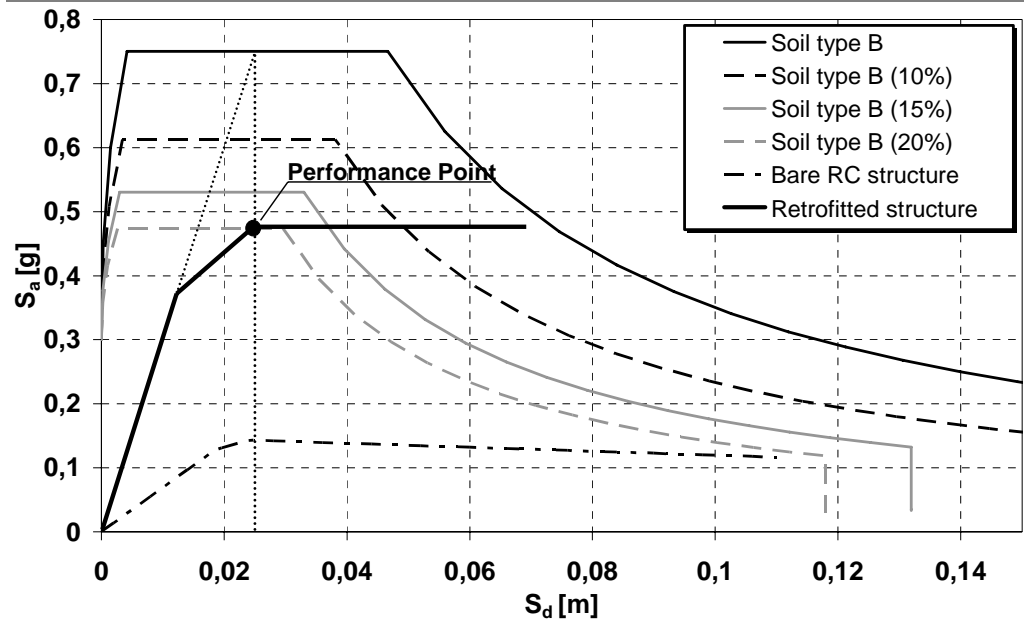


Figure 5.27: The design curve representative of the retrofitting intervention

The knowledge of both the strength and stiffness prerequisites that metal shear panels should present allows to perform the next study phase, which foresees the design of both steel and pure aluminium shear panels for improving the performances of the bare RC structure.

Chapter VI

Numerical and experimental activities on the RC structure upgraded with metal shear panels

6.1 INTRODUCTION

After the determination of both the strength and the stiffness prerequisites of the integrating system able to guarantee the satisfaction of the performances required to the upgraded RC module, the preliminary dimensioning of metal shear panels has to be carried out and then checked by more accurate non-linear analysis of the composite structure. In particular, two different metallic materials (mild steel and pure aluminium) have been selected for shear panels and, as a consequence, two different retrofitting interventions have been set-up. Therefore, the choice of such materials has addressed the definition of the panel dimensions to be employed and, consequently, on the basis of the actual strength of shear wall, all the components of the system foreseen for reinforcing the bare structure (reaction frame, panel-frame connections, steel wall – RC structure connections) have been designed according to the hierarchy criterion methodology, which is actually recognised within all modern seismic codes. Subsequently, the panel systems, positioned on both two longitudinal sides of the structure, have been opportunely studied by means of a non linear finite element program (ABAQUS), whose results have been compared with the ones obtained by adopting simpler models (Strip

model, theoretical PFI method) to check the capability of the latter procedures for interpreting the actual response of the system model.

Later on, the capacity spectra of the reinforced structure have been compared with the design one, aiming at evaluating the effectiveness of the proposed design procedure. Finally, the efficiency of the adopted upgrading intervention has been validated by means of cyclic experimental tests on the compound RC structure - metal shear panels systems, showing in both cases a considerable improvement of the structural capacity of the original structure in terms of initial stiffness, strength and dissipative capacity.

6.2 APPLICATION OF STEEL SHEAR PANELS

6.2.1 The base material

The material used for the characterization of shear walls is the DX56D steel, employed in the field of sheetings and cold-formed profiles according to the prescriptions given by the UNI EN 10142 italian code (1992). The material, which has been inkindly supplied by the MARCEGAGLIA iron and steel industrial group, is galvanized and is characterized by the nominal mechanical features reported in Table 6.1.

Table 6.1: Mechanical characteristics of the steel used for panels

Designation	Covering	$R_{p0,2}$ [Nmm ⁻²]	R_u [Nmm ⁻²]	ϵ_u	Hardening modulus
DX56	+Z	120÷180	270÷350	39	0.21

The panels have been provided under form of sheetings having dimensions of 400 x 2000 x 1.15 mm. Therefore, large attention has been paid to the dimensioning of the shear walls in order to respect the dimensional limit ratios provided by the Canadian code for guarantying the complete development of the tension field mechanism on the entire panel surface. The material has been subjected to tensile tests in order to characterise the actual behaviour,

considering that both a range of yielding and ultimate stresses has been provided by code. To this purpose, three dog-bone shaped specimens have been extracted from the same sheeting used for the panel (Figure 6.1 a) and have been tested under mono-axial regimen. Material tests have been carried out at the Department of Structural Analysis and Design of the University of Naples “Federico II” by using an universal tensile machine (MTS type) (Figure 6.1 b) able to apply tensile and compression actions up to 500 kN.

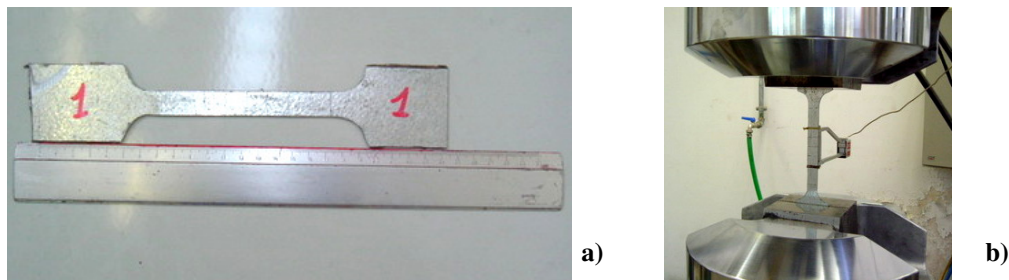


Figure 6.1: Steel specimen before (a) and in the initial phase of test (b)

A view of a specimen at the test end, in which both its elongation and failure is visible, is reported in Figure 6.2 a. The tensile tests performed on three steel specimens have provided the results reported in Figure 6.2 b. It can be observed that for the specimens n.1 and n.3 the recorded ultimate strain ϵ_u is significantly lower because the failure has been occurred externally to the applied displacement transducer.

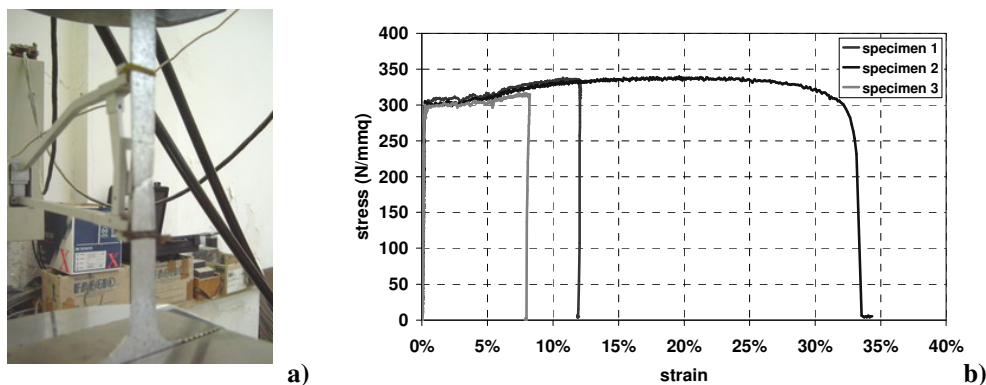


Figure 6.2: Specimen failure at the test end (a) and resulting stress-strain curves (b)

The obtained material characteristics are synthesised in Table 6.2, where it is apparent that the scatter respect to nominal values is really significant.

Table 6.2: Mechanical features of the material obtained from the test performed on specimen n. 2

Identification	f_y [Nmm ⁻²]	f_u [Nmm ⁻²]	ϵ_u	Strain hardening factor
Specimen n. 2	305	340	32.1%	1.15

6.2.2 The shear wall system

6.2.2.1 The shear panel design

Once the actual material features have been acquired, the geometry of the shear panel to be applied for the retrofitting of the existing RC structure can be identified, based on the strength and stiffness values that the rehabilitation system must introduce (De Matteis and Mistakidis, 2003). In order to use these parameters for determining the panel dimensions, reference will be made to the formulations given by Sabouri-Ghomi et al. (2003) and Berman and Bruneau (2003), neglecting the shear resistance in the pre-buckling stage. Therefore the following relationships can be applied:

$$V_p = \frac{1}{2} f_y t b \sin 2\alpha \quad (6.1)$$

$$K_p = \frac{E b \cdot t}{4 h_s} \quad (6.2)$$

Such relationships have been used to evaluate the width of the applied shear wall, being the whole height based on the inter-storey height of the analysed RC frame, given by the distance between the upper surface of the bottom beam and the lower surface of the upper one ($h=2800$ mm). Therefore, the panel depth is determined starting from this value, from which the depth of the beam of the surrounding steel frame, estimated in the first analysis as 400 mm, has to be deduced, thus obtaining a net depth $h_s = 2400$ mm. Therefore the panel width can be calculated by employing eqs. (6.1) and (6.2):

$$V_p = \frac{1}{2} f_y t (\sum b) \sin 2\alpha \quad \Rightarrow \quad \sum b = \frac{2 \cdot V_p}{f_y \cdot t} = 1095 \text{ mm}$$

$$K_p = \frac{E (\sum b) \cdot t}{4 h_s} \quad \Rightarrow \quad \sum b = \frac{4 \cdot h_s \cdot K_p}{E} = 536 \text{ mm}$$

being $\sum b$ the sum of the width of the two applied panels (each one on one side of the frame). In such a case it is observed that the determination of the panel width is governed from the strength rather than the stiffness. In particular, a width of 600 mm has been assumed for each panel, providing the external steel frame geometry depicted in Figure 6.3 a. Such a dimension has been selected due to the necessity to increase the b/d ratio up to 0.25. Since the b/d ratio results lower than the lower limit ($b/d = 0.8$) suggested by the Canadian code (CSA, 2001), intermediate stiffeners have to be applied. Therefore, 600 x 2400 x 1.15 mm shear panels with appropriate stiffeners to be designed have been selected, they being able to provide a contribution in terms of strength and stiffness equal to 214.9 kN and 14.81 kNmm⁻¹, respectively.

Finally it is interesting to observe that combining the two previous relationships (eqs. 6.1 and 6.2) the following expression can be obtained:

$$f_y = \frac{E \cdot V_p}{2 \cdot K_p \cdot h} \quad (6.3)$$

which allows to define, based on both the stiffness K_p and the shear resistance V_p , the optimum yielding strength of the adopted material, evidencing as this parameter is independent from the panel width.

6.2.2.2 Design of the external steel frame

Based on the knowledge of both the mechanical characteristics of the material used for the panel and its geometrical dimensions, it is possible to design the members characterising the reaction steel frame containing the steel plate shear walls (Formisano et al., 2006b). Since the panel has a b/d ratio equal to 0.25, with height of 2400 mm, the frame columns would be subjected to a bending action equal to:

$$M_{pf} = \frac{\sigma_{ty} \cdot t \cdot d^2 \cdot \cos^2 \Theta}{8} \quad (6.4)$$

which, combined with the presence of the axial load deriving from the same tension field mechanism developed by the panel, would determine the adoption of a very large profile. Therefore, also considering the low b/d ratio of the panel, an intermediate transversal beam able to subdivide the panel in two separate parts, having b/d ratio equal to 0.5, is introduced. The insertion of this intermediate beam allows to schematise the columns as a continuous beam on three supports, which presents in the section where the intermediate stiffener is present a maximum flexural moment given by the following relationship:

$$M_{pf} = \frac{\sigma_{ty} \cdot t \cdot \left(\frac{d}{2}\right)^2 \cdot \cos^2 \Theta}{8} \quad (6.5)$$

which is reduced to 1/4 of the previous one (eq. 6.4).

With this premise, the beams and columns have been firstly designed and then checked by means of the application of the CNR 10011 Italian code (1995). In particular, it has been assured that the columns, which have been designed in order to avoid any buckling phenomenon, are able to resist the effects induced by the tension field developing in the shear panel.

As design result, columns and beams obtained by coupling 2 Fe 430 UPN 180 profiles have been adopted, while for the intermediate beam two coupled UPN 240 profiles have been chosen (Figure 6.3), due to technological reasons that will be explained in the following.

Such members will be connected by means of hinged connections. The choice of coupled profiles for the frame elements has been determined by the type of connection between the panel and the surrounding steel frame, which will be based by interposing the panel between the two profiles and connecting them with bolted connections.

In Figure 6.4 the details of the connection between the external steel frame and the RC structure are reported.

The intermediate beam of the steel frame and the hinged beam-to-column connection of the steel frame are illustrated in Figures 6.5 and 6.6, respectively.

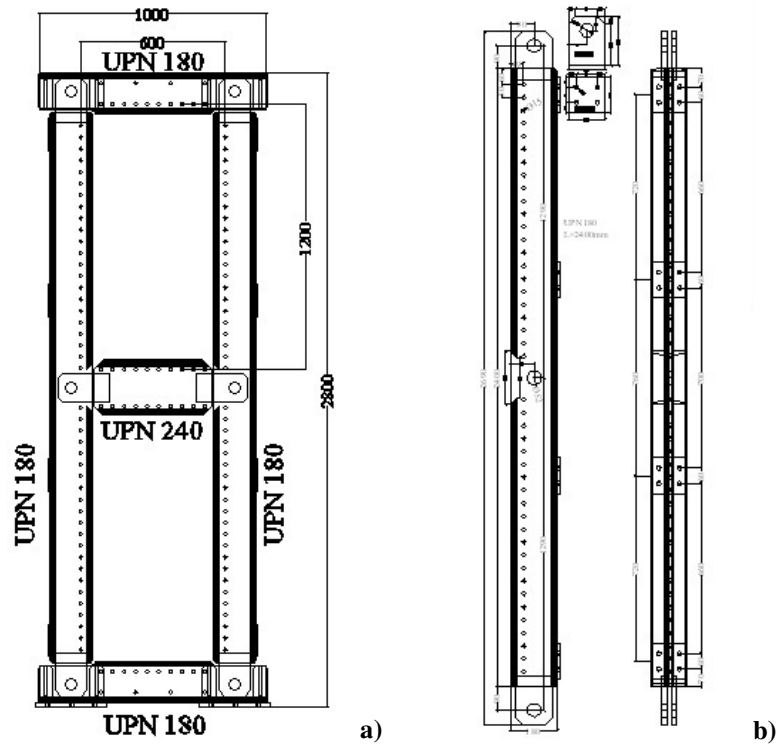


Figure 6.3: Reaction steel frame (a) and carpentry of columns (b)

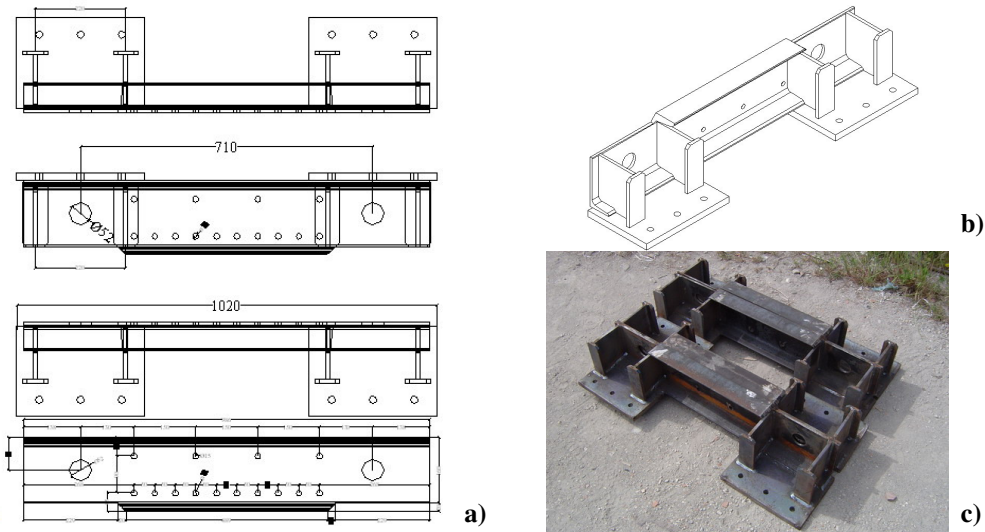


Figure 6.4: Details of the connection with the RC structure: carpentry (a), 3D graphical view (b) and the adopted system (c)

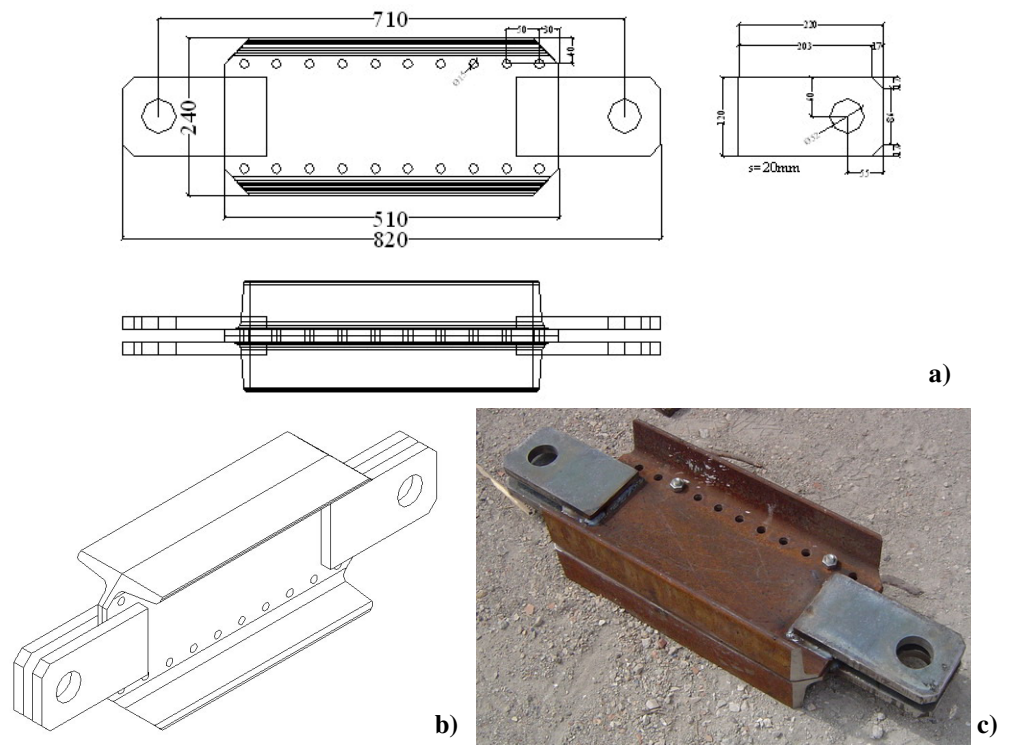


Figure 6.5: The intermediate beam: carpentry (a), 3D graphical view (b) and the adopted system (c)

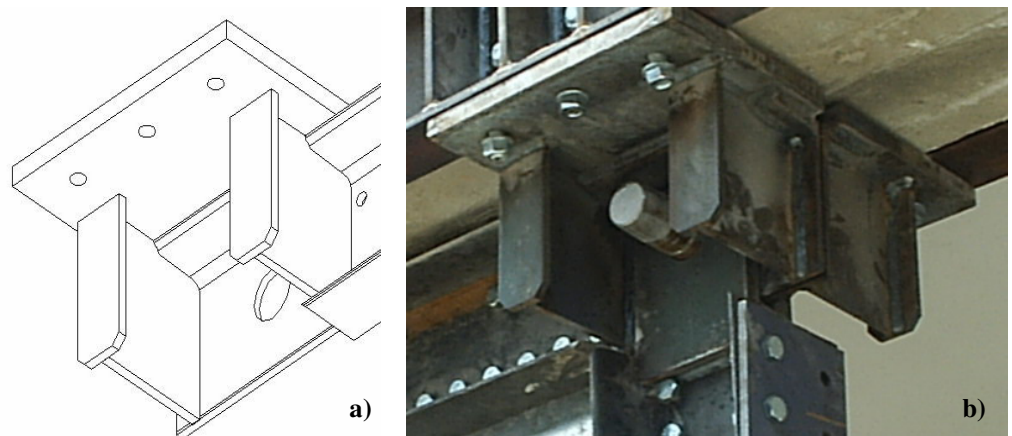


Figure 6.6: Beam-to-column hinged connection: 3D view (a) and the realised detail (b)

6.2.2.3 The steel frame insertion in the RC structure

After the design of the seismic retrofitting intervention of the RC module, the installation of the external steel frame within the original structure has been carried out.

The applied reinforcing system foresees at the foundation level the connection between the reaction steel frame and the RC beam by means of four UPN 220 profiles, which were opportunely stiffened through steel plates (Figures 6.7 a, b).

In particular, the connection among the steel parts (frame and members) has been performed by using six 8.8 steel grade M16 bolts, which have been designed in order to transfer the maximum shear load that the retrofitted structure should withstand. The interaction between the UPN 220 profiles and the RC foundation beam is carried out by means of ends threaded bars which pass the beam and transfer the shear action to the RC member (Figure 6.7c).

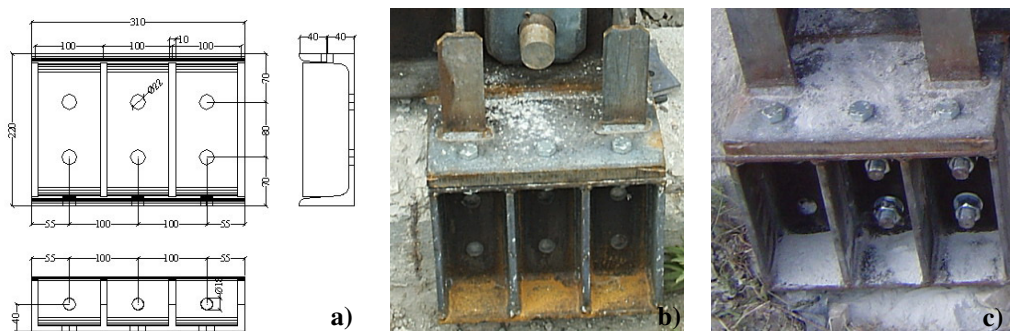


Figure 6.7: Steel frame – RC beam connection: a) carpentry; b) the system realization; c) the use of threaded bars

The connection of the steel shear wall with the first level RC beam is always realised by using UPN 200 profiles having the same length of the RC member (Figure 6.8 a). In such a way the reinforcing of the first level beam through jacketing operations has been performed, being necessary to avoid collapse phenomena in the beam due to the transfer of the forces carried out by the panel (about 10 times greater than the ones applied on the bare frame). In this context, it is important to note that the RC beams located along the two

sides of the structure have different dimensions, their width being equal to 25 and 30 cm, respectively. For this reason, in the reinforcement of the beam with base of 25 cm, next to the external UPN 220 profile, closure elements represented by UPN 100 steel members have been inserted in correspondence of the passing bars in order to provide the connection between the steel and the RC parts (Figure 6.8 b).

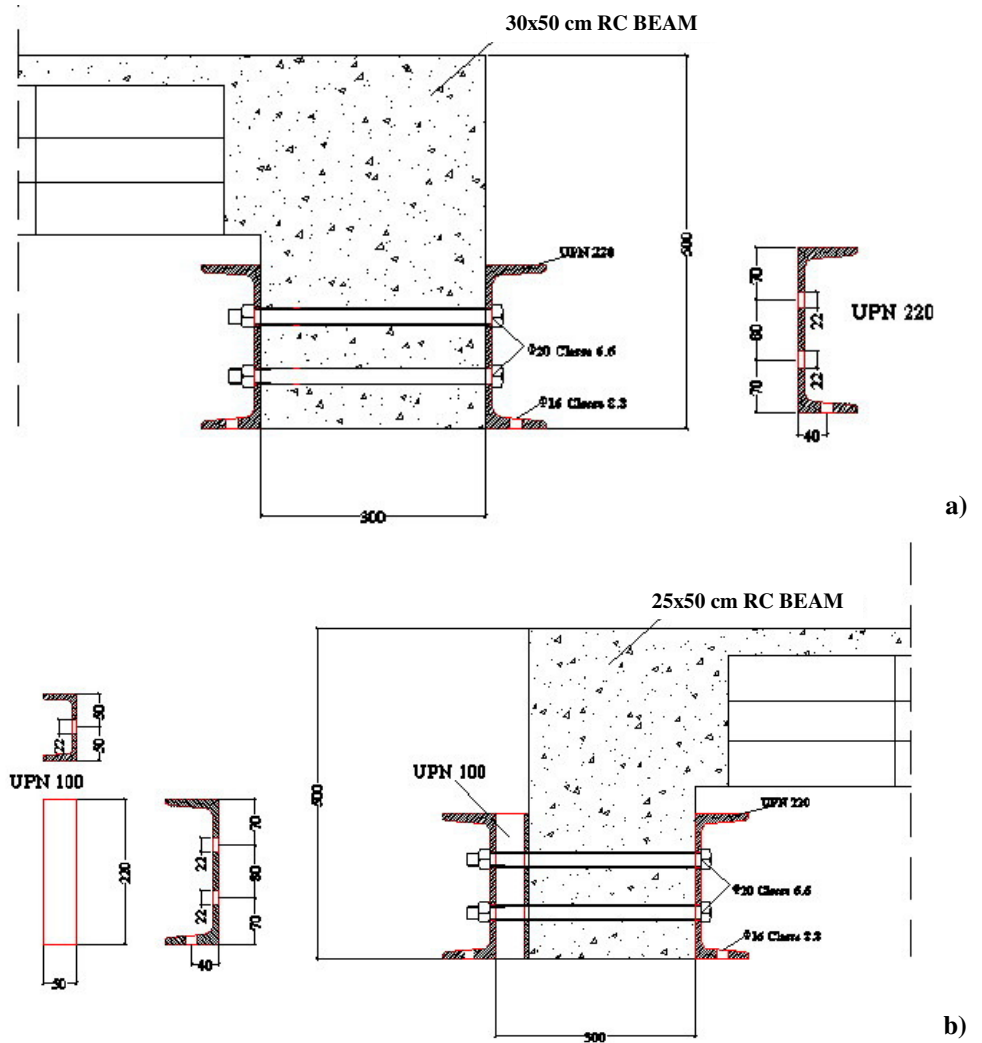


Figure 6.8: Reinforcement of the first level 30 x 50 cm (a) and 25 x 50 cm (b) RC beams

In the zone characterised by the connection between the steel beam and the shear wall, realised through 8.8 class M16 bolts, reinforcement stiffeners have been located in order to avoid buckling phenomena in the web of the beam (Figure 6.9 a). A three-dimensional view of the jacketing operation carried out on the first level RC beam is reported in Figure 6.9 b.

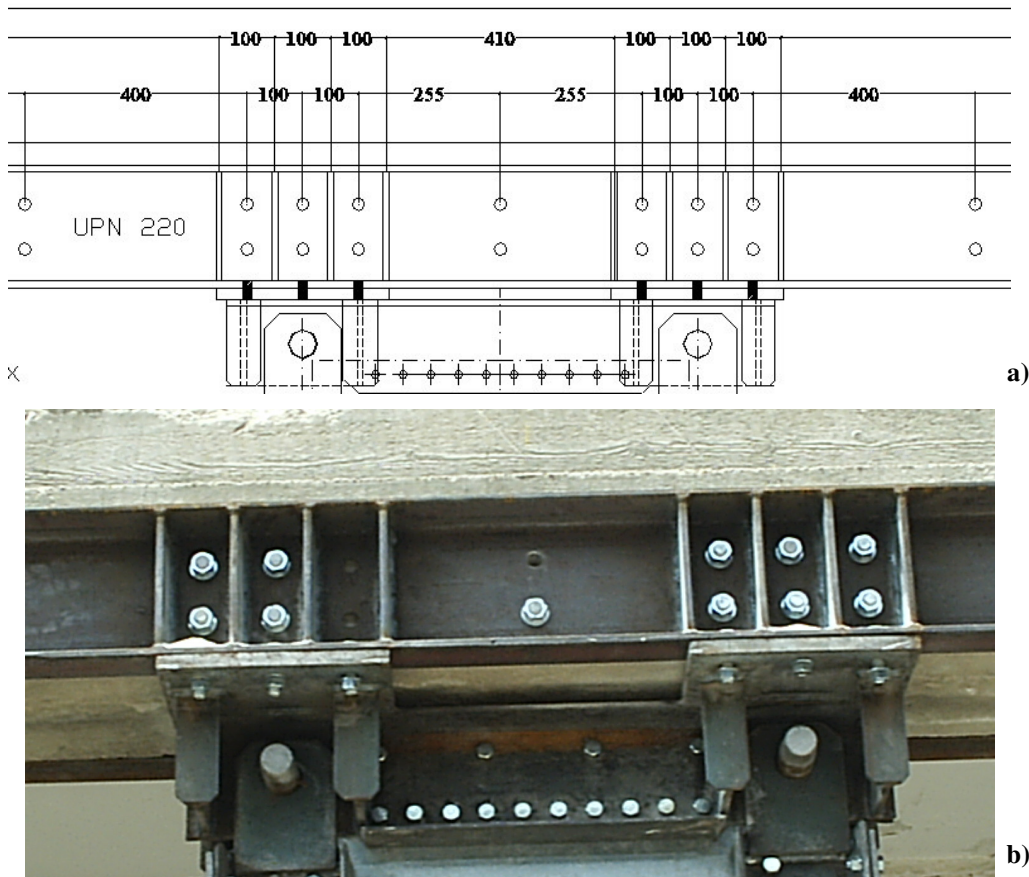


Figure 6.9: Shear wall – steel beam connection: design (a) and realization of the intervention (b)

After the design of the single connection elements between the steel plate shear wall and the RC building, the installation of the retrofitting systems foreseen for the seismic adjustment intervention has been done along the longitudinal direction of the module n. 5 (Figures 6.10 a, b).

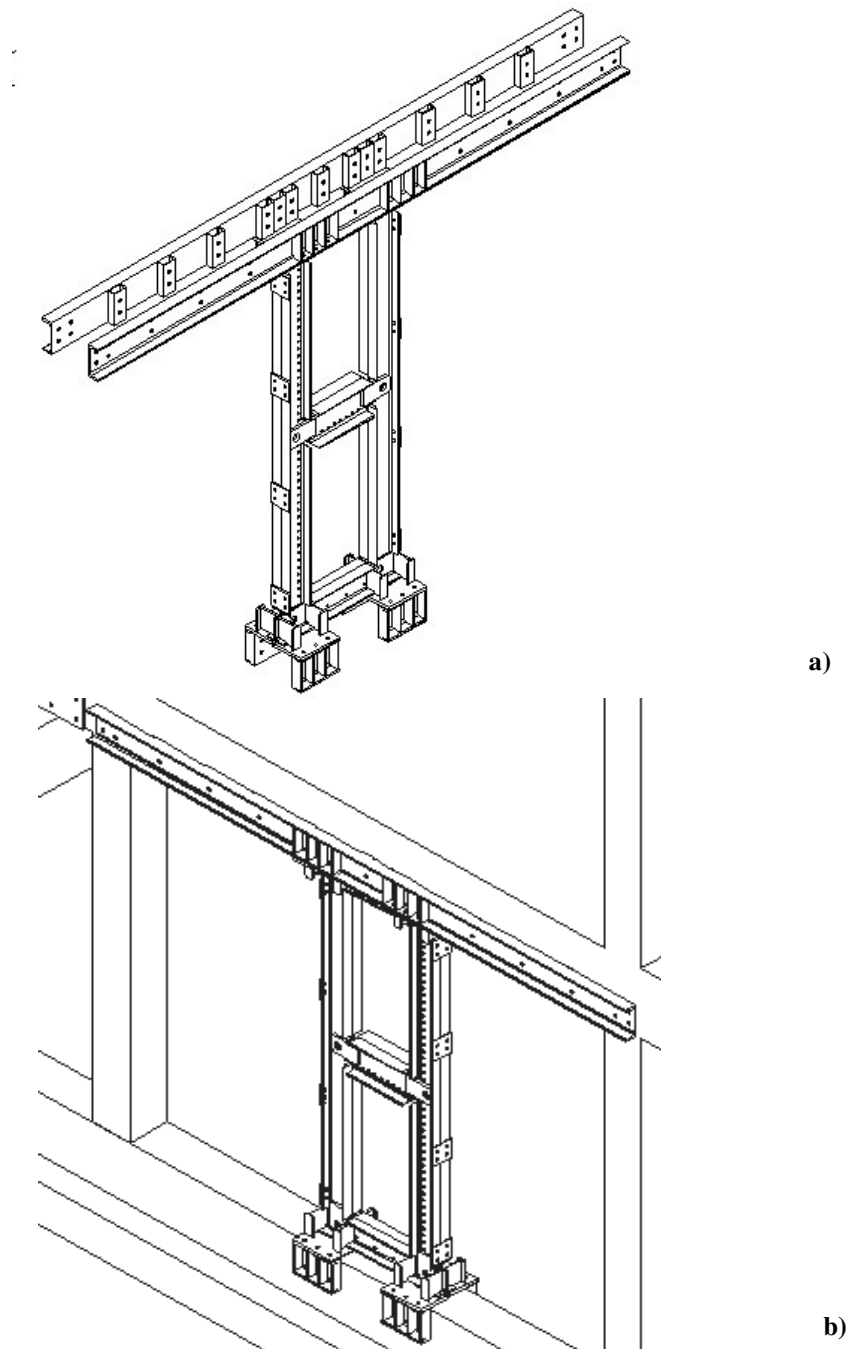


Figure 6.10: Global view of the designed reinforcing steel system (a) and its insertion into the RC structure (b)

Based on the above technical drawings, the real application of both the steel frame and the system used for reinforcing the RC structure, has been done (Figure 6.11).



Figure 6.11: Global view of the reinforcing intervention

6.2.2.4 The insertion of transversal stiffeners

From the design procedure used for the characterization of the shear wall two steel panels, having dimensions of 600 x 1200 x 1.15 mm and presenting a b/d ratio equal to 0.5, have been defined. In particular, considering that panels were provided under form of sheetings having plane dimensions of 400 x 2000 mm, it has not been possible to realise a full-height shear wall and, therefore, each of two panel fields has been composed by three sub-elements of 400 mm side length, which must be connected among them in order to restore the system continuity.

For this reason the insertion of opportune stiffeners, composed by two steel plates connected to the panel through bolted connections, has been foreseen. In addition, since the adopted shear panel would be very deformable without the possibility to develop a regular tension field in the whole loading phase, such stiffeners have been used aiming at both enhancing its response under lateral loads, acting as flexural stiffness, and serving as fishplates for the application of the bolted connection among the separate plates. With reference to the latter purpose, the use of M14 bolts has been foreseen. Such bolts, in conformity with prescriptions about edge distance, determine the employment of a connection plate having depth of 100 mm and length equal to the panel width. Then, the thickness of the plate is determined, checking that the stiffener behaves as rigid type. According to EC3 (EN 1993-1-1, 2005), since two stiffeners for each sub-panel are considered, the following value of the optimal second moment of area of the stiffener is obtained (see eq. 3.20):

$$a/h_w = 0,67 < \sqrt{2} \Rightarrow I_{st} \geq \frac{1,5 h_w^3 t^3}{a^2} = \frac{1,5 \cdot 600^3 \cdot 1,15^3}{400^2} = 3080 \text{ mm}^4$$

being a and h_w the height and the width of each sub-panel, respectively.

Such a value will be multiplied for the Massonet coefficient, drawn by the non linear theory, so that the post-buckling reserves of the panel can be fully exploited (see eq. 3.19), reaching the following value:

$$I_s^* = I_s \cdot \xi = 3080 \cdot 4 = 12320 \text{ mm}^4$$

Finally, the stiffeners thickness, that should guarantee a second moment of area greater than the optimal one, has been assumed equal to 4 mm. The stiffeners will have to act also as fishplate elements for the connection among the sheetings: for this reason the definitive dimension will be validated through experimental tests, which will be carried out for confirming the possibility to have a full strength connection.

6.2.2.5 Panel-to-frame and panel-to-panel connections

The sub-panels are connected to each other and to the reaction frame by means of M14 bolts, having a pitch of 50 mm and a edge distance of 25 mm (Figure 6.12 a). In order to assess the effectiveness of the adopted connecting systems, preliminary tensile tests on two 150 x 250 x 1.15 mm panel portions, connected by means of 100 x 150 x 4 mm stiffened plates and six M14 bolts,

have been carried out (Figure 6.12 b).

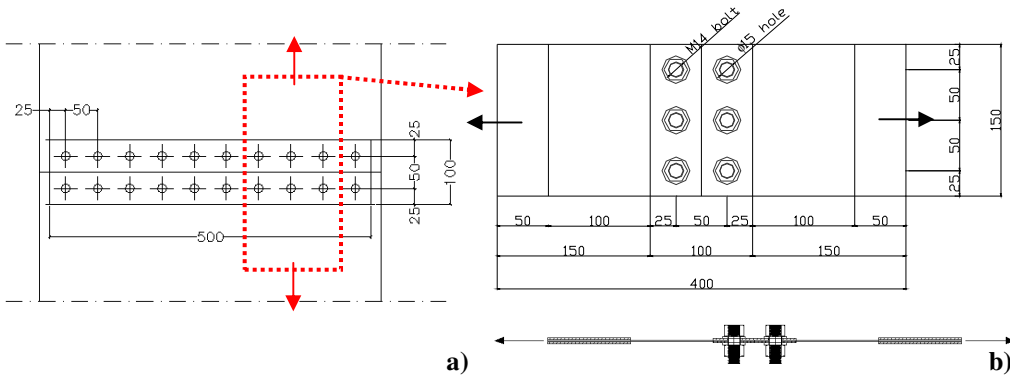


Figure 6.12: The connection among panels (a) and the tested connection specimen (b)

Such experimental tests have been executed at the Department of Structural Analysis and Design of the University of Naples “Federico II” by employing the same universal testing machine used for the determination of the panel material mechanical characteristics.

The different phases of the experimental test up to the collapse condition of the tested specimen are illustrated in Figure 6.13 and the corresponding results in terms of force (F) – relative displacement (Δ) are given in Figure 6.14.

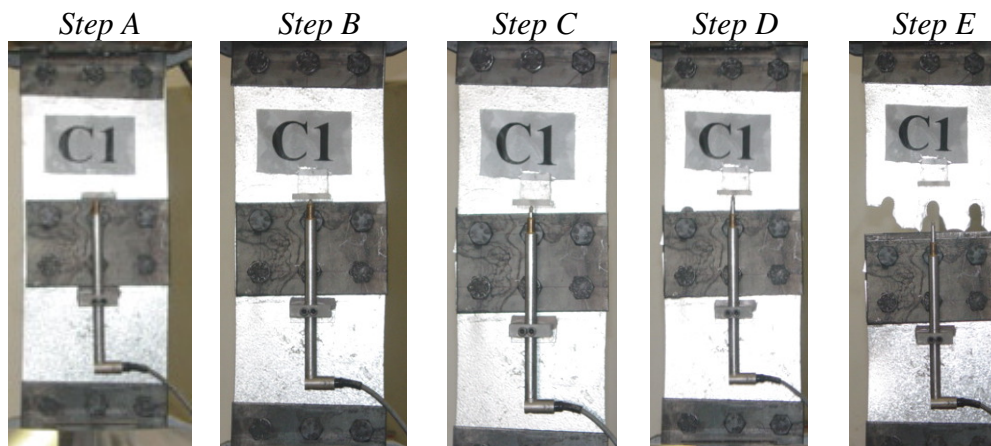


Figure 6.13: The connection behaviour during experimental test

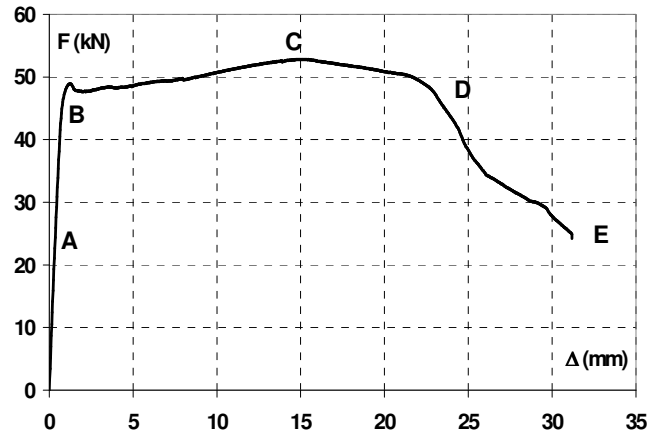


Figure 6.14: Experimental response of the tested connection specimen

The connection has been tested for a shear force acting in a specific direction, while actually it will be loaded by a load, deriving from the development of the tension field mechanism, which introduces two different components, acting in the normal and tangential direction of the connection line. The normal stress component can be obtained by the following relationship:

$$\sigma_n = f_y \cdot \cos^2 \Theta \quad (6.6)$$

On the other hand, the shear resistance before instability, due to the high slenderness of the shear panel ($b/t \approx 522$), can be neglected

Such a situation considers that the maximum tensile stress transferred by the tension field, whose inclination is equal to 45° , is obtained when the yielding of the shear panel occurs. Therefore, considering that the material plasticization occurs when the main tensile stress is equal to the steel yielding one, it is possible to evaluate the maximum force applied to the connection:

$$F_n = f_y \cdot \cos^2 \Theta \cdot t \cdot B = 305 \cdot \frac{1}{2} \cdot 1,15 \cdot 150 = 26.30 \text{ KN}$$

Comparing this value with the experimental one ($F_y = 48.63 \text{ KN}$), it is observed that the connection check for stress acting in normal direction is widely satisfied. Therefore, the shear connection strength is higher than the yielding resistance of the plate and this is due to the occurrence of the block tearing mechanism, which determines a significant increment of the effective

sheeting net section (Figure 6.13 – Step E). Also a significant ductility of the adopted connection, which make it able to restore the panel continuity, is noticeable.

Such results can be considered also valid for the connection between the plate and external reaction frame, since in this case only the fishplate is varied, it being represented by the profiles used for the columns and beams cross-sections. In this case, also the tangential action, representing the component of the tension field mechanism developed in the shear panel, has to be considered, but the total load applied to the connection, given by the resultant of applied forces, is always lesser than one obtained under experimental way.

6.2.2.6 Installation of shear walls

According to the provisions given by design steps presented in the above Sections, the insertion of steel plate shear wall systems at both longitudinal sides of the base RC structure has been performed. The global view of the intervention is illustrated in Figure 6.15, where the presence of six 600x400x1.15 mm sub-panels connected by bolts each other and to the steel frame members is visible (De Matteis et al., 2006a).



Figure 6.15: Insertion of steel plate shear walls within the RC module n.5

6.2.3 The numerical modeling

6.2.3.1 The ABAQUS model

After the preliminary design of the shear wall geometry, it is necessary to proceed with the detailed checking of the adopted shear panel. To this purpose, a sophisticated finite element model implemented through the ABAQUS v. 6.4 non linear numerical code (Hibbitt et al., 2004), has been set-up, allowing the correct evaluation of the influence of the main parameters on the performance of the system. The slender plates, which have been modelled with four nodes bi-dimensional elements having reduced integration (S4R type), are positioned within a hinged reaction Fe430 steel frame, composed by three beams (upper, intermediate and lower) and two columns characterised by HEB180 profiles, represented by two nodes linear elements (B31 type) (Formisano et al., 2005a).

In the numerical model, the stiffening effect produced by the connection fishplate has been simulated considering in that zones the correspondent increase of thickness given by the sum of the plate thickness and the two fishplates one.

The connection between the panel and the frame members has been modelled considering that among different parts slipping phenomena do not occur, according to the previous experimental tests previously reported. Such a condition has been introduced in the numerical model by employing the TIE constraint command. On the basis of preliminary sensibility studies, a mesh characterised by elements having dimensions of 20x20 mm, which represents the better compromise between time required by the elaboration and accuracy of the obtained results, has been used. The lateral load has been directly applied on the upper beam of the external steel frame. The analysis has been performed employing the modified Riks algorithm, which uses the Newton-Raphson procedure and results particularly suitable in the cases in which non linear problems due to the equilibrium instability are faced. The effect of the geometrical imperfections have been taken into account assuming an initial configuration according to the deformed shape corresponding to the first eigenvalue. The amplitude of such a configuration (maximum out-of-plane displacement) has been assumed conventionally equal to 1/1000 of the total depth of the panel, which corresponds to 2.4 mm. The result of the numerical

analysis performed on the system, in comparison with the theoretical PFI method one (Sabouri-Ghomi and Roberts, 1991), is shown in Figure 6.16.

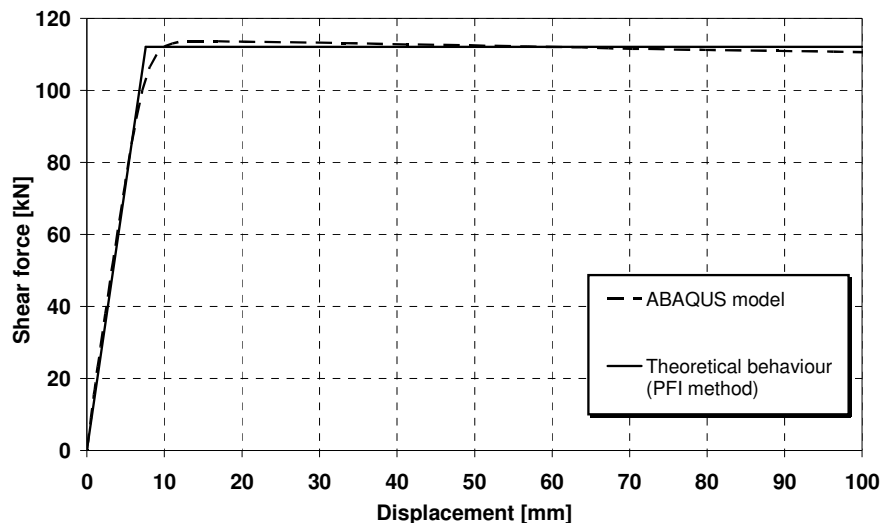


Figure 6.16: Comparison between numerical (ABAQUS) and theoretical results for the analysed shear panel

Based on the above comparison, since the ABAQUS model supply a strength of 113.64 kN, while the theoretical resistance is equal to 112.1 kN, a very good agreement is apparent. In particular, the above value of the theoretical strength has been obtained by means of the following relationship:

$$F_{wu} = b \cdot t \cdot \left(\tau_{cr} + \frac{\sigma_{ty} \cdot \sin 2\Theta}{2} \right) \quad (6.7)$$

where also the pre-buckling phase has been considered. In fact, the numerical analysis provided a not negligible critical shear, equal to 13.2 kN and therefore equal to 12% of the shear wall limit strength. In the above relationship the maximum tensile stress developed through the tension field mechanism (σ_{ty}) is provided by the following formula:

$$3 \cdot \tau_{cr}^2 + 3 \cdot \tau_{cr} \cdot \sigma_{ty} \cdot \sin 2\Theta + \sigma_{ty}^2 - \sigma_0^2 = 0 \quad (6.8)$$

where σ_0 is the yielding strength of the material.

Also, it should be observed that, although the system is very slender because of the low b/d ratio (equal to 0.25), due to the presence of both

intermediate beam and stiffeners, it provides a very good behaviour with a high stiffness. In the following some results of the numerical analysis phases are reported in terms of both the stress state and the deformed panel shape (Figures 6.17 and 6.18).

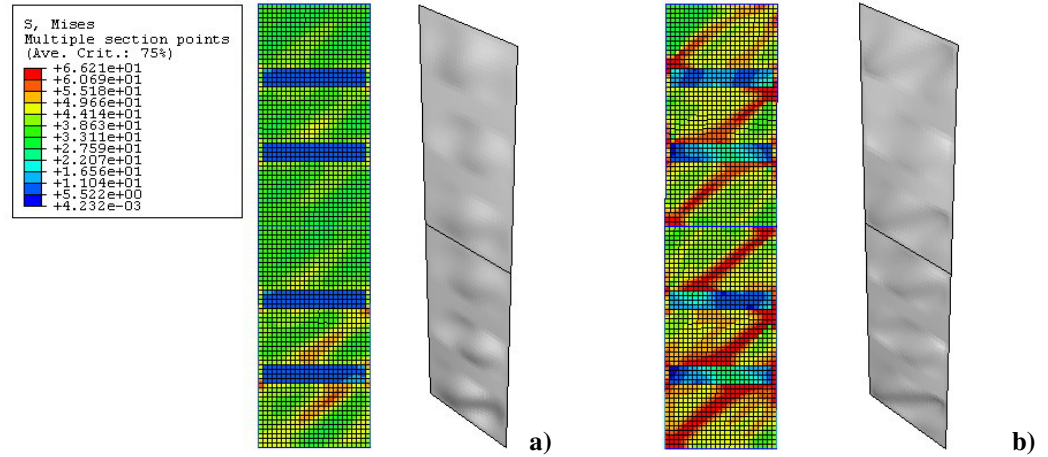


Figure 6.17: Stress state and deformed shape corresponding to the panel instability (amplification factor = 50) (a) and to the attainment of 73% of the maximum panel strength (amplification factor = 5) (b)

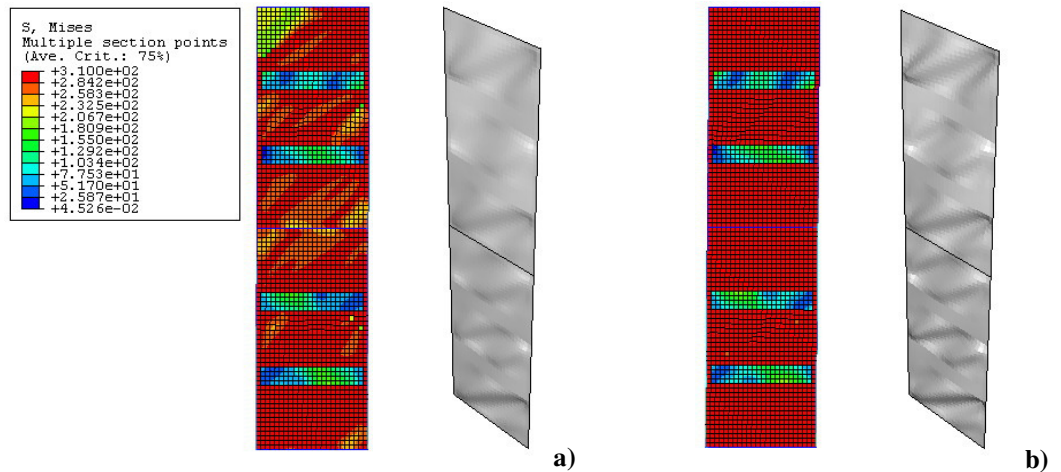


Figure 6.18: Stress state and deformed shape (amplification factor = 5) corresponding to the attainment of 94% (a) and of 100% (b) of the maximum panel strength

Finally, by summing the response provided by two steel shear walls with the numerical bare RC frame one, the capacity curve of the retrofitted structure has been determined and compared to the theoretical design one (Figure 6.19).

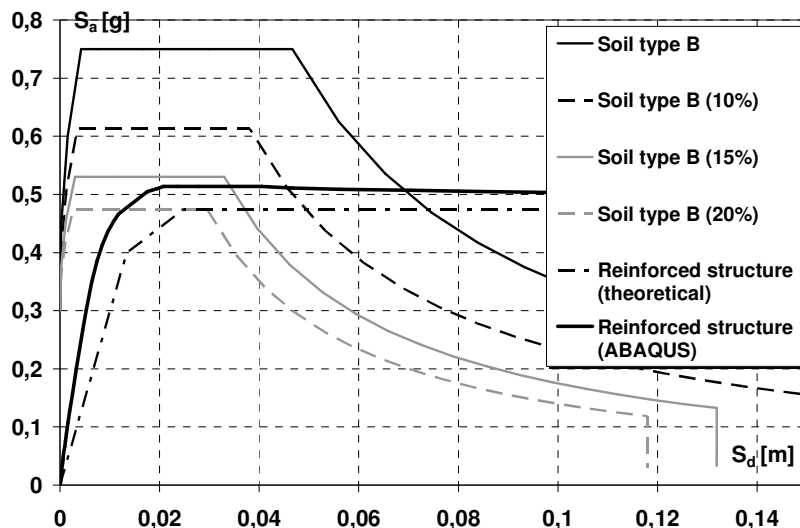


Figure 6.19: Comparison between numerical (ABAQUS) and theoretical design curves

From the comparison it is apparent that the numerical model provides a curve having both strength and stiffness larger than the ones given from the theoretical structure response. While the strength increase is obviously explained by the fact that a panel width larger than the nominal value has been adopted, the higher stiffness is probably caused by the lack of interaction between RC structure and steel panels. Aiming at investigating on the latter aspect, a more refined numerical analysis has been performed.

6.2.3.2 The SAP model

In order to confirm the validity of the proposed design solution and for estimating the possible interaction problems between the RC structure and the added steel parts, the numerical modelling of both the single steel shear wall and the retrofitted structure has been implemented by means of the SAP 2000 non linear program. In particular, in the first analysis phase, the obtained

results have been compared with the ones derived by the ABAQUS model.

The shear wall has been modelled by means of linear elements, according to the "strip model" theory, considering ten truss elements, inclined with the same slope of the main tensile directions (45°) and connected through hinged connections to the external steel frame. Moreover, in order to guarantee the correctness of the panel b/d ratio, in the external frame both an intermediate simply hinged beam and two truss elements, having sections equal to the stiffeners and connected with hinges to the columns, have been introduced (Figure 6.20 a).

The SAP analysis results are reported in Figure 6.20 b, where the comparison with both the theoretical and the numerical results obtained through the use of the ABAQUS model are depicted.

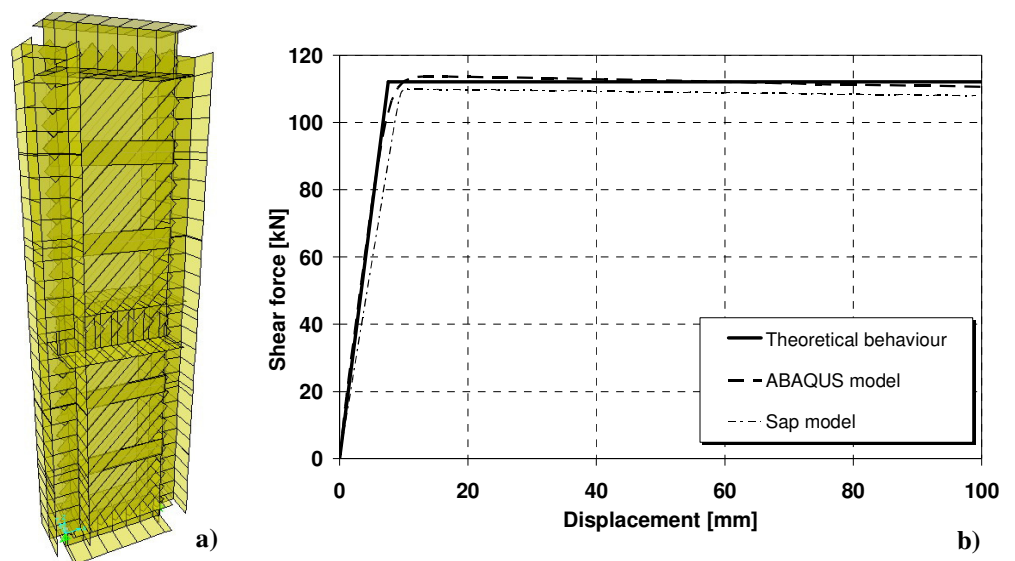


Figure 6.20: Modelling of the shear wall (SAP 2000) (a) and comparison between the theoretical behaviour and the numerical responses of the shear panel (b)

The results of the Sap model do not correspond perfectly to the Abaqus ones because the strip model neglects the shear effect before the occurrence of buckling phenomena, providing a 10% reduced panel strength. However, for the study of RC reinforced frame, the results can be considered to be acceptable.

In a second study phase, a global model of the reinforced module has been developed connecting the shear walls to the RC structure by means of the first level beam (Figure 6.21 a).

From the pushover analysis carried out on the reinforced structure, the response in the shear – displacement plane provided in Figure 6.21 b has been obtained. It can be transformed into the capacity curve of the retrofitted structure by applying the procedure reported in the Section 5.3.2.4 (Figure 6.22).

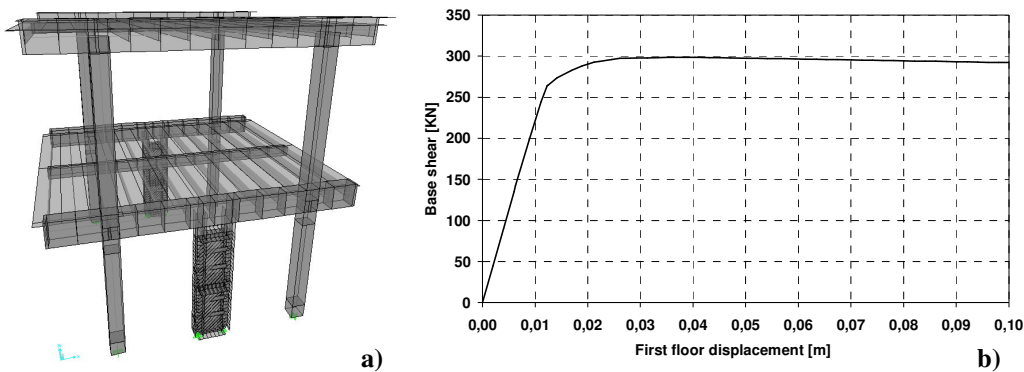


Figure 6.21: SAP 2000 model of the reinforced structure (a) and the obtained response in the shear force – displacement plane (b)

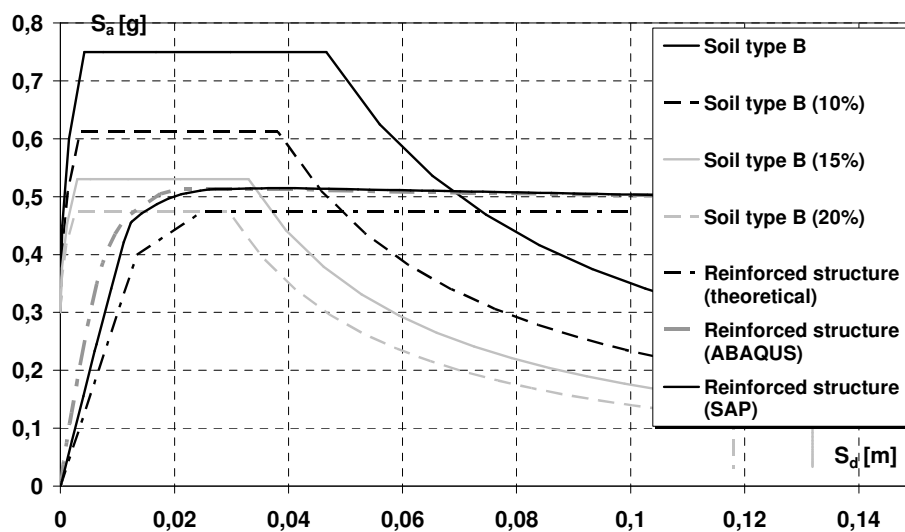


Figure 6.22: Comparison between the theoretical design curve and the numerical one (SAP 2000)

The comparison with the design curve evidences that the numerical curve (SAP 2000) provides higher strength, but, also in this case, this is due to the adoption of a panel width larger than the nominal value. In particular, a maximum strength of 298 kN for the retrofitted structure is obtained, which corresponds to a value about ten times greater than the one related to the expected real resistance of the bare RC module. Besides, although a slight scatter in terms of stiffness is still noticed, it is evident that the SAP model gives better results, taking into account with a major attention the real deformability of the structure.

6.2.4 The experimental test

6.2.4.1 Loading devices and measurement instruments

The retaining structure used for the execution of the experimental test is the same system employed for the pushover test carried out on the bare RC module. Such a system has been realised by connecting two coupled steel channel profiles at the foundation level and at first level of the module n. 6 of the RC building along the longitudinal direction (see Figure 4.45). In addition, for the execution of the experimental test on the retrofitted structure, the same two hydraulic jacks applied to the retaining structure and illustrated in Figure 4.46, able to apply tensile and compression actions equal to 200 and 300 kN, respectively, have been employed.

Since the test purpose is the evaluation of the system response under the load application in terms of both the displacements and the hysteretic behaviour, a series of measurement devices have been applied on the structure so to relieve all the main relative displacements occurring among different parts of the structure (Formisano et al., 2006c). Firstly, linear displacement transducers (LDTs) placed on the first storey beam, both on the RC frame (Figure 6.23 a) and on the reinforcing steel member (Figure 6.23 b), have been positioned in order to record the first storey displacement and the possible slips occurring between the RC beam and the reinforcing system.

The same instrumentation system has been also employed for checking the first storey displacements on the opposite side of the frame, where the second steel plate shear wall is located. In addition four continuous transducers have been installed aiming at determining the shear wall displacements at different

levels, particularly where the panel stiffeners and the intermediate UPN 240 beam are positioned (Figure 6.24).

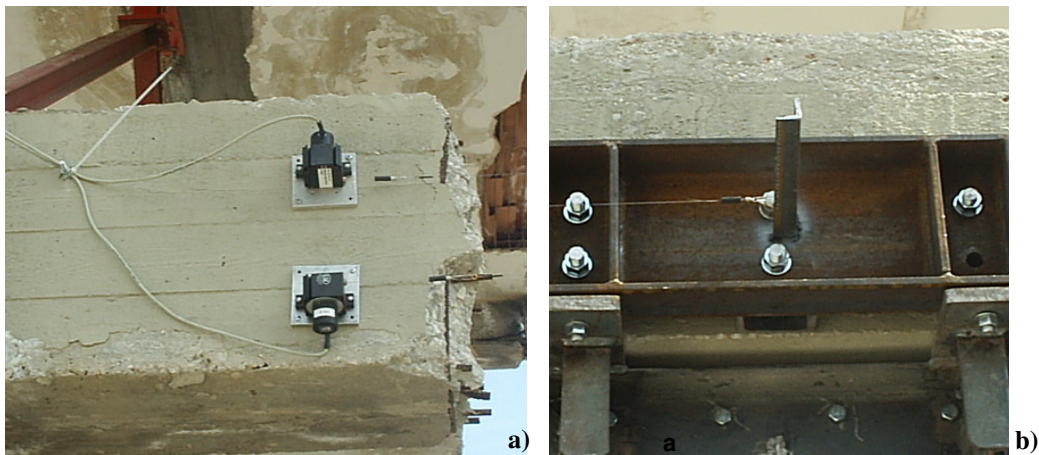


Figure 6.23: Transducers n.3 and 4 placed on the RC beam (a) and transducer n.4 applied on the steel beam (b)

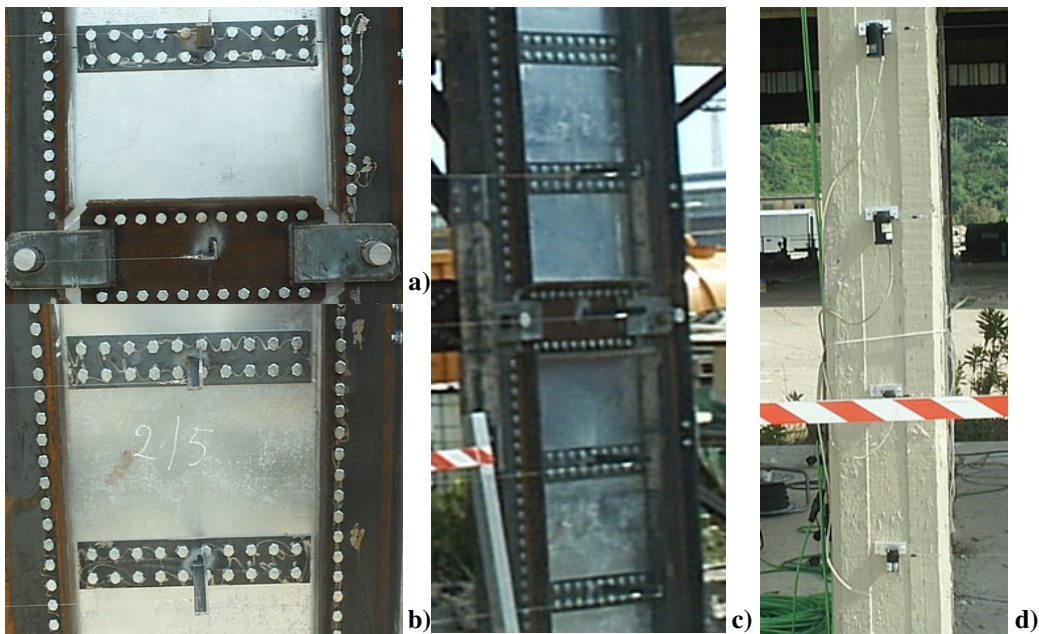


Figure 6.24: LDT location on the upper panel (a), LDT location on the bottom panel (b), global view of LDTs used to evaluate the shear wall displacements (c) and measurement instruments located on the adjacent module n.4 (d)

Additional instruments have been located at the base of the two shear walls in order to acquire the displacements occurring due to the slip of the connection at the foundation level (Figure 6.25 a).

The disposition of all the measurement instruments applied on one side of the structure during the experimental test is schematically reported in Figure 6.25 b. Also, it is interesting to observe that the displacement transducers P1 and P2 have to be intended positioned on the opposite side of the structure, at the same level of the P3 and P4 ones. A global view of the measurement devices applied on one side of the structure is reported in Figure 6.26.

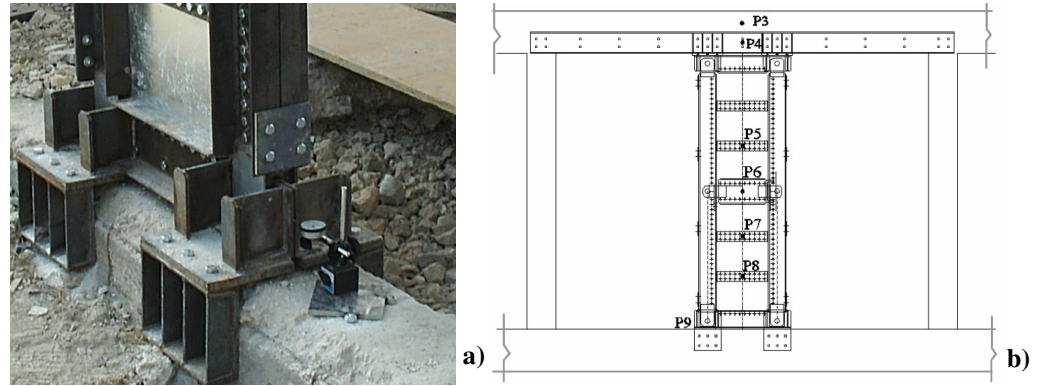


Figure 6.25: LDT location at the foundation level (a) and schematic view of LDTs location on one side of the structure (b)



Figure 6.26: Global view of the measurement devices applied on one side of the structure under investigation

6.2.4.2 The obtained results

In the experimental test, a cyclic loading history in quasi-static regime and under force control has been applied (Figure 6.27). The load has been increased of 20 kN for each cycle up to the last one, where the increment has been of 60 kN. Every cycle has been characterised by a symmetry condition up to the attainment of 200 kN; hence only the compression load has been increased up to 300 kN (Formisano et al., 2006b, c).

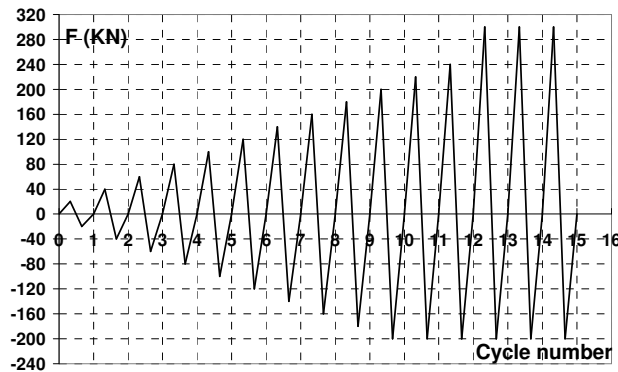


Figure 6.27: The applied loading history

The results of the experimental test in terms of force-first level displacement (P3 transducer) are reported in Figure 6.28 .

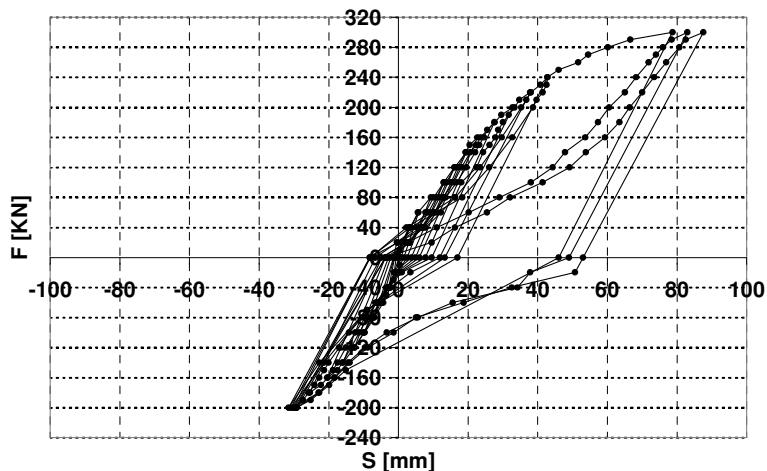
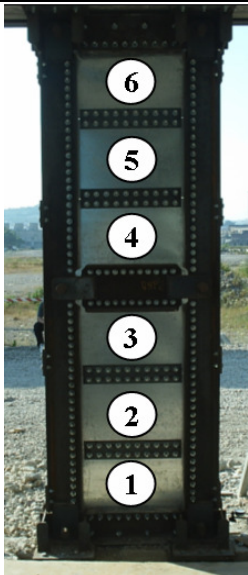
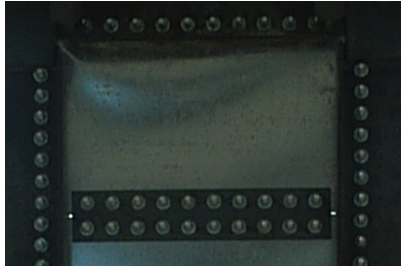



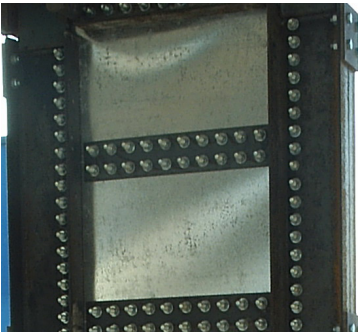
Figure 6.28: The experimental response of the RC structure retrofitted with steel shear panels


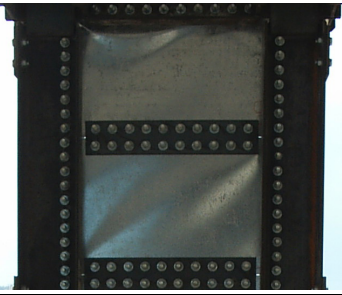
From the test results it is noticed that the retrofitted structure attains a maximum load of 300 kN for a displacement amplitude of 85 mm, which corresponds to an inter-storey drift equal to about 3.5%. Besides, the hysteretic cycles of the loaded structure are strongly affected by pinching phenomena, which do not allow to achieve a fully dissipative system behaviour. Therefore, according to the initial forecasts of the performed study, the used steel panels can be considered as strengthening and stiffening devices only for retrofitting operations.

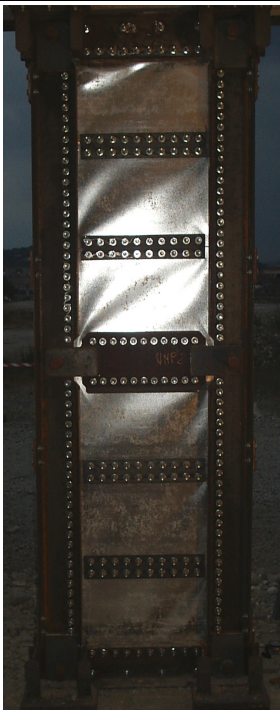
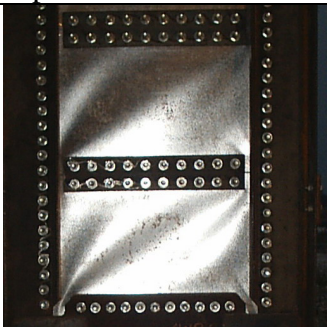
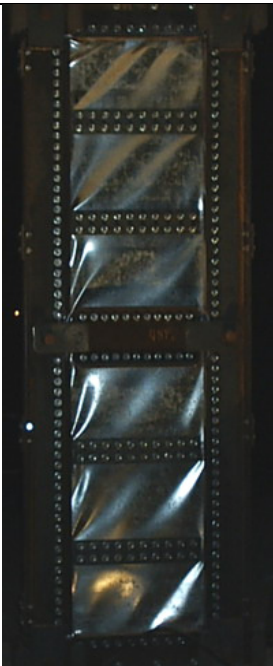

During the experimental test, any important difference between the displacements measured by two transducers located at the two opposite sides of the building occurred. In addition, the displacement transducers fixed on the RC beam and on the reinforcing steel profile provided the same results, confirming the effectiveness of the connection created among the members. Also the displacements detected at the base of the steel plate shear wall was not significant, assuming a maximum amplitude of 1 mm when a peak load of 300 kN was attained.

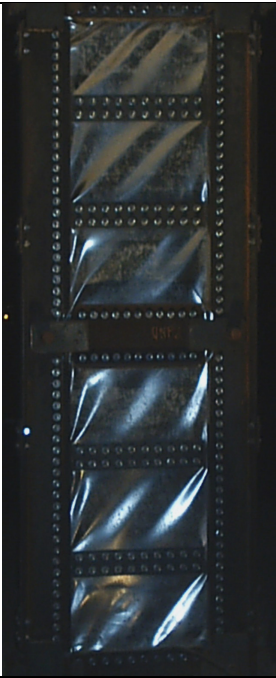
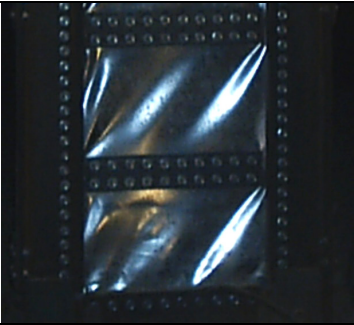
In the following several significant phases of the experimental test based on the use of steel panels, identifying with n.1 the lower element and assigning an increasing number proceeding upward (up to 6), are reported (Figure 6.29).

	Load cycle: 2
	Applied force: 40 KN
	Displacement: 2.94 mm
	Experimental evidence: Buckling phenomena of upper sub-panels, with the creation of a buckling wave.
	

	Load cycle: 3
	Applied force: 60 KN
	Displacement: 5.74 mm
	Experimental evidence: Shear buckling instability of all sub-panels, with development of significant waves in the upper ones.
	

	Load cycle: 5
	Applied force: 100 KN
	Displacement: 12.99 mm
	Experimental evidence: Significant buckling phenomena of every sub-panels. Sub-panel n.6 is characterised by a remarkable buckling wave, not allowing the development of the diagonal tension field mechanism. A similar buckling wave is also present in sub-panel n.1.
	

	Load cycle: 9
	Applied force: 180 KN
	Displacement: 27.59 mm
	Experimental evidence: Permanent waves on the surface of all the sub-panels, evidencing a wide plasticization mainly diffused along the diagonals. In sub-panel n.6 the first waves characterising the tension field mechanism begin to develop.
	
	Load cycle: 11
	Applied force: 220 KN
	Displacement: 37.90 mm
	Experimental evidence: The plastic behaviour of sub-panel is more evident. In sub-panel n.6 the activation of buckling waves confirms that the system is working mainly in shear.
	

	Load cycle: 12
	Applied force: 240 KN
	Displacement: 42.80 mm
	Experimental evidence: Plastic behaviour of shear panels. The characteristic buckling waves of the initial loading phase are disappearing both in the upper and lower sub-panels. The buckling waves are well visible.
	

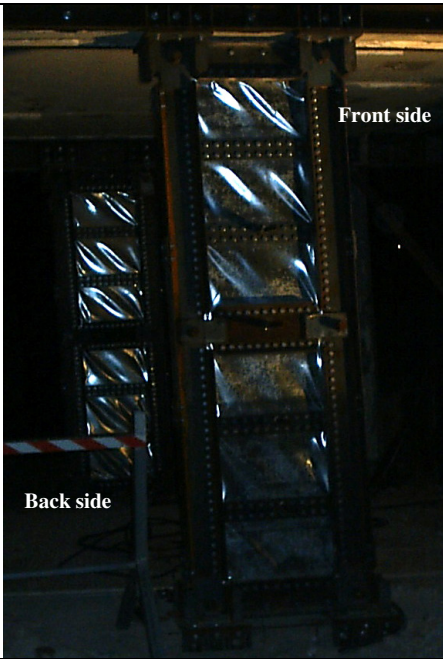
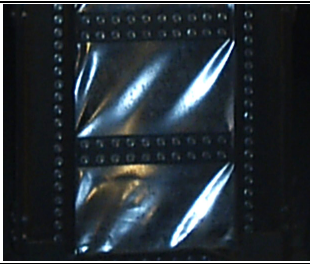
	Load cycle: 15
	Applied force: 300 KN
	Displacement: 87.55 mm
	Experimental evidence: The maximum panel strength, corresponding to the horizontal plateau of the loading curve, is attained. The panels have a completely plastic behaviour, showing the presence of permanent deformations.
	

Figure 6.29: Significant phases of the experimental test

Based on the analysis of the loading test phases, the presence of unforeseen deformations has been observed in bottom and upper sub-panels, which are responsible of the transfer of the shear action on the RC structure through the connections realized at the first level and at the foundation beams, probably causing a reduction of the global stiffness of the system.

In addition, the formation of foldings in the upper sub-panel determines a different behaviour of the retrofitted structure in terms of stiffness in the loading phases with respect to the unloading ones. Such a different structural behaviour makes the system less rigid and retards the activation of the tension field mechanism. Only in advanced loading phases, all the sub-panels presented diagonal waves, allowing the attainment of the expected maximum strength of the system. The final deformed configuration of each sub-panel (with its own number) of the two shear walls, located at both the front and back sides of the building (see Figure 6.29), is reported in Figures 6.30 and 6.31.

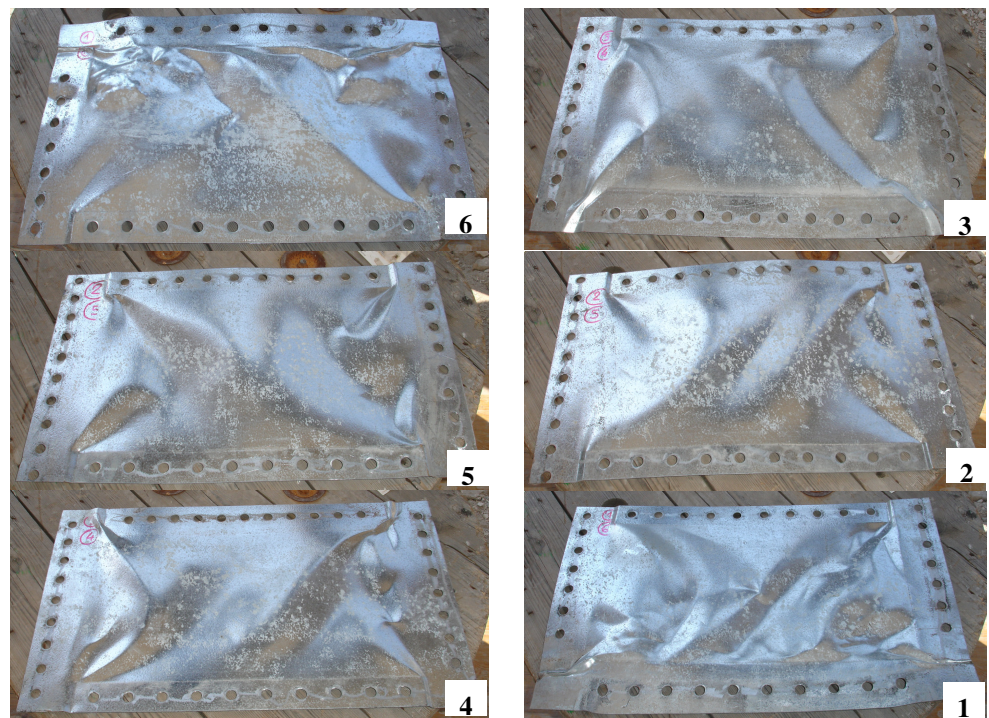


Figure 6.30: Deformed shapes of sub-panels belonging to the shear wall located at the front side of the RC structure

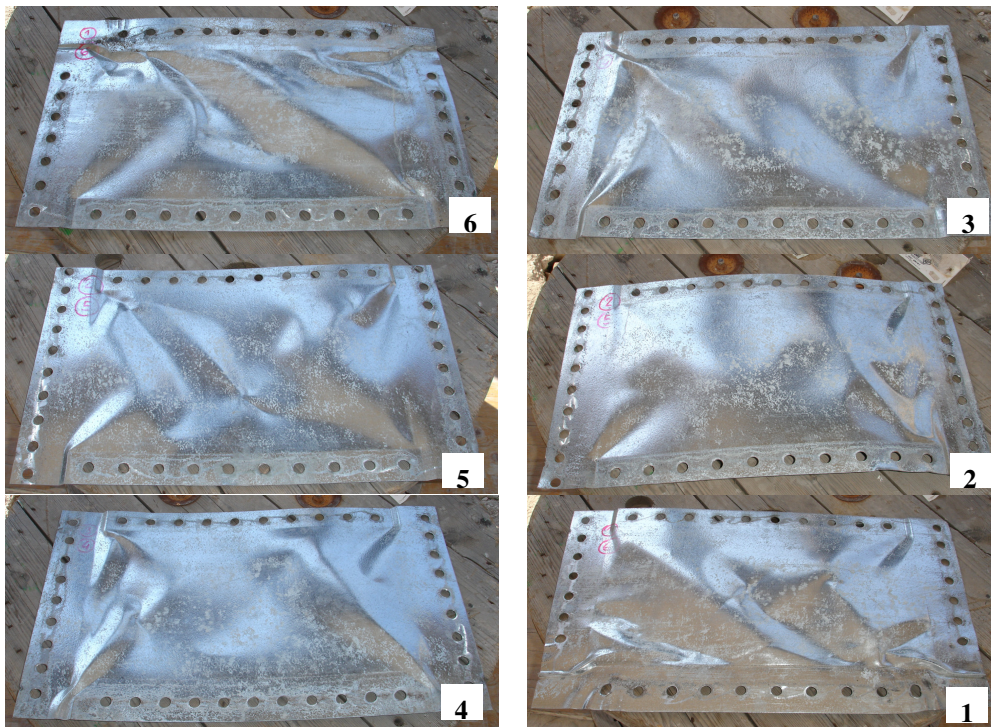


Figure 6.31: Deformed shapes of sub-panels belonging to the shear wall located at the back side of the RC structure

From the above figures it is apparent that panel portions of the two shear walls have similar deformations in terms of both amplitude and configuration, they being all characterised by the activation of a tension field mechanism having an inclination angle of about 45° . In particular, due to the combined flexural-shear behaviour of shear walls, the foldings produced from the compression loads applied to the columns in the end panel fields (n.1 and n.6) are evident. Besides, the effectiveness of the used connection system is clearly proved from the absence of significant deformations around bolt holes.

At the end of the experimental test any significant damages occurred into the structural members of the RC module. Slight cracks into foundation beams and expulsion of the columns cover concrete, together with buckling of some reinforcing steel bars, appeared only, as shown in Figure 6.32.

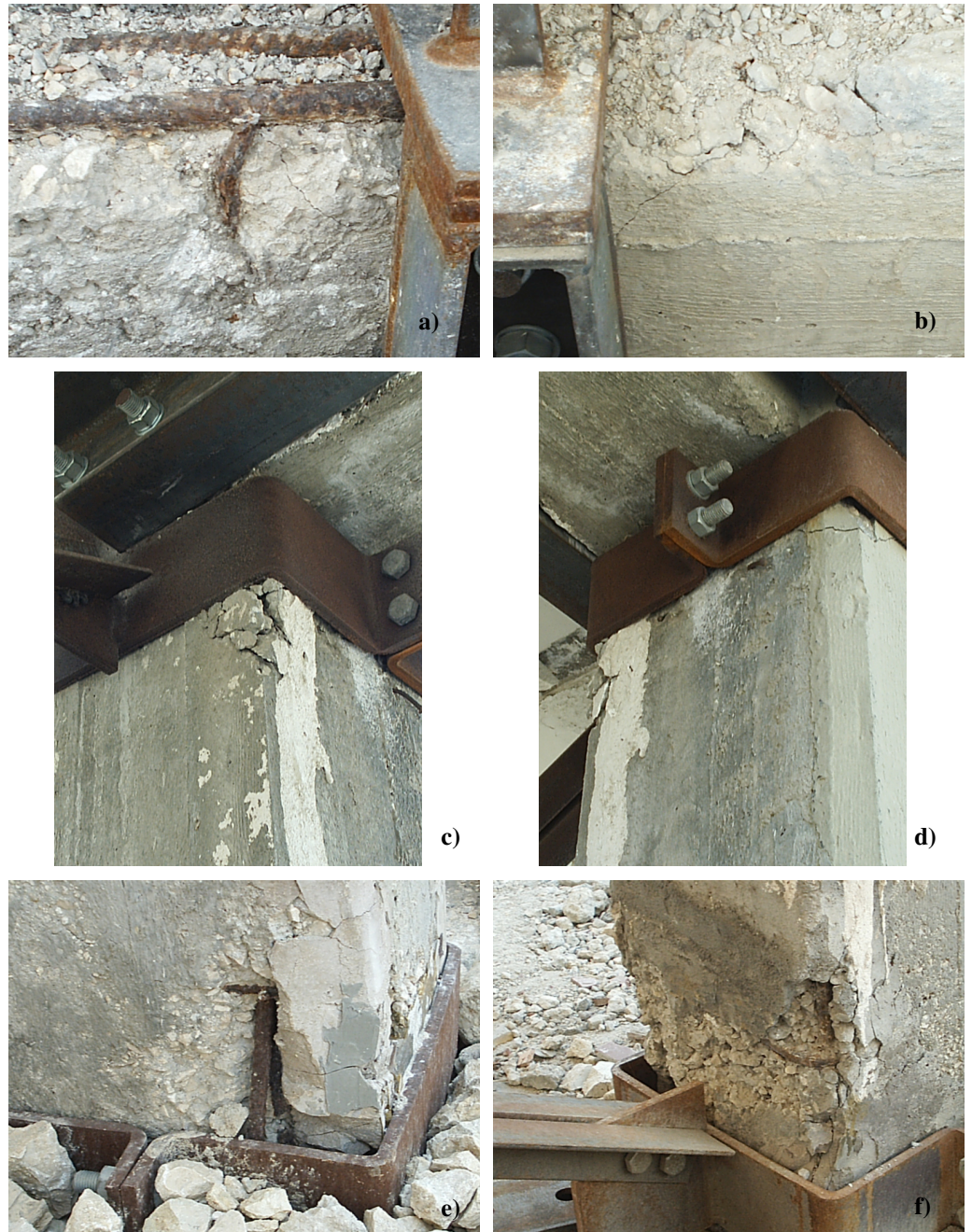


Figure 6.32: Damages occurred in the RC structure members at the test end: foundation beam (a, b) and top (c, d) and bottom (e, f) zones of columns

6.2.5 Interpretation of test results

From the results of the experimental test it is possible to obtain an envelope curve (Figure 6.33) which can be compared with the expected experimental response of the bare RC structure in the shear force – first floor displacement plane (Figure 6.34).

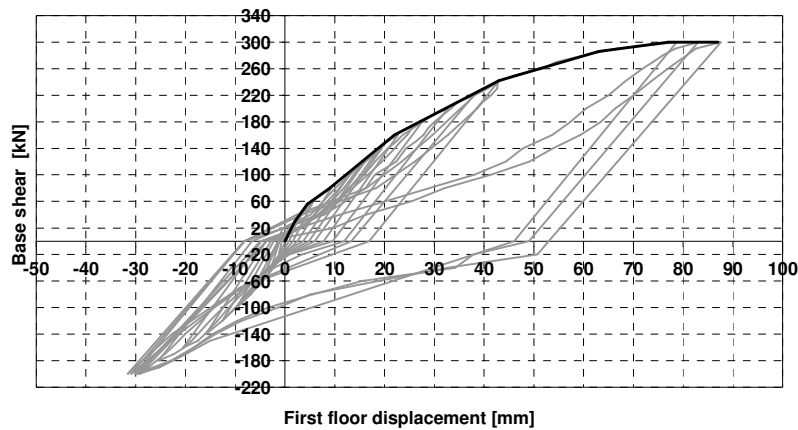


Figure 6.33: Envelope curve of the experimental test

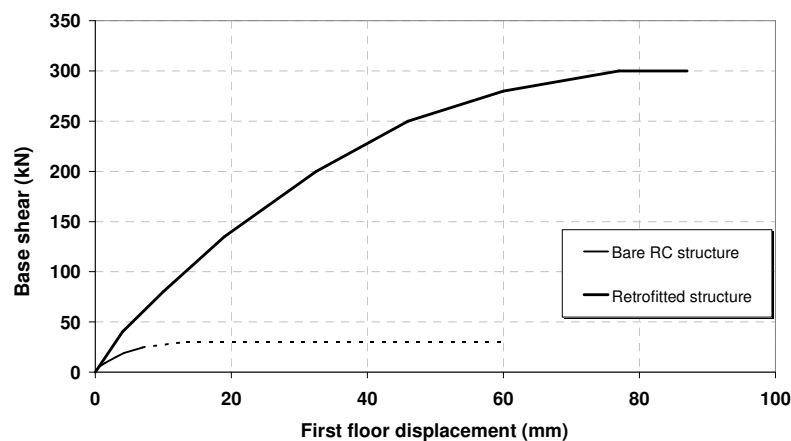


Figure 6.34: Comparison between the response of the structure retrofitted with steel panels and the bare RC structure one

From the comparison it is apparent that the response of the retrofitted structure is significantly improved, showing an increase of both initial

stiffness and ultimate strength equal to 2.5 and 10 times the bare RC structure ones. Also with reference to the numerical forecast of the bare RC structure response (see Figure 4.49), a significant increase of strength exhibited by the retrofitted structure is achieved, it being equal to about 4 times the structure resistance before intervention.

The deformation capacity of the structure appears to be very large, without the involvement of any brittle collapse mode up to a deformation amplitude corresponding to an inter-storey drift greater than 3.5%. Besides it is evident as a combined dissipative mechanism between plastic hinges in the beam-to-column joint of the RC frame and plastic deformation of tensile diagonals of the applied shear panels occurs.

The cyclic response of the RC structure retrofitted with steel shear panels can be interpreted by means of three numerical parameters characterising the system behaviour in terms of dissipated energy (E_{cycle}), secant shear stiffness (K_{sec}) and equivalent viscous damping factor (ν_{eq}), which are defined according to the relationships provided in the Chapter 3 (see Figure 3.12). Therefore, the experimental data have been processed by representing E_{cycle} , K_{sec} and ν_{eq} under form of bar diagrams as a function of the cycles number (Figure 6.35). In particular, both secant stiffness and damping ratio values have been plotted vs. the maximum load attained in each cycle.

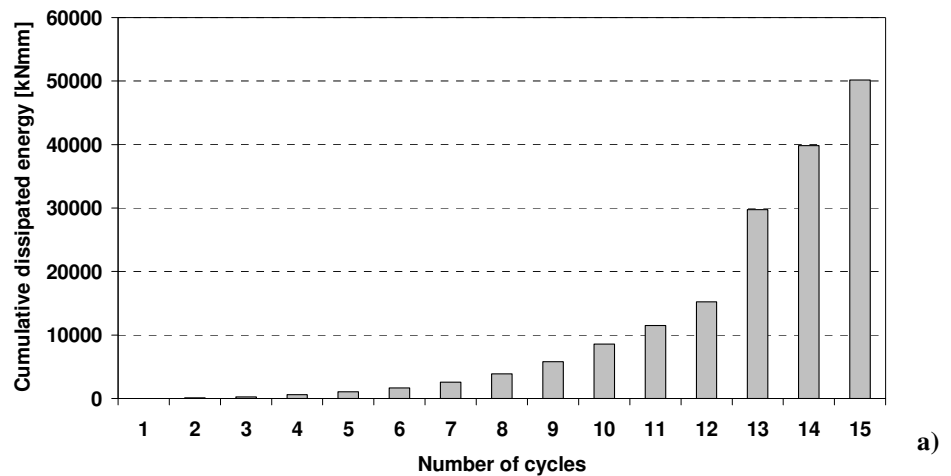


Figure 6.35: Interpretation of experimental results in terms of cumulative dissipated energy (a), secant stiffness (b) and equivalent viscous damping ratio (c) (continues)

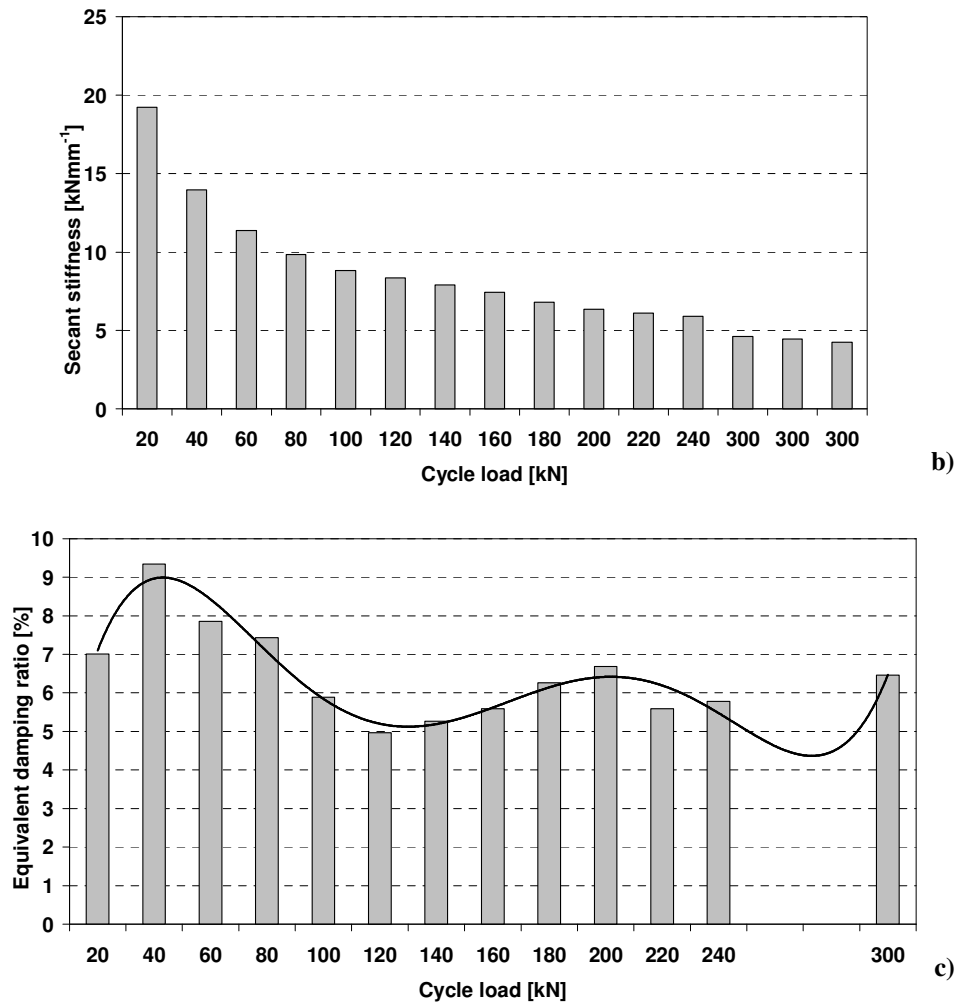


Figure 6.35: Interpretation of experimental results in terms of cumulative dissipated energy (a), secant stiffness (b) and equivalent viscous damping ratio (c)

From the above figure it is apparent that:

- 1) the experimental dissipation capacity of the RC structure upgraded with steel shear panels increases with cycle number in exponential way, showing a significant improvement of behaviour in the last three cycles, when the same maximum load (300 kN) is applied. This shows that buckling phenomena occurred into steel shear panels do not limit the

energy dissipation capacity of the compound structure thanks to the activation of the tensile bands developed within plates.

- 2) the secant stiffness of the composed structure attains its maximum value (19.2 kNmm^{-1}) at 20 kN, in the initial test phase, due to very small applied displacements. Then, such a parameter quickly decreases with a regular non linear trend as the number of cycles increases according to the following equation:

$$K_{\text{sec}} = 19.677n^{-0.492} \quad (6.9)$$

where n is the cycles number.

Such a behaviour is due to the fact that during test the structure displacement excursions due to the applied load and, therefore, the corresponding hysteretic loops, increase more than the total force variation, which is characterised cycle by cycle from a constant increment of 40 kN (up to the applied force of 200 kN), thanks to the inelastic properties of the used steel. Finally, it is apparent that secant stiffness remains practically constant as the applied load value is unchanged.

- 3) the equivalent viscous damping ratio of the upgraded structure, which is averagely equal to 6.7%, assumes maximum values of 9.3% for an applied lateral force equal to 40 kN, which corresponds to a displacement excursion equal to 5.73 mm (about 2 ‰ inter-storey drift). Starting from such a force, damping factor presents a strong oscillation of values, whose variation can be interpreted by means of a fifth order polynomial curve having the following equation:

$$v_{\text{eq}} = 0.001n^5 - 0.0419n^4 + 0.6161n^3 - 3.9442n^2 + 9.9805n + 0.49 \quad (6.10)$$

where n is the number of cycles performed during the experimental test.

Finally, the last three cycles performed in the experimental test, characterized by the same applied maximum load (300 kN) and not all reported in the diagram, show a very similar damping factor, which testifies the presence of hysteretic loops having dissipation capacity very close each other. In the whole, the variable trend of v_{eq} , together with its low average value, is a further confirm of the low dissipative capacity of the used steel shear panels.

6.3 APPLICATION OF PURE ALUMINIUM SHEAR PANELS

6.3.1 General

In the framework of the seismic retrofitting of the RC structure under study, besides the employment of steel plates, the performance of shear panels realised with pure aluminium has been evaluated (De Matteis et al., 2006a). In fact, such a material allows to increase the structural behaviour also in terms of ductility, in addition to the improvement provided in terms of strength and stiffness, which usually characterises the use of steel shear panels.

Also in this case, after the evaluation of the panels strength and stiffness characteristics, the retrofitting design, on the basis of the panel dimensions obtained by considering numerical models and theoretical methods, has been performed. Then, the reinforced structure has been studied by means of non linear programs and the achieved results have been compared with the theoretical design ones. Finally the experimental test on the panel-frame compound structure has been carried out, confirming the effectiveness of the adopted passive seismic protection devices.

6.3.2 Design of the shear wall system

In order to apply the seismic retrofitting intervention for the RC structure under consideration by using aluminium shear panels, which have the same geometry of the steel ones previously employed, a different plate thickness has to be determined according to the strength of the adopted material. The objective of the study is to realise a system that, besides introducing a good strength and stiffness, can also dissipate a greater amount of energy. For this reason, large attention has to be paid to the b/t ratio to be adopted; in such a way the shear panel can be defined as compact. Applying eq. (6.2), already used for the design of steel panels, it is possible to determine the aluminium plate area:

$$K_p = \frac{E}{4} \frac{2 \cdot b \cdot t}{h_s} \quad \Rightarrow \quad 2 \cdot b \cdot t = \frac{4 \cdot h_s \cdot K_p}{E} = \frac{4 \cdot 2400 \cdot 11500}{70000} = 1577 \text{ mm}^2$$

After the determination of the cross-sectional area, in order to provide the required initial stiffness, the aluminum panel should have a thickness of 1.5 mm. From eq. (6.1) it is possible to determine the yielding stress of the base material to respect the above prerequisites:

$$V_p = \frac{1}{2} f_y t \cdot 2 \cdot b \sin 2\alpha \quad \Rightarrow \quad f_y = \frac{2 \cdot V_p}{b \cdot t} = \frac{2 \cdot 192000}{2 \cdot 600 \cdot 1,5} = 213 \text{ N mm}^{-2}$$

The obtained resistance value would suggest the adoption of a typical aluminium alloy. On the other hand, it should be observed that, in order to have a shear panel with higher energy dissipation capacity, the b/t ratio should be reduced in such a way buckling phenomena occur for shear stresses larger than the conventional elastic limit of the material.

According to the studies carried out by some Authors (De Matteis et al., 2005b), compact aluminium shear panels should be characterised by a b/t ratio not larger than 80. Therefore, being the minimum panel dimension (namely the distance among the stiffeners) equal to 400 mm, a minimum plate thickness of 5 mm should be adopted. The critical shear stress corresponding to such a thickness value can be evaluated according to the following relationship:

$$\tau_{cr} = k \cdot \frac{\pi^2 \cdot E}{12 \cdot (1 - \nu^2)} \cdot \left(\frac{t}{d} \right)^2 \quad (6.11)$$

which provides a value of σ_{cr} equal to 92 Nmm^{-2} . As a consequence, the material limit conventional elastic strength ($f_{0.2}$) of the adopted aluminium alloy should be lower than 92 Nmm^{-2} .

6.3.3 The adopted base material

According to the above considerations, the base material selected for panels is the pure aluminium, effectively adopted as basic material to realise passive seismic protection devices and characterised both by a limited strength and a large ductility (De Matteis et al., 2005c).

Such a material, commercially known as the wrought aluminium alloy EN-AW 1050A, has a degree of purity of 99.50% and presents the chemical composition listed in Table 6.3.

Table 6.3: Chemical composition and mechanical properties of the used aluminium alloy 1050A H24

<i>Commercial Denomination</i>		<i>Impurities</i>
Aluminium	99.50%	0.02%Cu, 0.40%Fe, 0.31%Si, 0.07%Zn, 0.02%Ti, 0.02%other
<i>Mechanical properties</i>		
Tensile Strength (MPa)	Yield strength (0.2% offset, MPa)	Elongation on 5 cm (%)
70-100	30-70	20-40

In order to improve its mechanical features according to the purpose of this study, the panel after the fabrication, has been subjected to a heat treatment, favouring the increase of material ductility and the reduction of yielding stress (De Matteis et al., 2006b).

A number of specimens have been submitted to heat treatment cycles characterised by different phases with constant temperature, each one having a duration of four hours. At the end of each phase, measures of Brinell's hardness with weight of 31.2 daN and sphere with 2.5 mm of diameter have been carried out. Details of heat treatment are listed in Table 6.4.

Table 6.4: Cycle of heat treatment of the aluminium alloy

<i>No. phase</i>	<i>Temperature (°C)</i>	<i>Exposure time (hours)</i>	<i>Brinell's index</i>
initial	environment	/	69
1	150	4	68
2	230	4	67
3	280	4	44
4	330	4	35

For the sake of comparison, in Table 6.5, the mechanical features of the above aluminium alloy have been compared with the ones of other two metal materials, namely low-yield strength (LYS) steel and a different low-strength heat treated aluminium alloy, namely EN-AW 5154A.

Table 6.5: Mechanical features of considered metal materials

<i>Material</i>	$f_{0.2}$ (Nmm^{-2})	f_u (Nmm^{-2})	ϵ_u (%)	E (Nmm^{-2})	$E/f_{0.2}$	$\alpha =$ $f_u/f_{0.2}$
LYS steel	86	254	50	210000	2441	2.95
Pure aluminium (EN-AW 1050A)	21.3	80	45	70000	3286	3.76
Aluminium alloy (EN-AW 5154A)	75.2	203.6	18	70000	931	2.71

Typical stress-strain relationships for such materials are given in Figure 6.36. It should be noticed that the aluminium alloy EN-AW 1050A is more suitable for the application under consideration. In fact, it is characterised by a higher value of the $E/f_{0.2}$ ratio, which means higher attitude to undergo plastic deformation without incurring into buckling. Another important aspect is represented by the higher hardening ratio (over 3), which allows not only an added resource of resistance in the plastic field but also a dissipative capacity increasing with the applied strain.

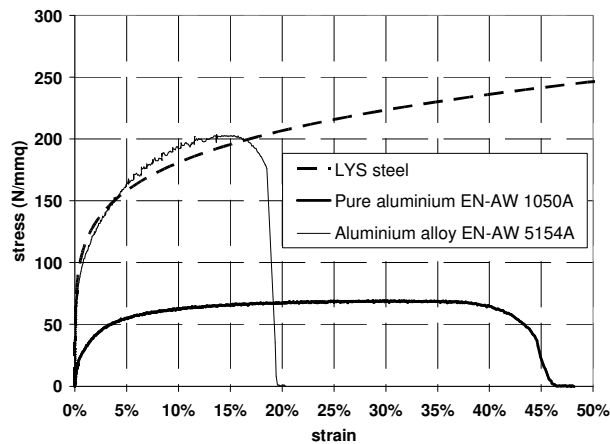


Figure 6.36: Comparison of stress-strain relationship between considered low-strength materials

6.3.4 The numerical modelling

6.3.4.1 The ABAQUS model

For the detailed characterization of the panel, the modelling phase has been intentionally postponed with respect to the experimental test because, being the considered aluminium alloy characterised by a high strain hardening factor, the simple monotonic test was not able to achieve the envelope curve of the cyclic test.

At this aim a sophisticated finite element model, implemented by means of the ABAQUS v. 6.4 non linear numerical code, has been set-up, by modelling the panel and the reaction steel frame as already stated for steel shear walls. Also, the interaction among parts, the geometrical imperfection effects, the adopted mesh and the analysis type have been selected according to the previously defined FEM model. The obtained results are provided in Figure 6.37, where it can be observed that the shear panel response is strongly characterised by the hardening behaviour of the base material. In Figure 6.38 two characteristics phases of the simulation carried out on the aluminium shear panel, both in terms of stresses and deformed shapes, are illustrated.

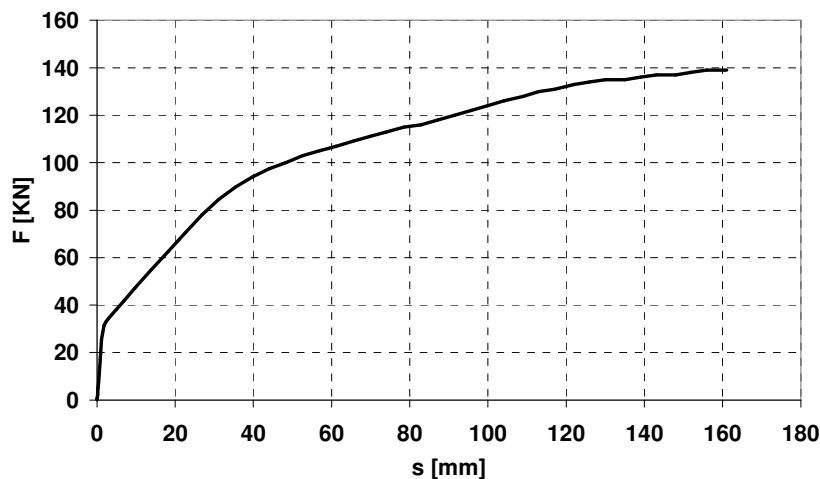


Figure 6.37: Numerical response (ABAQUS) of the analysed pure aluminium shear panel

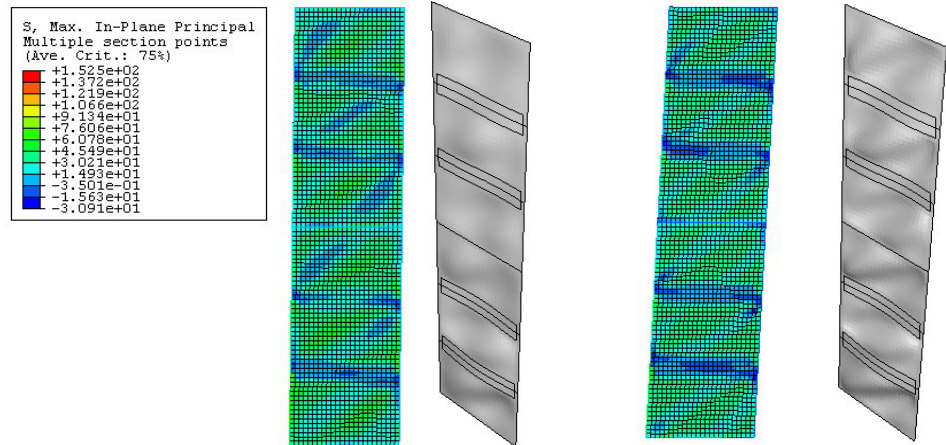


Figure 6.38: Stress state and deformed shape corresponding to the attainment of 73% (amplification factor = 5) (a) and of 92% (amplification factor = 1) (b) of the maximum panel strength

6.3.4.2 The SAP model

Also for aluminium shear panel a finite element model based on the strip model theory has been developed by means of the SAP 2000 program. The obtained result has been compared with the one resulting from the use of the ABAQUS model in the base shear – first floor displacement plane (Figure 6.39), showing a very good agreement.

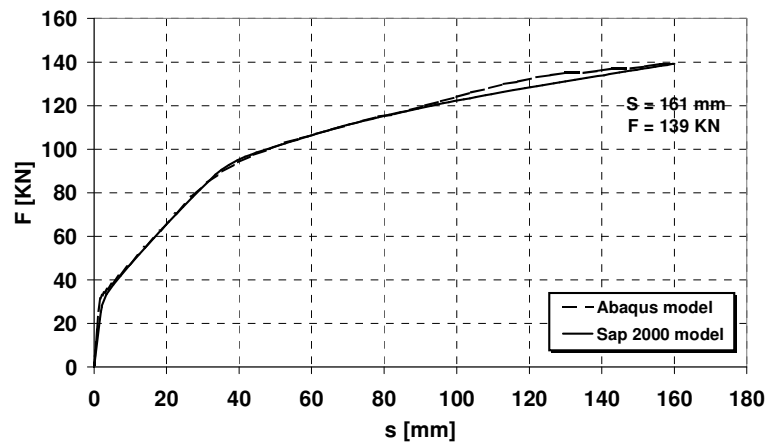


Figure 6.39: Comparison between numerical results for the analysed pure aluminium shear panel

In addition, the numerical model of the RC structure reinforced with pure aluminium shear panels has been implemented in order to foresee the experimental test results (Figure 6.40).

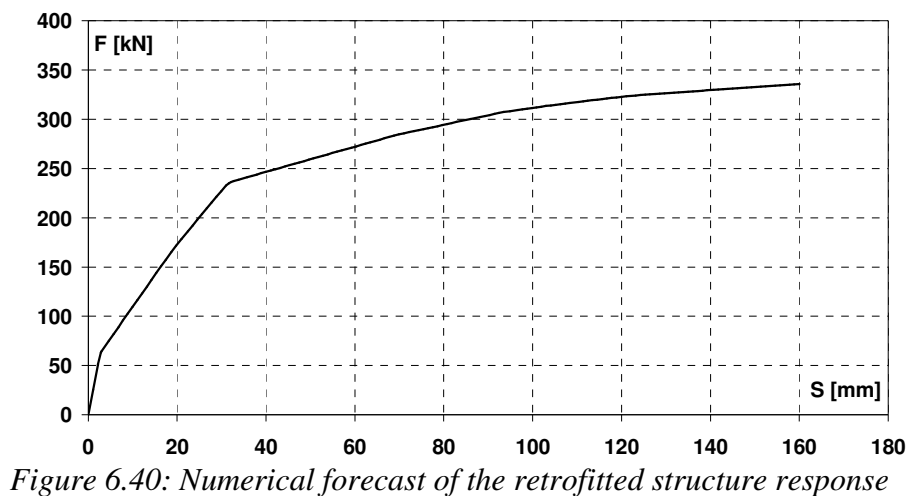


Figure 6.40: Numerical forecast of the retrofitted structure response

6.3.5 The experimental test

6.3.5.1 The intervention set-up

After the definition of the aluminium shear panel geometry, the experimental test on the retrofitted RC frame-aluminium panels structure has been carried out (Formisano et al., 2006e). In this context, all the equipments for the test set-up, namely the retaining structure, the RC - shear wall connections and the measuring devices, are the ones previously analysed for the retrofitting intervention based on the use of steel panels.

6.3.5.2 The obtained results

In the experimental test a cyclic loading history under quasi-static conditions and force control, followed by a final pushover test up to the attainment of a total force of 340 kN, has been applied at the first floor of the reinforced structure (Figure 6.41).

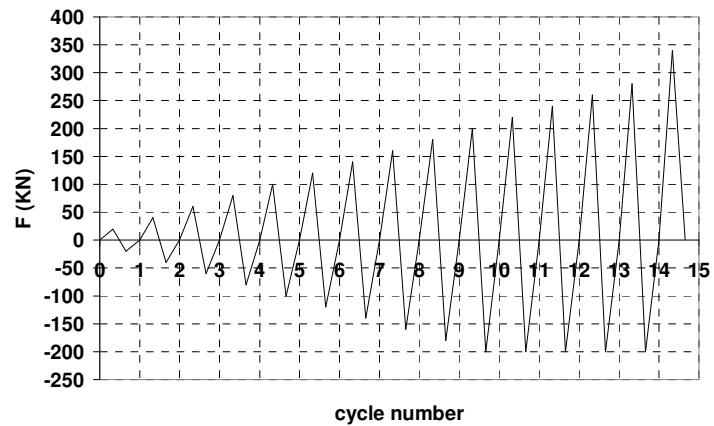


Figure 6.41: Loading history of the experimental test carried out on the RC structure reinforced with aluminium shear panels

In particular the displacements measurement were made for each step of 10 kN, so to obtain a detailed recording of the deformative structural state during the whole loading process. The results of the experimental test in terms of shear forces - first level displacements (P3 transducer - see Figure 6.25 b) are reported in Figure 6.42.

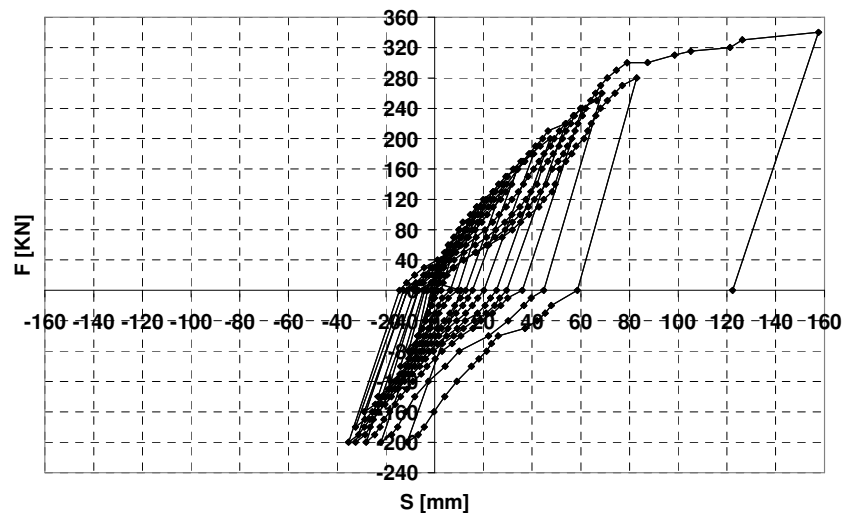
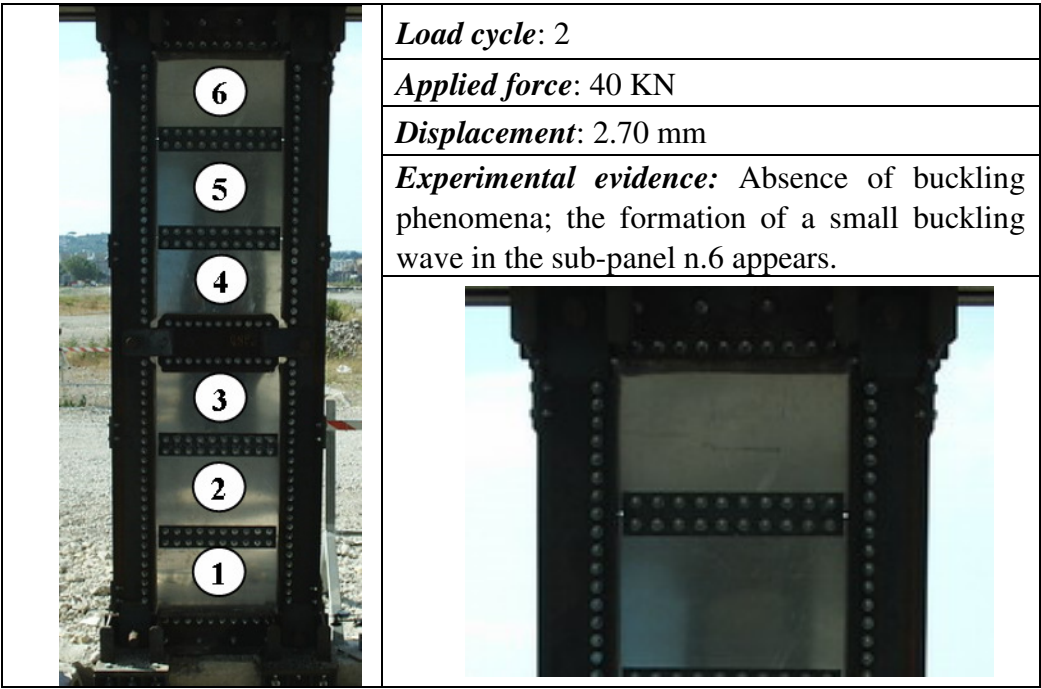



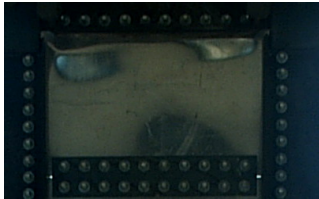
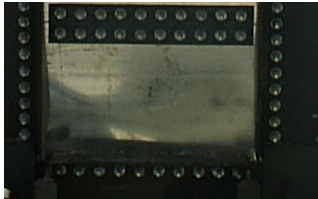
Figure 6.42: The experimental response of the RC structure retrofitted with pure aluminium shear panels


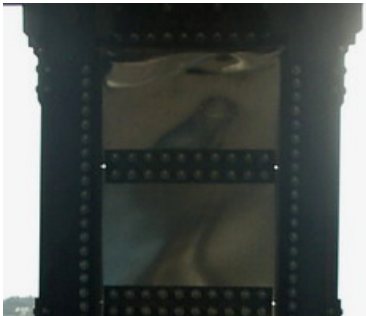
Also in this case, as detected during the previous test, the displacements of the transducers fixed on the RC beam and on the reinforcing steel profile have provided the same values, confirming the effectiveness of the connection system created among different members. Moreover, the displacements at the base of the steel plate shear wall have not provided any significant values, assuming a maximum amplitude of 1 mm when the peak load was attained.



In the experimental test the retrofitted structure attains a maximum load of 340 kN for a displacement amplitude of 158 mm, which corresponds to an inter-storey drift equal to about 6.5%. Besides, the hysteretic cycles of the compound RC frame - aluminium panels structure appear to be significantly more dissipative than the ones achieved in the previous experimental test, they allowing to exploit the plastic features of the used material. For this reason, pure aluminium shear panels can be also considered as dissipative systems, other than strengthening and stiffening devices, for retrofitting operations.


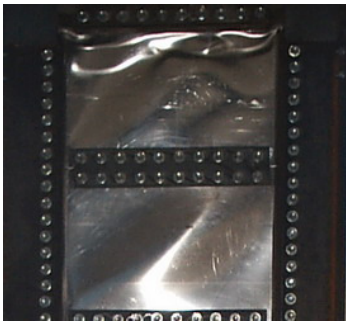
The more significant phases of the experimental test, by making reference to the behaviour of single sub-panels numbered in the same way used for steel ones, is illustrated in details in the following Figure 6.43.



	Load cycle: 4
	Applied force: 80 KN
	Displacement: 10.18 mm
	Experimental evidence: The presence of buckling waves due to compression forces appears in the bottom and upper sub-panels (n.1 and n.6), delaying the activation of the tension field mechanism.
	<div>   </div>

	Load cycle: 5
	Applied force: 100 KN
	Displacement: 16.75 mm
	Experimental evidence: Shear buckling of all sub-panels develops. Bottom and upper sub-panels are still characterised by the presence of buckling waves.
	

	Load cycle: 10
	Applied force: 200 KN
	Displacement: 47.48 mm
	Experimental evidence: Permanent waves, representative of a plastic mechanism occurred especially along the diagonals, are present on the whole panel surface. In the sub-panel n.6 the tension field mechanism develops.
	

	Load cycle: 14
	Applied force: 280 KN
	Displacement: 83.00 mm
	Experimental evidence: The shear panel presents a fully plastic behaviour, exhibiting the permanent deformations characterising the tension field, even if some buckling waves in the sub-panels n.1 and n.6 are present.
	

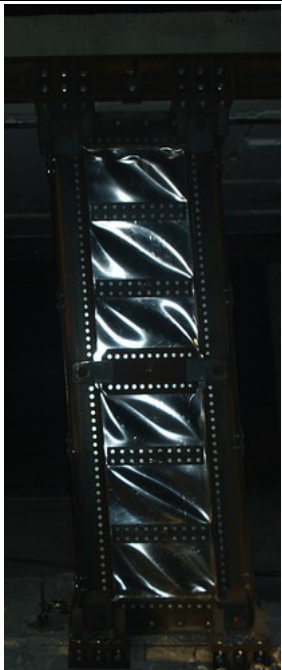
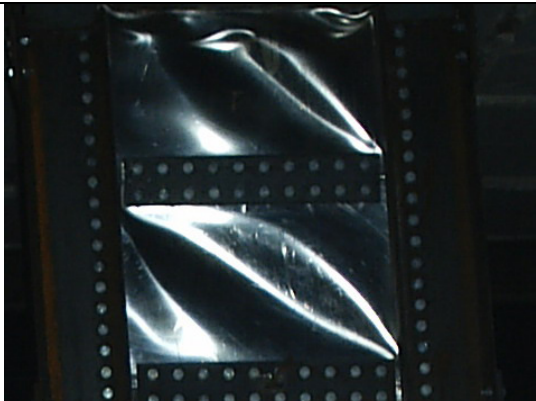
	Load cycle: 15
	Applied force: 340 KN
	Displacement: 157.64 mm
	Experimental evidence: Maximum panel deformations, with very evident plastic buckling phenomena in shear.
	

Figure 6.43: The progressive deformations of the pure aluminium shear panel during experimental test

As in the experimental test on the structure retrofitted with steel panels, also in this case the presence of buckling waves in the terminal panel fields determines, even if in less pronounced way due to a higher b/t plate ratio, a reduction of the system stiffness between the loading phases and the unloading ones. Nevertheless, when significant displacements are attained, permanent waves develop into each sub-panel.

The final deformed configuration of all panel fields of both the front side shear wall and the back side one, which are defined as in the test on steel panels (see Figure 6.29), is reported in Figures 6.44 and 6.45, respectively. From the comparison between figures it is shown that, as already seen in the previous test, the two pure aluminium plate shear walls behave in the same way, they always presenting foldings in the end plate portions.

Finally, considering that the RC structure has not been repaired after the experimental test on steel shear panels, the presence of further significant damages is not occurred, as testified in Figure 6.46.

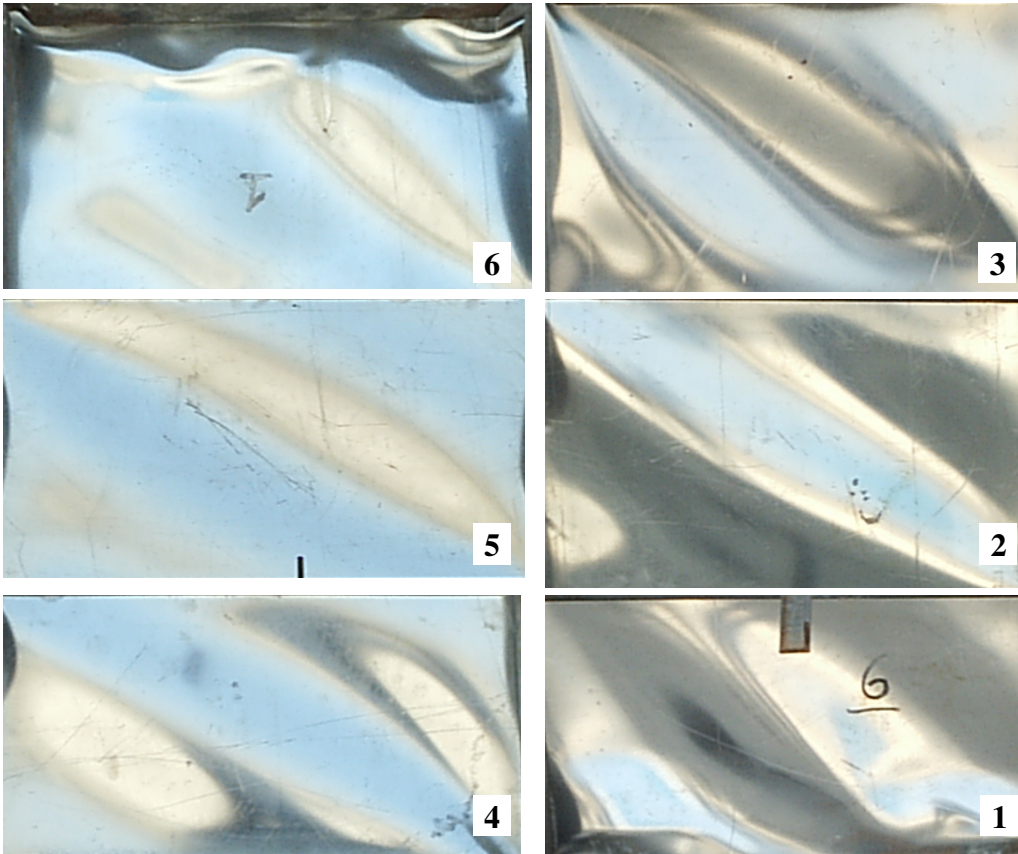


Figure 6.44: Deformed shapes of sub-panels (with their own number) belonging to the shear wall located at the front side of the RC structure

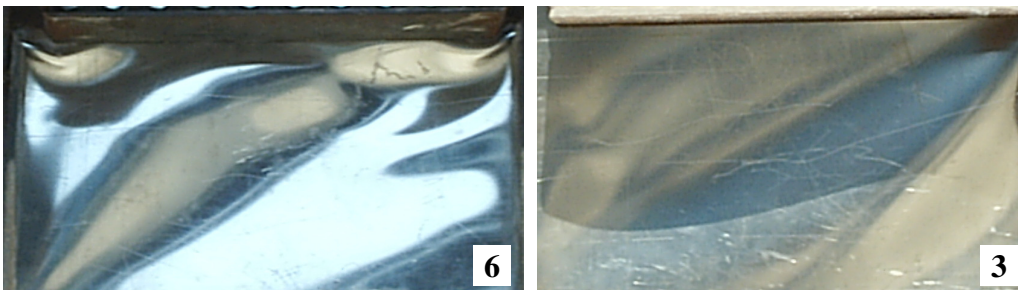


Figure 6.45: Deformed shapes of sub-panels (with their own number) belonging to the shear wall located at the back side of the RC structure (continues)

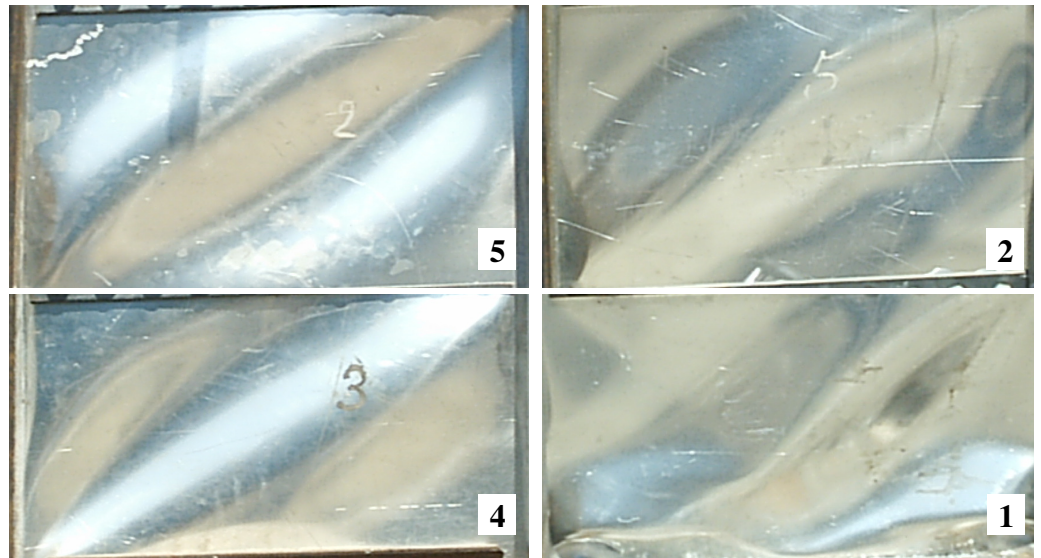


Figure 6.45: Deformed shapes of sub-panels (with their own number) belonging to the shear wall located at the back side of the RC structure



Figure 6.46: Damages occurred in the columns ends at the test conclusion

6.3.6 Interpretation of test results

Once the cyclic behaviour of the compound RC-pure aluminium structure has been determined, the corresponding envelope curve can be achieved (Figure 6.47) and then compared with the expected experimental response of the bare RC structure in the shear force – first floor displacement plane (Figure 6.48).

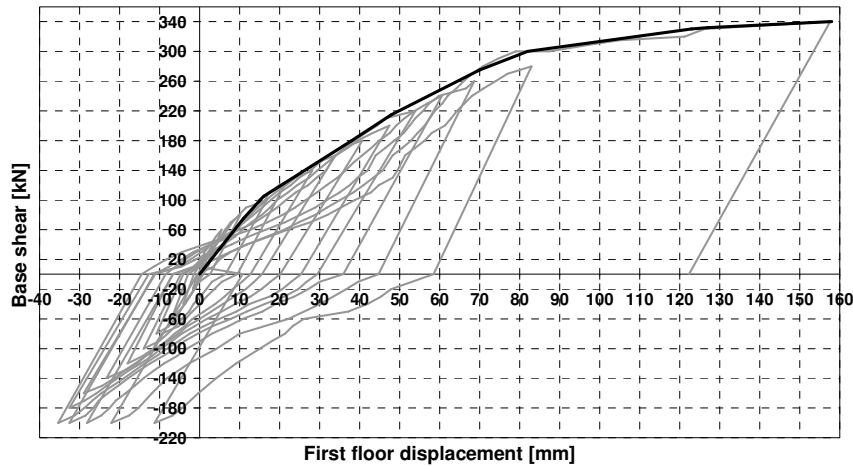


Figure 6.47: Envelope curve of the experimental test

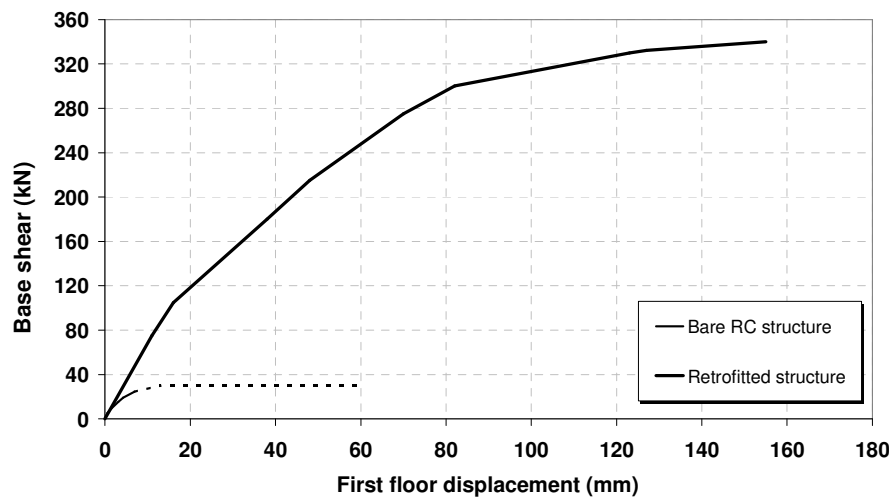


Figure 6.48: Comparison between the response of the structure retrofitted with pure aluminium panels and the bare RC structure one

From the comparison it is apparent that the response of the retrofitted structure is significantly improved, showing an increase of both initial stiffness and ultimate strength equal to 2 and 11.5 times the bare RC structure ones. Also with reference to the numerical forecast of the bare RC structure response (see Figure 4.49), a significant increase of strength exhibited by the retrofitted structure is achieved, it being equal to about 5 times the structure resistance before intervention.

The deformation capacity of the structure appears to be very large, without the involvement of any brittle collapse mode up to a deformation amplitude corresponding to an inter-storey drift greater than 6.5%. In addition, the same combined dissipative mechanism between plastic hinges in the beam-to-column joints of the RC frame and plastic deformation of tensile diagonals of the applied shear panels experienced in the previous test occurs.

The cyclic response of the RC structure retrofitted with pure aluminium shear panels can be evaluated by means of the same three parameters already used for interpreting the behaviour of the RC-steel panels one. Therefore, as in the previous case, the experimental data have been processed by representing E_{cycle} , K_{sec} and ν_{eq} under form of bar diagrams as a function of the cycles number (Figure 6.49). In particular, both secant stiffness and damping ratio values have been plotted vs. the maximum load attained in each cycle.

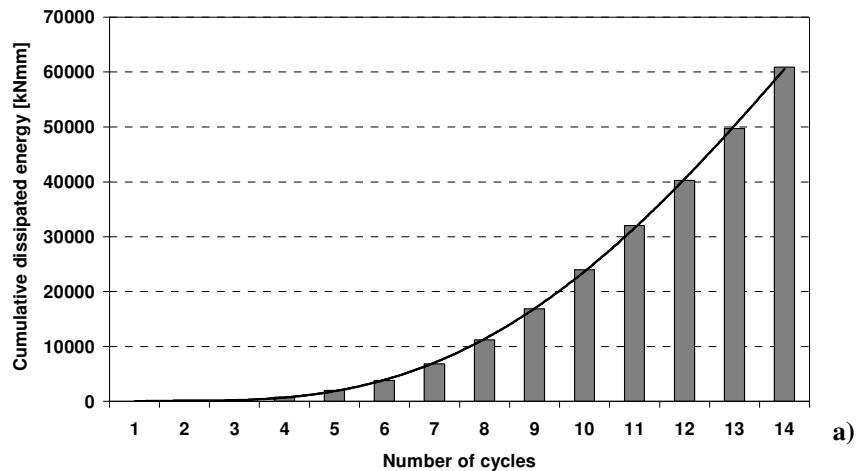


Figure 6.49: Interpretation of experimental results in terms of cumulative dissipated energy (a), secant stiffness (b) and equivalent viscous damping ratio (c) (continues)

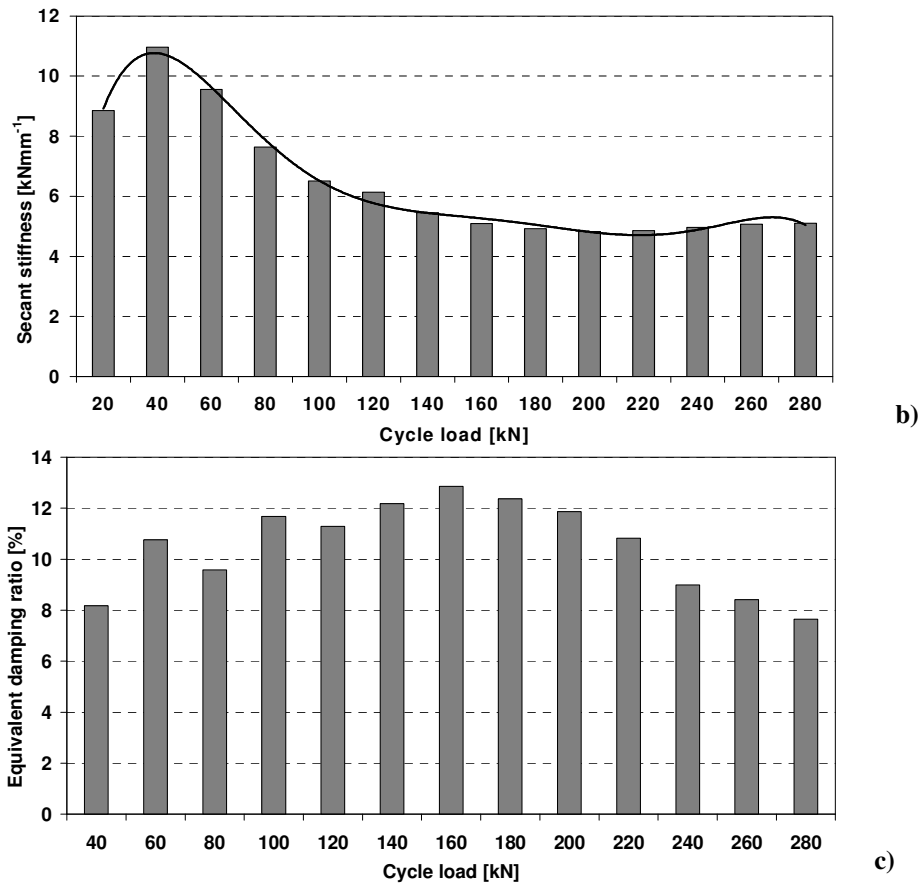


Figure 6.49: Interpretation of experimental results in terms of cumulative dissipated energy (a), secant stiffness (b) and equivalent viscous damping ratio (c)

From the above figure it is apparent that:

- 1) the experimental cumulative dissipation capacity of the RC structure upgraded with pure aluminium shear panels increases with cycle number following a second order polynomial curve, whose equation is:

$$E_{\text{cycle}} = 505.39n^2 - 3032.5n + 3874.6 \quad (6.12)$$

where n is the number of cycles.

As a consequence, the increase of displacements applied to the structure produces a progressive development of tension field into panel portions, determining the increment of the structural energy dissipation capacity.

- 2) the secant stiffness of the composed structure increases significantly

(about 20%) passing from 20 kN to 40 kN, where it attains its maximum value (10.96 kNmm^{-1}). This is due to the fact that in the initial phase of the loading test, due to the occurrence of buckling waves in the end plate portions, the shear panels displacements are very small. Then, as the number of cycles increases, secant stiffness quickly decreases with a quite regular non linear trend up to an applied total force of 180 kN. This is verified because the achieved structure displacement excursions and, therefore, the corresponding hysteretic loops, increase in significant way due to the excellent inelastic properties of the used aluminium alloy. Starting from this point an almost constant value of the secant stiffness is noticed. As a consequence, for these load cycles, the increase of the force variation (ΔF) is practically equal to the corresponding total displacement excursion (ΔS). In the whole, the trend assumed by secant stiffness can be very well interpreted by a fourth order polynomial interpolation curve, whose equation is:

$$K_{\text{sec}} = -2,5093n^4 + 83,49n^3 - 423,2n^2 + 803,27n - 433,21 \quad (6.13)$$

being the cycles number indicated with n .

- 3) the equivalent viscous damping ratio of the upgraded structure, which is averagely equal to 10%, assumes its maximum value of 12.85% for an applied lateral force equal to 160 kN. Starting from such a load, a reduction of values with non linear trend for lower and greater amplitude cycles occurs. In particular such a reduction is more relevant for three load cycles characterised by an applied total force greater than 220 kN, corresponding to a displacement of 89 mm. Nevertheless, the scatter detected in terms of the equivalent damping factor for these three cycles is very small. This is due to the fact that in the final phases of the loading process no significant increase of hysteretic loop areas occurs when larger displacements are applied to the structure. Such a phenomenon is caused by the occurrence of pinching phenomena. On the contrary, in the initial test phases, the increase of the damping factor is due to the remarkable difference detected in terms of dissipated energy among cycles when loads applied to the structure increase. Finally, the damping ratio variation with cycles number n is well approximated by the following expression:

$$v_{\text{eq}} = -0.1232n^2 + 1.6232n + 6.9097 \quad (6.14)$$

Chapter VII

Comparison of solutions and results: steel versus aluminium and numerical versus experimental

7.1 INTRODUCTION

In the present Chapter the experimental results deriving from tests on the RC structure upgraded with steel and pure aluminium shear panels have been compared each other in terms of energy dissipation capacity, secant stiffness and equivalent viscous damping ratio. Therefore, interesting preliminary conclusions on the use of metal shear panels for seismic upgrading interventions have been drawn. Finally, such results have been put in relation to the numerical forecasts of the retrofitted structures behaviour. In such a framework, the numerical-experimental differences detected in terms of stiffness have allowed to set-up a new FEM model able to interpret very well the metal plate shear walls behaviour evidenced during tests.

7.2 COMPARISON AMONG EXPERIMENTAL RESULTS

The experimental results illustrated in the previous Chapter can be compared each other in terms of both monotonic and cyclic behaviour. With reference to the first aspect, the comparison is performed by considering the envelope curves achieved from experimental tests (Figure 7.1).

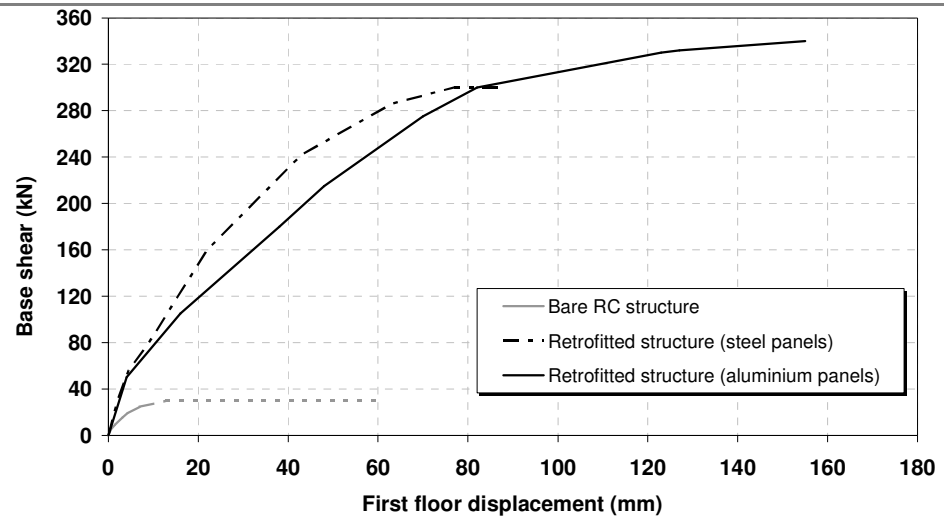


Figure 7.1: Comparison among experimental envelope curves

From the above figure, where the experimental results related to the application of steel and aluminium shear panels have been plotted together with the bare RC structure response, it can be noticed that:

- 1) the maximum final strength exhibited by reinforced structure in both tests is very similar, it being slightly predominant in the intervention based on the use of pure aluminium shear panels (340 kN vs. 300 kN). Therefore, with respect to the maximum resistance to lateral loads of the original structure, an increase of about 10 and 11.5 times is obtained with the employment of steel and aluminium panels, respectively.
- 2) the initial stiffness detected in both cases is also characterised by very close values, even if the best contribution is provided by the structure reinforced with steel shear plates (10 kNmm^{-1} vs. 8 kNmm^{-1}). During the test, when both loads and displacements increase, the stiffness of the structure retrofitted with aluminium shear panels decreases more rapidly than the one of the compound RC-steel panels system. In the whole, when steel and aluminium panels are used, the reinforced structure stiffness becomes about 2.5 and 2 times the one of the bare RC module, respectively. This behavioural difference is obviously due to the fact that the steel elasticity modulus is greater than the aluminium alloy one.

- 3) the ductile properties of the RC structure upgraded with aluminium panels are decidedly larger than the ones characterising the behaviour of the composed RC module - steel panels structure. In fact, for the same applied loads, the former structure presents displacements greater than the ones exhibited by the latter structure. Besides, in the final test phase, the composed RC-aluminium structure is subjected to a displacement of 158 mm, corresponding to an inter-storey drift equal to about 6.5%, while the maximum displacement carried by the RC-steel one under the maximum applied load is equal to 87 mm only, which corresponds to an inter-storey drift equal to about 3.5%. The different behaviour detected in terms of deformation capacity among two retrofitted structures is caused by the dissimilar ultimate strain of the used materials, which is significantly larger in the case of aluminium. Finally, considering that the original RC structure is not able to undergo any plastic displacement excursion, the results achieved in both experimental tests are really remarkable.

On the other hand, with reference to the cyclic behaviour of the strengthened structures, a first effective comparison between results can be performed by superposing the hysteretic loops achieved from experimental tests (Figure 7.2).

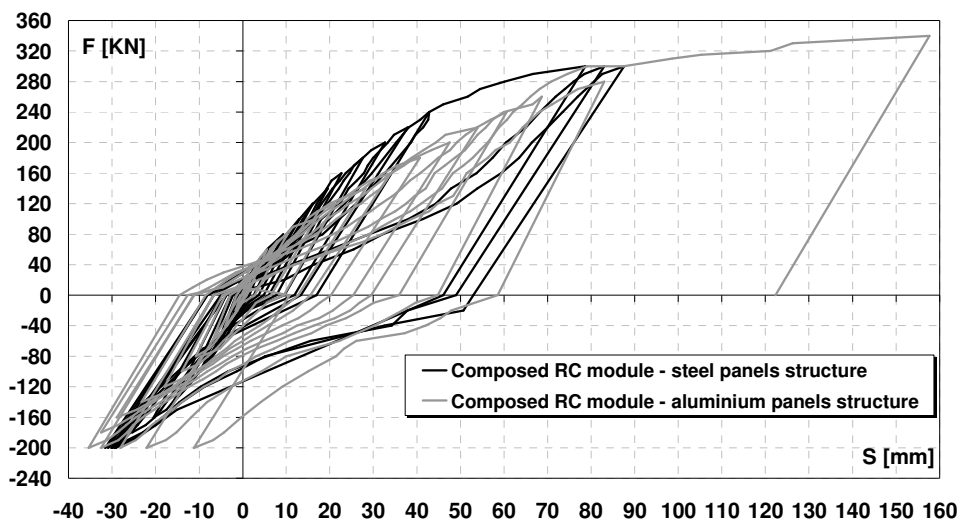


Figure 7.2: Comparison among experimental cyclic results

From the comparison it is apparent that hysteretic cycles obtained using aluminium panels (*APs*) are decidedly larger, evidencing a better dissipative behaviour with respect to the steel ones (*SPs*).

Such a condition occurs for two main reasons:

1) for the same applied load the displacement of the structure strengthened with aluminium panels is greater in comparison to the one of the structure endowed with steel plates;

2) the slenderness of shear panels is smaller in case of aluminium.

In addition, the cyclic response of the RC structure retrofitted before with steel and after with pure aluminium shear panels can be interpreted comparing the obtained results each other by means of the same three numerical parameters already introduced in the previous Chapter for evaluating the systems behaviour. So, the experimental data have been processed in terms of dissipated energy (E_{cycle}), secant shear stiffness (K_{sec}) and equivalent viscous damping factor (ν_{eq}), whose physical significance, together with the expressions used for their calculation, is depicted in Figure 3.12.

All the above parameters have been represented under form of histograms. In particular, the cumulative dissipated energy values have been plotted vs. the cycles number, whereas both secant stiffness and damping ratio values have been reported vs. the maximum load attained in each cycle. In this context it is important to observe that the comparison has been performed only with reference to the cycles characterised by the same force levels detected in both tests. In Figures 7.3, 7.4 and 7.5 such diagrams are shown, allowing a comparison of the performance of tested structures to be highlighted.

From the comparison carried out in terms of the experimental cyclic behaviour up to an applied total load of 240 kN, it is noticed that, as already shown in Figure 7.2, cumulative dissipated energy obtained using *APs* is decidedly larger than the one achieved by means of *SPs* (Figure 7.3 a). Such an observation is also justified by the interpolation curves of experimental data reported in Figure 7.3 b, where it is shown that a fourth order polynomial curve is used to interpret the behaviour of the composed RC-aluminium structure, while the trend assumed by energy for the RC-steel one can be well assimilated by a third order curve.

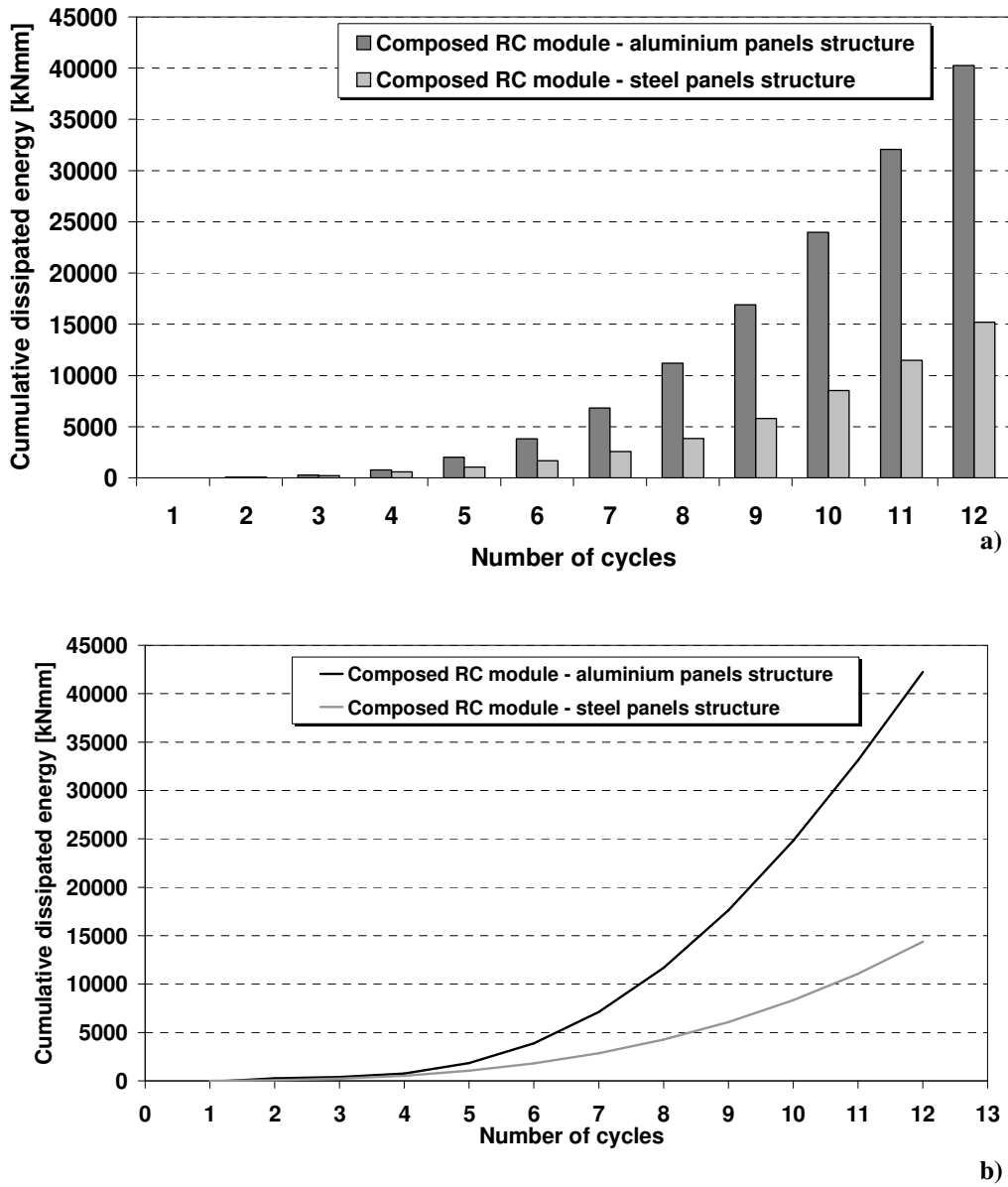


Figure 7.3: Comparison between experimental results in terms of cumulative dissipated energy reported under form of bar diagrams (a) and interpolation curves (b)

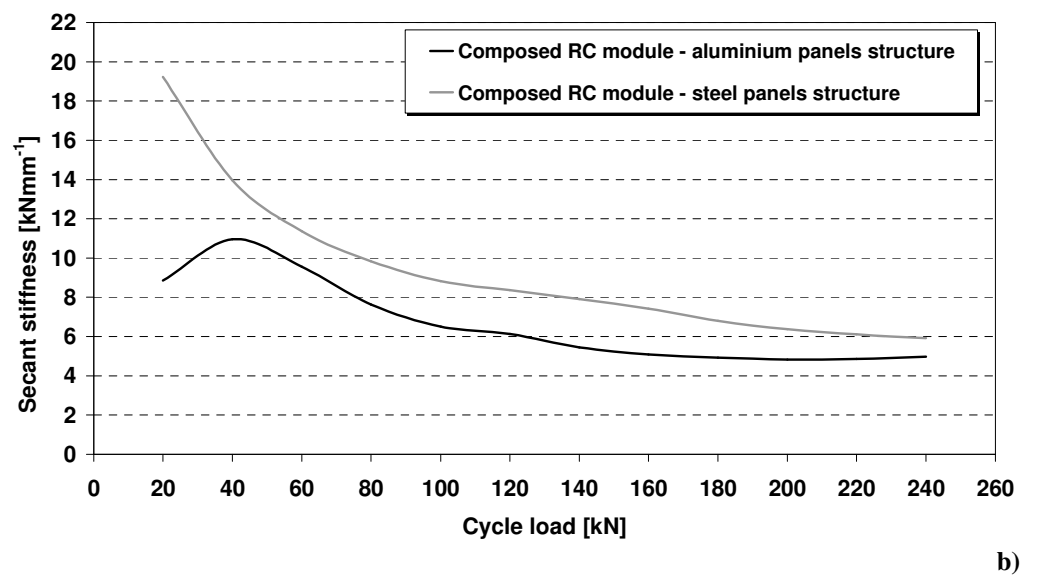
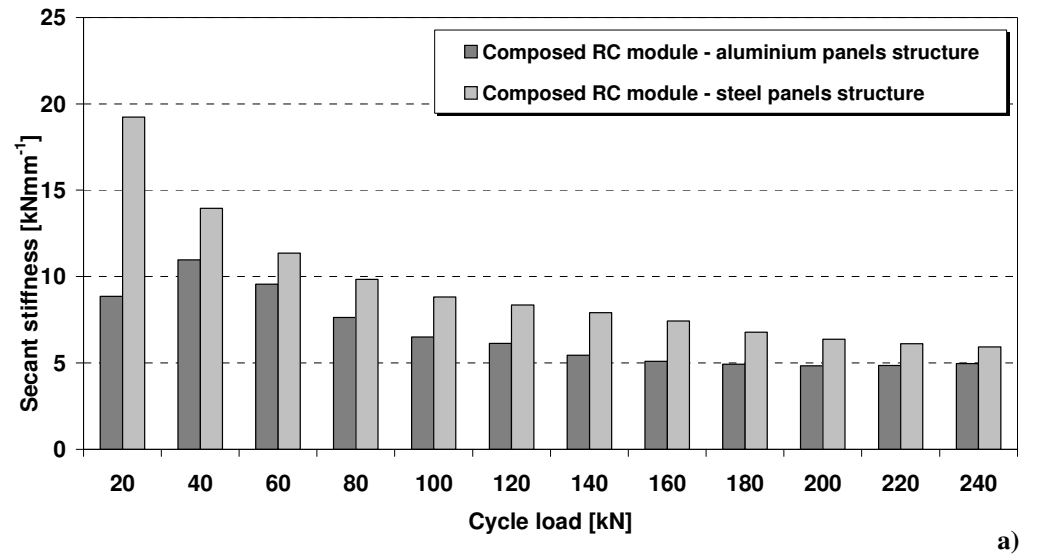


Figure 7.4: Comparison between experimental results in terms of secant stiffness reported under form of bar diagrams (a) and interpolation curves (b)

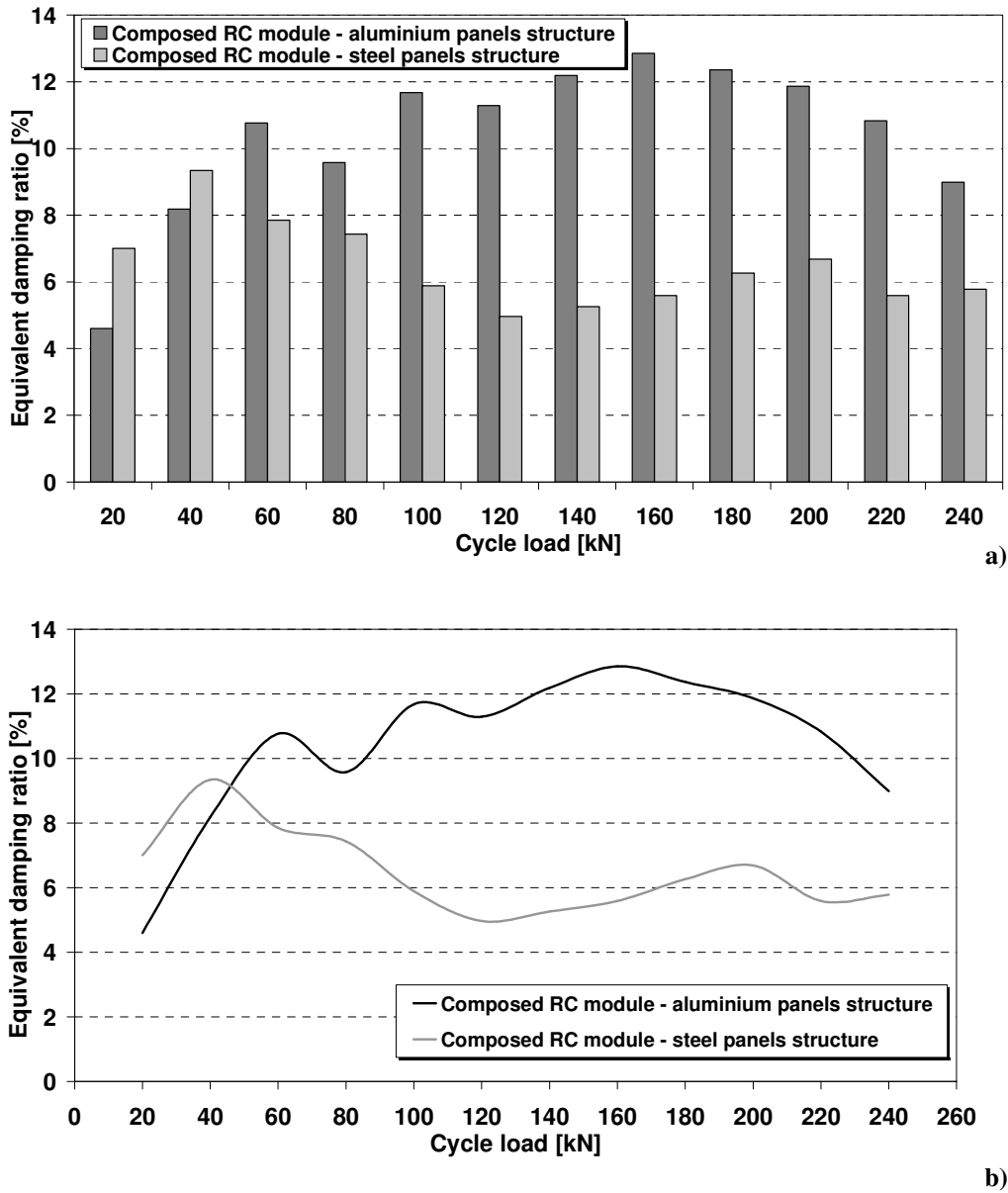


Figure 7.5: Comparison between experimental results in terms of equivalent viscous damping ratio reported under form of bar diagrams (a) and interpolation curves (b)

In particular, the retrofitted structures behaviour in terms of cumulative dissipated energy can be interpreted through the following equations:

$$E_{\text{cycle,APs}} = -4.0997n^4 + 124.26n^3 - 765.28n^2 + 1851n - 1317.7 \quad (7.1)$$

$$E_{\text{cycle,SPs}} = 8.4353n^3 \quad (7.2)$$

where n is the number of cycles.

It is important to underline that these relationships are appropriate in all cases where a constant load increment of 20 kN is applied per each cycle (that is the case under examination).

Finally, the different behaviour experienced by structures in terms of energy dissipation capacity can be explained by the fact that, for the same applied load, the displacements exhibited by the structure strengthened with APs are significantly larger than the ones of the structure retrofitted with SPs.

In addition, it is interesting to observe the trend assumed by G_{sec} during tests (Figure 7.4). It is apparent that in the initial test phase, up to a total force of 40 kN, corresponding to a displacement excursion of 5.73 mm, the global stiffness of the composed RC module - SPs structure increases due to the limited activation of the tension field mechanism into plate fields. Later on, it rapidly decreases as the applied deformation amplitude increases. On the other hand, the trend assumed by secant stiffness for the composed RC module - APs structure is well represented by a non linear decreasing curve with values always higher than the RC-SPs structure ones. For this reason pure aluminium shear panels are effective in stiffening the bare RC structure. Nevertheless, in the current case, the reduction of shear stiffness K_{sec} is more remarkable than the one exhibited by steel shear panels, showing the better attitude of the latter devices to be applied as stiffening rather than dissipative devices for seismic retrofitting interventions.

Finally, by observing the results shown in Figure 7.5, it can be noticed that the examined RC structures strengthened before with steel and after with aluminium panels present a different average equivalent viscous damping ratio, it being equal to 6.7% and 10%, respectively. In addition, while RC-SPs structure attains maximum damping ratio values in the initial and final phases of the loading process and presents a strong reduction of such a factor for intermediate amplitude cycles, RC-APs one has its peak value (12.85 %) in the middle test phase, when a displacement of 57 mm is applied, presenting a reduction of values for loads both greater and lower than 160 kN. In

particular, such a reduction is more significant for displacements smaller than 57 mm. This is due to the fact that in the final phase of the loading process the energy dissipation capacity of the structure retrofitted with aluminium panels increases. Also, it is interesting to observe that the retrofitted structures present the same equivalent damping factor for an applied force of about 50 kN. For loads lower than 50 kN the damping factors of the RC-SPs structure are greater than the RC-APs structure ones, whereas the opposite situation occurs when forces greater than 50 kN are applied. Such a phenomenon shows that a better dissipative behaviour of the composed RC-APs structure in comparison to the RC-SPs structure one occurs for loads larger than 50 kN, that is a displacement excursion equal to about 10 mm.

In conclusion, on the basis of the above considerations, it is possible to declare that pure aluminium shear panels result to have damping properties more remarkable than steel panels ones due to the higher ultimate strain of the base material. For this reason the use of aluminium shear panels is preferable when the improvement of the dissipative capacity of the primary structure where they are installed is requested.

7.3 EXPERIMENTAL-NUMERICAL COMPARISONS

7.3.1 RC structure retrofitted with steel shear panels

As it has been already shown, from the results of the experimental test it is possible to achieve an envelope curve (Figure 7.1) which can be compared with the response of the structure modelled with the SAP 2000 program, in which the panels system is represented through the strip model, in terms of the shear force – first level displacement curve (Figure 7.6).

The comparison underlines that the numerical response of the compound system is significantly different in terms of stiffness from the one obtained by the experimental test. Such a phenomenon, as already mentioned, is mainly due to the formation in bottom and upper sub-panels of buckling waves due to local compression forces. The formation of such waves can be explained by considering possible slips occurred at the beam-to-column connections of the external steel frame, as well as for the high compression stress transmitted by the columns in that zones.

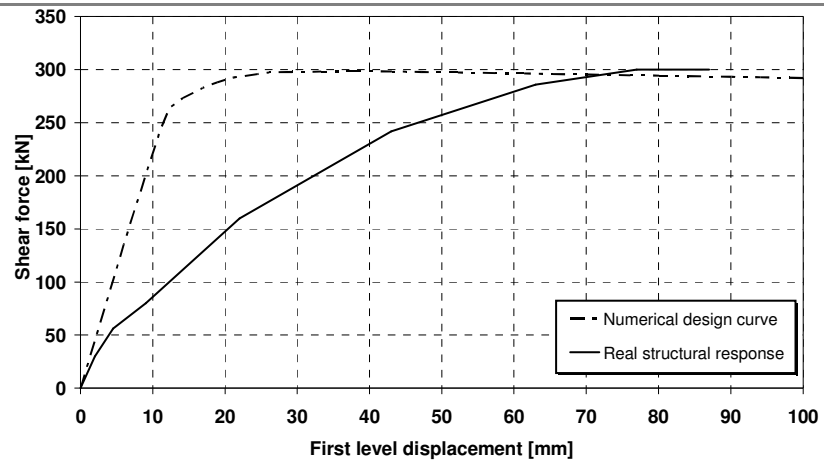


Figure 7.6: Comparison between numerical and experimental results in the force-displacement plane

On the other hand, the comparison with the theoretical design curve in the spectral acceleration-displacement plane depicted in Figure 7.7 shows a satisfactory agreement in terms of both initial stiffness (fundamental period) and maximum strength (spectral acceleration), confirming the effectiveness of the adopted design procedure.

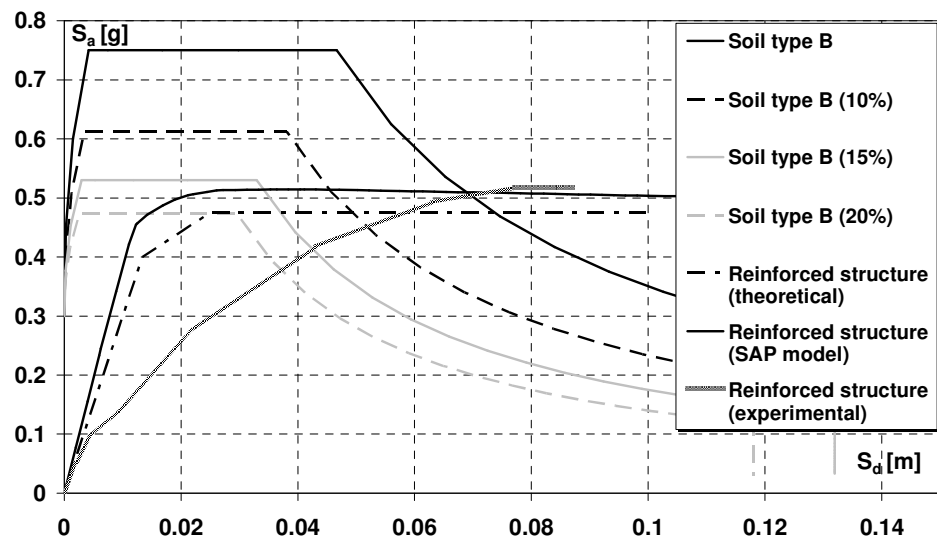


Figure 7.7: Comparison between numerical and experimental results in the spectral acceleration – spectral displacement (ADRS) plane

In addition, the reliability of the proposed FEM model developed by ABAQUS program is clearly evident in Figure 7.8, where the comparison between the numerical deformed shape with the real one shows a perfect similitude of results, evidencing the activation of a correct tension field mechanism.

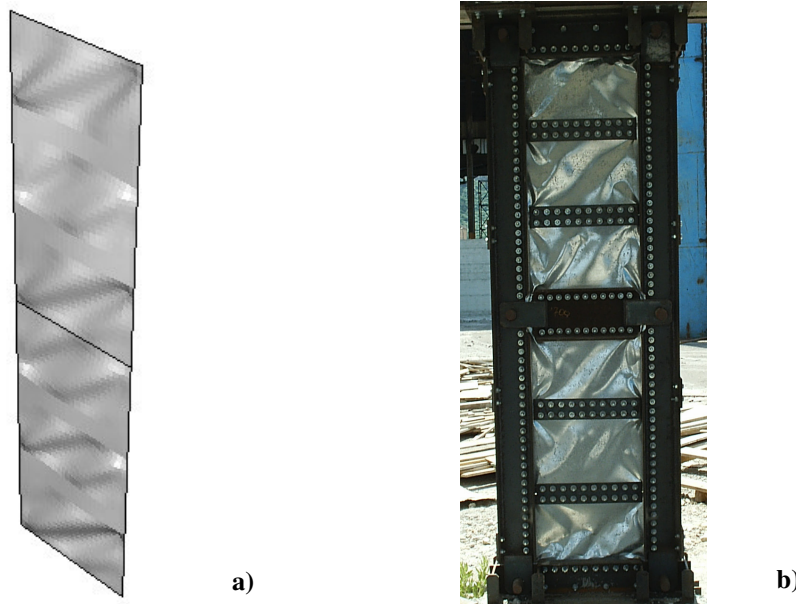


Figure 7.8: Deformed shape of the shear panel: numerical model (a) and real system (b)

Nevertheless, in order to improve the numerical results obtained through SAP non linear analysis software, the slips occurred at the beam-to-column connections of the external steel frame have been taken into account in the implementation of a new FEM model by introducing appropriate spring elements able to consider the real stiffness evidenced during the experimental test by the above joints.

The results of the performed new numerical simulation are represented in Figure 7.9, where a good agreement with the experimental stiffness of the retrofitted structure is detected. The effectiveness of such a final FEM model

is also illustrated in Figure 7.10, where different phases of the pushover test, together with the corresponding attained displacement Δ , are reported, they being able to simulate, according to the experimental evidence, the delayed activation of the tension field mechanism into end panel portions.

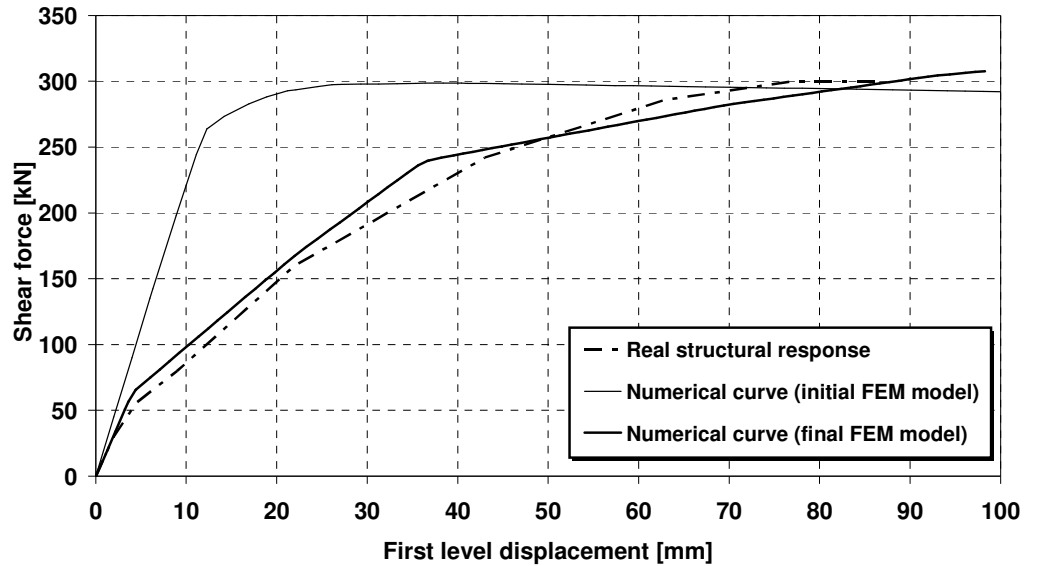


Figure 7.9: Comparison between numerical (initial and final FEM models) and experimental results

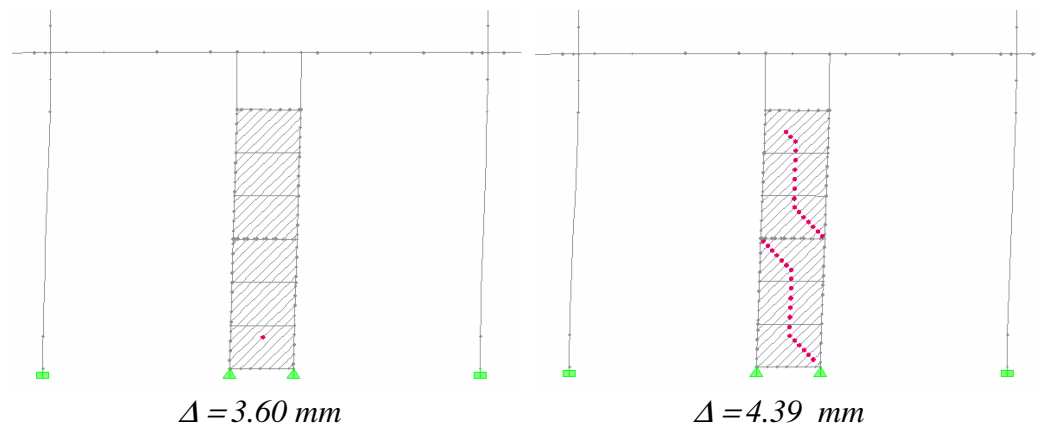


Figure 7.10: The progressive activation of the initial tension field mechanism into panel portions (continues)

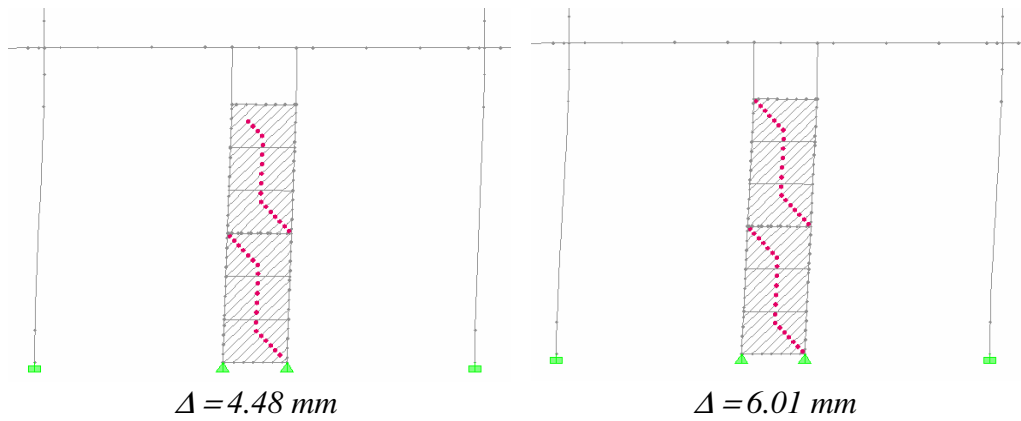


Figure 7.10: The progressive activation of the initial tension field mechanism into panel portions

7.3.2 RC structure retrofitted with pure aluminium shear panels

According to the study performed in the previous Section, also for the RC structure retrofitted with pure aluminium shear panels a comparison between experimental and numerical results has been done. Therefore, the envelope experimental curve of the RC structure response (Figure 7.1) has been compared with the retrofitting intervention numerical one, which is achieved from using SAP 2000 program, in the force-displacement plane (Figure 7.11).

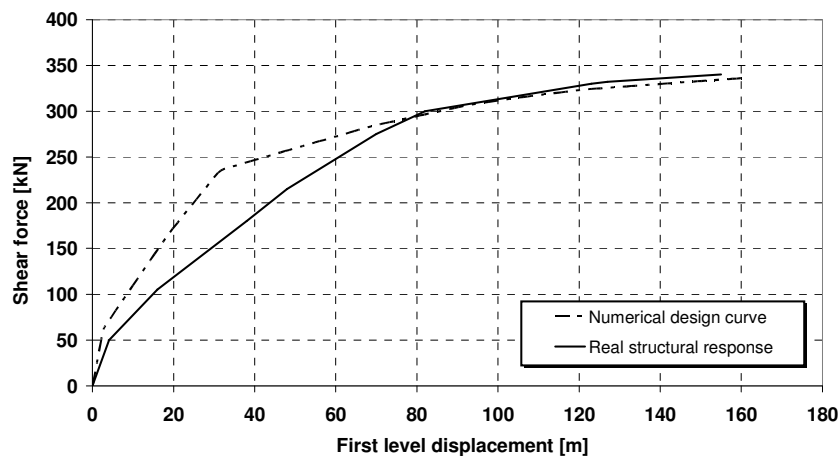


Figure 7.11: Comparison between numerical and experimental results in the force-displacement plane

The comparison underlines that, even if the same resistance is attained, the numerical response of the reinforced structure is different in terms of stiffness. Anyway such a discrepancy is lower than the one achieved when steel shear panels have been used (Figure 7.6) due to the lower slenderness (b/t ratio) of aluminium plates. Such a phenomenon, as mentioned in the previous experimental test, is due to the formation in the two extreme sub-panels of buckling waves, caused by the slips occurring in the beam-to-column connection of the external steel frame, which partially reduce the effectiveness of the proposed retrofitting system.

The same scatter in terms of stiffness is also detected from the comparison in the spectral acceleration - spectral displacement plane (Figure 7.12), where, as in the previous case, the good agreement of results in terms of both fundamental period and spectral acceleration confirms the effectiveness of the adopted design procedure. In fact, the FEM model of the shear panel derived from the application of such a procedure and developed by the ABAQUS program shows a final deformed shape perfectly similar to the final configuration of the real panel, evidencing a correct activation of the tension field mechanism (Figure 7.13).

Finally, also in this analysis phase, the same improved FEM model implemented in order to analyse the experimental behaviour of the compound RC-SPs structure has been used aiming at reducing the difference among curves detected in terms of stiffness.

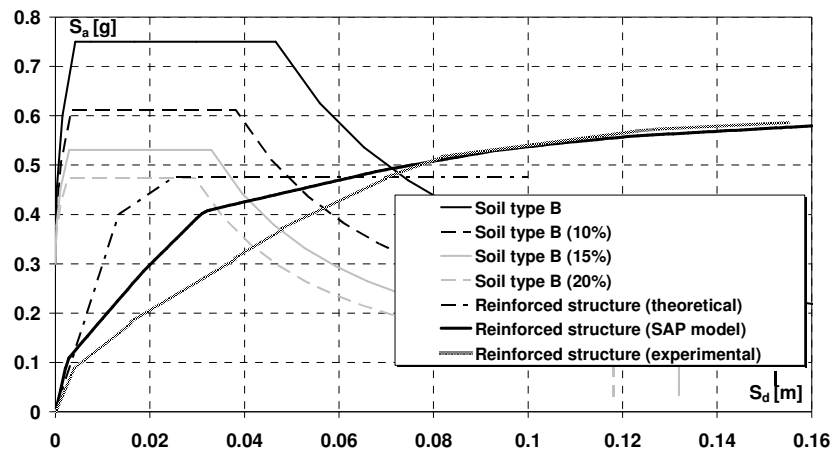


Figure 7.12: Comparison among the responses of the structure retrofitted with pure aluminium shear panels

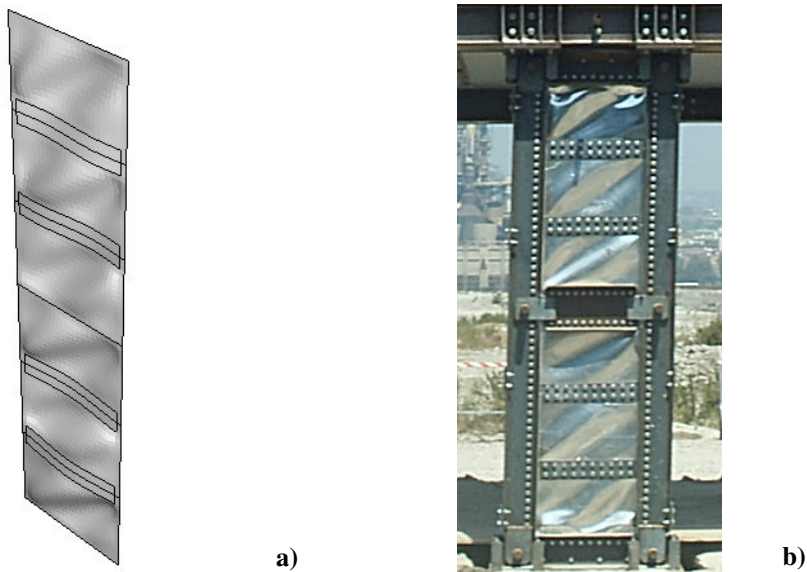


Figure 7.13: Deformed configuration of the aluminium shear panel: the numerical model (a) and the real system (b)

The results deriving from the employment of the new FEM model are represented in Figure 7.14, where a good agreement between the experimental stiffness exhibited by the retrofitted structure and the numerical one is observed.

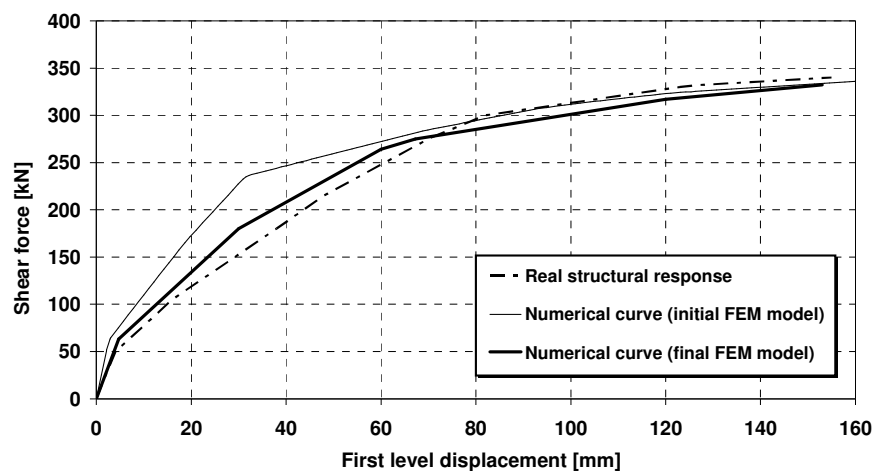


Figure 7.14: Comparison between numerical (initial and final FEM models) and experimental results

Concluding remarks

The current thesis work presents the study of metal shear panels for seismic upgrading of existing reinforced concrete (RC) buildings, which has been performed by means of both the implementation of theoretical and numerical design methods and the execution of full-scale experimental investigations.

In the last decades the occurrence of severe earthquakes worldwide confirmed the deficiencies of existing structures, with particular reference to the reinforced concrete ones. As a consequence, the experience collected from field observations and the related development of accurate analyses led to the improvement of both the knowledge level and the evolution of seismic codes.

As a first step of the research activity, a wide survey has been carried out on the seismic vulnerability sources detected in existing gravity-load designed (GLD) RC buildings and the analysis of related assessment techniques. The possible retrofiting solutions to be used, namely local and global intervention methods, have been presented aiming at improving their behaviour under earthquake attacks.

In such a framework, with reference to passive seismic protection systems, particular attention has been devoted to metal shear panels, under form of both slender and compact plates, which have been successfully applied into steel buildings, both new for earthquake protection and existing for retrofiting. No reference in the technical literature has been found on the possible use of metal shear panels for seismic upgrading of existing RC buildings. For this reason this subject has been selected as research objective and it represents the main target of the present dissertation.

In the preliminary phase of the investigation, a wide numerical investigation aiming at evaluating the performance of both compact and slender metal shear panels has been carried out.

First, both parametric numerical studies and numerical simulation of experimental tests on 1000x1500x5 mm aluminium stiffened shear panels have been performed. Two different aluminium alloys have been considered, namely EN-AW 1050A and EN-AW 5154A, the former being known as pure aluminium, and different arrangements of applied stiffeners, either welded or bolted to the base plate, have been used. Such an activity has provided appropriate design charts for these panels, allowing the determination of their optimal configurations with respect to the performance required in terms of strength and deformation capacity.

In addition, on the basis of the conclusions deriving from these first results, a wide numerical analysis has been carried out considering panels with different rib configurations, aiming at emphasizing the influence of the main behavioural parameters on the dissipative capacity of these systems subjected to different displacement demand levels. The out-put of this activity allows to obtain some economical data about the most suitable configuration to be adopted as passive control devices in case of new and existing structures in relation to the estimated displacement demand.

The second investigation phase was devoted to analyse the behaviour of slender steel shear panels, by using DX56D steel as base material, it being characterised by a nominal yield point lower than the one of ordinary structural steels. After the implementation of a refined FEM model calibrated on the basis of available experimental results, a parametric analysis on these panels has been carried out, in order to evaluate the influence of the geometry on the structural behaviour of shear plates. The theoretical behaviour of thin steel panels in shear, based on existing simplified methodologies, has been analysed and then compared with the results obtained by an extensive numerical study carried out by means of accurate finite element models. The comparison between theoretical and numerical results has been developed with reference to different values of thickness and by varying the aspect ratio of the plate, investigating also on the influence provided by intermediate stiffeners. In particular, the validity of the aspect ratio range provided by Canadian code for steel panels aiming at assuring the development of a

complete tension field mechanism on the plate surface has been proved. The obtained results have provided useful information for the correct design of slender steel plates in shear to be used as stiffening and strengthening devices in new and existing framed structures.

Starting from the above numerical survey, two types of metallic materials have been selected for seismic retrofitting purposes by means of shear panels: DX56D steel and pure aluminium. The former, which is used to produce cold-formed thin walled sheeting and profiles according to the UNI EN 10142 code provisions, is characterised by both nominal low yield stress followed by strain-hardening, whereas the choice of the latter, which is really innovative in the field of seismic engineering, is justified by both low conventional elastic limit and high ductility, which can be further improved through proper heat treatments.

The seismic upgrading intervention with shear panels made of the above selected metallic materials has been applied to a real RC building, which is located in the site of the former industrial plant ILVA in Bagnoli, a surrounding area of Naples, and has been used to analyse the effectiveness of different metal-based retrofitting techniques. The original building has been reduced to the bare RC structure by eliminating external and partition walls, and then has been subdivided into six sub-structures (modules), in order to increase the number of systems to be tested. Particular attention has been paid to the module where the application of metal shear panels has been done.

After the identification of the mechanical properties of structure materials, the dynamic behaviour of the bare RC module has been experimentally evaluated by means of both direct and indirect impulse tests. Then, the achieved results in terms of modal frequencies have been numerically reproduced by means of the calibration of a finite element model of the whole structure. A preliminary experimental cyclic test has been carried out on the bare RC structure, aiming at evaluating its initial stiffness, and pushover numerical analyses have been also carried out in order to evaluate the building performance under lateral loads.

Later on, the seismic retrofitting design of existing buildings has been deeply analysed and discussed with particular reference to the methodology given by both FEMA 273 and ATC-40 American guidelines. Therefore, in the framework of the “performance based design” methodology, the seismic

performance of the building under investigation has been evaluated and the theoretical design curve of the upgrading intervention has been achieved. Such a design curve, together with the selected metallic materials, led to the definition of appropriate shear panel configurations able to provide the strength and stiffness prerequisites requested for the seismic retrofitting intervention of the original RC structure. Subsequently, both steel and pure aluminium shear panels have been designed according to simplified analytical procedures and then checked by adopting a sophisticated FEM model. In particular, the panel dimensions have been determined as $b = 600$ mm and $d = 2400$ mm, with a thickness of 1.15 mm and 5 mm in case of steel and aluminium plates, respectively.

Then, in both cases, global numerical analyses of the whole retrofitted structure have been done, giving a refined simulation of the theoretical response as expected in the design phase.

When theoretical and numerical activities have been concluded, all the components of the reinforcing system (panel-frame connection, steel frame – RC structure connection) have been designed according to the hierarchy criterion methodology.

Since shear panels were provided under form of 400x600 mm sheetings, plate portions have been joined each other by means of bolted connections in order to built-up the whole shear wall. The effectiveness of panel-to-panel, as well as of panel-to-frame connections, has been proved by laboratory tests. The obtained results have shown that the shear connection strength was higher than the yielding resistance of the plate due to the occurrence of the block tearing mechanism, which has determined a significant increment of the effective sheeting net section. Also a significant ductility of the adopted connection has been noticed, together with its ability to restore the panel continuity.

The shear panels have been installed into external steel frames, which have been inserted within the RC structure. The efficiency of the adopted upgrading intervention has been validated by means of two cyclic experimental tests on the RC retrofitted structure: the first with steel and the second with pure aluminium shear panel systems.

In both cases a considerable improvement of the structural capacity of the original structure in terms of initial stiffness, strength and energy dissipation

has been achieved. Firstly, the comparison among structure performance has been carried out considering the envelope curves of the cyclic response. In particular, when steel plates have been used, the increase of the initial stiffness and ultimate strength has been equal to 2.5 and 10 times, respectively, the ones of the bare RC structure. Also the deformation capacity of the structure has been very large, without the involvement of any brittle collapse mode up to a sway deflection equal to 85 mm, which corresponds to an inter-storey drift equal to 3.5%. For the RC structure retrofitted with aluminium panels the increase of initial stiffness and ultimate strength has been 2 and 11.5 times greater than the ones of the bare module, respectively, exhibiting also a large deformation capacity up to an interstorey-drift of 6.5%. In both cases a combined dissipative mechanism between plastic hinges in the beam-to-column joints of the RC frame and plastic deformation of tension diagonals in the shear panels have been observed.

Finally, the comparison among proposed panel solutions has been performed with reference to the cyclic behaviour of the retrofitted structures by processing the obtained experimental data in terms of dissipated energy, secant stiffness and equivalent viscous damping ratio. In both tests, a non linear decreasing trend of secant stiffness as the number of cycles increase has been noticed, even if a more remarkable reduction has occurred when aluminium shear panels have been used. On the other hand, cumulative dissipated energy obtained using aluminium panels has been clearly larger than the one achieved by means of steel plates due to their excellent hysteretic features.

In conclusion, all the above results allow to recognize that steel shear panels can be considered as effective strengthening and stiffening devices for retrofitting intervention, whereas in addition the pure aluminium panels are also able to significantly increase the energy dissipation capacity of the retrofitted structure. Both systems are suitable in retrofitting existing RC buildings designed just for gravity loads.

References

- Aiken, I.D., Whittaker, A.S., (1993). Development and application of passive energy dissipation techniques in the USA. *Proceedings of the International Post-SmiRT Conference Seminar on Isolation, Energy Dissipation and Control of Vibration of Structures*, Capri, August 23-25.
- AISC, (1999). *Load and Resistance Factor Design Specification*. American Institute of Steel Construction Inc., Chicago.
- Applied Technology Council (ATC) - 24, (1992). *Guidelines for seismic testing of components of steel structures*. Redwood City, CA.
- Applied Technology Council (ATC) - 40, (1996). *Seismic evaluation and retrofit of concrete buildings*. Vol.1, Report No. SSC 96-01.
- Astaneh-Asl, A., (2001). Seismic Behavior and Design of Steel Shear Walls. *Steel TIPS Report*, Structural Steel Educational Council, Moraga, CA, January.
- Astaneh-Asl, A., Zhao, Q., (2002). Cyclic behaviour of traditional and an innovative composite shear wall. *Report No. UCB-Steel-01/2002*, Department of Civil and Env. Engineering, University of California, Berkeley.
- Bakker, M.C.M., Pekoz, T., (2001). The finite element method for thin-walled members – Basic principles. *Proceedings of the 3rd International Conference on Thin-Walled Structures*, Elsevier Science Ltd.
- Basler, K., (1961). Strength of plate girders in shear. *Journal of Structural Division*, ASCE, Vol. 87, No ST7, Proc. Paper 2967.
- Berman, J. W., Bruneau, M., (2003). Experimental Investigation of Light-Gauge Steel Plate Shear for the Seismic Retrofit of Buildings. *Technical Report No. MCEER-03-0001*, Multidisciplinary Center for Earthquake Engineering Research, Buffalo, NY.
- Berman, J. W., Celik, O. C., Bruneau, M., (2005). Comparating hysteretic behavior of light-gauge steel plate shear walls and braced frames. *Engineering Structures*, 27, pp. 474-485.
- Bleich, F., (1952). *Buckling strength of metal structures*. McGraw-Hill.

- Bracci, J. M. , Reinhorn, A. M., Mander, J. B., (1995). Seismic Resistance of Reinforced Concrete Frame Structures Designed for Gravity Loads: Performance of Structural System. *ACI Structural Journal*, Technical Paper, Title no.92-S58, September – October.
- Bruno, S., Valente, C., (2002). Comparative response analysis of conventional and innovative seismic protection strategies. *Earthquake Engineering and Structural Dynamics*, 31(5), pp. 1067-1092.
- Caccese, V., Elgaaly, M., Chen, R., (1993). Experimental Study of Thin Steel-Plate Shear Walls Under Cyclic Loads. *Journal of Structural Engineering*, ASCE, pp. 573-587.
- Cardone, D., Dolce, M., Marnetto, R., Nigro, D., Ponzo, F.C., Santarsiero, G., Mucciarelli, M., (2004). Experimental Static and Dynamic Response of a Real R/C Frame Upgraded with Sma Re-Centering and Dissipating Braces. *Proceedings of the 13th World Conference on Earthquake Engineering*, Vancouver, B.C., Canada, August 1-6.
- Canadian Standards Association (CSA), (2001). *Limit states design of steel structures*. CAN/CSA S16-01, Willowdale, Ontario, Canada.
- Chopra, A. K., (1995). *Dynamic of Structures – Theory and Applications to Earthquake Engineering*. Prentice-Hall, Inc., New Jersey.
- Clark, W., Kasai, K., Aiken, I.D., Kimura, I., (2000). Evaluation of design methodologies for structures incorporating steel unbonded braces for energy dissipation. *Proceedings of the 12th World Conference on Earthquake Engineering*, Auckland, New Zealand , Paper No. 2240, CD-ROM.
- Cohen, J.M., Powell, G. H., (1993). A Design Study of an Energy-Dissipating Cladding System. *Earthquake Engineering and Structural Dynamic*, 22, pp 617-32.
- City of Los Angeles (COLA), (1995). Earthquake hazard reduction in existing reinforced concrete frame buildings with masonry infills. *Technical Report*, Los Angeles.
- CNR 10011, (1995). *Steel structures: provisions for calculation, execution, testing and maintenance*. Research National Council (CNR), Italy.

- Computer and Structures, Inc., (2003). *SAP 2000 Non linear Version 8.23*. Berkeley, California, USA.
- D'Aniello, M., Della Corte, G., Mazzolani, F.M., (2006). Seismic upgrading of RC buildings by steel eccentric braces: experimental results vs. numerical modelling. *Proceedings of the 5th International Conference on Behaviour of Steel Structures in Seismic Areas (STESSA 2006)*, Yokohama, August 14-17.
- Della Corte, G., D'Aniello, M., Mazzolani, F.M., (2005). Seismic upgrading of RC buildings using buckling restrained braces: full-scale experimental tests. *Proceedings of the National Conference on "Advances in Steel Constructions" (XX C.T.A.)*, Lacco Ameno, September 26-28.
- De Matteis, G., (2002). Seismic performance of MR steel frames stiffened by light-weight cladding panels. *Proc. of the 12th European Conference on Earthquake Engineering*, London, UK, Elsevier, CD-ROM, Paper No. 308.
- De Matteis, G., Mistakidis, E.S., (2003). Seismic retrofitting of moment resisting frames using low yield steel panels as shear walls. *Proceedings of the 4th International Conference on Behaviour of Steel Structures in Seismic Areas (STESSA 2003)*, Naples, pp. 677-682.
- De Matteis, G., Mazzolani, F. M., Panico, S., (2003). Pure aluminium shear panels as passive control system for seismic protection of steel moment resisting frames. *Proceedings of the 4th International Conference on "Behaviour of Steel Structures in Seismic Areas" (STESSA '03)*, Naples, June 9-12, pp. 599-607.
- De Matteis, G., Addelio, F., Mazzolani, F. M., (2004a). Sul dimensionamento dei pannelli di alluminio puro per la protezione sismica dei telai di acciaio. *Proceedings of the 11th National Congress "L'Ingegneria Sismica in Italia" (ANIDIS '04)*, Genoa, January 25-29, CD-ROM.
- De Matteis, G., Mazzolani, F. M., Panico, S., (2004b). Numerical analysis of pure aluminium stiffened shear panels for design optimisation. *Proceedings of the 4th International Conference on "Coupled Instabilities in Metal Structures" (CIMS '04)*, Rome, September 27-29, pp. 365-384.
- De Matteis, G., Formisano, A., Mazzolani, F. M., Panico, S., (2005a). Experimental Tests and Numerical Simulation on Stiffened Pure

- Aluminium Shear Panels. *Proceedings of the 10th International Conference on Civil, Structural and Environmental Engineering Computing (CC '05)*, Rome, August 30 – September 2, CD-ROM, Paper No. 202.
- De Matteis, G., Formisano, A., Mazzolani, F. M., Panico, S., (2005b). Design of low-yield metal shear panels for energy dissipation. *Proceedings of the COST C12 Final Conference*, Innsbruck, January 20-22, pp. 665-675.
- De Matteis, G., Panico, S., Formisano, A., Mazzolani, F. M., (2005c). Experimental tests on pure aluminium shear panels under cyclic loading. *Proceedings of the International Conference on "Earthquake Engineering in 21st Century (EE-21C)"*, Skopje, August 27-31, CD-ROM.
- De Matteis, G., Formisano, A., Panico, S., Calderoni, B., Mazzolani, F. M., (2006a). Metal shear panels. *Seismic upgrading of RC buildings by advanced techniques – The ILVA-IDEM Research Project*. Mazzolani, F. M. co-ordinator & editor, Polimetrica International Scientific Publisher, Monza, pp. 361-449.
- De Matteis, G., Panico, S., Mazzolani, F. M., (2006b). Experimental tests on stiffened pure aluminium shear panels. *Proceedings of the 11th International Conference on Metal Structures (ICMS '06)*, Rzeszow, June, 21-23.
- Driver, R. G., Kulak, G. L., Kennedy, D. J. L., (1997). Seismic Behaviour of Steel Plate Shear Walls. *Struct. Engrg. Rep No. 215*, Dept. of Civ. Engrg., University of Alberta, Edmonton, Alta, Canada.
- ECCS - Technical Committee 1 - Working Group 1.3 - Seismic Design, (1988). *European Recommendations for Steel Structures in Seismic Zones*, First Edition.
- Elgaaly, M., Caccese, V., Du, C., (1993). Postbuckling Behaviour of Steel-Plate Shear Walls Under Cyclic Loads. *Journal of Structural Engineering*, ASCE, pp. 588-605.
- EN 1993-1-1, (2005). *Eurocode 3: Design of steel structures: general rules and rules for buildings*. CEN - European Committee for Standardization, Brussels.
- EN 1998-1-1, (2005). *Eurocode 8: Design of structures for earthquake*

- resistance*. CEN - European Committee for Standardization, Brussels.
- EN 1999-1-1, (2006). *Eurocode 9: Design of aluminium structures – Part 1-1: General structural rules*. CEN - European Committee for Standardization, Brussels.
- Faggiano, B., Fiorino, L., Della Corte, G., Calderoni, B., Landolfo, R., Mazzolani, F. M., (2006). “As built” data collection. *Seismic upgrading of RC buildings by advanced techniques – The ILVA-IDEM Research Project*. Mazzolani, F. M. co-ordinator & editor, Polimetrica International Scientific Publisher, Monza.
- Federal Emergency Management Agency (FEMA) - 154, (1988). *Rapid visual screening of buildings for potential seismic hazards: a handbook*. Washington (DC).
- Federal Emergency Management Agency (FEMA) - 178, (1992). *BSSC: NEHRP handbook for the seismic evaluation of existing buildings*. Washington (DC).
- Federal Emergency Management Agency (FEMA) - 273, (1997). *NEHRP Guidelines for the seismic rehabilitation of buildings*. Washington (DC).
- Federal Emergency Management Agency (FEMA) - 310, (1998). *Handbook for the seismic evaluation of buildings – a prestandard*. Washington (DC).
- Formisano, A., (2006). Experimental-numerical investigation on stiffened aluminium shear panels. *Accepted for publication in the Pollack Periodica review “An International Journal for Engineering and Information Sciences”*, Ivanyi, A. and Ivanyi M. (eds.), Pecs.
- Formisano, A., De Matteis, G., Panico S., Mazzolani, F.M., (2005). Adeguamento sismico di una struttura esistente in c.a. mediante pannelli a taglio in acciaio: la soluzione progettuale proposta. *Proceedings of the National Conference on “Advances in Steel Constructions” (XX C.T.A.)*, Lacco Ameno, September 26-28, pp. 475-482.
- Formisano, A., De Matteis, G., Maruzzelli, M., Mazzolani, F. M., (2006a). Design of slender steel shear panels: a numerical study. *Proceedings of the 3rd European Conference on “Computational Mechanics Solids, Structures*

- and Coupled Problems in Engineering*" (ECCM '06), Lisbon, June 5–8, CD-ROM.
- Formisano, A., De Matteis, G., Panico, S., Calderoni, B., Mazzolani, F.M., (2006b). Full-scale experimental study on the seismic upgrading of an existing RC frame by means of slender steel shear panels. *Proceedings of the International Conference on Metal Structures (ICMS '06)*, Poiana Brasov, September 16-18, pp. 609-617.
- Formisano, A., De Matteis, G., Panico, S., Calderoni, B., Mazzolani, F.M., (2006c). Full-scale test on existing RC frame reinforced with slender shear steel plates. *Proceedings of the 5th International Conference on the "Behaviour of Steel Structures in Seismic Areas" (STESSA '06)*, Yokohama, August 14-17, pp. 827-834.
- Formisano, A., Mazzolani, F. M., Brando, G., De Matteis, G., (2006d). Full numerical evaluation of the hysteretic performance of pure aluminium shear panels. *Proceedings of the 5th International Conference on "Behaviour of Steel Structures in Seismic Areas" (STESSA '06)*, Yokohama, August 14-17, pp. 211-217.
- Formisano, A., De Matteis, G., Panico, M., Mazzolani, F. M., (2006e). Full scale test of an existing RC frame reinforced with pure aluminium shear panels. *Proceedings of the International Conference on "Stability and Ductility of Steel Structures" (SDSS '06)*, Lisbon, September 6-8, pp. 903-910.
- Foti, D., Zambrano, A., (2004). Shear panel for seismic protection of structures. *Proceedings of the 13th World Conference on Earthquake Engineering*, Vancouver, B.C., Canada, August 1-6, Paper No. 1991.
- Fujitani, H., Yamanouchi, H., Okawa, I. Sawai, N., Uchida, N., Matsutani, T., (1996). Damage and performance of tall buildings in the 1995 Hyogoken Nanbu earthquake. *Proceedings of the 67th Regional Conference Council on Tall Building and Urban Habitat*, Chicago, pp. 103-125.
- Fukuyama, H., Sugano, S., (2000). Japanese seismic rehabilitation of concrete buildings after the Hyogoken-Nanbu Earthquake. *Cement & Concrete Composites*, 22, pp. 59-79.
- Gavarini, C., (1991). Earthquake protection of buildings. *Proceedings of the*

- International Meeting on Earthquake Protection of Buildings*. Ancona, June 6-8, pp. 3/A-22/A.
- Gioncu, V., Mazzolani, F. M., (2002). *Ductility of Seismic Resistant Steel Structures*. E & FN Spon, London.
- Gulkan, P., Sozen, M. A., (1999). Procedure for determining seismic vulnerability of building structures. *ACI Struct. Journal*, 96(3), pp. 336-342.
- Hamburger, R. O., Moehle, J. P., (2000). State of Performance Based-Engineering in the United States. *Proceedings of the 2nd US-Japan Workshop on Performance-Based Design Methodology for Reinforced Concrete Building Structures*, Sapporo, September.
- Hassan, A. F., Sozen, M. A., (1997). Seismic vulnerability assessment of low-rise buildings in regions with infrequent earthquakes. *ACI Structural Journal*, 94 (1), pp. 31-39.
- Hibbitt, Karlsson, Sorensen, Inc., (2004). *ABAQUS/Standard, version 6.4*. Patwucket, RI, USA.
- Höglund, T., (1997). Shear buckling resistance of steel and aluminium plate girders. *Thin-Walled Structures*, Vol.29 (1-4), pp. 13-30.
- Kanada, M., Astaneh-Asl, A., (1996). Seismic Performance of Steel Bridges During the 1995 Hanshin Earthquake. *Report No. UCB/CE-Steel-96-01*, Department of Civil and Environmental Engineering, Univ. of California, Berkeley.
- Katayama, T., Ito, S., Kamura, H., Ueki, T., Okamoto, H., (2000). Experimental Study on Hysteretic Damper with Low Yield Strength Steel Under Dynamic Loading. *Proceedings of the 12th World Conference on Earthquake Engineering*, Auckland, January 30 – February 4.
- Kulak, G.L., (1991). Unstiffened Steel Plate Shear Walls. *Structures subjected to repeated loading – stability and strength*. Narayanan, R. and Roberts, T. M. eds., Elsevier, London, pp. 237-276.
- Lew, H. S., (2005). Handbook for Seismic Rehabilitation of Existing Buildings. *Proceedings of 37th Joint Meeting on “Panel on wind and seismic effects”*, May 16-21.
- Liu, J., Astaneh-Asl, A., (2000). Cyclic tests on simple connections including

- slab effects. *Proceedings of the North American Steel Construction Conference*, AISC, Las Vegas.
- Lubell, A. S., Prion, H. G. L., Ventura, C. E., Rezai, M., (2000). Unstiffened Steel Plate Shear Wall Performance Under Cyclic Loading. *Journal of Structural Engineering*, ASCE, pp. 453-460, April.
- Masi, A., Vona, M., (2004). Seismic vulnerability of RC buildings realised during 70's (in italian). *Proceedings of the 11th National Conference "L'Ingegneria Sismica in Italia"*, Genoa, January 25-29.
- Mazzolani, F.M., (2006a). Experimental tests on real RC buildings for seismic upgrading by innovative techniques. *Proceedings of the International Symposium in honour of Jean Marie Aribert*.
- Mazzolani, F.M., (2006b). Foreword. *Seismic upgrading of RC buildings by advanced techniques – The ILVA-IDEM Research Project*. Mazzolani, F. M. co-ordinator & editor, Polimetrica International Scientific Publisher, Monza.
- Mazzolani, F.M., Della Corte, G., Faggiano, B., (2004). Seismic upgrading of RC buildings by means of advanced techniques: the ILVA-IDEM research project. *Proceedings of the 13th World Conference on Earthquake Engineering*, Vancouver, B.C., Canada, August 1-6, Paper No. 2703.
- Mazzolani, F.M., Gioncu, V. (eds), (2000). *Seismic Resistant Steel Structures (CISM Course)*. Springer - Verlag Wien - New York.
- Miller, C.J., Serag, A.E., (1978). Dynamic Response of Infilled Multi-Storey Steel Frames. *Proceedings of the 4th International Specialty Conference on Cold-formed Steel Structures*, Missouri-Rolla, pp. 557-586.
- Mimura, H., Akiyama, H., (1977). Load-Deflection Relationship of Earthquake Resistant Steel Shear Walls with a Developed Diagonal Tension Field. *Trans. Arch. Inst. of Japan*, Tokyo, Japan, pp. 109-114.
- Miranda, E., Bertero, V.V., (1990). Post-tensioning Techniques for Seismic Upgrading of Existing Low-Rise Buildings. *Proceedings of the 4th U.S. National Conference on Earthquake Engineering*, Vol. 3, pp. 393-402.
- Mistakidis, E.S., De Matteis, G., Formisano, A., (2004). Seismic Upgrade of Concrete Structures using Low Yield Metal Shear Panels. *Proceedings of*

- the 7th International Conference on Computational Structures Technology*, Topping, B.H.V., Mota Soares, C.A. (eds), Civil-Comp Press, Stirling, United Kingdom, CD-ROM, Paper No. 279.
- Mo, Y.L., Perng, S.F., (2000). Seismic Behavior of Reinforced Concrete Frames with Corrugated Steel Walls. *Advances in Structural Engineering*, Vol.3, No. 3, pp. 255-262.
- Moehle, J. P., (2000). State of Research on Seismic Retrofit of Concrete Building Structures in the US. *US-Japan Symposium and Workshop on Seismic Retrofit of Concrete Structures—State of Research and Practice*, September.
- Nakagawa, S., Kihara, H., Torii, S., Nakata, Y., Matsuoka, Y., Fujisawa, K., Fukuda, K., (1996). Hysteretic Behavior of Low Yield Strength Steel Panel Shear Walls – Experimental Investigation. *Proceedings of the 11th World Conference on Earthquake Engineering*, Acapulco, June 23-28.
- Nakashima, M., (1995). Strain-Hardening Behavior of Shear Panels Made of Low Yield Steel – I: Test. *Journal of Structural Engrg.*, ASCE, Vol. 121, No. 12, pp. 1742-1749, December.
- Nakashima, M., Akawaza, T., Tsuji, B., (1995). Strain-Hardening Behavior of Shear Panels Made of Low-Yield Steel - II: Model. *Journal of Structural Engrg.*, ASCE, Vol. 121, No. 12, pp. 1750-1757, December.
- Nakashima, M., Iwai, S., Iwata, M., Takeuchi, T., Konomi, S., Akazawa, T., Saburi, K., (1994). Energy Dissipation Behaviour of Shear Panels Made of Low Yield Steel. *Earthquake Engineering and Structural Dynamics*, Vol. 23, pp. 1299-1313.
- Nilson, H., (1960). Shear Diaphragms of Light Gauge Steel. *Journal of Structural Division*, ASCE, 86, No. ST1,1.
- OPCM 3431, (2005). *First elements in the matter of general criteria for seismic classification of the national territory and of technical codes for structures in seismic zones (in italian)*. Official Gazette of the Italian Republic.
- Pagano, M., Mazzolani, F. M., (1966). Indagine sperimentale al vero sull'instabilità elasto-plastica di due telai multipiani in acciaio. *Costruzioni*

Metalliche, 4-5-6.

- Panico, S., (2004). Aluminium shear panels for seismic protection: numerical analysis and experimental tests. *PhD Thesis in Structural Engineering*, University of Naples “Federico II”.
- Panico, S., De Matteis, G., Mazzolani, F. M., (2003). Numerical investigation on pure aluminium shear panels. *Proceedings of the 19th C. T. A. National Congress “Giornate Italiane della Costruzione in Acciaio”*, Genoa, September 28 – October 1.
- Paulay, T., Priestley, M.J.N., (1992). *Seismic Design of Reinforced Concrete and Masonry Buildings*. John Wiley and Sons, New York.
- Pecce, M., Di Sarno, L., Cosenza, E., (2004). Methodology for seismic vulnerability analysis of RC buildings (in italian). *Proceedings of the 15th C.T.E. Congress “Associazione dei tecnici della Prefabbricazione Edilizia”*, Bari, Novembre 4-6.
- Pinelli, J. P., Moor, C., Craig, J. I., Goodno, B. J., (1996). Testing of Energy Dissipating Cladding Connections. *Earthquake Engineering and Structural Dynamics*, 25, pp. 129-47.
- Rai, D., Wallace, B.J., (1998). Aluminium shear links for enhanced seismic resistance. *Earthquake Engineering and Structural Dynamics* 27, pp. 315-342.
- Rezai, M., (1999). Seismic Behaviour of Steel Plate Shear Walls by Shake Table Testing. *PhD dissertation*, Univ. of British Columbia, Vancouver, Canada.
- Sabouri-Ghomi, S., Roberts, T. M., (1991). Nonlinear Dynamic Analysis of Thin Steel Plate Shear Walls. *Computers & Structures*, Vol. 39, No. 1/2, pp. 121-127.
- Sabouri-Ghomi, S., Ventura, C., Kharrazi, M.H.K. (2003). Shear analysis and design of ductile steel plate walls. *Proceedings of the 4th International Conference on “Behaviour of Steel Structures in Seismic Areas” (STESSA 2003)*, Naples, Italy, June 9-12.
- SEAOC, (1995). *Performance-Based Seismic Engineering*. California.
- Stowell, E.Z., (1948). Critical shear stress of an infinitely long plate in the

plastic region. *NACA Tech. Note*.

Tanaka, K., Sasaki, Y., (2000). Hysteretic Performance of Shear Panel Dampers of Ultra Low Yield Strength Steel for Seismic Response Control of Buildings. *Proceedings of the 12th World Conference on Earthquake Engineering*, Auckland, January 30 – February 4.

Tanaka, K., Torii, T., Sasaki, Y., Miyama, T., Kawai, H., Iwata, M., Wada, A., (1998). Practical application of damage tolerant structures with seismic control panel using low yield point steel at a high-rise steel building. *Proceedings of the Structural Engineering World Wide*, Elsevier, CD-ROM, Paper T190-4.

Thermou, G. E., Elnashai, A. S., (2005). Seismic retrofit schemes for RC structures and local-global consequences. *Prog. Struct. Engrg Mater.*, 8, pp. 1-15.

Thorburn, L. J., Kulak, G. L., Montgomery, C. J., (1983). Analysis of Steel Plate Shear Walls. *Struct. Eng. Rep. No. 107*, Dept. of Civ. Engrg., University of Alberta, Edmonton, Alta, Canada.

Timler, P.A., (2000). Design Evolution and State-of-the-Art Development of Steel Plate Shear Wall Construction in North America. *Proceedings of the 69th Annual SEAOC Convention*, Vancouver, British Columbia, pp. 197-208.

Timler, P.A., Kulak, G.L., (1983). Experimental Study of Steel Plate Shear Walls. *Struct. Eng. Rep. No. 114*, University of Alberta, Edmonton, Alta, Canada.

Timoshenko, S.P., Gere, J.M., (1961). *Theory of elastic stability*. 2nd Ed. McGraw-Hill Book Co., New York (USA).

Timoshenko, S., Woinowsky-Krieger, S., (1959). *Theory of Plates and Shells, Second Edition*. McGraw- Hill, New York.

Tromposch, E. W., Kulak, G. L., (1987). Cyclic and Static Behaviour of Thin Panel Steel Plate Shear Walls. *Struct. Eng. Rep. No. 145*, Dept. of Civ. Engrg., University of Alberta, Edmonton, Alta, Canada.

Troy, R.G., Richard, R. M., (1988). Steel Plate Shear Wall Design. *Struct. Engrg. Review*, 1(1).

- UNI EN 10142, (1992). *Continuously hot-dip zinc coated low carbon steels strip and sheet for cold forming - Technical delivery conditions*. March.
- Valente, C., Spina, D., Nicoletti, M., (2006). Dynamic testing and modal identification. *Seismic upgrading of RC buildings by advanced techniques – The ILVA-IDEM Research Project*. Mazzolani, F. M. co-ordinator & editor, Polimetrica International Scientific Publisher, Monza.
- Vayas, I., Papantonopoulos, K., Marinelli, K., (2005). Greek contribution to Workpackage 3 : Risk Analysis. *Project Deliverable D3 “Assessment of seismic risk maps and evaluation of seismic vulnerability of historical building heritage in the mediterranean area” of the PROHITECH research project “Earthquake Protection of Historical Buildings by Reversible Mixed Technologies”*, March.
- Vian, D., Bruneau, M., (2004). Testing of special LYS steel plate shear walls. *Proceedings of the 13th World Conference on Earthquake Engineering*, Vancouver, B.C., Canada, August 1-6, Paper No. 978.
- Verderame, G. M., (1999). Seismic analysis of gravity-load designed RC buildings (in italian). *PhD Thesis in Structural Engineering*, University of Naples “Federico II”.
- Xue, M., Lu, L. W., (1994). Interaction of Infilled Steel Shear Wall Panels with Surrounding Frame Members. *Proceedings of the Structural Stability Research Council, Annual Technical Session*, Bethlehem, pp. 339-354.
- Yakut, A., (2004). Preliminary seismic performance assessment procedure for existing RC buildings. *Engineering Structures*, 26, pp. 1447-1461.
- Yamaguchi, T., et al., (1998). Seismic Control Devices Using Low-Yield-Point Steel. *Nippon Steel Technical Report No. 77*, pp.65-72.
- Wada, A., Connor, J.J., Kawai, H., Iwata, M., Watanabe, A., (1992). Damage Tolerant Structures. *Proceedings of the 5th US-Japan Workshop on the Improvement of Building Structural Design and Construction Practices*, ATC-15, California, USA.
- Wagner, H., (1931). Flat Sheet Metal Girders with Very Thin Webs, Part I - General Theories and Assumptions. *Tech. Memo. No. 604*, National Advisory Committee for Aeronautics, Washington, USA.